PROGRAMMED CELL DEATH 2.0: THE QUALITY OF CELL DEATH

EDITED BY: Michael Thomas Lotze, Yinan Gong, Jennifer Martinez and Na Dong
PUBLISHED IN: Frontiers in Cell and Developmental Biology

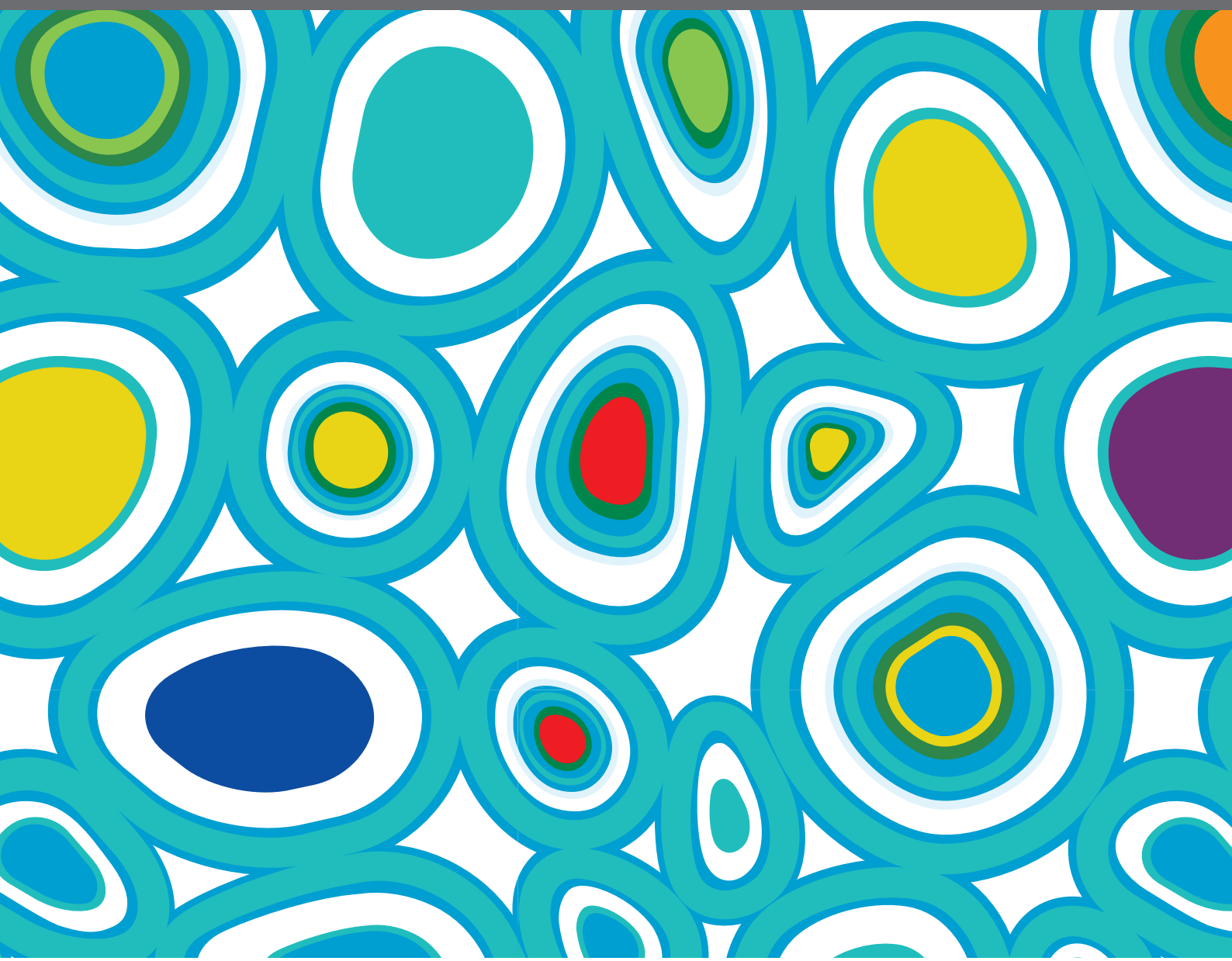

frontiers Research Topics

frontiers

ISSN 1664-8714
ISBN 978-2-88974-390-2
DOI 10.3389/978-2-88974-390-2

About Frontiers

Frontiers is more than just an open-access publisher of scholarly articles: it is a pioneering approach to the world of academia, radically improving the way scholarly research is managed. The grand vision of Frontiers is a world where all people have an equal opportunity to seek, share and generate knowledge. Frontiers provides immediate and permanent online open access to all its publications, but this alone is not enough to realize our grand goals.

Frontiers Journal Series

The Frontiers Journal Series is a multi-tier and interdisciplinary set of open-access, online journals, promising a paradigm shift from the current review, selection and dissemination processes in academic publishing. All Frontiers journals are driven by researchers for researchers; therefore, they constitute a service to the scholarly community. At the same time, the Frontiers Journal Series operates on a revolutionary invention, the tiered publishing system, initially addressing specific communities of scholars, and gradually climbing up to broader public understanding, thus serving the interests of the lay society, too.

Dedication to Quality

Each Frontiers article is a landmark of the highest quality, thanks to genuinely collaborative interactions between authors and review editors, who include some of the world's best academicians. Research must be certified by peers before entering a stream of knowledge that may eventually reach the public - and shape society; therefore, Frontiers only applies the most rigorous and unbiased reviews.
Frontiers revolutionizes research publishing by freely delivering the most outstanding research, evaluated with no bias from both the academic and social point of view. By applying the most advanced information technologies, Frontiers is catapulting scholarly publishing into a new generation.

What are Frontiers Research Topics?

Frontiers Research Topics are very popular trademarks of the Frontiers Journals Series: they are collections of at least ten articles, all centered on a particular subject. With their unique mix of varied contributions from Original Research to Review Articles, Frontiers Research Topics unify the most influential researchers, the latest key findings and historical advances in a hot research area! Find out more on how to host your own Frontiers Research Topic or contribute to one as an author by contacting the Frontiers Editorial Office: frontiersin.org/about/contact

PROGRAMMED CELL DEATH 2.0: THE QUALITY OF CELL DEATH

Topic Editors:
Michael Thomas Lotze, University of Pittsburgh Cancer Institute, United States
Yinan Gong, University of Pittsburgh, United States
Jennifer Martinez, National Institute of Environmental Health Sciences (NIEHS), United States
Na Dong, China Agricultural University, China

Citation: Lotze, M. T., Gong, Y., Martinez, J., Dong, N., eds. (2022). Programmed Cell Death 2.0: The Quality of Cell Death. Lausanne: Frontiers Media SA.
doi: 10.3389/978-2-88974-390-2

Table of Contents

frontiers in Cell and Developmental Biology

ORIGINAL RESEARCH
published: 17 July 2020
doi: 10.3389/fcell.2020.00641

Arg-GlcNAcylation on TRADD by NleB and SseK1 Is Crucial for Bacterial Pathogenesis

*Juan Xue[1,2,3], Shufan Hu[2,3], Yuxuan Huang[2,3], Qi Zhang[2,3], Xueying Yi[2,3], Xing Pan[1,2,3] and Shan Li[1,2,3]**

[1] Taihe Hospital, Institute of Infection and Immunity, Hubei University of Medicine, Shiyan, China, [2] College of Life Science and Technology, Huazhong Agricultural University, Wuhan, China, [3] College of Biomedicine and Health, Huazhong Agricultural University, Wuhan, China

Death receptor signaling is critical for cell death, inflammation, and immune homeostasis. Hijacking death receptors and their corresponding adaptors through type III secretion system (T3SS) effectors has been evolved to be a bacterial evasion strategy. NleB from enteropathogenic *Escherichia coli* (EPEC) and SseK1/2/3 from *Salmonella enterica* serovar Typhimurium (*S.* Typhimurium) can modify some death domain (DD) proteins through arginine-GlcNAcylation. Here, we performed a substrate screen on 12 host DD proteins with conserved arginine during EPEC and *Salmonella* infection. NleB from EPEC hijacked death receptor signaling through tumor necrosis factor receptor 1 (TNFR1)-associated death domain protein (TRADD), FAS-associated death domain protein (FADD), and receptor-interacting serine/threonine-protein kinase 1 (RIPK1), whereas SseK1 and SseK3 disturbed TNF signaling through the modification of TRADD Arg235/Arg245 and TNFR1 Arg376, respectively. Furthermore, mouse infection studies showed that SseK1 but not SseK3 rescued the bacterial colonization deficiency contributed by the deletion of NleBc (*Citrobacter* NleB), indicating that TRADD was the *in vivo* substrate. The result provides an insight into the mechanism by which attaching and effacing (A/E) pathogen manipulate TRADD-mediated signaling and evade host immune defense through T3SS effectors.

Keywords: enteropathogenic *Escherichia coli*, T3SS effectors, NleB, SseK, arginine GlcNAc transferase, TRADD

OPEN ACCESS

Edited by:
Yinan Gong,
University of Pittsburgh, United States

Reviewed by:
Liming Sun,
Shanghai Institute of Biochemistry and Cell Biology (CAS), China
Min Zheng,
St. Jude Children's Research Hospital, United States
Weihong Wang,
University of Pittsburgh, United States

***Correspondence:**
Shan Li
lishan@mail.hzau.edu.cn

Specialty section:
This article was submitted to Cell Death and Survival, a section of the journal Frontiers in Cell and Developmental Biology

Received: *16 May 2020*
Accepted: *25 June 2020*
Published: *17 July 2020*

Citation:
Xue J, Hu S, Huang Y, Zhang Q, Yi X, Pan X and Li S (2020) Arg-GlcNAcylation on TRADD by NleB and SseK1 Is Crucial for Bacterial Pathogenesis. Front. Cell Dev. Biol. 8:641. doi: 10.3389/fcell.2020.00641

INTRODUCTION

Death receptor signaling is crucial for cell death (Giogha et al., 2014; Luo et al., 2015; Galluzzi et al., 2018), inflammation (Park et al., 2007), and immune homeostasis (Wilson et al., 2009). It is mediated by homotypic or heterotypic interactions among death domains (DDs) of the TNFR family of transmembrane death receptors and the downstream adaptors, including TRADD (Hsu et al., 1995; Luo et al., 2015), RIPK1 (Stanger et al., 1995; Luo et al., 2015), and FADD (Chinnaiyan et al., 1995; Luo et al., 2015). TRADD is known as the initial adaptor for TNFR1-induced apoptosis and nuclear factor-κB (NF-κB) signaling (Hsu et al., 1995; Chen and Goeddel, 2002; Mak and Yeh, 2002; Chen et al., 2008; Pobezinskaya et al., 2008; Pobezinskaya and Liu, 2012). Recent studies have found that TRADD has a Goldilocks effect on the survival of $Ripk1^{-/-}Ripk3^{-/-}$ mice. Both $Tradd^{+/+}Ripk1^{-/-}Ripk3^{-/-}$ and $Tradd^{-/-}Ripk1^{-/-}Ripk3^{-/-}$ mice result in death through apoptosis, while a single allele of TRADD is optimal for survival of $Ripk1^{-/-}Ripk3^{-/-}$

mice (Dowling et al., 2019). RIPK1 and TRADD are synergistically required for TRAIL-induced NF-κB signaling and TNFR1-induced NF-κB signaling and apoptosis (Fullsack et al., 2019). Besides that, TRADD plays roles independent of TNFR1 signaling, such as downstream of Toll-like receptors (Chen et al., 2008; Pobezinskaya et al., 2008) and DR3 (Chinnaiyan et al., 1996; Kitson et al., 1996; Pobezinskaya et al., 2011; Pobezinskaya and Liu, 2012). Type III secretion system effector NleB from enteropathogenic *E. coli* (EPEC) was previously reported as an arginine GlcNAc transferase that inhibited multiple death receptor mediated inflammation and cell death by modifying a conserved arginine residue in some death domain proteins (Li et al., 2013; Pearson et al., 2013; Ding et al., 2019; Pan et al., 2020; Xue et al., 2020). The arginine GlcNAc transferase activity of NleB is critical for attaching and effacing (A/E) pathogen colonization in the mouse colon (Li et al., 2013; Pearson et al., 2013; Scott et al., 2017; Ding et al., 2019). Although modification of TRADD, FADD, and RIPK1 in *in vitro* reconstitution system and *ex vivo* epithelial cell infection system has been studied, the *in vivo* substrate preference of NleB remains elusive.

Intracellular pathogen *Salmonella entrica* strains secreted three *Salmonella* pathogenicity island 2 (SPI-2) effector SseK1, SseK2, and SseK3 (Kujat Choy et al., 2004; Brown et al., 2011; Baison-Olmo et al., 2015; El Qaidi et al., 2017; Gunster et al., 2017; Yang et al., 2018; Araujo-Garrido et al., 2020; Meng et al., 2020). Crystal structure studies show that NleB, SseK1, and SseK3 belong to the GT-A family glycosyltransferase (Esposito et al., 2018; Park et al., 2018; Ding et al., 2019; Araujo-Garrido et al., 2020; Pan et al., 2020). The crystal structures of NleB in complex with FADD-DD and the sugar donor, and NleB-GlcNAcylated DDs (TRADD-DD and RIPK1-DD) show that NleB is an inverting enzyme. NleB converts the α-configuration in the UDP-GlcNAc donor into the β-configuration toward the conserved arginine of DD proteins, namely, TRADD Arg235, FADD Arg117, and RIPK1 Arg603 (Ding et al., 2019; Xue et al., 2020). Previous *in vitro* studies have suggested that SseK1 could GlcNAcylate TRADD (Li et al., 2013; Gunster et al., 2017; Xue et al., 2020), FADD (Gunster et al., 2017), and GAPDH (Gao et al., 2013; El Qaidi et al., 2017) with different efficiency. However, the substrate specificity of SseK effectors remains controversial.

Therefore, this study applied a substrate screen of 12 conserved arginine-containing DD proteins during EPEC and *Salmonella* infection, finding that SseK1 and SseK3 selectively modify TRADD and TNFR1, respectively. SseK1 GlcNAcylated hTRADD at Arg235 and Arg245 while SseK3 targeted TNFR1 at Arg376. SseK1 but not SseK3 can inhibit TRADD-activated NF-κB and apoptosis. Taking advantage of the substrate specificity of SseK effectors, we found that only chimera SseK1 fully rescued the bacterial colonization deficiency contributed by the deletion of NleBc in *Citrobacter rodentium* (*C. rodentium*) infection animal model. This result indicates that TRADD is the preferred *in vivo* substrate corresponding to NleB/SseK1-induced bacterial virulence. More importantly, the TRADD$^{-/-}$ mice infection model confirmed this result. All these findings suggest that arginine GlcNAcylation in TRADD catalyzed by type III-translocated bacterial effector proteins NleB and SseK1 is crucial for the pathogenesis of A/E pathogen.

MATERIALS AND METHODS

Bacterial Strains and Growth Conditions

The EPEC strains, *Salmonella* strains, and *C. rodentium* strains used in this study, unless specially mentioned, were grown in LB broth at 37°C, shaking with the following antibiotics: nalidixic acid (50 μg/ml) (0677, AMRESCO), kanamycin (50 μg/ml) (1758-9316, INALCO), ampicillin (100 μg/ml) (1758-9314, INALCO), chloramphenicol (17 μg/ml) (1758-9321, INALCO), and streptomycin (50 μg/ml) (1758-9319, INALCO).

Plasmid Construction

nleB gene and *sseK1/2/3* genes were amplified from EPEC E2348/69, *C. rodentium* ICC168, and *S. enterica* Typhimurium SL1344 strains. These genes were inserted into pCS2-EGFP, pCS2-1Flag, and pCS2-3Flag for mammalian cell expression, and into pGEX-6P-2 and pET28a-His for protein expression in *E. coli*. The pTRC99A vector was used for complementation in EPEC (under the trc promoter) and the pET28a vector for complementation in *C. rodentium* (under the *C. rodentium nleB* signal peptide) and *S.* Typhimurium (with their upstream promoter regions). Human cDNAs for TRADD, TNFR1, FADD, DR3 DD, ANK1 DD, ANKDD1B, ANK2 DD, ANK3 DD, RIPKI DD, FAS DD, DR4 DD, DR5 DD were amplified from a HeLa cDNA library as previously described (Li et al., 2013). All single point mutants were generated by quick change and multiple point mutants and truncation mutants were generated by standard molecular biology procedures. NF-κB reporter plasmids were used as previously described (Li et al., 2007, 2013). All plasmids were verified by DNA sequencing and primers were synthesized by Sangon Biotech.

Antibodies and Reagents

The anti-GlcNAc arginine antibody (ab195033, Abcam) was described previously (Pan et al., 2014). Antibody for Flag M2 (F2426) and tubulin (T5186) were Sigma products. Antibodies for EGFP (sc8334) and DnaK 8E2/2 (ab69617) were purchased from Santa Cruz Biotechnology and Abcam, respectively. Horse radish peroxidase (HRP)-conjugated goat anti-mouse IgG (NA931V) and HRP-conjugated goat anti-rabbit IgG (NA934) were both from GE Healthcare. Unless specially mentioned, the cell culture products were purchased from Invitrogen, and all other reagents were Sigma-Aldrich products.

Recombinant Protein Expression and Purification

Protein expression was induced overnight in *E. coli* BL21 (DE3) strain at 22°C with 0.4 mM isopropyl-β-D-thiogalactopyranoside (IPTG) when OD600 reached 0.8˜1.0. Affinity purification of GST-TRADD DD and the site-directed mutants expression alone or co-expression with SseK1 were performed by using glutathione sepharose (GE Healthcare, United States), following the manufactures' instructions. Proteins were further purified by ion exchange chromatography. All the purified recombinant proteins were concentrated and stored in the buffer containing 20 mM Tris-HCl (pH 8.0), 150 mM NaCl, and 5 mM

dithiothreitol. The protein purity was examined by SDS-PAGE, followed by Coomassie Blue staining.

Cell Culture and NF-κB Luciferase Reporter Assay

293T cells and HeLa cells obtained from the American Type Culture Collection (ATCC) and MEF cells provided by S. Ghosh were grown in DMEM (GIBCO) medium supplemented with 10% FBS (GIBCO and BI), 2 mM L-glutamine (GIBCO), 100 U/ml penicillin, and 100 mg/ml streptomycin (GIBCO). These cells were cultivated at 37°C in the presence of 5% CO_2. Vigofect (Vigorus) was used for 293T cell transfection and jetPRIME (PolyPlus) for HeLa cell transfection, following the respective manufacturer's instructions. Luciferase activity was determined 24 h after transfection by using the dual luciferase assay kit (Promega) according to the manufacturer's instructions.

Immunoprecipitation

The 293T cells seeded in 6-well plates at a confluency of 60–80% were transfected with a total of 5 μg plasmids. Twenty-four hours after transfection, cells were washed in phosphate-buffered saline (PBS) and lysed in lysis buffer A containing 25 mM Tris-HCl, pH 7.6, 150 mM NaCl, 10% glycerol, and 1% Triton, supplemented with a protease inhibitor cocktail (Roche). Cells were collected and centrifuged under 13,200 rpm at 4°C for 15 min. Pre-cleared lysates were subjected to anti-Flag M2 immunoprecipitation following the manufacturer's instructions. After a 2 h incubation, the beads were washed four times with lysis buffer B containing 25 mM Tris-HCl, pH 7.6, 150 mM NaCl, 10% glycerol, and 0.5% Triton, and the immunoprecipitates were eluted by 1 × SDS sample buffer, followed by standard immunoblotting analysis. All the immunoprecipitation assays were performed more than three times, and representative results are shown in figures.

Bacterial Infection of Mammalian Cells and Cell Death Assay

Bacterial infection and cell death were performed as described previously (Li et al., 2013; Gunster et al., 2017; Ding et al., 2019; Newson et al., 2019; Xue et al., 2020). Briefly, MEF cells were seeded in 96-well plates at a concentration of 2×10^4 per well one day before infection. A single colony in 0.5 ml LB was incubated overnight in a static LB culture at 37°C. Bacterial strains were then diluted by 1:40 in antibiotic-free DMEM supplemented with 1 mM IPTG and cultured at 37°C in the presence of 5% CO_2 for an additional 4 h to OD600 approximately at 0.4∼0.6. Infection was performed at a multiplicity of infection (MOI) of 200 in the presence of 1 mM IPTG for 2 h, with centrifugation at 800 g for 10 min at room temperature to promote infection. After the infection, cells were washed four times with PBS, and the extra bacteria were killed with 200 μg/ml gentamicin. One-hour CHX pretreatment (2 μg/ml) was used to sensitize TNF (20 ng/ml)-stimulated cell death. Cell survival was then determined 15 h after treatment with TNF by using the CellTiter-Glo Luminescent Cell Viability Assay kit (Promega).

Liquid Chromatography-Mass Spectrometry Analysis of Intact Proteins

The method was performed as described previously (Xue et al., 2020). In brief, 10 μg of purified protein was injected and separated by reversed-phase liquid chromatography in a Dionex Ultimate 3000 HPLC system (Thermo Fisher Scientific, United States). Using a C4 capillary column (MAbPacTM RP, 4 μm, 2.1 × 50 mm, Thermo Fisher Scientific, United States), the flow rate was set at 0.3 ml/min and the linear 10 min gradient of buffer A (0.1% Formic acid) and buffer B (0.1% Formic acid, 80% acetonitrile) was from 5 to 100%. The eluted proteins were sprayed into a Q Exactive Plus mass spectrometer (Thermo Fisher Scientific, United States) equipped with a Heated Electrospray Ionization (HESI-II) Probe (Thermo Fisher Scientific, United States). Thermo Scientific Protein Deconvolution program was used to analyze the mass accuracy of the intact protein.

Mice Infection and *C. rodentium* Colonization Assays

All animal experiments were conducted following the Chinese National Ministry of Health guidelines for housing and care of laboratory animals, and the experiments were performed in accordance with institutional regulations made by the Institutional Animal Care and Use Committee at Taihe Hospital, Hubei University of Medicine. The 5–6 weeks old of C57BL/6 male mice and $TRADD^{-/-}$ mice were maintained in the specific pathogen-free environment. All the mice were randomly divided into each experimental group with no blind mice and were housed individually in high-efficiency particulate air (HEPA)-filtered cages with sterile bedding. Independent experiments were performed using 6–8 mice per group. The mice infection was performed as described previously (Li et al., 2013; Ding et al., 2019).

Caspase-3 Activity Assay

The activity of prepared cell lysates toward Ac-DEVD-AFC were conducted as previously described (Meng et al., 2016; Wang et al., 2020). Briefly, 293T cells transfected with the indicated plasmid combinations were washed and lysed. The pre-cleared cell lysates collected were mixed with Na-Citrate buffer (50 mM Tris-HCl, pH 7.4, 1 M Na-Citrate, 10 mM DTT, 0.05% CHAPS). Peptide substrates Ac-DEVD-AFC for caspase-3 was added to each well to a final concentration of 20 μM to start the reaction. Assay plates were incubated at 37°C and the caspase-3 activity was measured every 2 min for total 2 h. Substrate cleavage was monitored by measuring the emission signal at 510 nm wavelength by a 405 nm fluorescence excitation on a microplate reader (SpectraMax i3x, Molecular Devices). Fluorometric assays were conducted in white opaque tissue culture plates and all measurements were carried out in triplicate.

Statistical Analysis

All the values of at least three independent experiments were presented. Statistical analysis was performed using Student's *t*-test. The comparison of multiple groups was conducted by

using one-way analysis of variance (ANOVA) or two-way ANOVA. $P < 0.05$ was considered significant.

RESULTS

SseK1 and SseK3 Selectively Modify TRADD and TNFR1 During Pathogen Infection

Death domain (DD) is a subclass of protein motif known as the death fold (Park et al., 2007). DD-containing proteins are usually associated with programmed cell death and inflammation (Park et al., 2007; Park, 2011; Ferrao and Wu, 2012). Multiple sequence alignment of DDs in human genome revealed that Arg235 in TRADD (Arg117 in FADD) was conserved in one-third of the total 37 DD-containing proteins, including TNFR1, TRADD, FADD, RIPK1, FAS, DR3, DR4, DR5, ANK1, ANK2, ANK3, and ANKDD1B (**Figures 1A,B** and **Supplementary Figure 1**). The phylogenetic tree of the 12 DDs showed an evolutionary relationship based on protein sequence (**Figure 1C**). Previous studies show that the conserved arginine is critical for NleB mediated modification (Li et al., 2013; Ding et al., 2019; Pan et al., 2020). Here, we screened all the arginine-containing

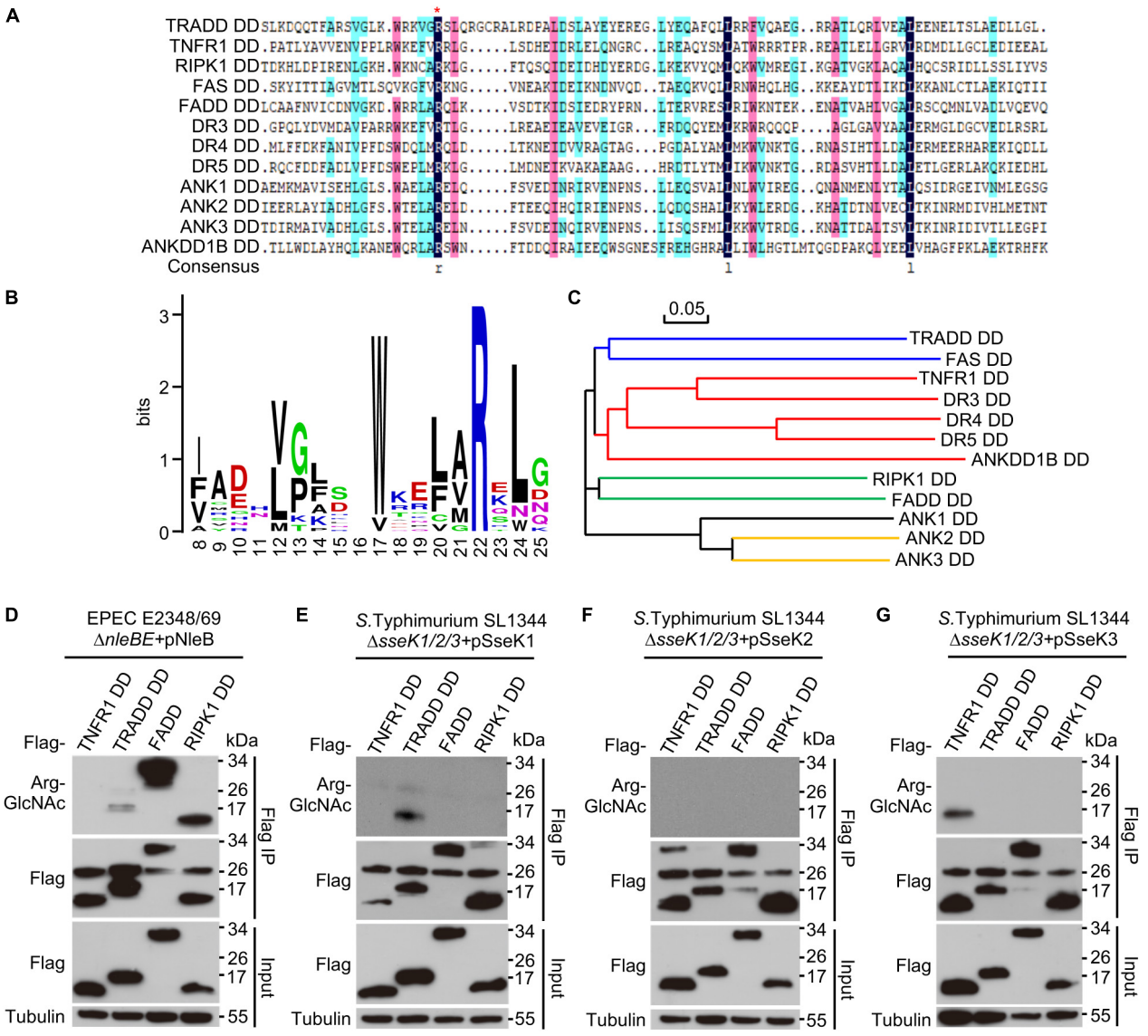

FIGURE 1 | SseK1 and SseK3 selectively modify TRADD and TNFR1 during pathogen infection. **(A)** Multiple sequence alignment of 12 DD proteins from 34 human DD-containing proteins. The red asterisk indicates the conserved arginine. **(B)** Site distribution of amino acids in 12 conserved arginine containing-DDs. **(C)** Phylogenetic tree of the 12 DDs constructed on the basis of sequence similarity. **(D–G)** Selective GlcNAcylation of DDs by NleB and SseK1/2/3 during bacterial infection. 293T cells transfected with the indicated Flag-DD plasmids were infected with EPEC or *Salmonella* strains. Cell lysates were subjected to anti-Flag immunoprecipitation and immunoblotting. Data in **(D–G)** are from at least three independent experiments.

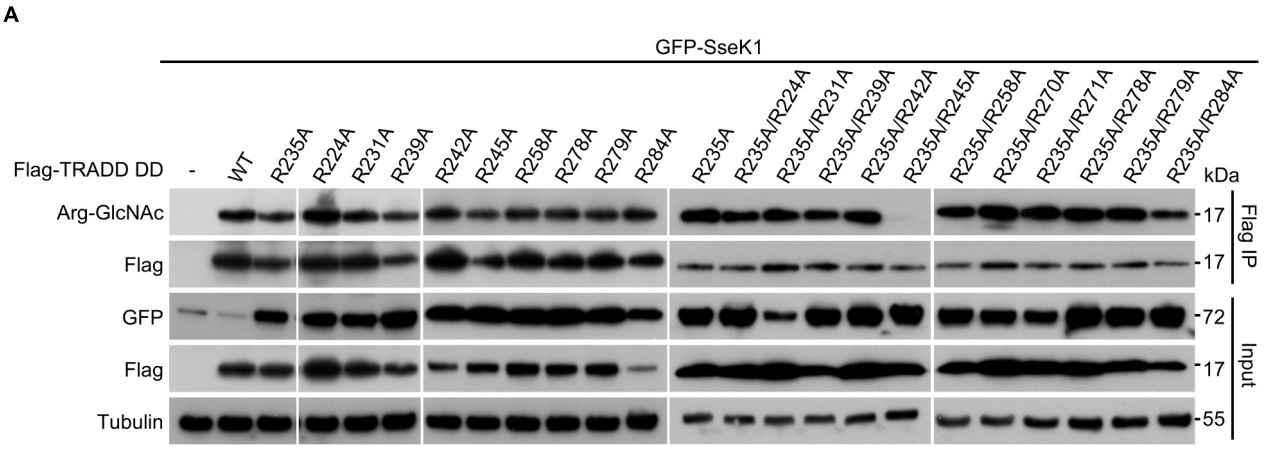

B

Protein	MW change (Da) (induced by SseK1)	Percentage (%)	Total GlcNAcylation (%)
TRADD(195-312)	+203	29	94
	+203-131	13	
	+203+203	34	
	+203+203-131	18	
TRADD(195-312) R235/245A	0	0	0

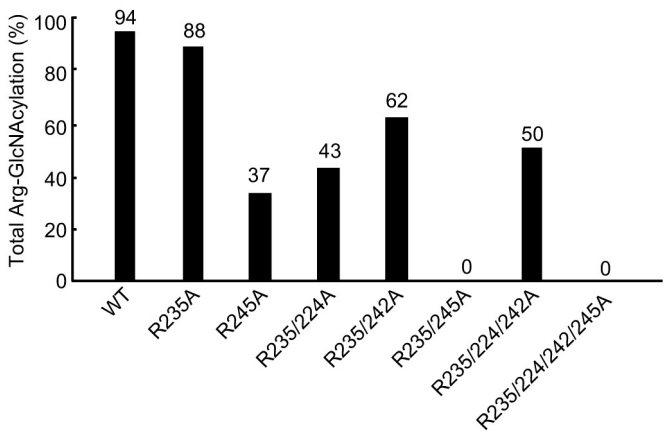

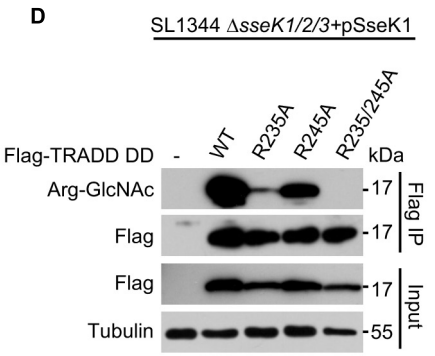

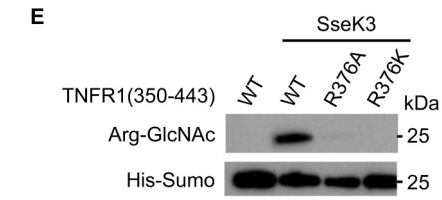

F

TNFR1 (350-443)	MW change(Da) (modified by Ssek3)
WT	+203
R376A	+0
R376K	+0

FIGURE 2 | SseK1 GlcNAcylates hTRADD at R235/R245and SseK3 GlcNAcylates TNFR1 at R376. **(A)** An arginine point mutation screen of hTRADD to investigate its ability to be GlcNAcylated by SseK1. 293T cells were transfected with the indicated plasmid combinations. The samples of anti-Flag immunoprecipitates (Flag IP) and total cell lysates (Input) were immunoblotted with the corresponding antibodies. Anti-tubulin was used as a loading control. **(B)** Mass spectrometry summary of the total molecular weight of TRADD DD and TRADD DD (Arg235Ala/Arg245Ala) mutant co-expressed with SseK1 in bacteria. " + 203" indicates a single GlcNAc modification. " + 203-131" indicates in addition to a single GlcNAc modification, one methionine is missing as well. " + 203 + 203" indicates two GlcNAc modifications. " + 203 + 203-131" indicates in addition to two GlcNAc modifications, one methionine is missing as well. **(C)** Total Arg-GlcNAcylation modification percentages of TRADD and TRADD arginine mutants catalyzed by SseK1. **(D)** Modification of TRADD and TRADD variants by SseK1 upon *S.* Typhimurium infection. Plasmids carrying genes for Flag-TRADD DD, Flag-TRADD DD R235A, Flag-TRADD DD R245A, and Flag-TRADD DD R235/245A transfected into 293T cells were infected with the indicated *Salmonella* strains. After infection, cells were lysed and proteins were immunoprecipitated with Flag beads, followed by standard immunoblotting analysis with the indicated antibodies. **(E)** TNFR1 WT and Arg376 mutants co-expressed with SseK3 in BL21. Bacterial lysates were subjected to SDS-PAGE, followed by immunoblotting analyses as shown. **(F)** Summary of ESI-MS determination of the total mass of TNFR1 and its mutants co-expressed with SseK3 in bacteria. Data in **(A–D)** are from at least three independent experiments.

DD proteins to be GlcNAcylated by NleB/SseKs in bacterial pathogen infection systems. Arginine GlcNAc transferase-deficient strains from EPEC and *Salmonella* were generated. NleB was expressed in EPEC strains, while SseK1, SseK2, and SseK3 were individually expressed in *Salmonella* strains. NleB from EPEC E2348/69 modified TRADD DD, FADD, and RIPK1 DD (**Figure 1D** and **Supplementary Figure 2**). SseK1 and SseK3 from *S. Typhimurium* SL1344 specifically modified TRADD DD and TNFR1 DD, respectively, while SseK2 exhibited no obvious arginine GlcNAcylation activity toward DD proteins during infection (**Figures 1E–G** and **Supplementary Figure 2**). Other arginine containing death domains could not be modified (**Supplementary Figure 2**).

SseK1 GlcNAcylates TRADD at Arg235 and Arg245

Arg235 was the only modification site on TRADD by NleB (Li et al., 2013). However, mutation of Arg235 in TRADD could not abolish the modification of human TRADD by SseK1 (**Figure 2A**). This was in accordance with the previous report on mouse TRADD (Gunster et al., 2017), suggesting that SseK1-mediated GlcNAcylation of TRADD occurred on either a different residue or on multiple arginine residues. We applied an arginine point mutation screen of human TRADD to explore the modification sites of TRADD by SseK1. 293T cells were co-transfected with SseK1 and wild-type or different point mutation variants of TRADD. Single point mutation of any arginines in the death domain of TRADD had no effects on the modification detected by the Arg-GlcNAc antibody (**Figure 2A**). Subsequently, we mutated all the arginine residues on the background of Arg235Ala mutation and found that GlcNAcylation of TRADD Arg235Ala/Arg245Ala mutant was significantly reduced in western blot (Pan et al., 2014; **Figure 2A**). To determine the modification ratio, recombinant TRADD DD and its mutants were co-expressed with SseK1 in *E. coli* BL21 (DE3) strain. Purified proteins were analyzed on the mass spectrometer, and the summary of the resulting total molecular weight of mass spectra was shown (**Figures 2B,C**). Electrospray ionization mass spectrometry (ESI-MS) analysis identified one GlcNAc moiety addition and two GlcNAc moieties addition on TRADD DD, suggesting two sites can be modified simultaneously. Double mutation of Arg235 and Arg245 exhibited the theoretical molecular weight (**Figure 2B**). Consistently, SseK1 delivered from a *Salmonella* derivative strain SL1344Δ*sseK1/2/3* by T3SS, could not modify TRADD DD (R235A/R245A) yet, even though single arginine mutation could be modified (**Figure 2D**). For the modification of TNFR1 by SseK3, mutation of Arg376 into Ala or Lys abolished the arginine-GlcNAcylation signal and molecular weight increase, suggesting that the conserved Arg376 was the bona fide modification site (**Figures 2E,F**). All these data showed that SseK1 GlcNAcylated hTRADD at Arg235 and Arg245 both in the co-expression system and in the pathogen infection process.

SseK1 Inhibits TRADD DD-Activated NF-κB and Cell Death Signaling in 293T Cells

Overexpression of TRADD protein can activate both NF-κB and cell death signaling (Li et al., 2013). SseK1 significantly

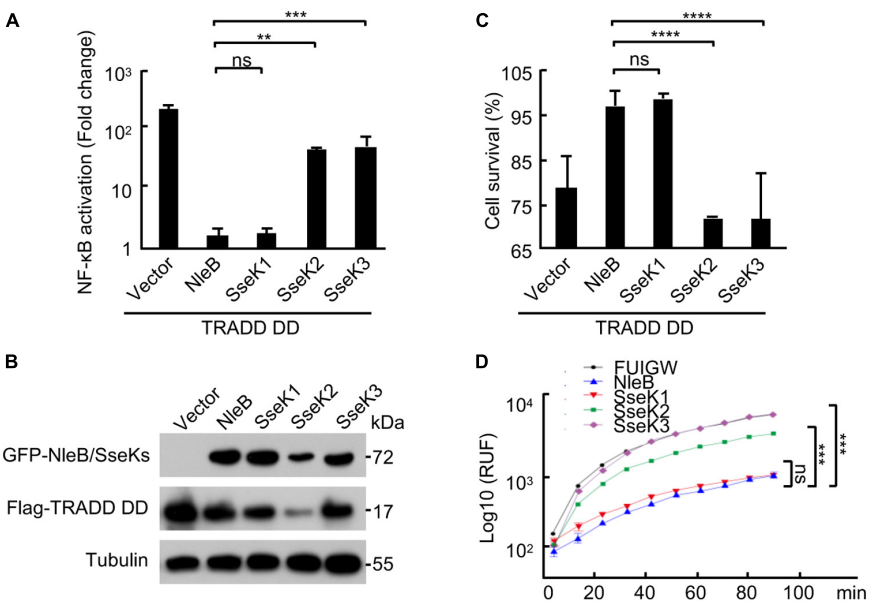

FIGURE 3 | SseK1 inhibits TRADD-activated NF-κB and cell death signaling. **(A–D)** Effects of NleB/SseK on TRADD DD-activated NF-κB **(A,B)**, cell survival **(C)**, and caspase-3 activation **(D)**. 293T cells were transfected with Flag-TRADD DD in combination with the indicated plasmids. NF-κB luciferase activation was indicated as fold change **(A)**. Cell viability was determined by measuring ATP levels **(C)**. Caspase-3 activity was assayed using an Ac-DEVD-AFC probe according to manufacturer's instructions **(D)**. For A and C, one-way ANOVA was used for statistical analysis. And for D, two-way ANOVA was used. $^{**}P < 0.01$, $^{***}P < 0.001$, $^{****}P < 0.0001$, ns, not statistically significant. All data are acquired at the same time and at least three independent experiments.

abolished TRADD DD overexpression-induced NF-κB activation (**Figures 3A,B**), cell death (**Figure 3C**), and caspase-3 activation in 293T cells (**Figure 3D**). However, SseK3 had no effects on these TRADD DD-activated signaling pathways (**Figures 3A–D**). Thus, SseK1 could target TRADD directly and disrupt multiple signaling pathways at the downstream of TRADD.

Chimera SseK1 and SseK3 Inhibits TNF-Induced Cell Death During *C. rodentium* Infection

Considering the broad substrate range of NleB during cell culture infection, it is intriguing to determine the target in *in vivo* infection system. Signal peptides of SseK1/2/3 were replaced with a signal peptide of NleBc to make the chimera SseK1/2/3, which harbor the substrate specificity and can be secreted as NleBc. Complementation strains of Δ*nleB* with *Citrobacter* NleBc or chimera SseK1/2/3 were generated. Chimera SseK1/2/3 expressed normally in *C. rodentium* strain. Chimera SseK1 and SseK3 exhibited their enzymatic activity to modify the substrates in bacteria, whereas the DxD mutants did not (**Figure 4A**). During MEF cell infection, complementation with chimera SseK1 and SseK3, but not SseK2, or respected DxD mutants, inhibited TNF-induced cell death. This inhibition was similar to the level of complementation of NleB (**Figure 4B**), which indicated chimera SseK1 and SseK3 were both translocated and played enzymatic roles in MEF cells. Collectively, these results suggested that chimera SseK1 and SseK3 were functionally secreted during *C. rodentium* infection.

Chimera SseK1 but Not Chimera SseK3 Rescues the Function of NleB in Animal Infection Model

Infection of mice with *C. rodentium* is a natural and physiologically relevant model to study pathogen-host

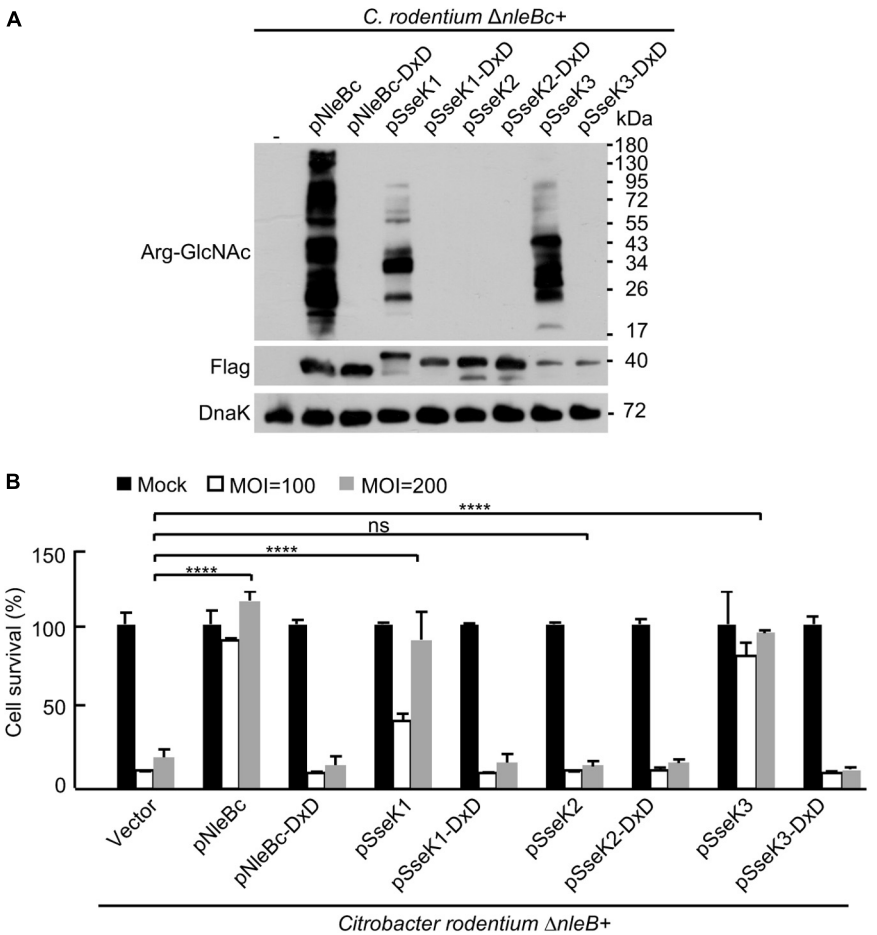

FIGURE 4 | Chimera SseK1 and chimera SseK3 inhibits TNF-induced cell death during *C. rodentium* infection on MEF cells. **(A)** Complementation strains of Δ*nleB* with *Citrobacter* NleBc or chimera SseK1/2/3 and their enzyme inactivated mutants were generated. Single colony of each strain was inoculated and incubated overnight with the corresponding antibiotics. Bacterial lysates were collected and samples were loaded onto SDS-PAGE gels, followed by standard immunoblotting analysis. **(B)** NleB and SseK1/3 mediate inhibition of TNF-induced cell death in MEF cells during *C. rodentium* infection. MEF cells infected with derivatives of *C. rodentium* strains were stimulated with TNF. Cell viability was determined by measuring ATP levels. $^{****}P < 0.0001$ (one-way ANOVA), ns, not statistically significant. Data are representative from at least three repetitions.

interactions for A/E pathogens (Kamada et al., 2012; Li et al., 2013; Pearson et al., 2013; Collins et al., 2014; Crepin et al., 2016; Ding et al., 2019). Previous studies showed that the arginine GlcNAc transferase activity of NleB was crucial for bacterial colonization and virulence in mice infection model (Li et al., 2013; Pearson et al., 2013; Ding et al., 2019). We performed mouse infection assays to investigate the preferred *in vivo* substrate of NleB by utilizing the substrate specificity of SseK1/3. In *C. rodentium*-inoculated C57BL/6 mice, the Δ*nleB* mutant showed a significantly reduced colonization compared to the wild-type strain, demonstrated by colony-forming units of bacteria recovered from stool samples and colons from infected mice. Complementation of Δ*nleB* with NleBc or SseK1, but not SseK2 or SseK3, recovered stool counts to the level of the wild-type strain and restored bacterial colonization in the intestinal tract of mice (**Figures 5A,B**). SseK1 exhibited substrate specificity to TRADD, indicating TRADD was the preferential *in vivo* substrate corresponding to NleB-induced bacterial virulence. We hypothesized that if NleB interfered with TRADD-mediated signaling during infection, then *C. rodentium* Δ*nleB* mutant bacteria would no longer be attenuated in mice with defects in TRADD. Indeed, TRADD$^{-/-}$ mice infected with the Δ*nleB* mutant showed comparable levels of bacterial colonization compared to wild-type mice infected with wild-type *C. rodentium* (**Figure 5C**).

DISCUSSION

Previous studies confirmed that the arginine GlcNAc transferase activity of NleB was essential for bacterial colonization in the mouse model of EPEC infection (Li et al., 2013; Pearson et al., 2013; Ding et al., 2019). Considering that NleB could modify the DDs of TRADD, FADD, and RIPK1 in cell culture infection system (Li et al., 2013; Lu et al., 2015; Scott et al., 2017; Ding et al., 2019; Xue et al., 2020), it is necessary to

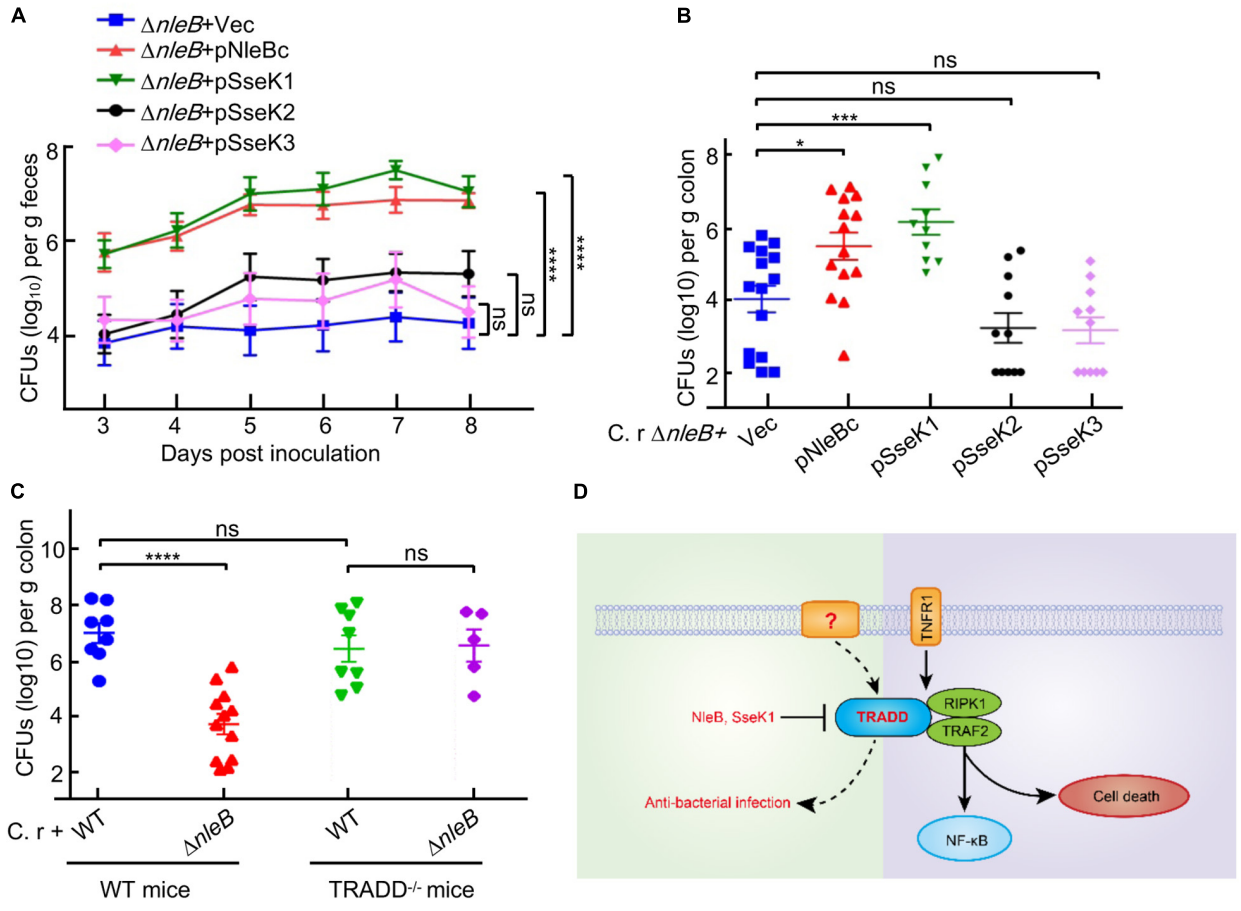

FIGURE 5 | Only SseK1 fully rescues the bacterial colonization contributed by NleBc in *C. rodentium* infection animal model. **(A,B)** 5–6 week-old C57BL/6 male mice were orally gavaged with the indicated *C. rodentium* derivatives. The viable stool bacteria count (log10 CFU/g feces) **(A)** and bacterial colonization in the colon (log10 CFU/g colon, $n > 6$) 8 days post-infection **(B)** were presented as mean ± s.e.m. pNleB(c), pSseK1, pSseK2, and pSseK3 are complementary plasmids expressing NleB(c), SseK1, SseK2, and SseK3, respectively. **(C)** 5–6 week-old TRADD$^{-/-}$ mice and parent mice were orally gavaged with wild type *C. rodentium* and *nleB* deletion mutant. Bacterial colonization in the colon (log10 CFU/g colon, $n > 6$) 8 days post-infection were presented. $^{*}P < 0.05$, $^{***}P < 0.001$, and $^{****}P < 0.0001$ (one-way ANOVA), ns, not statistically significant. Data in **(A–C)** are representative from at least three repetitions. **(D)** Schematic diagram of TRADD-mediated signaling.

determine the target *in vivo*. In *C. rodentium* infection animal model, we found that only SseK1 fully rescued the bacterial colonization deficiency contributed by NleB from *Citrobacter* or EPEC. The finding that SseK1 had substrate specificity to TRADD indicated that TRADD was the preferential *in vivo* substrate corresponding to NleB-induced bacterial colonization. TRADD$^{-/-}$ mice infection model confirmed this result, which might be correlated with its role of dynamic equilibrium in both cell death and NF-κB signaling. SseK3 disrupted TNF signaling by directly targeting TNFR1, which was the upstream receptor of TRADD. Inhibition of TRADD but not TNFR1 was beneficial for bacterial colonization, thus this provided insights into the non-TNFR1 signaling role of TRADD (**Figure 5D**; Chen et al., 2008; Pobezinskaya et al., 2008).

In summary, this study presented compelling evidence for distinct substrate specificities of NleB, SseK1, SseK2, and SseK3 among 12 death domains. SseK1 fully rescued the bacterial colonization deficiency contributed by NleBc in *C. rodentium* infection animal model. TRADD knockout diminished the colonization attenuation effect of NleB deletion. All the data suggest that TRADD is the preferential *in vivo* substrate corresponding to NleB-induced bacterial colonization.

AUTHOR'S NOTE

This manuscript has been released as a Pre-Print at bioRxiv (Xue et al., 2019).

DATA AVAILABILITY STATEMENT

All datasets presented in this study are included in the article/**Supplementary Material**.

ETHICS STATEMENT

The animal study was reviewed and approved by the Ethics Committee of Huazhong Agricultural University.

AUTHOR CONTRIBUTIONS

SL and JX conceived the overall study, designed the experiments, and wrote the manuscript. JX, SH, and YH conducted and performed the majority of the experiments, analyzed data with assistance from QZ, XP, and XY. All authors read and approved the final version of the manuscript.

FUNDING

This work was supported by the National Key Research and Development Programs of China 2018YFA0508000, Fundamental Research Funds for the Central Universities 2662017PY011, 2662018PY028, 2662019YJ014, 2662018JC001, Talent funding RCQD002 from Taihe Hospital, and Huazhong Agricultural University Scientific and Technological Self-Innovation Foundation 2017RC003 to SL.

ACKNOWLEDGMENTS

We thank members of the Li laboratory and the central laboratory of Taihe Hospital for helpful discussions and technical assistance.

SUPPLEMENTARY MATERIAL

The Supplementary Material for this article can be found online at: https://www.frontiersin.org/articles/10.3389/fcell.2020.00641/full#supplementary-material

REFERENCES

Araujo-Garrido, J. L., Bernal-Bayard, J., and Ramos-Morales, F. (2020). Type III secretion effectors with arginine N-glycosyltransferase activity. *Microorganisms* 8:357. doi: 10.3390/microorganisms8030357

Baison-Olmo, F., Galindo-Moreno, M., and Ramos-Morales, F. (2015). Host cell type-dependent translocation and PhoP-mediated positive regulation of the effector SseK1 of *Salmonella enterica*. *Front. Microbiol.* 6:396. doi: 10.3389/fmicb.2015.00396

Brown, N. F., Coombes, B. K., Bishop, J. L., Wickham, M. E., Lowden, M. J., Gal-Mor, O., et al. (2011). *Salmonella* phage ST64B encodes a member of the SseK/NleB effector family. *PLoS One* 6:e17824. doi: 10.1371/journal.pone.0017824

Chen, G., and Goeddel, D. V. (2002). TNF-R1 signaling: a beautiful pathway. *Science* 296, 1634–1635. doi: 10.1126/science.1071924

Chen, N. J., Chio, I. I., Lin, W. J., Duncan, G., Chau, H., Katz, D., et al. (2008). Beyond tumor necrosis factor receptor: TRADD signaling in toll-like receptors. *Proc. Natl. Acad. Sci. U.S.A.* 105, 12429–12434. doi: 10.1073/pnas.0806585105

Chinnaiyan, A. M., O'Rourke, K., Tewari, M., and Dixit, V. M. (1995). FADD, a novel death domain-containing protein, interacts with the death domain of Fas and initiates apoptosis. *Cell* 81, 505–512. doi: 10.1016/0092-8674(95)90071-3

Chinnaiyan, A. M., Orourke, K., Yu, G. L., Lyons, R. H., Garg, M., Duan, D. R., et al. (1996). Signal Transduction by DR3, a death domain-containing receptor related to TNFR-1 and CD95. *Science* 274, 990–992. doi: 10.1126/science.274.5289.990

Collins, J. W., Keeney, K. M., Crepin, V. F., Rathinam, V. A. K., Fitzgerald, K. A., Finlay, B. B., et al. (2014). Citrobacter rodentium: infection, inflammation and the microbiota. *Nat. Rev. Microbiol.* 12, 612–623. doi: 10.1038/nrmicro3315

Crepin, V. F., Collins, J. W., Habibzay, M., and Frankel, G. (2016). Citrobacter rodentium mouse model of bacterial infection. *Nat. Protoc.* 11, 1851–1876. doi: 10.1038/nprot.2016.100

Ding, J., Pan, X., Du, L., Yao, Q., Xue, J., Yao, H., et al. (2019). Structural and functional insights into host death domains inactivation by the bacterial arginine GlcNAcyltransferase effector. *Mol. Cell.* 74, 922.e6–935.e6. doi: 10.1016/j.molcel.2019.03.028

Dowling, J. P., Alsabbagh, M., Del Casale, C., Liu, Z. G., and Zhang, J. (2019). TRADD regulates perinatal development and adulthood survival in mice lacking RIPK1 and RIPK3. *Nat. Commun.* 10:705. doi: 10.1038/s41467-019-08584-5

El Qaidi, S., Chen, K., Halim, A., Siukstaite, L., Rueter, C., Hurtado-Guerrero, R., et al. (2017). NleB/SseK effectors from *Citrobacter rodentium*, *Escherichia coli*, and *Salmonella enterica* display distinct differences in host substrate specificity. *J. Biol. Chem.* 292, 11423–11430. doi: 10.1074/jbc.M117.790675

Esposito, D., Gunster, R. A., Martino, L., El Omari, K., Wagner, A., Thurston, T. L. M., et al. (2018). Structural basis for the glycosyltransferase activity of the *Salmonella* effector SseK3. *J. Biol. Chem.* 293, 5064–5078. doi: 10.1074/jbc.RA118.001796

Ferrao, R., and Wu, H. (2012). Helical assembly in the death domain (DD) superfamily. *Curr. Opin. Struct. Biol.* 22, 241–247. doi: 10.1016/j.sbi.2012.02.006

Fullsack, S., Rosenthal, A., Wajant, H., and Siegmund, D. (2019). Redundant and receptor-specific activities of TRADD, RIPK1 and FADD in death receptor signaling. *Cell Death Dis.* 10:122. doi: 10.1038/s41419-019-1396-5

Galluzzi, L., Vitale, I., Aaronson, S. A., Abrams, J. M., Adam, D., Agostinis, P., et al. (2018). Molecular mechanisms of cell death: recommendations of the Nomenclature Committee on Cell Death 2018. *Cell Death Differ.* 25, 486–541. doi: 10.1038/s41418-017-0012-4

Gao, X., Wang, X., Pham, T. H., Feuerbacher, L. A., Lubos, M. L., Huang, M., et al. (2013). NleB, a bacterial effector with glycosyltransferase activity, targets GAPDH function to inhibit NF-kappaB activation. *Cell Host Microbe* 13, 87–99. doi: 10.1016/j.chom.2012.11.010

Giogha, C., Lung, T. W., Pearson, J. S., and Hartland, E. L. (2014). Inhibition of death receptor signaling by bacterial gut pathogens. *Cytokine Growth Factor Rev.* 25, 235–243. doi: 10.1016/j.cytogfr.2013.12.012

Gunster, R. A., Matthews, S. A., Holden, D. W., and Thurston, T. L. M. (2017). SseK1 and SseK3 type III secretion system effectors inhibit NF-kappaB signaling and necroptotic cell death in *Salmonella*-infected macrophages. *Infect. Immun.* 85:e00010-17. doi: 10.1128/IAI.00010-17

Hsu, H., Xiong, J., and Goeddel, D. V. (1995). The TNF receptor 1-associated protein TRADD signals cell death and NF-kappa B activation. *Cell* 81, 495–504. doi: 10.1016/0092-8674(95)90070-5

Kamada, N., Kim, Y. G., Sham, H. P., Vallance, B. A., Puente, J. L., Martens, E. C., et al. (2012). Regulated virulence controls the ability of a pathogen to compete with the gut microbiota. *Science* 336, 1325–1329. doi: 10.1126/science.1222195

Kitson, J., Raven, T., Jiang, Y. P., Goeddel, D. V., Giles, K. M., Pun, K. T., et al. (1996). A death-domain-containing receptor that mediates apoptosis. *Nature* 384, 372–375. doi: 10.1038/384372a0

Kujat Choy, S. L., Boyle, E. C., Gal-Mor, O., Goode, D. L., Valdez, Y., Vallance, B. A., et al. (2004). SseK1 and SseK2 are novel translocated proteins of *Salmonella enterica* serovar typhimurium. *Infect. Immun.* 72, 5115–5125. doi: 10.1128/IAI.72.9.5115-5125.2004

Li, H., Xu, H., Zhou, Y., Zhang, J., Long, C., Li, S., et al. (2007). The phosphothreonine lyase activity of a bacterial type III effector family. *Science* 315, 1000–1003. doi: 10.1126/science.1138960

Li, S., Zhang, L., Yao, Q., Li, L., Dong, N., Rong, J., et al. (2013). Pathogen blocks host death receptor signalling by arginine GlcNAcylation of death domains. *Nature* 501, 242–246. doi: 10.1038/nature12436

Lu, Q., Li, S., and Shao, F. (2015). Sweet talk: protein glycosylation in bacterial interaction with the host. *Trends Microbiol.* 23, 630–641. doi: 10.1016/j.tim.2015.07.003

Luo, J., Hu, J., Zhang, Y., Hu, Q., and Li, S. (2015). Hijacking of death receptor signaling by bacterial pathogen effectors. *Apoptosis* 20, 216–223. doi: 10.1007/s10495-014-1068-y

Mak, T. W., and Yeh, W. C. (2002). Signaling for survival and apoptosis in the immune system. *Arthritis Res.* 4(Suppl. 3), S243–S252. doi: 10.1186/ar569

Meng, K., Li, X., Wang, S., Zhong, C., Yang, Z., Feng, L., et al. (2016). The strica homolog AaCASPS16 is involved in apoptosis in the yellow fever vector, *Aedes albopictus*. *PLoS One* 11:e0157846. doi: 10.1371/journal.pone.0157846

Meng, K., Zhuang, X., Peng, T., Hu, S., Yang, J., Wang, Z., et al. (2020). Arginine GlcNAcylation of Rab small GTPases by the pathogen *Salmonella* Typhimurium. *Commun. Biol.* 3:287. doi: 10.1038/s42003-020-1005-2

Newson, J. P. M., Scott, N. E., Yeuk Wah Chung, I., Wong Fok Lung, T., Giogha, C., Gan, J., et al. (2019). *Salmonella* effectors SseK1 and SseK3 target death domain proteins in the TNF and TRAIL signaling pathways. *Mol. Cell. Proteomics* 18, 1138–1156. doi: 10.1074/mcp.RA118.001093

Pan, M., Li, S., Li, X., Shao, F., Liu, L., and Hu, H. G. (2014). Synthesis of and specific antibody generation for glycopeptides with arginine N-GlcNAcylation. *Angew. Chem. Int. Ed. Engl.* 53, 14517–14521. doi: 10.1002/anie.201407824

Pan, X., Luo, J., and Li, S. (2020). Bacteria-catalyzed arginine glycosylation in pathogens and host. *Front. Cell. Infect. Microbiol.* 10:185.

Park, H. H. (2011). Structural analyses of death domains and their interactions. *Apoptosis* 16, 209–220. doi: 10.1007/s10495-010-0571-z

Park, H. H., Lo, Y. C., Lin, S. C., Wang, L., Yang, J. K., and Wu, H. (2007). The death domain superfamily in intracellular signaling of apoptosis and inflammation. *Annu. Rev. Immunol.* 25, 561–586. doi: 10.1146/annurev.immunol.25.022106.141656

Park, J. B., Kim, Y. H., Yoo, Y., Kim, J., Jun, S. H., Cho, J. W., et al. (2018). Structural basis for arginine glycosylation of host substrates by bacterial effector proteins. *Nat. Commun.* 9:4283. doi: 10.1038/s41467-018-06680-6

Pearson, J. S., Giogha, C., Ong, S. Y., Kennedy, C. L., Kelly, M., Robinson, K. S., et al. (2013). A type III effector antagonizes death receptor signalling during bacterial gut infection. *Nature* 501, 247–251. doi: 10.1038/nature12524

Pobezinskaya, Y. L., Choksi, S., Morgan, M. J., Cao, X., and Liu, Z.-G. (2011). The adaptor protein TRADD is essential for TNF-like ligand 1A/death receptor 3 signaling. *J. Immunol.* 186, 5212–5216. doi: 10.4049/jimmunol.1002374

Pobezinskaya, Y. L., Kim, Y. S., Choksi, S., Morgan, M. J., Li, T., Liu, C., et al. (2008). The function of TRADD in signaling through tumor necrosis factor receptor 1 and TRIF-dependent Toll-like receptors. *Nat. Immunol.* 9, 1047–1054. doi: 10.1038/ni.1639

Pobezinskaya, Y. L., and Liu, Z. (2012). The role of TRADD in death receptor signaling. *Cell Cycle* 11, 871–876. doi: 10.4161/cc.11.5.19300

Scott, N. E., Giogha, C., Pollock, G. L., Kennedy, C. L., Webb, A. I., Williamson, N. A., et al. (2017). The bacterial arginine glycosyltransferase effector NleB preferentially modifies Fas-associated death domain protein (FADD). *J. Biol. Chem.* 292, 17337–17350. doi: 10.1074/jbc.M117.805036

Stanger, B. Z., Leder, P., Lee, T. H., Kim, E., and Seed, B. (1995). RIP: a novel protein containing a death domain that interacts with Fas/APO-1 (CD95) in yeast and causes cell death. *Cell* 81, 513–523. doi: 10.1016/0092-8674(95)90072-1

Wang, K., Sun, Q., Zhong, X., Zeng, M., Zeng, H., Shi, X., et al. (2020). Structural mechanism for GSDMD targeting by autoprocessed caspases in pyroptosis. *Cell* 180, 941.e20–955.e20. doi: 10.1016/j.cell.2020.02.002

Wilson, N. S., Dixit, V., and Ashkenazi, A. (2009). Death receptor signal transducers: nodes of coordination in immune signaling networks. *Nat. Immunol.* 10, 348–355. doi: 10.1038/ni.1714

Xue, J., Pan, X., Du, L., Zhuang, X., Cai, X., and Li, S. (2019). Arginine-GlcNAcylation of death domain and NleB/SseK proteins is crucial for bacteria pathogenesis by regulating host cell death. *bioRxiv* [Preprint]. doi: 10.1101/746883

Xue, J., Pan, X., Peng, T., Duan, M., Du, L., Zhuang, X., et al. (2020). Auto arginine-GlcNAcylation is crucial for bacterial pathogens in regulating host cell death. *Front. Cell. Infect. Microbiol.* 10:197.

Yang, Y., Yu, C., Ding, K., Zhang, C., Liao, C., Jia, Y., et al. (2018). Role of the sseK1 gene in the pathogenicity of *Salmonella enterica* serovar enteritidis *in vitro* and *in vivo*. *Microb. Pathog.* 117, 270–275. doi: 10.1016/j.micpath.2018.02.030

Conflict of Interest: The authors declare that the research was conducted in the absence of any commercial or financial relationships that could be construed as a potential conflict of interest.

frontiers in Cell and Developmental Biology

ORIGINAL RESEARCH
published: 28 July 2020
doi: 10.3389/fcell.2020.00702

Dihydromyricetin Protects Against Gentamicin-Induced Ototoxicity via PGC-1α/SIRT3 Signaling *in vitro*

*Hezhou Han†, Yaodong Dong† and Xiulan Ma**

Department of Otolaryngology Head and Neck Surgery, Shengjing Hospital of China Medical University, Shenyang, China

Aminoglycoside-induced ototoxicity can have a major impact on patients' quality of life and social development problems. Oxidative stress affects normal physiologic functions and has been implicated in aminoglycoside-induced inner ear injury. Excessive accumulation of reactive oxygen species (ROS) damages DNA, lipids, and proteins in cells and induces their apoptosis. Dihydromyricetin (DHM) is a natural flavonol with a wide range of health benefits including anti-inflammatory, antitumor, and antioxidant effects; however, its effects and mechanism of action in auditory hair cells are not well understood. The present study investigated the antioxidant mechanism and anti-ototoxic potential of DHM using House Ear Institute-Organ of Corti (HEI-OC)1 auditory cells and cochlear explant cultures prepared from Kunming mice. We used gentamicin to establish aminoglycoside-induced ototoxicity models. Histological and physiological analyses were carried out to determine DHM's pharmacological effects on gentamicin-induced ototoxicity. Results showed DHM contributes to protecting cells from apoptotic cell death by inhibiting ROS accumulation. Western blotting and quantitative RT-PCR analyses revealed that DHM exerted its otoprotective effects by up-regulating levels of peroxisome proliferator activated receptor γ-coactivator (PGC)-1α and Sirtuin (SIRT)3. And the role of PGC-1α and SIRT3 in the protective effects of DHM was evaluated by pharmacologic inhibition of these factors using SR-18292 and 3-(1*H*-1,2,3-triazol-4-yl) pyridine, respectively, which indicated DHM's protective effect was dependent on activation of the PGC-1α/SIRT3 signaling. Our study is the first report to identify DHM as a potential otoprotective drug and provides a basis for the prevention and treatment of hearing loss caused by aminoglycoside antibiotic-induced oxidative damage to auditory hair cells.

Keywords: dihydromyricetin, aminoglycosides, ototoxicity, PGC-1α, sirtuin 3, reactive oxygen species

OPEN ACCESS

Edited by:
Yinan Gong,
University of Pittsburgh, United States

Reviewed by:
Pengfei Guo,
University of Texas Southwestern Medical Center, United States
Shan Li,
Huazhong Agricultural University, China

****Correspondence:***
Xiulan Ma
xiulan_ma1964@163.com

† These authors have contributed equally to this work

Specialty section:
This article was submitted to Cell Death and Survival, a section of the journal Frontiers in Cell and Developmental Biology

Received: *04 May 2020*
Accepted: *10 July 2020*
Published: *28 July 2020*

Citation:
Han H, Dong Y and Ma X (2020) Dihydromyricetin Protects Against Gentamicin-Induced Ototoxicity via PGC-1α/SIRT3 Signaling in vitro. Front. Cell Dev. Biol. 8:702. doi: 10.3389/fcell.2020.00702

INTRODUCTION

Oxidative stress results from the perturbation of cellular redox balance (Kandola et al., 2015) caused by excessive levels of reactive oxygen species (ROS) that exceed antioxidant defense mechanisms, leading to the destruction of cellular structures and cell death (Sies, 2015). Oxidative stress has been linked to diseases of the nervous system (Liu et al., 2015) and cardiovascular system

(Madamanchi and Runge, 2013); aging (Stefanatos and Sanz, 2018); and neurologic hearing loss (Someya et al., 2010; Chen et al., 2015; Esterberg et al., 2016) caused by aminoglycoside-induced damage (Cheng et al., 2005) and apoptosis of hair cells from the base to the apex of the organ of Corti (Jiang et al., 2016). Aminoglycosides exert this effect by stimulating ROS production in hair cells (Mangiardi et al., 2004; Coffin et al., 2013). Mammalian hair cells are not regenerated; as such, research on therapeutic interventions for hearing loss has focused the regulation of genes responsible for hair cell proliferation and differentiation, as well as stem cell therapy (Chen et al., 2019; Czajkowski et al., 2019).

Sirtuin (SIRT)3 is a member of the Sirtuin family of NAD^+-dependent class III histone deacetylases and/or protein ADP-ribosyl transferases that mediates adaptive responses to a variety of stressors. SIRT3 regulates mitochondrial function (Salvatori et al., 2017) and inhibits ROS production in cochlear tissue, and protects against ototoxicity (A pharmacological adverse reaction that affects the inner ear or auditory nerve, characterized by cochlear or vestibular dysfunction) induced by the aminoglycoside antibiotic gentamicin (Finkel et al., 2009; Quan et al., 2015). It was recently reported that SIRT3 can prevent hair cell apoptosis by inhibiting ROS production (Brown et al., 2014; Quan et al., 2015). Peroxisome proliferator activated receptor γ coactivator (PGC)-1α, a regulator of SIRT3 (Palacios et al., 2009; Wang et al., 2015; Li et al., 2016; Song et al., 2017), stabilizes mitochondria and regulates fatty acid oxidation and glucose metabolism (Cheng et al., 2018). PGC-1α can suppress ROS production and protect nerve cells from oxidative stress-induced damage by stimulating mitochondrial biosynthesis, enhancing the activity of the electron transport chain, and inducing the expression of a variety of ROS-detoxifying enzymes (Zhang Y. et al., 2018).

Antioxidant compounds have been investigated for their potential to protect hair cells from injury (Ylikoski et al., 2002; Tabuchi et al., 2007; Dong et al., 2015; Quan et al., 2015), but most have adverse effects, which limit their clinical applicability. As the most abundant natural flavonoid in rattan tea, dihydromyricetin (DHM) has wide-ranging pharmacologic properties, with demonstrated cardioprotective, antidiabetic, antitumor, and anti-inflammatory effects (Zhang J. et al., 2018) and no adverse effects in humans (Tong et al., 2020). DHM regulates mitochondrial function via PGC-1α in skeletal muscle and functions as an antioxidant (Zou et al., 2014); it was shown to regulate blood lipid and lipoprotein levels and protect PC12 cells from methylglyoxal-induced toxicity and endothelial cells from oxidative damage by eliminating ROS (Le et al., 2016). However, the mechanism underlying the latter effect is not well understood.

We speculated that the antioxidant property of DHM can protect against gentamicin-induced ototoxicity. To test this hypothesis, we established aminoglycoside-induced ototoxicity models using House Ear Institute-Organ of Corti (HEI-OC)1 auditory cells and cochlear explant cultures prepared from mice, and examined whether DHM pretreatment could reduce oxidative stress and apoptosis in these models. We also evaluated the role of PGC-1α and SIRT3 in the protective effects of DHM.

MATERIALS AND METHODS

Ethics Statement

The study was approved by the Institutional Animal Care and Use Committee of China Medical University. All animals were treated in accordance with institutional guidelines.

Cell Culture and Reagents

The HEI-OC1 auditory cell line is a widely used *in vitro* model for evaluating the ototoxicity as well as the protective effects of various agents (Jadidian et al., 2015; Kalinec et al., 2016; Park et al., 2016). HEI-OC1 cells were obtained from House Ear Institute (Los Angeles, CA, United States) and cultured in high-glucose Dulbecco's modified Eagle's medium (DMEM) supplemented with 10% fetal bovine serum at 33°C and 5% CO_2. All cell culture reagents were purchased from NEST Biotech (Wuxi, China).

Cell Viability Assay

Cell viability was assayed using 3-(4,5-dimethyl-2-thiazoyl)-2,5-diphenyltetrazoliumbromide (MTT) (Roche, Basel, Switzerland) according to the manufacturer's instructions. HEI-OC1 cells were cultured in 96-well plates and incubated with gentamicin for 24 or 48 h before treatment with 10, 100, or 1,000 μM DHM for 24 h. MTT (0.5 mg/ml) was then added to each well for 4 h, followed by overnight incubation with lysis buffer. Optical density at 570 nm was measured using a microplate reader (Bio-Rad, Hercules, CA, United States).

Cochlear Explant Cultures

Cochlear explant cultures were prepared from postnatal day 3 Kunming mice (Changsheng Biological Co, Liaoning Institutes for Biological Science, Shenyang, China). All animal procedures were carried out in accordance with the guidelines of the Institutional Animal Care and Use Committee of China Medical University. Before cochlea dissection, 10-mm round glass coverslips in 4-well dishes were coated with 0.012 mg/ml rat tail tendon collagen type I (Solarbio, Beijing, China). The collagen gel was allowed to solidify in air for several minutes. Cochlear explants were placed on the coverslips with DMEM-F12 (∼100 μl/dish). To evaluate whether DHM protects hair cells from gentamicin-induced ototoxicity, the cultures were divided into three groups: explants were maintained in normal DMEM-F12 for 36 h; maintained in normal medium for 24 h and then treated with 0.5 mM gentamicin for 12 h; or pretreated with DHM for 24 h followed by 0.5 mM gentamicin in the presence of DHM for 12 h.

Immunofluorescence Analysis

Cultured cochlear explants were fixed with 4% paraformaldehyde for 15 min and washed three times for 15 min each in phosphate-buffered saline (PBS). They were then blocked for 1 h in PBS containing 0.1% Triton X-100, 5% donkey serum, and 1% bovine serum albumin (BSA). The explants were incubated overnight at 4°C with anti-myosin-VIIa antibody

(1:500; Proteus Biosciences, Ramona, CA, United States), followed by Alexa Fluor 488-conjugated secondary antibody (1:200; Abcam, Cambridge, MA, United States) and Alexa Fluor 546 phalloidin (1:1000; Thermo Fisher Scientific, Waltham, MA, United States) to label hair cells; they were then examined by confocal microscopy (LSM 880; Zeiss, Oberkochen, Germany). Photographs were taken from the same area of tissue in each group (middle turn of the cochlea). The number of hair cells that were immunopositive for myosin VIIa antibody and phalloidin were counted.

Real-Time (RT)-PCR

Total RNA was extracted from 6 cochlear explants per group using TRIzol reagent (Tiangen Biotech, Beijing, China). First-strand cDNA was synthesized using reverse transcriptase (Tiangen Biotech), and RT-PCR was performed using the SuperReal PreMix Plus kit (Tiangen Biotech) on an ABI7500 Real-time PCR system (Applied Biosystems, Foster City, CA, United States). The forward and reverse primers used in this study were synthesized by Takara Bio (Beijing, China) and had the following sequences: glyceraldehyde 3-phosphate dehydrogenase, 5′-AAATGGTGAAGGTCGGYGYGAAC-3′ and 5′-CAACAATCTCCACTTTGCCACTG-3′; PGC-1α, 5′-ACCG CAATTCTCCCTTGTATG-3′ and 5′-CTTCTGCCTCTCTCT CTGTTTGG-3′; and SIRT3, 5′-ATGCACGGTCTGTCGAA GGTC-3′ and 5′-AGAACACAATGTCGGGTTTCACAA-3′.

Western Blotting

Cultured HEI-OC1 cells were washed three times with PBS and lysed on ice using ice-cold radioimmunoprecipitation buffer for 30 min (Millipore, Billerica, MA, United States). Protein concentration was determined using a bicinchoninic acid assay kit (Beyotime, Shanghai, China). Proteins were resolved by SDS-PAGE and transferred to a polyvinylidene difluoride

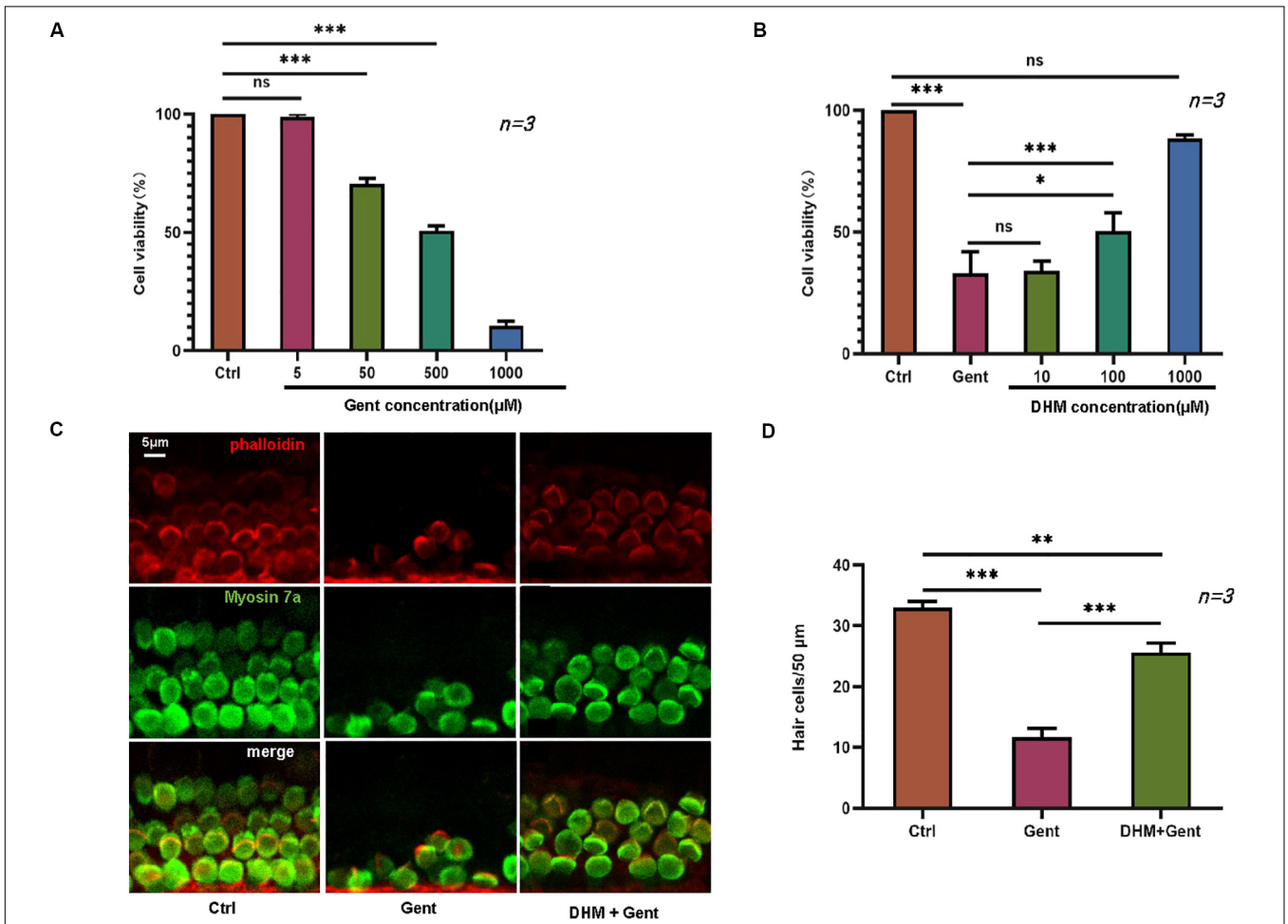

FIGURE 1 | DHM protects against gentamicin-induced ototoxicity in HEI-OC1 cells and cochlear explants. **(A)** HEI-OC1 cells treated with increasing concentrations of gentamicin (0, 5, 50, and 500 μM) for 12 h. **(B)** Effect of DHM pretreatment at 0, 10, 100, and 1,000 μM for 24 h on the survival of HEI-OC1 cells exposed to 500 μM gentamicin, measured with the MTT assay. **(C,D)** Cochlear explants were divided into three groups: Ctrl (no treatment), Gent (no treatment for 24 h and 500 μM gentamicin for 12 h), and DHM + Gent (1 mM DHM pretreatment for 24 h and 500 μM gentamicin for 12 h). Samples were labeled with myosin VIIa (green) and phalloidin (red); merged images obtained by confocal microscopy are shown. Scale bar, 5 μm. Experiments were repeated three times. NS, not significant; $^{*}P < 0.05$, $^{**}P < 0.01$, $^{***}P < 0.001$ (one-way analysis of variance followed by Tukey's multiple comparisons test).

membrane that was blocked with 5% BSA for 2 h and incubated overnight at 4°C with rabbit anti-SIRT3 (1:1000) and anti-PGC-1α (1:1000) antibodies (both from Affinity Biologicals, Ancaster, ON, Canada). After washing three times with Tris-buffered saline containing 0.1% Tween-20, the membrane was incubated for 2 h at room temperature with secondary antibody (1:10000; Absin Biotechnology, Shanghai, China). Anti-Bax (1:2000; Abcam, United States, anti-Bcl-2 (1:2000; Abcam, United States), cleaved PARP (1:1000; Abcam, United States) and cleaved caspase-3 (1:1000; Abcam, United States) also did the same. Protein bands were visualized with enhanced chemiluminescence reagent (Affinity Biologicals). The experiment was repeated three times. Protein levels were quantified using ImageJ software (National Institutes of Health, Bethesda, MD, United States) by analyzing gray values.

Drug Treatment

Ototoxicity models were established in HEI-OC1 cells and cochlear explants by treatment for 12 h with 500 μM gentamicin (Meilun Biotechnology, Dalian, China). To evaluate the effects of DHM, samples were pretreated with 1 mM DHM (Meilun Biotechnology) for 24 h before adding gentamicin. To evaluate the role(s) of PGC-1α and SIRT3 in the protective effect of DHM against gentamicin-induced ototoxicity, samples were pretreated with the PGC-1α and SIRT3 inhibitors SR-18292 (20 μM; MedChemExpress, Princeton, NJ, United States) and 3-(1*H*-1,2,3-triazol-4-yl) pyridine (3-TYP, 50 μM; Absin Biotechnology), respectively, for 2 h before the addition of DHM and exposure to gentamicin.

Flow Cytometry

Cells were stained with 2′-7′ dichlorofluorescin diacetate (DCFH-DA) solution (Abcam). Cells were incubated for 1 h at 37°C, followed by 2 washes with PBS for 5 min each. We used a FACSCalibur flow cytometer (BD Biosciences, Franklin Lakes, NJ, United States) to measure ROS levels. The fraction of apoptotic HEI-OC1 cells was quantitated by flow cytometry after staining with annexin V-fluorescein isothiocyanate (FITC)/propidium iodide (PI) (Sigma-Aldrich, St. Louis, MO, United States). The cells were seeded in 6-well culture plates and incubated with 1 mM DHM for 24 h, followed by application of 500 μM gentamicin for 12 h.

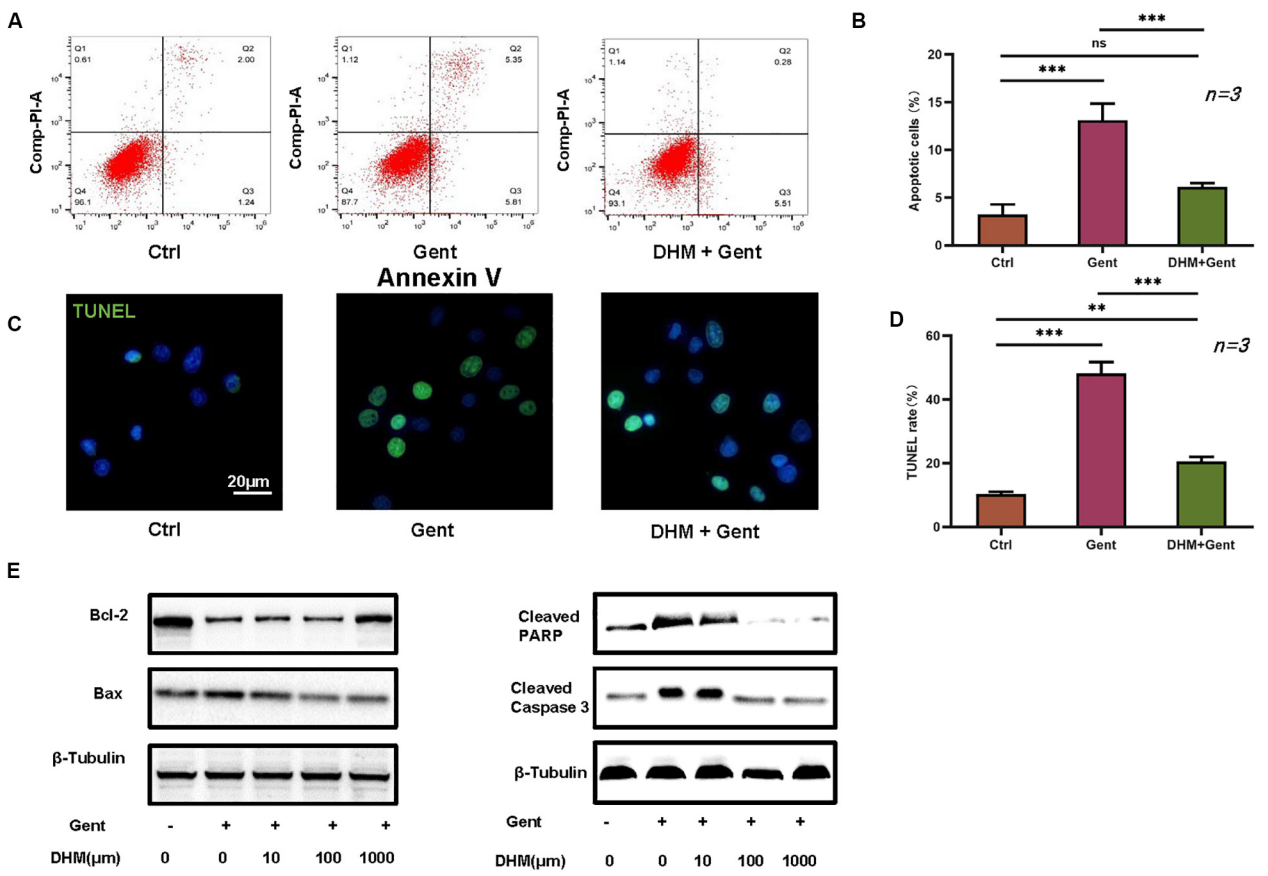

FIGURE 2 | DHM attenuates gentamicin-induced HEI-OC1 cell apoptosis. **(A,B)** HEI-OC1 cells were divided into three groups: Ctrl (no treatment), Gent (500 μM gentamicin treatment for 12 h), and DHM + Gent (1,000 μM DHM pretreatment for 24 h and gentamicin treatment for 12 h). Apoptotic cells were detected by flow cytometry. **(C,D)** Quantitative analysis of TUNEL-positive cells. Scale bar, 20 μm. **(E)** Western blot analysis of B-cell lymphoma 2-associated X protein (Bax), cleaved caspase-3, and cleaved PARP expression as a function of DHM concentration. β-Tubulin was used as a loading control. Experiments were repeated three times. NS, not significant; $^{**}P < 0.01$, $^{***}P < 0.001$ (1-way analysis of variance followed by Tukey's multiple comparisons test).

Control cells were treated with culture medium containing vehicle (Cells without treatment). The cells were collected and washed with PBS and resuspended in 500 ml of 1 × binding buffer, transferred to fluorescence-activated cell sorting tubes, and stained with annexin V in accordance with the protocol for the apoptosis detection kit (Sigma-Aldrich). After incubation for 15 min at room temperature, apoptotic cells were detected by flow cytometry. Data were analyzed with Prism software (GraphPad, La Jolla, CA, United States). The experiment was repeated three times.

Terminal Deoxynucleotidyl Transferase dUTP Nick End Labeling (TUNEL) Assay

Cultured HEI-OC1 cells were washed once with PBS and fixed with 4% paraformaldehyde for 30 min. After washing with PBS, the cells were incubated for 5 min with PBS containing 0.3% Triton X-100. After two washes with PBS, 50 μl TUNEL detection solution (Beyotime) was added to each well, and samples were incubated at 37°C in the dark for 1 h. After three washes with PBS, the samples were mounted with anti-fade solution (Beyotime) and observed under a fluorescence microscope (E800; Nikon, Japan). Cells from 10 visual fields from the same part of each of the three slides per sample were counted and averaged. Data were analyzed using Prism software.

Quantitative Analysis

The normality of the data was confirmed with the K-S test and Q-Q figure test using SPSS software (SPSS Inc., Chicago, IL, United States). Differences between group means were evaluated by one-way analysis of variance followed by Tukey's multiple comparisons test, and a P value <0.05 was considered statistically significant.

RESULTS

DHM Protects Against Gentamicin-Induced Ototoxicity in HEI-OC1 Cells and Cochlear Explants

We first established an *in vitro* gentamicin-induced ototoxicity model by exposing HEI-OC1 cells to increasing concentrations of gentamicin (0, 5, 50, and 500 μM) for 12 h. The viability of HEI-OC1 cells was reduced in a dose-dependent manner by gentamicin treatment (**Figure 1A**), confirming that the

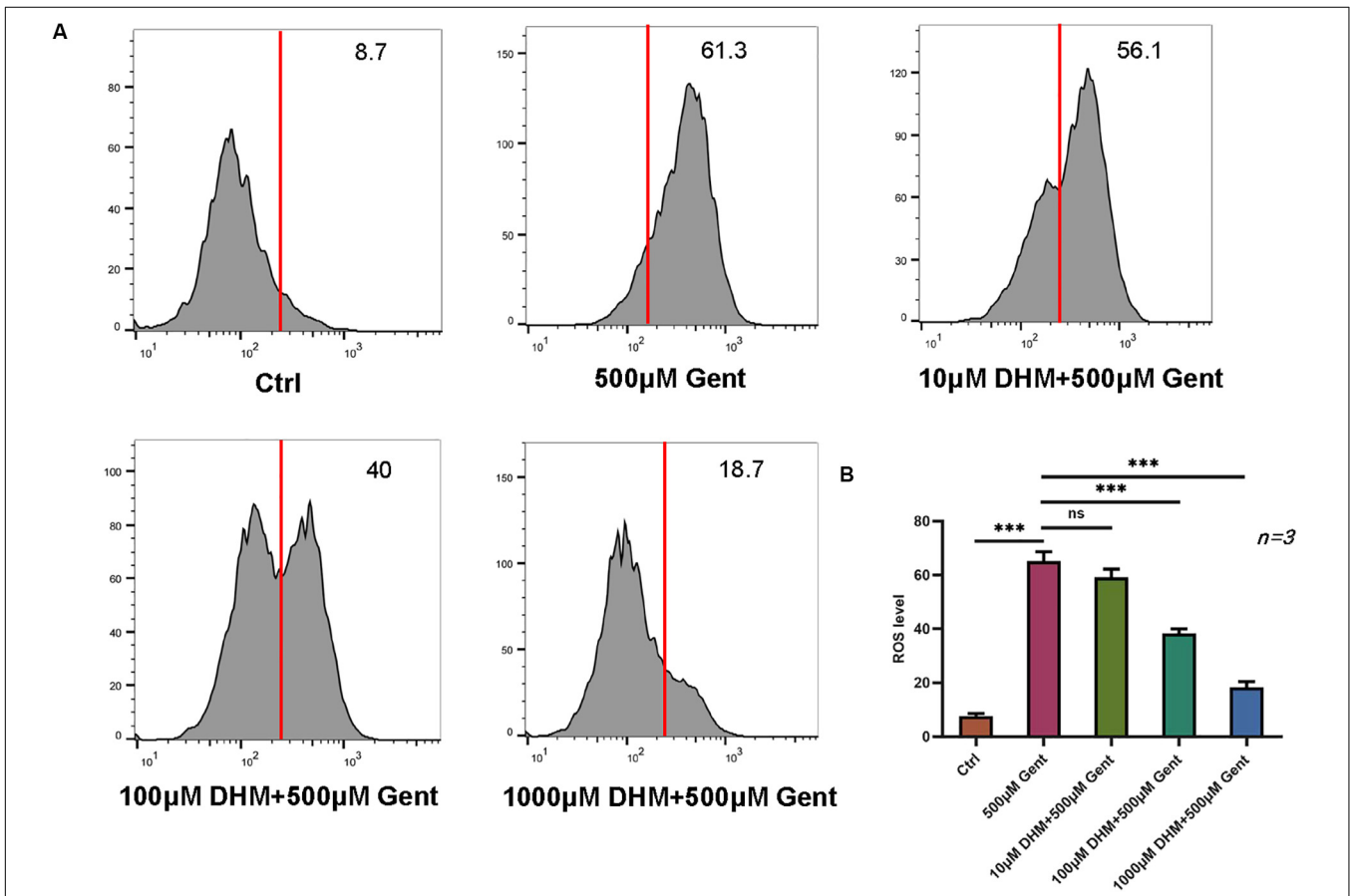

FIGURE 3 | DHM attenuates gentamicin-induced oxidative stress in HEI-OC1 cells. **(A,B)** HEI-OC1 cells were incubated with increasing concentrations of DHM. ROS levels after gentamicin treatment with or without DHM pretreatment were evaluated by DCFH-DA staining combined with flow cytometry. The experiment was repeated three times. NS, not significant; ***P < 0.001 (one-way analysis of variance followed by Tukey's multiple comparisons test).

ototoxicity model was successfully established. To evaluate the protective effect of DHM against gentamicin-induced toxicity, cells were treated with 500 μM gentamicin to cause substantial cell damage (∼50% reduction in viability) along with pre-treatment of 10, 100, or 1,000 μM DHM. Unexpectedly, there was no obvious improvement in viability at DHM concentrations below 100 μM; treatment with 1,000 μM DHM and 500 μM gentamicin yielded cell numbers that were comparable to the control group (**Figure 1B**), demonstrating that DHM abrogates the cytotoxic effects of gentamicin in a dose-dependent manner.

We also carried out a similar experiment using mouse cochlear explants cultured in regular medium or in medium supplemented with 500 μM gentamicin alone or in combination with 1,000 μM DHM, after determining the optimal concentrations of the 2 agents. Stereociliary bundles of hair cells were identified by phalloidin staining and myosin VIIa immunolabeling. In explants cultured in normal medium, there was a single row of inner hair cells and three rows of outer hair cells with polarized hair bundles protruding from the apical surface of the cell body (**Figure 1C**). In explants exposed to gentamicin, most hair cells were damaged and immunonegative for myosin VIIa and phalloidin staining; even the few positive cells were disorganized and fragmented. In contrast, in explants treated with both gentamicin and DHM, most hair cells were intact, with only slight disorganization of stereocilia. These observations were confirmed by quantification of surviving hair cell numbers in each group (**Figure 1D**), which indicated that DHM acts as an anti-ototoxic agent.

DHM Decreases Gentamicin-Induced HEI-OC1 Cell Apoptosis

We evaluated the effect of DHM on HEI-OC1 cell apoptosis by flow cytometry and with the TUNEL assay. Dead cells were labeled by PI and those undergoing apoptosis were labeled by annexin V. The proportion of apoptotic cells was increased after gentamicin treatment compared to the control group; however, the effect was reversed by pretreatment with DHM compared to the gentamicin-only group (**Figures 2A,B**). Additionally, while few TUNEL-positive cells were detected in the control group, numerous cells were observed following gentamicin treatment; the number was reduced by DHM pretreatment (**Figures 2C,D**). Western blot analysis revealed the downregulation of B-cell lymphoma 2-associated X protein, cleaved PARP, and cleaved caspase-3 over time following DHM pretreatment relative to control cells (**Figure 2E**).

DHM Alleviates Gentamicin-Induced Oxidative Stress in HEI-OC1 Cells

Given that gentamicin-induced hair cell apoptosis is mediated by ROS (Yang et al., 2011), we investigated the effect of DHM on ROS levels in HEI-OC1 cells by flow cytometry. The ototoxicity

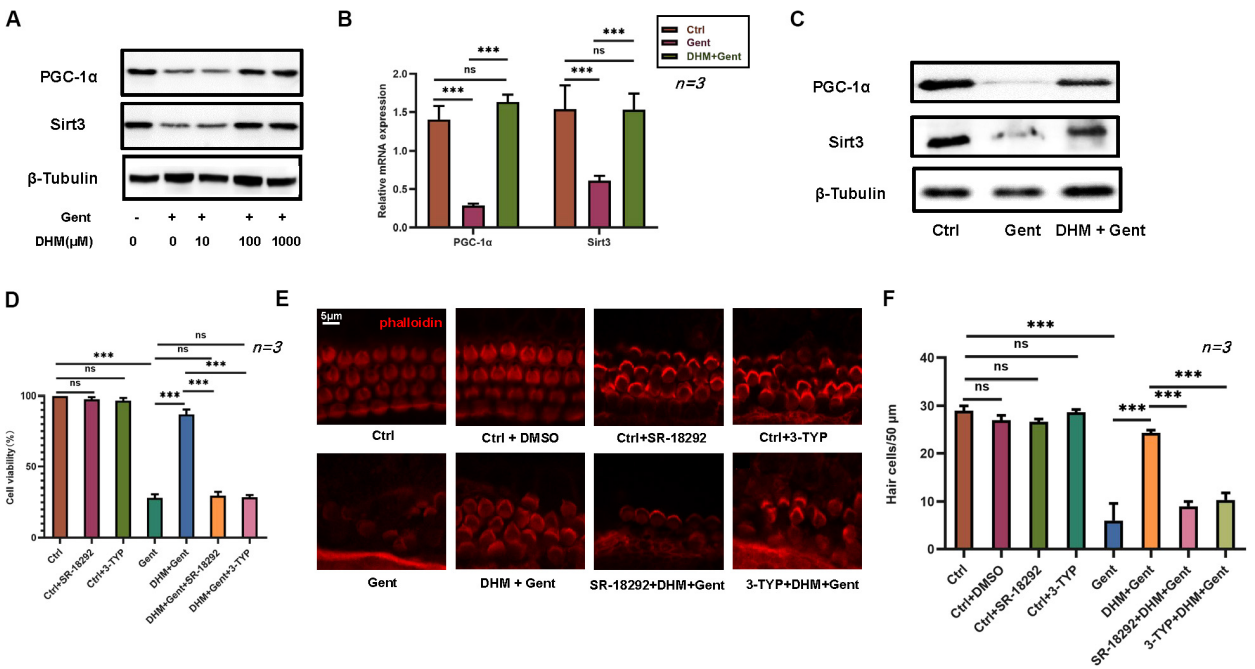

FIGURE 4 | PGC-1α and SIRT3 mediate the protective effect of DHM against gentamicin-induced hair cell damage. **(A)** Endogenous PGC-1α and SIRT3 protein expression in HEI-OC1 cells as determined by western blotting; β-tubulin was used as a loading control. **(B)** RT-PCR detection of PGC-1α and SIRT3 transcript levels in cochlear explants after gentamicin treatment with or without DHM (1 mM) pretreatment; glyceraldehyde 3-phosphate dehydrogenase (GAPDH) was used as an internal control. **(C)** Western blot analysis of PGC-1α and SIRT3 protein expression after DHM (1 mM) pretreatment; β-tubulin was used as a loading control. **(D–F)** Effect of PGC-1α and SIRT3 inhibition (with SR-18292 and 3-TYP, respectively) on the viability of HEI-OC1 cells **(D)** and hair cells in cochlear explants **(E,F)** treated with gentamicin with or without DHM pretreatment. Experiments were repeated three times NS, not significant; ***$P < 0.001$ (one-way analysis of variance followed by Tukey's multiple comparisons test).

model was established with a gentamicin concentration of 500 μM. The results showed that ROS levels were increased after gentamicin treatment compared to control cells; the levels were reduced in the presence of increasing concentrations of DHM starting at 100 μM (**Figures 3A,B**).

Protection Against Gentamicin-Induced Hair Cell Damage by DHM Involves PGC-1α and SIRT3

We investigated the mechanisms underlying the effects of DHM by evaluating PGC-1α and SIRT3 levels by RT-PCR and western blotting. Expression of PGC-1α and SIRT3 proteins in HEI-OC1 cells markedly increased with DHM concentration (**Figure 4A**). In cochlear explants, pretreatment with DHM for 24 h prior to gentamicin application increased both mRNA and protein levels of PGC-1α and SIRT3 compared to samples treated with gentamicin only (**Figures 4B,C**). To confirm the involvement of PGC-1α and SIRT3 in the protective effects of DHM, we treated HEI-OC1 cells and cochlear explants with pharmacologic inhibitors of PGC-1α (SR-18292) and SIRT3 (3-TYP) prior to DHM pretreatment and exposure to gentamicin (**Figures 4D–F**). Inhibiting PGC-1α and SIRT3 attenuated the effects of DHM without altering the survival of HEI-OC1 cells, although some deformation of hair cell cilia was observed.

To examine the functions of PGC-1α and SIRT3 in greater detail, HEI-OC1 cells were treated with SR-18292 and 3-TYP and the fraction of apoptotic cells was evaluated by flow cytometry and with the TUNEL assay. Inhibitor pretreatment increased the number of apoptotic cells compared to the DHM + gentamicin group (**Figures 5A,B**); the same trend was observed by quantifying the number of TUNEL-positive cells (**Figures 5C,D**). These results indicate that PGC-1α and SIRT3 are involved in the protective effects of DHM in hair cells.

The Antioxidant Effect of DHM in HEI-OC1 Cells Is Mediated by PGC-1α and SIRT3

The above results showed that DHM inhibits apoptosis in HEI-OC1 cells induced by gentamicin by suppressing ROS production. To determine whether this involves PGC-1α and SIRT3, SR-18292 and 3-TYP were added to HEI-OC1 cell cultures, prior to DHM and gentamicin treatment; ROS levels were then assessed by DCFH-DA staining and flow cytometry. We found that PGC-1α and SIRT3 inhibition markedly increased ROS levels compared to cells without SR-18292 and 3-TYP treatment (**Figure 6**). Thus, DHM prevents ototoxicity via the PGC-1α/SIRT3 axis.

PGC-1α Regulates SIRT3 Expression in HEI-OC1 Cells and Cochlear Explants

The relationship between PGC-1 α and SIRT3 in the auditory system has not been previously reported.

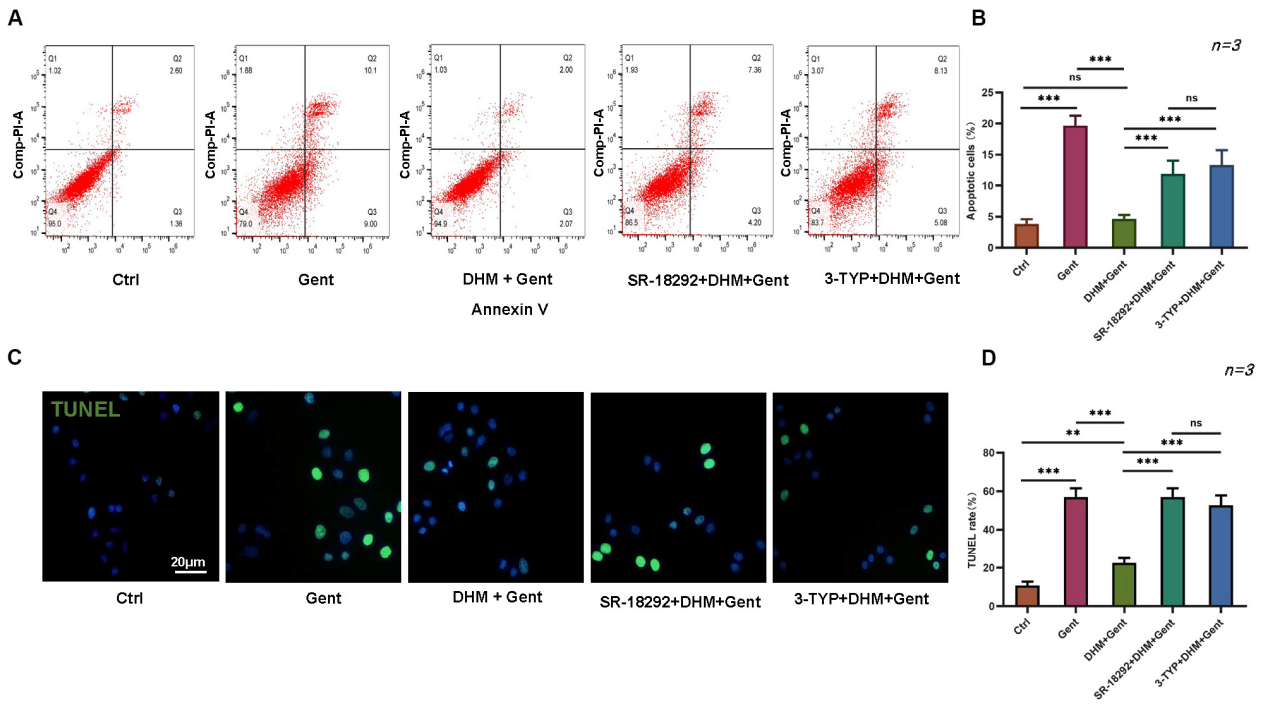

FIGURE 5 | PGC-1α and SIRT3 mediate the protective effect of DHM against gentamicin-induced HEI-OC1 cell apoptosis. **(A,B)** Flow cytometry detection of apoptosis in HEI-OC1 cells treated with PGC-1α and SIRT3 inhibitors (SR-18292 and 3-TYP, respectively) prior to DHM and gentamicin treatment. **(C,D)** Quantitative analysis of TUNEL-positive cells following pretreatment with 20 μM SR-18292 and 50 μM 3-TYP for 2 h prior to 1 mM DHM treatment and gentamicin exposure. Experiments were repeated three times. NS, not significant; $^{**}P < 0.01$, $^{***}P < 0.001$ (one-way analysis of variance followed by Tukey's multiple comparisons test).

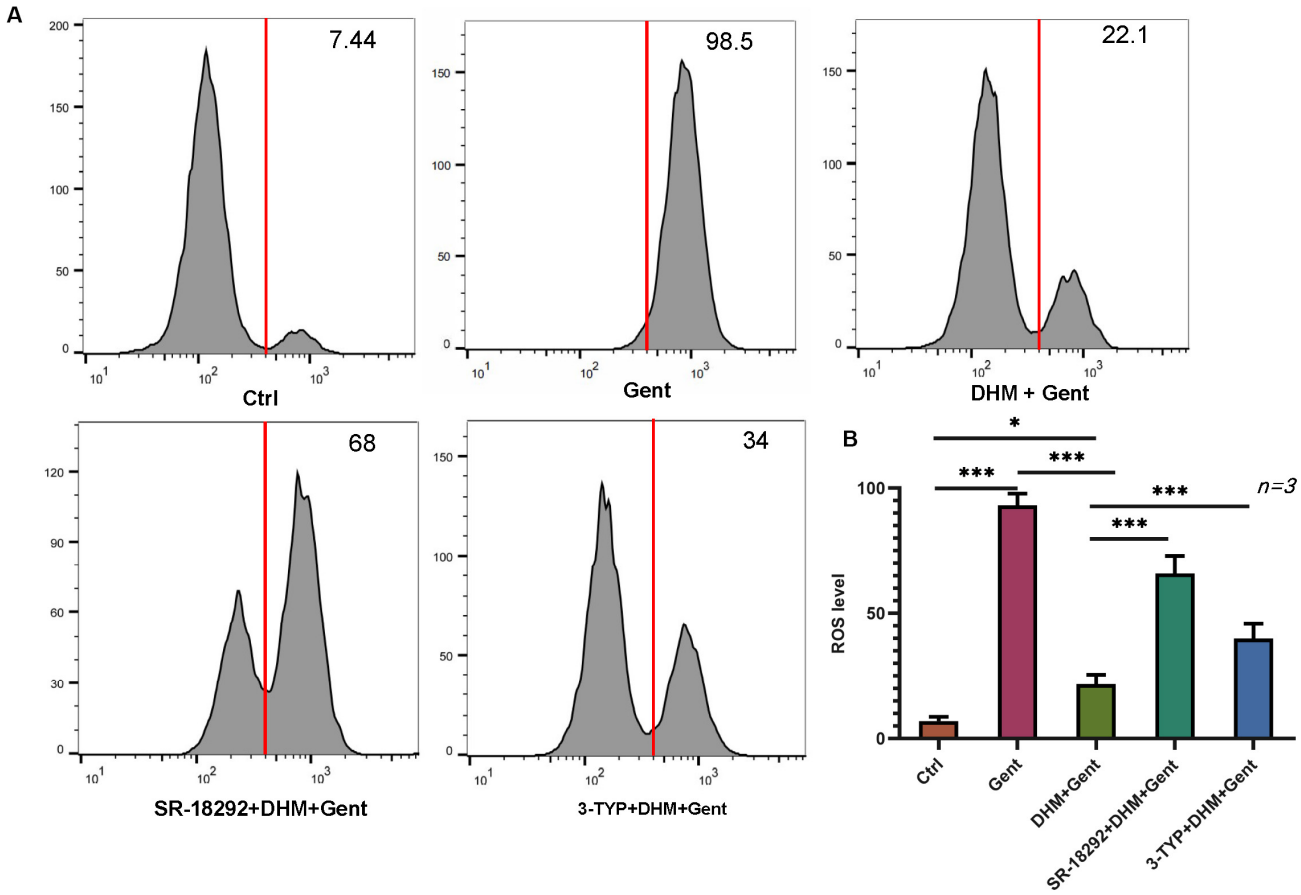

FIGURE 6 | PGC-1α and SIRT3 mediate the protective effect of DHM against gentamicin-induced oxidative stress in HEI-OC1 cells. **(A,B)** HEI-OC1 cells were pretreated with PGC-1α and SIRT3 inhibitors (SR-18292 and 3-TYP, respectively) before treatment with 1 mM DHM followed by 500 μM gentamicin for 12 h. Intracellular ROS levels were measured by DCFH-DA staining combined with flow cytometry. The experiment was repeated three times. $^{*}P < 0.05$, $^{***}P < 0.001$ (one-way analysis of variance followed by Tukey's multiple comparisons test).

We therefore investigated the expression of PGC-1α signaling pathway components, including SIRT3. Treatment with the PGC-1α inhibitor SR-18292 resulted in the downregulation of PGC-1α and SIRT3, whereas SIRT3 inhibition by 3-TYP application had no effect on the protein expression of PGC-1α (**Figures 7A,B**). Similar results were obtained in cochlear explants (**Figures 7C,D**). Thus, DHM exerts its protective against gentamicin-induced ototoxicity via PGC-1α/SIRT3 signaling, with PGC-1α acting as an upstream regulator of SIRT3 expression.

DISCUSSION

Aminoglycosides can induce excessive ROS production in cells; this activates caspase-dependent and -independent apoptosis signaling cascades (Chan, 2005; Genestra, 2007) and leads to ototoxicity (Esterberg et al., 2016; Sheth et al., 2017; Desa et al., 2018; Guo et al., 2018) and hearing loss. From a clinical standpoint, it is important to identify new therapeutic strategies to prevent or treat ototoxicity caused by aminoglycoside antibiotics.

DHM exerts antioxidant effects via multiple signaling pathways including AMP-activated protein kinase (AMPK), mitogen-activated protein kinase, nuclear factor E2-related factor 2, ATP-binding cassette transporter A1, and peroxisome proliferator-activated receptor γ (Zhang J. et al., 2018). DHM was shown to suppress ROS production and H_2O_2-induced apoptosis in human pulmonary arterial smooth muscle cells (Hou et al., 2015). In the present study, we established ototoxicity models using HEI-OC1 cells and mouse cochlear explants and investigated whether DHM can protect against hair cell injury caused by gentamicin. We found that DHM pretreatment improved HEI-OC1 cell viability and the survival of hair cells in cochlear explants, and determined that the underlying mechanism involves inhibition of apoptosis via suppression of ROS production mediated by PGC-1α/SIRT3 signaling.

The cytoprotective effects of DHM in a variety of pathologic conditions including non-alcoholic fatty liver disease (NAFLD) (Zeng et al., 2019), osteoarthritis (Wang et al., 2018), cardiac

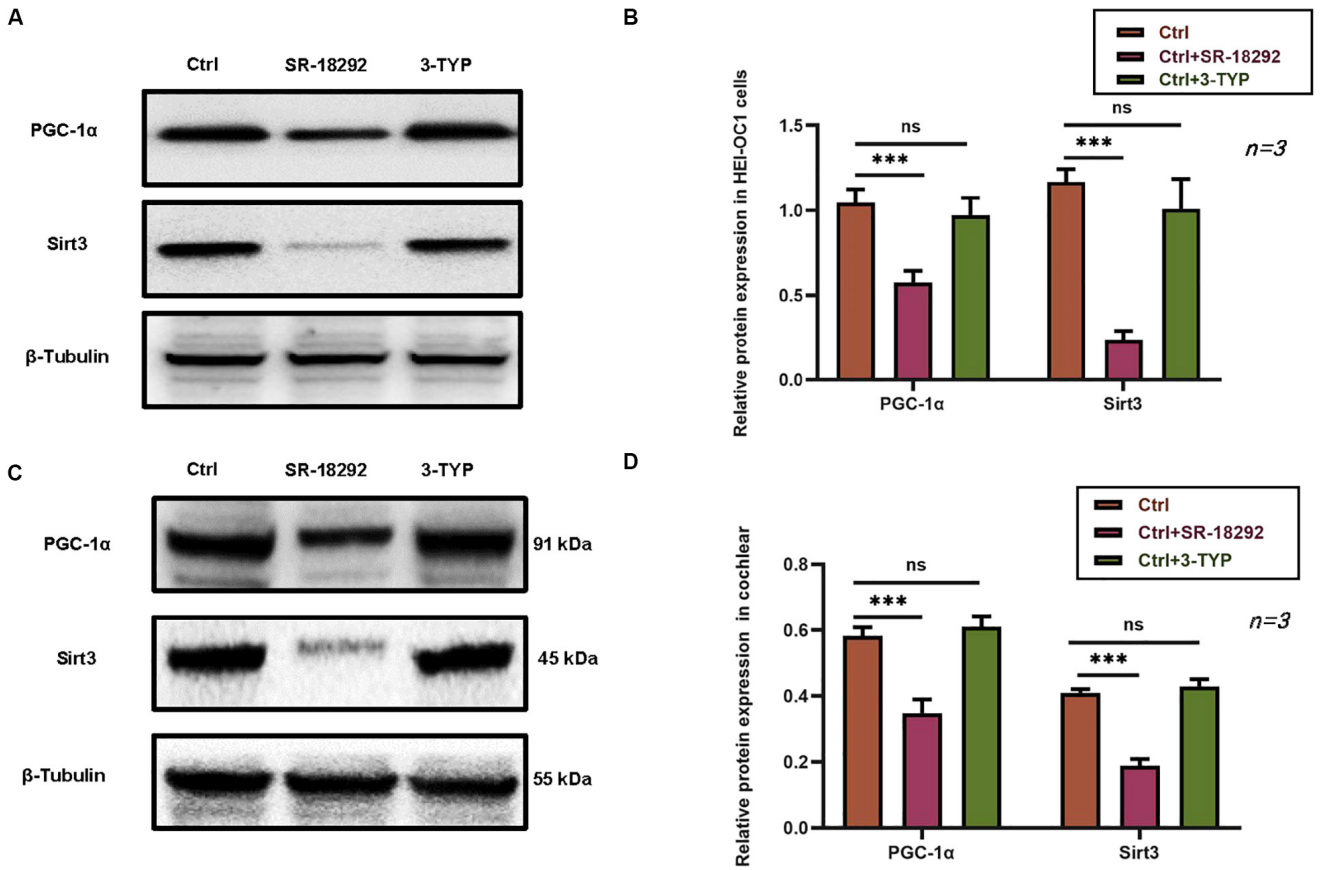

FIGURE 7 | PGC-1α regulates SIRT3 expression in HEI-OC1 cells and cochlear explants. **(A–D)** Effect of pretreatment with the PGC-1α inhibitor SR-18292 and SIRT3 inhibitor 3-TYP on PGC-1α and SIRT3 protein levels in HEI-OC1 cells **(A,B)** and cochlear explants **(C,D)**, as determined by western blotting. The experiment was repeated three times. NS, not significant; ***$P < 0.001$ (one-way analysis of variance followed by Tukey's multiple comparisons test).

ischemia/reperfusion injury (Wei et al., 2019), and hypobaric hypoxia-induced memory impairment involve the modulation of SIRT3 expression and/or activity. SIRT3 has been reported to protect hair cells against gentamicin-induced ototoxicity by stimulating the conversion of $NADP^+$ to NADPH in mitochondria, thereby suppressing ROS production (Quan et al., 2015). Accordingly, we observed that SIRT3 protein expression was enhanced by pretreatment with DHM, which has known antioxidant effects. However, the mechanism by which DHM regulates SIRT3 has not been reported. In previous studies, DHM was found to increase the expression of PGC-1α in skeletal muscle (Zhou et al., 2015; Huang et al., 2018). PGC-1α is a transcription factor that regulates lipid metabolism by inducing the expression of multiple genes in the tricarboxylic acid cycle and mitochondrial fatty acid oxidation pathway (Cheng et al., 2018). Additionally, PGC-1α regulates mitochondrial gene expression and oxidative metabolism (Islam et al., 2018). However, the function of PGC-1α in aminoglycoside-induced ototoxcity models has never been studied. Most previous research on the regulatory relationship between PGC-1α and Sirtuin family proteins have focused on SIRT1. It was reported that DHM inhibited lipid accumulation in hepatocytes by activating AMPK/PGC-1α/estrogen related receptor α signaling to increase SIRT3 expression and reduce oxidative stress, thereby preventing the development of NAFLD (Zeng et al., 2019). Our data showed that PGC-1α and SIRT3 expression increased with DHM concentration, suggesting that the anti-ototoxic effect of DHM involves these factors. To assess this possibility, we used pharmacologic inhibitors of PGC-1 α and SIRT3 prior to DHM pretreatment. The alleviation of apoptosis and oxidative stress by DHM was abrogated by both agents, providing support for our hypothesis.

The regulatory relationship between PGC-1α and SIRT3 has been previously described (Zhang et al., 2016; Song et al., 2017; Yu et al., 2017), but not in the context of the auditory system. We determined that PGC-1α functions as a transcriptional regulator of SIRT3 expression in HEI-OC1 cells and cochlear explants, providing additional evidence that PGC-1α/SIRT3 signaling mediates the effects of DHM. However, rescue experiments are needed in future studies to validate these findings.

It is worth noting that the working concentration of DHM varies across experimental systems and tissues. In palmitic acid-treated human umbilical vein endothelial cells (HUVECs), application of 1 μM DHM for 12 h suppressed apoptosis and

ROS production but in H_2O_2-treated HUVECs, a concentration of 300 μM was required to achieve the same effect (Tong et al., 2020). In our study, 100 μM DHM had statistically significant but mild effects on cell viability, apoptosis, and gene expression in both HEI-OC1 cells and cochlear explants; we therefore used a working concentration of 1 mM DHM and observed more robust effects. One major limitation of our study was the lack of *in vivo* experiments; therefore, it is unclear whether DHM has the same protective effects in living animals.

In conclusion, this is the first demonstration that DHM protects against gentamicin-induced ototoxicity PGC-1α/SIRT3 signaling. Our findings indicate that DHM may be effective in the prevention or treatment of hearing loss caused by aminoglycoside antibiotics as well as other oxidative stress-related diseases.

DATA AVAILABILITY STATEMENT

All datasets presented in this study are included in the article/**Supplementary Material**.

ETHICS STATEMENT

This study was approved by the Institutional Animal Care and Use Committee, China Medical University, and all animals were treated in accordance with the institutional guidelines.

AUTHOR CONTRIBUTIONS

XM designed the study. HH performed the experiments. HH and YD analyzed the data and wrote the manuscript. All authors contributed to the article and approved the submitted version.

FUNDING

This work was supported by the National Natural Science Foundation of China (grant no. 81800904, YD); Shenyang Science and Technology Plan Project (grant no. 18-014-4-09, XM); 345 Talent Project of Shengjing Hospital (YD); and Natural Science Foundation of Liaoning Province (grant no. 20180550477, XM).

ACKNOWLEDGMENTS

We thank Shengjing Hospital for providing laboratory and laboratory instruments. We thank Dr. Yang Fan for her technical guidance.

SUPPLEMENTARY MATERIAL

The Supplementary Material for this article can be found online at: https://www.frontiersin.org/articles/10.3389/fcell.2020.00702/full#supplementary-material

REFERENCES

Brown, K. D., Maqsood, S., Huang, J. Y., Pan, Y., Harkcom, W., Li, W., et al. (2014). Activation of SIRT3 by the NAD? precursor nicotinamide riboside protects from noise-induced hearing loss. *Cell Metab.* 20, 1059–1068. doi: 10.1016/j.cmet.2014.11.003

Chan, P. H. (2005). Mitochondrial dysfunction and oxidative stress as determinants of cell death/survival in stroke. *Ann. N. Y. Acad. Sci.* 1042, 203–209. doi: 10.1196/annals.1338.022

Chen, Y., Li, L., Ni, W., Zhang, Y., Sun, S., Miao, D., et al. (2015). Bmi1 regulates auditory hair cell survival by maintaining redox balance. *Cell Death Dis.* 6:e1605. doi: 10.1038/cddis.2014.549

Chen, Y., Zhang, S., Chai, R., and Li, H. (2019). Hair cell regeneration. *Adv. Exp. Med. Biol.* 1130, 1–16. doi: 10.1007/978-981-13-6123-4_1

Cheng, A. G., Cunningham, L. L., and Rubel, E. W. (2005). Mechanisms of hair cell death and protection. *Curr. Opin. Otolaryngol. Head Neck. Surg.* 13, 343–348. doi: 10.1097/01.moo.0000186799.45377.63

Cheng, C. F., Ku, H. C., and Lin, H. (2018). PGC-1α as a pivotal factor in lipid and metabolic regulation. *Int. J. Mol. Sci.* 19:3447. doi: 10.3390/ijms19113447

Coffin, A. B., Rubel, E. W., and Raible, D. W. (2013). Bax, Bcl2, and p53 differentially regulate neomycin- and gentamicin-induced hair cell death in the zebrafish lateral line. *J. Assoc. Res. Otolaryngol.* 14, 645–659. doi: 10.1007/s10162-013-0404-1

Czajkowski, A., Mounier, A., Delacroix, L., and Malgrange, B. (2019). Pluripotent stem cell-derived cochlear cells: a challenge in constant progress. *Cell Mol. Life Sci.* 76, 627–635. doi: 10.1007/s00018-018-2950-5

Desa, D., Nichols, M. G., and Smith, H. J. (2018). Aminoglycosides rapidly inhibit NAD(P)H metabolism increasing reactive oxygen species and cochlear cell demise. *J. Biomed. Opt.* 24, 1–14. doi: 10.1117/1.JBO.24.5.051403

Dong, Y., Liu, D., Hu, Y., and Ma, X. (2015). NaHS protects cochlear hair cells from gentamicin-induced ototoxicity by inhibiting the mitochondrial apoptosis pathway. *PLoS One* 10:e0136051. doi: 10.1371/journal.pone.0136051

Esterberg, R., Linbo, T., Pickett, S. B., Wu, P., Ou, H. C., Rubel, E. W., et al. (2016). Mitochondrial calcium uptake underlies ROS generation during aminoglycoside-induced hair cell death. *J. Clin. Invest.* 126, 3556–3566. doi: 10.1172/JCI84939

Finkel, T., Deng, C. X., and Mostoslavsky, R. (2009). Recent progress in the biology and physiology of sirtuins. *Nature* 460, 587–591. doi: 10.1038/nature08197

Genestra, M. (2007). Oxyl radicals, redox-sensitive signalling cascades and antioxidants. *Cell. Signal.* 19, 1807–1819. doi: 10.1016/j.cellsig.2007.04.009

Guo, X., Bai, X., Li, L., Li, J., and Wang, H. (2018). Forskolin protects against cisplatin-induced ototoxicity by inhibiting apoptosis and ROS production. *Biomed. Pharmacother.* 99, 530–536. doi: 10.1016/j.biopha.2018.01.080

Hou, X., Tong, Q., Wang, W., Xiong, W., Shi, C., and Fang, J. (2015). Dihydromyricetin protects endothelial cells from hydrogen peroxide-induced oxidative stress damage by regulating mitochondrial pathways. *Life Sci.* 130, 38–46. doi: 10.1016/j.lfs.2015.03.007

Huang, Y., Chen, K., Ren, Q., Yi, L., Zhu, J., Zhang, Q., et al. (2018). Dihydromyricetin attenuates dexamethasone-induced muscle atrophy by improving mitochondrial function via the PGC-1α pathway. *Cell Physiol. Biochem.* 49, 758–779. doi: 10.1159/000493040

Islam, H., Edgett, B. A., and Gurd, B. J. (2018). Coordination of mitochondrial biogenesis by PGC-1α in human skeletal muscle: a re-evaluation. *Metab. Clin. Exp.* 79, 42–51. doi: 10.1016/j.metabol.2017.11.001

Jadidian, A., Antonelli, P. J., and Ojano-Dirain, C. P. (2015). Evaluation of apoptotic markers in HEI-OC1 cells treated with gentamicin with and without the mitochondria-targeted antioxidant mitoquinone. *Otol. Neurotol.* 36, 526–530. doi: 10.1097/MAO.0000000000000517

Jiang, P., Ray, A., Rybak, L. P., and Brenner, M. J. (2016). Role of STAT1 and oxidative stress in gentamicin-induced hair cell death in organ of Corti. *Otol. Neurotol.* 37, 1449–1456. doi: 10.1097/MAO.0000000000001192

Kalinec, G. M., Park, C., Thein, P., and Kalinec, F. (2016). Working with auditory HEI-OC1 cells. *J. Vis. Exp.* 2016:54425. doi: 10.3791/54425

Kandola, K., Bowman, A., and Birch-Machin, M. A. (2015). Oxidative stress – a key emerging impact factor in health, ageing, lifestyle and aesthetics. *Int. J. Cosmet. Sci.* 37, 1–8. doi: 10.1111/ics.12287

Le, L., Jiang, B., Wan, W., Zhai, W., Xu, L., Hu, K., et al. (2016). Metabolomics reveals the protective of Dihydromyricetin on glucose homeostasis by enhancing insulin sensitivity. *Sci. Rep.* 6:36184. doi: 10.1038/srep36184

Li, L. L., Zhang, P., Bao, Z. X., Wang, T. X., Liu, S., Huang, F. R., et al. (2016). PGC-1α promotes ureagenesis in mouse periportal hepatocytes through SIRT3 and SIRT5 in response to glucagon. *Sci. Rep.* 6:24156. doi: 10.1038/srep24156

Liu, L., Zhang, K., Sandoval, H., Yamamoto, S., Jaiswal, M., Sanz, E., et al. (2015). Glial lipid droplets and ROS induced by mitochondrial defects promote neurodegeneration. *Cell* 160, 177–190. doi: 10.1016/j.cell.2014.12.019

Madamanchi, N. R., and Runge, M. S. (2013). Redox signaling in cardiovascular health and disease. *Free Radic. Biol. Med.* 61, 473–501. doi: 10.1016/j.freeradbiomed.2013.04.001

Mangiardi, D. A., McLaughlin-Williamson, K., May, K. E., Messana, E. P., Mountain, D. C., and Cotanche, D. A. (2004). Progression of hair cell ejection and molecular markers of apoptosis in the avian cochlea following gentamicin treatment. *J. Comp. Neurol.* 475, 1–18. doi: 10.1002/cne.20129

Palacios, O. M., Carmona, J. J., Michan, S., Chen, K. Y., Manabe, Y., Ward, J. L., et al. (2009). Diet and exercise signals regulate SIRT3 and activate AMPK and PGC-1alpha in skeletal muscle. *Aging* 1, 771–783. doi: 10.18632/aging.100075

Park, C., Thein, P., Kalinec, G., and Kalinec, F. (2016). HEI-OC1 cells as a model for investigating prestin function. *Hear. Res.* 335, 9–17. doi: 10.1016/j.heares.2016.02.001

Quan, Y., Xia, L., Shao, J., Yin, S., Cheng, C. Y., Xia, W., et al. (2015). Adjudin protects rodent cochlear hair cells against gentamicin ototoxicity via the SIRT3-ROS pathway. *Sci. Rep.* 5:8181. doi: 10.1038/srep0818

Salvatori, I., Valle, C., Ferri, A., and Carrì, M. T. (2017). SIRT3 and mitochondrial metabolism in neurodegenerative diseases. *Neurochem. Int.* 109, 184–192. doi: 10.1016/j.neuint.2017.04.012

Sheth, S., Mukherjea, D., Rybak, L. P., and Ramkumar, V. (2017). Mechanisms of cisplatin-induced ototoxicity and otoprotection. *Front. Cell. Neurosci.* 11:338. doi: 10.3389/fncel.2017.00338

Sies, H. (2015). Oxidative stress: a concept in redox biology and medicine. *Redox Biol.* 4, 180–183. doi: 10.1016/j.redox.2015.01.002

Someya, S., Yu, W., Hallows, W. C., Xu, J., Vann, J. M., Leeuwenburgh, C., et al. (2010). Sirt3 mediates reduction of oxidative damage and prevention of age-related hearing loss under caloric restriction. *Cell* 143, 802–812. doi: 10.1016/j.cell.2010.10.002

Song, C., Zhao, J., Fu, B., Li, D., Mao, T., Peng, W., et al. (2017). Melatonin-mediated upregulation of Sirt3 attenuates sodium fluoride-induced hepatotoxicity by activating the MT1-PI3K/AKT-PGC-1α signaling pathway. *Free Radic. Biol. Med.* 112, 616–630. doi: 10.1016/j.freeradbiomed.2017.09.005

Stefanatos, R., and Sanz, A. (2018). The role of mitochondrial ROS in the aging brain. *FEBS Lett.* 592, 743–758. doi: 10.1002/1873-3468.12902

Tabuchi, K., Pak, K., Chavez, E., and Ryan, A. F. (2007). Role of inhibitor of apoptosis protein in gentamicin-induced cochlear hair cell damage. *Neuroscience* 149, 213–222. doi: 10.1016/j.neuroscience.2007.06.061

Tong, H., Zhang, X., Tan, L., Jin, R., Huang, S., and Li, X. (2020). Multitarget and promising role of dihydromyricetin in the treatment of metabolic diseases. *Eur. J. Pharmacol.* 870:172888. doi: 10.1016/j.ejphar.2019.172888

Wang, J., Wang, K., Huang, C., Lin, D., Zhou, Y., Wu, Y., et al. (2018). SIRT3 activation by dihydromyricetin suppresses chondrocytes degeneration via maintaining mitochondrial homeostasis. *Int. J. Biol. Sci.* 14, 1873–1882. doi: 10.7150/ijbs.27746

Wang, Q., Li, L., Li, C. Y., Pei, Z., Zhou, M., and Li, N. (2015). SIRT3 protects cells from hypoxia via PGC-1α- and MnSOD-dependent pathways. *Neuroscience* 286, 109–121. doi: 10.1016/j.neuroscience.2014.11.045

Wei, L., Sun, X., Qi, X., Zhang, Y., Li, Y., and Xu, Y. (2019). Dihydromyricetin ameliorates cardiac ischemia/reperfusion injury through Sirt3 activation. *Biomed. Res. Int.* 2019:6803943. doi: 10.1155/2019/6803943

Yang, T. H., Young, Y. H., and Liu, S. H. (2011). EGb 761 (Ginkgo biloba) protects cochlear hair cells against ototoxicity induced by gentamicin via reducing reactive oxygen species and nitric oxide-related apoptosis. *J. Nutr. Biochem.* 22, 886–894. doi: 10.1016/j.jnutbio.2010.08.009

Ylikoski, J., Xing-Qun, L., Virkkala, J., and Pirvola, U. (2002). Blockade of c-Jun N-terminal kinase pathway attenuates gentamicin-induced cochlear and vestibular hair cell death. *Hear. Res.* 166, 33–43. doi: 10.1016/s0378-5955(01)00380-x

Yu, L., Gong, B., Duan, W., Fan, C., Zhang, J., Li, Z., et al. (2017). Melatonin ameliorates myocardial ischemia/reperfusion injury in type 1 diabetic rats by preserving mitochondrial function: role of AMPK-PGC-1α-SIRT3 signaling. *Sci. Rep.* 7:41337. doi: 10.1038/srep41337

Zeng, X., Yang, J., Hu, O., Huang, J., Ran, L., Chen, M., et al. (2019). Dihydromyricetin ameliorates nonalcoholic fatty liver disease by improving mitochondrial respiratory capacity and redox homeostasis through modulation of SIRT3 signaling. *Antioxid. Redox. Signal.* 30, 163–183. doi: 10.1089/ars.2017.7172

Zhang, J., Chen, Y., Luo, H., Sun, L., Xu, M., Yu, J., et al. (2018). Recent update on the pharmacological effects and mechanisms of dihydromyricetin. *Front. Pharmacol.* 9:1204. doi: 10.3389/fphar.2018.01204

Zhang, X., Ren, X., Zhang, Q., Li, Z., Ma, S., Bao, J., et al. (2016). PGC-1α/ERRα-Sirt3 pathway regulates DAergic neuronal death by directly deacetylating SOD2 and ATP synthase β. *Antioxid. Redox. Signal.* 24, 312–328. doi: 10.1089/ars.2015.6403

Zhang, Y., Wang, C., Jin, Y., Yang, Q., Meng, Q., Liu, Q., et al. (2018). Activating the PGC-1/TERT pathway by catalpol ameliorates atherosclerosis via modulating ROS production, DNA damage, and telomere function: implications on mitochondria and telomere link. *Oxid. Med. Cell. Longev.* 2018:2876350. doi: 10.1155/2018/2876350

Zhou, Q., Chen, K., Liu, P., Gao, Y., Zou, D., Deng, H., et al. (2015). Dihydromyricetin stimulates irisin secretion partially via the PGC-1α pathway. *Mol. Cell. Endocrinol.* 412, 349–357. doi: 10.1016/j.mce.2015.05.036

Zou, D., Chen, K., Liu, P., Chang, H., Zhu, J., and Mi, M. (2014). Dihydromyricetin improves physical performance under simulated high altitude. *Med. Sci. Sports Exerc.* 46, 2077–2084. doi: 10.1249/MSS.0000000000000336

Conflict of Interest: The authors declare that the research was conducted in the absence of any commercial or financial relationships that could be construed as a potential conflict of interest.

frontiers in Cell and Developmental Biology

REVIEW
published: 15 September 2020
doi: 10.3389/fcell.2020.574338

The Multifaceted Roles of the BCL-2 Family Member BOK

*Samara Naim and Thomas Kaufmann**

Institute of Pharmacology, University of Bern, Bern, Switzerland

BCL-2–related ovarian killer (BOK) is—despite its identification over 20 years ago—an incompletely understood member of the BCL-2 family. BCL-2 family proteins are best known for their critical role in the regulation of mitochondrial outer membrane permeabilization during the intrinsic apoptotic pathway. Based on sequence and structural similarities to BAX and BAK, BOK is grouped with these "killers" within the effector subgroup of the family. However, the mechanism of how exactly BOK exerts apoptosis is not clear and controversially discussed. Furthermore, and in accordance with reports on several other BCL-2 family members, BOK seems to be involved in the regulation of a variety of other, "apoptosis-independent" cellular functions, including the unfolded protein response, cellular proliferation, metabolism, and autophagy. Of note, compared with other proapoptotic BCL-2 family members, BOK levels are often reduced in cancer by various means, and there is increasing evidence for BOK modulating tumorigenesis. In this review, we summarize and discuss apoptotic- and non–apoptotic-related functions of BOK, its regulation as well as its physiological and pathophysiological roles.

Keywords: apoptosis, BCL-2 family, Bok, cell death, cancer, metabolism, autophagy, er stress

OPEN ACCESS

Edited by:
Yinan Gong,
University of Pittsburgh School of Medicine, United States

Reviewed by:
Ben A. Croker,
University of California, San Diego, United States
Gustavo P. Amarante-Mendes,
University of São Paulo, Brazil

***Correspondence:**
Thomas Kaufmann
thomas.kaufmann@pki.unibe.ch

Specialty section:
This article was submitted to Cell Death and Survival, a section of the journal Frontiers in Cell and Developmental Biology

Received: *19 June 2020*
Accepted: *18 August 2020*
Published: *15 September 2020*

Citation:
Naim S and Kaufmann T (2020) The Multifaceted Roles of the BCL-2 Family Member BOK. Front. Cell Dev. Biol. 8:574338. doi: 10.3389/fcell.2020.574338

INTRODUCTION: THE BCL-2 PROTEIN FAMILY IN APOPTOSIS

Apoptosis, the first described and probably best understood form of programed cell death, is a physiological process that actively leads to the death of a cell. Apoptosis is critical for the removal of old, unwanted or critically damaged cells, both during development and for the maintenance of cellular homeostasis in adult multicellular organisms. Its regulation reaches the complexity of cell growth and cell proliferation, and a fine-tuned and self-regulatory balance between cell growth and cell death guarantees the healthy state of individual organisms (Singh et al., 2019). Cellular turnover in adult humans is estimated to be around 1 million per second (Reed, 2006). Given the massive number of cells constantly dying in our bodies, it is not surprising that nature has ensured a highly efficient, fast, and safe removal process of dying cells. However, there is a strong connection between the imbalance in apoptosis regulation and various pathophysiologies (Favaloro et al., 2012). Many cancer cells, for example, increase their prosurvival activity during the process of malignant transformation or in the course of radiotherapeutic/chemotherapeutic intervention, contributing to the development of resistance against apoptotic stimuli. One commonly observed way to achieve this is through upregulation of antiapoptotic BCL-2 family members, such as BCL-2, BCL-XL, or MCL-1 (Campbell and Tait, 2018). To overcome such apoptosis resistance of cancer cells, great interest in developing specific inhibitors of antiapoptotic BCL-2 proteins, so-called BH3 mimetics, has arisen over the past years, with a first compound [the BCL-2–specific inhibitor venetoclax (Venclexta)] approved by the US Food and Drug and Administration for

chronic lymphocytic leukemia and acute myeloid leukemia (Montero and Letai, 2018; Timucin et al., 2019). On the other hand, excessive apoptosis is described in neurodegenerative diseases such as Alzheimer and Huntington disease (Mattson, 2000; Ghavami et al., 2014).

Central to apoptosis induction are cysteine aspartate–specific proteases, called caspases. Caspases form an evolutionary conserved family of cysteine proteases involved in cell death (apoptotic caspases), as well as inflammatory responses (inflammatory caspases) (Zheng et al., 1999; Van Opdenbosch and Lamkanfi, 2019). Apoptotic caspases can be subdivided into initiator (caspases-8, -9, and -10) and effector caspases (caspases-3, -6, and -7) (Van Opdenbosch and Lamkanfi, 2019). Caspases are mainly abundant in their inactive state as procaspases (Mcilwain et al., 2013). Once autoactivated following intrinsic or extrinsic initiation of apoptosis, initiator caspases activate effector caspases through proteolytic cleavage (Shi, 2004). Activated effector caspases then cleave cellular substrates leading to cell death (Julien and Wells, 2017).

Members of the BCL-2 family are central regulators of the so-called intrinsic, or mitochondrial, apoptotic pathway, a pathway that can be activated in possibly all cell types in response to a plethora of intrinsic stress ("apoptotic") stimuli. These include DNA damaging insults, oxidative stress, aberrant calcium fluxes, endoplasmic reticulum (ER) stress, nutrient deprivation, or infection by pathogens, among others (Lopez and Tait, 2015). Once activated, the intrinsic apoptotic pathway results in the BCL-2 family regulated discrete permeabilization of the mitochondrial outer membrane (MOMP), with subsequent release of many proteins from the mitochondrial intermembrane space into the cytoplasm. Among the latter are apoptogenic proteins (such as cytochrome c or SMAC/DIABLO), which are needed for—or facilitate—the downstream activation of apoptotic caspases (Lopez and Tait, 2015).

The members of the BCL-2 family are small globular proteins that contain up to four rather loosely conserved Bcl-2 homology (BH) domains, BH1–BH4. All family members contain the hydrophobic BH3 domain, which is important for protein–protein interaction between the various BCL-2 proteins, and most members contain a C-terminal α-helical transmembrane domain (TMD) that serves to tail-anchor the protein to intracellular membranes (Schinzel et al., 2004; Wilfling et al., 2012). Based on structural and functional homologies, the family is classified into three subgroups: the antiapoptotic proteins (BCL-2, BCL-XL, BCL-W, MCL-1, BFL-1/BCL-2A1, and BCL-B), the proapoptotic BH3-only proteins (BAD, BID, BIK, BIM, BMF, HRK, NOXA, PUMA), and the proapoptotic effector proteins BAX, BAK, and BCL-2–related ovarian killer (BOK) (Adams and Cory, 2018).

The interaction of the BCL-2 proteins depends on the abundance, the attraction, and the affinity of the proteins. The affinity between different proteins on its part results from conformational changes of the proteins (Kale et al., 2018). There are three main types of interaction: (1) binding of the BH3 domain of so-called "activator" BH3-only proteins (such as BIM or BID) to the BH3-binding groove of the effectors BAX and/or BAK, leading to their direct activation; (2) binding of the BH3-binding groove of antiapoptotic proteins to the BH3 domain of BAX/BAK or activator BH3-only proteins, leading to their sequestration; (3) binding of the BH3 domain of so-called "sensitizer" BH3-only proteins (such as BAD or NOXA) to the BH3-binding groove of antiapoptotic proteins, leading to their inactivation (Kale et al., 2018).

The ultimate goal of the early initiation phase of intrinsic apoptosis is MOMP. Whether or not MOMP occurs depends on the ratio between proapoptotic and antiapoptotic proteins, or more precisely, on their activation status and the interactions between them (Kale et al., 2018). Equally important seems the composition of the lipid bilayer of the mitochondrial outer membrane (MOM), where most of the previously described interactions take place and which has an active role in facilitating structural changes of the BCL-2 proteins, resulting in affinity changes and consequently alterations of interactions (Kale et al., 2018).

Once activated, the effector proteins BAX and BAK oligomerize to form pores leading to MOMP (Cosentino and Garcia-Saez, 2017), a process described as point of no return during the initiation of intrinsic apoptosis. While BAK is already located at the MOM, BAX translocates from the cytosol to the mitochondrial membrane upon activation (Wolter et al., 1997; Todt et al., 2015).

Whereas regulation of the intrinsic apoptotic pathway, specifically MOMP, is the best understood role of BCL-2 family members, it is important to mention that for most—if not all—members, other, distinct non-apoptotic roles have been described. These range from modulating mitochondrial shape and metabolism, calcium flux, the unfolded protein response (UPR), DNA damage response, glucose and lipid metabolism to cellular proliferation and autophagy [reviewed in (Gross and Katz, 2017)].

A SHORT HISTORY OF BOK

BOK was first discovered in 1997 by Hsu et al. (1997) in a yeast two-hybrid screen of a rat ovarian fusion library using MCL-1 as a bait and by Inohara et al. (1998) by sequence homology prediction screening, naming it "matador" (MTD), meaning *killer* in Spanish. Hsu et al. (1997) initially described BOK as highly and restrictedly expressed in rat ovaries, testis and uterus, hence the name "Bcl-2–related ovarian killer." Within the first years after its discovery, only a few articles on BOK were published. Besides classifying it as a proapoptotic BCL-2 protein based on transient overexpression experiments and describing first interaction partners (MCL-1, BHRF1, and BFL-1, but not BCL-2, BCL-XL, or BCL-W) (Hsu et al., 1997), sequence analyses revealed BOK as an evolutionarily highly conserved BCL-2 member (Zhang et al., 2000). Not only was it reported to be important for apoptosis regulation in normal B-cell development in chicken (Brown et al., 2004) but also for the increased trophoblast cell death found in preeclampsia, regulated by the MCL-1/MTD (BOK) rheostat (Soleymanlou et al., 2005; Soleymanlou et al., 2007). The interest in BOK rapidly increased in 2010 upon the discovery that the locus containing the *BOK*

gene is frequently deleted across human cancers, thus indicating a possible tumor suppressor role for BOK (Beroukhim et al., 2010) as well as the characterization of the first *Bok*-deficient mouse model in 2012 (Ke et al., 2012). This latter study showed that the expression of BOK is, in contrast to earlier assumptions (Hsu et al., 1997), not restricted to reproductive organs but rather widely distributed across tissues, in which it is detectable both at mRNA and protein levels (Ke et al., 2012). Because of its proapoptotic potential and its considerable amino acid sequence homologies with BAX and BAK, BOK was clustered in the effector ("killer") subgroup of the BCL-2 family of proteins (Hsu et al., 1997). Until recently, there was no structural information available on BOK. The structural similarities between BOK and BAX/BAK were substantiated in 2018 by two independent studies using X-ray crystallography on chicken BOK and NMR spectroscopy on human BOK, respectively (Ke et al., 2018; Moldoveanu and Zheng, 2018; Zheng et al., 2018). However, as discussed in more detail below, there are several important differences that distinguish BOK properties and functions from those of BAX or BAK. More than 20 years after its discovery, the role of BOK in apoptosis is not entirely understood and to some extent controversially discussed (Yakovlev et al., 2004; Jaaskelainen et al., 2010; Carpio et al., 2015; D'Orsi et al., 2016; Einsele-Scholz et al., 2016; Llambi et al., 2016; Fernandez-Marrero et al., 2017; Moldoveanu and Zheng, 2018; Schulman et al., 2019). There is increasing evidence supporting roles of BOK in cellular functions other than cell death regulation, namely, uridine metabolism and cellular proliferation (Ray et al., 2010; Moravcikova et al., 2017; Rabachini et al., 2018; Srivastava et al., 2019), autophagy (Kalkat et al., 2013), mitochondrial physiology (D'Orsi et al., 2017; Ausman et al., 2018; Schulman et al., 2019), ER homeostasis, and modulation of the UPR (Echeverry et al., 2013; Carpio et al., 2015; Schulman et al., 2016; Moravcikova et al., 2017; Kang et al., 2019). Thus, there are many open questions remaining to fully understand the different roles and functions of this protein.

BOK GENE TARGETING IN MICE

The first $Bok^{-/-}$ mouse was published in 2012 by Ke et al., using homologous recombination in C57BL/6-derived embryonic stem cells targeting half of exon 1 and exon 2 of *Bok* (with exon 2 containing the ATG start site) (Ke et al., 2012). BOK knockout mice did not show an overt phenotype and were produced at the expected Mendelian frequency (**Table 1**; Ke et al., 2012). Investigated organs of $Bok^{-/-}$ mice appeared normal, and there was no difference in hematopoietic cell subset composition (Ke et al., 2012). An important message of this study was that BOK is widely expressed in mouse tissues and readily detectable at the protein level in most tissues analyzed. Expression in the bone marrow, however, was shown to be low. Among the hematopoietic subsets, BOK expression was highest in myeloid cells but very low in lymphoid cells. These expression profiles may explain the finding that loss of BOK did not accelerate lymphoma development in Eμ-myc transgenic mice (Ke et al., 2012). Along the same line, *Bok*-deficient lymphoid and myeloid cells were found to respond normally to the classic apoptotic stimuli etoposide, dexamethasone, FasL, or the BH3 mimetic ABT-737 (Ke et al., 2012).

Lack of a spontaneous phenotype was confirmed in two independently derived *Bok*-deficient mouse models (Carpio et al., 2015; Llambi et al., 2016). This finding was no great surprise, also given that neither BAX nor BAK single knockout mice display major phenotypes, with the exception of testicular atrophy and infertility seen in $Bax^{-/-}$ males (Knudson et al., 1995; Lindsten et al., 2000).

While loss of either BAK or BAX alone is compatible with the development of mice, $Bax^{-/-}Bak^{-/-}$ double-knockout (DKO) mice are obtained at less than 10% of the expected Mendelian frequency, and only few survive into adulthood (Lindsten et al., 2000; Mason et al., 2013). Those surviving mice develop severe neurological and hematopoietic abnormalities, splenomegaly, and lymphadenopathy (Lindsten et al., 2000). On the other hand, combined gene knockouts of *Bok* and *Bax*, or *Bok* and *Bak*, respectively, did not worsen the phenotype of $Bak^{-/-}$ or $Bax^{-/-}$ single knockout mice, except for an increased oocyte count in $Bax^{-/-}Bok^{-/-}$ DKO females (Ke et al., 2013). Mice lacking BAX, BAK, and BOK [triple-knockout (TKO)] in the hematopoietic system showed a slightly more severe phenotype compared to respective $Bax^{-/-}Bak^{-/-}$ DKO controls, including increased levels of autoantibodies and leukocyte infiltration in several organs (Ke et al., 2015). These data were an early indication that BOK may have redundant functions with BAX and BAK. The proof that BOK indeed has overlapping functions with BAX and BAK also beyond the hematopoietic compartment came with the generation of full-body $Bax^{-/-}Bak^{-/-}Bok^{-/-}$ TKO mice in 2018 by Ke et al. (2018). This article showed that TKO mice develop more severe defects and die earlier compared with $Bax^{-/-}Bak^{-/-}$ DKO mice, with 99% developing lethal abnormalities. With developmental defects starting from E11.5, TKO pups at E18.5 showed, among others, multiple midline defects and aortic arch defects, as well as abnormal tissue growth in multiple organs, all of which were thought to be a consequence of inactivated intrinsic apoptosis (Ke et al., 2018). Besides providing the current best evidence for a physiologically relevant role of BOK in apoptosis and embryogenesis, this study also demonstrated that multiple organs develop more or less normally in TKO mice and that a small proportion (1%) of TKO mice even survives into adulthood, indicating that intrinsic apoptosis is not strictly required for the development of mice (Ke et al., 2018).

INTERACTION PARTNERS AND SUBCELLULAR LOCALIZATION OF BOK

So far, only a few BOK interacting partners have been described (**Figure 1**). Using yeast two-hybrid screens, BOK was found to interact with some selected antiapoptotic members of the BCL-2 family, i.e., MCL-1, BFL-1/BCL-2A1, and the Epstein-Barr virus BCL-2 homolog BHRF1, but neither with BCL-2, BCL-XL, or BCL-W, nor with BAX or BAK (Hsu et al., 1997; Srivastava et al., 2019). Using co-immunoprecipitation assays of

TABLE 1 | *Bok*-deficient mouse models.

Model	Targeting strategy/comments	Characteristics	References
Bok$^{-/-}$	• Homologous recombination in C57BL/6 derived ES cells; C57BL/6J genetic background • Deletion of half of exon 1 and exon 2	• No overt phenotype • Reproduction at expected Mendelian frequency	Ke et al., 2012
Bok$^{-/-}$	• Homologous recombination in 129-derived ES cells; backcrossed to C57BL/6 genetic background • Deletion of exons 2 and 3	• Normal development	Carpio et al., 2015
Bok$^{-/-}$	• Homologous recombination in 129/SvEv derived ES cells; backcrossed to C57BL/6N genetic background • Deletion of exons 2–5	• No overt phenotype	Llambi et al., 2016
Eμ-myc/Bok$^{-/-}$	• Crossing *Eμ-myc* transgenic mice with full-body *Bok*$^{-/-}$ mice (Ke et al., 2012)	• No acceleration of lymphoma development and no impact on disease severity compared to *Eμ-myc* transgenic mice	Ke et al., 2012
Nup98-HoxD13 (NHD13)/*Bok*$^{-/-}$	• Crossing NHD13 transgenic mice with full-body *Bok*$^{-/-}$ mice (Carpio et al., 2015)	• Acute myeloid leukemia development in 36.7% of mice • Development of progressive anemia: lower hemoglobin, lower mean cell hemoglobin concentration, higher mean cell volume	Kang et al., 2019
Bok$^{-/-}$*Bak*$^{-/-}$ *DKO*	• Crossing *Bak*$^{-/-}$ mice with *Bok*$^{-/-}$ mice	• No noticeable defects compared to *BAK*$^{-/-}$ single knockout	Ke et al., 2013
Bok$^{-/-}$*Bax*$^{-/-}$ *DKO*	• Crossing *Bax*$^{-/-}$ mice with *Bok*$^{-/-}$ mice	• Increased ovarian follicle numbers at 1 year of age	Ke et al., 2013
Bok$^{-/-}$*Bax*$^{-/-}$*Bak*$^{-/-}$ *TKO* in the hematopoietic system	• Bone marrow chimeras obtained by injection of TKO fetal liver cells (FLC, E14) into lethally irradiated wild-type recipients	• Slightly more severe phenotype compared to mice reconstituted with FLCs of *Bax*$^{-/-}$*Bak*$^{-/-}$ *DKO* mice • Increased numbers of leukocytes in the periphery, as well as in several organs • Lymphocytic infiltration in multiple organs and organ-specific autoantibodies	Ke et al., 2015
Bok$^{-/-}$*Bax*$^{-/-}$*Bak*$^{-/-}$ full-body *TKO*	• Crossing *Bok*$^{-/-}$ (Ke et al., 2012), *Bax*$^{-/-}$ (Knudson et al., 1995) and *Bak*$^{-/-}$ (Lindsten et al., 2000) mice; C57BL/6J genetic background	• 1% of mice survive into adulthood • Developmental defects at E11.5 • Multiple midline defects at E18.5 • Pups develop abnormal tissue growth in multiple locations	Ke et al., 2018

overexpressed proteins, Echeverry et al. reported failure of BOK to interact with any tested BCL-2 family member (BCL-2, BCL-XL, MCL-1, BAX, BAK), with the exception of BOK itself, an interaction that is dependent on critical amino acids within the BH3 domain (Echeverry et al., 2013). However, there currently are no convincing data published that BOK forms dimers or higher homo-oligomers or hetero-oligomers. Moreover, both yeast two-hybrid screens and co-immunoprecipitation assays are error-prone; thus, more reliable assays are needed to clarify the interactions of BOK with other family members. Like most BCL-2 proteins, BOK contains a C-terminal TMD that serves as a tail-anchor domain for the posttranslational insertion at the cytoplasmic side of intracellular membranes (Hsu et al., 1997; Schinzel et al., 2004). Tail anchors are both necessary and sufficient to target a protein to the ER, the MOM, or to other intracellular membranes, whereas they are not always specific for a single compartment with known examples of dual targeting of ER and MOM (Borgese and Fasana, 2011). Echeverry et al. (2013) have demonstrated that the TMD of BOK has a high affinity for the ER, Golgi, and associated membranes, into which it integrally inserts. However, whereas the majority of BOK is located at the ER, BOK can also be found at the mitochondria (Ray et al., 2010; Echeverry et al., 2013; Einsele-Scholz et al., 2016; Ausman et al., 2018) and has further been reported to localize to the nucleus, where its role is still rather enigmatic (Bartholomeusz et al., 2006; Echeverry et al., 2013). In contrast to most other multi–BH-domain BCL-2 proteins, which contain a classic hydrophobic TMD, the TMD of BOK is peculiar in that it comprises two positively charged amino acids (aa) in its center (R^{200} and K^{203} in mouse BOK) (Lindsay et al., 2011). The functions of these polar aa are not clear, but may affect the topology of the BOK TMD and its membrane insertion; on the other hand, it may also be speculated that these polar aa mediate intramembranous homodimerization or heterodimerization with polar TMDs of interaction partners.

BOK's dominant localization at the ER is an important distinction from BAX or BAK and is much in line with increasing evidence for a role of BOK in the modulation of ER stress responses (see below). This is also strongly supported by the direct interaction of BOK with inositol 1,4,5-trisphosphate receptors (IP3R), in particular with IP3R1 and IP3R2, as identified by the Wojcikiewicz laboratory (Schulman et al., 2013, 2016). This interaction was shown to be strong and constitutive and mediated by the N-terminal BH4 domain of BOK binding to a region within the IP3R coupling domain, a region to which no other BCL-2 family member has been reported to bind. Through this interaction, BOK protects IP3R from caspase-3–mediated degradation during apoptosis (Schulman et al., 2013). However, no direct effect of BOK in altering Ca^{2+} mobilization by IP3Rs was observed (Schulman et al., 2013). Nevertheless, a role for

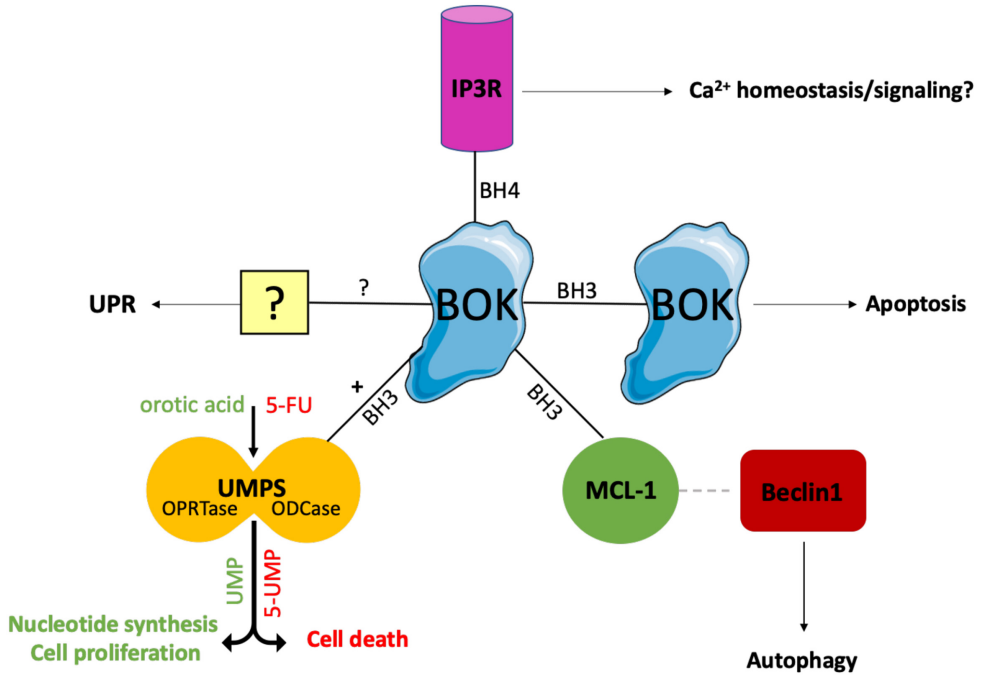

FIGURE 1 | Interaction partners of BOK. Only few BOK interacting partners have been described so far. Using yeast two-hybrid screens, BOK was found to interact with MCL-1. This interaction has been proposed to promote autophagy, as BOK binding to MCL-1 frees MCL-1–bound Beclin-1, which in turn initiates the autophagy machinery. Moreover, BOK is constitutively bound to IP3Rs (IP3R1 and IP3R2) at the ER via its BH4 domain. IP3Rs may act as a regulatory sink for BOK to keep the levels of unbound ("free") BOK low. Furthermore, co-immunoprecipitation experiments indicated that BOK may interact with itself in a BH3 domain–dependent manner. Whether BOK truly forms dimers or homo-oligomers and whether this oligomerization induces MOMP need to be further investigated. Recently, BOK was found to interact with and increase the activity of the enzyme UMPS via its BH3 domain. UMPS catalyzes the last two steps of the *de novo* synthesis of UMP and is central for metabolizing the chemotherapeutic drug 5-FU into its active metabolites. As a result, cells lacking BOK have a defect in uridine metabolism, leading to decreased cellular proliferation compared to WT controls. On the other hand, *Bok*$^{-/-}$ cells are resistant toward 5-FU treatment. Losing BOK seems to confer a selective advantage to CRC cells, and consequently, BOK expression levels are suggested to be useful as a prognostic marker in CRC and as a predictive marker for the efficacy of 5-FU treatment in CRC. While there is increasing evidence for a UPR-modulating role for BOK, the exact mechanism and possible interaction partners for UPR modulation and the ER stress response are still unknown.

BOK in maintaining Ca^{2+} homeostasis in response to excitotoxic stimulation has been described in neurons, and this phenotype was linked to a decreased protein stability of MCL-1 observed in the absence of BOK (D'Orsi et al., 2016). Importantly, Schulman et al. (2016) showed that BOK is stabilized when bound to IP3R and that its proapoptotic activity is thereby likely limited, whereas unbound ("free") BOK is rapidly degraded by the ubiquitin proteasome pathway. In consideration of the potent proapoptotic activity of BOK reported by Llambi et al. (2016), it can be argued that IP3Rs may act as a regulatory sink for BOK to keep the levels of unbound ("free") BOK low (**Figure 2**). Furthermore, Schulman et al. (2016) also identified an alternative start site for BOK at Met^{15}, resulting in a shorter protein that should not be mistaken for BOK's shorter isoform, BOK-S. Regulation and functional relevance of the resulting N-terminally truncated BOK protein is currently unknown and needs further investigation.

Recently, BOK was identified to interact with uridine monophosphate synthetase (UMPS) (**Figure 1**; Srivastava et al., 2019). UMPS, which in higher eukaryotes is a bifunctional enzyme consisting of the orotate phosphoribosyltransferase (OPRTase) and orotidine decarboxylase (ODCase) domains, is a central enzyme catalyzing the final steps in the *de novo* synthesis of orotate to uridine monophosphate (UMP) (Qumsiyeh et al., 1989). BOK binds to the ODCase domain at its dimer interface in a BH3-dependent manner (Srivastava et al., 2019). Intriguingly, it was found that, through this interaction, BOK increases the enzymatic activity of UMPS approximately threefold (Srivastava et al., 2019). As a consequence, cells lacking BOK have a defect in uridine metabolism, which affects crucial metabolic pathways including pyrimidine nucleotide synthesis, resulting in decreased cellular proliferation of *Bok*$^{-/-}$ cells compared with WT controls (Rabachini et al., 2018; Srivastava et al., 2019). On the other hand, loss of BOK confers resistance to 5-fluorouracil (5-FU)–induced apoptosis, as UMPS catalyzes the biotransformation of 5-FU into its active downstream metabolites. As discussed below, there are important implications of these findings for cancer biology, as colorectal cancer (CRC) cells may have a selective advantage from losing BOK expression (Srivastava et al., 2019). The study by Srivastava et al. provides the first link between BOK and uridine metabolism. Along that line, a connection from BOK to mitochondrial bioenergetics, fusion/fission and morphology has recently been reported also, further supporting apoptosis-independent roles of BOK (D'Orsi et al., 2016; Ausman et al., 2018; Schulman et al., 2019). Taken together, there is solid

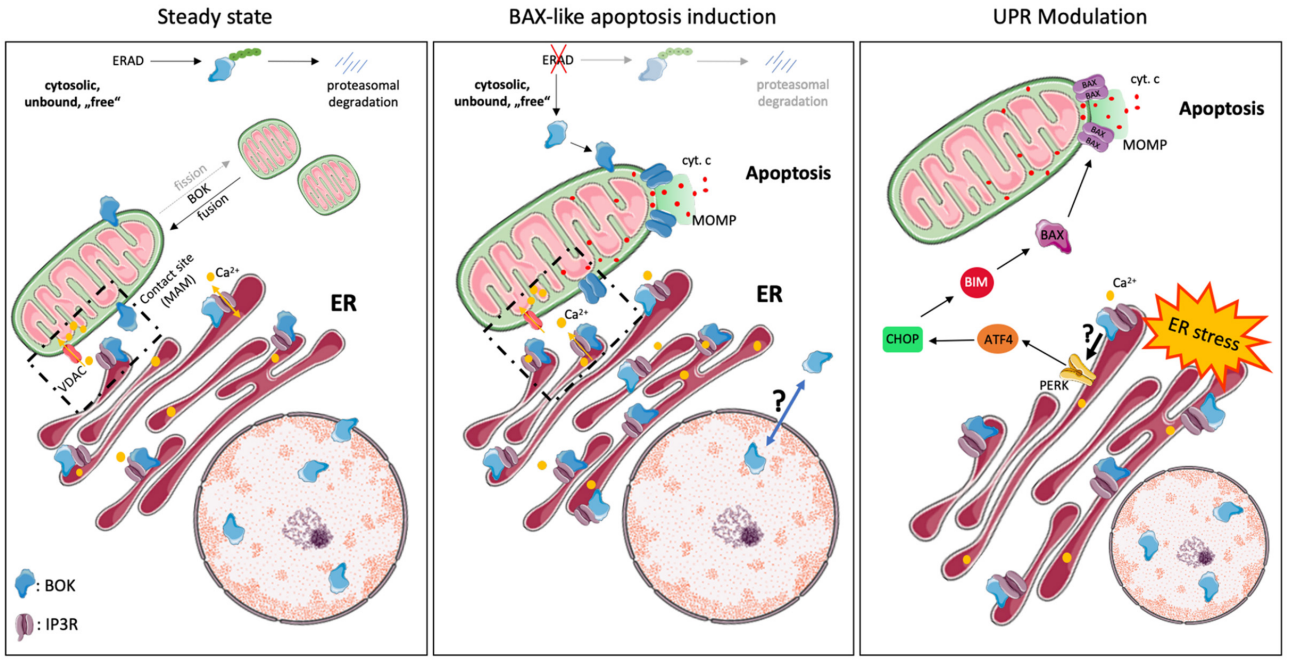

FIGURE 2 | Intracellular localization and cellular functions of BOK. BOK was described to exert various cellular functions at steady state and upon stress exposure, probably dependent on its various subcellular localizations. At steady state, the majority of BOK is bound to the ER, Golgi, and associated membranes. However, it can also be found within the nucleus, where its role is unclear, as well as on the MOM and ER-mitochondrial contact sites. ER-localized BOK is bound to IP3R and stabilizes the latter from caspase-3–mediated cleavage. IP3R-bound BOK, on the other hand, is stabilized from proteasomal turnover, as unbound, "free" BOK is ubiquitinated and degraded by the ERAD pathway. IP3R-bound BOK may thus not be available for mitochondrial apoptosis induction. No direct effect of BOK in altering Ca^{2+} mobilization by IP3Rs has been observed so far. Recently, BOK was found to be important for mitochondrial fission and morphology and thus to affect mitochondrial membrane potential. BOK has furthermore been described to exert a BAX-like killing function. Disturbance of components of the ERAD pathway thereby results in the stabilization of "free" BOK protein, which then directly induces MOMP and apoptosis in a BAX-like manner, independently of other BCL-2 family members. Under certain stress conditions, e.g., under hypoxia, BOK is upregulated and translocates from the nucleus into the cytoplasm and to mitochondrial membranes by a still unknown mechanism, where it may induce apoptosis. Increasing evidence points toward a UPR-modulating function by BOK, following ER stress, by a yet unknown mechanism. In that respect, BOK was described to regulate the PERK > ATF4 arm along with CHOP, which induces the BH3-only protein BIM (and PUMA). BIM directly activates BAX/BAK, leading to MOMP and subsequent apoptosis, suggesting an apoptosis-inducing role of BOK upstream of MOMP in that context.

evidence published for the interaction of BOK with IP3R1/-2, as well as with UMPS. Regarding the BCL-2 proteins, the best evidence for interaction is with MCL-1 (**Figure 1**).

VARIOUS MODELS OF BOK-INDUCED APOPTOSIS

The role and exact molecular function of BOK in apoptosis is still not fully understood. Since its discovery, BOK has been grouped together with BAX and BAK as "killer"; however, whether BOK induces MOMP in the absence of BAX or BAK and how relevant BOK-induced apoptosis is for (patho)physiology are currently controversially discussed. Earlier reports provided evidence that BOK induces intrinsic apoptosis, but these studies were restricted to transient overexpression and were performed in BAX/BAK-proficient cell lines (Hsu et al., 1997; Yakovlev et al., 2004; Rodriguez et al., 2006). Whereas it seems to be clear that high levels of BOK can induce apoptosis, two studies reported that cell death induced by overexpressed BOK is much reduced in $Bax^{-/-}Bak^{-/-}$ DKO cells (SV40-immortalized MEF, Hoxb8-immortalized growth factor–dependent myeloid progenitors) compared to WT controls (Echeverry et al., 2013; Carpio et al., 2015). These data implied that BOK may act upstream of BAX/BAK-mediated MOMP, which is in line with its predominant subcellular localization at the ER and its role in modulating ER stress responses (Echeverry et al., 2013; Carpio et al., 2015; Llambi et al., 2016). On the other hand, several studies reported that increased BOK levels are able to kill $Bax^{-/-}Bak^{-/-}$ DKO cells (HCT116, SV40 MEF) and to induce MOMP in the absence of BAX and BAK, implying a true BAX-like effector function of BOK at the MOM (**Figure 2**; Einsele-Scholz et al., 2016; Llambi et al., 2016; Zheng et al., 2018). While these latter reports are in strong support for BOK-induced MOMP, biophysical evidence for an oligomerization of BOK and direct pore formation in the MOM is currently missing. Of note, while recombinant forms of BOK readily permeabilized artificial membrane vesicles, in particular when their composition mimicked the MOM, it failed to do so on isolated mitochondria lacking BAX and BAK, even in the presence of the activator BH3-only protein tBID (Fernandez-Marrero et al., 2017). A possible alternative explanation was put forward by Llambi et al. (2016)

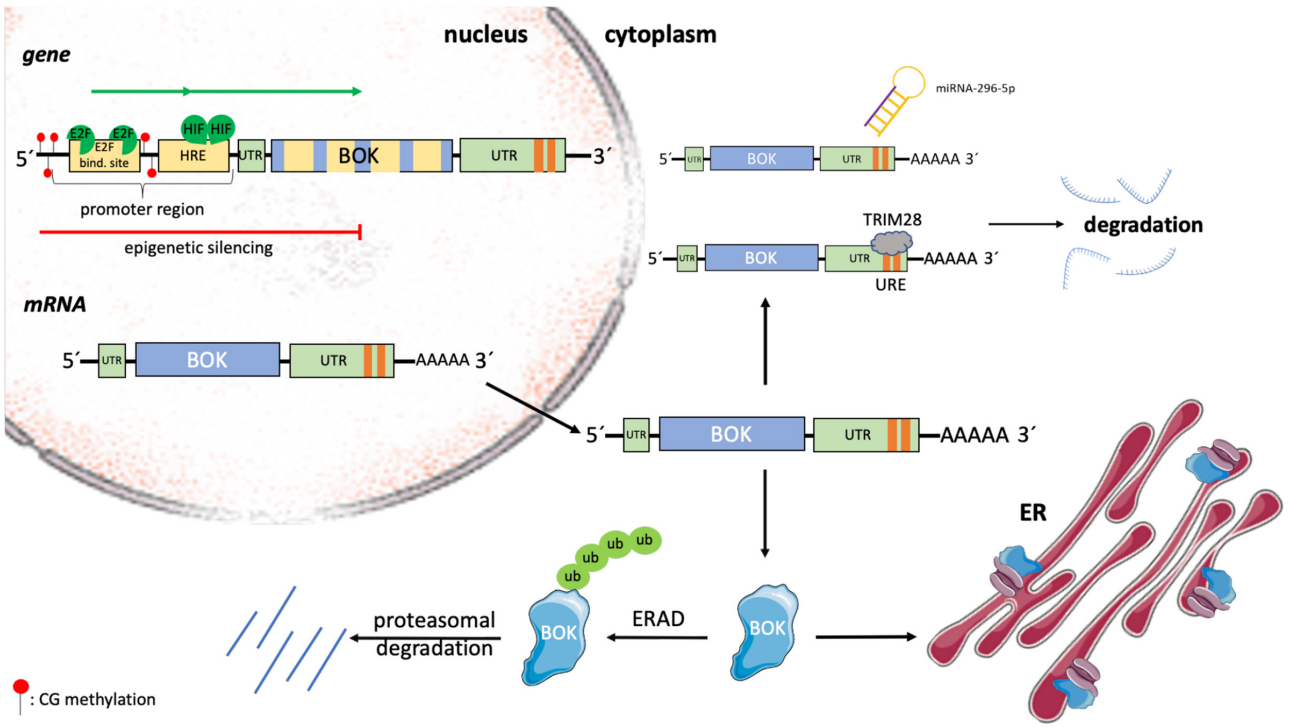

FIGURE 3 | Transcriptional and posttranslational regulation of BOK. The expression of BOK is regulated at transcriptional, epigenetic, translational, and posttranslational levels. In a variety of human cancers, the genomic region containing the BOK locus on chromosome 2 is deleted. Within its promoter region, BOK contains HREs, as well as a conserved E2F1-binding site. Upon binding by hypoxia-inducible factors (HIFs) and the cell cycle–regulating transcription factor E2F1, respectively, BOK transcription is induced. On the other hand, by means of promoter methylation, BOK can be epigenetically silenced. BOK comprises five exons. Alternative splicing leads to the development of the poorly understood BOK isoforms BOK-S and BOK-P. The expression of BOK is furthermore regulated at the level of mRNA stability. The miRNA miR-296-5p has been shown to bind to the 3' UTR of BOK mRNA, leading to its degradation. Moreover, strongly destabilizing (AU/U)–rich elements (one ARE site in mouse *Bok* mRNA, two URE sites in human *BOK* mRNA) were described in the 3' UTR of BOK. Tripartite motif containing 28 (TRIM28) was identified to bind to this region, leading to destabilization and subsequent degradation of human *BOK* mRNA. Once translated, BOK is mainly localized at ER membranes, where it is bound to IP3Rs. Unbound BOK is quickly turned over by the ERAD pathway, resulting in ubiquitin-proteasomal degradation.

and Zheng et al. (2018), who proposed a unique mechanism for BOK-induced MOMP, which is independent of interaction with tBID or other BCL-2 family members. Interestingly, this mechanism relies on an intrinsic instability of BOK (hydrophobic groove and helix α1), which results in its spontaneous association with mitochondria and MOMP, independent of the activation by BH3 ligands of other BCL-2 family members. Because of this model, BOK is expected to be a very potent inducer of MOMP and apoptosis, and thus, BOK levels need to be tightly controlled. One way to control BOK levels is through ER-associated degradation (ERAD), with a high turnover of BOK via ubiquitination and proteasomal degradation (**Figures 2**, **3**; Llambi et al., 2016). However, several reports have shown that many cell types or tissues can tolerate high levels of BOK protein (Ke et al., 2012; Moravcikova et al., 2017; Srivastava et al., 2019; Zhang et al., 2019), indicating that other posttranslational mechanisms are in place to control BOK activity and/or to sequester it away from mitochondria.

Whether loss of BOK protects cells from specific apoptotic stresses cannot be generalized and may be highly specific on the cell type or the nature of the apoptotic stress. Ke et al. (2012) showed that hematopoietic cells derived from *Bok*$^{-/-}$ mice are normally sensitive to dexamethasone, etoposide, FasL, or ABT-737–induced apoptosis. Likewise, various cell types, including MEF, were shown to respond normally to etoposide or staurosporine in the absence of BOK (Echeverry et al., 2013; Carpio et al., 2015; Fernandez-Marrero et al., 2016). On the other hand, however, Einsele-Scholz et al. (2016) reported that knocking down BOK leads to decreased drug-induced (taxol, cisplatin, camptothecin) cell death of ovarian carcinoma cells, OVCAR-3, OVCAR-4, and OVCAR-8. This seeming discrepancy in the involvement of BOK in response to DNA damaging agents may be explained by cell-intrinsic differences (e.g., amount of endogenous BOK, cancer cells vs. normal cells) and requires further investigation. However, what seems to be emerging is that BOK has important functions at the ER in response to ER stress (Echeverry et al., 2013; Carpio et al., 2015; Moravcikova et al., 2017). Carpio et al. (2015) described BOK as a promoter of cell death in SV40-immortalized MEF in response to various kinds of ER stress. The authors reported that BOK connects ER stress signaling to the intrinsic apoptotic machinery through modulating the UPR, in particular the PERK > ATF4 arm along with CHOP, which induces the BH3-only protein BIM (Carpio et al., 2015). Similarly, Kang et al. (2019) found decreased ATF4

and CHOP expression in erythrocytes derived from $Bok^{-/-}$ mice compared to WT mice, also suggesting a role for BOK in modulating the UPR in response to ER stress. In line with these findings, Rabachini et al. (2018) showed that chemical [diethylnitrosamine (DEN)]–induced upregulation of CHOP and BIM, and consequently hepatocellular apoptosis, is reduced in livers of $Bok^{-/-}$ mice. These studies are supportive of a proapoptotic role of BOK at the level of the ER and upstream of mitochondrial apoptotic events (**Figure 2**). It should also be mentioned that, in some instances, BOK has been attributed a protective or apoptosis-unrelated role in response to ER stress or other stressors and has also been shown to affect other arms of the UPR, namely, the IRE1α branch (Echeverry et al., 2013; D'Orsi et al., 2016). Taken together, based on the current literature, there is increasing evidence to put an important place of action of BOK at the ER membrane and it seems that—at the ER—BOK may be best described as a modulator of UPR signaling in response to ER stress (Carpio et al., 2016; Fernandez-Marrero et al., 2016). Whereas most of the previously described effects were derived from cell lines, the recent study by Ke et al. (2018) provides the up to now most convincing evidence for a relevant proapoptotic role of BOK *in vivo*. One key finding of that study was a more severe developmental phenotype in $Bax^{-/-}Bak^{-/-}Bok^{-/-}$ full-body TKO mice compared with $Bax^{-/-}Bak^{-/-}$ DKO controls, demonstrating overlapping roles of BOK with BAX and BAK during mouse embryogenesis.

REGULATION OF BOK EXPRESSION

Regulation of BOK expression in health and disease has been described at transcriptional, epigenetic, and posttranslational levels, but is overall only incompletely understood (**Figure 3**). Within the promoter of human and mouse BOK, a conserved E2F-binding site has been described (Rodriguez et al., 2006; Luo et al., 2014). Consequently, Rodriguez et al. (2006) described BOK to be cell cycle regulated by the transcription factor E2F1, which upon binding to the promoter activates transcription. E2F1 plays a crucial role in the control of the cell cycle but is not only involved in cellular proliferation but also regulates the expression of BH3-only proteins such as BIM and NOXA and furthermore mediates p53-dependent apoptosis (Hershko and Ginsberg, 2004; Zhang et al., 2020). In the model of Rodriguez et al., starvation followed by serum treatment, which stimulates quiescent cells to enter S phase, and overexpression of E2F1, respectively, led to an increase of *BOK* mRNA in H1299 cells (Rodriguez et al., 2006). In contrast to the above findings, Ha et al. (2001) found an increase in *BOK* mRNA upon serum starvation, rather than serum stimulation in HC11 mammary epithelial cells as well as in mouse mammary glands. Yet, the mechanism behind the observed BOK upregulation in this report has not been resolved. In all cases, however, the increase in BOK was correlated with an increase in apoptosis. But, while apoptosis induction in the mouse mammary gland was described as a physiological process after weaning, the increased induction of apoptosis in H1299 cells was observed only in response to an extrinsic stressor (Ha et al., 2001; Rodriguez et al., 2006). Within the *BOK* promoter region, Luo et al. (2014) described the presence of hypoxia response elements (HREs). Hypoxia-inducible factors play an important role in adapting the cellular metabolism in response to cellular stress caused by hypoxia (Vanderhaeghen et al., 2020) and were shown to bind to HRE in the promoter region of BOK, leading to an induction of BOK expression and increase in mitochondrial apoptosis (Soleymanlou et al., 2005, 2007; Luo et al., 2014). Furthermore, the expression of BOK, as well as of BAX, has been reported to be controlled by Wnt signaling in intestinal cancer (Zeilstra et al., 2011). Dysregulated Wnt signaling, which is frequently observed in sporadic CRC patients, was correlated with an increase in *BOK* and *BAX* mRNAs and accordingly with increased apoptotic activity (Zeilstra et al., 2011).

In a variety of human cancers, BOK is frequently found to be downregulated. Often, this downregulation can be associated with the deletion of the genomic region containing the BOK locus (Beroukhim et al., 2010). Moreover, epigenetic silencing by promoter methylation has been described in non–small cell lung carcinoma (NSCLC) (Moravcikova et al., 2017). In colorectal carcinoma tissue, in which BOK protein was also found to be decreased compared to matched healthy tissue, promoter hypomethylation rather than hypermethylation has been observed, thus excluding epigenetic downregulation in CRC (Carberry et al., 2018; Srivastava et al., 2019). Hence, so far, only little is known about the epigenetic regulation of the *BOK* gene.

At the level of mRNA stability and translation, *BOK* was found to be downregulated by binding of the miRNA miR-296-5p to its 3' UTR in breast cancer cells (Onyeagucha et al., 2017). Furthermore, destabilizing (AU/U)–rich elements [one AU-rich element (ARE) site in mouse *Bok*, two U-rich element (URE) sites in human *BOK*] were recently described in the 3' UTR of BOK (Fernandez-Marrero et al., 2018). In that study, the authors identified tripartite motif containing 28 (TRIM28), a large pleiotropic protein that is known for its many roles at the genomic level in the nucleus (Czerwinska et al., 2017), as a novel URE-binding protein triggering the degradation of human *BOK* mRNA (**Figure 3**; Fernandez-Marrero et al., 2018).

At the protein level, little is known about BOK activation or how possible changes in subcellular localization are regulated. BOK protein stability is regulated by ubiquitination and proteasomal degradation and may be cell type specific (Schulman et al., 2013, 2016; Llambi et al., 2016; Moravcikova et al., 2017; Sopha et al., 2017). Schulman et al. (2013, 2016) showed that major portions of cellular BOK are constitutively bound to IP3R and protected from degradation, whereas newly synthesized BOK is quickly degraded by the ubiquitin–proteasome pathway. More specifically, BOK is rapidly turned over by the ERAD components AMFR/gp78, by which BOK is ubiquitylated, and VCP/p97, a complex that processes ubiquitylated BOK further for proteasomal degradation. Upon inhibition of ERAD, or of proteasome activity, BOK protein gets stabilized and induces MOMP (Llambi et al., 2016). Whether and how BOK translocates from the ER to mitochondria are not known. One possibility is that BOK is already present at mitochondria–ER contact sites, such as mitochondria-associated membranes (MAM), which

again needs further investigation (**Figure 2**; Giacomello and Pellegrini, 2016).

ROLE OF BOK IN PATHOPHYSIOLOGY AND CANCER

There is increasing evidence pointing toward BOK as a prognostic or predictive marker in cancer. Interestingly, the genomic region containing BOK was identified to be relatively frequently deleted across many types of human cancers (Beroukhim et al., 2010). Given the evidence for a proapoptotic role of BOK, this finding could hint toward a tumor suppressor–like activity of BOK. However, the peak region of the genomic deletion in question contains 18 other genes (Beroukhim et al., 2010) and hard evidence that BOK is indeed a tumor suppressor is currently missing. Nevertheless, the finding that BOK is one of the most frequently deleted genes among the proapoptotic family members was unexpected and merits further investigation. Besides loss of BOK through somatic copy-number variations, epigenetic repression of BOK expression was proposed from studies in NSCLC cell lines (Moravcikova et al., 2017). Here, analysis of primary NSCLC patient samples revealed that BOK protein levels are reduced in NSCLC tumors compared with matched healthy lung tissue. Importantly, in poorly differentiated tumors, as well as in tumors of patients with lymph node infiltrations and metastases, BOK protein was even further decreased. For those patients, a weak positive correlation between BOK protein and overall survival was identified. Hence, these data do support a tumor-suppressing action of BOK and suggest that BOK protein levels may be useful as a prognostic marker in late-stage NCSLC patients (Moravcikova et al., 2017). Of note, that study also provided evidence that BOK does not directly induce apoptosis or affect apoptotic responses toward chemotherapeutic drugs, but rather that high BOK levels antagonize transforming growth factor β–induced epithelial-to-mesenchymal transition and may thus slow down malignant transformation (metastasization) of NSCLC. Mechanistically, it was suggested that this function is mediated via the modulation of the PERK > ATF4 arm of the UPR, a function of BOK first described by Carpio and colleagues (Carpio et al., 2015; Moravcikova et al., 2017). In line with this, Kang et al. (2019) described BOK to be important for erythropoiesis in the context of Nup98-HoxD13 (NHD13)–driven myelodysplastic syndrome. In this study, the induction of ATF4 and CHOP was significantly reduced in erythrocytes derived from $Bok^{-/-}$ mice compared to WT mice. While erythropoiesis in $Bok^{-/-}$ mice was not affected compared to WT mice, NHD13 transgenic mice showed reduced BFU-E (blast-forming units–erythroid) colonies and a progressive anemia when BOK was lost (Kang et al., 2019). It was concluded that BOK contributes to erythropoiesis under stress conditions, probably via modulation of the ATF4 pathway (**Table 1**; Kang et al., 2019).

BOK mRNA stability is negatively regulated by the presence of one ARE in the mouse and two URE in the human 3' UTR (Fernandez-Marrero et al., 2018). TRIM28 was identified as one of the factors binding to the UREs in human *BOK* mRNA, leading to its degradation. TRIM28 is overexpressed in various cancers in which it is associated with poor prognosis (Czerwinska et al., 2017). Of note, TRIM28 and BOK levels were found to be negatively correlated in selected cancers such as hepatocellular carcinoma and kidney cancer. In those cancers, high *BOK* and low *TRIM28* mRNA levels correlated with increased survival, and low *BOK* and high *TRIM28* levels with decreased survival (Fernandez-Marrero et al., 2018). Translational silencing of *BOK* mRNA by miRNA miR-296-5p was reported by Onyeagucha et al. (2017) in human breast cancer cell lines. This study also describes an miR-296-5p–mediated regulatory feedback loop between *MCL-1* and *BOK* levels that determines whether the breast cancer cells die by apoptosis or survive. Like in NSCLC, BOK protein levels were again found to be significantly lower in tumor tissue compared to matched normal tissue, and higher BOK expression positively correlated with overall as well as with relapse-free survival of breast cancer patients (Onyeagucha et al., 2017).

Besides NSCLC and breast cancer, BOK has been shown to be downregulated in CRC and to be of potential prognostic and predictive value, respectively (Carberry et al., 2018; Srivastava et al., 2019). Srivastava et al. (2019) reported increased resistance of BOK-deficient CRC cells and MEFs toward 5-FU and showed that CRC cells lose BOK expression when becoming resistant to 5-FU. Mechanistically, that study showed that BOK directly interacts and thereby activates the enzymatic activity of UMPS and provided the first connection of BOK to uridine and nucleotide metabolism (Srivastava et al., 2019). UMPS is a central enzyme in both the conversion of 5-FU into its active metabolites, as well as in the *de novo* synthesis of UMP and hence pyrimidine nucleotides. A consequence of the latter was that BOK-deficient cells show a proliferation defect that is likely caused by an increase in p53 activity at steady state. Importantly, this growth defect of $BOK^{-/-}$ cells could be rescued by reintroduction of WT BOK, but not of a BOK mutant that fails to interact with UMPS (Srivastava et al., 2019). Overall, this study identified BOK as a double-edged sword in CRC. On the one hand, 5-FU–treated CRC cells acquire a selective advantage by losing BOK; on the other hand, this advantage costs them proliferative potential. The latter may put selective pressure on the BOK-deficient cells to lose cell cycle inhibitors and/or p53 activity, eventually resulting in a faster-growing and likely more aggressive phenotype. BOK is therefore suggested to serve as a predictive marker in CRC, and the authors proposed to explore the potential of BOK-mimetic compounds to sensitize resistant CRC to 5-FU treatment (Srivastava et al., 2019). The observation by Carberry et al. (2018) that high BOK levels in CRC surprisingly correlate with reduced overall survival may be dependent on the time of biopsy (tumor stage) and could possibly be explained by the decreased proliferation of BOK-deficient, yet still p53 proficient, tumors.

The role of BOK in affecting cellular proliferation, cancer development, and progression was also reported in a chemical-induced hepatocellular carcinoma model in the mouse (Rabachini et al., 2018). The carcinogen DEN triggers acute hepatic injury and a subsequent inflammatory response that is followed by compensatory hepatocyte proliferation. Regarding the acute phase, livers from $Bok^{-/-}$ mice were shown to

be protected from hepatocellular apoptosis induced by DEN through induction of CHOP, BIM, and PUMA (Rabachini et al., 2018). These data provided evidence for a proapoptotic role of BOK in a pathophysiologically relevant setting, whereas it suggested at the same time an "indirect" killing mechanism, with BOK inducing cell death upstream of CHOP and BH3-only proteins, and thus likely upstream of MOMP. Because of the protection during the acute phase, $Bok^{-/-}$ mice developed fewer tumors at the endpoint of 9 months. Of note, the tumors in $Bok^{-/-}$ mice were also smaller and showed a reduced proliferative index. Furthermore, BOK-deficient HCC cells and MEF proliferated slower compared to BOK proficient cells, which is in line with the growth defect reported in the study of Srivastava et al. (2019) and others (Ray et al., 2010; Moravcikova et al., 2017; Zhang et al., 2019).

Besides cancer, BOK expression and regulation have been connected with preeclampsia, a placental disease that may occur during pregnancies and that is characterized by a reduced oxygenation of trophoblast cells, increased trophoblast cell death, and trophoblast hyperproliferation (Chaiworapongsa et al., 2014). The Caniggia laboratory reported physiological BOK expression in proliferating trophoblast cells that is further increased in preeclampsia, where it contributes to the hyperproliferative state of the trophoblasts (Ray et al., 2010). Of note, in this context, it seems that nuclear localized BOK is important for cellular proliferation of trophoblast cells during placental development, while cytoplasmic BOK induces cell death (Ray et al., 2010). Moreover, in patients suffering from preeclampsia, a splice variant of BOK, BOK-P, was described (Soleymanlou et al., 2005; Ray et al., 2010). BOK-P results from skipping exon 2 (Soleymanlou et al., 2005), which contains the first of the two existing ATG start codons within the human *BOK* gene (a second start codon is localized within human, but not mouse, exon 3). The resulting BOK isoform lacks the BH4 and parts of the BH3 domain, as well as parts of the 5' UTR (Soleymanlou et al., 2005). Apart from cellular proliferation (Ray et al., 2010) and apoptosis induction (Soleymanlou et al., 2005), several observations point toward an autophagy regulating role of BOK in preeclampsia (Kalkat et al., 2013; Melland-Smith et al., 2015; Ausman et al., 2018). In this setting, upregulation of BOK due to hypoxic conditions (Kalkat et al., 2013) or due to ceramide accumulation within the mitochondria (Melland-Smith et al., 2015; Ausman et al., 2018) leads to an increase in autophagic flux (Kalkat et al., 2013; Melland-Smith et al., 2015; Ausman et al., 2018). The involvement of BOK in autophagy regulation can be explained by the observation that BOK disrupts the interaction between MCL-1 and Beclin-1, which ultimately leads to the induction of autophagy (Kalkat et al., 2013). Beclin-1 has been described to interact with different antiapoptotic members of the BCL-2 family of proteins via its BH3 domain, namely, with MCL-1, BCL-2, and BCL-XL (Marino et al., 2014). These interactions can be disrupted by several BH3-only proteins of the Bcl-2 family–like NOXA and PUMA (Marino et al., 2014) and supposedly also by BOK (Kalkat et al., 2013), leading to an increase in freely available Beclin-1 and subsequent autophagy induction (Kalkat et al., 2013; Marino et al., 2014). However, the model that the interaction of different BCL-2 family members with Beclin-1 is sufficient to regulate autophagy under physiological conditions has been challenged (Lindqvist et al., 2014). Lindqvist et al. (2014) proposed that endogenous levels of the BCL-2 family proteins are not able to directly influence autophagy, since the binding of Beclin-1 with the BH3 domain of different BCL-2 family members is rather weak and thus insufficient to lead to the sequestration of Beclin-1. They concluded that the impact of the BCL-2 family on autophagy is indirect through BAX and BAK inhibition by prosurvival BCL-2 family members rather than direct through effects on Beclin-1 (Lindqvist et al., 2014). In their model, the inhibition of BAX/BAK and the resulting inhibition of apoptosis lead to the activation of autophagy by a yet unknown mechanism (Lindqvist et al., 2014). Nevertheless, given that several other groups ascribe a role of various members of the BCL-2 family not only to apoptosis but also to autophagy induction and repression, respectively, it seems likely that BOK may likewise play a role in the regulation of autophagy initiation. Whether this regulation is important under physiological or only under pathophysiological conditions needs further investigation.

CONCLUSION

Over the last years, various functions have been described for BOK. However, its main function (or functions) remains elusive, and there are still many riddles to be answered. What exactly is its role in apoptosis? Does the function of BOK depend on the intracellular organelle it localizes to, i.e., does it exert different functions at the ER membrane, mitochondrion, or in the nucleus, respectively? What is its role in cancer progression, and why do many types of human cancer lose BOK expression? Does it act as tumor suppressor and, if so, in which cancer subtypes and by what mechanism? Currently, a lot of discordance on BOK and its function can be found in the literature, which makes it difficult to fully grasp the key roles of this protein. In part, this problem may be explained by different cellular systems, mouse models, and different disease settings that have been used by different groups. It, however, also indicates that—more than 20 years after its discovery—there remain lots of open questions and work to be done to understand this fascinating and multifaceted member of the BCL-2 family.

AUTHOR CONTRIBUTIONS

TK and SN wrote the manuscript.

FUNDING

TK is supported the Swiss National Science Foundation (#31003A_173006). SN is supported by the Graduate School of Cellular and Biomedical Sciences of the University of Bern. Cartoon Figures were created using modified graphical elements provided by smart Servier Medical Art (https://smart.servier.com).

REFERENCES

Adams, J. M., and Cory, S. (2018). The BCL-2 arbiters of apoptosis and their growing role as cancer targets. *Cell Death Differ.* 25, 27–36. doi: 10.1038/cdd.2017.161

Ausman, J., Abbade, J., Ermini, L., Farrell, A., Tagliaferro, A., Post, M., et al. (2018). Ceramide-induced BOK promotes mitochondrial fission in preeclampsia. *Cell Death Dis.* 9:298.

Bartholomeusz, G., Wu, Y., Ali Seyed, M., Xia, W., Kwong, K. Y., Hortobagyi, G., et al. (2006). Nuclear translocation of the pro-apoptotic Bcl-2 family member Bok induces apoptosis. *Mol. Carcinog.* 45, 73–83. doi: 10.1002/mc.20156

Beroukhim, R., Mermel, C. H., Porter, D., Wei, G., Raychaudhuri, S., Donovan, J., et al. (2010). The landscape of somatic copy-number alteration across human cancers. *Nature* 463, 899–905.

Borgese, N., and Fasana, E. (2011). Targeting pathways of C-tail-anchored proteins. *Biochim. Biophys. Acta* 1808, 937–946. doi: 10.1016/j.bbamem.2010.07.010

Brown, C. Y., Bowers, S. J., Loring, G., Heberden, C., Lee, R. M., and Neiman, P. E. (2004). Role of Mtd/Bok in normal and neoplastic B-cell development in the bursa of *Fabricius*. *Dev. Comp. Immunol.* 28, 619–634. doi: 10.1016/j.dci.2003.09.017

Campbell, K. J., and Tait, S. W. G. (2018). Targeting BCL-2 regulated apoptosis in cancer. *Open Biol.* 8:180002. doi: 10.1098/rsob.180002

Carberry, S., D'orsi, B., Monsefi, N., Salvucci, M., Bacon, O., Fay, J., et al. (2018). The BAX/BAK-like protein BOK is a prognostic marker in colorectal cancer. *Cell Death Dis.* 9:125.

Carpio, M. A., Michaud, M., Zhou, W., Fisher, J. K., Walensky, L. D., and Katz, S. G. (2015). BCL-2 family member BOK promotes apoptosis in response to endoplasmic reticulum stress. *Proc. Natl. Acad. Sci. U.S.A.* 112, 7201–7206. doi: 10.1073/pnas.1421063112

Carpio, M. A., Michaud, M., Zhou, W., Fisher, J. K., Walensky, L. D., and Katz, S. G. (2016). Reply to Fernandez-Marrero et al.: role of BOK at the intersection of endoplasmic reticulum stress and apoptosis regulation. *Proc. Natl. Acad. Sci. U.S.A.* 113, E494–E495.

Chaiworapongsa, T., Chaemsaithong, P., Yeo, L., and Romero, R. (2014). Pre-eclampsia part 1: current understanding of its pathophysiology. *Nat. Rev. Nephrol.* 10, 466–480. doi: 10.1038/nrneph.2014.102

Cosentino, K., and Garcia-Saez, A. J. (2017). Bax and bak pores: are we closing the circle? *Trends Cell Biol.* 27, 266–275. doi: 10.1016/j.tcb.2016.11.004

Czerwinska, P., Mazurek, S., and Wiznerowicz, M. (2017). The complexity of TRIM28 contribution to cancer. *J. Biomed. Sci.* 24:63.

D'Orsi, B., Engel, T., Pfeiffer, S., Nandi, S., Kaufmann, T., Henshall, D. C., et al. (2016). Bok is not pro-apoptotic but suppresses poly ADP-ribose polymerase-dependent cell death pathways and protects against excitotoxic and seizure-induced neuronal injury. *J. Neurosci.* 36, 4564–4578. doi: 10.1523/jneurosci.3780-15.2016

D'Orsi, B., Mateyka, J., and Prehn, J. H. M. (2017). Control of mitochondrial physiology and cell death by the Bcl-2 family proteins Bax and Bok. *Neurochem. Int.* 109, 162–170. doi: 10.1016/j.neuint.2017.03.010

Echeverry, N., Bachmann, D., Ke, F., Strasser, A., Simon, H. U., and Kaufmann, T. (2013). Intracellular localization of the BCL-2 family member BOK and functional implications. *Cell Death Differ.* 20, 785–799. doi: 10.1038/cdd.2013.10

Einsele-Scholz, S., Malmsheimer, S., Bertram, K., Stehle, D., Johanning, J., Manz, M., et al. (2016). Bok is a genuine multi-BH-domain protein that triggers apoptosis in the absence of Bax and Bak. *J. Cell Sci.* 129:3054. doi: 10.1242/jcs.193946

Favaloro, B., Allocati, N., Graziano, V., Di Ilio, C., and De Laurenzi, V. (2012). Role of apoptosis in disease. *Aging* 4, 330–349.

Fernandez-Marrero, Y., Bachmann, D., Lauber, E., and Kaufmann, T. (2018). Negative Regulation of BOK expression by recruitment of TRIM28 to regulatory elements in Its 3' untranslated region. *iScience* 9, 461–474. doi: 10.1016/j.isci.2018.11.005

Fernandez-Marrero, Y., Bleicken, S., Das, K. K., Bachmann, D., Kaufmann, T., and Garcia-Saez, A. J. (2017). The membrane activity of BOK involves formation of large, stable toroidal pores and is promoted by cBID. *FEBS J.* 284, 711–724. doi: 10.1111/febs.14008

Fernandez-Marrero, Y., Ke, F., Echeverry, N., Bouillet, P., Bachmann, D., Strasser, A., et al. (2016). Is BOK required for apoptosis induced by endoplasmic reticulum stress? *Proc. Natl. Acad. Sci. U.S.A.* 113, E492–E493.

Ghavami, S., Shojaei, S., Yeganeh, B., Ande, S. R., Jangamreddy, J. R., Mehrpour, M., et al. (2014). Autophagy and apoptosis dysfunction in neurodegenerative disorders. *Prog. Neurobiol.* 112, 24–49.

Giacomello, M., and Pellegrini, L. (2016). The coming of age of the mitochondria-ER contact: a matter of thickness. *Cell Death Differ.* 23, 1417–1427. doi: 10.1038/cdd.2016.52

Gross, A., and Katz, S. G. (2017). Non-apoptotic functions of BCL-2 family proteins. *Cell Death Differ.* 24, 1348–1358. doi: 10.1038/cdd.2017.22

Ha, S. H., Lee, S. R., Lee, T. H., Kim, Y. M., Baik, M. G., and Choi, Y. J. (2001). The expression of Bok is regulated by serum in HC11 mammary epithelial cells. *Mol Cells* 12, 368–371.

Hershko, T., and Ginsberg, D. (2004). Up-regulation of Bcl-2 homology 3 (BH3)-only proteins by E2F1 mediates apoptosis. *J. Biol. Chem.* 279, 8627–8634. doi: 10.1074/jbc.m312866200

Hsu, S. Y., Kaipia, A., Mcgee, E., Lomeli, M., and Hsueh, A. J. (1997). Bok is a pro-apoptotic Bcl-2 protein with restricted expression in reproductive tissues and heterodimerizes with selective anti-apoptotic Bcl-2 family members. *Proc. Natl. Acad. Sci. U.S.A.* 94, 12401–12406. doi: 10.1073/pnas.94.23.12401

Inohara, N., Ekhterae, D., Garcia, I., Carrio, R., Merino, J., Merry, A., et al. (1998). Mtd, a novel Bcl-2 family member activates apoptosis in the absence of heterodimerization with Bcl-2 and Bcl-XL. *J. Biol. Chem.* 273, 8705–8710. doi: 10.1074/jbc.273.15.8705

Jaaskelainen, M., Nieminen, A., Pokkyla, R. M., Kauppinen, M., Liakka, A., Heikinheimo, M., et al. (2010). Regulation of cell death in human fetal and adult ovaries–role of Bok and Bcl-X(L). *Mol. Cell Endocrinol.* 330, 17–24. doi: 10.1016/j.mce.2010.07.020

Julien, O., and Wells, J. A. (2017). Caspases and their substrates. *Cell Death Differ.* 24, 1380–1389. doi: 10.1038/cdd.2017.44

Kale, J., Osterlund, E. J., and Andrews, D. W. (2018). BCL-2 family proteins: changing partners in the dance towards death. *Cell Death Differ.* 25, 65–80. doi: 10.1038/cdd.2017.186

Kalkat, M., Garcia, J., Ebrahimi, J., Melland-Smith, M., Todros, T., Post, M., et al. (2013). Placental autophagy regulation by the BOK-MCL1 rheostat. *Autophagy* 9, 2140–2153. doi: 10.4161/auto.26452

Kang, S. H., Perales, O., Michaud, M., and Katz, S. G. (2019). BOK promotes erythropoiesis in a mouse model of myelodysplastic syndrome. *Ann. Hematol.* 98, 2089–2096. doi: 10.1007/s00277-019-03726-7

Ke, F., Bouillet, P., Kaufmann, T., Strasser, A., Kerr, J., and Voss, A. K. (2013). Consequences of the combined loss of BOK and BAK or BOK and BAX. *Cell Death Dis.* 4:e650. doi: 10.1038/cddis.2013.176

Ke, F., Grabow, S., Kelly, G. L., Lin, A., O'reilly, L. A., and Strasser, A. (2015). Impact of the combined loss of BOK, BAX and BAK on the hematopoietic system is slightly more severe than compound loss of BAX and BAK. *Cell Death Dis.* 6:e1938. doi: 10.1038/cddis.2015.304

Ke, F., Voss, A., Kerr, J. B., O'reilly, L. A., Tai, L., Echeverry, N., et al. (2012). BCL-2 family member BOK is widely expressed but its loss has only minimal impact in mice. *Cell Death Differ.* 19, 915–925. doi: 10.1038/cdd.2011.210

Ke, F. F. S., Vanyai, H. K., Cowan, A. D., Delbridge, A. R. D., Whitehead, L., Grabow, S., et al. (2018). Embryogenesis and adult life in the absence of intrinsic apoptosis effectors BAX, BAK, and BOK. *Cell* 173, 1217–1230. doi: 10.1016/j.cell.2018.04.036

Knudson, C. M., Tung, K. S., Tourtellotte, W. G., Brown, G. A., and Korsmeyer, S. J. (1995). Bax-deficient mice with lymphoid hyperplasia and male germ cell death. *Science* 270, 96–99. doi: 10.1126/science.270.5233.96

Lindqvist, L. M., Heinlein, M., Huang, D. C., and Vaux, D. L. (2014). Prosurvival Bcl-2 family members affect autophagy only indirectly, by inhibiting Bax and Bak. *Proc. Natl. Acad. Sci. U.S.A.* 111, 8512–8517. doi: 10.1073/pnas.1406425111

Lindsay, J., Esposti, M. D., and Gilmore, A. P. (2011). Bcl-2 proteins and mitochondria–specificity in membrane targeting for death. *Biochim. Biophys. Acta* 1813, 532–539. doi: 10.1016/j.bbamcr.2010.10.017

Lindsten, T., Ross, A. J., King, A., Zong, W. X., Rathmell, J. C., Shiels, H. A., et al. (2000). The combined functions of proapoptotic Bcl-2 family members bak and bax are essential for normal development of multiple tissues. *Mol. Cell* 6, 1389–1399. doi: 10.1016/s1097-2765(00)00136-2

Llambi, F., Wang, Y. M., Victor, B., Yang, M., Schneider, D. M., Gingras, S., et al. (2016). BOK is a non-canonical BCL-2 family effector of apoptosis regulated by ER-associated degradation. *Cell* 165, 421–433. doi: 10.1016/j.cell.2016.02.026

Lopez, J., and Tait, S. W. (2015). Mitochondrial apoptosis: killing cancer using the enemy within. *Br. J. Cancer* 112, 957–962. doi: 10.1038/bjc.2015.85

Luo, D., Caniggia, I., and Post, M. (2014). Hypoxia-inducible regulation of placental BOK expression. *Biochem. J.* 461, 391–402. doi: 10.1042/bj20140066

Marino, G., Niso-Santano, M., Baehrecke, E. H., and Kroemer, G. (2014). Self-consumption: the interplay of autophagy and apoptosis. *Nat. Rev. Mol. Cell Biol.* 15, 81–94. doi: 10.1038/nrm3735

Mason, K. D., Lin, A., Robb, L., Josefsson, E. C., Henley, K. J., Gray, D. H., et al. (2013). Proapoptotic Bak and Bax guard against fatal systemic and organ-specific autoimmune disease. *Proc. Natl. Acad. Sci. U.S.A.* 110, 2599–2604. doi: 10.1073/pnas.1215097110

Mattson, M. P. (2000). Apoptosis in neurodegenerative disorders. *Nat. Rev. Mol. Cell Biol.* 1, 120–129.

Mcilwain, D. R., Berger, T., and Mak, T. W. (2013). Caspase functions in cell death and disease. *Cold Spring Harb. Perspect. Biol.* 5:a008656.

Melland-Smith, M., Ermini, L., Chauvin, S., Craig-Barnes, H., Tagliaferro, A., Todros, T., et al. (2015). Disruption of sphingolipid metabolism augments ceramide-induced autophagy in preeclampsia. *Autophagy* 11, 653–669. doi: 10.1080/15548627.2015.1034414

Moldoveanu, T., and Zheng, J. H. (2018). Metastability, an emerging concept governing BOK-mediated apoptosis initiation. *Oncotarget* 9, 30944–30945. doi: 10.18632/oncotarget.25801

Montero, J., and Letai, A. (2018). Why do BCL-2 inhibitors work and where should we use them in the clinic? *Cell Death Differ.* 25, 56–64. doi: 10.1038/cdd.2017.183

Moravcikova, E., Krepela, E., Donnenberg, V. S., Donnenberg, A. D., Benkova, K., Rabachini, T., et al. (2017). BOK displays cell death-independent tumor suppressor activity in non-small-cell lung carcinoma. *Int. J. Cancer* 141, 2050–2061. doi: 10.1002/ijc.30906

Onyeagucha, B., Subbarayalu, P., Abdelfattah, N., Rajamanickam, S., Timilsina, S., Guzman, R., et al. (2017). Novel post-transcriptional and post-translational regulation of pro-apoptotic protein BOK and anti-apoptotic protein Mcl-1 determine the fate of breast cancer cells to survive or die. *Oncotarget* 8, 85984–85996. doi: 10.18632/oncotarget.20841

Qumsiyeh, M. B., Valentine, M. B., and Suttle, D. P. (1989). Localization of the gene for uridine monophosphate synthase to human chromosome region 3q13 by in situ hybridization. *Genomics* 5, 160–162. doi: 10.1016/0888-7543(89)90103-1

Rabachini, T., Fernandez-Marrero, Y., Montani, M., Loforese, G., Sladky, V., He, Z., et al. (2018). BOK promotes chemical-induced hepatocarcinogenesis in mice. *Cell Death Differ.* 25, 708–720. doi: 10.1038/s41418-017-0008-0

Ray, J. E., Garcia, J., Jurisicova, A., and Caniggia, I. (2010). Mtd/Bok takes a swing: proapoptotic Mtd/Bok regulates trophoblast cell proliferation during human placental development and in preeclampsia. *Cell Death Differ.* 17, 846–859. doi: 10.1038/cdd.2009.167

Reed, J. C. (2006). Drug insight: cancer therapy strategies based on restoration of endogenous cell death mechanisms. *Nat. Clin. Pract. Oncol.* 3, 388–398. doi: 10.1038/ncponc0538

Rodriguez, J. M., Glozak, M. A., Ma, Y., and Cress, W. D. (2006). Bok, Bcl-2-related ovarian killer, is cell cycle-regulated and sensitizes to stress-induced *Apoptosis*. *J. Biol. Chem.* 281, 22729–22735. doi: 10.1074/jbc.m604705200

Schinzel, A., Kaufmann, T., and Borner, C. (2004). Bcl-2 family members: integrators of survival and death signals in physiology and pathology [corrected]. *Biochim. Biophys. Acta* 1644, 95–105.

Schulman, J. J., Szczesniak, L. M., Bunker, E. N., Nelson, H. A., Roe, M. W., Wagner, L. E., et al. (2019). Bok regulates mitochondrial fusion and morphology. *Cell Death Differ.* 26, 2682–2694. doi: 10.1038/s41418-019-0327-4

Schulman, J. J., Wright, F. A., Han, X., Zluhan, E. J., Szczesniak, L. M., and Wojcikiewicz, R. J. (2016). The stability and expression level of Bok are governed by binding to inositol 1,4,5-trisphosphate receptors. *J. Biol. Chem.* 291, 11820–11828. doi: 10.1074/jbc.m115.711242

Schulman, J. J., Wright, F. A., Kaufmann, T., and Wojcikiewicz, R. J. (2013). The Bcl-2 protein family member Bok binds to the coupling domain of inositol 1,4,5-trisphosphate receptors and protects them from proteolytic cleavage. *J. Biol. Chem.* 288, 25340–25349. doi: 10.1074/jbc.m113.496570

Shi, Y. (2004). Caspase activation, inhibition, and reactivation: a mechanistic view. *Protein Sci.* 13, 1979–1987. doi: 10.1110/ps.04789804

Singh, R., Letai, A., and Sarosiek, K. (2019). Regulation of apoptosis in health and disease: the balancing act of BCL-2 family proteins. *Nat. Rev. Mol. Cell Biol.* 20, 175–193. doi: 10.1038/s41580-018-0089-8

Soleymanlou, N., Jurisicova, A., Wu, Y., Chijiiwa, M., Ray, J. E., Detmar, J., et al. (2007). Hypoxic switch in mitochondrial myeloid cell leukemia factor-1/Mtd apoptotic rheostat contributes to human trophoblast cell death in preeclampsia. *Am. J. Pathol.* 171, 496–506. doi: 10.2353/ajpath.2007.070094

Soleymanlou, N., Wu, Y., Wang, J. X., Todros, T., Ietta, F., Jurisicova, A., et al. (2005). A novel Mtd splice isoform is responsible for trophoblast cell death in pre-eclampsia. *Cell Death Differ.* 12, 441–452. doi: 10.1038/sj.cdd.4401593

Sopha, P., Ren, H. Y., Grove, D. E., and Cyr, D. M. (2017). Endoplasmic reticulum stress-induced degradation of DNAJB12 stimulates BOK accumulation and primes cancer cells for apoptosis. *J. Biol. Chem.* 292, 11792–11803. doi: 10.1074/jbc.m117.785113

Srivastava, R., Cao, Z., Nedeva, C., Naim, S., Bachmann, D., Rabachini, T., et al. (2019). BCL-2 family protein BOK is a positive regulator of uridine metabolism in mammals. *Proc. Natl. Acad. Sci. U.S.A.* 116, 15469–15474. doi: 10.1073/pnas.1904523116

Timucin, A. C., Basaga, H., and Kutuk, O. (2019). Selective targeting of antiapoptotic BCL-2 proteins in cancer. *Med. Res. Rev.* 39, 146–175. doi: 10.1002/med.21516

Todt, F., Cakir, Z., Reichenbach, F., Emschermann, F., Lauterwasser, J., Kaiser, A., et al. (2015). Differential retrotranslocation of mitochondrial Bax and Bak. *EMBO J.* 34, 67–80. doi: 10.15252/embj.201488806

Van Opdenbosch, N., and Lamkanfi, M. (2019). Caspases in cell death, inflammation, and disease. *Immunity* 50, 1352–1364. doi: 10.1016/j.immuni.2019.05.020

Vanderhaeghen, T., Vandewalle, J., and Libert, C. (2020). Hypoxia-inducible factors in metabolic reprogramming during sepsis. *FEBS J.* 287, 1478–1495. doi: 10.1111/febs.15222

Wilfling, F., Weber, A., Potthoff, S., Vogtle, F. N., Meisinger, C., Paschen, S. A., et al. (2012). BH3-only proteins are tail-anchored in the outer mitochondrial membrane and can initiate the activation of Bax. *Cell Death Differ.* 19, 1328–1336. doi: 10.1038/cdd.2012.9

Wolter, K. G., Hsu, Y. T., Smith, C. L., Nechushtan, A., Xi, X. G., and Youle, R. J. (1997). Movement of Bax from the cytosol to mitochondria during apoptosis. *J. Cell Biol.* 139, 1281–1292. doi: 10.1083/jcb.139.5.1281

Yakovlev, A. G., Di Giovanni, S., Wang, G., Liu, W., Stoica, B., and Faden, A. I. (2004). BOK and NOXA are essential mediators of p53-dependent apoptosis. *J. Biol. Chem.* 279, 28367–28374. doi: 10.1074/jbc.m313526200

Zeilstra, J., Joosten, S. P., Wensveen, F. M., Dessing, M. C., Schutze, D. M., Eldering, E., et al. (2011). WNT signaling controls expression of pro-apoptotic BOK and BAX in intestinal cancer. *Biochem. Biophys. Res. Commun.* 406, 1–6. doi: 10.1016/j.bbrc.2010.12.070

Zhang, F., Ren, L., Zhou, S., Duan, P., Xue, J., Chen, H., et al. (2019). Role of B-cell lymphoma 2 ovarian killer (BOK) in acute toxicity of human lung epithelial cells caused by cadmium chloride. *Med. Sci. Monit.* 25, 5356–5368. doi: 10.12659/msm.913706

Zhang, H., Holzgreve, W., and De Geyter, C. (2000). Evolutionarily conserved Bok proteins in the Bcl-2 family. *FEBS Lett.* 480, 311–313. doi: 10.1016/s0014-5793(00)01921-9

Zhang, K., Zhang, B., Bai, Y., and Dai, L. (2020). E2F1 promotes cancer cell sensitivity to cisplatin by regulating the cellular DNA damage response through miR-26b in esophageal squamous cell carcinoma. *J. Cancer* 11, 301–310. doi: 10.7150/jca.33983

Zheng, J. H., Grace, C. R., Guibao, C. D., Mcnamara, D. E., Llambi, F., Wang, Y. M., et al. (2018). Intrinsic instability of BOK enables membrane permeabilization in *Apoptosis*. *Cell Rep.* 23, 2083–2094. doi: 10.1016/j.celrep.2018.04.060

Zheng, T. S., Hunot, S., Kuida, K., and Flavell, R. A. (1999). Caspase knockouts: matters of life and death. *Cell Death Differ.* 6, 1043–1053. doi: 10.1038/sj.cdd.4400593

Conflict of Interest: The authors declare that the research was conducted in the absence of any commercial or financial relationships that could be construed as a potential conflict of interest.

frontiers in Cell and Developmental Biology

REVIEW
published: 17 September 2020
doi: 10.3389/fcell.2020.586578

Oxidative Damage and Antioxidant Defense in Ferroptosis

Feimei Kuang[1], Jiao Liu[1], Daolin Tang[1,2] and Rui Kang[2]**

[1] *The Third Affiliated Hospital, Guangzhou Medical University, Guangzhou, China,* [2] *Department of Surgery, UT Southwestern Medical Center, Dallas, TX, United States*

Many new types of regulated cell death have been recently implicated in human health and disease. These regulated cell deaths have different morphological, genetic, biochemical, and functional hallmarks. Ferroptosis was originally described as a carcinogenic RAS-dependent non-apoptotic cell death, and is now defined as a type of regulated necrosis characterized by iron accumulation, lipid peroxidation, and the release of damage-associated molecular patterns (DAMPs). Multiple oxidative and antioxidant systems, acting together autophagy machinery, shape the process of lipid peroxidation during ferroptosis. In particular, the production of reactive oxygen species (ROS) that depends on the activity of nicotinamide adenine dinucleotide phosphate (NADPH) oxidases (NOXs) and the mitochondrial respiratory chain promotes lipid peroxidation by lipoxygenase (ALOX) or cytochrome P450 reductase (POR). In contrast, the glutathione (GSH), coenzyme Q10 (CoQ10), and tetrahydrobiopterin (BH_4) system limits oxidative damage during ferroptosis. These antioxidant processes are further transcriptionally regulated by nuclear factor, erythroid 2-like 2 (NFE2L2/NRF2), whereas membrane repair during ferroptotic damage requires the activation of endosomal sorting complexes required for transport (ESCRT)-III. A further understanding of the process and function of ferroptosis may provide precise treatment strategies for disease.

Keywords: ferroptosis, cell death, ROS, antioxidant, redox

OPEN ACCESS

Edited by:
Yinan Gong,
University of Pittsburgh, United States

Reviewed by:
Jennifer Martinez,
National Institute of Environmental Health Sciences (NIEHS), United States
Giovanni Quarato,
St. Jude Children's Research Hospital, United States

****Correspondence:***
Daolin Tang
daolin.tang@utsouthwestern.edu
Rui Kang
rui.kang@utsouthwestern.edu

Specialty section:
This article was submitted to Cell Death and Survival, a section of the journal Frontiers in Cell and Developmental Biology

Received: *23 July 2020*
Accepted: *28 August 2020*
Published: *17 September 2020*

Citation:
Kuang F, Liu J, Tang D and Kang R (2020) Oxidative Damage and Antioxidant Defense in Ferroptosis. Front. Cell Dev. Biol. 8:586578. doi: 10.3389/fcell.2020.586578

INTRODUCTION

The survival and death of cells are strictly controlled by various signals and molecules (Fulda et al., 2010). Physiological cell death is essential for normal function and tissue development. But pathological cell death may have side effects that cause inflammation and threaten our health. The first classification of cell death was based on morphological criteria proposed by pathologists in the 1970s. The pathologists suggested that cell death has three main forms, namely apoptosis (type I), autophagy (type II), and necrosis (type III) (Schweichel and Merker, 1973). The typical morphological changes of apoptosis are nuclear chromatin concentration and the formation of apoptotic bodies in the cytoplasm (Elmore, 2007). This is different from cell swelling and membrane rupture in necrosis (Golstein and Kroemer, 2007) and the formation of cytoplasmic double membrane vesicles in autophagy (a lysosome-dependent degradation process) (Xie et al., 2015). The latest cell death classification was formulated and is recommended by the Cell Death Nomenclature Committee. Generally, cell death is divided into accidental cell death and regulated cell death (Galluzzi et al., 2018). Accidental cell death is a passive process, whereas regulated

cell death is an active process that plays an important role in the pathogenesis of the disease (Galluzzi et al., 2018). In the past 20 years, many new types of regulated cell death (e.g., necroptosis, pyroptosis, ferroptosis, entotic cell death, netotic cell death, parthanatos, lysosome-dependent cell death, autophagy-dependent cell death, alkaliptosis, and oxeiptosis) have been identified in various models (Tang et al., 2019). Although they may share several common signals (e.g., redox signals), different forms of regulated cell death require special molecular machinery to trigger cell death (Tang et al., 2019). In this review, we summarize the major ways in which oxidative stress and antioxidant defense regulate ferroptosis, which is a form of iron-dependent cell death driven by lipid peroxidation (**Figure 1**).

THE BASIC PROPERTIES OF FERROPTOSIS

The concept of ferroptosis is derived from precision medicine for tumors that targeted RAS mutation signals (Dolma et al., 2003; Yang and Stockwell, 2008). RAS is a proto-oncogene and is frequently mutated in human cancer, leading to tumorgenesis and therapy resistance. Drug screening identified that the small molecular compounds erastin and RSL3 can selectively kill RAS-mutant cancer cells, but not RAS wild-type cells (Dolma et al., 2003; Yang and Stockwell, 2008). Later, it was proved that the anticancer activity of erastin and RSL3 depends on the induction of a new type of iron-dependent cell death, termed ferroptosis (Dixon et al., 2012). Although initial research showed that ferroptosis may be different from the classical cell death (e.g., apoptosis, necrosis, and autophagy-dependent cell death) (Dixon et al., 2012), recent studies demonstrate that there is a close relationship between ferroptosis, necrosis, and autophagy (Chen M.S. et al., 2017; Muller et al., 2017; Li et al., 2020; Lin et al., 2020; Liu et al., 2020c; Xie et al., 2020a). Ferroptotic cells usually exhibit cell membrane rupture and the release of intracellular contents, especially damage-associated molecular patterns (DAMPs) (Wen et al., 2019; Dai et al., 2020b), and are therefore classified as a type of regulated necrosis (Conrad et al., 2016). Increased autophagy, especially several types of selective autophagy [e.g., ferritinophagy (Hou et al., 2016), lipophagy (Bai et al., 2019), clockophagy (Yang M. et al., 2019), and chaperone-mediated autophagy (Wu et al., 2019)], promotes ferroptosis, indicating that ferroptosis is related to an abnormal intracellular degradation pathway.

Although the direct effectors of ferroptosis are unclear, iron accumulation and lipid peroxidation seem to play a central role in regulating the process of ferroptosis (Dixon et al., 2012; Yang et al., 2016; Shintoku et al., 2017; Wenzel et al., 2017; Li et al., 2020). Iron is an essential nutrient for cell proliferation, but iron overload can cause iron toxicity and lead to cell damage, even death. The balance of iron in cells and in the body is controlled by an integrated system. Pathways for abnormal iron metabolism, such as increasing the iron absorption and reducing iron storage or iron output, may cause ferroptosis through at least two ways. One is iron-mediated reactive oxygen species (ROS) production through the Fenton reaction (Dixon et al., 2012). The other is involved in the activation of iron-containing enzymes, such as lipoxygenase (ALOX) (Yang et al., 2016; Shintoku et al., 2017; Wenzel et al., 2017; Li et al., 2020). Finally, the accumulation of iron causes lipid peroxidation, which is the process of oxidative degradation in lipids [especially polyunsaturated fatty acids (PUFAs)] (Yuan et al., 2016; Doll et al., 2017; Kagan et al., 2017), leading to subsequent membrane damage and rupture. In contrast, an increased membrane repair ability through the activation of charged multivesicular body protein 5 (CHMP5) and charged multivesicular body protein 6 (CHMP6), which then mediate the endosomal sorting complexes required for transport (ESCRT)-III pathway, limits ferroptosis (Dai et al., 2020c). Notably, multiple oxidative stress and antioxidant defense pathways are involved in shaping ferroptotic responses (discussed later). This process is further regulated by epigenetic, transcriptional, posttranscriptional, and posttranslational mechanisms (Dai et al., 2020a; Wu et al., 2020). In particular, the activation of nuclear factor, erythroid 2-like 2 (NFE2L2/NRF2) plays a major transcriptional regulatory role in the suppression of ferroptosis through the induction of expression of antioxidants or iron metabolism genes (Sun et al., 2016a,b). Functionally, impaired ferroptosis (due to its excessive activation or cellular defects) is increasingly recognized as the cause of human diseases, especially neurodegenerative diseases, cancer, and infectious diseases as well as tissue damage (Xie et al., 2016; Stockwell et al., 2017).

OXIDATIVE DAMAGE IN FERROPTOSIS

Oxidative damage results from an imbalance between the generation of free radicals and the body's ability to neutralize or eliminate their harmful effects through antioxidants. ROS-mediated lipid peroxidation is the key step that drives ferroptosis. Below, we describe the main cellular sources of ROS and the main regulators of lipid peroxidation during ferroptosis (**Figure 1**).

Mitochondria-Mediated ROS Production

Mitochondria play a key role in regulating cell energy and cell death signal transduction. In addition to producing adenosine triphosphate, mitochondria are also the main source of ROS production (Zorov et al., 2014). The production of mitochondrial ROS mainly occurs during the oxidative phosphorylation in the electron transport chain located on the inner membrane of the mitochondria. Electrons leak from complex I and complex III on the electron transport chain, resulting in a partial reduction of oxygen to form superoxide anion ($O_2^{\cdot -}$). Subsequently, $O_2^{\cdot -}$ is rapidly disproportionated into hydrogen peroxide (H_2O_2) by the superoxide dismutase 2 (SOD2) in the mitochondrial matrix and superoxide dismutase 1 (SOD1) in the intermembrane space. Overall, $O_2^{\cdot -}$ and H_2O_2 produced during this process are called mitochondrial ROS, which is related to the loss of mitochondrial membrane potential ($\Delta\Psi m$) (Zorov et al., 2014). The reduction of $\Delta\Psi m$ is a common sign of apoptosis and ferroptosis, but their regulatory mechanisms are different. In

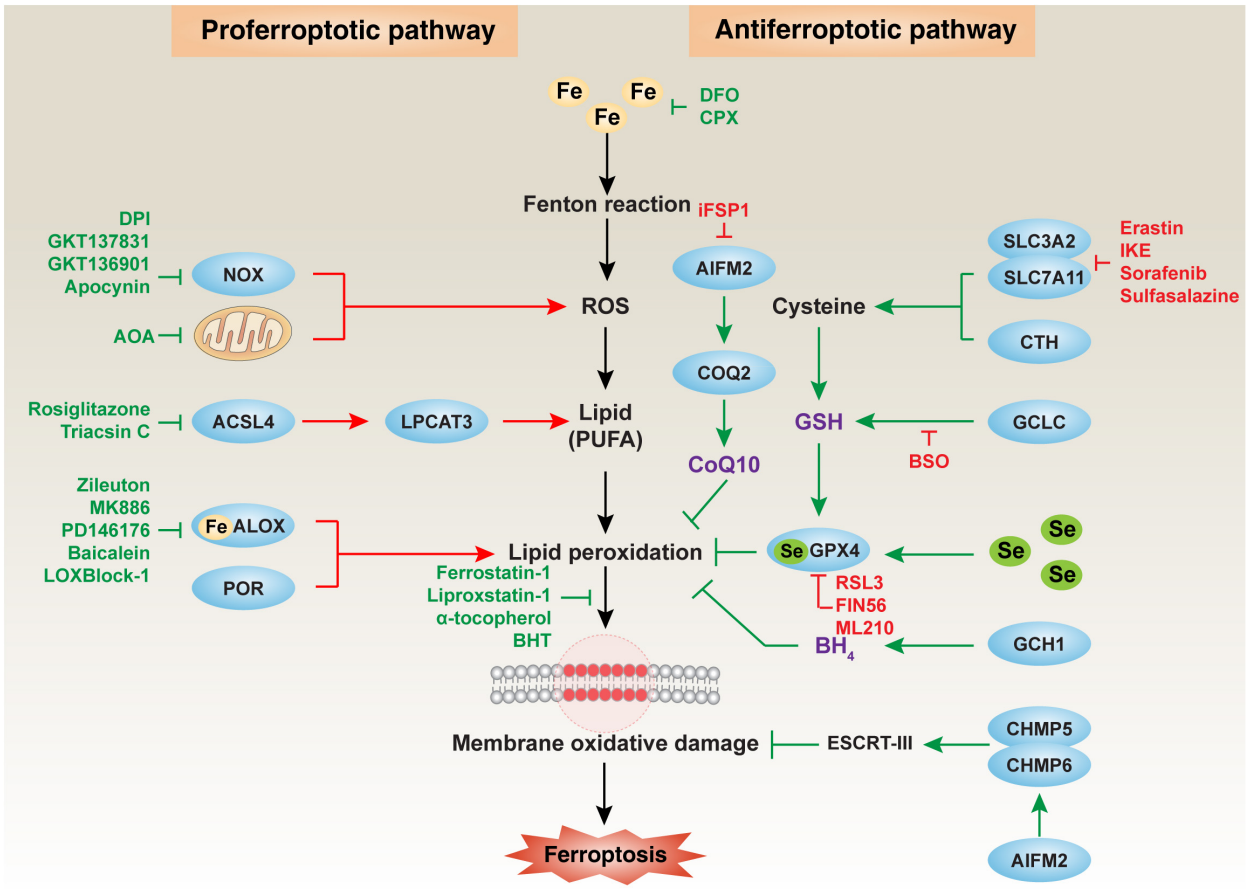

FIGURE 1 | The major mechanism of oxidative damage and antioxidant defense in ferroptosis. Ferroptosis is an iron-dependent oxidative cell death caused by ROS from the Fenton reaction and subsequent lipid peroxidation. Multiple oxidative and antioxidant systems control the process of membrane oxidative damage during ferroptosis. In particular, NOX-dependent and mitochondrial respiratory chain-dependent ROS production promotes lipid peroxidation by ALOX or POR. The production of lipids, especially PUFA, requires the activation of the ACSL4-LPCAT3 pathway. In contrast, the GSH, CoQ10, and BH_4 systems limit oxidative damage during ferroptosis. Membrane repair during ferroptotic damage requires the activation of the ESCRT-III pathway. ACSL4, acyl-CoA synthetase long-chain family member 4; AIFM2, apoptosis-inducing factor mitochondria-associated 2; ALOX, lipoxygenase; BH_4, tetrahydrobiopterin; CHMP5, charged multivesicular body protein 5; CHMP6, charged multivesicular body protein 6; COQ2, coenzyme Q2, polyprenyltransferase; CoQ10, coenzyme Q10; CTH, cystathionine gamma-lyase; ESCRT-III, endosomal sorting complexes required for transport-III; GCH1, GTP cyclohydrolase 1; GCLC, glutamate-cysteine ligase catalytic subunit; GPX4, glutathione peroxidase 4; GSH, glutathione; LPCAT3, lysophosphatidylcholine acyltransferase 3; NOX, nicotinamide adenine dinucleotide phosphate (NADPH) oxidase; POR, cytochrome P450 oxidoreductase; ROS, reactive oxygen species; Se, selenium; SLC3A2, solute carrier family 3 member 2; SLC7A11, solute carrier family 7 member 11.

mitochondria, cytochrome C, somatic (CYCS) plays an essential role in generating $\Delta\Psi m$. The translocation of CYCS from the mitochondria to the cytoplasm is an important event that initiates the loss of $\Delta\Psi m$ in the process of apoptosis induced by mitochondrial ROS (Yang et al., 1997). However, changes in CYCS position and the subsequent activation of apoptosis effector caspases are not observed during ferroptosis (Dixon et al., 2012), indicating that different mechanisms control $\Delta\Psi m$ during ferroptosis.

Some important mitochondrial apoptosis regulators, such as those in the voltage-dependent anion channel (VDAC) family and BCL2 family, are also involved in the regulation of ferroptosis in a context-dependent manner. VDAC, also known as mitochondrial porin, is the most abundant protein in the outer mitochondrial membrane. In the VDAC family, VDAC2 and VDAC3 are considered to be directly targeted by erastin to induce ferroptosis (**Figure 2**; Yagoda et al., 2007). As a negative feedback mechanism, the proteasome degradation of VDAC2 and VDAC3 that depends on NEDD4 E3 ubiquitin protein ligase can block erastin-induced ferroptosis in melanoma cells (Yang et al., 2020b). NEDD4-like E3 ubiquitin protein ligase (NEDD4L) inhibits ferroptosis by degrading lactotransferrin protein (Wang et al., 2020). VDAC2 is also a direct target of lipid-derived electrophile-induced carbonylation proteins during ferroptosis caused by RSL3 (Chen et al., 2018). Therefore, posttranslational modulation of VDAC2 or VDAC3 may weaken or exacerbate ferroptosis sensitivity. In addition to VDAC, the BCL2 family is also an important regulator of mitochondrial outer membrane permeability, which consists of many members that promote or inhibit apoptosis (Youle and Strasser, 2008). Pro-apoptotic BCL2

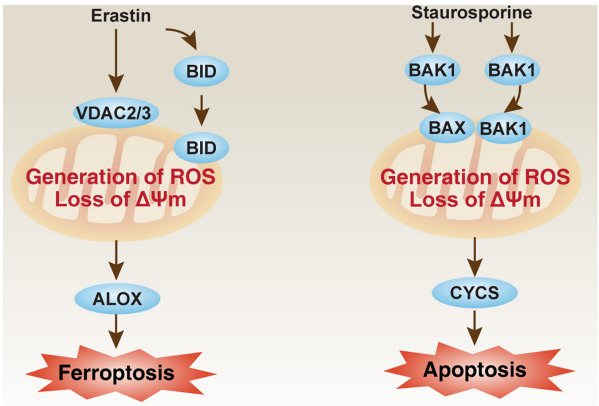

FIGURE 2 | The role of mitochondria in ferroptosis and apoptosis. The loss of mitochondrial membrane potential (ΔΨm) and the production of ROS are implicated in ferroptosis and apoptosis by different pathways. Erastin can bind VDAC2 and VDAC3 to induce BID-dependent ferroptosis through ALOX, whereas BAK1 and BAX are required for staurosporine-induced apoptosis through CYCS. ALOX, lipoxygenase; BAK1/BAK, BCL2 antagonist/killer 1; BAX, BCL2-associated X, apoptosis regulator; BID, BH3 interacting domain death agonist; CYCS, cytochrome C, somatic; ROS, reactive oxygen species; VDAC, voltage-dependent anion channel.

family members, such as BCL2 antagonist/killer 1 (BAK1/BAK) and BCL2-associated X, apoptosis regulator (BAX), are required for staurosporine-induced apoptosis (Wei et al., 2001), but not required for erastin-induced ferroptosis in fibroblasts (Dixon et al., 2012; **Figure 2**). However, BH3 interacting domain death agonist (BID), a pro-apoptotic BCL2 family member, mediates mitochondrial ROS-induced ferroptosis in neuronal cells (Neitemeier et al., 2017; Jelinek et al., 2018). These findings increase the likelihood that apoptotic or ferroptotic death requires different types of changes in mitochondrial membrane, which are further regulated by different members of VDAC and BCL2 families.

In addition, mitochondrial energy sensors or mitochondrial quality control systems plays a dual role in ferroptosis. AMP-activated protein kinase (AMPK) is a key sensor of cellular energy and regulates ferroptosis through its phosphorylated substrate. AMPK-mediated BECN1 (a key autophagy regulator) phosphorylation promotes ferroptosis through the inhibition of system xc^- activity (Song et al., 2018). In contrast, AMPK-mediated acetyl-CoA carboxylase alpha (ACACA) phosphorylation blocks ferroptosis through the inhibition of fatty acid biosynthesis (Lee et al., 2020). Additional signals, currently unknown, are needed to explain the substrate selectivity of AMPK-related ferroptosis regulation. Although many types of selective autophagy promote ferroptosis, mitophagy (an important mitochondrial quality control system) may play a context-dependent role in ferroptosis. On the one hand, mitophagy can maintain a healthy number of mitochondria to promote survival against ferroptosis (Gao et al., 2019). On the other hand, excessive mitophagy may cause metabolic stress and subsequent production of mitochondrial ROS, leading to ferroptosis (Basit et al., 2017). The interaction of mitochondria and other organelles in ferroptosis remains to be explored.

NOX-Mediated ROS Production

For a long time, the production of $O_2^{\cdot -}$ by transmembrane nicotinamide adenine dinucleotide phosphate (NADPH) oxidase (NOX) has been regarded as an important function in professional phagocytes, such as macrophages and dendritic cells (Bedard and Krause, 2007). In addition to phagocytes, other cells also express NOX to produce $O_2^{\cdot -}$ or H_2O_2 by transporting electrons across the membrane. The human genome encodes seven members of the NOX family, including five NOX proteins [NOX1, cytochrome B-245 beta chain (CYBB/NOX2), NOX3, NOX4, and NOX5] and two dual oxidases (DUOX1 and DUOX2). NOX-derived ROS plays a broad role in various physiological and pathological conditions (e.g., development, infection, immunity, and cell death) (Bedard and Krause, 2007). As an important regulator of lipid raft-derived redox signaling platforms, NOX participates in the induction of apoptosis (Jin et al., 2011). Similarly, NOX1-, CYBB-, and NOX4-mediated ROS production is also involved in the initiation of ferroptotic cancer cell death by inducing lipid peroxidation (Xie et al., 2017; Chen et al., 2019; Yang W.H. et al., 2019; Yang et al., 2020a), indicating a wide role for NOXs in cell death. In cancer cells, the activity of NOXs in ferroptosis is further affected by oncogenes and tumor suppressors. For example, the loss of tumor suppressor TP53 inhibits the accumulation of dipeptidyl-peptidase-4 (DPP4/CD26) in the nucleus, thereby increasing plasma-membrane associated DPP4-dependent lipid peroxidation and subsequent ferroptosis via the formation of the DPP4-NOX1 complex (Xie et al., 2017). During the activation of oncogenic RAS, NOX1 mediates the production of ROS (Adachi et al., 2008), which may promote ferroptosis through the activation of the extracellular signal-regulated kinase (ERK) pathway (Yagoda et al., 2007). More research is needed to clearly define how different NOX members, coupled with impaired genetic signals in tumors, cause ferroptosis.

ALOX-Mediated Lipid Peroxidation

Reactive oxygen species-mediated lipid peroxidation is mainly accomplished by ALOX, which is a dioxygenase that contains non-heme iron. ALOX includes six members (ALOXE3, ALOX5, ALOX12, ALOX12B, ALOX15, and ALOX15B) and catalyzes the stereotactic insertion of oxygen into PUFAs, especially arachidonic acid (AA) and adrenic acid (AdA), in a tissue- or cell-dependent manner. For example, ALOX5, ALOXE3, ALOX15, or ALOX15B mediates ferroptosis caused by erastin or RSL3 in BJeLR, HT1080, or PANC1 cells (Yang et al., 2016; Shintoku et al., 2017; Wenzel et al., 2017; Li et al., 2020). ALOX15 or ALOX12 mediates TP53-induced ferroptosis in cancer cells following different stimuli (Ou et al., 2016; Chu et al., 2019). Phosphatidylethanolamine-binding protein 1 (PEBP1) can be used as an adaptor protein for ALOX15 and enhances the activity of ALOX15 in the induction of ferroptosis *in vitro* (Wenzel et al., 2017). However, ALOX12/15 may not be important for ferroptotic damage in mice caused by glutathione peroxidase 4 (GPX4)

depletion in kidney (Friedmann Angeli et al., 2014) or T cells (Matsushita et al., 2015). Therefore, when evaluating the sensitivity of ferroptosis, it is necessary to first detect the basic expression levels of different ALOX members.

Lipoxygenase-mediated lipid peroxidation is firstly initiated by the generation of AA/AdA derivatives mediated by ACSL4 and LPCAT3 (Yuan et al., 2016; Doll et al., 2017; Kagan et al., 2017). ACSL4 catalyzes the combination of free AA/AdA and CoA to form AA/AdA-CoA derivatives and promotes their esterification to phospholipids, while LPCAT3 then catalyzes the biosynthesis of AA/AdA-CoA and membrane phosphatidylethanolamine (PE) to form AA/AdA-PE. ALOX then mediates the peroxidation of AA/AdA-PE to generate AA/AdA-PE-OOH (e.g., 5-HETE, 11-HETE, and 15-HETE, but not 12-HETE), which leads to membrane injury during ferroptosis. Therefore, the genetic or pharmacological inhibition of the ACSL4-LPCAT3-ALOX pathway inhibits ferroptosis *in vitro* and *in vivo*. Although ACSL4-independent ferroptosis may exist, increased ACSL4 expression is a biomarker of ferroptosis (Yuan et al., 2016).

POR-Mediated Lipid Peroxidation

Cytochrome P450 reductase (POR) plays a major role in the metabolism of drugs and steroids. POR supplies electrons to microsomal cytochrome P450 from NADPH (Riddick et al., 2013). Consequently, the destruction of POR affects the activity of all microsomal P450 enzymes. In addition to ALOX-mediated lipid peroxidation, POR-mediated lipid peroxidation plays an alternative role in mediating ferroptosis. In particular, POR binds its cofactors, such as flavin mononucleotide (FMN) and flavin adenine dinucleotide (FAD). This complex mediated electron supplementation to cytochrome P450 from NADPH is required for erastin-, FIN56-, ML210-, or RSL3-induced lipid peroxidation and subsequent ferroptosis in melanoma and other cancer cells (Zou et al., 2020). Although the exact mechanism of POR-mediated lipid peroxidation is still unknown, POR may accelerate the cycling between ferrous and ferric iron in the heme component of cytochrome P450 (Zou et al., 2020). Given that the conditional knockout of POR in the liver leads to a decrease in the metabolism and lipid accumulation in mice (Henderson et al., 2003), the pathological role of POR-mediated ferroptosis in tissue damage and metabolism disease is worthy of further study.

ANTIOXIDANT DEFENSE IN FERROPTOSIS

Cellular protection against oxidative damage in ferroptosis is organized at multiple levels. The synthesis of antioxidants, such as glutathione (GSH), coenzyme Q10 (CoQ10) and tetrahydrobiopterin (BH_4), is the main defense strategy in the process of ferroptosis, which is related to multiple enzymes or proteins (**Figure 1**). In addition to the antioxidant systems discussed below, some antioxidant proteins, such as peroxiredoxins (PRDXs) (Lu et al., 2019; Qi et al., 2019; Lovatt et al., 2020) and thioredoxin (Llabani et al., 2019), can also block ferroptotic cell death. Therefore, an integrated antioxidant defense network exists in different cells.

GSH System

Glutathione is an active tripeptide, formed by the condensation of glutamic acid, cysteine, and glycine. As an important antioxidant, glutathione is used to treat liver diseases, tumors, poisoning, cataracts, and aging diseases. The pharmacological inhibition of GSH synthesis and utilization is a classic method of inducing ferroptosis (Dixon et al., 2012; Yang et al., 2014). There are two main sources of cysteine production for GSH synthesis, namely the system xc^- pathway and the transsulfuration pathway (McBean, 2012; Lewerenz et al., 2013). System xc^- is a transmembrane sodium-independent and chloride-independent transporter of cystine and glutamic acid, which contains two key components [solute carrier family 7 member 11 (SLC7A11/xCT) and solute carrier family 3 member 2 (SLC3A2/CD98)] (Lewerenz et al., 2013). After being transported into the cell by system xc^-, cystine is oxidized to cysteine, which is then used for glutamate-cysteine ligase catalytic subunit (GCLC/GCL)-mediated GSH synthesis. The inhibition of system xc^- (using erastin, sorafenib, and sulfasalazine) or GCL (using buthionine sulfoximine) triggers ferroptosis in various cells (Conrad and Pratt, 2019). The expression or activity of system xc^- is affected by epigenetics, transcription, and posttranscriptional and posttranslational regulators, such as TP53 (Jiang et al., 2015), NFE2L2 (Chen D. et al., 2017), BRCA1-associated protein 1 (BAP1) (Zhang Y. et al., 2018), mucin 1, cell surface-associated (MUC1) (Hasegawa et al., 2016), or BECN1 (Song et al., 2018), leading to complex feedback mechanisms to control GSH levels in ferroptosis. The transsulfuration pathway is a metabolic pathway that involves the interconversion of cysteine and homocysteine through intermediate cystathionine (McBean, 2012). Cystathionine gamma-lyase (CTH/CGL)-mediated decomposition of cystathionine is required for cysteine production. This process is inhibited by cysteinyl tRNA synthetase 1 (CARS1/CARS), an enzyme that charges $tRNA^{Cys}$ with cysteine in the cytoplasm. In contrast, knocking down CARS1 increases resistance to ferroptosis by activating the transsulfuration pathway (Hayano et al., 2016).

The main anti-ferroptotic activity of GSH is related to GPX4, which reduces phospholipid hydroperoxide production (AA/AdA-PE-OOH) to AA/AdA-PE-OH (Yang et al., 2014). GPX4 is a selenium-containing protein whose activity is regulated by GSH. As an essential trace element, the function of selenium depends on a unique functional group, namely the selenol (-SeH) group. In the catalytic cycle of GPX4, active selenol (-SeH) is oxidized by peroxide to selenic acid (-SeOH), and then reduced by GSH to intermediate selenide disulfide (-Se-SG) (Ingold et al., 2018). GPX4 is further activated by the second GSH, releasing glutathione disulfide (GS-SG) (Ingold et al., 2018). GPX4 inhibitors (e.g., RSL3, ML162, ML210, FIN56, and FINO2) are also known as classic ferroptosis activators, although their activities and effects are still different (Conrad and Pratt, 2019). In addition to ferroptosis, GPX4 also mediates antioxidant defense in apoptosis (Ran et al., 2003), necroptosis (Canli et al., 2016), and

pyroptosis (Kang et al., 2018), suggesting a context-dependent role of GPX4 in cell death.

CoQ10 System

Coenzyme Q10 is a vitamin-like endogenously produced isoprenyl benzoquinone compound that occurs naturally in the human body and is highest in the heart, liver, kidney, and pancreas (Hernandez-Camacho et al., 2018). CoQ10 exists in oxidized form (ubiquinone) and reduced form (ubiquinol). The effective function of mitochondria depends on various cofactors, such as L-carnitine, α-lipoic acid, and CoQ10 (Pagano et al., 2014). CoQ10 is particularly interesting because it not only supports the mitochondrial respiratory chain, but also acts as a powerful antioxidant by neutralizing free radicals in various membrane structures (Teran et al., 2018). CoQ10 not only inhibits apoptosis (Chen et al., 2011), but also ferroptosis (Shimada et al., 2016). For example, the application of farnesyl pyrophosphate (an upstream product of CoQ10 synthesis) or idebenone (a hydrophilic analog of CoQ10) prevents ferroptosis caused by FIN56 (Shimada et al., 2016). In contrast, inhibiting the production of CoQ10 may accelerate ferroptotic cell death. In particular, apoptosis-inducing factor mitochondrial-related 2 (AIFM2/FSP1/AMID), a traditional regulator of apoptosis in the mitochondria (Wu et al., 2002), can mediate the production of CoQ10 to inhibit ferroptosis in a GSH-independent manner (Bersuker et al., 2019; Doll et al., 2019). This process requires the N-myristoylation of AIFM2, which results in the translocation of AIFM2 to the cell membrane (Bersuker et al., 2019; Doll et al., 2019). The depletion of CoQ10 biosynthesis enzyme [e.g., coenzyme Q2, polyprenyltransferase (COQ2)] may reverse the anti-ferroptotic activity of AIFM2 (Bersuker et al., 2019; Doll et al., 2019). Of note, the increased accumulation of AIFM2 in the cell membrane may also inhibit ferroptosis by activating CHMP5- and CHMP6-mediated ESCRT-III membrane repair mechanisms, which are independent of CoQ10 (Dai et al., 2020d). Statin drugs inhibit 3-hydroxy-3-methylglutaryl–coenzyme A reductase (HMG-CoA), a rate-limiting step that converts HMG-CoA to mevalonate in the production of cholesterol. Interestingly, statins can cause a decrease in CoQ10, thereby increasing the sensitivity of ferroptosis (Shimada et al., 2016). Further understanding of the antioxidant capacity of CoQ10 may provide benefits for reducing ferroptosis-related damage.

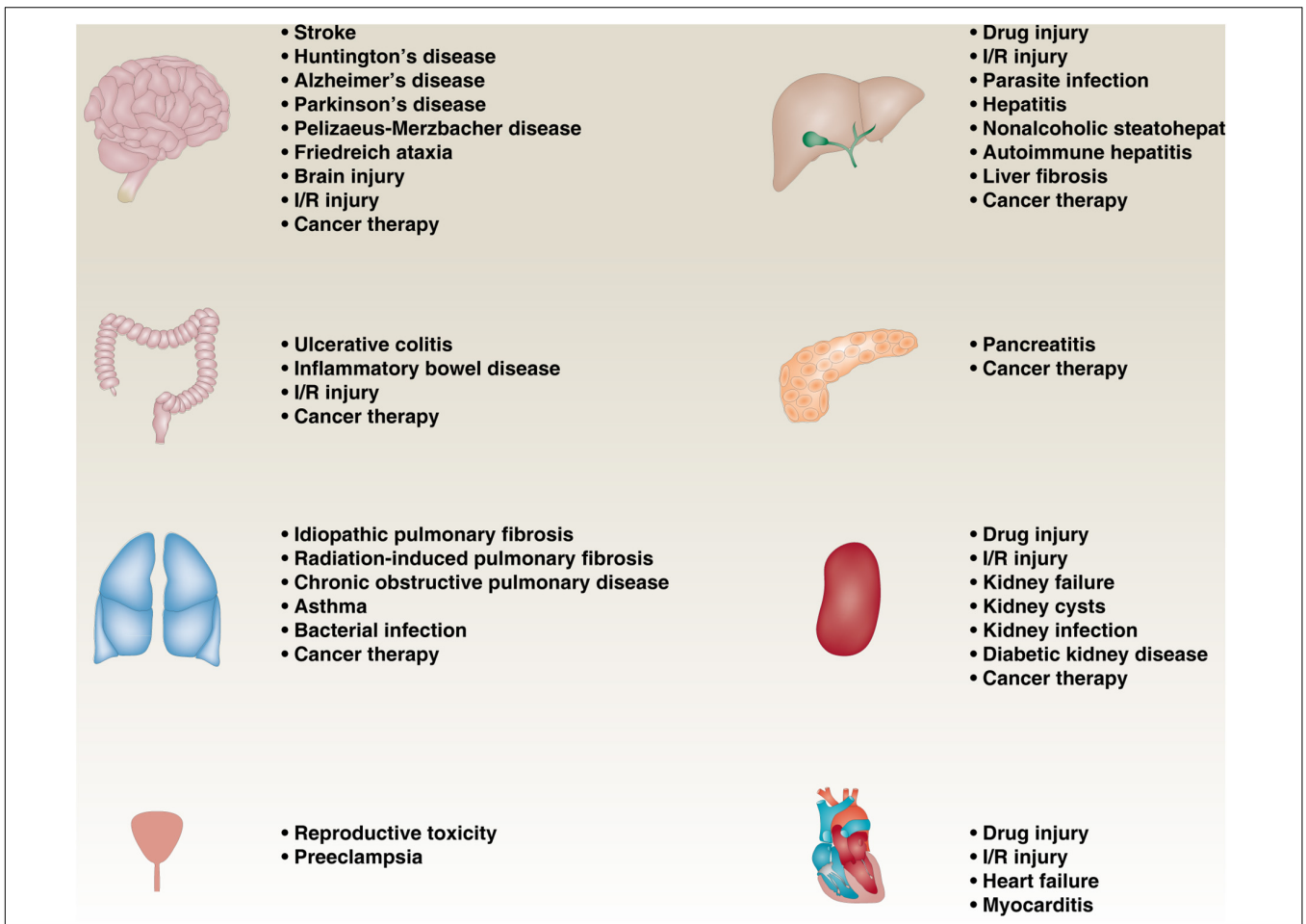

FIGURE 3 | The role of ferroptosis in diseases. Impaired or excessive ferroptotic pathway is involved in various diseases, such as neurodegenerative diseases, infectious diseases, cancers, and ischemia-reperfusion (I/R) injury diseases.

BH_4 System

Tetrahydrobiopterin is a natural nutrient that can be used as a cofactor for various enzymes, such as tryptophan hydroxylase, phenylalanine hydroxylase, tyrosine hydroxylase, nitric oxide (NO) synthase, and glyceryl ether mono-oxygenase (Werner et al., 2011). Functionally, BH_4 is involved in the biosynthesis of some neurotransmitters, such as 5-hydroxytryptamine, dopamine, noradrenaline, adrenaline, and melatonin (Werner et al., 2011). Exogenous dopamine or melatonin has been shown to suppress erastin- or hemin-induced ferroptosis in various cells (NaveenKumar et al., 2019; Wang et al., 2016), but it remains unclear whether BH_4-mediated endogenous dopamine or melatonin production regulates ferroptosis. In addition, BH_4 plays a redox role in the catalysis of L-arginine, O_2, and NADPH to form NO. The oxidation of BH_4 to BH_2 causes an uncoupling of NOS, thereby forming $O_2^{\cdot -}$ instead of NO. $O_2^{\cdot -}$ reacts rapidly with NO to form peroxynitrite, and nitrite can further uncouple NOS (Werner et al., 2011). The activation of the NO pathway is implicated in ferroptosis-related tissue injury (Deng et al., 2020). In particular, L-arginine induces acute pancreatitis in mice through the activation of ferroptosis-induced sterile inflammation, which is further regulated by circadian rhythms (Liu et al., 2020d). The synthesis and recycling of BH_4 is a dynamic process, and GTP cyclohydrolase-1 (GCH1) is the rate-limiting enzyme for the biosynthesis of BH_4. GCH1-mediated BH_4 production prevents ferroptosis by inhibiting lipid peroxidation (Kraft et al., 2020), indicating that BH_4 has antioxidant activity during cell death. Overall, these findings demonstrate the prosurvival role of BH_4 in protecting against ferroptotic damage.

FERROPTOSIS IN DISEASE

More and more reports showing that impaired or excessive ferroptotic pathway in various diseases, such as neurodegenerative diseases, infectious diseases, cancers, and ischemia-reperfusion (I/R) injury diseases (**Figure 3**). In cancer pathology, ferroptosis not only inhibits tumor growth (Daher et al., 2019), but also promotes tumor formation (Dai et al., 2020b), depending on the type, stage, and microenvironment of the tumor. Iron-induced ferroptotic damage is implicated in Huntington's disease (HD), Alzheimer's disease (AD), and Parkinson's disease (PD) (Skouta et al., 2014; Do Van et al., 2016; Zhang Y.H. et al., 2018; Hirata et al., 2019), although oxytosis has long been considered to be the main mode leading to neuronal cell damage caused by glutamate toxicity (Tan et al., 2001). Inflammation mediated by ferroptotic cell death can promote pancreatitis (Liu et al., 2020d), liver fibrosis (Tsurusaki et al., 2019; Zeng et al., 2020), chronic obstructive pulmonary disease (COPD) (Park et al., 2019; Wang and Tang, 2019; Yoshida et al., 2019), inflammatory bowel disease (Mayr et al., 2020), and preeclampsia (Zhang et al., 2020). In addition, inhibiting ferroptosis can prevent I/R damage to various tissues, especially liver, kidney, brain, and heart (Linkermann et al., 2014; Skouta et al., 2014; Martin-Sanchez et al., 2017; Muller et al., 2017; Fang et al., 2019). Therefore, the development of pharmacological agents that regulate ferroptosis under these pathological conditions is crucial.

CONCLUSION AND PERSPECTIVES

Ferroptosis was discovered not long ago, and there have been more and more studies related to it in recent years. This is because the core signals of ferroptosis (iron accumulation and lipid peroxidation) are often observed abnormally in various diseases and pathological conditions. Like other types of regulated cell death, ferroptosis may be caused by an imbalance between oxidation and antioxidant systems (Chen et al., 2020). In particular, NOX-dependent and mitochondrial respiratory chain-dependent ROS formation facilitates lipid peroxidation, whereas the GSH, CoQ10, and BH_4 systems play a major role in limiting oxidative damage during ferroptosis. However, the process and function of ferroptosis needs to be explored. An unresolved central issue is that these oxidative damage, antioxidant defense mechanisms, and membrane repair mechanisms are also involved in the regulation of other kinds of non-ferroptotic cell death (Bae et al., 2011; Liu et al., 2020a). Thus, although they may share a common upstream mechanism, the identification of unique downstream effectors may distinguish ferroptosis from non-ferroptotic cell death. Similarly, it remains a challenge to distinguish the pathological role of ferroptosis and non-ferroptotic cell death in disease (Hotchkiss et al., 2009). In addition, the complexity of autophagy and lipid metabolism in the regulation of ferroptosis should be further clarified (Liu et al., 2020b; Xie et al., 2020b) and therefore provide a reasonable explanation for regulating ferroptosis in a context-dependent manner.

AUTHOR CONTRIBUTIONS

All authors conceptualized and wrote the manuscript.

ACKNOWLEDGMENTS

We thank Dave Primm (Department of Surgery, University of Texas Southwestern Medical Center) for his critical reading of the manuscript.

REFERENCES

Adachi, Y., Shibai, Y., Mitsushita, J., Shang, W. H., Hirose, K., and Kamata, T. (2008). Oncogenic Ras upregulates NADPH oxidase 1 gene expression through MEK-ERK-dependent phosphorylation of GATA-6. *Oncogene* 27, 4921–4932. doi: 10.1038/onc.2008.133

Bae, Y. S., Oh, H., Rhee, S. G., and Yoo, Y. D. (2011). Regulation of reactive oxygen species generation in cell signaling. *Mol. Cells* 32, 491–509. doi: 10.1007/s10059-011-0276-3

Bai, Y., Meng, L., Han, L., Jia, Y., Zhao, Y., Gao, H., et al. (2019). Lipid storage and lipophagy regulates ferroptosis. *Biochem. Biophys. Res. Commun.* 508, 997–1003. doi: 10.1016/j.bbrc.2018.12.039

Basit, F., van Oppen, L. M., Schockel, L., Bossenbroek, H. M., van Emst-de Vries, S. E., Hermeling, J. C., et al. (2017). Mitochondrial complex I inhibition triggers a mitophagy-dependent ROS increase leading to necroptosis and ferroptosis in melanoma cells. *Cell Death Dis.* 8:e2716. doi: 10.1038/cddis.2017.133

Bedard, K., and Krause, K. H. (2007). The NOX family of ROS-generating NADPH oxidases: physiology and pathophysiology. *Physiol. Rev.* 87, 245–313. doi: 10.1152/physrev.00044.2005

Bersuker, K., Hendricks, J. M., Li, Z., Magtanong, L., Ford, B., Tang, P. H., et al. (2019). The CoQ oxidoreductase FSP1 acts parallel to GPX4 to inhibit ferroptosis. *Nature* 575, 688–692. doi: 10.1038/s41586-019-1705-2

Canli, O., Alankus, Y. B., Grootjans, S., Vegi, N., Hultner, L., Hoppe, P. S., et al. (2016). Glutathione peroxidase 4 prevents necroptosis in mouse erythroid precursors. *Blood* 127, 139–148. doi: 10.1182/blood-2015-06-654194

Chen, C. C., Liou, S. W., Chen, C. C., Chen, W. C., Hu, F. R., Wang, I. J., et al. (2011). Coenzyme Q10 reduces ethanol-induced apoptosis in corneal fibroblasts. *PLoS One* 6:e19111. doi: 10.1371/journal.pone.0019111

Chen, D., Tavana, O., Chu, B., Erber, L., Chen, Y., Baer, R., et al. (2017). NRF2 is a major target of ARF in p53-independent tumor suppression. *Mol. Cell* 68, 224.e4–232.e4. doi: 10.1016/j.molcel.2017.09.009

Chen, M. S., Wang, S. F., Hsu, C. Y., Yin, P. H., Yeh, T. S., Lee, H. C., et al. (2017). CHAC1 degradation of glutathione enhances cystine-starvation-induced necroptosis and ferroptosis in human triple negative breast cancer cells via the GCN2-eIF2alpha-ATF4 pathway. *Oncotarget* 8, 114588–114602. doi: 10.18632/oncotarget.23055

Chen, X., Li, J., Kang, R., Klionsky, D. J., Tang, D. (2020). Ferroptosis: machinery and regulation. *Autophagy* 1–28. doi: 10.1080/15548627.2020.1810918 [Epub ahead of print].

Dai, C., Chen, X., Li, J., Comish, P., Kang, R., and Tang, D. (2020a). Transcription factors in ferroptotic cell death. *Cancer Gene Ther.* doi: 10.1038/s41417-020-0170-2 [Epub ahead of print].

Dai, E., Han, L., Liu, J., Xie, Y., Kroemer, G., Klionsky, D. J., et al. (2020b). Autophagy-dependent ferroptosis drives tumor-associated macrophage polarization via release and uptake of oncogenic KRAS protein. *Autophagy* 16, 1–15. doi: 10.1080/15548627.2020.1714209

Dai, E., Meng, L., Kang, R., Wang, X., and Tang, D. (2020c). ESCRT-III-dependent membrane repair blocks ferroptosis. *Biochem. Biophys. Res. Commun.* 522, 415–421. doi: 10.1016/j.bbrc.2019.11.110

Dai, E., Zhang, W., Cong, D., Kang, R., Wang, J., and Tang, D. (2020d). AIFM2 blocks ferroptosis independent of ubiquinol metabolism. *Biochem. Biophys. Res. Commun.* 523, 966–971. doi: 10.1016/j.bbrc.2020.01.066

Chen, X., Xu, S., Zhao, C., and Liu, B. (2019). Role of TLR4/NADPH oxidase 4 pathway in promoting cell death through autophagy and ferroptosis during heart failure. *Biochem. Biophys. Res. Commun.* 516, 37–43. doi: 10.1016/j.bbrc.2019.06.015

Chen, Y., Liu, Y., Lan, T., Qin, W., Zhu, Y., Qin, K., et al. (2018). Quantitative profiling of protein carbonylations in ferroptosis by an aniline-derived probe. *J. Am. Chem. Soc.* 140, 4712–4720. doi: 10.1021/jacs.8b01462

Chu, B., Kon, N., Chen, D., Li, T., Liu, T., Jiang, L., et al. (2019). ALOX12 is required for p53-mediated tumour suppression through a distinct ferroptosis pathway. *Nat. Cell Biol.* 21, 579–591. doi: 10.1038/s41556-019-0305-6

Conrad, M., Angeli, J. P., Vandenabeele, P., and Stockwell, B. R. (2016). Regulated necrosis: disease relevance and therapeutic opportunities. *Nat. Rev. Drug Discov.* 15, 348–366. doi: 10.1038/nrd.2015.6

Conrad, M., and Pratt, D. A. (2019). The chemical basis of ferroptosis. *Nat. Chem. Biol.* 15, 1137–1147. doi: 10.1038/s41589-019-0408-1

Daher, B., Parks, S. K., Durivault, J., Cormerais, Y., Baidarjad, H., Tambutte, E., et al. (2019). Genetic Ablation of the Cystine Transporter xCT in PDAC Cells Inhibits mTORC1, Growth, Survival, and Tumor Formation via Nutrient and Oxidative Stresses. *Cancer Res.* 79, 3877–3890. doi: 10.1158/0008-5472.CAN-18-3855

Deng, G., Li, Y., Ma, S., Gao, Z., Zeng, T., Chen, L., et al. (2020). Caveolin-1 dictates ferroptosis in the execution of acute immune-mediated hepatic damage by attenuating nitrogen stress. *Free Radic. Biol. Med.* 148, 151–161. doi: 10.1016/j.freeradbiomed.2019.12.026

Dixon, S. J., Lemberg, K. M., Lamprecht, M. R., Skouta, R., Zaitsev, E. M., Gleason, C. E., et al. (2012). Ferroptosis: an iron-dependent form of nonapoptotic cell death. *Cell* 149, 1060–1072. doi: 10.1016/j.cell.2012.03.042

Do Van B, Gouel, F., Jonneaux, A., Timmerman, K., Gele, P., Petrault, M., et al. (2016). Ferroptosis, a newly characterized form of cell death in Parkinson's disease that is regulated by PKC. *Neurobiol. Dis.* 94, 169–178. doi: 10.1016/j.nbd.2016.05.011

Doll, S., Freitas, F. P., Shah, R., Aldrovandi, M., da Silva, M. C., Ingold, I. A. G., et al. (2019). FSP1 is a glutathione-independent ferroptosis suppressor. *Nature* 575, 693–698. doi: 10.1038/s41586-019-1707-0

Doll, S., Proneth, B., Tyurina, Y. Y., Panzilius, E., Kobayashi, S., Ingold, I. M., et al. (2017). ACSL4 dictates ferroptosis sensitivity by shaping cellular lipid composition. *Nat. Chem. Biol.* 13, 91–98. doi: 10.1038/nchembio.2239

Dolma, S., Lessnick, S. L., Hahn, W. C., and Stockwell, B. R. (2003). Identification of genotype-selective antitumor agents using synthetic lethal chemical screening in engineered human tumor cells. *Cancer Cell* 3, 285–296. doi: 10.1016/s1535-6108(03)00050-3

Elmore, S. (2007). Apoptosis: a review of programmed cell death. *Toxicol. Pathol.* 35, 495–516. doi: 10.1080/01926230701320337

Fang, X., Wang, H., Han, D., Xie, E., Yang, X., Wei, J., et al. (2019). Ferroptosis as a target for protection against cardiomyopathy. *Proc. Natl. Acad. Sci. U.S.A.* 116, 2672–2680. doi: 10.1073/pnas.1821022116

Friedmann Angeli, J. P, Schneider, M., Proneth, B., Tyurina, Y. Y., Tyurin, V. A., Hammond, V. J., et al. (2014). Inactivation of the ferroptosis regulator Gpx4 triggers acute renal failure in mice. *Nat. Cell Biol.* 16, 1180–1191. doi: 10.1038/ncb3064

Fulda, S., Gorman, A. M., Hori, O., and Samali, A. (2010). Cellular stress responses: cell survival and cell death. *Int. J. Cell Biol.* 2010:214074. doi: 10.1155/2010/214074

Galluzzi, L., Vitale, I., Aaronson, S. A., Abrams, J. M., Adam, D., Agostinis, P., et al. (2018). Molecular mechanisms of cell death: recommendations of the nomenclature committee on cell death 2018. *Cell Death Differ.* 25, 486–541. doi: 10.1038/s41418-017-0012-4

Gao, M., Yi, J., Zhu, J., Minikes, A. M., Monian, P., Thompson, C. B., et al. (2019). Role of mitochondria in ferroptosis. *Mol. Cell* 73, 354.e3–363.e3. doi: 10.1016/j.molcel.2018.10.042

Golstein, P., and Kroemer, G. (2007). Cell death by necrosis: towards a molecular definition. *Trends Biochem. Sci.* 32, 37–43. doi: 10.1016/j.tibs.2006.11.001

Hasegawa, M., Takahashi, H., Rajabi, H., Alam, M., Suzuki, Y., Yin, L., et al. (2016).). Functional interactions of the cystine/glutamate antiporter, CD44v and MUC1-C oncoprotein in triple-negative breast cancer cells. *Oncotarget* 7, 11756–11769. doi: 10.18632/oncotarget.7598

Hayano, M., Yang, W. S., Corn, C. K., Pagano, N. C., and Stockwell, B. R. (2016). Loss of cysteinyl-tRNA synthetase (CARS) induces the transsulfuration pathway and inhibits ferroptosis induced by cystine deprivation. *Cell Death Differ.* 23, 270–278. doi: 10.1038/cdd.2015.93

Henderson, C. J., Otto, D. M., Carrie, D., Magnuson, M. A., McLaren, A. W., Rosewell, I., et al. (2003). Inactivation of the hepatic cytochrome P450 system by conditional deletion of hepatic cytochrome P450 reductase. *J. Biol. Chem.* 278, 13480–13486. doi: 10.1074/jbc.M212087200

Hernandez-Camacho, J. D., Bernier, M., Lopez-Lluch, G., and Navas, P. (2018). Coenzyme Q10 supplementation in aging and disease. *Front. Physiol.* 9:44. doi: 10.3389/fphys.2018.00044

Hirata, Y., Iwasaki, T., Makimura, Y., Okajima, S., Oh-Hashi, K., and Takemori, H. (2019). Inhibition of double-stranded RNA-dependent protein kinase prevents oxytosis and ferroptosis in mouse hippocampal HT22 cells. *Toxicology* 418, 1–10. doi: 10.1016/j.tox.2019.02.012

Hotchkiss, R. S., Strasser, A., McDunn, J. E., and Swanson, P. E. (2009). Cell death. *N. Engl. J. Med.* 361, 1570–1583. doi: 10.1056/NEJMra0901217

Hou, W., Xie, Y., Song, X., Sun, X., Lotze, M. T., Zeh, H. J. III, et al. (2016). Autophagy promotes ferroptosis by degradation of ferritin. *Autophagy* 12, 1425–1428. doi: 10.1080/15548627.2016.1187366

Ingold, I., Berndt, C., Schmitt, S., Doll, S., Poschmann, G., Buday, K., et al. (2018). Selenium utilization by GPX4 is required to prevent hydroperoxide-induced ferroptosis. *Cell* 172, 409.e21–422.e21. doi: 10.1016/j.cell.2017.11.048

Jelinek, A., Heyder, L., Daude, M., Plessner, M., Krippner, S., Grosse, R., et al. (2018). Mitochondrial rescue prevents glutathione peroxidase-dependent ferroptosis. *Free Radic. Biol. Med.* 117, 45–57. doi: 10.1016/j.freeradbiomed.2018.01.019

Jiang, L., Kon, N., Li, T., Wang, S. J., Su, T., Hibshoosh, H., et al. (2015). Ferroptosis as a p53-mediated activity during tumour suppression. *Nature* 520, 57–62. doi: 10.1038/nature14344

Jin, S., Zhou, F., Katirai, F., and Li, P. L. (2011). Lipid raft redox signaling: molecular mechanisms in health and disease. *Antioxid Redox Signal.* 15, 1043–1083. doi: 10.1089/ars.2010.3619

Kagan, V. E., Mao, G., Qu, F., Angeli, J. P., Doll, S., Croix, C. S., et al. (2017). Oxidized arachidonic and adrenic PEs navigate cells to ferroptosis. *Nat. Chem. Biol.* 13, 81–90. doi: 10.1038/nchembio.2238

Kang, R., Zeng, L., Zhu, S., Xie, Y., Liu, J., Wen, Q., et al. (2018). Lipid peroxidation drives gasdermin d-mediated pyroptosis in lethal polymicrobial sepsis. *Cell Host Microbe* 24, 97.e4–108.e4. doi: 10.1016/j.chom.2018.05.009

Kraft, V. A. N., Bezjian, C. T., Pfeiffer, S., Ringelstetter, L., Muller, C., Zandkarimi, F., et al. (2020). GTP Cyclohydrolase 1/Tetrahydrobiopterin counteract ferroptosis through lipid remodeling. *ACS Cent. Sci.* 6, 41–53. doi: 10.1021/acscentsci.9b01063

Lee, H., Zandkarimi, F., Zhang, Y., Meena, J. K., Kim, J., Zhuang, L., et al. (2020). Energy-stress-mediated AMPK activation inhibits ferroptosis. *Nat. Cell Biol.* 22, 225–234. doi: 10.1038/s41556-020-0461-8

Lewerenz, J., Hewett, S. J., Huang, Y., Lambros, M., Gout, P. W., Kalivas, P. W., et al. (2013). The cystine/glutamate antiporter system x(c)(-) in health and disease: from molecular mechanisms to novel therapeutic opportunities. *Antioxid Redox Signal.* 18, 522–555. doi: 10.1089/ars.2011.4391

Li, C., Zhang, Y., Liu, J., Kang, R., Klionsky, D. J., and Tang, D. (2020). Mitochondrial DNA stress triggers autophagy-dependent ferroptotic death. *Autophagy* 18, 1–13. doi: 10.1080/15548627.2020.1739447

Lin, P. L., Tang, H. H., Wu, S. Y., Shaw, N. S., and Su, C. L. (2020). Saponin formosanin C-induced ferritinophagy and ferroptosis in human hepatocellular carcinoma cells. *Antioxidants* 9:682. doi: 10.3390/antiox9080682

Linkermann, A., Skouta, R., Himmerkus, N., Mulay, S. R., Dewitz, C., De Zen, F., et al. (2014).). Synchronized renal tubular cell death involves ferroptosis. *Proc. Natl. Acad. Sci. U.S.A.* 111, 16836–16841. doi: 10.1073/pnas.1415518111

Liu, J., Kang, R., and Tang, D. (2020a). ESCRT-III-mediated membrane repair in cell death and tumor resistance. *Cancer Gene Ther.* doi: 10.1038/s41417-020-0200-0 [Epub ahead of print].

Liu, J., Kuang, F., Kroemer, G., Klionsky, D. J., Kang, R., and Tang, D. (2020b). Autophagy-dependent ferroptosis: machinery and regulation. *Cell Chem. Biol.* 27, 420–435. doi: 10.1016/j.chembiol.2020.02.005

Liu, Y., Wang, Y., Liu, J., Kang, R., and Tang, D. (2020c). Interplay between MTOR and GPX4 signaling modulates autophagy-dependent ferroptotic cancer cell death. *Cancer Gene Ther.* doi: 10.1038/s41417-020-0182-y [Epub ahead of print].

Liu, Y., Wang, Y., Liu, J., Kang, R., and Tang, D. (2020d). The circadian clock protects against ferroptosis-induced sterile inflammation. *Biochem. Biophys. Res. Commun.* 525, 620–625. doi: 10.1016/j.bbrc.2020.02.142

Llabani, E., Hicklin, R. W., Lee, H. Y., Motika, S. E., Crawford, L. A., Weerapana, E., et al. (2019). Diverse compounds from pleuromutilin lead to a thioredoxin inhibitor and inducer of ferroptosis. *Nat. Chem.* 11, 521–532. doi: 10.1038/s41557-019-0261-6

Lovatt, M., Adnan, K., Kocaba, V., Dirisamer, M., Peh, G. S. L., and Mehta, J. S. (2020). Peroxiredoxin-1 regulates lipid peroxidation in corneal endothelial cells. *Redox Biol.* 30:101417. doi: 10.1016/j.redox.2019.101417

Lu, B., Chen, X. B., Hong, Y. C., Zhu, H., He, Q. J., Yang, B., et al. (2019). Identification of PRDX6 as a regulator of ferroptosis. *Acta Pharmacol. Sin.* 40, 1334–1342. doi: 10.1038/s41401-019-0233-9

Martin-Sanchez, D., Ruiz-Andres, O., Poveda, J., Carrasco, S., Cannata-Ortiz, P., Sanchez-Nino, M. D., et al. (2017). Ferroptosis, but not necroptosis, is important in nephrotoxic folic acid-induced AKI. *J. Am. Soc. Nephrol.* 28, 218–229. doi: 10.1681/ASN.2015121376

Matsushita, M., Freigang, S., Schneider, C., Conrad, M., Bornkamm, G. W., and Kopf, M. (2015). T cell lipid peroxidation induces ferroptosis and prevents immunity to infection. *J. Exp. Med.* 212, 555–568. doi: 10.1084/jem.20140857

Mayr, L., Grabherr, F., Schwarzler, J., Reitmeier, I., Sommer, F., Gehmacher, T., et al. (2020). Dietary lipids fuel GPX4-restricted enteritis resembling Crohn's disease. *Nat. Commun.* 11:1775. doi: 10.1038/s41467-020-15646-6

McBean, G. J. (2012). The transsulfuration pathway: a source of cysteine for glutathione in astrocytes. *Amino Acids* 42, 199–205. doi: 10.1007/s00726-011-0864-8

Muller, T., Dewitz, C., Schmitz, J., Schroder, A. S., Brasen, J. H., Stockwell, B. R., et al. (2017). Necroptosis and ferroptosis are alternative cell death pathways that operate in acute kidney failure. *Cell Mol. Life Sci.* 74, 3631–3645. doi: 10.1007/s00018-017-2547-4

NaveenKumar, S. K., Hemshekhar, M., Kemparaju, K., and Girish, K. S. (2019). Hemin-induced platelet activation and ferroptosis is mediated through ROS-driven proteasomal activity and inflammasome activation: protection by melatonin. *Biochim. Biophys. Acta Mol. Basis Dis.* 1865, 2303–2316. doi: 10.1016/j.bbadis.2019.05.009

Neitemeier, S., Jelinek, A., Laino, V., Hoffmann, L., Eisenbach, I., Eying, R., et al. (2017). BID links ferroptosis to mitochondrial cell death pathways. *Redox Biol.* 12, 558–570. doi: 10.1016/j.redox.2017.03.007

Ou, Y., Wang, S. J., Li, D., Chu, B., and Gu, W. (2016). Activation of SAT1 engages polyamine metabolism with p53-mediated ferroptotic responses. *Proc. Natl. Acad. Sci. U.S.A.* 113, E6806–E6812. doi: 10.1073/pnas.1607152113

Pagano, G., Aiello Talamanca, A., Castello, G., Cordero, M. D., d'Ischia, M., Gadaleta, M. N., et al. (2014). Current experience in testing mitochondrial nutrients in disorders featuring oxidative stress and mitochondrial dysfunction: rational design of chemoprevention trials. *Int. J. Mol. Sci.* 15, 20169–20208. doi: 10.3390/ijms151120169

Park, E. J., Park, Y. J., Lee, S. J., Lee, K., and Yoon, C. (2019). Whole cigarette smoke condensates induce ferroptosis in human bronchial epithelial cells. *Toxicol. Lett.* 303, 55–66. doi: 10.1016/j.toxlet.2018.12.007

Qi, W., Li, Z., Xia, L., Dai, J., Zhang, Q., Wu, C., et al. (2019). LncRNA GABPB1-AS1 and GABPB1 regulate oxidative stress during erastin-induced ferroptosis in HepG2 hepatocellular carcinoma cells. *Sci. Rep.* 9:16185. doi: 10.1038/s41598-019-52837-8

Ran, Q., Van Remmen, H., Gu, M., Qi, W., Roberts, L. J. II, Prolla, T., et al. (2003). Embryonic fibroblasts from Gpx4+/- mice: a novel model for studying the role of membrane peroxidation in biological processes. *Free Radic. Biol. Med.* 35, 1101–1109. doi: 10.1016/s0891-5849(03)00466-0

Riddick, D. S., Ding, X., Wolf, C. R., Porter, T. D., Pandey, A. V., Zhang, Q. Y., et al. (2013). NADPH-cytochrome P450 oxidoreductase: roles in physiology, pharmacology, and toxicology. *Drug Metab. Dispos.* 41, 12–23. doi: 10.1124/dmd.112.048991

Schweichel, J. U., and Merker, H. J. (1973). The morphology of various types of cell death in prenatal tissues. *Teratology* 7, 253–266. doi: 10.1002/tera.1420070306

Shimada, K., Skouta, R., Kaplan, A., Yang, W. S., Hayano, M., Dixon, S. J., et al. (2016). Global survey of cell death mechanisms reveals metabolic regulation of ferroptosis. *Nat. Chem. Biol.* 12, 497–503. doi: 10.1038/nchembio.2079

Shintoku, R., Takigawa, Y., Yamada, K., Kubota, C., Yoshimoto, Y., Takeuchi, T., et al. (2017). Lipoxygenase-mediated generation of lipid peroxides enhances ferroptosis induced by erastin and RSL3. *Cancer Sci.* 108, 2187–2194. doi: 10.1111/cas.13380

Skouta, R., Dixon, S. J., Wang, J., Dunn, D. E., Orman, M., Shimada, K., et al. (2014). Ferrostatins inhibit oxidative lipid damage and cell death in diverse disease models. *J. Am. Chem. Soc.* 136, 4551–4556. doi: 10.1021/ja411006a

Song, X., Zhu, S., Chen, P., Hou, W., Wen, Q., Liu, J., et al. (2018). AMPK-mediated BECN1 phosphorylation promotes ferroptosis by directly blocking system Xc(-) Activity. *Curr. Biol.* 28, 2388.e5–2399.e5. doi: 10.1016/j.cub.2018.05.094

Stockwell, B. R., Friedmann Angeli, J. P, Bayir, H., Bush, A. I., Conrad, M., Dixon, S. J., et al. (2017). Ferroptosis: a regulated cell death nexus linking metabolism, redox biology, and disease. *Cell* 171, 273–285. doi: 10.1016/j.cell.2017.09.021

Sun, X., Niu, X., Chen, R., He, W., Chen, D., Kang, R., et al. (2016a). Metallothionein-1G facilitates sorafenib resistance through inhibition of ferroptosis. *Hepatology* 64, 488–500. doi: 10.1002/hep.28574

Sun, X., Ou, Z., Chen, R., Niu, X., Chen, D., Kang, R., et al. (2016b). Activation of the p62-Keap1-NRF2 pathway protects against ferroptosis in hepatocellular carcinoma cells. *Hepatology* 63, 173–184. doi: 10.1002/hep.28251

Tan, S., Schubert, D., and Maher, P. (2001). Oxytosis: a novel form of programmed cell death. *Curr. Top. Med. Chem.* 1, 497–506. doi: 10.2174/1568026013394741

Tang, D., Kang, R., Berghe, T. V., Vandenabeele, P., and Kroemer, G. (2019). The molecular machinery of regulated cell death. *Cell Res.* 29, 347–364. doi: 10.1038/s41422-019-0164-5

Teran, E., Hernandez, I., Tana, L., Teran, S., Galaviz-Hernandez, C., Sosa-Macias, M., et al. (2018). Mitochondria and coenzyme Q10 in the pathogenesis of preeclampsia. *Front. Physiol.* 9:1561. doi: 10.3389/fphys.2018.01561

Tsurusaki, S., Tsuchiya, Y., Koumura, T., Nakasone, M., Sakamoto, T., Matsuoka, M., et al. (2019). Hepatic ferroptosis plays an important role as the trigger for initiating inflammation in nonalcoholic steatohepatitis. *Cell Death Dis.* 10:449. doi: 10.1038/s41419-019-1678-y

Wang, D., Peng, Y., Xie, Y., Zhou, B., Sun, X., Kang, R., et al. (2016). Antiferroptotic activity of non-oxidative dopamine. *Biochem. Biophys. Res. Commun.* 480, 602–607. doi: 10.1016/j.bbrc.2016.10.099

Wang, Y., Liua, Y., Liua, J., Kang, R., and Tang, D. (2020). NEDD4L-Mediated LTF protein degradation limits ferroptosis. *Biochem. Biophys. Res. Commu.* 13, 506–515. doi: 10.1021/acschembio.7b01082

Wang, Y., and Tang, M. (2019). PM2.5 induces ferroptosis in human endothelial cells through iron overload and redox imbalance. *Environ. Pollut.* 254:112937. doi: 10.1016/j.envpol.2019.07.105

Wei, M. C., Zong, W. X., Cheng, E. H., Lindsten, T., Panoutsakopoulou, V., Ross, A. J., et al. (2001). Proapoptotic BAX and BAK: a requisite gateway to mitochondrial dysfunction and death. *Science* 292, 727–730. doi: 10.1126/science.1059108

Wen, Q., Liu, J., Kang, R., Zhou, B., and Tang, D. (2019). The release and activity of HMGB1 in ferroptosis. *Biochem. Biophys. Res. Commun.* 510, 278–283. doi: 10.1016/j.bbrc.2019.01.090

Wenzel, S. E., Tyurina, Y. Y., Zhao, J., St Croix, C. M, Dar, H. H., Mao, G., et al. (2017). PEBP1 wardens ferroptosis by enabling lipoxygenase generation of lipid death signals. *Cell* 171, 628.e26–641.e26. doi: 10.1016/j.cell.2017.09.044

Werner, E. R., Blau, N., and Thony, B. (2011). Tetrahydrobiopterin: biochemistry and pathophysiology. *Biochem. J.* 438, 397–414. doi: 10.1042/BJ20110293

Wu, M., Xu, L. G., Li, X., Zhai, Z., and Shu, H. B. (2002). AMID, an apoptosis-inducing factor-homologous mitochondrion-associated protein, induces caspase-independent apoptosis. *J. Biol. Chem.* 277, 25617–25623. doi: 10.1074/jbc.M202285200

Wu, Y., Zhang, S., Gong, X., Tam, S., Xiao, D., Liu, S., et al. (2020). The epigenetic regulators and metabolic changes in ferroptosis-associated cancer progression. *Mol. Cancer* 19:39. doi: 10.1186/s12943-020-01157-x

Wu, Z., Geng, Y., Lu, X., Shi, Y., Wu, G., Zhang, M., et al. (2019). Chaperone-mediated autophagy is involved in the execution of ferroptosis. *Proc. Natl. Acad. Sci. U.S.A.* 116, 2996–3005. doi: 10.1073/pnas.1819728116

Xie, Y., Hou, W., Song, X., Yu, Y., Huang, J., Sun, X., et al. (2016). Ferroptosis: process and function. *Cell Death Differ.* 23, 369–379. doi: 10.1038/cdd.2015.158

Xie, Y., Kang, R., Sun, X., Zhong, M., Huang, J., Klionsky, D. J., et al. (2015). Posttranslational modification of autophagy-related proteins in macroautophagy. *Autophagy* 11, 28–45. doi: 10.4161/15548627.2014.984267

Xie, Y., Kuang, F., Liu, J., Tang, D., and Kang, R. (2020a). DUSP1 blocks autophagy-dependent ferroptosis in pancreatic cancer. *J. Pancreatol.* 319, 322–332. doi: 10.1016/j.jconrel.2020.01.008

Xie, Y., Li, J., Kang, R., and Tang, D. (2020b). Interplay between lipid metabolism and autophagy. *Front. Cell Dev. Biol.* 8:431. doi: 10.3389/fcell.2020.00431

Xie, Y., Zhu, S., Song, X., Sun, X., Fan, Y., Liu, J., et al. (2017). The tumor suppressor p53 limits ferroptosis by blocking DPP4 activity. *Cell Rep.* 20, 1692–1704. doi: 10.1016/j.celrep.2017.07.055

Yagoda, N., von Rechenberg, M., Zaganjor, E., Bauer, A. J., Yang, W. S., Fridman, D. J., et al. (2007). RAS-RAF-MEK-dependent oxidative cell death involving voltage-dependent anion channels. *Nature* 447, 864–868. doi: 10.1038/nature05859

Yang, J., Liu, X., Bhalla, K., Kim, C. N., Ibrado, A. M., Cai, J., et al. (1997). Prevention of apoptosis by Bcl-2: release of cytochrome c from mitochondria blocked. *Science* 275, 1129–1132. doi: 10.1126/science.275.5303.1129

Yang, M., Chen, P., Liu, J., Zhu, S., Kroemer, G., Klionsky, D. J., et al. (2019). Clockophagy is a novel selective autophagy process favoring ferroptosis. *Sci. Adv.* 5:eaaw2238. doi: 10.1126/sciadv.aaw2238

Yang, W. H., Ding, C. C., Sun, T., Rupprecht, G., Lin, C. C., Hsu, D., et al. (2019). The hippo pathway effector TAZ regulates ferroptosis in renal cell carcinoma. *Cell Rep.* 28, 2501.e4–2508.e4. doi: 10.1016/j.celrep.2019.07.107

Yang, W. H., Huang, Z., Wu, J., Ding, C. C., Murphy, S. K., and Chi, J. T. (2020a). A TAZ-ANGPTL4-NOX2 axis regulates ferroptotic cell death and chemoresistance in epithelial ovarian cancer. *Mol. Cancer Res.* 18, 79–90. doi: 10.1158/1541-7786.MCR-19-0691

Yang, Y., Luo, M., Zhang, K., Zhang, J., Gao, T., Connell, D. O., et al. (2020b). Nedd4 ubiquitylates VDAC2/3 to suppress erastin-induced ferroptosis in melanoma. *Nat. Commun.* 11:433. doi: 10.1038/s41467-020-14324-x

Yang, W. S., Kim, K. J., Gaschler, M. M., Patel, M., Shchepinov, M. S., and Stockwell, B. R. (2016). Peroxidation of polyunsaturated fatty acids by lipoxygenases drives ferroptosis. *Proc. Natl. Acad. Sci. U.S.A.* 113, E4966–E4975. doi: 10.1073/pnas.1603244113

Yang, W. S., SriRamaratnam, R., Welsch, M. E., Shimada, K., Skouta, R., Viswanathan, V. S., et al. (2014). Regulation of ferroptotic cancer cell death by GPX4. *Cell* 156, 317–331. doi: 10.1016/j.cell.2013.12.010

Yang, W. S., and Stockwell, B. R. (2008). Synthetic lethal screening identifies compounds activating iron-dependent, nonapoptotic cell death in oncogenic-RAS-harboring cancer cells. *Chem. Biol.* 15, 234–245. doi: 10.1016/j.chembiol.2008.02.010

Yoshida, M., Minagawa, S., Araya, J., Sakamoto, T., Hara, H., Tsubouchi, K., et al. (2019). Involvement of cigarette smoke-induced epithelial cell ferroptosis in COPD pathogenesis. *Nat. Commun.* 10:3145. doi: 10.1038/s41467-019-10991-7

Youle, R. J., and Strasser, A. (2008). The BCL-2 protein family: opposing activities that mediate cell death. *Nat. Rev. Mol. Cell Biol.* 9, 47–59. doi: 10.1038/nrm2308

Yuan, H., Li, X., Zhang, X., Kang, R., and Tang, D. (2016). Identification of ACSL4 as a biomarker and contributor of ferroptosis. *Biochem. Biophys. Res. Commun.* 478, 1338–1343. doi: 10.1016/j.bbrc.2016.08.124

Zeng, T., Deng, G., Zhong, W., Gao, Z., Ma, S., Mo, C., et al. (2020). Indoleamine 2, 3-dioxygenase 1enhanceshepatocytes ferroptosis in acute immune hepatitis associated with excess nitrative stress. *Free Radic. Biol. Med.* 58, 974–986. doi: 10.1016/j.freeradbiomed.2020.01.009

Zhang, H., He, Y., Wang, J. X., Chen, M. H., Xu, J. J., Jiang, M. H., et al. (2020). miR-30-5p-mediated ferroptosis of trophoblasts is implicated in the pathogenesis of preeclampsia. *Redox Biol.* 29: 101402. doi: 10.1016/j.redox.2019.101402

Zhang, Y. H., Wang, D. W., Xu, S. F., Zhang, S., Fan, Y. G., Yang, Y. Y., et al. (2018). Alpha-Lipoic acid improves abnormal behavior by mitigation of oxidative stress, inflammation, ferroptosis, and tauopathy in P301S Tau transgenic mice. *Redox Biol.* 14, 535–548. doi: 10.1016/j.redox.2017.11.001

Zhang, Y., Shi, J., Liu, X., Feng, L., Gong, Z., Koppula, P., et al. (2018). BAP1 links metabolic regulation of ferroptosis to tumour suppression. *Nat. Cell Biol.* 20, 1181–1192. doi: 10.1038/s41556-018-0178-0

Zorov, D. B., Juhaszova, M., and Sollott, S. J. (2014). Mitochondrial reactive oxygen species (ROS) and ROS-induced ROS release. *Physiol. Rev.* 94, 909–950. doi: 10.1152/physrev.00026.2013

Zou, Y., Li, H., Graham, E. T., Deik, A. A., Eaton, J. K., Wang, W., et al. (2020). Cytochrome P450 oxidoreductase contributes to phospholipid peroxidation in ferroptosis. *Nat. Chem. Biol.* 16, 302–309. doi: 10.1038/s41589-020-0472-6

Conflict of Interest: The authors declare that the research was conducted in the absence of any commercial or financial relationships that could be construed as a potential conflict of interest.

frontiers in Cell and Developmental Biology

ORIGINAL RESEARCH
published: 30 October 2020
doi: 10.3389/fcell.2020.595253

ICP6 Prevents RIP1 Activation to Hinder Necroptosis Signaling

Hong Hu[1,2,3], Guoxiang Wu[1,3], Zhaoqian Shu[1,3], Dandan Yu[1,3], Ning Nan[1,3], Feiyang Yuan[1,3], Xiaoyan Liu[1] and Huayi Wang[1]**

[1] School of Life Science and Technology, ShanghaiTech University, Shanghai, China, [2] CAS Center for Excellence in Molecular Cell Science, Shanghai Institute of Biochemistry and Cell Biology, Chinese Academy of Sciences, Shanghai, China, [3] University of Chinese Academy of Sciences, Beijing, China

Necroptosis is a type of programmed necrosis which depends on the activation of receptor-interacting protein kinase 3 (RIP3). Herpes simplex virus type 1 (HSV-1) is known to block necroptosis by the viral protein ICP6 in human cells, but its specific inhibitory mechanism is not fully understood. Here we reported that ICP6 could promote rather than suppress the formation of necrosome, the necroptosis signaling complex containing RIP3 and upstream regulator receptor-interacting protein kinase 1 (RIP1), but blocked RIP3 activation. Moreover, ICP6 could reduce the necroptosis-specific auto-phosphorylation of RIP1 regardless of the presence of RIP3. These results indicate that ICP6 block necroptosis through preventing RIP1 activation dependent signal transduction in necrosome.

Keywords: necrosome, RIP3, necroptosis, RIP1, ICP6

OPEN ACCESS

Edited by:
Yinan Gong,
University of Pittsburgh, United States

Reviewed by:
Xin Chen,
Xiamen University, China
Sudan He,
Chinese Academy of Medical Sciences, Suzhou Institute of Systems Medicine (ISM), China
Tudor Moldoveanu,
St. Jude Children's Research Hospital, United States

****Correspondence:***
Hong Hu
huhong@shanghaitech.edu.cn;
huhongdcjz@163.com
Huayi Wang
wanghuayi@shanghaitech.edu.cn

Specialty section:
This article was submitted to Cell Death and Survival, a section of the journal Frontiers in Cell and Developmental Biology

Received: *15 August 2020*
Accepted: *13 October 2020*
Published: *30 October 2020*

Citation:
Hu H, Wu G, Shu Z, Yu D, Nan N, Yuan F, Liu X and Wang H (2020) ICP6 Prevents RIP1 Activation to Hinder Necroptosis Signaling. Front. Cell Dev. Biol. 8:595253. doi: 10.3389/fcell.2020.595253

INTRODUCTION

Under the selection pressure, the pathogen and the host are engaging in a long-term defense and counter-defense war (Mocarski et al., 2012; Mossman and Weller, 2015). Cell death play an important role in the mammalian host defense system when pathogens invade (Wang X. et al., 2014). There are two classical forms of programmed cell death: apoptosis and programmed necrosis. Apoptosis is characterized by cell shrinkage, chromosomal DNA fragmentation, and the formation of apoptotic bodies (Kerr et al., 1972). But the cell membrane is intact and does not cause inflammation. While necrosis is characterized by swelling of cells and organelles, rupturing cell membranes and releasing of contents and triggering inflammation and immune response (Festjens et al., 2006). Apoptosis can be stimulated by the intrinsic or extrinsic signaling pathways which depend on caspase-9 and caspase-8, respectively (Li et al., 1997; Du et al., 2000; Verhagen et al., 2000; Peter and Krammer, 2003). The extrinsic apoptosis pathway is initiated by various cytokines including tumor necrosis factor (TNF). Interestingly, TNF can also induce cell necroptosis, a type of programmed necrosis when caspase-8 is inhibited (Vercammen et al., 1998). The signaling of necroptosis is dependent of a protein complex called necrosome, which contains receptor-interacting protein kinase 1 (RIP1), receptor-interacting protein kinase 3 (RIP3), and mixed lineage kinase domain-like protein (MLKL) (Holler et al., 2000; Degterev et al., 2005; Cho et al., 2009; He et al., 2009; Zhang et al., 2009; Sun et al., 2012; Zhao et al., 2012). The necrosome is initiated with the binding of RIP1-RIP3 through their RIP homotypic interaction motif (RHIM) (Sun et al., 2002). In necrosome, the RIP1 and RIP3 is sequentially activated (He et al., 2009). Then MLKL is recruited and phosphorylated by RIP3, which induce MLKL to form oligomers and migrate to the

membrane (Wang H. et al., 2014). Finally, MLKL destroys the integrity of the cell membrane and causes cell rupture (Su et al., 2014; Wang H. et al., 2014).

Pathogens and hosts are constantly evolving for survival. Upon virus infection, the conventional strategy of host is to initiate apoptosis of infected cells, thus limiting the amplification and spread of the virus (Chan et al., 2015; Mossman and Weller, 2015). However, many viruses have evolved counteractive effectors such as the inhibitors of caspase (IAPs) to inhibit apoptosis (Kaiser et al., 2013). Usually, necroptosis signaling is supervised by caspase-8 which can cleavage RIP1 and RIP3 to prevent necrosome formation (Lin et al., 1999; Feng et al., 2007). Therefore, the expression of viral IAPs will sensitize infected cells to necroptosis. Consisted with that, RIP3-deficent mice are developmental normal but exhibited severely impaired virus-induced necrosis and restriction of viral amplification (Cho et al., 2009). Necroptosis is regarded as an alternative defense pathway in the infected cells, when apoptosis is inhibited (Chan et al., 2015; Mossman and Weller, 2015). Although necroptosis is effective to inhibit many virus amplifications, some viruses such as herpes simplex virus type 1 (HSV-1) and murine cytomegalovirus (MCMV) can block necroptosis signaling by special viral effectors, ICP6 and M45 (Upton et al., 2010; Guo et al., 2015; Huang et al., 2015; Yu et al., 2016). The ICP6 (from HSV-1) and M45 (from MCMV) are homologous, with similar domain structures, which contain an N-terminal RHIM domain and a C-terminal ribonucleotide reductase (RNR) large subunit (R1)–homology domain (Lembo and Brune, 2009). The inhibitory function of M45 in necroptosis pathway is solely dependent on its RHIM, which binds with RIP3-RHIM and form hetero-amyloids to prevent RIP3 activation by disturbing inter-filament assembly of RIP3-RHIM (Hu et al., 2020). But the ICP6-RHIM alone do not block RIP3 activation, suggesting a different mechanism to disrupt necroptosis signaling (Hu et al., 2020).

In this study, we confirmed the previous finding that both the N-terminal RHIM and C-terminal R1 domains of ICP6 are required for its inhibitory function. And ICP6 block necroptosis is not due to prevent RIP1-RIP3 binding and necrosome initiation. ICP6 could participate in necrosome formation with interaction with both RIP1 and RIP3 upon necroptosis induction. Interestingly, ICP6 can attenuate necroptosis signal induced auto-phosphorylation of RIP1 regardless of the presence of RIP3, suggesting ICP6 hinder necroptosis signaling through preventing RIP1 activation.

MATERIALS AND METHODS

Reagents and Antibodies

The Z-VAD and Smac mimetic were used as described previously (Wang H. et al., 2014). Recombinant TNF was purified in our laboratory, AP20187 (HY-13992) was purchased from MCE. ICP6 polyclonal antibodies can be obtained by injecting His-ICP6 (1-177 amino acids) expressed in *E. coli* into rabbits. The following antibodies were used in this study: anti-Flag M2 (F3165), anti-Myc (SAB4700448) (Sigma); anti-RIP1 (610459) (BD Biosciences); anti-RIP1 (D94C12), anti-phospho-RIP1 (65746S) and anti-hRIP3 (13526S) (Cell Signaling Technology); anti-FKBP (ab108420) (Abcam); and anti-actin (PM053-7) (MBL).

Cell Survival Assay

Drugs were diluted and added into cell culture plate. Necroptosis was induced by adding the final concentrations of 10 ng/ml TNF-α (T), 100 nM Smac mimetics (S), and 20 μM Z-VAD (Z). Cell survival assay was performed by using the CellTiter-Glo Luminescent Cell viability Assay Kit and performed according to the manufacturer's instructions. Luminescence was recorded with an EnSpire Multimode Plate Reader from PerkinElmer.

Cell Culture and Stable Cell Lines

HEK293T cells, HeLa cells, and HT-29 human colon cancer cells were obtained from cell bank of CAS (Shanghai). HeLa-RIP3 (HeLa with exogenous Flag-tagged RIP3 expression) cells were established as described previously (He et al., 2009; Sun et al., 2012; Wang H. et al., 2014). HT-29 (*RIP3*-KO) cells were generated by using the CRISPR/Cas9 editing technique. KO cells were identified by target site sequencing. Cells would stably express related proteins after lentivirus infection. All cells were cultured in DMEM/L-glutamine without sodium pyruvate (HyClone). All media were supplemented with 10% Foundation^{TM} FBS (Gemini) and 100 units/ml penicillin/streptomycin (HyClone). All cells were cultured at 37°C, 5% CO_2, and the standard PCR method was negative for mycoplasma. EZ transfection (Shanghai Life iLab Biotech Co., Ltd.) was used for cell transfection according to the instructions.

Plasmids and Molecular Cloning

ICP6 cDNA was amplified by PCR from a reverse transcription cDNA library. Standard PCR and cloning methods were used to clone the full-length or mutated cDNAs of ICP6 into the lentiviral vector pCDH-CMV-MCS-EF1-copGFP (Addgene). All plasmids have been verified by DNA sequencing. The detailed information of primer sequence can be provided upon request.

Lentivirus Preparation and Infection

For lentivirus production, HEK293T cells were transfected with lentiviral vectors (pCDH-CMV-MCS-EF1-copGFP/copRFP) and virus packing plasmids (psPAX2 and pMD2.g, Addgene) by using EZ transfection reagents (Shanghai Life-iLab Biotech Co., Ltd.). After 48 h, the virus-containing medium was collected and added to the cells according to the instructions and the final concentration of polybrene was 10 μg/ml. After 24 h, the infection medium was replaced with fresh medium.

CRISPR/Cas9

The Cas9-target sites are as follows: human RIP3: 5′-GACAGGGTCCGGGGAGCCAG-3′ and 5′-GCAAGCCGGGCCTGAGACTCC-3′. The Cas9-target sites were cloned into the PX330 (Addgene) vector. All plasmids were verified by DNA sequencing. The details of the primer sequences are available upon request.

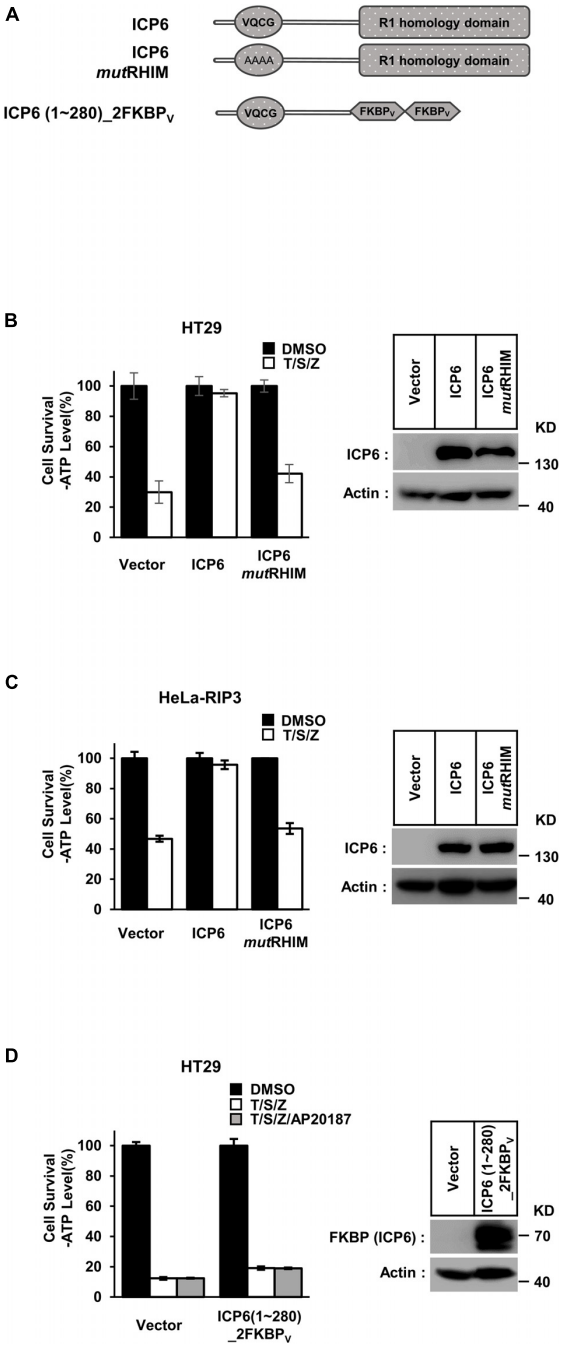

FIGURE 1 | Either RHIM or R1 domain of ICP6 is indispensable for necroptosis blockage. **(A)** Schematic representation of full-length ICP6 with or without RHIM mutations (upper). ICP6 N-terminal portion (1-280) was fused with tandem FKBPv domain at its C-terminus (lower). **(B,C)** The RHIM of ICP6 is essential for inhibition of necroptosis. The HT29 and HeLa-RIP3 (HeLa with exogenous Flag-tagged RIP3 expression) cells stably expressing ICP6 protein by lentivirus infection were stimulated with T/S/Z for 10 h. The number of surviving cells were analyzed by measuring ATP levels using CellTiter-Glo kit **(left)**. The data are represented as the mean ± standard deviation (SD) from at least three independent experiments. Abbreviations are as follows: T, TNF-α; S, Smac mimetic; Z, Z-VAD. The final concentrations of 10 ng/ml TNF-α, 100 nM Smac mimetic, and 20 μM Z-VAD were used. Identical

(Continued)

FIGURE 1 | Continued

concentrations of these necroptosis-inducing agents were used in subsequent experiments unless otherwise stated. The untreated cells were harvested and whole cell extracts were prepared and normalized to the same concentration. Aliquots of 20 μg whole-cell lysates were subjected to SDS-PAGE followed by western blot analysis of ICP6 and β-Actin which is shown as a loading control **(right)**. **(D)** The R1-homology domain of ICP6 has a unique function in inhibiting necroptosis. HT29 cells were infected with lentiviruses encoding ICP6 (1-280)_2FKBPv and treated with indicated stimuli. The number of surviving cells was determined by measuring ATP levels **(left)**. The ICP6 (1-280)_2FKBPv expression level was measured by western blot analysis **(right)**.

Immunoprecipitation and Immunoblotting

Cells were cultured on 10 cm dishes and grown to confluence. Cells at 90% confluence were washed once with DPBS and harvested and centrifuged at 900 rpm for 3 min. The harvested cells were lysed by lysis buffer [25 mM HEPES-NaOH (pH 7.5), 150 mM NaCl, 1% Triton, 10% glycerol, and complete protease inhibitor (Roche) and phosphatase inhibitor (Roche) cocktails] on ice for 30 min. Cell lysates were centrifuged at 15000 rpm at 4°C for 10 min. The soluble fraction was collected. The protein solution were incubated overnight with anti-Flag or anti-Myc magnetic beads at 4°C. The beads were washed three times with lysis buffer. Finally, the samples were subjected to western blotting analysis.

Immunofluorescence Staining and Confocal Microscopy

HeLa-RIP3 and HT29 cells infected with lentivirus were plated on the coverslip overnight and then treated as shown. The cells were washed once with PBS, and then fixed with 4% paraformaldehyde (PFA). The primary antibody (Flag, RIP1 or ICP6) was incubated. Then, the cells were incubated with goat anti-mouse IgG labeled with Alexa Fluor 555 (Invitrogen) for RIP1 or 633 (Invitrogen) for Flag and goat anti-rabbit IgG labeled with Alexa Fluor 647 (Invitrogen) for ICP6. Finally, the nuclei were stained with DAPI (Southern Biotech) and using the same settings for image capture and processing on the Zeiss LSM 710 laser scanning confocal microscope (63×).

Quantification and Statistical Analysis

All cell survival data are shown as the mean ± standard deviation (SD) of duplicate wells, and similar results were obtained from at least three independent experiments.

RESULTS

The R1 Domain of ICP6 Is Unique and Essential in Inhibiting Necroptosis

According to previous reports, full-length ICP6 can effectively inhibit necroptosis in human cells, but induce mouse cell necroptosis (Huang et al., 2015). It requires the structural integrity of both RHIM and R1 domain. First, we constructed

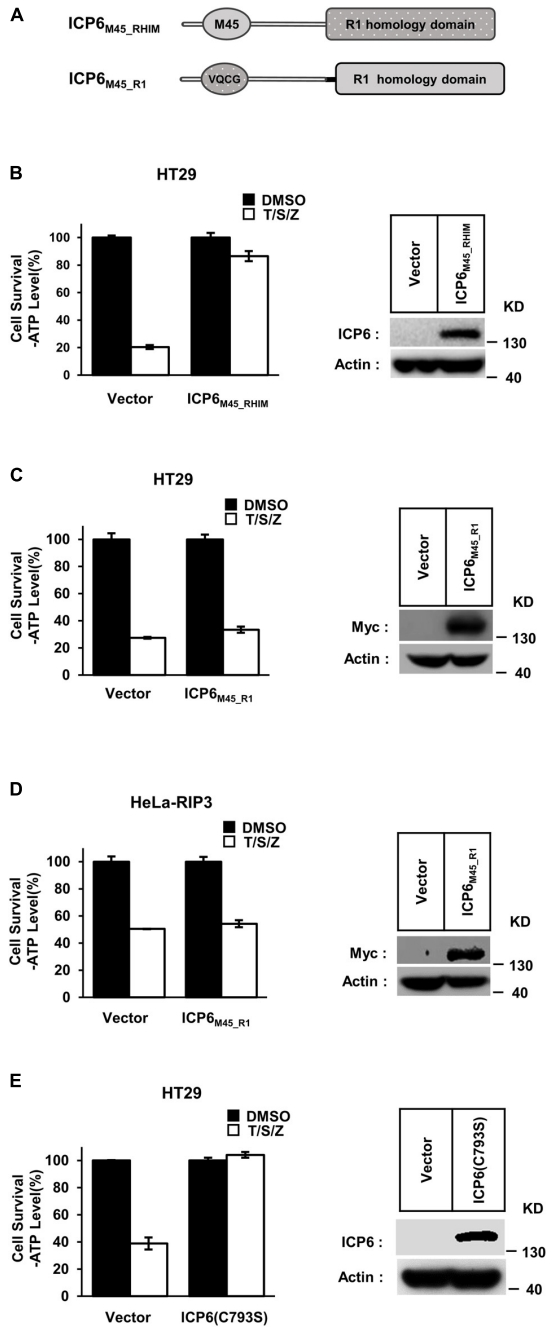

FIGURE 2 | The R1 domain of ICP6 is unique in inhibiting necroptosis. **(A)** Schematic representation of chimaeric ICP6 containing M45 RHIM and R1-homology domain. **(B)** The chimaeric ICP6 containing M45 RHIM has no effect on the inhibition of necroptosis. Necroptosis was induced by T/S/Z for 10 h. Then the cells were lysed and subjected to western blotting analysis using the indicated antibodies. **(C,D)** The R1 homology domain is important to ICP6 function. The HT29 **(C)** and Hela-RIP3 **(D)** cells with indicated lentivirus infection were treated with T/S/Z for 10 h. Cell viability was determined by measuring ATP levels **(left)**. The data are represented as the mean ± SD of duplicate wells. The expression level of $ICP6_{M45\_R1}$ was measured by western blot analysis **(right)**. **(E)** The ICP6 (C793S) has no effect on the inhibition of necroptosis. Necroptosis was induced by T/S/Z for 10 h. Then the cells were lysed and subjected to western blotting analysis using the indicated antibodies.

wild-type and RHIM-mutated ICP6 to confirm the requirement of intact ICP6-RHIM (**Figure 1A**, upper). In either human colon cancer HT29 cells with endogenously RIP3 expression or HeLa-RIP3 cells with exogenously expressed Flag-tagged RIP3, necroptosis could be induced by TNF plus a pan-caspase inhibitor Z-VAD-FMK (Z-VAD) and Smac-mimic small molecule compound (Smac-mimic). We confirmed that the expression of wild-type rather than RHIM-mutant of ICP6 could inhibit necroptosis in HT-29 and HeLa-RIP3 cells (**Figures 1B,C**). The importance of R1 domain of ICP6 has also been suggested by previous studies (Guo et al., 2015). And the function of R1 domain in ICP6-induced mouse cell necroptosis depends on the oligomeric state of R1 domain (Huang et al., 2015). So that the function of ICP6-R1 in mouse cells could be mimic by chemical (AP20187)-induced oligomerization of the tandem FKBPv domain. To investigate if oligomeric state of R1 domain could contribute its necroptosis inhibitory function in human cells. We constructed ICP6 with the R1 domain replaced by tandem FKBPv domain [ICP6 (1∼280)_2FKBP$_V$] (**Figure 1A**, lower). In HT-29 cells even if the oligomerization is induced by AP20187 (**Figure 1D**) and it also doesn't inhibition necroptosis. These results indicate that the R1 domain is essential for the inhibitory function of ICP6.

Different from ICP6, the inhibitory role of M45 in necroptosis signaling does not require R1 domain of M45. But it still needs to reveal that if the function of R1 in necroptosis repression is universal in different R1 domains. We then constructed the chimaeric ICP6 containing M45 RHIM or R1 domain ($ICP6_{M45\_RHIM}$ and $ICP6_{M45\_R1}$) (**Figure 2A**). We found that $ICP6_{M45\_RHIM}$ could effectively inhibit necroptosis in HT29 cells (**Figure 2B**). This suggests that the RHIM domain of ICP6 can be replaced by the RHIM domain of M45 in inhibiting necroptosis. In $ICP6_{M45\_R1}$ expression HT29 or HeLa-RIP3 cells, TNF-induced necroptosis was not inhibited (**Figures 2C,D**). It suggested again that the oligomeric state of R1 domain did not contribute to necroptosis inhibition since both M45-R1 and ICP6-R1 could form oligomers. Besides that, it also indicated that the R1 domain of ICP6 is special in necroptosis inhibition. The difference of R1 domain between ICP6 and M45 is that the ICP6-R1 has but M45-R1 loses the ribonucleotide reductase activity. To investigate how the enzyme activity of ICP6-R1 is necessary for necroptosis inhibition. The enzyme-dead form of ICP6 mutant (C793S) was introduced to HT-29 cells. But it showed that the mutant form of ICP6 still block necroptosis efficiently (**Figure 2E**). It suggested the function of ICP6-R1 do not require its enzyme activity.

ICP6 Promotes Necrosome Initiation but Block Necrosome Maturation

It is well known that the necrosome formed by RIP1 and RIP3 is essential for TNF-induced necroptosis. And this necroptosis signal complex is initiated by RHIM-RHIM interactions between RIP1 and RIP3. Since ICP6-RHIM is required for its function, confirmed by our data shown that RHIM-mutated ICP6 lost

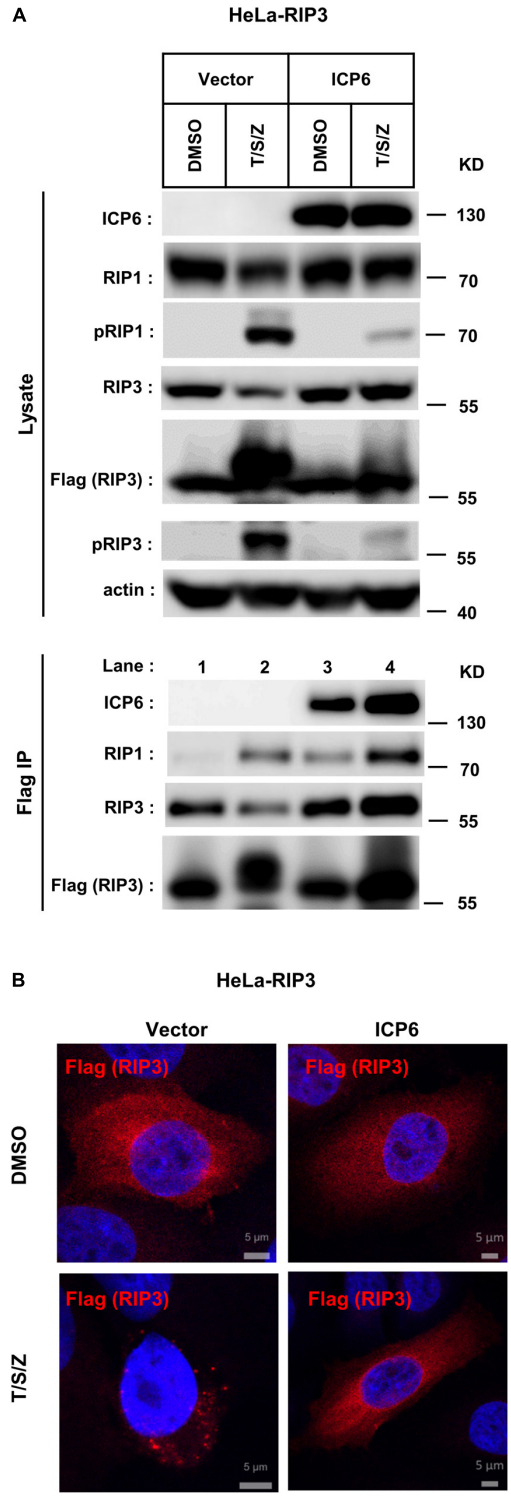

FIGURE 3 | ICP6 promotes necrosome initiation but block necrosome maturation. **(A)** HeLa-RIP3 cells (HeLa with exogenous Flag-tagged RIP3 expression) infected with empty virus (Vector) or lentiviral virus encoding ICP6 were cultured in the presence of T/S/Z for 6 h. Whole-cell lysates were subjected to immunoprecipitation with anti-Flag M2 beads. The total cell lysates and immunoprecipitates were immunoblotted with the indicated antibodies. **(B)** ICP6 inhibits the formation of RIP3 puncta. HeLa-RIP3 cells infected with empty virus (Vector) or lentiviral virus encoding ICP6 were stimulated as indicated for 6 h, and then immunostained for Flag and counterstained with DAPI. The distribution of Flag-RIP3 (Alexa Fluor 633 dye, red) was detected by immunofluorescence as described in "Materials and Methods." The scale bar represents 5 μm.

the ability to inhibit TSZ-induced necroptosis (**Figures 1B,C**), We proposed that RIP1-RIP3 interactions maybe disturbed by ICP6-RHIM, so that it inhibited the necrosome formation and necroptosis signal transduction. To verify that, we performed co-immunoprecipitation by Flag-tagged RIP3 in HeLa-RIP3 cells. It showed that the protein level of co-immunoprecipitated RIP1 is not reduced but increased in TSZ treated cells with ICP6 expression (**Figure 3A**, lane 3 vs. lane 4). Moreover, compared with empty vector, the presence of ICP6 enhanced the interaction between RIP1 and RIP3 in the DMSO-treated cells (**Figure 3A**, lane 1 vs. lane 3). Different from the binding of RIP1-RIP3 which depended on necroptosis stimuli (lane 2), ICP6 could bind with RIP3 in normal conditions (lane 3), but was also enhanced upon necroptosis induction (lane 4). Altogether, these data suggested that ICP6 did not disturb but promoted RIP1-RIP3 binding and necrosome initiation. Then, the effect of ICP6 at step of necrosome maturation was investigated. The necrosome maturation is featured by RIP3 self-assembly as puncta in necrotic cells (He et al., 2009). As shown that TSZ-induced RIP3 puncta were observed in control cells transfected with empty vector. However, in ICP6-expressing cells, RIP3 remained uniformly diffuse in the cytosol, no matter whether necroptosis was induced or not (**Figure 3B**). The co-immunoprecipitation results showed that necrosomes are made of RIP1-RIP3 or RIP1-RIP3-ICP6 (when ICP6 was expressed) complexes (**Figure 3A**). We then using RIP1 antibody to detect the necrosome puncta in both Hela-RIP3 and HT-29 cells, the RIP1 puncta appeared after necroptosis induction, and ICP6 expression blocked the T/S/Z-induced RIP1 puncta formation (**Figures 4A,B**). Besides that, the RIP1 and ICP6 signals partially overlapped and were diffused in cytosol (**Figures 4A,B**). It confirmed the necrosome puncta only reflect the matured necrosome. So that, ICP6 promotes necrosome initiation but block necrosome maturation. The premature state of necrosome was featured as decreased auto-phosphorylation of RIP1 and RIP3 (**Figure 3A**, lane 2 vs. lane 4). Since the RIP1 activation (indicted by auto-phosphorylation) is upstream of RIP3 activation, it suggested ICP6 blocks necroptosis signaling by targeting on RIP1.

The Inhibition of RIP1 Auto-Phosphorylation by ICP6 Is RIP3-Independent

ICP6 does not inhibit the formation of RIP1-RIP3 necrosome but invade into this necroptosis signal complex. Then we want to know if the blockage of RIP1 activation by ICP6 needs RIP3. We first examined the binding between ICP6 and RIP1 in HT29 cells with *RIP3* knockout. The co-immunoprecipitation results

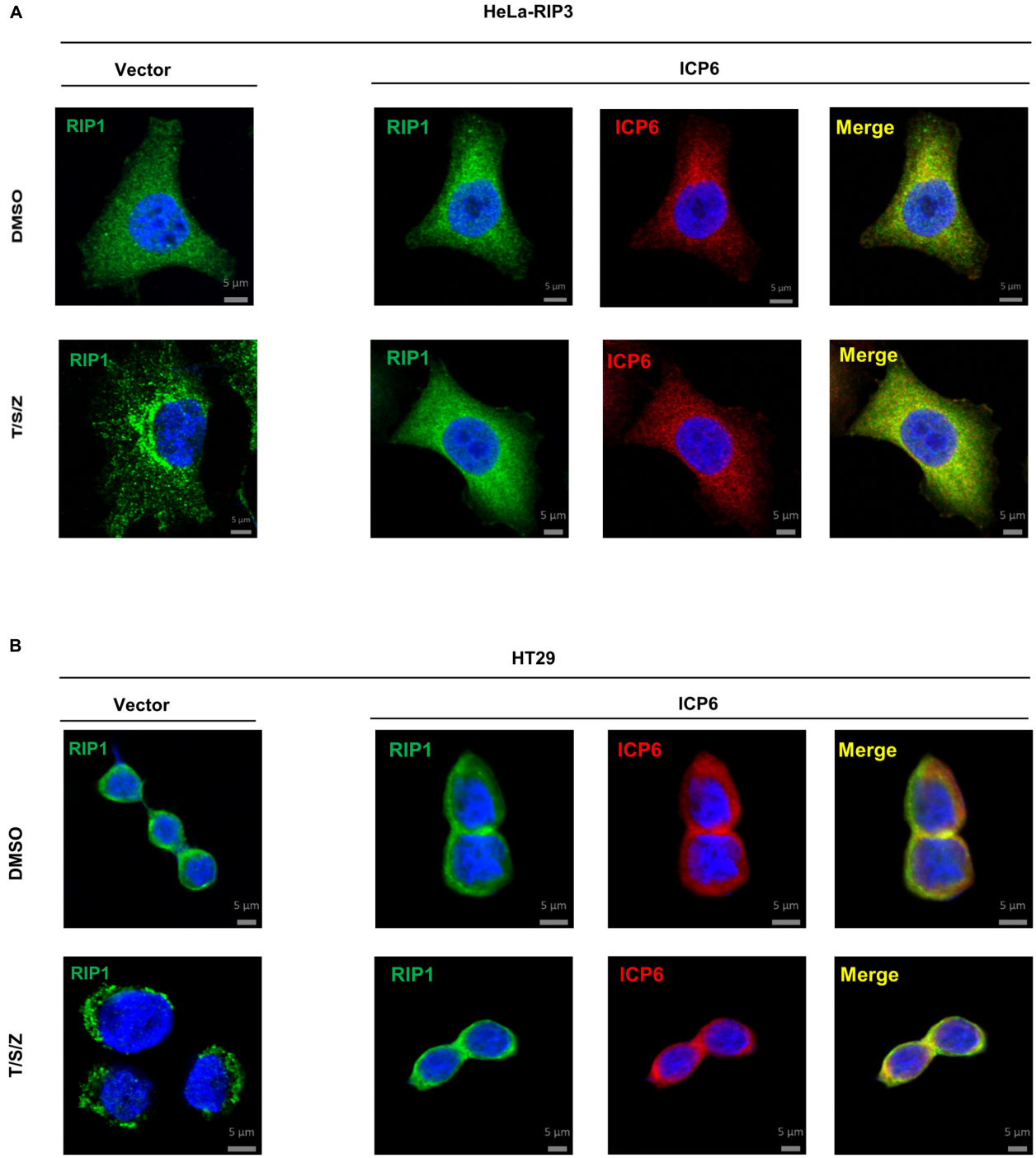

FIGURE 4 | ICP6 inhibits the formation of RIP1 puncta. **(A,B)** HeLa-RIP3 and HT29 cells infected with empty virus (Vector) or lentiviral virus encoding ICP6 were stimulated as indicated for 6 h, and then immunostained for RIP1, ICP6, and counterstained with DAPI. The distribution of RIP1 (Alexa Fluor 555 dye, green) and ICP6 (Alexa Fluor 647 dye, red) were detected by immunofluorescence as described in "Materials and Methods". The scale bar represents 5 μm.

showed that wild-type rather than RHIM mutant of ICP6 bind with RIP1 in DMSO treated control cells (**Figure 5A**, lane 3 vs. lane 5). Interestingly, both wild-type and RHIM mutant form of ICP6 interact with RIP1 upon necroptosis induction (**Figure 5A**, lane 4 vs. lane 6). Thus, these results demonstrated that ICP6 could directly interact with RIP1 in absence of RIP3. Then, the inhibition of RIP1 auto-phosphorylation by ICP6 was checked in *Rip3* knockout HT29 cells. The results showed that whether RIP3 is present or not, the increment of RIP1 auto-phosphorylation level was attenuated when ICP6

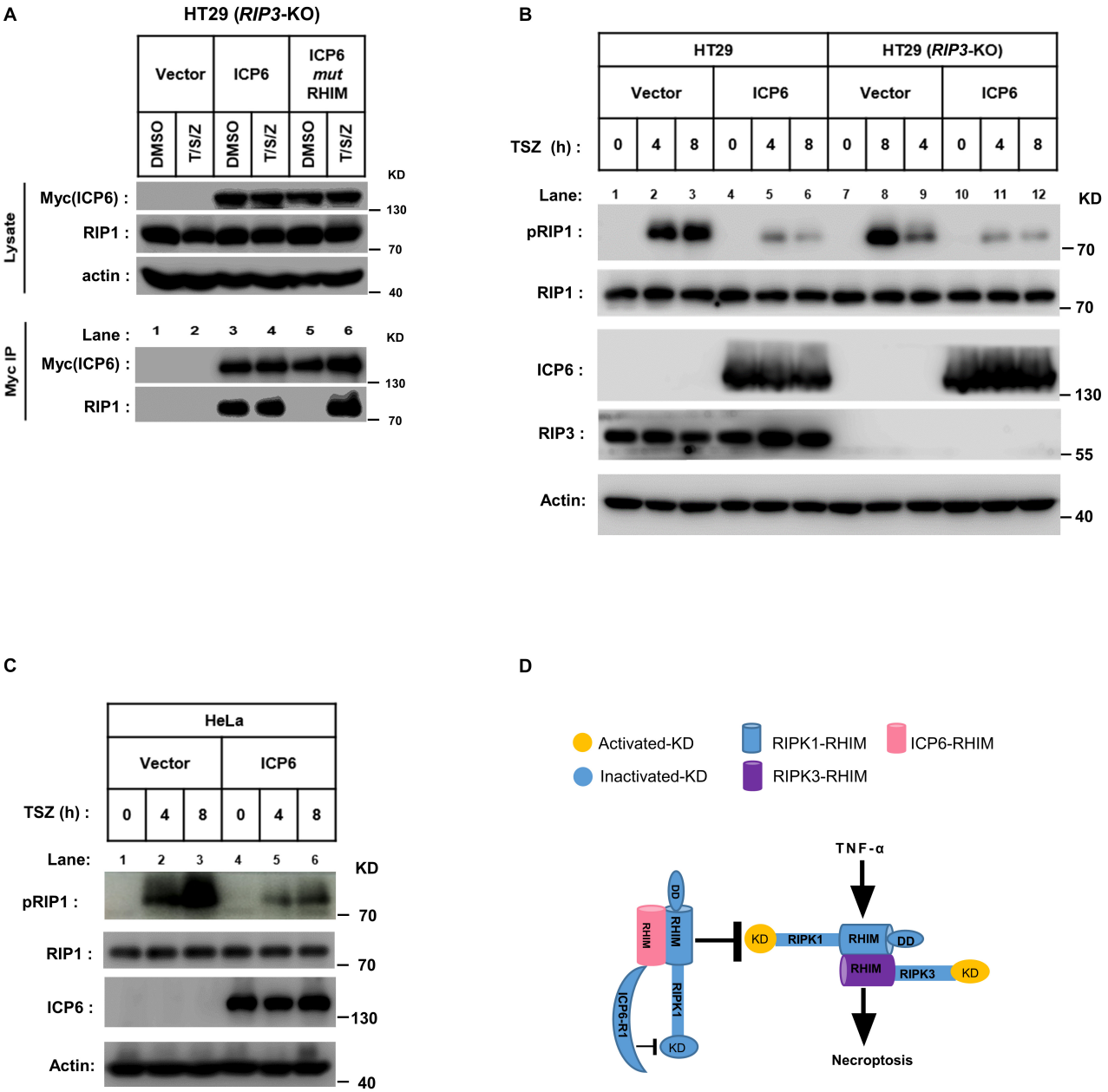

FIGURE 5 | The inhibition of RIP1 auto-phosphorylation by ICP6 is *RIP3*-independent. **(A)** HT29 (*RIP3*-KO) cells were infected with empty virus (Vector) or lentiviral virus encoding Myc-tagged ICP6. Then these cells were treated with T/S/Z for 6 h. Whole-cell lysates were subjected to immunoprecipitation with anti-Myc. The total cell lysates and immunoprecipitates were analyzed by western blot with the indicated antibodies. **(B,C)** ICP6 reduces the phosphorylation of RIP1. HT29, HT29 (*RIP3*-KO) **(B)** and HeLa **(C)** cells with indicated lentivirus infection were treated with T/S/Z for indicated time. The cells were then harvested, and the whole-cell extracts were analyzed by western blotting to check the RIP1 activation with anti-phospho-hRIP1 (S166). β-Actin and total RIP1 were shown as loading control. **(D)** The proposed mechanism of ICP6 inhibited necroptosis. KD, kinase domain; RHIM, RIP homotypic interaction motifs; DD, death domain; R1, C-terminal R1 homology domain of ICP6. Cells with necroptosis induction (TNF) undergo RIP1-*RIP3* interaction and kinase activation which are indispensable for necrosome maturation and cell necroptosis. ICP6 block necroptosis through ICP6-RIP1/3 RHIM domain interaction, then the ICP6-R1 could block RIP1 kinase activation to necrosome maturation.

was expressed (**Figure 5B**). Similar results were obtained in HeLa cells which are absent of endogenous RIP3-expression (**Figure 5C**). These results suggested the necroptosis signal induced RIP1 activation was attenuated by ICP6. So, we proposed the model of ICP6 blocking necroptosis. ICP6 binds with both RIP1 and RIP3 through RHIM-RHIM interaction to promote necrosome initiation. But in necrosome, ICP6 (probably using its R1 domain) block RIP1 activation, so that the ICP6 containing necrosome could not maturate and process cell necroptosis (**Figure 5D**).

DISCUSSION

Receptor-interacting protein kinase 1 (RIP1) is composed of kinase domain, RHIM domain and death domain. In TNF-induced cell death pathways, the kinase activity is required for both RIP1 dependent apoptosis (RDA) and necroptosis (Yuan et al., 2019). Our present work reveals that ICP6 could attenuate necroptosis signal induced RIP1 activation (**Figures 5B,C**), so that the necroptosis signaling is blocked by ICP6 on RIP1. Interestingly, the inhibitory function of ICP6 needs both of RHIM domain and R1 domain. The RHIM domain of ICP6 is responsible for efficient binding to RIP1 (**Figure 5A**). For R1 domain of ICP6, our data ruled out the possibilities that the enzymatic activity or oligomeric state of R1 domain contribute necroptosis inhibition (**Figures 1D**, **2E**). Therefore, how R1 domain of ICP6 functions in necroptosis blockage still needed to be studied.

ICP6 is encoded by a viral gene HSV-1. It is known that HSV-1 is a human-hosted virus belonging to the alpha herpesvirus subfamily. Infection with HSV-1 mainly causes herpes, and sporadic encephalitis for severe cases (Steiner and Benninger, 2013). Other symptoms by HSV-1 infection were reported, such as a latent infection in the peripheral nervous system of the host. It is reported that after infection with HSV, the immune system is destroyed and ulcers in the affected area increase the probability and risk of HIV infection (van Velzen et al., 2013). In epithelial cells, HSV-1 can induce the secretion of TNFα, IL-1β and other inflammatory factors, that is, the inflammatory response participates in the host's resistance to pathogen infection (Muscolino et al., 2020). RIP1 plays a very important role in inflammation through NF-κB or p38 MAPK pathways which is independent of its kinase activity. Our data showed that ICP6 attenuate RIP1 activation, and it is interesting to study if other functions of RIP1 are affected by HSV-1 infection or ICP6 expression.

DATA AVAILABILITY STATEMENT

The raw data supporting the conclusions of this article will be made available by the authors, without undue reservation.

AUTHOR CONTRIBUTIONS

HH and HW conceived and designed the experiments, drafted the manuscript, discussed the results, and edited the manuscript. HH performed and analyzed most of the experiments. GW contributed to the performance of the experiments. ZS, DY, NN, FY, and XL generated essential tools and reagents for the study. All authors contributed to the article and approved the submitted version.

FUNDING

This study was supported by the National Natural Science Foundation of China (31571427 to HW) and the Start-up Grant from ShanghaiTech University.

ACKNOWLEDGMENTS

We thank the Pengyu Huang Laboratory (pCDH-CMV-MCS-EF1-copGFP) and the Liming Sun Laboratory (PX330) for the Vectors. We also thank the Molecular Imaging Core Facility (MICF), School of Life Sciences and Technology, ShanghaiTech University for our Microscopy work, and we would be grateful to Ziwei Yang for her help of taking images.

REFERENCES

Chan, F. K.-M., Luz, N. F., and Moriwaki, K. (2015). Programmed necrosis in the cross talk of cell death and inflammation. *Annu. Rev. Immunol.* 33, 79–106. doi: 10.1146/annurev-immunol-032414-112248

Cho, Y. S., Challa, S., Moquin, D., Genga, R., Ray, T. D., Guildford, M., et al. (2009). Phosphorylation-driven assembly of the RIP1-RIP3 complex regulates programmed necrosis and virus-induced inflammation. *Cell* 137, 1112–1123. doi: 10.1016/j.cell.2009.05.037

Degterev, A., Huang, Z. H., Boyce, M., Li, Y. Q., Jagtap, P., Mizushima, N., et al. (2005). Chemical inhibitor of nonapoptotic cell death with therapeutic potential for ischemic brain injury. *Nat. Chem. Biol.* 1, 112–119. doi: 10.1038/nchembio711

Du, C. Y., Fang, M., Li, Y. C., Li, L., and Wang, X. D. (2000). Smac, a mitochondrial protein that promotes cytochrome c-dependent caspase activation by eliminating IAP inhibition. *Cell* 102, 33–42. doi: 10.1016/s0092-8674(00)00008-8

Feng, S. S., Yang, Y. H., Mei, Y., Ma, L., Zhu, D. E., Hoti, N., et al. (2007). Cleavage of RIP3 inactivates its caspase-independent apoptosis pathway by removal of kinase domain. *Cell. Signal.* 19, 2056–2067. doi: 10.1016/j.cellsig.2007.05.016

Festjens, N., Vanden Berghe, T., and Vandenabeele, P. (2006). Necrosis, a well-orchestrated form of cell demise: signalling cascades, important mediators and concomitant immune response. *Biochim. Biophys. Acta Bioenerg.* 1757, 1371–1387. doi: 10.1016/j.bbabio.2006.06.014

Guo, H., Omoto, S., Harris, P. A., Finger, J. N., Bertin, J., Gough, P. J., et al. (2015). Herpes simplex virus suppresses necroptosis in human cells. *Cell Host Microbe* 17, 243–251. doi: 10.1016/j.chom.2015.01.003

He, S., Wang, L., Miao, L., Wang, T., Du, F., Zhao, L., et al. (2009). Receptor interacting protein kinase-3 determines cellular necrotic response to TNF-alpha. *Cell* 137, 1100–1111. doi: 10.1016/j.cell.2009.05.021

Holler, N., Zaru, R., Micheau, O., Thome, M., Attinger, A., Valitutti, S., et al. (2000). Fas triggers an alternative, caspase-8-independent cell death pathway using the kinase RIP as effector molecule. *Nat. Immunol.* 1, 489–495. doi: 10.1038/82732

Hu, H., Wu, X., Wu, G., Nan, N., Zhang, J., Zhu, X., et al. (2020). RIP3-mediated necroptosis is regulated by inter-filament assembly of RIP homotypic interaction motif. *Cell Death Diff.* [Epub ahead of print].

Huang, Z., Wu, S.-Q., Liang, Y., Zhou, X., Chen, W., Li, L., et al. (2015). RIP1/RIP3 binding to HSV-1 ICP6 initiates necroptosis to restrict virus propagation in mice. *Cell Host Microbe* 17, 229–242. doi: 10.1016/j.chom.2015.01.002

Kaiser, W. J., Upton, J. W., and Mocarski, E. S. (2013). Viral modulation of programmed necrosis. *Curr. Opin. Virol.* 3, 296–306. doi: 10.1016/j.coviro.2013.05.019

Kerr, J. F., Wyllie, A. H., and Currie, A. R. (1972). Apoptosis: a basic biological phenomenon with wide-ranging implications in tissue kinetics. *Br. J. Cancer* 26, 239–257. doi: 10.1038/bjc.1972.33

Lembo, D., and Brune, W. (2009). Tinkering with a viral ribonucleotide reductase. *Trends Biochem. Sci.* 34, 25–32. doi: 10.1016/j.tibs.2008.09.008

Li, P., Nijhawan, D., Budihardjo, I., Srinivasula, S. M., Ahmad, M., Alnemri, E. S., et al. (1997). Cytochrome c and dATP-dependent formation of Apaf-1/caspase-9 complex initiates an apoptotic protease cascade. *Cell* 91, 479–489. doi: 10.1016/s0092-8674(00)80434-1

Lin, Y., Devin, A., Rodriguez, Y., and Liu, Z. G. (1999). Cleavage of the death domain kinase RIP by caspase-8 prompts TNF-induced apoptosis. *Genes Dev.* 13, 2514–2526. doi: 10.1101/gad.13.19.2514

Mocarski, E. S., Upton, J. W., and Kaiser, W. J. (2012). Viral infection and the evolution of caspase 8-regulated apoptotic and necrotic death pathways. *Nat. Rev. Immunol.* 12, 79–88. doi: 10.1038/nri3131

Mossman, K. L., and Weller, S. K. (2015). HSV cheats the executioner. *Cell Host Microbe* 17, 148–151. doi: 10.1016/j.chom.2015.01.013

Muscolino, E., Schmitz, R., Loroch, S., Caragliano, E., Schneider, C., Rizzato, M., et al. (2020). Herpesviruses induce aggregation and selective autophagy of host signalling proteins NEMO and RIPK1 as an immune-evasion mechanism. *Nat. Microbiol.* 5, 331–342. doi: 10.1038/s41564-019-0624-1

Peter, M. E., and Krammer, P. H. (2003). The CD95(APO-1/Fas) DISC and beyond. *Cell Death Diff.* 10, 26–35. doi: 10.1038/sj.cdd.4401186

Steiner, I., and Benninger, F. (2013). Update on herpes virus infections of the nervous system. *Curr. Neurol. Neurosci. Rep.* 13:414.

Su, L., Quade, B., Wang, H., Sun, L., Wang, X., and Rizo, J. (2014). A plug release mechanism for membrane permeation by MLKL. *Structure* 22, 1489–1500. doi: 10.1016/j.str.2014.07.014

Sun, L., Wang, H., Wang, Z., He, S., Chen, S., Liao, D., et al. (2012). Mixed lineage kinase domain-like protein mediates necrosis signaling downstream of RIP3 kinase. *Cell* 148, 213–227. doi: 10.1016/j.cell.2011.11.031

Sun, X. Q., Yin, J. P., Starovasnik, M. A., Fairbrother, W. J., and Dixit, V. M. (2002). Identification of a novel homotypic interaction motif required for the phosphorylation of receptor-interacting protein (RIP) by RIP3. *J. Biol. Chem.* 277, 9505–9511. doi: 10.1074/jbc.m109488200

Upton, J. W., Kaiser, W. J., and Mocarski, E. S. (2010). Virus inhibition of RIP3-dependent necrosis. *Cell Host Microbe* 7, 302–313. doi: 10.1016/j.chom.2010.03.006

van Velzen, M., Jing, L. C., Osterhaus, A., Sette, A., Koelle, D. M., and Verjans, G. (2013). Local CD4 and CD8 T-cell reactivity to HSV-1 antigens documents broad viral protein expression and immune competence in latently infected human trigeminal ganglia. *PLoS Pathog.* 9:11.

Vercammen, D., Brouckaert, G., Denecker, G., Van de Craen, M., Declercq, W., Fiers, W., et al. (1998). Dual signaling of the Fas receptor: initiation of both apoptotic and necrotic cell death pathways. *J. Exp. Med.* 188, 919–930. doi: 10.1084/jem.188.5.919

Verhagen, A. M., Ekert, P. G., Pakusch, M., Silke, J., Connolly, L. M., Reid, G. E., et al. (2000). Identification of DIABLO, a mammalian protein that promotes apoptosis by binding to and antagonizing IAP proteins. *Cell* 102, 43–53. doi: 10.1016/s0092-8674(00)00009-x

Wang, H., Sun, L., Su, L., Rizo, J., Liu, L., Wang, L. F., et al. (2014). Mixed lineage kinase domain-like protein MLKL causes necrotic membrane disruption upon phosphorylation by RIP3. *Mol. Cell.* 54, 133–146. doi: 10.1016/j.molcel.2014.03.003

Wang, X., Li, Y., Liu, S., Yu, X., Li, L., Shi, C., et al. (2014). Direct activation of RIP3/MLKL-dependent necrosis by herpes simplex virus 1 (HSV-1) protein ICP6 triggers host antiviral defense. *Proc. Natl. Acad. Sci. U.S.A.* 111, 15438–15443. doi: 10.1073/pnas.1412767111

Yu, X. L., Li, Y., Chen, Q., Su, C. H., Zhang, Z. L., Yang, C. K., et al. (2016). Herpes Simplex Virus 1 (HSV-1) and HSV-2 mediate species-specific modulations of programmed necrosis through the viral ribonucleotide reductase large subunit R1. *J. Virol.* 90, 1088–1095. doi: 10.1128/jvi.02446-15

Yuan, J. Y., Amin, P., and Ofengeim, D. (2019). Necroptosis and RIPK1-mediated neuroinflammation in CNS diseases. *Nat. Rev. Neurosci.* 20, 19–33. doi: 10.1038/s41583-018-0093-1

Zhang, D. W., Shao, J., Lin, J., Zhang, N., Lu, B. J., Lin, S. C., et al. (2009). RIP3, an energy metabolism regulator that switches TNF-induced cell death from apoptosis to necrosis. *Science* 325, 332–336. doi: 10.1126/science.1172308

Zhao, J., Jitkaew, S., Cai, Z., Choksi, S., Li, Q., Luo, J., et al. (2012). Mixed lineage kinase domain-like is a key receptor interacting protein 3 downstream component of TNF-induced necrosis. *Proc. Natl. Acad. Sci. U.S.A.* 109, 5322–5327. doi: 10.1073/pnas.1200012109

Conflict of Interest: The authors declare that the research was conducted in the absence of any commercial or financial relationships that could be construed as a potential conflict of interest.

frontiers in Cell and Developmental Biology

ORIGINAL RESEARCH
published: 08 December 2020
doi: 10.3389/fcell.2020.606119

Discovery of a Potent RIPK3 Inhibitor for the Amelioration of Necroptosis-Associated Inflammatory Injury

Kaijiang Xia[1†], Fang Zhu[2,3,4,5†], Chengkui Yang[2,3,4], Shuwei Wu[1], Yu Lin[1], Haikuo Ma[1], Xiaoliang Yu[2,3,4], Cong Zhao[2,3,4], Yuting Ji[2,3,4,6], Wenxiang Ge[2,3,4], Jingrui Wang[2,3,4], Yayun Du[2,3,4,5], Wei Zhang[2,3,4], Tao Yang[2,3,4,5], Xiaohu Zhang[1] and Sudan He[2,3,4,5]**

[1] Jiangsu Key Laboratory of Neuropsychiatric Diseases and College of Pharmaceutical Sciences, Soochow University, Suzhou, China, [2] Center of Systems Medicine, Institute of Basic Medical Sciences, Chinese Academy of Medical Sciences & Peking Union Medial College, Beijing, China, [3] Suzhou Institute of Systems Medicine, Suzhou, China, [4] Key Laboratory of Synthetic Biology Regulatory Elements, Chinese Academy of Medical Sciences, Beijing, China, [5] Cyrus Tang Hematology Center and Collaborative Innovation Center of Hematology, State Key Laboratory of Radiation Medicine and Protection, Soochow University, Suzhou, China, [6] School of Life Sciences and Technology, China Pharmaceutical University, Nanjing, China

Necroptosis is a form of regulated necrosis that requires the activation of receptor-interacting kinase 3 (RIPK3 or RIP3) and its phosphorylation of the substrate MLKL (mixed lineage kinase domain-like protein). Necroptosis has emerged as important cell death involved in the pathogenesis of various diseases including inflammatory diseases, degenerative diseases, and cancer. Here, we discovered a small molecule Zharp-99 as a potent inhibitor of necroptosis through blocking the kinase activity of RIPK3. Zharp-99 efficiently blocks necroptosis induced by ligands of the death receptor and Toll-like receptor as well as viral infection in human, rat and mouse cells. Zharp-99 strongly inhibits cellular activation of RIPK3, and MLKL upon necroptosis stimuli. Zharp-99 directly blocks the kinase activity of RIPK3 without affecting RIPK1 kinase activity at the tested concentration. Importantly, Zharp-99 exerts effective protection against TNF-α induced systemic inflammatory response syndrome in the mouse model. Zharp-99 displays favorable *in vitro* safety profiles and *in vivo* pharmacokinetic parameters. Thus, our study demonstrates Zharp-99 as a potent inhibitor of RIPK3 kinase and also highlights its potential for further development of new approaches for treating necroptosis-associated inflammatory disorders.

Keywords: necroptosis, RIPK3, kinase inhibitor, inflammatory diseases, Zharp-99

OPEN ACCESS

Edited by:
Yinan Gong,
University of Pittsburgh, United States

Reviewed by:
Xizhi Guo,
Brigham and Women's Hospital and Harvard Medical School, United States
Beiyun Liu,
St. Jude Children's Research Hospital, United States
Yi-Chieh Perng,
Washington University School of Medicine in St. Louis, United States

***Correspondence:**
Xiaohu Zhang
xiaohuzhang@suda.edu.cn
Sudan He
hesudan2018@163.com

[†] These authors have contributed equally to this work

Specialty section:
This article was submitted to Cell Death and Survival, a section of the journal Frontiers in Cell and Developmental Biology

Received: *14 September 2020*
Accepted: *16 November 2020*
Published: *08 December 2020*

Citation:
Xia K, Zhu F, Yang C, Wu S, Lin Y, Ma H, Yu X, Zhao C, Ji Y, Ge W, Wang J, Du Y, Zhang W, Yang T, Zhang X and He S (2020) Discovery of a Potent RIPK3 Inhibitor for the Amelioration of Necroptosis-Associated Inflammatory Injury. Front. Cell Dev. Biol. 8:606119. doi: 10.3389/fcell.2020.606119

INTRODUCTION

Necroptosis is a form of regulated cell death that shows necrotic features including cell swelling and disrupted cell membrane. Necroptosis is tightly regulated by the activation of receptor-interacting protein kinase 1 (RIPK1 or RIP1) and RIPK3 (RIP3; Linkermann and Green, 2014; He and Wang, 2018; Mifflin et al., 2020). In TNF-induced necroptosis, RIPK1 interacts with RIPK3 through their RIP homotypic interaction motif (RHIM) domains, leading to RIPK3 activation and

phosphorylation (Holler et al., 2000; Cho et al., 2009; He et al., 2009; Zhang et al., 2009). Active RIPK3 phosphorylates its substrate mixed lineage kinase domain-like protein (MLKL; Sun et al., 2012; Zhao et al., 2012). The phosphorylation of MLKL results in MLKL oligomerization and membrane translocation to mediate cell rupture (Murphy et al., 2013; Cai et al., 2014; Chen et al., 2014; Wang et al., 2014a). As a lytic cell death, necroptosis elicits inflammatory responses via the release of cellular contents including damage-associated molecular patterns (DAMPs; Linkermann and Green, 2014; He and Wang, 2018; Mifflin et al., 2020). Necroptosis plays important roles in a variety of pathological conditions including inflammatory disorders, ischemia-reperfusion-induced injury, degenerative diseases and cancer. Thus, strategies to interfere with the necroptosis signaling pathway could be potentially developed for the treatment of necroptosis-related diseases.

Receptor-interacting kinase 3 has emerged as a key molecule of necroptosis that can be initiated by various signals including activation of death receptors, Toll-tike receptors, interferon receptors as well as pathogen infection3 (Linkermann and Green, 2014; He and Wang, 2018; Mifflin et al., 2020). Receptor-interacting kinase 3 contains an N-terminal serine/threonine kinase domain and a C-terminal RHIM domain. The kinase activity of RIPK3 is essential for its activation and phosphorylation of MLKL (Cho et al., 2009; He et al., 2009; Sun et al., 2012; Zhang et al., 2009; Zhao et al., 2012). Increasing evidence suggests that RIPK3 can be activated for necroptosis by other RHIM-containing proteins including ZBP1/DAI/ DLM1 (Z-nucleic acid binding protein) (Upton et al., 2012; Samir et al., 2020)and TRIF/TICAM-1 (Toll/IL-1 receptor domain-containing adaptor inducing IFN-β) (He et al., 2011; Kaiser et al., 2013) in addition to RIPK1. Thus, necroptosis can proceed independent of RIPK1, leading to the assumption that RIPK3 may protect cell from a broader range of necroptotic pathologies. The combination of tractability and broad dedicated role in necroptosis makes RIPK3 an attractive target for modulating necroptosis and its related diseases.

Considering the essential role of RIPK3 kinase activity in necroptosis, the kinase domain of RIPK3 is an interesting target for intervention with small molecule inhibitors. A number of RIPK3 inhibitors have been reported including the FDA approved drugs dabrafenib, sorafenib, and ponatinib (Kaiser et al., 2013; Li et al., 2014; Mandal et al., 2014; Fauster et al., 2015; Park et al., 2018; Zhang et al., 2019; Hart et al., 2020). Inhibition of RIPK3 was discovered as an off-target effect of these drugs as opposed to the intended targets such as Braf, VEGRF, and Bcr-Abl (Fauster et al., 2015; Li et al., 2014). The classical work on GSK'840, GSK'843, GSK'872 established RIPK3 as a potential drug target with a caveat: inhibition of RIPK3 kinase activity induced apoptosis in a concentration-dependent manner (Kaiser et al., 2013; Mandal et al., 2014). The interaction of compound with RIPK3 imposed a conformation change which drove the recruitment of RIPK1 via the RHIM domain and activated caspase 8 for the initiation of apoptosis (Mandal et al., 2014). It is not clear what structural features of a compound may avoid the induction of apoptotic RIPK3 conformational change. Reflecting these challenges, there is no RIPK3 inhibitor currently under clinical investigation. We have a long standing interest in studying RIPK3 and its role in necroptosis. Our ultimate goal is to identify novel RIPK3 inhibitors with high efficacy and low toxicity. Here, we wish to report the discovery of Zharp-99 as a novel inhibitor of RIPK3 kinase activity. Zharp-99 exhibits potent cellular efficacy of inhibiting necroptosis induced by multiple necroptotic stimuli in human, mouse, and rat cells. Zharp-99 displays favorable in vitro safety profiles and in vivo pharmacokinetic parameters. Importantly, pre-treatment of Zharp-99 significantly ameliorates TNF-induced systemic inflammatory response syndrome (SIRS) in the mouse model. These findings highlight Zharp-99 as a potent RIPK3 inhibitor and suggest the potential of Zharp-99 as a starting point for the development of new approaches to treat necroptosis-associated disorders.

MATERIALS AND METHODS

Cell Culture

Human colon cancer HT-29 and mouse fibrosarcoma L929 cells were from ATCC. Mouse embryonic fibroblasts (MEF), HT-29 cells stably expressing RIPK3-shRNA and shRNA resistant scramble Flag-tagged RIPK3 (W46), and NIH3T3 cell line stably expressing RIPK3 fused to mutant FK506-binding protein (NIH3T3-RIPK3) were kindly provided by Dr. Xiaodong Wang [National Institute of Biological Sciences (NIBS), Beijing]. HeLa-MLKL (1-190) cell line was a gift from Dr. Zhigao Wang (University of Texas Southwestern Medical Center at Dallas). These cells were cultured in Dulbecco's modified Eagle's medium (Hyclone) supplemeted with 10% fetal bovine serum (Invitrogen) and 2 mM L-glutamine (Invitrogen) in a humidified incubator at 37°C and 5% CO_2. NIH3T3-RIPK3 was cultured in complete medium containing 2 μg/ml G418 (Calbiochem). HeLa-MLKL (1–190) stable line were cultured in complete medium containing 10 μg/ml Blasticidin plus 1 μg/ml puromycin. Bone marrow-derived macrophages were isolated from the bone marrow of 6–8 week old mice and rats, and cultured for 7 days in the medium containing 30% L929-cell conditioned medium, 20% FBS, and 50% RPMI-1640. L929 cell conditioned medium containing colony stimulating factor was collected after growing L929 cells in DMEM plus 10% FBS for 7 to 10 days previously described (He et al., 2011).

Cell Viability Assay

Cells were seeded in 96-well plates and then treated as indicated. The cell viability was determined by assessment of ATP levels using the CellTiter-Glo Luminescent Cell Viability Assay kit following the manufacture's instructions (Promega). Luminescence was calculated with SpectraMax i3x (Molecular Devices).

Reagents and Antibodies

Human TNF-α recombinant protein was generated as previously described (Wang et al., 2008). Mouse TNF-α recombinant

protein was purchased from Genscript. The Smac mimetic compound and anti-human RIPK3 antibody were kindly provided by Dr. Xiaodong Wang (National Institute of Biological Sciences, Beijing). z-VAD was purchased from Bachem respectively. Lipopolysaccharide (LPS) was purchased from Sigma. Mouse recombinant RIPK1 and RIPK3 were purchased from SignalChem. The cellTiter-Glo Luminescent cell viability assay kit and ADP-Glo kinase assay kit were purchased from Promega. The following antibodies were used: RIPK1 (BD Biosciences, 610458), p-hRIPK1 (CST, 65746), p-hRIPK3 (Abcam, 209384), hMLKL (Abcam, 184718), p-hMLKL (Abcam, 187091), p-mRIPK1 (CST, 31122S), mRIPK3 (Prosci, 2283), p-mRIPK3 (CST, 91702), mMLKL (Abgent, 14272b), p-mMLKL (Abcam, 196436), β-actin (Sigma, A2066). Mouse IL-6 ELISA kit was from MultiSciences (Lianke).

Western Blot Analysis

The cell pellets were harvested and dissolved in lysis buffer (20 mM Tris–HCl, pH 7.4 150 mM NaCl, 1% Triton X-100, 1 mM Na_3VO_4, 10% glycerol, 25 mM β-glycerol-phosphate, 0.1 mM PMSF, with the Sigma phosphatase inhibitors and the Roche Pierce protease inhibitor set). The re-suspended cell pellet was then incubated on ice for 20 min, followed by centrifugation at 13000 × *g* for 20 min at 4°C. The supernatants were collected and protein concentrations were measured using the BCA Protein Assay Kit (Thermo Fisher Scientifc, United States). Finally, cell lysates were subjected for western-blot analysis of the indicated antibodies.

RNA Extraction and Real-Time PCR

Total RNA was extracted using TRIzol Reagent (Invitrogen) from cell pellets. cDNA was synthesized using a Revert Aid First Strand cDNA kit (Thermo Fisher Scientifc). Real-time PCR was performed using corresponding primers and Power SYBR® Green PCR Master Mix (Invitrogen). The data were normalized to GAPDH. The primer sequences are as follows: ICP6 Forward: GGCTGCAATCGGCCCTGAAGTA, Reverse: GGT GGTCGTAGAGGCGGTGGAA; TNFα Forward: CCCTCACAC TCAGATCATCTTCT, Reverse: GCTACGACGTGGGCTACAG; CCL3 Forward: TTCTCTGTACCATGACACTCTGC, Reverse: CGTGGAATCTTCCGGCTGTAG; CXCL1 Forward: GCACCC AAACCGAAGTCATAG, Reverse: AGAAGCCAGCGTTCAC CAGA; GAPDH Forward: CAAGAAGGTGGTGAAGCAGGC, Reverse: CATACCAGGAAATGAGCTTGAC.

In vitro Kinase Activity Assay

The recombinant human RIPK1 or RIPK3 protein was incubated with the control DMSO or the indicated compound for around 15 min in the assay buffer (25 mM HEPES PH7.2, 12.5 mM $MnCl_2$, 5 mM EGTA, 20 mM $MgCl_2$, 12.5 mM β-glycerol phosphate, 2 mM EDTA, and 2 mM DTT). ATP (50 μM) and the substrate MBP (20 μM) were then added to the reaction at room temperature for 2 h. The kinase activity was calculated by the measuring the luminescence after the addition of the ADP-Glo Kinase Assay kit according to the manufacture's instructions (Promega).

Source of Animals

C57BL/6 male mice were purchased from Suzhou JOINN Clinical Co., Ltd. All male mice were bred under standard conditions and used at the age of 6–7 weeks with about 18–20 g body weight. All animal experiments were performed in accordance with protocols approved by the Institutional Animal Care and Use Committee at Suzhou Institute of Systems Medicine.

TNF-Induced Systemic Inflammatory Response Syndrome

Zharp-99 was diluted into sterile PBS containing 40% PEG400. C57BL/6 mice were pretreated with vehicle or Zharp-99 (5 mg/kg) via intraperitoneal injection for around 15 min, followed by the administration of mouse TNF-α (6.5 μg/mouse) via tail intravenous injection. The status of mice was monitored by measuring anal temperature. Mice mortality was continuously monitored till 60 h after TNF-α administration. Blood was collected 4 h post TNF-α challenge and serum was isolated for further examination.

Methods for Determination of CYP/hERG Inhibition and Pharmacokinetic Parameters

Cytochrome P450 (CYP) inhibitory potency was determined by industrial standard methods as reported previously (Dong et al., 2015). Methods to determine potassium channel hERG inhibition and in vivo pharmacokinetic parameters have been previously published (Lu et al., 2017).

Synthesis of Zharp-99

The synthetic scheme and detailed experimental procedure as well as spectroscopic characterizations of Zharp-99 can be found in the supporting information.

Statistical Analyses

Data of cell survival rate are represented as the mean ± standard deviation of duplicates or triplicates from one representative experiment ($n \geq 2$ independent experiments). Significance was analyzed using *t*-tests of GraphPad Prism software. *P*-values were defined by ONE-way ANOVA and multi-comparison test for statistics analysis. $^{*}P < 0.05$, $^{**}P < 0.01$, $^{***}P < 0.001$.

RESULTS

Zharp-99 Efficiently Blocks TNF-Induced Necroptosis in Both Human and Mouse Cells

To discover novel inhibitors of necroptosis, we designed and synthesized a focused library with novel structures based on the GSK'872 scaffold. Human colon cancer HT-29 cells were treated with these compounds for 2 h prior to the treatment of necroptotic stimuli (TNFα, Smac mimetic and z-VAD), which are widely used to trigger TNF-induced necroptosis (He et al., 2009). Zharp-99 turned out to be the most efficient inhibitor of TNF-induced necroptosis in HT-29 cells with higher efficacy compared

to the well-known RIPK3 inhibitor GSK'872 (**Figures 1A–C**). We further examined the effect of Zharp-99 on TNF-induced necroptosis in MEFs. Zharp-99 exhibited efficient inhibition of TNF-induced necroptosis in MEFs at concentrations ranging from 0.15 to 1.2 μM (**Figures 1D,E**). We also observed obvious toxicity of Zharp-99 at higher concentrations ranging from 2.5 to 20 μM (**Figure 1D**). Collectively, these results demonstrate that Zharp-99 is an effective inhibitor of TNF-induced necroptosis in human and mouse cells.

Zharp-99 Inhibits Necroptosis Induced by TLR and HSV-1 Infection

It is known that necroptosis can be initiated by activation of TLR3 or TLR4 as well as pathogen infection in addition to activation of death receptors (Linkermann and Green, 2014; He and Wang, 2018; Mifflin et al., 2020). We examined the impact of Zharp-99 on TLR4-mediated necroptosis induced by LPS/z-VAD. Zharp-99 potently blocked TLR4-mediated necroptosis in both mouse and rat bone marrow derived macrophages (**Figures 2A–C**). Infection of herpes simplex virus (HSV)-1 infection can trigger necroptosis in mouse cells (Huang et al., 2015; Wang et al., 2014c). We further evaluated the effect of Zharp-99 on HSV-1-induced necroptosis and found that Zharp-99 significantly inhibited HSV-1 induced necroptosis in L929 cells (**Figure 2D**). We examined the effect of Zharp-99 on viral genome extracted from cell culture supernatants 5h post HSV-1 infection and found that Zharp-99 did not affect the expression of viral gene ICP6 (**Figures 2E,F**). These results suggest that Zharp-99 has a common mechanism of blocking conserved necroptosis signaling pathways activated by various stimuli in different species.

Zharp-99 Blocks Cellular Activation of RIPK3 and MLKL Upon Necroptotic Stimuli

Having established that Zharp-99 is a novel inhibitor of necroptosis, we next investigate the molecular mechanism underlying Zharp-99-mediated necroptosis inhibition. It is well understood that RIPK1, RIPK3, and MLKL are activated during TNF-induced necroptosis, as indicated by their phosphorylation (Sun et al., 2012; Mifflin et al., 2020; Wang et al., 2014a). We examined the effect of Zharp-99 on the phosphorylation of RIPK1, RIPK3, and MLKL upon necroptotic stimuli. Treatment of Zharp-99 abolished phosphorylation of RIPK3 and MLKL in human HT-29 cells, but did not reduce RIPK1 phosphorylation at S166 (**Figure 3A**). Consistently, Zharp-99 blocked phosphorylation of RIPK3, and MLKL in mouse L929 cells, but not phosphorylation of RIPK1 (**Figure 3B**). We further examined the effect of Zharp-99 on the formation of RIPK1/RIPK3 complex in HT-29 cells stably expressing Flag-RIPK3. Zharp-99 did not affect the RIPK1/RIPK3 necrosome formation (**Figure 3C**). Collectively, these results demonstrate that Zharp-99 blocks necroptosis through the suppression of RIPK3 function or signaling upstream of RIPK3 activation.

Zharp-99 Is an Inhibitor of RIPK3 Kinase Domain

Having shown that Zharp-99 can block activation of RIPK3 and MLKL during TNF-induced necroptosis, we further asked whether Zharp-99 could directly target RIPK3 by performing

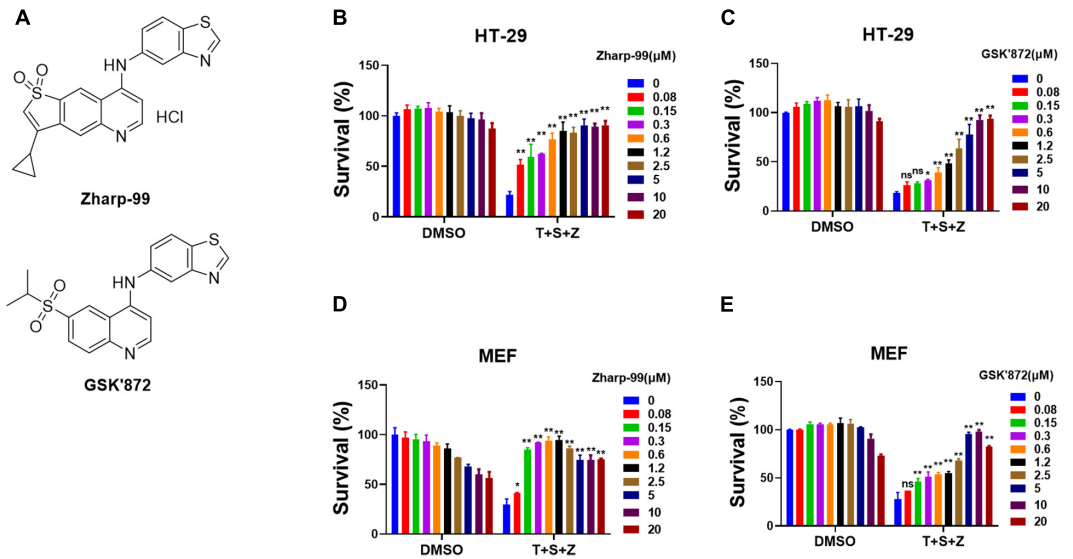

FIGURE 1 | Zharp-99 efficiently blocks TNF-induced necroptosis in both human and mouse cells. **(A)** Chemical structure of Zharp-99 and GSK'872. **(B–E)** The effects of Zharp-99 and GSK'872 on TNF-induced necroptosis were examined in HT-29 cells and MEF cells. **(B,C)** HT-29 cells were pretreated with indicated concentrations of Zharp-99 and GSK'872 for 2 h prior to the treatment with TNF-α (40 ng/ml), Smac mimetic (100 nM) and z-VAD (20 μM) for 48 h. Cell viability was assessed by measuring ATP levels. Data are represented as the mean ± standard deviation of triplicates. **(D,E)** MEF cells were pretreated with indicated concentrations of Zharp-99 and GSK'872 for 2 h followed by the treatment with TNF-α (40 ng/ml), Smac mimetic (100 nM), and z-VAD (20 μM) for 24 h. T, TNF-α; S, Smac mimetic; Z, z-VAD. Data are represented as the mean ± standard deviation of dipartites. $^{*}P < 0.05$. $^{**}P < 0.01$.

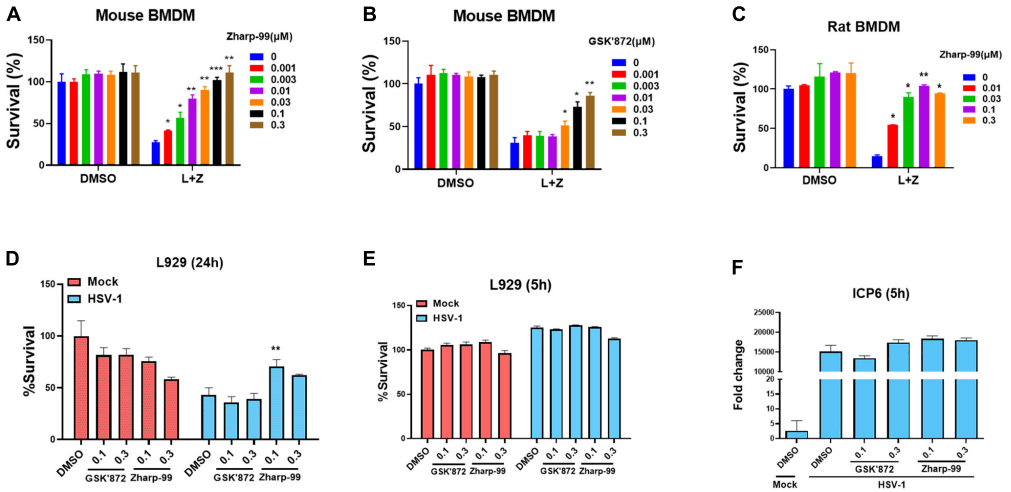

FIGURE 2 | Zharp-99 blocks necroptosis induced by TLR and HSV-1 infection. **(A–C)** Bone marrow-derived macrophages (BMDM) from mouse and rat was pretreated with DMSO, Zharp-99 or GSK'872 for 2 h prior to the treatment of DMSO, LPS (20 ng/ml) plus z-VAD (20 μM) or z-VAD (10 μM) for 24 h. Cell viability was determined by measuring ATP levels. L, LPS; Z, z-VAD. Data are represented as the mean ± standard deviation of dipartites. **(D)** L929 cells were pretreated with DMSO, Zharp-99 or GSK'872 for 2h prior to HSV-1 infection. After 24 h, cell viability was determined by measuring ATP levels. Data are represented as the mean ± standard deviation of triplicates. **(E,F)** L929 cells were pretreated with DMSO, Zharp-99 or GSK'872 for 2 h prior to HSV-1 infection. After 5 h, cell viability was determined by measuring ATP levels and ICP6 mRNA expression was detected using viral genome extracted from cell culture supernatant. $^{*}P < 0.05$. $^{**}P < 0.01$. $^{***}P < 0.001$.

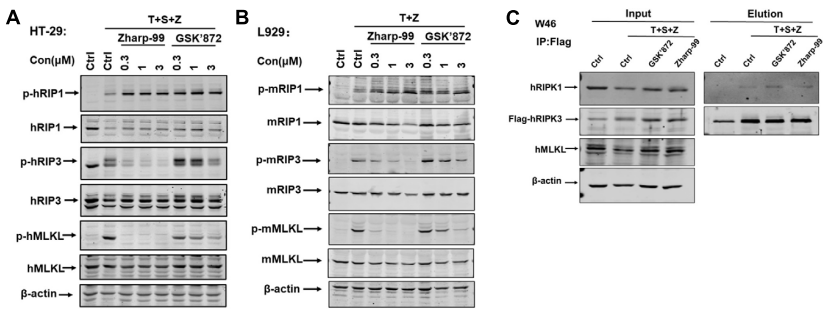

FIGURE 3 | Zharp-99 blocks cellular activation of RIPK3 and MLKL upon necroptotic stimuli. **(A)** HT-29 cells were treated with the indicated compound for 2 h prior to the treatment of TNF-α (40 ng/ml), Smac mimetic (100 nM) and z-VAD (20 μM) for additional 8 h. Cell lysates were harvest and subjected to western-blot analysis for phosphorylation of RIPK1, RIPK3, and MLKL. **(B)** L929 cells were pretreated with DMSO, Zharp-99 or GSK'872 for 2 h prior to TNF-α (40 ng/ml) and z-VAD (20 μM) for additional 4 h. Cell lysates were harvest and subjected to western-blot analysis for phosphorylation of RIPK1, RIPK3, and MLKL. **(C)** HT-29 cells stably expressing RIPK3-shRNA and shRNA resistant scramble Flag-tagged RIPK3 (W46) were pretreated Zharp-99 or GSK'872 for 2 h prior to treatment of TNF-α (40 ng/ml), Smac (100 nM) and z-VAD (20 μM) for 8 h. Cell lysates were prepared for immunoprecipitation using an anti-Flag antibody. The levels of RIPK3 and RIPK1 in the immunocomplex were determined by western blot analysis.

in vitro kinase assay. Zharp-99 inhibited the kinase activity of human RIPK3 *in vitro* with higher inhibitory activity compared to GSK'872 (**Figure 4A**). In contrast, Zharp-99 did not affect RIPK1 kinase activity even at 10 μM, displaying a similar effect as GSK'872 (**Figure 4B**). Moreover, Zharp-99 exhibited efficient binding to human recombinant RIPK3 with Kd of 1.35 nM (**Figure 4C**). These results indicate that Zharp-99 is an inhibitor of RIPK3 by targeting the kinase activity.

Previous studies have shown that enforced dimerization/polymerization of RIPK3 or MLKL triggers necroptosis bypassing the upstream signals (Chen et al., 2014; Orozco et al., 2014). We further evaluated the effect of Zharp-99 on necroptosis induced by RIPK3 dimerization or MLKL polymerization. Consistent with previous observation, NIH3T3 cells expressing mouse RIPK3 fused to mutant FK506-binding protein (FKBP) were committed to necroptosis upon the treatment of the dimerizer AP20187 (**Figure 4D**). This RIPK3 dimerization-induced necroptosis was efficiently blocked by Zharp-99 (**Figure 4D**). It has been reported that HeLa cells expressing MLKL (1–190aa) fused to DmrB could undergo MLKL polymerization-induced necroptosis upon AP20187 treatment (Liu et al., 2017; **Figure 4E**). Treatment of Zharp-99 did not affect this polymerized MLKL-induced necroptosis, while the cell death phenotype was blocked by MLKL inhibitor necrosulfonamide (NSA), suggesting that Zharp-99 does not affect MLKL function or signaling downstream of MLKL.

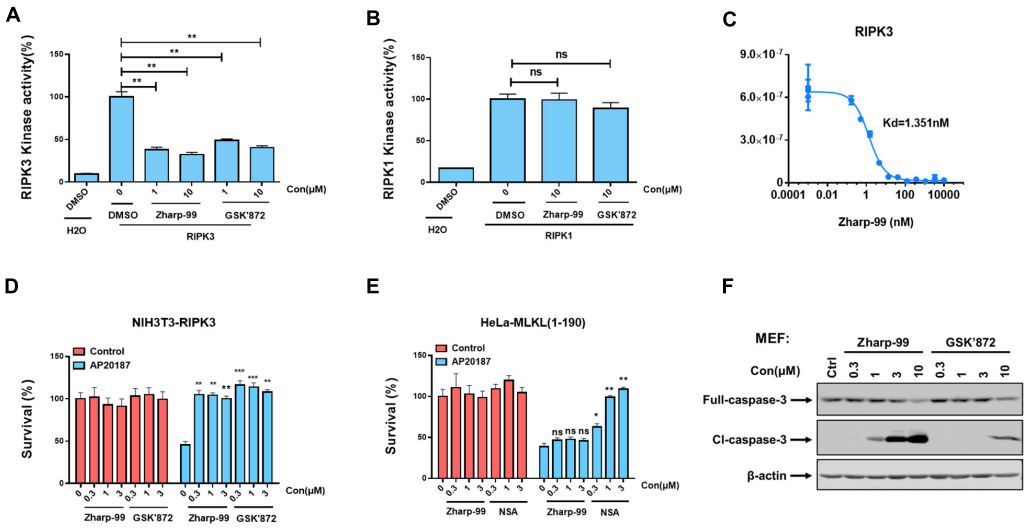

FIGURE 4 | Zharp-99 is a potent inhibitor of RIPK3. **(A,B)** The effect of Zharp-99 on the kinase activities of RIPK3 and RIPK1. In vitro kinase activity assays using recombinant RIPK3 and RIPK1 were performed as described in the section "Materials and Methods." Data represent mean value ± standard deviation. **(C)** Binding constants (Kds) of Zharp-99 with recombinant human RIPK3 in collaboration with Discover X Corporation. **(D)** Zharp-99 inhibits RIPK3 dimerization-induced cell death in NIH3T3-RIPK3 cells that stably express RIPK3 fused to FKBP F36V mutant. NIH3T3-RIPK3 cells were pretreated with indicated compounds for 2 h and subsequently treated with AP20187 (60 nM) for 24 h. Cell viability was determined by measuring ATP levels. **(E)** Zharp-99 has no effect on MLKL dimerization-induced cell death in HeLa-MLKL (1–190) cells that stably express MLKL (1–190aa) fused to DmrB. HeLa-MLKL (1–190) cells were induced by doxycycline (1 μg/ml) for 24 h. Cells were pretreated with indicated compounds for 2 h and subsequently treated with AP20187 (60nM) for 24h. Cell viability was determined by measuring ATP levels. Data are represented as the mean ± standard deviation of triplicates. $^{*}P < 0.05$. $^{**}P < 0.01$. $^{***}P < 0.001$. **(F)** MEFs were treated as indicated for 3 h. Cell lysates were harvest and subjected to western-blot analysis for full length and cleaved caspase 3.

Taken together, these results demonstrate that Zharp-99 inhibits necroptosis via the blockage of RIPK3 kinase activity. It has been demonstrated that GSK'872 is able to induce on-target apoptosis (Mandal et al., 2014). Consistently, Zharp-99 induced activation of caspase-3 and cell death in a dose-dependent manner especially in mouse cells (**Figures 1D,4F**). Compared to GSK'872, Zharp-99 was more potent in inducing apoptosis in MEFs (**Figures 1D,E, 4F**).

Zharp-99 Effectively Alleviates TNF-Induced SIRS

Based on the strong biochemical and cellular anti-necroptosis activity of Zharp-99, we sought to test the therapeutic potential of Zharp-99 in the mouse model of necroptosis-associated diseases. Necroptosis is associated with various pathological conditions such as TNF-induced SIRS (Berger et al., 2014; Duprez et al., 2011). We evaluated the protective effect of Zharp-99 in TNF-induced SIRS in vivo. Female C57BL/6 mice were treated with vehicle or Zharp-99 for 15 min, followed by the intravenous injection of mouse TNFα at 6.5 μg/mouse. Treatment with 5 mg/kg Zharp-99 significantly protected mice against TNFα-induced lethal shock (**Figure 5A**). Zharp-99 treatment also ameliorated TNFα-induced temperature loss in mice (**Figure 5B**). Moreover, Zharp-99 reduced TNFα-induced production of IL-6 in the serum (**Figure 5C**). Collectively, these results demonstrate that RIPK3 inhibition by Zharp-99 provides effective protection against TNF-induced SIRS. The kinase activity of RIPK3 was shown to be required for RIPK3-mediated expression of inflammatory cytokines in mouse BMDM treated with LPS plus z-VAD (Najjar et al., 2016). We found that Zharp-99 could inhibit LPS/z-VAD-induced expression of inflammatory cytokines including TNFα, CCL3, and CXCL1 in mouse BMDM (**Figure 5D**). Taken together, these results suggest that Zharp-99 inhibits RIPK3-mediated cytokine production both *in vitro* and *in vivo*.

Zharp-99 Displays Favorable *in vitro* Safety Profiles and *in vivo* Pharmacokinetic Parameters

Encouraged by the *in vitro* and *in vivo* efficacy data, we sought to evaluate the preliminary drugability profile of Zharp-99. Zharp-99 did not inhibit major human cytochrome P450 isozymes (CYP3A4, 2D6, 1A2, 2C9, 2C19) at 10 μM concentration, suggesting low liability for potential drug/drug interactions. Moreover, Zharp-99 exhibited low inhibition (IC50 > 10 μM) of hERG (standard patch clamp), indicating minimal cardiotoxicity associated with blockade of this key potassium channel (**Figure 6A**). When evaluated for its in vitro metabolic stability in mouse, rat and human liver microsomes, Zharp-99 demonstrated moderate intrinsic clearance across rodent and human species, leading to half-lives ranging from 26 min (MLM) to 37 min (RLM, **Figure 6B**). This data was recapitulated in the standard in vivo mouse pharmacokinetic study. When dosed orally at 10 mg/kg in mice, Zharp-99 was quickly absorbed with a T_{max} of 1 h and C_{max} of 2650 ng/mL. Zharp-99 exhibited a

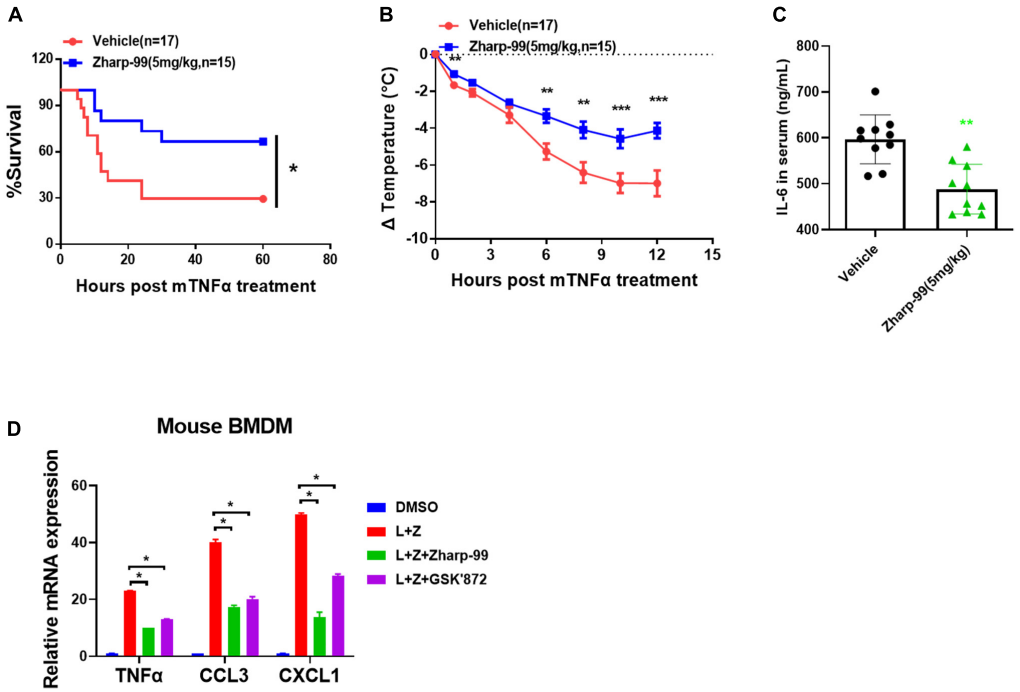

FIGURE 5 | Zharp-99 effectively alleviates TNF-induced systemic inflammatory response syndrome. C57BL/6 mice were injected with vehicle or Zharp-99 (5 mg/kg) via intraperitoneal injection for around 15 min, followed by the tail intravenous injection of mouse TNF-α (6.5 μg/mouse). **(A,B)** The survival rate **(A)** and body temperature loss **(B)** were monitored. The body temperature changes (means ± SEM) for each group are shown. *P*-values were determined using the ONE-way ANOVA and multi-comparison test for statistics analysis. **(C)** After 4 h, serum was collected for mouse IL6 level analysis by ELISA. Data are represented as the mean ± standard deviation. **(D)** Mouse BMDM were pretreated with DMSO, Zharp-99 or GSK'872 for 2 h prior to the treatment of DMSO or LPS (20 ng/ml) plus z-VAD (20 μM) as indicated. After 7 h, cell were harvested for analysis of mRNA expression of TNFα, CCL3, CXCL1 or IL-6 by Q-PCR. $^{*}P < 0.05$. $^{**}P < 0.01$. $^{***}P < 0.001$.

moderate clearance (33 mL/min/kg) and volume of distribution (4.4 L/kg) with a short half-life (1.5 h). The exposure was 8220 h ng/mL, leading to an estimated oral bioavailability over 100% (**Figure 6C**).

DISCUSSION

Necroptosis plays a pivotal role in the pathogenesis of diseases including inflammatory diseases, neurodegenerative diseases, ischemia-reperfusion induced tissue injury and cancer (Linkermann and Green, 2014; He and Wang, 2018; Mifflin et al., 2020). Although RIPK1 is considered as a promising therapeutic targets, emerging evidence suggests that RIPK1-independent necroptosis proceeds when RIPK3 is activated by other RHIM-containing proteins (Mifflin et al., 2020). In the present study, we discovered Zharp-99 as a novel necroptosis inhibitor that directly blocks the kinase activity of RIPK3 and efficiently inhibits necroptosis *in vitro* and *in vivo*.

The kinase activity of RIPK3 is essential for necroptosis (Cho et al., 2009; He et al., 2009; Zhang et al., 2009). Therefore, inhibition of RIPK3 kinase activity is an attractive strategy for interfering with necroptosis and necroptosis-related injury. Our study has demonstrated that Zharp-99 is a potent inhibitor of RIPK3 kinase activity with Kd of 1.35nM. Zharp-99 exhibits higher efficacy in the inhibition of necroptosis and RIPK3 kinase activity compared to GSK872, a well characterized RIPK3 inhibitor (Kaiser et al., 2013; Mandal et al., 2014). It has been noted that mice expressing catalytically inactive RIPK3 D161N leads to caspase8-dependent embryonic lethality (Newton et al., 2014). This phenomenon raises concerns regarding the possible toxic effect in the whole animal when RIPK3 kinase activity is impaired. Unlike RIPK3 D161N knock-in mice, RIPK3 kinase inactive mice which carry a RIPK3 K51A knock-in mutation develop normally and are fertile (Mandal et al., 2014), providing the evidence that inhibition of RIPK3 kinase activity can be tolerated in mice depending on the context. Moreover, the kinase-inactive mutant forms of RIPK3 K51A, D143N, and D161G do not induce apoptosis (Mandal et al., 2014). These findings suggest that the kinase activity of RIP3 kinase is not vital for cell survival. It has been reported that several RIPK3 kinase inhibitors trigger apoptosis by exposing its RHIM domain, therefore facilitating RIPK1 recruitment and activation of caspase-8 for apoptosis (Mandal et al., 2014). Although Zharp-99 does not cause obvious cell death at the tested concentrations when it completely blocks necroptosis, it induces apoptosis at higher concentrations.

Importantly, Zharp-99 provides strong protection against TNF-induced lethal shock and inflammatory responses in the mouse model. This result supports an essential role of RIPK3

A

Compd	hERG	% of CYP inhibiton(10 μM)				
		1A2	2C9	2C19	2D6	CYP3A4
Zharp-99	>10	9.26	-5.59	4.15	-0.44	5.04

B

Zharp-99[a]	$T_{1/2}$(min)	H[b]	28
		R[c]	37
		M[d]	26
	Cl_{int} (mL/min/Kg)	H	63
		R	67
		M	212

[a]Compounds tested at 1 μM.
[b]H = human livermicrosomes.
[c]R = rat liver microsomes.
[d]M = mouse liver microsomes.

C

Zharp-99 Parameter	2 mg/kg (iv)	10 mg/kg (po)
$t_{1/2}$ (h)	1.5	1.2
T_{max} (h)		1.0
C_{max} (ng/mL)	1387	2650
AUC (h*ng/mL)	990	8220
Vz (L/kg)	4.4	
CL (mL/min/kg)	33	
F (%)		166

FIGURE 6 | Zharp-99 displays favorable in vitro safety profiles and in vivo pharmacokinetic parameters. **(A)** CYP and hERG inhibition of Zharp-99. **(B)** Metabolic stability of Zharp-99 in human, rat, and mouse liver microsomes. **(C)** Pharmacokinetic parameters of Zharp-99 determined in male ICR mouse.

kinase activity in the pathogenesis of TNF-induced systemic inflammatory injury. Our work highlights the potential of Zharp-99 for the development of novel anti-inflammatory therapies based on RIPK3 inhibition. It is worth noting that RIPK3 has been shown to regulate inflammatory signaling pathways via a necroptosis-independent mechanism (Wang et al., 2014b; Lawlor et al., 2015; Yatim et al., 2015; Moriwaki and Chan, 2016; Najjar et al., 2016; Daniels et al., 2017). Therefore, further investigation in various mouse models of human disease using RIPK3 kinase-dead mice and RIPK3 inhibitors will provide crucial insights for developing valuable therapies targeting RIPK3.

DATA AVAILABILITY STATEMENT

The original contributions presented in the study are included in the article/**Supplementary Materials**, further inquiries can be directed to the corresponding authors.

ETHICS STATEMENT

The animal study was reviewed and approved by The Institutional Animal Care and Use Committee at Suzhou Institute of Systems Medicine.

AUTHOR CONTRIBUTIONS

SH and XZ designed the study and revised the manuscript. KX and FZ performed the molecular biology and chemistry studies and animal model, analyzed the data, and drafted the manuscript. CY XY, CZ, YJ, WG, JW, and YD performed the cell culture, biochemistry, kinase assay, and HSV infection. SW, YL, and HM performed the chemical synthesis. TY and WZ performed the cell culture and viability assay. All authors contributed to the article and approved the submitted version.

FUNDING

This work was supported by the National Natural Science Foundation of China (31671436, 31830051, 81973161, 81773561, 31900526, 31771533, and 31600133), the Priority Academic Program Development of the Jiangsu Higher Education Institutes (PAPD), the Jiangsu Key Laboratory of Neuropsychiatric Diseases (BM2013003), Natural Science Foundation of Jiangsu Province Grant (BK20160314), Fok Ying Tung Education Foundation for Young Teachers (151020), the CAMS Innovation Fund for Medical Sciences (CIFMS; 2019-I2M-1-004, 2019-I2M-1-003, and 2016-I2M-1-005), Non-profit Central Research Institute Fund of Chinese Academy of Medical Sciences (2019PT310028, 2017NL31004, and 2017NL31002), and China Postdoctoral Science Foundation funded Project (2019M650563).

SUPPLEMENTARY MATERIAL

The Supplementary Material for this article can be found online at: https://www.frontiersin.org/articles/10.3389/fcell.2020.606119/full#supplementary-material

REFERENCES

Berger, S. B., Kasparcova, V., Hoffman, S., Swift, B., Dare, L., Schaeffer, M., et al. (2014). Cutting Edge: RIP1 kinase activity is dispensable for normal development but is a key regulator of inflammation in SHARPIN-deficient mice. *J. Immunol.* 192, 5476–5480. doi: 10.4049/jimmunol.1400499

Cai, Z., Jitkaew, S., Zhao, J., Chiang, H. C., Choksi, S., Liu, J., et al. (2014). Plasma membrane translocation of trimerized MLKL protein is required for TNF-induced necroptosis. *Nat. Cell Biol.* 16, 55–65. doi: 10.1038/ncb2883

Chen, X., Li, W., Ren, J., Huang, D., He, W. T., Song, Y., et al. (2014). Translocation of mixed lineage kinase domain-like protein to plasma membrane leads to necrotic cell death. *Cell Res.* 24, 105–121. doi: 10.1038/cr.2013.171

Cho, Y. S., Challa, S., Moquin, D., Genga, R., Ray, T. D., Guildford, M., et al. (2009). Phosphorylation-driven assembly of the RIP1-RIP3 complex regulates programmed necrosis and virus-induced inflammation. *Cell* 137, 1112–1123. doi: 10.1016/j.cell.2009.05.037

Daniels, B. P., Snyder, A. G., Olsen, T. M., Orozco, S., Oguin, T. H. III, Tait, S. W. G., et al. (2017). RIPK3 restricts viral pathogenesis via cell death-independent neuroinflammation. *Cell* 169:e11. doi: 10.1016/j.cell.2017.03.011

Dong, Y., Li, K., Xu, Z., Ma, H., Zheng, J., Hu, Z., et al. (2015). Exploration of the linkage elements of porcupine antagonists led to potent Wnt signaling pathway inhibitors. *Bioorg. Med. Chem.* 23, 6855–6868. doi: 10.1016/j.bmc.2015.09.048

Duprez, L., Takahashi, N., Van Hauwermeiren, F., Vandendriessche, B., Goossens, V., Vanden Berghe, T., et al. (2011). RIP kinase-dependent necrosis drives lethal systemic inflammatory response syndrome. *Immunity.* 35, 908–918. doi: 10.1016/j.immuni.2011.09.020

Fauster, A., Rebsamen, M., Huber, K. V., Bigenzahn, J. W., Stukalov, A., Lardeau, C. H., et al. (2015). A cellular screen identifies ponatinib and pazopanib as inhibitors of necroptosis. *Cell Death Dis.* 6:e1767. doi: 10.1038/cddis.2015.130

Hart, A. C., Abell, L., Guo, J., Mertzman, M. E., Padmanabha, R., Macor, J. E., et al. (2020). Identification of RIPK3 type II inhibitors using high-throughput mechanistic studies in hit triage. *ACS Med. Chem. Lett.* 11, 266–271. doi: 10.1021/acsmedchemlett.9b00065

He, S., and Wang, X. (2018). RIP kinases as modulators of inflammation and immunity. *Nat. Immunol.* 19, 912–922. doi: 10.1038/s41590-018-0188-x

He, S., Liang, Y., Shao, F., and Wang, X. (2011). Toll-like receptors activate programmed necrosis in macrophages through a receptor-interacting kinase-3-mediated pathway. *Proc. Natl. Acad. Sci. U S A.* 108, 20054–20059. doi: 10.1073/pnas.1116302108

He, S., Wang, L., Miao, L., Wang, T., Du, F., Zhao, L., et al. (2009). Receptor interacting protein kinase-3 determines cellular necrotic response to TNF-alpha. *Cell* 137, 1100–1111. doi: 10.1016/j.cell.2009.05.021

Holler, N., Zaru, R., Micheau, O., Thome, M., Attinger, A., Valitutti, S., et al. (2000). Fas triggers an alternative, caspase-8-independent cell death pathway using the kinase RIP as effector molecule. *Nat. Immunol.* 1, 489–495. doi: 10.1038/82732

Huang, Z., Wu, S. Q., Liang, Y., Zhou, X., Chen, W., Li, L., et al. (2015). RIP1/RIP3 binding to HSV-1 ICP6 initiates necroptosis to restrict virus propagation in mice. *Cell Host. Microbe.* 17, 229–242. doi: 10.1016/j.chom.2015.01.002

Kaiser, W. J., Sridharan, H., Huang, C., Mandal, P., Upton, J. W., Gough, P. J., et al. (2013). Toll-like receptor 3-mediated necrosis via TRIF. RIP3, and MLKL. *J. Biol. Chem.* 288, 31268–31279. doi: 10.1074/jbc.M113.462341

Lawlor, K. E., Khan, N., Mildenhall, A., Gerlic, M., Croker, B. A., D'Cruz, A. A., et al. (2015). RIPK3 promotes cell death and NLRP3 inflammasome activation in the absence of MLKL. *Nat. Commun.* 6:6282. doi: 10.1038/ncomms7282

Li, J. X., Feng, J. M., Wang, Y., Li, X. H., Chen, X. X., Su, Y., et al. (2014). The B-Raf(V600E) inhibitor dabrafenib selectively inhibits RIP3 and alleviates acetaminophen-induced liver injury. *Cell Death Dis.* 5:e1278. doi: 10.1038/cddis.2014.241

Linkermann, A., and Green, D. R. (2014). Necroptosis. *N. Engl. J. Med.* 370, 455–465. doi: 10.1056/NEJMra1310050

Liu, S., Liu, H., Johnston, A., Hanna-Addams, S., Reynoso, E., Xiang, Y., et al. (2017). MLKL forms disulfide bond-dependent amyloid-like polymers to induce necroptosis. *Proc. Natl. Acad. Sci. U S A.* 114, E7450–E7459. doi: 10.1073/pnas.1707531114

Lu, W., Liu, Y., Ma, H., Zheng, J., Tian, S., Sun, Z., et al. (2017). Design. synthesis, and structure-activity relationship of tetrahydropyrido[4,3-d]pyrimidine derivatives as potent smoothened antagonists with in vivo activity. *ACS Chem. Neurosci.* 8, 1980–1994. doi: 10.1021/acschemneuro.7b00153

Mandal, P., Berger, S. B., Pillay, S., Moriwaki, K., Huang, C., Guo, H., et al. (2014). RIP3 induces apoptosis independent of pronecrotic kinase activity. *Mol. Cell* 56, 481–495. doi: 10.1016/j.molcel.2014.10.021

Mifflin, L., Ofengeim, D., and Yuan, J. (2020). Receptor-interacting protein kinase 1 (RIPK1) as a therapeutic target. *Nat. Rev. Drug. Discov.* 19, 553–571. doi: 10.1038/s41573-020-0071-y

Moriwaki, K., and Chan, F. K. (2016). Necroptosis-independent signaling by the RIP kinases in inflammation. *Cell Mol. Life Sci.* 73, 2325–2334. doi: 10.1007/s00018-016-2203-4

Murphy, J. M., Czabotar, P. E., Hildebrand, J. M., Lucet, I. S., Zhang, J. G., Alvarez-Diaz, S., et al. (2013). The pseudokinase MLKL mediates necroptosis via a molecular switch mechanism. *Immunity* 39, 443–453. doi: 10.1016/j.immuni.2013.06.018

Najjar, M., Saleh, D., Zelic, M., Nogusa, S., Shah, S., Tai, A., et al. (2016). RIPK1 and RIPK3 kinases promote cell-death-independent inflammation by toll-like receptor 4. *Immunity* 45, 46–59. doi: 10.1016/j.immuni.2016.06.007

Newton, K., Dugger, D. L., Wickliffe, K. E., Kapoor, N., de Almagro, M. C., Vucic, D., et al. (2014). Activity of protein kinase RIPK3 determines whether cells die by necroptosis or apoptosis. *Science* 343, 1357–1360. doi: 10.1126/science.1249361

Orozco, S., Yatim, N., Werner, M. R., Tran, H., Gunja, S. Y., Tait, S. W., et al. (2014). RIPK1 both positively and negatively regulates RIPK3 oligomerization and necroptosis. *Cell Death Differ.* 21, 1511–1521. doi: 10.1038/cdd.2014.76

Park, H. H., Park, S. Y., Mah, S., Park, J. H., Hong, S. S., Hong, S., et al. (2018). HS-1371, a novel kinase inhibitor of RIP3-mediated necroptosis. *Exp. Mol. Med.* 50:125. doi: 10.1038/s12276-018-0152-8

Samir, P., Malireddi, R. K. S., and Kanneganti, T. D. (2020). The PANoptosome: a deadly protein complex driving pyroptosis. apoptosis, and necroptosis (PANoptosis). *Front. Cell Infect. Microbiol.* 10:238. doi: 10.3389/fcimb.2020.00238

Sun, L., Wang, H., Wang, Z., He, S., Chen, S., Liao, D., et al. (2012). Mixed lineage kinase domain-like protein mediates necrosis signaling downstream of RIP3 kinase. *Cell* 148, 213–227. doi: 10.1016/j.cell.2011.11.031

Upton, J. W., Kaiser, W. J., and Mocarski, E. S. (2012). DAI/ZBP1/DLM-1 complexes with RIP3 to mediate virus-induced programmed necrosis that is targeted by murine cytomegalovirus vIRA. *Cell Host. Microbe.* 11, 290–297. doi: 10.1016/j.chom.2012.01.016

Wang, H., Sun, L., Su, L., Rizo, J., Liu, L., Wang, L. F., et al. (2014a). Mixed lineage kinase domain-like protein MLKL causes necrotic membrane disruption upon phosphorylation by RIP3. *Mol. Cell* 54, 133–146. doi: 10.1016/j.molcel.2014.03.003

Wang, L., Du, F., and Wang, X. (2008). TNF-alpha induces two distinct caspase-8 activation pathways. *Cell* 133, 693–703. doi: 10.1016/j.cell.2008.03.036

Wang, X., Jiang, W., Yan, Y., Gong, T., Han, J., Tian, Z., et al. (2014b). RNA viruses promote activation of the NLRP3 inflammasome through a RIP1-RIP3-DRP1 signaling pathway. *Nat. Immunol.* 15, 1126–1133. doi: 10.1038/ni.3015

Wang, X., Li, Y., Liu, S., Yu, X., Li, L., Shi, C., et al. (2014c). Direct activation of RIP3/MLKL-dependent necrosis by herpes simplex virus 1 (HSV-1) protein ICP6 triggers host antiviral defense. *Proc. Natl. Acad. Sci. U S A.* 111, 15438–15443. doi: 10.1073/pnas.1412767111

Yatim, N., Jusforgues-Saklani, H., Orozco, S., Schulz, O., and Barreira, R. (2015). da Silva. C Reis e Sousa, et al. RIPK1 and NF-kappaB signaling in dying cells determines cross-priming of CD8(+) T cells. *Science* 350, 328–334. doi: 10.1126/science.aad0395

Zhang, D. W., Shao, J., Lin, J., Zhang, N., Lu, B. J., Lin, S. C., et al. (2009). RIP3, an energy metabolism regulator that switches TNF-induced cell death from apoptosis to necrosis. *Science* 325, 332–336. doi: 10.1126/science.1172308

Zhang, H., Xu, L., Qin, X., Chen, X., Cong, H., Hu, L., et al. (2019). N-(7-Cyano-6-(4-fluoro-3-(2-(3-(trifluoromethyl)phenyl)acetamido)phenoxy)benzo[d]thiazol-2-yl)cyclopropanecarboxamide (TAK-632) analogues as novel necroptosis inhibitors by targeting receptor-interacting protein kinase 3 (RIPK3): synthesis. structure-activity relationships, and in vivo efficacy. *J. Med. Chem.* 62, 6665–6681. doi: 10.1021/acs.jmedchem.9b00611

Zhao, J., Jitkaew, S., Cai, Z., Choksi, S., Li, Q., Luo, J., et al. (2012). Mixed lineage kinase domain-like is a key receptor interacting protein 3 downstream component of TNF-induced necrosis. *Proc. Natl. Acad. Sci. U S A.* 109, 5322–5327. doi: 10.1073/pnas.1200012109

Conflict of Interest: XZ and SH are co-founders, consultants and shareholders of Accro Bioscience Inc., which supports research in their labs.

The remaining authors declare that the research was conducted in the absence of any commercial or financial relationships that could be construed as a potential conflict of interest.

frontiers in Cell and Developmental Biology

REVIEW
published: 23 December 2020
doi: 10.3389/fcell.2020.610022

Caspase-2 Substrates: To Apoptosis, Cell Cycle Control, and Beyond

Alexandra N. Brown-Suedel[1,2] *and Lisa Bouchier-Hayes*[1,2]*

[1] *Hematology-Oncology Section, Department of Pediatrics, Department of Molecular Cell Biology, Baylor College of Medicine, Houston, TX, United States,* [2] *William T. Shearer Center for Human Immunobiology, Texas Children's Hospital, Houston, TX, United States*

Caspase-2 belongs to the caspase family of proteins responsible for essential cellular functions including apoptosis and inflammation. Uniquely, caspase-2 has been identified as a tumor suppressor, but how it regulates this function is still unknown. For many years, caspase-2 has been considered an "orphan" caspase because, although it is able to induce apoptosis, there is an abundance of conflicting evidence that questions its necessity for apoptosis. Recent evidence supports that caspase-2 has non-apoptotic functions in the cell cycle and protection from genomic instability. It is unclear how caspase-2 regulates these opposing functions, which has made the mechanism of tumor suppression by caspase-2 difficult to determine. As a protease, caspase-2 likely exerts its functions by proteolytic cleavage of cellular substrates. This review highlights the known substrates of caspase-2 with a special focus on their functional relevance to caspase-2's role as a tumor suppressor.

Keywords: caspase-2, PIDD, Raidd, BID, MDM2, apoptosis, cell cycle, tumor suppressor

OPEN ACCESS

Edited by:
Yinan Gong,
University of Pittsburgh, United States

Reviewed by:
Andreas Villunger,
Innsbruck Medical University, Austria
Elodie Lafont,
INSERM U1242 Laboratoire COSS, France

***Correspondence:**
Lisa Bouchier-Hayes
bouchier@bcm.edu;
lxbouchi@txch.org

Specialty section:
This article was submitted to Cell Death and Survival, a section of the journal Frontiers in Cell and Developmental Biology

Received: *24 September 2020*
Accepted: *03 December 2020*
Published: *23 December 2020*

Citation:
Brown-Suedel AN and Bouchier-Hayes L (2020) Caspase-2 Substrates: To Apoptosis, Cell Cycle Control, and Beyond. Front. Cell Dev. Biol. 8:610022. doi: 10.3389/fcell.2020.610022

INTRODUCTION

Members of the caspase family of proteases are essential for the initiation and execution of apoptosis. When caspases are activated, they cleave a wide variety of substrates that bring about the death of the cell and are responsible for the morphological hallmarks of apoptosis, including membrane blebbing and nuclear condensation. Certain caspase targets have more specific functions that can even regulate non-apoptotic functions of caspases. The classical example of this is the cleavage of pro-IL-1β by caspase-1 to initiate the inflammatory response (Bolivar et al., 2019). Caspase-2 is considered a pro-apoptotic caspase that has a unique role as a tumor suppressor in multiple tissue types. Emerging evidence demonstrates that caspase-2 not only has an apoptotic role, but that it can also contribute to the regulation of other cellular events including cell division. However, there are only a few fully verified caspase-2 substrates that are known and, therefore, how caspase-2 can regulate both apoptosis and non-apoptotic processes to suppress tumors has been difficult to unravel. In this review, we highlight the substrates of caspase-2 and explore possible mechanisms of substrate selection that may regulate the tumor suppressive function of caspase-2.

THE MECHANISM OF CASPASE-2 ACTIVATION

Caspase-2 is classified as an initiator caspase, which respond to apoptotic stimuli by initiating the apoptotic cascade. Like other caspases, caspase-2 is comprised of an N-terminal prodomain and a large and small catalytic subunit. A defining characteristic of initiator caspases, the long

prodomain of caspase-2 contains a protein interaction motif, specifically a caspase activation recruitment domain (CARD) (Hofmann et al., 1997). This prodomain is essential for initiating caspase-2 activation because it facilitates dimerization of caspase monomers, which is the apical step in initiator caspase activation (Baliga et al., 2004). Dimerization of initiator caspases occurs through induced proximity upon recruitment to high molecular weight complexes called activation platforms. This occurs through protein-protein interactions mediated by conserved domains. For example, caspase-8 is recruited to and is dimerized at the DISC (death inducing signaling complex) by interaction between death effector domains (DEDs) present in caspase-8 and its adaptor protein FADD (Fas-associated protein with death domain). In the APAF-1 (Apoptotic protease activating factor 1) apoptosome, caspase-9 is activated by dimerization mediated by interactions between the CARDs present in APAF-1 and caspase-9 (Boatright and Salvesen, 2003). Caspase-2 is activated in a similar fashion. The activation platform for caspase-2 appears to be the PIDDosome, a molecular complex containing the proteins PIDD1 (p53-inducible protein with a death domain 1) and RAIDD (receptor-interacting protein-associated ICH-1/CED-3 homologous protein with a death domain) (Tinel and Tschopp, 2004; **Figure 1**). PIDD1 is a p53 response gene that serves as a scaffold for PIDDosome assembly. Upon expression, PIDD1 is constitutively processed by an autocatalytic mechanism into three fragments: PIDD-N, PIDD-C, and PIDD-CC (Tinel et al., 2007). Cleavage of full length PIDD1 to PIDD-N and PIDD-C occurs first, followed by a second cleavage of PIDD-C to yield PIDD-CC. It is the death domain (DD) containing PIDD-CC fragment that is responsible for assembly of the PIDDosome and activation of caspase-2. RAIDD serves as the adaptor molecule to mediate the PIDDosome's assembly. RAIDD contains both a CARD domain and a DD (death domain) and binds caspase-2 via a CARD-CARD interaction (Duan and Dixit, 1997). Similarly, the DD of RAIDD binds a DD in PIDD1 (Tinel and Tschopp, 2004). A cleavage defective mutant of PIDD1 that could not be processed to PIDD-CC failed to bind RAIDD and did not induce apoptosis after treatment with doxorubicin, demonstrating the necessity of PIDD-CC for PIDDosome assembly and caspase-2-mediated death (Tinel et al., 2007). Assembly of this complex facilitates proximity-induced dimerization, and thus, activation of caspase-2 (Bouchier-Hayes et al., 2009). The crystal structure of the PIDD1 DD/RAIDD DD interaction reveals an asymmetric, oligomeric complex containing five PIDD1 death domains bound to 7 RAIDD death domains (Park et al., 2007). This structure would potentially allow up to seven caspase-2 monomers to be recruited via an interaction with RAIDD. This asymmetry is odd, because only six monomers could dimerize at one time, resulting in three active caspase-2 dimers. The significance of this asymmetry is unknown, but evidence from the asymmetric CARD interactions between initiator caspase-9 and the apoptosome suggests that asymmetric assembly may allow for enhanced stabilization of the complex (Dorstyn et al., 2018).

The primary evidence that caspase-2 belongs to the initiator caspase subgroup is that, similar to caspase-8 and caspase-9, caspase-2 is activated by dimerization and not cleavage

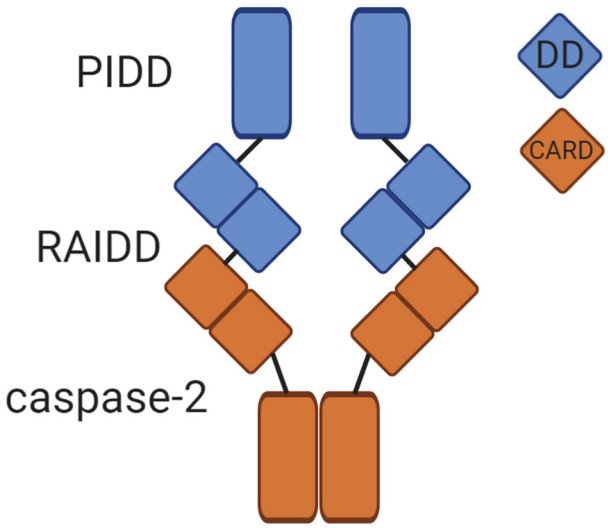

FIGURE 1 | The caspase-2 PIDDosome. The PIDDosome is the best characterized caspase-2 activation platform. PIDD-CC and RAIDD form the scaffold for complex formation via an interaction between their corresponding death domains (DD, blue squares). The CARD of caspase-2 binds the CARD of RAIDD (orange squares), promoting proximity-induced dimerization of caspase-2 monomers. This allows caspase-2 to become fully catalytically active.

(Baliga et al., 2004). *In vitro* studies using recombinant caspase-2 showed that monomeric caspase-2 had no catalytic activity, while a dimeric version of caspase-2 was fully active. When the cleavage site of caspase-2 was mutated to prevent cleavage, the dimeric full length protein retained up to 20% of its catalytic efficiency. This demonstrates that dimerization must occur for activation of caspase-2 (Baliga et al., 2004). After dimerization, cleavage of caspase-2 occurs auto-catalytically. This functions to stabilize the active dimer, resulting in enhanced catalytic efficiency. This is similar to the activation mechanisms for caspase-8 and caspase-9 (Boatright et al., 2003), and distinct to that of the executioner caspases, caspase-3 and caspase-7, which are activated by cleavage (Boatright and Salvesen, 2003). While caspase-2 can be cleaved by caspase-3 (Harvey et al., 1996), unlike executioner caspases, it is not dependent on additional caspases for its proteolytic processing. For example, caspase-2 cleavage induced by PIDD1 overexpression is not impaired in MCF-7 cells lacking caspase-3 (Tinel and Tschopp, 2004). In contrast, in thymocytes deficient in APAF-1 or caspase-9, caspase-2 processing was defective in response to intrinsic apoptosis stimuli like actinomycin D, but loss of caspase-2 did not impair apoptosis (O'Reilly et al., 2002). Together, these studies provide evidence that caspase-2 processing downstream of caspase-3, in the absence of dimerization, is dispensable for cell death in response to stimuli that directly engage the mitochondrial pathway, while caspase-2 cleavage that results from auto-processing following dimerization is more representative of caspase-2 activation.

Despite structural evidence that classifies caspase-2 as an initiator caspase, it possesses unique qualities that set it apart from the other initiator caspases and clouded its initial

categorization. The canonical function of initiator caspases is to activate downstream executioner caspases by proteolytic cleavage (Boatright and Salvesen, 2003). Caspase-2 has no detectable enzymatic activity toward other caspases; instead, it cleaves other cellular substrates to promote its functions and indirect activation of downstream caspases (Guo et al., 2002). Early studies of peptide libraries showed that the cleavage specificity of caspase-2 is more similar to executioner caspases than other initiator caspases (Talanian et al., 1997; Thornberry et al., 1997). The most efficiently cleaved caspase-2 substrate peptide, VDVAD, is also efficiently cleaved by executioner caspases (Talanian et al., 1997; Thornberry et al., 1997). A more recent degradomics approach revealed that caspase-2, caspase-3, and caspase-7 were nearly identical in their substrate cleavage motif preference, DEVD, demonstrating the overlap between caspase-2 and executioner caspase substrate specificity (Wejda et al., 2012). This overlap has made it challenging to not only categorize caspase-2, but also to identify its unique physiological substrate pool responsible for executing its functions. Without a full understanding of caspase-2's targets and their impact on cell death, it has been difficult to correctly place caspase-2 in the apoptotic cascade and to fully understand its physiological functions.

CASPASE-2 IS A TUMOR SUPPRESSOR

Somewhat unique among the caspase family is caspase-2's proposed function as a tumor suppressor (Boice and Bouchier-Hayes, 2020). Caspase-2 has been identified as a tumor suppressor in multiple murine models of oncogene-driven cancers. While caspase-2 deficiency alone is not competent to induce tumor formation, its role as a tumor suppressor has been recapitulated by independent groups and in various cancer models. The first demonstration of the tumor suppressor ability of caspase-2 was in an *Eμ-Myc* model of lymphoma (Ho et al., 2009). *Eμ-Myc* transgenic mice develop spontaneous B cell lymphomas due to MYC expression from the strong immunoglobulin μ enhancer (Adams et al., 1985). Both partial and complete loss of caspase-2 in combination with the *Eμ-Myc* transgene accelerated the rate of growth of these tumors (Ho et al., 2009; Manzl et al., 2012). These findings were recapitulated in a second lymphoma model using *Atm*-deficient mice (Puccini et al., 2013). Dual caspase-2/ATM deficiency increased the incidence of tumor formation from 31% in control *Atm*-deficient mice to nearly 64% in *Casp2/Atm* double knockout mice. Further, the average age of tumor onset was decreased in *Casp2/Atm* double knockout mice compared to *Atm* knockout alone. This suggests that loss of caspase-2 not only increased overall tumor incidence but also increased the rate of tumorigenesis. This increased tumorigenesis also resulted in significantly poorer survival of *Casp2/Atm* knockout mice in comparison to loss of *Atm* alone. Caspase-2 also acts as a tumor suppressor in non-hematologic malignancies. Using a model of MMTV/*c-neu* mammary tumor formation, we demonstrated that caspase-2 can also act as a tumor suppressor in the context of an epithelial cancer (Parsons et al., 2013). Deletion of caspase-2 increased tumor incidence and significantly decreased cancer free survival in multiparous female mice. Similarly, loss of caspase-2 has been linked to increased tumor burden in the *Kras*-driven lung cancer model (Terry et al., 2015). In this model, *Kras* lung tumors deficient in caspase-2 were both more numerous and had a higher average volume than tumors induced by Kras alone. This difference in tumor burden has also been observed in a chemically induced model of liver cancer, where caspase-2 deficiency promoted both higher incidence and a significantly increased number of cancerous nodes in the liver after injection with the DNA-alkylating and reactive oxygen species carcinogen Diethylnitrosamine (DEN) (Shalini et al., 2016). However, a more recent article showed results in direct opposition to this where DEN-induced liver tumors were more abundant in wild type mice than in mice deficient in either caspase-2, PIDD1, or RAIDD (Sladky et al., 2020b). The reason for this difference is unclear, as the only notable difference in these models is the use of slightly different mouse strains. Shalini et al. used all male mice on a C57BL/6J background, which has a mutation in the NNT gene associated with glucose-mediated insulin secretion, whereas Sladky et al. used all male C57BL/6N mice, which are wild type for this gene (Freeman et al., 2006). However, the significance of this small difference is uncertain. This is not the only model where caspase-2 has been implicated in tumor progression rather than suppression. In a model of *ThMycn*-induced neuroblastoma, *Th-Mycn/Casp2* null mice had delayed onset of tumor formation, suggesting that caspase-2 potentiated tumor growth in this model (Dorstyn et al., 2014). Finally, loss of caspase-2 had no effect on tumor incidence or growth in irradiation-induced lymphoma or 3-methylcholanthrene-induced fibrosarcoma murine models (Peintner et al., 2015). These distinct effects of caspase-2 on different tumor types strongly suggests that caspase-2 functions in different capacities depending on the cellular context.

The mechanism of tumor suppression by caspase-2 has been difficult to determine. As an established mediator of apoptosis, it may be expected that the caspase-2-deficient tumors described above are more resistant to apoptosis and that this defect in cell death underlies their accelerated tumorigenesis. However, this has been difficult to determine. Caspase-2 was initially identified as a conserved pro-apoptotic cysteine protease. Upon its discovery, it was shown that overexpression of caspase-2 resulted in apoptotic cell death in fibroblasts and neuroblastoma cells (Kumar et al., 1994). It has been implicated in apoptosis induced by a variety of damaging stimuli including heat shock, DNA damage, aneuploidy, and microtubule disruption (Robertson et al., 2002; Tu et al., 2006; Ho et al., 2008; Dawar et al., 2017). However, the importance of caspase-2 for cell death is complicated by observations that loss of caspase-2 is not universally protective from cell death induced by these stimuli in all cell types (reviewed in Bouchier-Hayes and Green, 2012). Indeed, much of the controversy in the caspase-2 field has largely resulted from inconsistencies in the apparent necessity for caspase-2 during apoptosis.

For example, caspase-2-deficient splenocytes are resistant to heat shock-induced death, while Jurkat cells are not (Tu et al., 2006; Shelton et al., 2010). In another example, *E1A/Ras* transformed caspase-2-deficient mouse embryonic fibroblasts (MEF) were found to be resistant to apoptosis induced by

irradiation, while their primary counterparts were not (Ho et al., 2009). Further clouding the contribution of caspase-2 to apoptosis, is the comparatively normal phenotype of caspase-2-deficient mice. While knockout of the other initiator caspases results in lethality (Zheng et al., 1999), caspase-2 knockout mice are viable, fertile, and are born at expected Mendelian ratios (Bergeron et al., 1998). These animals have few apoptotic defects, but females do have excess oocytes. With the exception of oocytes, most primary cells from these animals are not particularly resistant to apoptosis. Intriguingly, and in direct contrast with a pro-apoptotic role for caspase-2, facial motor neurons die at an accelerated rate in caspase-2-deficient mice. A second, independently generated, caspase-2-deficient knockout line showed similar phenotypes where primary thymocytes and dorsal root ganglion neurons did not display defects in apoptosis in the absence of caspase-2 (O'Reilly et al., 2002).

Consistent with the unclear apoptotic function for caspase-2, few apoptotic defects are reported in caspase-2-deficient tumor models. In *Atm*-deficient lymphomas, loss of caspase-2 had no effect on cell death, both in terms of background death, and death induced by irradiation as measured by TUNEL staining and gating of sub-G1 DNA content cells, respectively (Puccini et al., 2013). In contrast, sub-cultured primary lymphoma cells from *Eμ-Myc* lymphomas lacking caspase-2 showed a decreased sensitivity to apoptosis induced by cytoskeletal disruption and irradiation as measured by Annexin V binding (Ho et al., 2009). Whether these results contradict due to the mechanism of action of their respective driver genes (*Eμ-Myc* vs. *Atm* deficiency) or due to differences in the measurement of cell death (TUNEL staining vs. Annexin V binding) is unclear. It is possible that measurement of a more upstream marker of apoptosis would reveal a more profound apoptotic defect in caspase-2-deficient tumors. Terry et al. (2015) used cleaved caspase-3 as a marker of apoptotic cells in their model of *Kras*-driven lung cancer. Surprisingly, they found that caspase-2-deficient *Kras*-driven lung tumors had a significant increase in apoptotic cells after cisplatin treatment that was not observed in caspase-2 wild-type tumors. This result suggests that caspase-2-deficient tumor cells may be more susceptible to apoptosis and is at odds with the role of caspase-2 as a pro-apoptotic protease. However, this result could be due to other phenomena associated with the loss of caspase-2 as discussed below. In the *Th-Mycn* neuroblastoma model, no difference in cell death was observed, although no treatment was administered (Dorstyn et al., 2014). This could potentially be explained by findings that the neuronal activity of caspase-2 requires RAIDD and not PIDD1 (Ribe et al., 2012). Although this was determined in the context of treatment with damaging stimuli, and proposed that RAIDD was required for caspase-2 mediated death of neurons, it provides a potential mechanism for the disparate effects of caspase-2 in different cell types. The difficulty in uncovering the impact of caspase-2 on apoptosis in a tumor setting is reminiscent of the lack of apoptotic phenotypes in caspase-2-deficient mice (Bergeron et al., 1998). In all tumor models discussed above, tumors were generated on a caspase-2-deficient background. The ability of caspase-2 to suppress tumors by assessing tumorigenesis resulting from acute loss of caspase-2, rather than in fully caspase-2-deficient animals has not yet been assessed. Such an acute model of caspase-2 loss could allow for tissue specific effects of caspase-2 to be revealed. Ultimately, the true contribution of apoptosis to the mechanism of tumor suppression by caspase-2 is still largely unknown. These disparate findings of caspase-2's varying capacities in inducing apoptosis suggest that, while caspase-2 can induce apoptosis, it may perform other non-apoptotic functions that contribute to tumor suppression.

In the paper by Ho et al. (2009) that first identified caspase-2 as a tumor suppressor, the authors also noted that caspase-2-deficient MEF proliferated significantly faster than their wild-type counterparts, suggesting a defect in cell cycle control in the absence of caspase-2. Investigation of this phenotype revealed that a significantly higher proportion of caspase-2 deficient cells continued to proliferate after irradiation compared to wild-type cells. This suggests that caspase-2 deficient cells failed to arrest after DNA damage. It is generally thought that highly proliferative tumors are subject to replication stress, which can culminate in various forms of DNA damage (Negrini et al., 2010). Whether loss of caspase-2 causes a failure to arrest due to replication stress in tumors is still unknown, but this could be a potential explanation for faster proliferation. This accelerated growth mirrors the more rapid tumorigenesis and increased tumor burden seen in many of the tumor models discussed here. MMTV/*c-neu* mammary tumors that lacked caspase-2 had a higher mitotic index than caspase-2 wild-type tumors (Parsons et al., 2013). In *Atm*-deficient lymphomas, loss of caspase-2 conferred a proliferative advantage without impacting apoptosis (Puccini et al., 2013). This enhanced proliferation was also observed in *Kras*-driven lung tumors deficient in caspase-2 (Terry et al., 2015). However, in non-transformed primary MEF the effect of caspase-2 loss on proliferation was not as dramatic (Manzl et al., 2009). Therefore, similar to the apoptotic phenotypes associated with caspase-2, an oncogenic trigger may be required for this function of caspase-2. Similarly, in the neuroblastoma model, where caspase-2 appeared to act more like an oncogene, defects in proliferation were not observed (Dorstyn et al., 2014). The increased proliferation seen in the absence of caspase-2 in some but not all tumor models suggests that this effect could be tissue or cell type dependent. Identifying the mechanism of this increased proliferation could reveal the mechanism of tumor suppression by caspase-2.

A prevalent phenotype in caspase-2-deficient tumor models results from features associated with increased genomic instability. Genomic instability is a hallmark of cancer (Hanahan and Weinberg, 2000), and is thought to promote tumor heterogeneity and overall tumor survival (Burrell et al., 2013), so this could also be a potential mechanism to explain the tumor suppressor function of caspase-2. MMTV/*c-neu* mammary tumors from caspase-2-deficient animals had a higher proportion of cells with karyomegaly, aneuploidy, and chromosomal aberrations in the form of bizarre mitoses (Parsons et al., 2013). *Atm*-deficient lymphomas display a low level of chromosomal instability, but this was significantly exacerbated in the absence of caspase-2 (Puccini et al., 2013). Incidence of both low and high grade aneuploidy was increased in dual *Casp2*/*Atm*-deficient lymphomas, suggesting that caspase-2

protects against aneuploidy. In support of this function, it was shown that when caspase-2 expression is suppressed in a model of colorectal cancer, aneuploidy increased (Lopez-Garcia et al., 2017). It is possible that prevention of genomic instability is tied to caspase-2's apoptotic role. In primary splenocytes, it was shown that caspase-2 is required for cell death induced by aneuploidy (Dawar et al., 2017). Aneuploidy was induced by inhibition of PLK1, which is important for centrosome maturation and mitotic spindle formation. *Casp2* knockout cells were more resistant to treatment with a PLK1 inhibitor and became multinucleated. Increased resistance to death and a higher incidence of multinucleation was also observed when caspase-2-deficient cells were treated with the microtubule disruptor Taxol, which also impacts mitotic spindle formation. Primary MEF cells lacking caspase-2 had previously been shown to be more resistant to Taxol, suggesting that caspase-2 is required for death induced by cytoskeletal disruption (Ho et al., 2008). While more recent studies have shown no requirement for caspase-2 in cytoskeletal disruption-induced cell death (Manzl et al., 2009), cytoskeletal disruptors like Taxol and Vincristine are inducers of caspase-2 activation (Bouchier-Hayes et al., 2009; Ando et al., 2017). Thus, aneuploidy resulting from cytoskeletal disruption may be a trigger for caspase-2-mediated apoptosis or may lead to an alternative caspase-2-mediated functional outcome. Therefore, caspase-2 may prevent aneuploidy and genomic instability due to its role in the cell cycle and the increased genomic instability observed in caspase-2-deficient tumors is a result of defective cell cycle regulation as a result of cytokinesis failure.

So, how can an ostensibly pro-apoptotic protein regulate both apoptosis and cell division and how does it have such disparate effects on different tumor models? In the remaining part of this review, we propose that this is achieved through differential targeting of caspase-2 substrates. In short, caspase-2 gains access to different subsets of proteolytic targets in a context-dependent manner, and this access is determined by how caspase-2 is regulated.

CASPASE-2 SUBSTRATES

There has been a distinct lack of investigation into the substrates of caspase-2, which has hampered our understanding of how this caspase functions. For example, the MEROPS database of proteases and substrates has cataloged 244 caspase-2 substrates (Rawlings et al., 2018). Caspase-3 has nearly twice the number of recorded substrates in the MEROPS database. However, the more telling comparison lies elsewhere. The over 400 caspase-3 substrates listed in the MEROPS database have been compiled from 222 individual studies. In comparison, the 244 caspase-2 substrates come from a mere 13 studies. Of these, 95% come from a single study, performed by Julien et al. (2016). While this landmark study identified the majority of known caspase-2 substrates, it highlights the lack of attention caspase-2 substrates have received in the field.

To date, the largest-scale characterization of caspase-2 substrates was performed using N-terminal degradomics (Julien et al., 2016). Not only were many unique caspase-2 substrates identified, but by performing quantitative enzymology on the top hits from the degradomics screen, the potential physiological relevance of these substrates was addressed. BID, MDM2, and Golgin-160, the three known substrates for caspase-2, were not identified in this screen, highlighting the limitations of this type of *in vitro* approach for identifying caspase substrates. In addition, the relevance and veracity of the majority of the substrates that were identified have not yet been validated in physiological settings. Due to these problems, there are only a few verified substrates for caspase-2 that have been identified and characterized *in vivo*. Because of this, it is not our intention to provide an extensive list of every substrate that has been published as a putative caspase-2 substrate. Rather, we provide a discussion of the more well-studied caspase-2 substrates, with attention paid to how these substrates may be executing the functions of caspase-2 that could contribute to tumor suppression (**Table 1**). We contend that there exists a number of additional, as yet unidentified, caspase-2 substrates, the access

TABLE 1 | Caspase-2 substrates.

Substrate	Caspase-2 cleavage motif (human)	Position (human)	Conserved in mouse (Y/N)	Mouse cleavage motif	Position (mouse)	Cleaved by other caspases?
MDM2	DVPD	362	Yes	DVPD	359	Caspase-3
Golgin-160	ESPD	59	Yes	GSPD	59	No
Golgin-160	SEVD	311	Yes	SEAD	308	Caspase-3 and caspase-7
Bid	LQTD	60	Yes	LQTD	59	Caspase-8 and caspase-3
Ku80	GDVD	726	Yes	GDVD	725	Unknown
ICAD	?	?	?	?	?	Caspase-3
Rictor	?	?	?	?	?	Unknown
eIF4B	DRKD	563	Yes	DRKD	563	Caspase-3*
HDAC4	DVTD	289	Yes	DVTD	288	Caspase-3 and caspase-7
Tau	KPVD	314	Yes	KEQD	289	Unknown
HTT	NGKD	213	Yes	NGKD	212	Caspase-3
S1P	LYGD	846	Yes	LYGD	846	Unknown

**With a much lower efficiency than caspase-2.*

to which provides critical decision points for the execution of caspase-2 function.

BID—The Primary Mediator of Caspase-2 Induced Apoptosis

Early demonstrations of caspase-2 as an apoptotic protease also yielded the first clue that caspase-2 functions in the intrinsic apoptotic pathway. Apoptosis induced by overexpression of caspase-2 was blocked by expression of BCL-2, which prevents mitochondrial outer membrane permeabilization (MOMP) (Kumar et al., 1995). The primary way caspase-2 initiates apoptosis through the mitochondrial pathway is by proteolytic cleavage of the BH3-only domain protein BID (Guo et al., 2002; Bonzon et al., 2006). Caspase-mediated cleavage of BID results in its conversion to tBID, which promotes MOMP, cytochrome c release, executioner caspase activation, and apoptosis (Luo et al., 1998). Accordingly, *Bid*-deficient MEF were resistant to cell death induced by caspase-2 overexpression, and heat shock (Bonzon et al., 2006). In addition, it has been shown that heat shock induces caspase-2 dimerization prior to MOMP (Bouchier-Hayes et al., 2009). Inhibition of caspase-2-induced cell death by BCL-2 and cleavage of BID places caspase-2 upstream of the mitochondria.

Although BID is one of the few caspase-2 substrates with a clear function, BID is not exclusively cleaved by caspase-2 (Luo et al., 1998; Slee et al., 2000). Caspase-8 can also cleave BID, with up to four times greater efficiency than caspase-2 (Bonzon et al., 2006). Although this higher cleavage efficiency would seem to suggest a redundant function for caspase-2 in BID cleavage, caspase-8 is an initiator caspase that is activated by extrinsic rather than intrinsic stimuli (Varfolomeev et al., 1998). Cleavage of BID by caspase-8 represents a point of convergence between the intrinsic and extrinsic apoptotic cascades (Li et al., 1998). One report suggests that in certain cell types, caspase-2 may participate in extrinsic apoptosis induced by TRAIL upstream of BID cleavage (Wagner et al., 2004). This study showed that in HCT116 and T3M4 cells, knockdown of caspase-2 significantly reduced TRAIL induced apoptosis, though not to as great an extent as knockdown of caspase-8 or BID. This suggests that caspase-2 could have a redundant role to caspase-8 in the TRAIL pathway. However, these effects were not recapitulated in Hela cells, suggesting that this is not a general mechanism of caspase-2 activation (Wagner et al., 2004).

Because cleavage of BID is a well-established contributor to apoptosis, BID proteolysis could be a potential mechanism to explain tumor suppression by caspase-2. Therefore, BID would induce MOMP to induce apoptosis, which would promote removal of cancerous cells (**Figure 2**). Although there are few clear examples of an apoptotic defect in caspase-2 deficient tumor models, BID cleavage has not been examined in these models. Determining if BID cleavage is defective in these models would be valuable in determining the true mechanism of tumor suppression by caspase-2 as it would suggest that apoptosis is impaired in these tumors, even though it may be masked *in vivo*. However, there is limited information as to whether BID phenocopies the tumor suppressive properties of caspase-2. One study showed that *Bid*-deficient mice

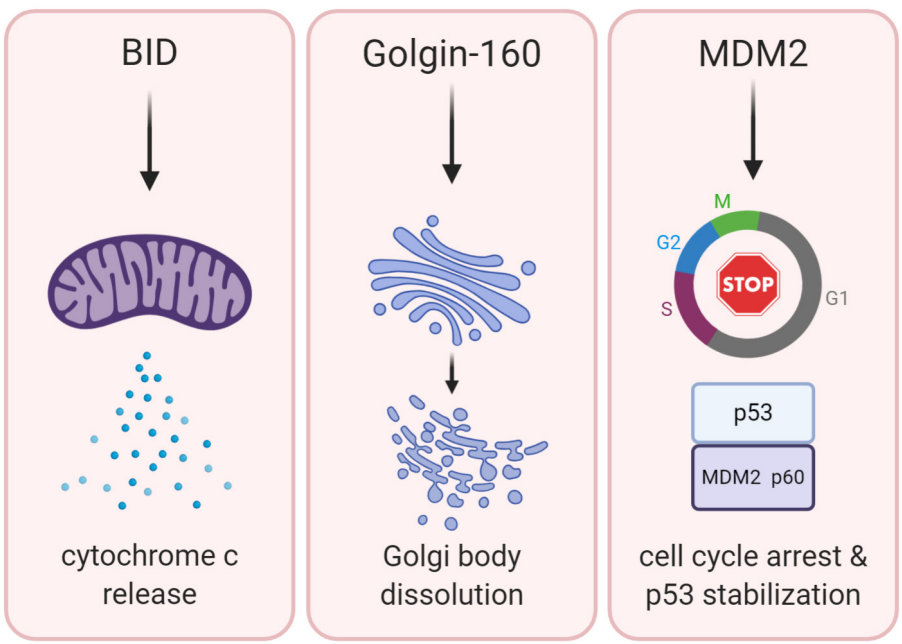

FIGURE 2 | BID, Golgin-160, and MDM2 are established caspase-2 substrates. The potential downstream functions of caspase-2-mediated cleavage of these substrates are shown. Cleavage of BID (*left panel*) promotes permeabilization of the outer mitochondrial membrane, releasing cytochrome c and activating downstream executioner caspases inducing apoptosis. Cleavage of Golgin-160 (*center panel*) induces Golgi fragmentation during apoptosis. MDM2 cleavage by caspase-2 (*right panel*) leads to the stabilization of p53 and promotion of cell cycle arrest.

develop a myeloproliferative disorder that resembles chronic myelomonocytic leukemia (CMML) as it progresses (Zinkel et al., 2003). Further, this study showed that *Bid*-deficient cells were resistant to the extrinsic death-inducing ligands, anti-Fas and TNF-α. Their resistance to intrinsic apoptotic damage was not investigated, so the contribution of caspase-2 is difficult to extrapolate. However, metaphase spreads from BID-deficient tumors displayed advanced chromosomal aberrations, including trisomy and translocation. These chromosomal abnormalities are similar to the genomic instability observed in caspase-2-deficient tumors, but it is unclear if caspase-2 is involved in BID-deficient tumorigenesis or how generalized this phenomenon is.

While cleavage of BID appears to be the main route for caspase-2-induced apoptosis, evidence of caspase-2-dependent apoptosis that does not require BID exists. For example, in *Tp53* null cells, caspase-2 has been linked to apoptosis independent of both mitochondrial permeabilization and downstream activation of caspase-3. This cell death only occurred when the cell cycle checkpoint protein Chk1 was inhibited, and was not inhibited by overexpression of BCL2 (Sidi et al., 2008). In another example, purified caspase-2 was shown to trigger cytochrome-c release from isolated mitochondria without the addition of cytosolic factors (Robertson et al., 2004). Caspase-8, which can also cleave BID, was not able to replicate this effect, suggesting that cytochrome c release did not occur simply due to cytosolic contamination. Therefore, additional caspase-2 substrates may exist that induce apoptosis independent of MOMP or BID.

MDM2—A Key Link to the p53 Pathway

MDM2 is a caspase-2 substrate that has the potential to reveal the mechanism of tumor suppression by caspase-2 due to its own ability to regulate both apoptosis and cell cycle (**Figure 2**). Best known as the E3 ubiquitin ligase responsible for targeting p53 to the proteasome for degradation, MDM2 is cleaved by caspase-2 at Asparagine 367 (Oliver et al., 2011). MDM2 is a key negative regulator of p53 levels and stability (Horn and Vousden, 2007). Furthermore, MDM2 is a p53 target gene, comprising a negative feedback loop that mediates levels of both p53 and MDM2 itself (Momand et al., 1992). Cleavage of MDM2 by caspase-2 removes the critical RING finger domain, which is responsible for the ubiquitination of p53 by MDM2 (Fang et al., 2000). Oliver et al. (2011) showed that both PIDD1 and RAIDD expression generates a p60 MDM2 fragment that is abolished by mutation of the Asp367 cleavage site. They further showed that while both caspase-2 and caspase-3 can directly cleave MDM2 *in vitro*, caspase-3 was not activated by their experimental conditions, suggesting that, in their study, MDM2 is primarily cleaved by caspase-2. Caspase-2 also cleaved MDM2 in response to DNA damage induced by doxorubicin, showing that MDM2 is a physiologically relevant substrate. Because cleavage of MDM2 removes the RING domain, this results in reduced degradation of p53, increasing both the levels and activity of p53. Furthermore, immunoprecipitation experiments have shown that the MDM2 p60 fragment binds p53, and even outcompetes full-length MDM2 for p53 binding. Binding of MDM2 p60 to p53 stabilizes rather than degrades p53. Therefore, cleavage of MDM2 by caspase-2 appears to be important for the maintenance of p53 levels after DNA damage. In support of this, a recent study demonstrated that activation of caspase-2 after DNA damage promotes sustained levels of p53 rather than oscillatory protein dynamics (Tsabar et al., 2020). This sustained p53 response prevented continual cell cycling in the presence of DNA damage. Importantly, this was reported to be dependent on caspase-2-mediated cleavage of MDM2, allowing p53 levels to rise. Again, this shows that caspase-2 has an important role in protection from aberrant cell cycling, which could be critical for its ability to suppress tumor formation.

The discovery of MDM2 as a caspase-2 substrate revealed an important connection to the critical p53 tumor suppressor pathway. The tumor suppressing functions of p53 are linked to its ability to trigger both apoptosis and cell cycle arrest (Chen, 2016), key processes that may also underlie tumor suppression by caspase-2. However, current evidence suggests that the caspase-2/MDM2/p53 axis may serve to promote cell cycle arrest, rather than apoptosis. It has been reported that caspase-2-mediated MDM2 cleavage leads to p53 accumulation and p21-dependent cell cycle arrest in human lung cancer cells (Fava et al., 2017). This was observed under conditions of "mitotic catastrophe," a variety of conditions including cytokinesis failure, increased mitotic duration, and microtubule disruption. Inhibitors generating these phenotypes resulted in activation of caspase-2 as monitored by the appearance of cleaved MDM2, which was reportedly produced in a caspase-2 specific manner. Although these conditions resulted in robust cleavage of MDM2, this occurred in the absence of notable cell death. Cytokinesis failure resulted in increased polyploidy, which was less severe in the presence of caspase-2, suggesting that caspase-2 limits the extent of this phenotype. This is consistent with observations that caspase-2-deficient tumors display enhanced aneuploidy and mitotic aberrations (Parsons et al., 2013; Lopez-Garcia et al., 2017). Caspase-2 has also been implicated in the constraint of polyploidy in the liver during organogenesis and regeneration (Sladky et al., 2020a). Cytokinesis failure in human lung cancer cells led to MDM2 cleavage, p53 accumulation, and p21-mediated cell cycle arrest (Fava et al., 2017). Caspase-2 deficiency completely blocked MDM2 cleavage, and resulted in a failure to accumulate p53 and arrest after inhibition of cytokinesis. It is proposed that this failure to arrest is what leads to the enhanced polyploidy seen in caspase-2-deficient lung cancer cells. This suggests that caspase-2 mediates cell cycle arrest – and limits polyploidy—by acting through p53. However, there was no observed defect in p53 accumulation when caspase-2-deficient cells were exposed to DNA damage or increased mitotic duration triggered by nocodazole (Fava et al., 2017). Therefore, caspase-2-mediated stabilization of p53 leading to cell cycle arrest as a mechanism to limit polyploidy may be specific to stimuli resulting in cytokinesis failure. This may also be a cell-type specific phenomenon, as it was reported that caspase-2-deficient U2OS cells still effectively induce p53 and cell cycle arrest in response to the same inhibitors used by Lim et al. (2018).

Ultimately, it is unlikely that cleavage of MDM2 represents the sole mechanism of tumor suppression by caspase-2. While caspase-2-deficient cells failed to induce p53 in response to cytokinesis failure, it was clear that caspase-2 was not

required for p53 induction under other conditions (Fava et al., 2017). Furthermore, while *Tp53*-deficient animals develop severe spontaneous tumors, dual loss of caspase-2 does not exacerbate this phenotype (Manzl et al., 2013), suggesting that these tumor suppressors may function independently of each other. However, based on the evidence that suggests caspase-2 is necessary for cell cycle arrest following cytokinesis failure, it is possible that a failure to cleave MDM2 may be at least partially responsible for the observable ploidy defects in caspase-2-deficient tumors (Parsons et al., 2013; Puccini et al., 2013).

While MDM2 represents a direct link between caspase-2 and p53, other reports point to a connection between caspase-2 and p53 independent of MDM2. Terry et al. (2015) found that in a cohort of lung cancer patients, caspase-2 mRNA levels were significantly lower in patients with wild type p53 than in patients with a mutation in p53. This suggests that p53 may act to suppress caspase-2, and is in agreement with an earlier report that showed lower caspase-2 transcript levels in the presence of p53 in H1299 tumor cells (Baptiste-Okoh et al., 2008). This report also showed lower protein levels of caspase-2 in the presence of p53, but since cells were treated with daunorubicin to induce p53, this may be due to processing of full length caspase-2, which was not shown. Caspase-2 has also been suggested to be required for the expression of *p21*, a key p53 target gene responsible for mediating cell cycle arrest (Sohn et al., 2011). Interestingly, this was reported to be independent of the catalytic activity of caspase-2, which suggests a potential non-catalytic function for caspase-2. However, the tumor suppression of caspase-2 has been shown to be dependent on caspase-2's catalytic activity (Ren et al., 2012), so it is unlikely that this contributes to tumor suppression in the absence of an additional enzymatic function of caspase-2.

Caspase-2 has been implicated in an alternative "Chk1 suppressed" apoptotic pathway in p53 null cells (Sidi et al., 2008). Chk1 is a key G2/M cell cycle checkpoint, responsible for arresting cells with DNA damage before the completion of cell division (Zhang and Hunter, 2014). It was shown that when Chk1 is inhibited, caspase-2 restores apoptosis in both zebrafish and human p53 null cells induced by irradiation (Sidi et al., 2008). However, Chk1 inhibition failed to significantly restore DNA damage-induced cell death in cells from various *Tp53* null mouse tissues (Manzl et al., 2013). Moreover, the cell death that did occur was shown to be independent of caspase-2 in *Casp2*/*Tp53* double knockout cells. MDM2 cleavage was not investigated in these p53-deficient models, so it is unclear if caspase-2 targets MDM2 as a substrate in these conditions. Furthermore, although MDM2 is primarily recognized for its degradation of p53, it does not exclusively act on p53 (Riley and Lozano, 2012). In the absence of p53, cleavage of MDM2 could still have an effect by failing to degrade other targets, although this has not yet been investigated.

Golgin-160—A Surprising Mediator of Cell Fate?

Golgin-160 is a member of a superfamily of structural Golgi body proteins. While Golgins are generally thought to be important for maintenance of Golgi structure, siRNA studies for Golgin-160 suggest that it is dispensable for the structural integrity of this organelle (Hicks et al., 2006). Rather, it has been suggested that it may be important for correct transport and shuttling of certain cellular proteins like the beta-1 Adrenergic Receptor (Hicks et al., 2006; Gilbert et al., 2014). Golgin-160 was identified as a caspase-2 substrate following observations that showed endogenous caspase-2 co-localized with Golgi body markers (Mancini et al., 2000). Upon investigation, it was revealed that caspase-2 cleaves Golgin-160 in two locations. The first of these, Asparagine 59, is exclusive to caspase-2, while the second cleavage site, Asp 311, can also be cleaved by caspases -3 and -7. Caspase-generated fragments of Golgin-160 were observed after induction of apoptosis with staurosporine, suggesting that Golgin-160 may be an apoptotic substrate. It was also shown that the caspase-2 specific fragment of Golgin-160 (D59 cleavage) appeared at an earlier time point than other caspase generated Golgin fragments. This is consistent with the role of caspase-2 as an initiator caspase, which would be activated prior to executioner caspases. A D59 mutant of Golgin-160 that could not be cleaved by caspase-2 significantly delayed the normal fragmentation of the Golgi body that occurs during apoptosis. This suggests that caspase-2 participates in the dissolution of the Golgi body during apoptosis, supporting a role for caspase-2 in the apoptotic cascade (**Figure 2**). However, this is incongruous with the findings that Golgin-160 is dispensable for maintenance of Golgi body architecture (Hicks et al., 2006), suggesting a potential other outcome of this cleavage.

Interestingly, multiple studies have reported finding caspase-generated fragments of Golgi proteins in the nucleus (Hicks and Machamer, 2002; Sbodio et al., 2006; Mukherjee and Shields, 2009). Indeed, the N-terminal domain of Golgin-160 contains a cryptic nuclear localization signal that is hidden in the full length protein (Hicks and Machamer, 2002). Mutants of Golgin-160 representing various caspase cleavage products demonstrate that multiple Golgin-160 fragments localize readily to the nucleus. Of these, two fragments have the potential to be generated exclusively by caspase-2, and one has the potential to be cooperatively produced by caspase-2 and caspase-3 (Mancini et al., 2000). A study in Hela cells showed that this cooperatively produced fragment could be prevented from localizing to the nucleus by expression of another Golgi protein, GCP60, which bound to the Golgin-160 fragment, preventing its translocation (Sbodio et al., 2006). Preventing this translocation actually rendered the cells significantly more sensitive to staurosporine, suggesting that nuclear translocation of Golgin-160 fragments may actually exert a pro-survival effect. While this was only determined for a specific Golgin-160 fragment in which caspase-2 only plays a supporting role (and is not strictly required, as the fragment could also be produced by caspase-3 alone or caspase-3 in tandem with caspase-7), it is tempting to speculate that caspase-2 and Golgin-160 could be part of a cell fate-determining signaling pathway. There is a precedent for this seemingly unusual signaling mechanism. Another Golgi protein, p115, can also be cleaved by caspases after apoptotic stimuli, yielding fragments that localize to the nucleus (Mukherjee and Shields, 2009). In the case of p115, the nuclear fragments were actually found to potentiate apoptosis, suggesting that there is a complex network of signaling between the Golgi

body and nucleus that regulates cell fate. While it is unknown how these Golgi body protein fragments impact cell fate from the nucleus, it has been speculated that this could be due to a change in transcriptional programs (Mukherjee and Shields, 2009). While this is certainly a possibility, it would be important to determine if this a specific, targeted transcriptional reprogramming, or a general non-specific interference with existing transcription. In addition, it will also be important to determine which protein fragments promote either death or survival, and which caspases are responsible for generating these fragments.

Other Substrates Point to Alternative Functions for Caspase-2

In addition to the substrates discussed above, there are several other caspase-2 substrates proposed in the literature (**Table 1**). While cleavage of many of these by caspase-2 has only been shown *in vitro* or in overexpression-based experiments, some are worth discussing here based on their potential functional relevance. For example, two proposed substrates, Ku80 and ICAD, could link caspase-2 to the DNA damage response, which could underlie the observations of increased genomic instability in caspase-2-deficient tumors. Ku80 is a key member of the complex responsible for mediating non-homologous end joining (NHEJ). It interacts with another member of the complex, DNA-PK_{cs}, to repair DNA breaks that occur throughout the cell cycle (Gottlieb and Jackson, 1993). It has been reported that caspase-2 promotes repair of double-stranded DNA breaks through non-homologous end joining (NHEJ) by cleaving Ku80 (Yan et al., 2017). The last 12 residues of the C-terminal end of Ku80 are reported to be important for this interaction with DNA-PK_{cs} (Gell and Jackson, 1999). Caspase-2 cleaves Ku80 at D726 at the extreme C-terminus and the removal of these few amino acids was reported to increase the affinity of the interaction between Ku80 and DNA-PK_{cs} (Yan et al., 2017). Importantly, this enhanced interaction increased the ability of cells to repair etoposide-induced DNA damage. This finding provides a potential explanation for the genomic instability observed in caspase-2-deficient tumors. However, many of these experiments were done using a C-terminally tagged version of Ku80, so further investigation is needed to determine if the tag impacted the cleavage of Ku80 and to see if this occurs physiologically and promotes the tumor suppressor effect of caspase-2. ICAD (Inhibitor of caspase-activated DNase) is an inhibitor of one of the key mediators of apoptosis, CAD, and is inactivated by caspase-mediated cleavage (Sakahira et al., 1998). When ICAD is unable to bind CAD, CAD degrades DNA, resulting in the characteristic nuclear condensation at the terminal stages of apoptosis (Sakahira et al., 1998). Lower levels of CAD activation resulting from minimal caspase activity have been shown to induce DNA damage and promote genomic instability (Ichim et al., 2015). It has been shown that caspase-2 can cleave ICAD *in vitro*, albeit with much less efficiency than caspase-3 (Dahal et al., 2007). Therefore, caspase-2 could promote DNA damage or even apoptosis through ICAD cleavage. However, the only study to demonstrate caspase-2-dependent ICAD cleavage used a Tat-caspase-2 fusion protein that had a higher cleavage efficiency toward ICAD than recombinant caspase-2 (Dahal et al., 2007) and this observation has yet to be confirmed in cells by endogenous caspase-2.

Substrates that contribute to caspase-2's role in cancer may do so through more indirect mechanisms by regulating transcription or translation. Two examples of these are translation initiation factor eIF4B, and transcriptional corepressor histone deacetylase 4 (HDAC4) (Paroni et al., 2004; Wejda et al., 2012). HDAC4 cleavage at D289 by caspase-2 produces an N-terminal fragment that when expressed leads to transcriptional repression and also appears to induce apoptosis (Paroni et al., 2004). eIF4B has been shown to have a caspase-2 specific cleavage site at D563, but the functional impact of this cleavage on translation has not been assessed (Wejda et al., 2012). The global changes in transcription and translation caused by cleavage of these substrates is unknown, but could represent a potential mechanism to impact cell division or other physiological processes in which caspase-2 has been implicated, like autophagy, metabolism, or differentiation, that may contribute to its regulation of tumor growth.

Additional putative caspase-2 substrates may be linked to other potential functions of caspase-2 that may not have an obvious cancer relevance. For example, caspase-2 has been linked to neurodegeneration (Hermel et al., 2004; Zhao et al., 2016). Caspase-2 reportedly cleaves Huntingtin (HTT), a neuroprotective protein of the central nervous system (Hermel et al., 2004). Cleavage of HTT generates a cytotoxic protein fragment thought to contribute to the neuronal cell death characteristic of Huntington's disease. Expression of a catalytically inactive caspase-2 inhibited cleavage of HTT and reduced cell death, suggesting that caspase-2 may participate in cell death associated with neurodegeneration caused by Huntington's disease. Caspase-2 has also been reported to cleave tau, a fibril forming protein thought to contribute to Alzheimer's pathology (Zhao et al., 2016). In a mouse model, cleavage of tau by caspase-2 had a detrimental effect on cognitive function, again pointing to a link between caspase-2 and neurodegenerative diseases. Cleavage of Rictor (rapamycin-insensitive companion of mTOR) by caspase-2 has been implicated in the inhibition of an mTOR/Akt signaling cascade to promote the normal progression of synaptic pruning (Xu et al., 2019). In humans, impaired synaptic pruning has been linked to mental disorders such as autism and schizophrenia, and indeed, loss of caspase-2 is associated with incomplete synaptic pruning and dysfunctional behavioral traits in mice (Xu et al., 2019). However, in these studies, cleavage of Rictor was only observed after overexpression of caspase-2 and the cleavage site has not been identified. This does not necessarily mean that Rictor is not a physiologically relevant substrate, as the authors note that endogenous levels of Rictor are low, so overexpression of caspase-2 may have increased the detection threshold of its cleavage products. Degradation of Rictor by caspase-2 had a similar effect on synaptic pruning as knockdown of Rictor, suggesting that cleavage by caspase-2 renders the protein inactive. Interestingly, Rictor amplification has been noted in a number of different cancer types such as small cell

lung cancer, colorectal cancer and esophageal squamous cell carcinoma (Zhao et al., 2020), indicating that cleavage of this putative substrate may play a role outside of neuronal processes to impact cancer progression.

Caspase-2 has also been implicated in obesity, metabolism, and the development of non-alcoholic fatty liver disease (Machado et al., 2016). Interestingly, caspase-2-deficient mice fed a high-fat diet were protected from the development of obesity and associated phenotypes like diabetes and hepatic steatosis (Machado et al., 2016). Further, caspase-2 is required for the progression from non-alcoholic fatty liver disease to non-alcoholic steatohepatitis, which is considered a risk factor for further liver damage that promotes hepatocellular carcinoma (Kim et al., 2018). One of the mechanisms that has been explored to explain this is elevated endoplasmic reticulum (ER) stress (Kim et al., 2018). ER stress has been found to upregulate caspase-2 expression, which in turn activated sterol regulatory element-binding proteins (SREBP) leading to the buildup of cholesterol and triglycerides. Notably, an earlier report suggests that caspase-2 is under transcriptional control of SREBP2, which could form a positive feedback loop promoting further SREBP activation (Logette et al., 2005). This activation of SREBP was reportedly due to caspase-2-dependent cleavage of site 1 protease (S1P), which once cleaved, becomes active and competent to activate SREBP. Given the relationship between non-alcoholic fatty liver disease and liver cancer, it is interesting to speculate that via this S1P/SREBP mechanism, caspase-2 could ultimately be potentiating the risk of liver cancer. However, this has not yet been investigated, and there is other evidence suggesting that caspase-2 may have a more specialized role in liver development as discussed below (Sladky et al., 2020a).

Like the substrates discussed in more detail above, a primary problem in making definitive conclusions about the function of substrates cleaved by caspase-2 is the lack of evidence suggesting that these substrate cleavage sites are exclusive to caspase-2. For example, while enzymology suggests that eIF4B is cleaved most efficiently by caspase-2, it can still be cleaved by caspase-3 and -7 *in vitro* (Wejda et al., 2012). HDAC4 on the other hand, appears to be much more efficiently cleaved by caspase-3 *in vitro*. Neither of these scenarios is enough to determine whether a substrate is exclusive to caspase-2 (or not*) in vivo*. Indeed, while there is enough evidence to suggest that the substrates of caspase-2 play critical roles in apoptosis, cell cycle control, and beyond, the key question remains: how does caspase-2 select these substrates to moderate different functions?

DOES SUBSTRATE SELECTION BY CASPASE-2 DIRECT ITS FUNCTION?

Given the insufficiency of studies on caspase-2 substrates, it is not surprising that there is even less literature that directly examines the regulation of caspase-2 substrate selection. However, the existing body of work on caspase-2 does present several possible mechanisms that could be harnessed to regulate substrate selection (**Figure 3**).

Regulation of Caspase-2 Gene and Protein Expression

The first of these potential mechanisms is temporal regulation of caspase-2 activity via either transcriptional or translational mechanisms (**Figure 3A**). While caspase-2 is generally thought to be a ubiquitously expressed protein, there is some evidence that suggests it may be regulated in these ways. As previously discussed, data from lung cancer patients suggested that caspase-2 mRNA levels were lower in patients with mutated p53, suggesting a level of transcriptional control (Terry et al., 2015). However, whether this is directly controlled by p53 is unknown. A recent report examining caspase-2 in liver development and regeneration places caspase-2 and its activating component PIDD1 under transcriptional control of E2F family members E2F1, E2F7, and E2F8 (Sladky et al., 2020a). E2F1 induced robust expression of both PIDD1 and caspase-2, while E2F7 and E2F8 resulted in transcriptional repression (Sladky et al., 2020a). In support of these findings, caspase-2 transcript levels were higher in E2F7/E2F8 null mouse liver extracts. Furthermore, E2F1 also upregulates E2F7 and E2F8, producing a negative feedback loop to control caspase-2 and PIDD1 expression. It is important to note that not only does this mechanism control expression of caspase-2, but also its ability to be activated by its canonical activating platform by regulating PIDD1 transcription. Ultimately, this loop was reported to activate caspase-2 to constrain polyploidization in the liver that occurs during development (Sladky et al., 2020a). While this phenomenon has not yet been studied in the tumor models where caspase-2 has been shown to play a role, E2F1 is known to promote tumorigenic properties like proliferation, drug resistance, and metastasis (Putzer and Engelmann, 2013). In a study of colorectal cancer patients, Lopez-Garcia et al. (2017) reported that mutation of the transcriptional activator BCL9L was associated with increased aneuploidy. Using a colorectal cancer cell line, this group demonstrated that BCL9L represses caspase-2 at the transcriptional level, resulting in lower protein levels. This transcriptional repression was linked to the inhibition of transcription factor TCF4, which promotes caspase-2 expression by binding near the transcriptional start site of caspase-2. This repression of caspase-2 resulted in increased aneuploidy in colorectal cancer cell lines, thought to exacerbate genetic variability and drug resistance in tumors. Interestingly, BCL9L mutations were highly correlated with p53 mutations, which have also been reported to reduce caspase-2 expression levels (Terry et al., 2015). Therefore, it is possible that this is a cooperative repression between p53 and BCL9L.

Post-translational Regulation of Caspase-2

Caspase-2 can also be regulated by post-translational modification (**Figure 3B**). In *Xenopus* oocytes, it was found that nutrient stores regulate cell death via caspase-2 (Nutt et al., 2005). Excess NADPH resulted in an inhibitory phosphorylation event on caspase-2 at S135, while deprivation of NADPH resulted in reduced phosphorylation at this site and enhanced caspase-2 activity and cell death. This phosphorylation was

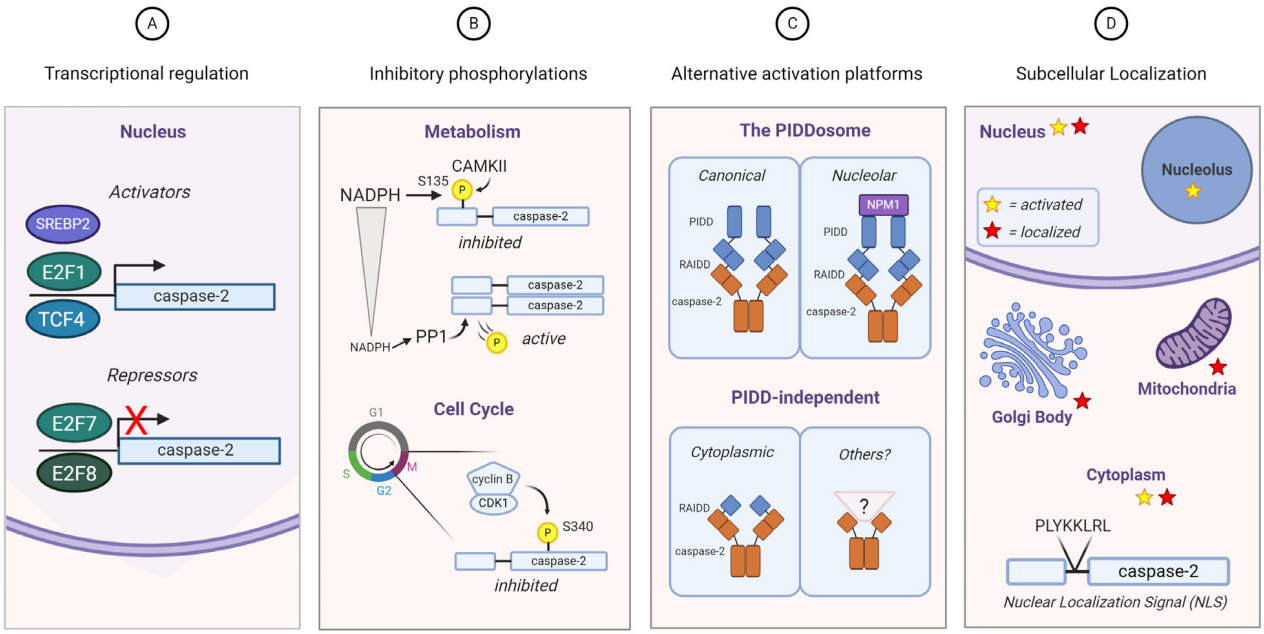

FIGURE 3 | Regulation of caspase-2 expression, activity, and localization. Substrate selection by caspase-2 could be directed by **(A)** transcriptional regulation: E2F family transcription factors both activate (E2F1) and repress (E2F7 and E2F8) caspase-2 transcription. TCF4 and SREBP2 activate caspase-2 transcription; **(B)** phosphorylation: Caspase-2 is phosphorylated on multiple residues. The known phosphorylation events of caspase-2 result in its inhibition, which can be regulated by metabolism (*top*) and the cell cycle (*bottom*); **(C)** differential activation platform assembly: The canonical PIDDosome contains both PIDD1 and RAIDD. Caspase-2 can be activated by complexes lacking one or both of these elements. NPM1 is required for the nucleolar activation complex; **(D)** subcellular localization: Caspase-2 contains a classical nuclear localization signal and it has been found outside the nucleus associated with the Golgi body and mitochondria. Activation of caspase-2 has also been observed specifically in the nucleolus induced by DNA damage, as well as more generally throughout cytoplasm induced by heat shock and microtubule disruption. Red stars represent sites where caspase-2 is expressed and yellow stars represent sites where caspase-2 is activated.

mediated by calcium/calmodulin-dependent protein kinase II (CaMKII). This finding was recapitulated in mouse oocytes, suggesting an important, conserved regulatory mechanism (Nutt et al., 2009). This site can be dephosphorylated by a direct interaction with protein phosphatase-1 (PP1) and can be protected from dephosphorylation by protein 14-3-3zeta, which binds phosphorylated caspase-2, thus preventing interaction with PP1. Phosphorylation of caspase-2 at a different site, S340, has been linked to cell cycle control. It has been observed that the morphological changes seen during mitosis are notably similar to those that occur during apoptosis, like nuclear membrane dissolution. Andersen et al. (2009) showed that caspase-2 is spontaneously processed to its mature form in interphase cell extracts. However, in mitotic cell extracts, this processing is inhibited, preventing caspase-2 mediated cell death during mitosis. Furthermore, they showed that this inhibition is dependent on caspase-2 being phosphorylated on S340. Because caspase-2 phosphorylation on S135 is regulated by metabolism of NADPH (Nutt et al., 2005), nutrient availability was examined in interphase and mitotic extracts, but there was no difference (Andersen et al., 2009). Rather, caspase-2 phosphorylation on S340 was regulated by the mitotic cycle itself. The mitosis promoting kinase cdk1-cyclinB1 was responsible for phosphorylating caspase-2 at S340, resulting in its inhibition. Interestingly, this site was vulnerable to dephosphorylation by PP1, but the action of PP1 appeared to be repressed during mitosis. This regulatory mechanism seems to be important for the demonstrated role of caspase-2 in mitotic catastrophe (Vitale et al., 2017). Mutation of the S340 phospho-site resulted in significantly enhanced cell death in cells arrested in mitosis compared to wild-type cells (Andersen et al., 2009). This finding suggests the existence of an important caspase-2-mediated safeguard against improper cell division. Because S340 is vulnerable to PP1 dephosphorylation, but PP1 is suppressed during mitosis, it may be that extended mitotic duration (symptomatic of mitotic damage) allows PP1 to be re-activated, allowing caspase-2 to be activated. This would promote apoptosis of a cell that is unable to sufficiently repair any mitotic damage, suggesting that caspase-2 could be a "mitotic timer."

Recently, another phosphorylation event has been demonstrated to be important for successful progression through mitosis. This site, S384, is highly conserved and is phosphorylated by Aurora B kinase, a critical mitotic kinase that controls cytokinesis (Lim et al., 2020). Phosphorylation at this site was induced by PLK1 inhibition, resulting in mitotic catastrophe as described earlier. Interestingly, phosphorylation at S384 prevented cleavage of both MDM2 and BID, suggesting that this modification prevents caspase-2 activation. Interestingly, a phospho-mimetic mutant of this site was still able to be recruited to its activation platform, as measured by a fluorescent readout of caspase-2 induced proximity dimerization. It did, however, reduce auto-processing of caspase-2, which could

explain the abrogation of MDM2 and BID cleavage. This study also performed structural analysis that suggests that S384 phosphorylation impacts the conformation of the substrate binding pocket of caspase-2, providing a potential explanation for the reduced auto-cleavage and MDM2/Bid cleavage. Importantly, this study ultimately showed that a S348 phospho-mimetic mutant of caspase-2 resulted in increased ploidy and resistance to cell death after mitotic stress. In contrast to this, another group recently showed that mutation of the S384 phosphorylation site to alanine to prevent phosphorylation blocks caspase-2 processing after DNA damage with cisplatin. This suggests that, in the context of DNA damage, phosphorylation at S384 is actually necessary for caspase-2 processing. However, this group was not able to identify phosphorylation at this site under these conditions, and importantly, a phospho-mimetic mutant did not restore the processing of caspase-2. It is possible that this site is differently regulated during mitosis and DNA damage, which could account for these conflicting findings. However, this more recent study did corroborate the idea that S384 is critical for substrate binding; not by forming a bond with the substrate itself, but by stabilizing Arg-378, which is responsible for binding to the critical Aspartate reside of the target substrate. These studies highlight the importance of caspase-2 phosphorylation at the same residue in different cellular contexts, and demonstrate that post-transcriptional modifications can impact substrate cleavage.

Regulation of caspase-2 expression and activation by post-translational modifications could provide a level of substrate specificity by modulating the amount of available active caspase-2. Thus, substrates that are cleaved most efficiently by caspase-2 would be targeted at the lowest doses of caspase-2, while others would not be cleaved unless caspase-2 was maximally active. However, few studies have explored if there is a dosage dependent effect of caspase-2 on different substrates. In the latter study exploring S384 phosphorylation, both BID and MDM2 cleavage was completely abrogated by S384 phosphorylation suggesting, at least in this case, that it is a binary on-off effect on caspase-2 activation rather than a dynamic response.

Assembly of Distinct Activation Platforms

Caspase-2 may be regulated toward cleaving different substrate targets through the assembly of distinct caspase-2 activation platforms (**Figure 3C**). While the PIDDosome is considered the canonical activation platform for caspase-2, its necessity for caspase-2 activation and subsequent physiological outcomes such as cell death has been debated in the literature (Bouchier-Hayes and Green, 2012). For example, primary thymocytes from PIDD1-deficient mice did not display reduced susceptibility to apoptosis induced by a variety of damaging stimuli including DNA damage (Manzl et al., 2009). Further, loss of PIDD1, RAIDD, or caspase-2 had no effect on cytochrome c release in SV40 immortalized fibroblasts induced by etoposide (Manzl et al., 2009), which is at odds with the established role for caspase-2 as an upstream mediator of cytochrome c release in response to DNA damage (Robertson et al., 2002). Caspase-2 was also found to elute in high-molecular weight complexes in the absence of both PIDD1 and RAIDD (Manzl et al., 2009), suggesting that it may have other activating complexes that are still unknown. Tumor suppression by caspase-2 has also been reported to be independent of both PIDD1 and RAIDD in certain models. In a model of c-*Myc*-induced lymphomagenesis, loss of caspase-2 accelerated tumor growth, but loss of PIDD1 suppressed tumor formation, suggesting that caspase-2 does not depend on PIDD1 to suppress tumors (Manzl et al., 2012). The observation that loss of PIDD1 suppressed tumor formation may be due to PIDD1's known role in activating the pro-survival NFκB pathway in response to genotoxic stress (Janssens et al., 2005). Similarly, loss of RAIDD does not phenocopy the effects of loss of caspase-2 on tumor suppression since RAIDD deficiency had no impact on Eμ-Myc-induced lymphomagenesis (Peintner et al., 2015).

Other potential activators of caspase-2 have been reported. For example, caspase-2 has been proposed to be a component of the TNFR complex, the TRAIL receptor complex, and the CD95 complex (Duan and Dixit, 1997; Droin et al., 2001; Wagner et al., 2004; Lavrik et al., 2006). However, the requirement for caspase-2 for TNF, TRAIL, or CD95-induced apoptosis is unclear. Although antisense-mediated downregulation of caspase-2 has been shown to decrease CD95-induced apoptosis in U937 cells (Droin et al., 2001), caspase-2 failed to facilitate CD95-induced apoptosis in the absence of caspase-8 in Jurkat cells (Lavrik et al., 2006). A more recent study suggests that caspase-2 augments CD95-associated STAT1 activation, suggesting a potential alternate function for caspase-2 at the DISC (Qadir et al., 2020). In the TRAIL pathway, siRNA-mediated silencing of caspase-2 was shown to reduce TRAIL-induced apoptosis in certain cell types (Wagner et al., 2004). A subsequent report suggested that caspase-2 can prime cancer cells for TRAIL-induced death and that caspase-2 is required for TRAIL-induced caspase-8 cleavage (Shin et al., 2005). Although the authors suggested that caspase-2 directly cleaved caspase-8, they did not provide evidence for this and other reports have demonstrated that caspase-2 has no catalytic activity toward other caspase family members (de Craen et al., 1999; Guo et al., 2002). In addition, the latter two TRAIL studies relied heavily on an siRNA oligo that was later shown to have off-target effects (Lassus et al., 2002). Therefore, the exact function, if any, that caspase-2 plays in the TRAIL complex is unclear.

Additional components of caspase-2 activation platforms have been described. TRAF2 has been shown to bind to caspase-2 in a complex that appears to be devoid of PIDD1 (Robeson et al., 2018). In contrast, BubR1 has been proposed as a negative regulator of PIDDosome formation by competing with RAIDD for binding to PIDD1 (Thompson et al., 2015). It is possible that the assembly of different caspase-2 activation platforms or the presence or absence of regulatory molecules in the PIDDosome could result in a caspase-2 enzyme that has variable activity and therefore has variable targeting efficiency for different substrates. Interestingly, there are non-canonical functions of caspase-2 where the activation platform remains unknown. One such report places caspase-2 at the heart of an ER-stress driven inflammatory response (Bronner et al., 2015). In this mechanism, ER stress triggers activation of NLRP3,

which translocates to the mitochondria and activates caspase-2 to promote the release of cytochrome c and mitochondrial DNA, resulting in activation of caspase-1, an inflammatory caspase (Bronner et al., 2015). Whether this results in either apoptosis or another form of cell death is not clear, but given the release of mitochondrial factors, it is certainly possible that caspase-2 promotes cell death in this mechanism. This is thought to occur independently of NLRP3's canonical role as a key member of the NLRP3 inflammasome signaling platform (Bronner et al., 2015). Because NLRP3 functions as part of an activation platform for caspase-1, it would be interesting to determine if NLRP3 participates directly or indirectly in the activation of caspase-2 at the mitochondria. Notably, it is thought that ER stress is a common feature across many types of cancers. Although the pro- vs. anti-tumor impacts of ER stress are still debated in the field (reviewed in Oakes, 2020), it is possible that caspase-2 has been overlooked as a contributor to cell death resulting from this phenotype.

Regulation of Caspase-2 Localization

Caspase-2 expression has been localized to the nucleus, cytoplasm, mitochondria, and Golgi body (Mancini et al., 2000; Paroni et al., 2002; Lopez-Cruzan et al., 2016; **Figure 3D**). Caspase-2 contains a classical nuclear localization signal (NLS), located in the C-terminus of its prodomain (Baliga et al., 2003). Mutation of a critical, conserved lysine residue in this NLS abolishes the nuclear localization of caspase-2 but how localization of caspase-2 impacts activation and downstream functions is still unclear. Although caspase-2 has this NLS, and has been reported to induce apoptosis from the nucleus (Paroni et al., 2002), stimuli such as heat shock and cytoskeletal disruption have been shown to activate caspase-2 in the cytoplasm and not in the nucleus (Bouchier-Hayes et al., 2009). To resolve this confusion, we investigated the localization of caspase-2 activation following DNA damage and reported that caspase-2 is activated by the PIDDosome in the nucleolus, while its activation in the cytoplasm is PIDD1-independent but RAIDD-dependent (Ando et al., 2017). This activation is highly stimulus specific, where DNA damaging agents are most efficient at activating caspase-2 in the nucleolus, while other stimuli such as cytoskeletal disrupters only activated caspase-2 in the cytoplasm or nucleus. We found that nucleolar caspase-2 activation is dependent on inclusion of nucleophosmin (NPM1) in the PIDDosome complex by interacting with PIDD1 itself. Surprisingly, in PIDD1 or NPM1-deficient cells, overall levels of caspase-2 activation were not impacted, but activation of caspase-2 specifically within the nucleolar compartment was significantly reduced. This finding suggests that PIDD1 is dispensable for general caspase-2 activation, in agreement with other published work (Manzl et al., 2009), but is required for DNA damage-induced activation specifically within the nucleolus. Consistent with the identification of a nucleolar PIDDosome, PIDD-CC, the fragment responsible for activating caspase-2, has been shown to localize to the nucleus and cytoplasm in unstimulated cells but was concentrated in the nucleolus after UV-irradiation (Pick et al., 2006). This shift could represent either translocation or degradation of PIDD1 following an activating stimulus.

This bifurcation between caspase-2 activation in the cytoplasm and nucleolus could allow access to different substrates in each location. However, the possibility of a nucleolar substrate pool for caspase-2 has not been investigated. Together with the stimuli specific localization patterns of caspase-2 activation, distinct activation platforms in different locations in the cell suggests that the localization of caspase-2 activation is a regulated process and this may be critically important for its downstream functions. The ability of caspase-2 or upstream PIDDosome components to translocate between different cellular compartments is a potential mechanism of caspase-2 regulation. For example, while NPM1 is a predominantly nucleolar protein, it has many roles that necessitate shuttling throughout the cell. Notably, it can localize to the centrosome, where it is thought to suppress centrosome duplication (Wang et al., 2005; Liu et al., 2007). This could also allow NPM1 to play a role in the activation of caspase-2 via the PIDDosome in response to supernumerary centrosomes as reported by Fava et al. (2017), but this has not been investigated. The primary localization of caspase-2 expression, as opposed to activation, has been difficult to determine. GFP-tagged caspase-2 localizes primarily to the nucleus, but does not appreciably translocate out of the nucleus until late in the apoptotic process, presumably due to compromised nuclear integrity (Paroni et al., 2002). One report in HeLa cells suggested that caspase-2 can translocate out of the nucleus in response to hydrogen peroxide and etoposide, but the activation status of this translocated caspase-2 was not determined (Tinnikov and Samuels, 2013). It was shown that this translocation occurred despite treatment with Leptomycin B, a well-established Exportin I inhibitor but was abrogated by another inhibitor, N-Ethylmaleimide (NEM), which alkylates cysteine thiol groups in proteins. How and why NEM specifically prevents caspase-2 translocation was not determined. In direct contrast to this, findings from immortalized MEF suggest that caspase-2 translocated into the nucleus after DNA damage induced by irradiation (Manzl et al., 2009). A more recent structural analysis suggested that the protein 14-3-3, masks the nuclear localization signal of caspase-2 when bound (Smidova et al., 2018). This would suggest that 14-3-3 binding would promote caspase-2 localization in the cytoplasm, but this was not tested in cells. These mechanisms of potentially restricting the activation of caspase-2 to a specific localization in the cell highlights the importance of substrate access. Even if a substrate is readily cleaved by caspase-2, if the localization of either of these is restricted, it introduces a level of regulation determined by the localization of this protease.

CLOSING REMARKS

The investigations into caspase-2 substrates to date have failed to provide evidence that a single substrate is responsible for all the functions of caspase-2. However, in contrast to the many caspase-3 substrates that have been identified, it is likely that the limited

number of caspase-2 substrates is indicative of a more directed function of this caspase. So rather than "death by a thousand cuts" for caspase-3 (Martin and Green, 1995), it may be a case of "death by 20 cuts" for caspase-2. Or, given the non-apoptotic roles of caspase-2, we could possibly paraphrase this to "life by 20 cuts." While catalytic independent functions of caspase-2 have been described, such as in the regulation of p21 expression (Sohn et al., 2011), tumor suppression associated with caspase-2 can be blocked by mutation of its catalytic cysteine (Ren et al., 2012). Therefore, the most likely route to tumor suppression is through proteolytic cleavage of substrates. It is only through the identification and investigation of additional caspase-2 substrates that we will reveal the cellular processes in which caspase-2 is actively involved, to clarify the important role of this caspase as a safeguard against cancer.

AUTHOR CONTRIBUTIONS

ANB-S wrote the manuscript and generated the figures. LB-H wrote and edited the manuscript. Both authors contributed to the article and approved the submitted version.

FUNDING

The Bouchier-Hayes lab was funded by T32 GM008231 (ANB-S) and NIH/NIGMS R01GM121389 (LB-H).

ACKNOWLEDGMENTS

Figures were generated using Biorender software.

REFERENCES

Adams, J. M., Harris, A. W., Pinkert, C. A., Corcoran, L. M., Alexander, W. S., Cory, S., et al. (1985). The c-myc oncogene driven by immunoglobulin enhancers induces lymphoid malignancy in transgenic mice. *Nature* 318, 533–538. doi: 10.1038/318533a0

Andersen, J. L., Johnson, C. E., Freel, C. D., Parrish, A. B., Day, J. L., Buchakjian, M. R., et al. (2009). Restraint of apoptosis during mitosis through interdomain phosphorylation of caspase-2. *EMBO J.* 28, 3216–3227. doi: 10.1038/emboj.2009.253

Ando, K., Parsons, M. J., Shah, R. B., Charendoff, C. I., Paris, S. L., Liu, P. H., et al. (2017). NPM1 directs PIDDosome-dependent caspase-2 activation in the nucleolus. *J. Cell. Biol.* 216, 1795–1810. doi: 10.1083/jcb.201608095

Baliga, B. C., Colussi, P. A., Read, S. H., Dias, M. M., Jans, D. A., and Kumar, S. (2003). Role of prodomain in importin-mediated nuclear localization and activation of caspase-2. *J. Biol. Chem.* 278, 4899–4905. doi: 10.1074/jbc.m211512200

Baliga, B. C., Read, S. H., and Kumar, S. (2004). The biochemical mechanism of caspase-2 activation. *Cell Death Differ.* 11, 1234–1241. doi: 10.1038/sj.cdd.4401492

Baptiste-Okoh, N., Barsotti, A. M., and Prives, C. (2008). Caspase 2 is both required for p53-mediated apoptosis and downregulated by p53 in a p21-dependent manner. *Cell Cycle* 7, 1133–1138. doi: 10.4161/cc.7.9.5805

Bergeron, L., Perez, G. I., Macdonald, G., Shi, L., Sun, Y., Jurisicova, A., et al. (1998). Defects in regulation of apoptosis in caspase-2-deficient mice. *Genes Dev.* 12, 1304–1314. doi: 10.1101/gad.12.9.1304

Boatright, K. M., Renatus, M., Scott, F. L., Sperandio, S., Shin, H., Pedersen, I. M., et al. (2003). A unified model for apical caspase activation. *Mol. Cell.* 11, 529–541. doi: 10.1016/s1097-2765(03)00051-0

Boatright, K. M., and Salvesen, G. S. (2003). Mechanisms of caspase activation. *Curr. Opin. Cell. Biol.* 15, 725–731. doi: 10.1016/j.ceb.2003.10.009

Boice, A., and Bouchier-Hayes, L. (2020). Targeting apoptotic caspases in cancer. Biochimica et biophysica acta. *Mol. Cell Res.* 1867:118688. doi: 10.1016/j.bbamcr.2020.118688

Bolivar, B. E., Vogel, T. P., and Bouchier-Hayes, L. (2019). Inflammatory caspase regulation: maintaining balance between inflammation and cell death in health and disease. *FEBS J.* 286, 2628–2644.

Bonzon, C., Bouchier-Hayes, L., Pagliari, L. J., Green, D. R., and Newmeyer, D. D. (2006). Caspase-2-induced apoptosis requires bid cleavage: a physiological role for bid in heat shock-induced death. *Mol. Biol. Cell.* 17, 2150–2157. doi: 10.1091/mbc.e05-12-1107

Bouchier-Hayes, L., and Green, D. R. (2012). Caspase-2: the orphan caspase. *Cell Death Differ.* 19, 51–57. doi: 10.1038/cdd.2011.157

Bouchier-Hayes, L., Oberst, A., McStay, G. P., Connell, S., Tait, S. W., Dillon, C. P., et al. (2009). Characterization of cytoplasmic caspase-2 activation by induced proximity. *Mol. Cell.* 35, 830–840. doi: 10.1016/j.molcel.2009.07.023

Bronner, D. N., Abuaita, B. H., Chen, X., Fitzgerald, K. A., Nunez, G., He, Y., et al. (2015). Endoplasmic reticulum stress activates the inflammasome via NLRP3- and caspase-2-driven mitochondrial damage. *Immunity* 43, 451–462. doi: 10.1016/j.immuni.2015.08.008

Burrell, R. A., McGranahan, N., Bartek, J., and Swanton, C. (2013). The causes and consequences of genetic heterogeneity in cancer evolution. *Nature* 501, 338–345. doi: 10.1038/nature12625

Chen, J. (2016). The cell-cycle arrest and apoptotic functions of p53 in tumor initiation and progression. *Cold Spring Harb. Perspect. Med.* 6:a026104. doi: 10.1101/cshperspect.a026104

Dahal, G. R., Karki, P., Thapa, A., Shahnawaz, M., Shin, S. Y., Lee, J. S., et al. (2007). Caspase-2 cleaves DNA fragmentation factor (DFF45)/inhibitor of caspase-activated DNase (ICAD). *Arch. Biochem. Biophys.* 468, 134–139. doi: 10.1016/j.abb.2007.09.007

Dawar, S., Lim, Y., Puccini, J., White, M., Thomas, P., Bouchier-Hayes, L., et al. (2017). Caspase-2-mediated cell death is required for deleting aneuploid cells. *Oncogene* 36, 2704–2714. doi: 10.1038/onc.2016.423

de Craen, M. Van, Declercq, W., Van den brande, I., Fiers, W., and Vandenabeele, P. (1999). The proteolytic procaspase activation network: an in vitro analysis. *Cell Death Differ.* 6, 1117–1124. doi: 10.1038/sj.cdd.4400589

Dorstyn, L., Akey, C. W., and Kumar, S. (2018). New insights into apoptosome structure and function. *Cell Death Differ.* 25, 1194–1208. doi: 10.1038/s41418-017-0025-z

Dorstyn, L., Puccini, J., Nikolic, A., Shalini, S., Wilson, C. H., Norris, M. D., et al. (2014). An unexpected role for caspase-2 in neuroblastoma. *Cell Death Dis.* 5:e1383. doi: 10.1038/cddis.2014.342

Droin, N., Bichat, F., Rebe, C., Wotawa, A., Sordet, O., Hammann, A., et al. (2001). Involvement of caspase-2 long isoform in Fas-mediated cell death of human leukemic cells. *Blood* 97, 1835–1844. doi: 10.1182/blood.v97.6.1835

Duan, H., and Dixit, V. M. (1997). RAIDD is a new 'death' adaptor molecule. *Nature* 385, 86–89. doi: 10.1038/385086a0

Fang, S., Jensen, J. P., Ludwig, R. L., Vousden, K. H., and Weissman, A. M. (2000). Mdm2 is a RING finger-dependent ubiquitin protein ligase for itself and p53. *J. Biol. Chem.* 275, 8945–8951. doi: 10.1074/jbc.275.12.8945

Fava, L. L., Schuler, F., Sladky, V., Haschka, M. D., Soratroi, C., Eiterer, L., et al. (2017). The PIDDosome activates p53 in response to supernumerary centrosomes. *Genes Dev.* 31, 34–45. doi: 10.1101/gad.289728.116

Freeman, H. C., Hugill, A., Dear, N. T., Ashcroft, F. M., and Cox, R. D. (2006). Deletion of nicotinamide nucleotide transhydrogenase: a new quantitive trait locus accounting for glucose intolerance in C57BL/6J mice. *Diabetes* 55, 2153–2156. doi: 10.2337/db06-0358

Gell, D., and Jackson, S. P. (1999). Mapping of protein-protein interactions within the DNA-dependent protein kinase complex. *Nucleic Acids Res.* 27, 3494–3502. doi: 10.1093/nar/27.17.3494

Gilbert, C. E., Zuckerman, D. M., Currier, P. L., and Machamer, C. E. (2014). Three basic residues of intracellular loop 3 of the beta-1 adrenergic receptor are required for golgin-160-dependent trafficking. *Int. J. Mol. Sci.* 15, 2929–2945. doi: 10.3390/ijms15022929

Gottlieb, T. M., and Jackson, S. P. (1993). The DNA-dependent protein kinase: requirement for DNA ends and association with Ku antigen. *Cell* 72, 131–142. doi: 10.1016/0092-8674(93)90057-w

Guo, Y., Srinivasula, S. M., Druilhe, A., Fernandes-Alnemri, T., and Alnemri, E. S. (2002). Caspase-2 induces apoptosis by releasing proapoptotic proteins from mitochondria. *J. Biol. Chem.* 277, 13430–13437. doi: 10.1074/jbc.m108029200

Hanahan, D., and Weinberg, R. A. (2000). The hallmarks of cancer. *Cell* 100, 57–70.

Harvey, N. L., Trapani, J. A., Fernandes-Alnemri, T., Litwack, G., Alnemri, E. S., and Kumar, S. (1996). Processing of the Nedd2 precursor by ICE-like proteases and granzyme B. *Genes Cells* 1, 673–685. doi: 10.1046/j.1365-2443.1996.00255.x

Hermel, E., Gafni, J., Propp, S. S., Leavitt, B. R., Wellington, C. L., Young, J. E., et al. (2004). Specific caspase interactions and amplification are involved in selective neuronal vulnerability in Huntington's disease. *Cell Death Differ.* 11, 424–438. doi: 10.1038/sj.cdd.4401358

Hicks, S. W., Horn, T. A., McCaffery, J. M., Zuckerman, D. M., and Machamer, C. E. (2006). Golgin-160 promotes cell surface expression of the beta-1 adrenergic receptor. *Traffic* 7, 1666–1677. doi: 10.1111/j.1600-0854.2006.00504.x

Hicks, S. W., and Machamer, C. E. (2002). The NH2-terminal domain of Golgin-160 contains both Golgi and nuclear targeting information. *J. Biol. Chem.* 277, 35833–35839. doi: 10.1074/jbc.m206280200

Ho, L. H., Read, S. H., Dorstyn, L., Lambrusco, L., and Kumar, S. (2008). Caspase-2 is required for cell death induced by cytoskeletal disruption. *Oncogene* 27, 3393–3404. doi: 10.1038/sj.onc.1211005

Ho, L. H., Taylor, R., Dorstyn, L., Cakouros, D., Bouillet, P., and Kumar, S. (2009). A tumor suppressor function for caspase-2. *Proc. Natl. Acad. Sci. U.S.A.* 106, 5336–5341.

Hofmann, K., Bucher, P., and Tschopp, J. (1997). The CARD domain: a new apoptotic signalling motif. *Trends Biochem. Sci.* 22, 155–156. doi: 10.1016/s0968-0004(97)01043-8

Horn, H. F., and Vousden, K. H. (2007). Coping with stress: multiple ways to activate p53. *Oncogene* 26, 1306–1316. doi: 10.1038/sj.onc.1210263

Ichim, G., Lopez, J., Ahmed, S. U., Muthalagu, N., Giampazolias, E., Delgado, M. E., et al. (2015). Limited mitochondrial permeabilization causes DNA damage and genomic instability in the absence of cell death. *Mol. Cell.* 57, 860–872. doi: 10.1016/j.molcel.2015.01.018

Janssens, S., Tinel, A., Lippens, S., and Tschopp, J. (2005). PIDD mediates NF-kappaB activation in response to DNA damage. *Cell* 123, 1079–1092. doi: 10.1016/j.cell.2005.09.036

Julien, O., Zhuang, M., Wiita, A. P., O'Donoghue, A. J., Knudsen, G. M., Craik, C. S., et al. (2016). Quantitative MS-based enzymology of caspases reveals distinct protein substrate specificities, hierarchies, and cellular roles. *Proc. Natl. Acad. Sci. U.S.A.* 113, E2001–E2010.

Kim, J. Y., Garcia-Carbonell, R., Yamachika, S., Zhao, P., Dhar, D., Loomba, R., et al. (2018). Lipogenesis and Steatohepatitis via Caspase-2 Activation of S1P. *Cell* 175, 133.e15–145.e15.

Kumar, S., Kinoshita, M., Noda, M., Copeland, N. G., and Jenkins, N. A. (1994). Induction of apoptosis by the mouse Nedd2 gene, which encodes a protein similar to the product of the *Caenorhabditis elegans* cell death gene ced-3 and the mammalian IL-1 beta-converting enzyme. *Genes Dev.* 8, 1613–1626. doi: 10.1101/gad.8.14.1613

Kumar, S., White, D. L., Takai, S., Turczynowicz, S., Juttner, C. A., and Hughes, T. P. (1995). Apoptosis regulatory gene NEDD2 maps to human chromosome segment 7q34-35, a region frequently affected in haematological neoplasms. *Hum. Genet.* 95, 641–644.

Lassus, P., Opitz-Araya, X., and Lazebnik, Y. (2002). Requirement for caspase-2 in stress-induced apoptosis before mitochondrial permeabilization. *Science* 297, 1352–1354. doi: 10.1126/science.1074721

Lavrik, I. N., Golks, A., Baumann, S., and Krammer, P. H. (2006). Caspase-2 is activated at the CD95 death-inducing signaling complex in the course of CD95-induced apoptosis. *Blood* 108, 559–565. doi: 10.1182/blood-2005-07-007096

Li, H., Zhu, H., Xu, C. J., and Yuan, J. (1998). Cleavage of BID by caspase 8 mediates the mitochondrial damage in the Fas pathway of apoptosis. *Cell* 94, 491–501. doi: 10.1016/s0092-8674(00)81590-1

Lim, Y., De Bellis, D., Dorstyn, L., and Kumar, S. (2018). p53 accumulation following cytokinesis failure in the absence of caspase-2. *Cell Death Differ.* 25, 2050–2052. doi: 10.1038/s41418-018-0161-0

Lim, Y., De Bellis, D., Sandow, J. J., Capalbo, L., D'Avino, P. P., Murphy, J. M., et al. (2020). Phosphorylation by Aurora B kinase regulates caspase-2 activity and function. *Cell Death Differ.* [Epub ahead of print].

Liu, X., Liu, Z., Jang, S. W., Ma, Z., Shinmura, K., Kang, S., et al. (2007). Sumoylation of nucleophosmin/B23 regulates its subcellular localization, mediating cell proliferation and survival. *Proc. Natl. Acad. Sci. U.S.A.* 104, 9679–9684. doi: 10.1073/pnas.0701806104

Logette, E., Le Jossic-Corcos, C., Masson, D., Solier, S., Sequeira-Legrand, A., Dugail, I., et al. (2005). Caspase-2, a novel lipid sensor under the control of sterol regulatory element binding protein 2. *Mol. Cell. Biol.* 25, 9621–9631. doi: 10.1128/mcb.25.21.9621-9631.2005

Lopez-Cruzan, M., Sharma, R., Tiwari, M., Karbach, S., Holstein, D., Martin, C. R., et al. (2016). Caspase-2 resides in the mitochondria and mediates apoptosis directly from the mitochondrial compartment. *Cell Death Discov.* 2:16005.

Lopez-Garcia, C., Sansregret, L., Domingo, E., McGranahan, N., Hobor, S., Birkbak, N. J., et al. (2017). BCL9L dysfunction impairs caspase-2 expression permitting aneuploidy tolerance in colorectal cancer. *Cancer Cell* 31, 79–93. doi: 10.1016/j.ccell.2016.11.001

Luo, X., Budihardjo, I., Zou, H., Slaughter, C., and Wang, X. (1998). Bid, a Bcl2 interacting protein, mediates cytochrome c release from mitochondria in response to activation of cell surface death receptors. *Cell* 94, 481–490. doi: 10.1016/s0092-8674(00)81589-5

Machado, M. V., Michelotti, G. A., Jewell, M. L., Pereira, T. A., Xie, G., Premont, R. T., et al. (2016). Caspase-2 promotes obesity, the metabolic syndrome and nonalcoholic fatty liver disease. *Cell Death Dis.* 7:e2096. doi: 10.1038/cddis.2016.19

Mancini, M., Machamer, C. E., Roy, S., Nicholson, D. W., Thornberry, N. A., Casciola-Rosen, L. A., et al. (2000). Caspase-2 is localized at the Golgi complex and cleaves golgin-160 during apoptosis. *J. Cell. Biol.* 149, 603–612. doi: 10.1083/jcb.149.3.603

Manzl, C., Fava, L. L., Krumschnabel, G., Peintner, L., Tanzer, M. C., Soratroi, C., et al. (2013). Death of p53-defective cells triggered by forced mitotic entry in the presence of DNA damage is not uniquely dependent on Caspase-2 or the PIDDosome. *Cell Death Dis.* 4:e942. doi: 10.1038/cddis.2013.470

Manzl, C., Krumschnabel, G., Bock, F., Sohm, B., Labi, V., Baumgartner, F., et al. (2009). Caspase-2 activation in the absence of PIDDosome formation. *J. Cell. Biol.* 185, 291–303. doi: 10.1083/jcb.200811105

Manzl, C., Peintner, L., Krumschnabel, G., Bock, F., Labi, V., Drach, M., et al. (2012). PIDDosome-independent tumor suppression by Caspase-2. *Cell Death Differ.* 19, 1722–1732. doi: 10.1038/cdd.2012.54

Martin, S. J., and Green, D. R. (1995). Protease activation during apoptosis: death by a thousand cuts? *Cell* 82, 349–352. doi: 10.1016/0092-8674(95)90422-0

Momand, J., Zambetti, G. P., Olson, D. C., George, D., and Levine, A. J. (1992). The mdm-2 oncogene product forms a complex with the p53 protein and inhibits p53-mediated transactivation. *Cell* 69, 1237–1245. doi: 10.1016/0092-8674(92)90644-r

Mukherjee, S., and Shields, D. (2009). Nuclear import is required for the pro-apoptotic function of the Golgi protein p115. *J. Biol. Chem.* 284, 1709–1717. doi: 10.1074/jbc.m807263200

Negrini, S., Gorgoulis, V. G., and Halazonetis, T. D. (2010). Genomic instability–an evolving hallmark of cancer. *Nat. Rev. Mol. Cell. Biol.* 11, 220–228. doi: 10.1038/nrm2858

Nutt, L. K., Buchakjian, M. R., Gan, E., Darbandi, R., Yoon, S. Y., Wu, J. Q., et al. (2009). Metabolic control of oocyte apoptosis mediated by 14-3-3zeta-regulated dephosphorylation of caspase-2. *Dev. Cell.* 16, 856–866. doi: 10.1016/j.devcel.2009.04.005

Nutt, L. K., Margolis, S. S., Jensen, M., Herman, C. E., Dunphy, W. G., Rathmell, J. C., et al. (2005). Metabolic regulation of oocyte cell death through the CaMKII-mediated phosphorylation of caspase-2. *Cell* 123, 89–103. doi: 10.1016/j.cell.2005.07.032

Oakes, S. A. (2020). Endoplasmic reticulum stress signaling in cancer cells. *Am. J. Pathol.* 190, 934–946. doi: 10.1016/j.ajpath.2020.01.010

Oliver, T. G., Meylan, E., Chang, G. P., Xue, W., Burke, J. R., Humpton, T. J., et al. (2011). Caspase-2-mediated cleavage of Mdm2 creates a p53-induced positive feedback loop. *Mol. Cell.* 43, 57–71. doi: 10.1016/j.molcel.2011.06.012

O'Reilly, L. A., Ekert, P., Harvey, N., Marsden, V., Cullen, L., Vaux, D. L., et al. (2002). Caspase-2 is not required for thymocyte or neuronal apoptosis even

though cleavage of caspase-2 is dependent on both Apaf-1 and caspase-9. *Cell Death Differ.* 9, 832–841. doi: 10.1038/sj.cdd.4401033

Park, H. H., Logette, E., Raunser, S., Cuenin, S., Walz, T., Tschopp, J., et al. (2007). Death domain assembly mechanism revealed by crystal structure of the oligomeric PIDDosome core complex. *Cell* 128, 533–546. doi: 10.1016/j.cell.2007.01.019

Paroni, G., Henderson, C., Schneider, C., and Brancolini, C. (2002). Caspase-2 can trigger cytochrome C release and apoptosis from the nucleus. *J. Biol. Chem.* 277, 15147–15161. doi: 10.1074/jbc.m112338200

Paroni, G., Mizzau, M., Henderson, C., Del Sal, G., Schneider, C., and Brancolini, C. (2004). Caspase-dependent regulation of histone deacetylase 4 nuclear-cytoplasmic shuttling promotes apoptosis. *Mol. Biol. Cell.* 15, 2804–2818. doi: 10.1091/mbc.e03-08-0624

Parsons, M. J., McCormick, L., Janke, L., Howard, A., Bouchier-Hayes, L., and Green, D. R. (2013). Genetic deletion of caspase-2 accelerates MMTV/c-neu-driven mammary carcinogenesis in mice. *Cell Death Differ.* 20, 1174–1182. doi: 10.1038/cdd.2013.38

Peintner, L., Dorstyn, L., Kumar, S., Aneichyk, T., Villunger, A., and Manzl, C. (2015). The tumor-modulatory effects of Caspase-2 and Pidd1 do not require the scaffold protein Raidd. *Cell Death Differ.* 22, 1803–1811. doi: 10.1038/cdd.2015.31

Pick, R., Badura, S., Bosser, S., and Zornig, M. (2006). Upon intracellular processing, the C-terminal death domain-containing fragment of the p53-inducible PIDD/LRDD protein translocates to the nucleoli and interacts with nucleolin. *Biochem. Biophys. Res. Commun.* 349, 1329–1338. doi: 10.1016/j.bbrc.2006.08.176

Puccini, J., Shalini, S., Voss, A. K., Gatei, M., Wilson, C. H., Hiwase, D. K., et al. (2013). Loss of caspase-2 augments lymphomagenesis and enhances genomic instability in Atm-deficient mice. *Proc. Natl. Acad. Sci. U.S.A.* 110, 19920–19925. doi: 10.1073/pnas.1311947110

Putzer, B. M., and Engelmann, D. (2013). E2F1 apoptosis counterattacked: evil strikes back. *Trends Mol. Med.* 19, 89–98. doi: 10.1016/j.molmed.2012.10.009

Qadir, A. S., Stults, A. M., Murmann, A. E., and Peter, M. E. (2020). The mechanism of how CD95/Fas activates the Type I IFN/STAT1 axis, driving cancer stemness in breast cancer. *Sci. Rep.* 10:1310.

Rawlings, N. D., Barrett, A. J., Thomas, P. D., Huang, X., Bateman, A., and Finn, R. D. (2018). The MEROPS database of proteolytic enzymes, their substrates and inhibitors in 2017 and a comparison with peptidases in the PANTHER database. *Nucleic Acids Res.* 46, D624–D632.

Ren, K., Lu, J., Porollo, A., and Du, C. (2012). Tumor-suppressing function of caspase-2 requires catalytic site Cys-320 and site Ser-139 in mice. *J. Biol. Chem.* 287, 14792–14802. doi: 10.1074/jbc.m112.347625

Ribe, E. M., Jean, Y. Y., Goldstein, R. L., Manzl, C., Stefanis, L., Villunger, A., et al. (2012). Neuronal caspase 2 activity and function requires RAIDD, but not PIDD. *Biochem. J.* 444, 591–599. doi: 10.1042/bj20111588

Riley, M. F., and Lozano, G. (2012). The many faces of MDM2 binding partners. *Genes Cancer* 3, 226–239. doi: 10.1177/1947601912455322

Robertson, J. D., Enoksson, M., Suomela, M., Zhivotovsky, B., and Orrenius, S. (2002). Caspase-2 acts upstream of mitochondria to promote cytochrome c release during etoposide-induced apoptosis. *J. Biol. Chem.* 277, 29803–29809. doi: 10.1074/jbc.m204185200

Robertson, J. D., Gogvadze, V., Kropotov, A., Vakifahmetoglu, H., Zhivotovsky, B., and Orrenius, S. (2004). Processed caspase-2 can induce mitochondria-mediated apoptosis independently of its enzymatic activity. *EMBO Rep.* 5, 643–648. doi: 10.1038/sj.embor.7400153

Robeson, A. C., Lindblom, K. R., Wojton, J., Kornbluth, S., and Matsuura, K. (2018). Dimer-specific immunoprecipitation of active caspase-2 identifies TRAF proteins as novel activators. *EMBO J.* 37:e97072.

Sakahira, H., Enari, M., and Nagata, S. (1998). Cleavage of CAD inhibitor in CAD activation and DNA degradation during apoptosis. *Nature* 391, 96–99. doi: 10.1038/34214

Sbodio, J. I., Hicks, S. W., Simon, D., and Machamer, C. E. (2006). GCP60 preferentially interacts with a caspase-generated golgin-160 fragment. *J. Biol. Chem.* 281, 27924–27931. doi: 10.1074/jbc.m603276200

Shalini, S., Nikolic, A., Wilson, C. H., Puccini, J., Sladojevic, N., Finnie, J., et al. (2016). Caspase-2 deficiency accelerates chemically induced liver cancer in mice. *Cell Death Differ.* 23, 1727–1736. doi: 10.1038/cdd.2016.81

Shelton, S. N., Dillard, C. D., and Robertson, J. D. (2010). Activation of caspase-9, but not caspase-2 or caspase-8, is essential for heat-induced apoptosis in Jurkat cells. *J. Biol. Chem.* 285, 40525–40533. doi: 10.1074/jbc.m110.167635

Shin, S., Lee, Y., Kim, W., Ko, H., Choi, H., and Kim, K. (2005). Caspase-2 primes cancer cells for TRAIL-mediated apoptosis by processing procaspase-8. *EMBO J.* 24, 3532–3542. doi: 10.1038/sj.emboj.7600827

Sidi, S., Sanda, T., Kennedy, R. D., Hagen, A. T., Jette, C. A., Hoffmans, R., et al. (2008). Chk1 suppresses a caspase-2 apoptotic response to DNA damage that bypasses p53, Bcl-2, and caspase-3. *Cell* 133, 864–877. doi: 10.1016/j.cell.2008.03.037

Sladky, V. C., Knapp, K., Soratroi, C., Heppke, J., Eichin, F., Rocamora-Reverte, L., et al. (2020a). E2F-family members engage the PIDDosome to limit hepatocyte ploidy in liver development and regeneration. *Dev. Cell.* 52, 335.e7–349.e7.

Sladky, V. C., Knapp, K., Szabo, T. G., Braun, V. Z., Bongiovanni, L., van den Bos, H., et al. (2020b). PIDDosome-induced p53-dependent ploidy restriction facilitates hepatocarcinogenesis. *EMBO Rep.* 21:e50893. doi: 10.15252/embr.202050893

Slee, E. A., Keogh, S. A., and Martin, S. J. (2000). Cleavage of BID during cytotoxic drug and UV radiation-induced apoptosis occurs downstream of the point of Bcl-2 action and is catalysed by caspase-3: a potential feedback loop for amplification of apoptosis-associated mitochondrial cytochrome c release. *Cell Death Differ.* 7, 556–565. doi: 10.1038/sj.cdd.4400689

Smidova, A., Alblova, M., Kalabova, D., Psenakova, K., Rosulek, M., Herman, P., et al. (2018). 14-3-3 protein masks the nuclear localization sequence of caspase-2. *FEBS J.* 285, 4196–4213. doi: 10.1111/febs.14670

Sohn, D., Budach, W., and Janicke, R. U. (2011). Caspase-2 is required for DNA damage-induced expression of the CDK inhibitor p21(WAF1/CIP1). *Cell Death Differ.* 18, 1664–1674. doi: 10.1038/cdd.2011.34

Talanian, R. V., Quinlan, C., Trautz, S., Hackett, M. C., Mankovich, J. A., Banach, D., et al. (1997). Substrate specificities of caspase family proteases. *J. Biol. Chem.* 272, 9677–9682. doi: 10.1074/jbc.272.15.9677

Terry, M. R., Arya, R., Mukhopadhyay, A., Berrett, K. C., Clair, P. M., Witt, B., et al. (2015). Caspase-2 impacts lung tumorigenesis and chemotherapy response in vivo. *Cell Death Differ.* 22, 719–730. doi: 10.1038/cdd.2014.159

Thompson, R., Shah, R. B., Liu, P. H., Gupta, Y. K., Ando, K., Aggarwal, A. K., et al. (2015). An inhibitor of PIDDosome formation. *Mol. Cell.* 58, 767–779. doi: 10.1016/j.molcel.2015.03.034

Thornberry, N. A., Rano, T. A., Peterson, E. P., Rasper, D. M., Timkey, T., Garcia-Calvo, M., et al. (1997). A combinatorial approach defines specificities of members of the caspase family and granzyme B. Functional relationships established for key mediators of apoptosis. *J. Biol. Chem.* 272, 17907–17911. doi: 10.1074/jbc.272.29.17907

Tinel, A., Janssens, S., Lippens, S., Cuenin, S., Logette, E., Jaccard, B., et al. (2007). Autoproteolysis of PIDD marks the bifurcation between pro-death caspase-2 and pro-survival NF-kappaB pathway. *EMBO J.* 26, 197–208. doi: 10.1038/sj.emboj.7601473

Tinel, A., and Tschopp, J. (2004). The PIDDosome, a protein complex implicated in activation of caspase-2 in response to genotoxic stress. *Science* 304, 843–846. doi: 10.1126/science.1095432

Tinnikov, A. A., and Samuels, H. H. (2013). A novel cell lysis approach reveals that caspase-2 rapidly translocates from the nucleus to the cytoplasm in response to apoptotic stimuli. *PLoS One* 8:e61085. doi: 10.1371/journal.pone.0061085

Tsabar, M., Mock, C. S., Venkatachalam, V., Reyes, J., Karhohs, K. W., Oliver, T. G., et al. (2020). in p53 dynamics marks cells that escape from dsb-induced cell cycle arrest. *Cell Rep.* 33:108392. doi: 10.1016/j.celrep.2020.108392

Tu, S., McStay, G. P., Boucher, L. M., Mak, T., Beere, H. M., and Green, D. R. (2006). In situ trapping of activated initiator caspases reveals a role for caspase-2 in heat shock-induced apoptosis. *Nat. Cell. Biol.* 8, 72–77. doi: 10.1038/ncb1340

Varfolomeev, E. E., Schuchmann, M., Luria, V., Chiannilkulchai, N., Beckmann, J. S., Mett, I. L., et al. (1998). Targeted disruption of the mouse Caspase 8 gene ablates cell death induction by the TNF receptors, Fas/Apo1, and DR3 and is lethal prenatally. *Immunity* 9, 267–276. doi: 10.1016/s1074-7613(00)80609-3

Vitale, I., Manic, G., Castedo, M., and Kroemer, G. (2017). Caspase 2 in mitotic catastrophe: the terminator of aneuploid and tetraploid cells. *Mol. Cell. Oncol.* 4:e1299274. doi: 10.1080/23723556.2017.1299274

Wagner, K. W., Engels, I. H., and Deveraux, Q. L. (2004). Caspase-2 can function upstream of bid cleavage in the TRAIL apoptosis pathway. *J. Biol. Chem.* 279, 35047–35052. doi: 10.1074/jbc.m400708200

Wang, W., Budhu, A., Forgues, M., and Wang, X. W. (2005). Temporal and spatial control of nucleophosmin by the Ran-Crm1 complex in centrosome duplication. *Nat. Cell. Biol.* 7, 823–830. doi: 10.1038/ncb1282

Wejda, M., Impens, F., Takahashi, N., Van Damme, P., Gevaert, K., and Vandenabeele, P. (2012). Degradomics reveals that cleavage specificity profiles of caspase-2 and effector caspases are alike. *J. Biol. Chem.* 287, 33983–33995. doi: 10.1074/jbc.m112.384552

Xu, Z. X., Tan, J. W., Xu, H., Hill, C. J., Ostrovskaya, O., Martemyanov, K. A., et al. (2019). Caspase-2 promotes AMPA receptor internalization and cognitive flexibility via mTORC2-AKT-GSK3beta signaling. *Nat. Commun.* 10:3622.

Yan, Q., Zhu, H., Lan, L., Yi, J., and Yang, J. (2017). Cleavage of Ku80 by caspase-2 promotes non-homologous end joining-mediated DNA repair. *DNA Repair* 60, 18–28. doi: 10.1016/j.dnarep.2017.10.001

Zhang, Y., and Hunter, T. (2014). Roles of Chk1 in cell biology and cancer therapy. *Int. J. Cancer* 134, 1013–1023. doi: 10.1002/ijc.28226

Zhao, D., Jiang, M., Zhang, X., and Hou, H. (2020). The role of RICTOR amplification in targeted therapy and drug resistance. *Mol. Med.* 26:20.

Zhao, X., Kotilinek, L. A., Smith, B., Hlynialuk, C., Zahs, K., Ramsden, M., et al. (2016). Caspase-2 cleavage of tau reversibly impairs memory. *Nat. Med.* 22, 1268–1276. doi: 10.1038/nm.4199

Zheng, T. S., Hunot, S., Kuida, K., and Flavell, R. A. (1999). Caspase knockouts: matters of life and death. *Cell Death Differ.* 6, 1043–1053. doi: 10.1038/sj.cdd.4400593

Zinkel, S. S., Ong, C. C., Ferguson, D. O., Iwasaki, H., Akashi, K., Bronson, R. T., et al. (2003). Proapoptotic BID is required for myeloid homeostasis and tumor suppression. *Genes Dev.* 17, 229–239. doi: 10.1101/gad.1045603

Conflict of Interest: The authors declare that the research was conducted in the absence of any commercial or financial relationships that could be construed as a potential conflict of interest.

frontiers in Cell and Developmental Biology

REVIEW
published: 11 February 2021
doi: 10.3389/fcell.2021.628330

The P2X7 Receptor in Osteoarthritis

*Zihao Li[1], Ziyu Huang[2] and Lunhao Bai[1]**

[1] Department of Orthopedic Surgery, Shengjing Hospital of China Medical University, Shenyang, China, [2] Foreign Languages College, Shanghai Normal University, Shanghai, China

Osteoarthritis (OA) is the most common joint disease. With the increasing aging population, the associated socio-economic costs are also increasing. Analgesia and surgery are the primary treatment options in late-stage OA, with drug treatment only possible in early prevention to improve patients' quality of life. The most important structural component of the joint is cartilage, consisting solely of chondrocytes. Instability in chondrocyte balance results in phenotypic changes and cell death. Therefore, cartilage degradation is a direct consequence of chondrocyte imbalance, resulting in the degradation of the extracellular matrix and the release of pro-inflammatory factors. These factors affect the occurrence and development of OA. The P2X7 receptor (P2X7R) belongs to the purinergic receptor family and is a non-selective cation channel gated by adenosine triphosphate. It mediates Na^+, Ca^{2+} influx, and K^+ efflux, participates in several inflammatory reactions, and plays an important role in the different mechanisms of cell death. However, the relationship between P2X7R-mediated cell death and the progression of OA requires investigation. In this review, we correlate potential links between P2X7R, cartilage degradation, and inflammatory factor release in OA. We specifically focus on inflammation, apoptosis, pyroptosis, and autophagy. Lastly, we discuss the therapeutic potential of P2X7R as a potential drug target for OA.

Keywords: osteoarthritis, P2X7 receptor, inflammation, apoptosis, pyroptosis, autophagy

OPEN ACCESS

Edited by:
Yinan Gong,
University of Pittsburgh, United States

Reviewed by:
Yansheng Feng,
The University of Texas Health Science Center at San Antonio, United States
Hu Zeng,
Mayo Clinic, United States

****Correspondence:***
Lunhao Bai
lunhaobai_ace@163.com

Specialty section:
This article was submitted to Cell Death and Survival, a section of the journal Frontiers in Cell and Developmental Biology

Received: *11 November 2020*
Accepted: *22 January 2021*
Published: *11 February 2021*

Citation:
Li Z, Huang Z and Bai L (2021) The P2X7 Receptor in Osteoarthritis. Front. Cell Dev. Biol. 9:628330. doi: 10.3389/fcell.2021.628330

INTRODUCTION

Osteoarthritis (OA), as an age-related degenerative joint disease, presents with physical pain and disability in patients. Finding effective therapies for OA remains a pertinent health problem (Carr et al., 2012). The occurrence and development of OA can be attributed to multifaceted factors, such as age, obesity, exercise, and trauma (Uthman et al., 2013). From a clinical perspective, its features include articular cartilage loss, synovitis, subchondral bone sclerosis, and osteophyte formation. From a cellular perspective, it is attributed to morphological, biochemical, and biomechanical changes affecting the extracellular matrix (ECM).

The most important structural part of the joint is the cartilage, and its condition directly affects the occurrence and development of OA. Cartilage consists of structural proteins, such as collagen (primarily type II collagen), non-collagen proteins, proteoglycan, elastin, and aminoglycan, which form a stable network structure providing elasticity and compression resistance to joints. In OA tissues, this network structure loses its integrity with a resulting loss of tensile strength (Speziali et al., 2015). The composition and integrity of the cartilage matrix can be maintained by chondrocytes—which account for a small proportion of the total cartilage volume—to provide mechanical support and joint lubrication (Archer and Francis-West, 2003). In response to certain

chemical and mechanical factors, chondrocytes produce and release inflammatory factors (IL-1β, IL-6, and TNF-α) and secrete matrix-degrading enzymes [metalloproteinases (MMPs)] and proteoglycan-degrading enzymes (ADAMTS), to regulate the shape and structure of cartilage. Unfortunately, these inflammatory factors and enzymes are the primary contributors to cartilage degradation. Therefore, the occurrence and development of OA can be ascribed to the state and the catabolism balance of chondrocytes and cartilage. In OA, the changes in the chondrocytes can be categorized into three groups, namely: (i) cell proliferation (early stage)/cell death (late stage); (ii) anabolic and catabolic balance disorder (production of matrix-degrading enzymes); and (iii) phenotypic change (Sandell and Aigner, 2001). The influence of the cell phenotypic changes in the development of OA is particularly critical. In this article, we focus on chondrocyte inflammation, apoptosis, pyroptosis, and autophagy, and analyze the correlation between these phenotypes and cartilage degradation in OA.

The P2X7 purinergic receptor (P2X7R) is a trimeric adenosine triphosphate (ATP)-gated cation channel, which is expressed in several eukaryotic cells, such as immune cells and bone cells. As a key inflammatory switch, the activation of P2X7R mediates several downstream reactions, including the release of inflammatory factors, cell proliferation, death, and phenotypic changes (North, 2002). Owing to the important role of P2X7R in various immune, inflammatory, musculoskeletal, and nervous system diseases, it could be a potential drug treatment target for OA. In this article, we review the association between P2X7R and OA. We explain the structure and function and the inhibitory effect of P2X7R and emphasize the correlation and intersection between P2X7R, inflammation, and OA. From the perspective of apoptosis, pyroptosis, and autophagy, we discuss the possible association between P2X7R, cartilage degradation, and inflammatory factor release in OA. Further, we summarize the possible treatment methods, including the use of P2X7R as a drug target, and highlight the potential future mechanistic research.

ELUCIDATION OF OA AND ITS TREATMENT

Focus on Preventing Inflammation

Most studies on OA focus on the synovium-mediated development of inflammation. Synoviocytes identify the foreign fragments that fall into the joint cavity as byproducts of cartilage degradation. This results in synovial angiogenesis, an increase in the release of auto-inflammatory factors, and the stimulation of chondrocytes to synthesize and secrete MMPs. Through this mechanism, synovitis can promote cartilage degradation and aggravate OA (van Lent et al., 2004). Synovial fluid factors are increased in the damaged cartilage of OA patients (Kim et al., 2006), including toll-like receptor (TLR)-2 and TLR-4 ligands, such as alarm proteins [S100 protein and high mobility group protein B1 (HMGB1)], low molecular weight hyaluronic acid, tenascin C, and fibronectin (Scanzello et al., 2008; García-Arnandis et al., 2010; van Lent et al., 2012). These mediators, together with low-grade inflammation present in the compromised joints, induce inflammation of the synoviocytes and affect the catabolism balance of the chondrocytes (Wang et al., 2011). Therefore, the innate immunity may be a key factor driving the development of OA. As for mild systemic inflammation, plasma and peripheral white blood cells can reflect the level of inflammation in the joint tissues. Adipokines secreted from visceral fat, such as leptin, resistin, and adiponectin also play an important role (Gomez et al., 2011), having both pro- or anti-inflammatory effects on OA development (Distel et al., 2009). The release of inflammatory factors into the blood can cause diseases in other parts as well, such as the inflammation of the nervous system and Alzheimer's disease (Kyrkanides et al., 2011).

Clinical Treatment Options

Although our understanding of the mechanism underlining OA has improved, limited progress has been made with respect to its treatment. Currently, analgesia and joint replacement are primarily used to treat end-stage OA (Bijlsma et al., 2011; Carr et al., 2012; Pivec et al., 2012) which neglects the problem of early disease incidence. Fortunately, the continuous advancement in our understanding of OA pathogenesis and the improvement in detection methods have shifted the focus toward the prevention and treatment of early OA. Lifestyle adjustments, such as weight loss and exercise for obese individuals, can enhance muscle strength and joint stability, improve cardiovascular function, and reduce the risk of OA (Felson et al., 1992; Gudbergsen et al., 2012; Uthman et al., 2013).

Drug treatment often goes hand-in-hand with prevention, with commonly used drugs in clinical practice, such as paracetamol (acetaminophen) and non-steroidal anti-inflammatory drugs (NSAIDs) also being able to effectively relieve pain symptoms (Palmer et al., 2013). Furthermore, the anti-inflammatory and anti-catabolism properties of chondroitin and glucosamine have been proven in clinical trials to alleviate the occurrence and development of OA (Henrotin and Lambert, 2013). Hyaluronic acid, a glycosaminoglycan, can also act as a lubricant in the synovial fluid. In patients with OA, the concentration of hyaluronic acid in the joint cavity is low, and the friction experienced by the joint surfaces during limb movement increases pain. It must be noted, however, the clinical efficacy and safety of injecting hyaluronic acid into the joint cavity remains controversial (Rutjes et al., 2012). Another lubricating element, lubricin, has been shown to work synergistically with hyaluronic acid with limited effects (Schmidt et al., 2007). Several targeted drugs have also been developed to treat OA, such as MMP inhibitors (doxycycline) (da Costa et al., 2012), osteoclast inhibitors (bisphosphonates and strontium ranelate) (Henrotin et al., 2001), IL-1R inhibitors (anakinra) (Chevalier et al., 2009), immunoglobulins (AMG 108) (Cohen et al., 2011), TNF-α inhibitors (adalimumab) (Verbruggen et al., 2012), cartilage repair factors [recombinant osteogenic protein-1 (Nishida et al., 2004) and kartogenin (Johnson et al., 2012)]. The application of these drugs still needs improvement as there is still a gap between the desired therapeutic effect and the clinical outcomes. This implies that more effective and targeted drugs are

required in the prevention and treatment of OA. Therefore, an in-depth exploration of the particular etiology and pathogenesis of OA is critical.

THE P2X7 RECEPTOR

P2X7R Structure and Function

Purine receptors can be divided into two categories: adenosine (ADO) activated P1 receptors and purine and pyrimidine nucleotides (ATP and ADP) activated P2 receptors. P2 receptors can further be divided into P2X ion channel receptors and P2Y metabotropic receptors. There are seven different members of the P2X family (P2X1-7), of which the P2X7 receptor (P2X7R, encoded by the *P2RX7* gene) is most closely related to inflammation and immunity, and belongs to the trimeric ligand-gated cation channel. Compared with other P2X receptors, P2X7R requires a higher concentration of ATP for activation and has a higher affinity for the selective agonist BzATP, with 10–30 times more potency than ATP (North, 2002). In addition, natural splice variants (P2X7A-J) and (P2X7a, P2X7k, P2X713b, and P2X713c) were found in human and rodent tissues, respectively, with P2X7R sharing 77–85% sequence identity. Therefore, several experiments have used rodent models to study the function of P2X7R.

Structurally, P2X7R contains relatively short intracellular amino- (N) and long carboxyl- (C) termini, and two hydrophobic transmembrane fragments separated by glycosylated extracellular ATP binding domains (transmembrane domains); its topology is similar to that of other ionic P2X receptors (Khakh and North, 2006; Karasawa and Kawate, 2016). The functional channel toward the plasma membrane is composed of stable trimers (Nicke, 2008; Jiang et al., 2013). Moderate activation occurs when the receptor is bound to ATP. The gated state of P2X7R is opened, mediating non-inactivated Na^+ and Ca^{2+} influx and K^+ efflux, resulting in rapid depolarization (Surprenant et al., 1996). When the activation time is prolonged, P2X7R can induce the formation of membrane pores, allowing molecules up to hundreds of Da to pass (Pelegrin and Surprenant, 2006).

P2X7R Activation and Regulation

The transcription and expression of P2X7R can be regulated by microRNAs [e.g., miR-373 (Zhang et al., 2018)], long-coding RNAs (e.g., lncRNA NONRATT021972), and transcription factors [e.g., specific protein 1 (Sp1)], and P2X7R will also undergo post-translational modifications, including N-linked glycosylation, palmitoylation, and ADP-ribosylation (Sluyter, 2017). The most important mediator for the activation of receptors is ATP and its role in inflammation and immunity has been proven. Cell death in inflammatory tissues releases large amounts of ATP, increasing the extracellular ATP concentration to hundreds of μM, which is enough to activate P2X7R. In contrast, the extracellular ATP concentration in healthy tissues is very low (Pellegatti et al., 2008; Wilhelm et al., 2010; Barbera-Cremades et al., 2012). In addition to passive release, ATP can also cross incomplete cell membranes through specific membrane protein channels, or can be stored in cytoplasmic vesicles and secreted outside the cell (Burnstock, 2006). Other mechanisms, such as the one mediated by the gap junction protein pannexin-1, control the release of ATP from living or apoptotic cells. Under certain conditions, such as hypoxia, increased extracellular K^+ concentration, and mechanical stress stimulation, pannexin-1 has high ATP permeability (Wang and Dahl, 2018). In undamaged tissues, a small amount of ATP in the extracellular environment will be rapidly degraded by enzymes (Plesner, 1995). Therefore, to activate P2X7R, the ATP release channel and the receptor should be in close proximity, which explains the closely related protein functions and structures of pannexin-1 and P2X7R (Bao et al., 2004; Pelegrin and Surprenant, 2006; Locovei et al., 2007).

The P2X7 receptor activation mediates numerous signaling pathways and cellular responses, such as the activation of the NLRP3 inflammasome via K^+ efflux, which induces IL-1β release; the formation of mitochondrial reactive oxygen species (mtROS) via ATP signaling, which can also regulate the activity of P2X7 ion channels; the regulation of caspase, cathepsin, and MMP release; and the regulation of the pro-inflammatory mediator prostaglandin E2 (PGE-2). PGE-2 is an important downstream inflammatory pathway of P2X7R, which may make P2X7R a potential anti-inflammatory target to replace cyclo-oxygenase that regulates the activation of transcription factors, such as NF-κB p65, HIF-1α, and PI3K-AKT; glutamate efflux; endocytosis; cell proliferation; and cell death. Briefly, P2X7R regulates ion flow, protease activation, and various secretory responses, which constitute the most common signaling pathways in inflammation (Bartlett et al., 2014). Therefore, P2X7R is also known as an inflammatory switch.

P2X7R AND OSTEOARTHRITIS

The importance of P2X7R in inflammation has recently attracted attention in the field of bone-related diseases. It has critical influence on OA, synovitis, and rheumatoid arthritis. This has opened a way for P2X7R inhibitors (as a specific target-directed approach) to serve as potential new therapeutics for these diseases.

P2X7R as an Inflammatory Switch

When OA occurs, the most significant cellular response is inflammation, which can be triggered by external and internal mechanisms. External factors include mechanical stress (compression, stretching, hydrostatic pressure, and shear stress), while the mechanoreceptors (ion channels and integrins) present on the surface of joint cells convert abnormal mechanical stress into activated intracellular signals (Guilak, 2011). Accordingly, the activation of the NF-κB and mitogen-activated protein kinase (MAPK) signaling pathways is commonly observed (Signaling, 2004).

Exercise as an Anti-inflammatory Mechanism

In daily life, physical exercise causes mechanical stress on joints that can be beneficial. Studies have shown that regular exercise can alleviate low-intensity inflammatory conditions, as are observed in OA, cancer, and cardiovascular disease, and

reduce the risks associated with a high-fat diet. P2X7R is one of the factors that determine the level of IL-1β in the plasma after exercise. Furthermore, P2X7R, NF-κB, NLRP3, and caspase-1 levels have been shown to progressively increase between sedentary individuals, trained athletes, and endurance athletes (Comassi et al., 2017). Post-exercise, NLRP3 and caspase-1 levels increased in sedentary individuals (pro-inflammatory), while they decreased in endurance athletes (anti-inflammatory). Regardless of the degree of fitness, acute exercise increased P2X7R expression and function. In another study, exercise reduced the expression levels of P2X7R, NLRP3, caspase-1, and IL-1β in plasma caused by a high-fat diet in Sprague Dawley rats, inhibiting inflammation and apoptosis, enhancing autophagy, and reducing myocardial damage (Chen et al., 2019). It is thus evident that P2X7R plays an important role during exercise to relieve inflammation and other risk factors.

Cytokine Secretion During Inflammation

The P2X7 receptor regulates the intensity and duration of several inflammatory reactions (Ferrari et al., 2006; Khakh and North, 2006; Dubyak, 2012). In macrophages, monocytes, and microglia, P2X7R mediates Ca^{2+} influx and K^{+} efflux inducing the activation and release of cytokines (Kahlenberg and Dubyak, 2004; Ferrari et al., 2006). This initiates inflammasome assembly, while caspase-1 pro-IL-1β cleavage releases a large amount of mature IL-1β (MacKenzie et al., 2001; Pelegrin et al., 2008; Dubyak, 2012). IL-1β can induce reactive oxygen species (ROS) and the expression of protein-degrading enzymes, leading to the loss of type II collagen and proteoglycans, thereby destroying cartilage structure and affecting joint function and stability (Sitia and Rubartelli, 2020). IL-1β is an atypical cytokine lacking secreted fragments which does not follow the standard endoplasmic reticulum-Golgi pathway for extracellular release (Dinarello, 2002). Instead, it functions via an ATP-dependent P2X7R-inflammasome pathway by TLR stimulation-induced accumulation of pro-IL-1β in the cytoplasm followed by its subsequent release (Perregaux et al., 2000; Ferrari et al., 2006). Other mechanisms of cytokine release occur through passive release after cell death, and secretion by modified lysosomes, exosomes, or plasma membrane-derived microvesicles (MacKenzie et al., 2001; Lopez-Castejon and Brough, 2011; Piccioli and Rubartelli, 2013). In all these instances, P2X7R is the main driver (Bianco et al., 2005; Pizzirani et al., 2007; Qu et al., 2007), further emphasizing its key role in the release of biologically active IL-1β.

Oxidative Stress in Inflammation

Among the internal factors contributing to the development of OA, ROS play a pivotal role. ROS comprise molecules containing free radicals, including oxygen free radicals (OH^{-}), hypochlorite ions (OCl^{-}), superoxide anions (O_2^{-}), nitric oxide (NO), and hydrogen peroxide (H_2O_2). ROS is mainly produced through the following pathways: mitochondrial (through oxidative phosphorylation) and non-mitochondrial membrane-bound nicotinamide adenine dinucleotide phosphate (NADPH) oxidase and xanthine oxidase (XO) pathways (Turrens, 2003). When the catabolic cell balance is disturbed, the accumulation of ROS leads to an increase in the production of inflammatory mediators, and an ineffective elimination of the oxidized proteins. This ultimately triggers oxidative damage that exacerbates inflammation (Licastro et al., 2005). Oxidative stress can promote cell senescence, especially affecting chondrocytes (Loeser, 2011). Chondrocytes have a low ability to divide and proliferate with high ability to synthesize and secrete, a circumstance called the senescence-associated secretory phenotype (SASP) (Coppe et al., 2010). ROS normally occurs at low levels in chondrocytes but can still regulate gene expression, affect ECM synthesis and catabolism balance, drive the production of cytokines, such as IL-1β (Forsyth et al., 2005), and induce cell apoptosis. The exacerbated oxidative stress in chondrocytes inhibits the PI3K/Akt pathway; activates the NF-κB pathway to promote the transcription of MMPs; activates the extracellular signal-regulated kinase (ERK)/MAPK pathway to reduce the expression of type II collagen, proteoglycans, and Sox-9; reduces ECM synthesis (Yin et al., 2009; Yu and Kim, 2015); and acts as a signal transduction intermediate for IL-1β and TNF-α in the c-Jun N-terminal kinase (JNK) pathway activation (Lo et al., 1996). Therefore, ROS plays an important role in the intracellular signal transduction mechanisms and is closely related to cartilage homeostasis (Rathakrishnan et al., 1992; Henrotin et al., 1993; Henrotin et al., 2003).

Significance of P2X7R in Inflammation

Summarily, the ion flow mediated by P2X7R activation is closely related to the homeostasis of the intracellular environment. Mitochondrial dysfunction caused by Ca^{2+} overload can induce the production of ROS. Activation of inflammasomes triggered by K^{+} efflux can induce the production of IL-1β and the activation of inflammation-related pathways. This indicates the important role of P2X7R in inflammation and its potential influence on the occurrence and development of OA. In terms of preventive treatment and cytokine treatments were not found to significantly improve the symptoms of OA or relieve the deterioration of bone structure. The results of pilot and controlled studies using anti-IL-1 and anti-TNF molecules lack credibility (Chevalier et al., 2009; Verbruggen et al., 2012). In this context, P2X7R-targeted therapy could present as a new direction for the prevention and treatment of OA.

P2X7R Induces Apoptosis in OA

When a cell undergoes apoptosis, the chromatin condenses around the nucleus, the cell membrane shrinks and bubbles, and apoptotic bodies with intact membranes form around organelles (Kerr et al., 1972). Upon recognition by the immune system, inflammation is induced. This can be prevented, however, by the phagocytic engulfment of these vesicles (Kurosaka et al., 2003). Apoptosis is a programmed cell death, which differs from passive necrosis (or cell membrane disintegration) caused by pyroptosis. At the molecular level, initiation, execution, degradation, and clearance are the established sequential steps of apoptosis.

Apoptotic Pathways

Apoptosis can be induced via extrinsic mediation by death receptors and via intrinsic mediation by mitochondria

(Elmore, 2007). The extrinsic pathways include damage or pathogen-related molecular patterns (DAMPs or PAMPs) and cytokines that activate the TNF superfamily (e.g., death receptors). The death receptor Fas and its ligand FasL combine to drive the assembly of the death-inducing signaling complex (DISC). Thereafter, the recruitment and activation of caspase-8 are mediated by Fas-related proteins and death domain (FADD) adaptor molecules, which leads to caspase-3 activation, and finally apoptosis (Fuentes-Prior and Salvesen, 2004). P2X7R is closely related to apoptosis. IL-1β, mediated by P2X7R, can further induce the production of TNF-α, both having pro-apoptotic effects (Lee et al., 2016). The membrane pores formed by P2X7R (Donnelly-Roberts et al., 2004), together with its mediated K^+ efflux (Delarasse et al., 2009; Aguirre et al., 2013), can induce the activation of caspase-8 and subsequently cleave caspase-3, the key executor of apoptosis.

Intrinsic pathways include those mediated by DNA damage, cytoplasmic Ca^{2+} overload, oxidative or endoplasmic reticulum stress (ERS), decreased cytokine levels, and the response to intracellular damage (Vanden Berghe et al., 2015). Bcl-2 family members respond by changing the permeability of the mitochondrial outer membrane (Kroemer and Reed, 2000). The activation of its priming members (e.g., Bid) not only inhibit survival supervisory members (e.g., Bcl-2), but also oligomerize pro-apoptotic members (e.g., Bax), thereby destroying the mitochondrial outer membrane. A large number of proteins are released into the cytoplasm, such as cytochrome c (Cyt c) (Qiu et al., 2000), activating a key component of apoptotic bodies, namely the apoptotic protease activator factor-1 (APAF-1) (Green, 2003). Cyt c combines with oligomeric APAF-1 to form a multimeric structure, recruiting and activating caspase-9 in the mitochondrial pathway (Bao and Shi, 2007). Caspase-9 directly activates downstream caspase-3, 6, and 7, ultimately leading to substrate cleavage and apoptosis. In addition to the inflammasome assembly caused by the intracellular K^+ consumption, K^+ efflux can also induce apoptosis by promoting APAF-1 (Bortner et al., 1997; Karki et al., 2007). Furthermore, Ca^{2+} influx can lead to mitochondrial dysfunction and caspase-3 activation. As P2X7R plays a crucial role ion transport, P2X7R inhibitors have shown promise in preventing cell death dependent on these mechanisms (Nishida et al., 2012).

Oxidative Stress in Apoptosis

Reactive oxygen species (e.g., H_2O_2) damages mitochondria as part of the apoptotic intrinsic pathway, destroying its DNA integrity and repair ability (Grishko et al., 2009). This can induce chondrocyte apoptosis through PI3K/Akt, p38 MAPK, and JNK signaling pathways (Yu and Kim, 2014; Li and Dong, 2016; Rao et al., 2017). As mentioned earlier, P2X7R can induce the generation of ROS, and the activation of P2X7 will increase the phosphorylation of tyrosine protein, activating MAPK (Panenka et al., 2001; Papp et al., 2007), including ERK, JNK, and p38 MAPK. ERK is essential for cell survival, while JNK and p38 MAPK can be activated under stress stimulation (Wada and Penninger, 2004; Yang et al., 2012). JNK phosphorylates Bcl-2 to reduce its anti-apoptotic activity (Cui et al., 2007), and p38 MAPK reduces the expression of Bcl-2 and induces the production of caspase-3, leading to apoptosis (Nishida et al., 2012). The NF-κB signaling pathway closely relates to P2X7R involvement in chondrocyte apoptosis, since it can affect the expression of apoptosis-related proteins (Bcl-2, Bax, Cyt c, and caspase-3) (Pan et al., 2018).

Chondrocyte Apoptosis

Unregulated apoptosis can lead to pathological changes, such as tumors and inflammation. Apoptosis is both the initiator (Hashimoto et al., 1998) and feedback in the development of OA (Blanco et al., 1998; Heraud et al., 2000). Specifically, chondrocyte apoptosis is considered a prerequisite for the development of OA. Compared with the normal cartilage, the number of apoptotic chondrocytes is increased in the cartilage of OA patients (Hashimoto et al., 1998), while that of normal chondrocytes is decreased (Aigner et al., 2006), and a dysregulation of apoptosis-related genes occurs (Bobinac et al., 2003). In addition, animal studies showed that low levels of mechanical stress stimulation can induce chondrocyte apoptosis, with high levels of mechanical stress stimulation leading to the degradation of the cartilage matrix (Loening et al., 2000). This indicates that chondrocyte apoptosis occurs first, followed by tissue damage, reflecting early features of OA. Therefore, chondrocyte apoptosis also represents the feedback of the outcome of OA (Zamli et al., 2013). In transgenic mice with type II collagen gene knockout, chondrocytes undergo increased apoptosis, have lower survival, and no longer interact with the surrounding matrix, and there is presentation of severe cartilage degradation, compared to the wild-type mice (Zemmyo et al., 2003). Several studies have confirmed the positive relationship between the severity of cartilage degradation and the rate of chondrocyte apoptosis (Blanco et al., 1998; Hashimoto et al., 1998; Thomas et al., 2007). Some studies used collagenase to destroy the matrix, increasing cell permeability to expose the chondrocytes to apoptosis inducers (NO and cytokines) secreted by either synoviocytes or other chondrocytes, ultimately leading to cell apoptosis (Zamli and Sharif, 2011). Taken together, although the sequence of cartilage degradation and chondrocyte death is still controversial, they are undeniably closely related in OA (Zamli and Sharif, 2011).

Interplay With Pyroptosis

Apoptosis does not always occur in isolation and often accompanies other phenotypes. In the early stage of OA, autophagy plays a protective role to prevent cell death on the surface and middle layers of cartilage (Almonte-Becerril et al., 2010; Carames et al., 2010); while in the late stage of OA, autophagy induces apoptosis and accelerates cell death (Almonte-Becerril et al., 2010). In the cartilage of patients with OA, the apoptotic bodies that have not been engulfed in time, together with increasing cartilage calcification, aggravate OA through secondary pyroptosis (Roach et al., 2004). The cell death caused by apoptosis and pyroptosis have also been confirmed in a model of OA induced by mechanical stress (Chen et al., 2001; Stolberg-Stolberg et al., 2013). *In vivo* and *in vitro* experiments showed that the application of mechanical stress to the chondrocytes of human cartilage explants (D'Lima et al., 2001),

end plates (Kong et al., 2013), or growth plates (Sun et al., 2017) can lead to the loss of type II collagen, proteoglycans, and glycosaminoglycans, accompanied by cell death. The protective role of antioxidants must briefly be mentioned as they can reduce cell death caused by shear stress (Martin and Buckwalter, 2006) and abnormal cyclic loading (Beecher et al., 2007).

Significance of P2X7R in Apoptosis

In summary, P2X7R-mediated ion flow, oxidative stress, and related signaling pathways are closely related to apoptosis. Apoptosis is complemented by OA under the action of autophagy and pyroptosis. Thus, P2X7R plays an important role in the interaction between apoptosis and OA. It participates in cartilage degradation and inflammatory factor release, aiding the progression to OA.

P2X7R Drives Pyroptosis in OA

Apoptosis and pyroptosis can occur independently, sequentially, and simultaneously (Zeiss, 2003). Both have common triggers and biochemical networks. The intensity and duration of different stimuli, the amount of ATP that can be consumed in the cell, and the potency of caspases can convert the ongoing process of apoptosis into pyroptosis (Leist et al., 1997; Denecker et al., 2001; Zeiss, 2003). The process of accidental and passive cell death caused by harmful stimuli (ultraviolet radiation, heat, hypoxia, and cytotoxic drugs), accompanied by cytoplasmic granulation, mitochondrial swelling, cell swelling, rupture of the plasma membrane, and uncontrolled release of intracellular substances (including pro-inflammatory cytokines, DAMPs, and lysosomal enzymes), causes an inflammatory response called pyroptosis (Festjens et al., 2006; Kaczmarek et al., 2013).

NLRP3 as the Initiator of Pyroptosis

NLRP3, as one of the components of the inflammasome (the core component of pyroptosis) exists in the cytoplasm and can recognize PAMPs (such as pore-forming toxins and microbial cell wall components) or DAMPs (such as ATP derived from endogenous stress and uric acid crystals) (McGilligan et al., 2013; Guo et al., 2015; Sharma and Kanneganti, 2016). NLRP3 activates caspase-1, promoting the secretion of IL-1β and IL-18 to exacerbate inflammation (Shao et al., 2015), resulting in rapid cell death (Latz et al., 2013). There are two main ways to activate inflammasomes. The first is through the recognition of PAMPs or DAMPs by TLRs to activate the NF-κB signaling pathway, increasing the synthesis of NLRP3, pro-IL-1β, and pro-IL-18; the second is by initiating oligomerization, leading to the assembly of inflammasomes (Shao et al., 2015). Both kinase activity and autophagy can regulate the activity of the NLRP3 inflammasome (Yang et al., 2017). Autophagy relieves pyroptosis by degrading pro-IL-1β, inflammasome components, and damaged mitochondria (Zhou et al., 2011; Shi et al., 2012).

As a key activator of inflammasomes, P2X7R participates in both the classical pathway (e.g., NLRP3) and non-classical pathway (e.g., caspase-11). The latter induces cell death similar to pyroptosis (Vigano and Mortellaro, 2013; de Gassart and Martinon, 2015). The C-terminal part of pannexin-1 can be cleaved by caspase-11, leading to ATP release and K^+ efflux (Yang et al., 2015). Hypoxia-induced caspase-11 expression and activation (Kim et al., 2003) are involved in ERS-dependent cell death (Fradejas et al., 2010). P2X7R and NLRP3 can also interact physically. Immunoprecipitation and confocal microscopy studies have found that changes in the local ionic microenvironment in cells caused by P2X7R or by a membrane pore opening can result in inflammasome assembly (Franceschini et al., 2015).

Under normal circumstances, inflammasomes activate the innate immune system, producing IL-1β, IL-18, and other pro-inflammatory cytokines to protect cells from infection and reduce damage (Man and Kanneganti, 2015). However, excessive activation of inflammasomes overproduce cytokines, causing inflammation and metabolic disorders (Strowig et al., 2012). NLRP3 is an established potential target for diseases, such as atherosclerosis, rheumatoid arthritis, and gout. NLRP3 is also activated in the synovial tissue contributing to cartilage degradation (Bougault et al., 2012). In patients with OA, high NLRP3 expression in tissue has been linked to high XO levels (an enzyme producing ROS and uric acid), further confirming the association between OA and NLRP3 inflammasomes (Clavijo-Cornejo et al., 2016).

As stated before, cartilage degradation in OA can result from disrupted anabolic and catabolic chondrocyte balance (Bijlsma et al., 2011). Once initiated, the primary cartilage-degrading enzymes, IL-1β and TNF-α, are produced by the NLRP3 inflammasome (Mueller and Tuan, 2011; Haseeb and Haqqi, 2013). IL-1β both induces cell apoptosis (Haseeb and Haqqi, 2013) and stimulates the secretion of other cartilage-degrading enzymes, such as MMP3/13 and ADAMTS-4/5 (Mueller and Tuan, 2011), leading to the degradation of the type II collagen and the proteoglycans of the ECM (Haseeb and Haqqi, 2013). The released collagen and proteoglycan particles stimulate the production of IL-18 (Olee et al., 1999; Man and Mologhianu, 2014), which inhibits proteoglycan synthesis and chondrocyte proliferation, promotes prostaglandin production, and further induces apoptosis (Jin et al., 2011).

Significance of P2X7R in Pyroptosis

Targeting the components of inflammasomes and upstream and downstream pathways, such as K^+ efflux, ROS, mitochondrial-, and lysosome dysfunction, is an important approach in the treatment of OA (Di Virgilio, 2013; He et al., 2016). The small molecule inhibitor MCC950 inhibits the oligomerization of inflammasomes and IL-1β release (Coll et al., 2015). Drugs that target IL-1R, such as rilonacept, anakinra, and canakinumab, can also reduce cartilage destruction (Dinarello et al., 2012). As an important driving force of the inflammasome pathway, P2X7R has potential as a drug target treatment to alleviate cartilage damage caused by pyroptosis.

P2X7R Regulates Autophagy in OA

Cells degrade excess or damaged lipids, proteins, and organelles, to maintain cell viability through autophagy. Autophagy also plays a role in maintaining mitochondrial function (Lo Verso et al., 2014), as the downregulation of autophagy will induce the accumulation of damaged mitochondria, increase the levels of

ROS, and lead to tissue degeneration (Mizushima and Komatsu, 2011). Autophagic flux can be divided into five stages: (i) induction, (ii) nucleation, (iii) extension, (iv) maturation, and (v) lysis. A complex is formed in each of the first three stages. In the induction phase, the Atg1 complex (including Atg1/Ulk1, Atg13, and Atg17/FIP200) and the activity of mammalian target of rapamycin complex 1 (mTORC1) is inhibited, Atg13 phosphorylation level is reduced, and the complex is formed (Ganley et al., 2009). The Vps34 (PI3K)-Atg6 (Beclin-1) complex acts on the nucleation of the membrane vesicles and mediates the formation of the pre-autophagosome structure. The extension of autophagosomes mainly depends on two ubiquitin-like systems: the binding process of Atg12-Atg5 and the modification process of LC3. LC3-II is a multi-signal transduction regulatory protein that is located on the autophagy vesicle membrane and is often used as a marker for autophagy formation.

Chondrocyte Autophagy

Cartilage lacks blood vessels to supply oxygen, thus cells exist in a somewhat hypoxic environment. Hypoxia promotes autophagy (e.g., through an increase in *Ulk1* and *Atg5* mRNA levels), maintains the chondrocyte phenotype (e.g., increased *Sox9* and *type II collagen* mRNA levels, decreased *MMP13* and *ADAMTS-5* mRNA levels), and further induces hypoxia factors (HIFs) (Coimbra et al., 2004), which play important roles as key regulators of autophagy in chondrocytes. HIF-1 is a heterodimer composed of two different subunits, HIF-1α and HIF-1β. Under hypoxic conditions, HIF-1α degradation is prevented and transferred to the nucleus, where it combines with β subunits to form an active HIF-1 transcription factor. HIF-1α is essential for cell survival, and its knockout induces mass chondrocyte death in the cartilage growth plate (Schipani et al., 2001). Bcl-2 plays a role in HIF-1α-mediated autophagy (Zhang F. et al., 2015), while HIF-1α modulates the Beclin-1/Bcl-2 complex (Bohensky et al., 2007), activates AMPK, inhibits mTOR (Bohensky et al., 2010), induces chondrocyte autophagy, and prevents apoptosis. P2X7R is also closely related to HIF-1α and autophagy (Mascanfroni et al., 2015). The ATP-P2X7R signal axis driven by oxidative metabolism participates in the differentiation of bone marrow-derived macrophages into their M2 type (Barbera-Cremades et al., 2016). HIF-1α also plays a key role in this process. For example, HIF-1α promotes lactic acid-dependent M2 polarization in the tumor microenvironment (Colegio et al., 2014). Interestingly, P2X7R is a strong stimulator of aerobic glycolysis and lactic acid production (Amoroso et al., 2012). P2X7R receives ATP signals to stimulate the alkalinization of lysosomes (Guha et al., 2013), which leads to an increase in the lysosomal pH. The accumulated autophagosomes cannot be fused with lysosomes for degradation and release outside the cell, thereby reducing autophagy flux (Takenouchi et al., 2009a,b). P2X7R activation downregulates the expression of glutamate transporter and promotes neuro-autophagy, which increases excitatory amino acids (Zhang et al., 2008; Działo et al., 2013; Kulbe et al., 2014) caused by an abnormal stimulation of glutamate receptors, ultimately resulting in cognitive impairment (Sun et al., 2015). P2X7R activates PI3K/Akt/GSK3β/β-catenin and/or mTOR/HIF1α/VEGF pathways to promote the proliferation and metastasis of osteosarcoma and increase bone destruction (Zhang et al., 2019).

Significance of P2X7R in Autophagy

Whether P2X7R promotes or inhibits autophagy is still controversial (Sluyter, 2017). For instance, one study showed ATP-activated P2X7R to inhibit the PI3K/AKT pathway, activate the AMPK-PRAS40-mTOR pathway, promote autophagy, inhibit cell proliferation, and exert anti-tumor effects (Bian et al., 2013). In another study, LL-37 activated AMPK and PI3K through P2X7R-mediated Ca^{2+} influx, promoted autophagy, and aided in inducing resistence against *Mycobacterium tuberculosis* in macrophages (Rekha et al., 2015). In another case, P2X7R-mediated Ca^{2+} influx activated mTOR and inhibited Treg cell conversion (Bohensky et al., 2010). However, to the contrary, in memory CD8+ T cells, P2X7R receives extracellular ATP signals to activate AMPK through Ca^{2+} influx and increase the AMP/ATP ratio, inhibit mTOR, and enhance mitochondrial function (Borges da Silva et al., 2018).

The level of autophagy is also related to the activation state of P2X7R. In the early stage of activation, P2X7R-mediated K^+ efflux and Ca^{2+} influx activate mtROS, and Ca^{2+} activates CaMK, which in turn activates the AMPK pathway, inhibits mTOR, and promotes mitophagy and lysosome biogenesis. In the late stage of activation, lysosome stability decreases and cell death occurs (Sekar et al., 2018). Energy receptor AMPK (Garcia and Shaw, 2017) is also regulated by exercise (Garber, 2012). High-intensity exercise activates AMPKα to increase autophagic flux (Schwalm et al., 2015). In skeletal muscle, exercise induces mitophagy to degrade damaged mitochondria through the AMPK-Ulk1 signaling pathway (Laker et al., 2017). When energy is severely lacking, exercise inhibits AMPK/Ulk1/Beclin-1 phosphorylation, and the accumulated p62/SQATM1 inhibits autophagy to reduce muscle loss (Martin-Rincon et al., 2019). As an important downstream signaling molecule of P2X7R, AMPK is involved in the regulation of several physiological and pathological functions (Jeon, 2016), including autophagy in OA.

AUTOPHAGY IS A DOUBLE-EDGED SWORD IN OA

Compared with microautophagy and chaperone-mediated autophagy, macroautophagy is most studied and understood (Parzych and Klionsky, 2014). However, the relationship between cartilage damage, the degree of autophagy, and cell death remains unclear (Caramés et al., 2015).

The Positive Side of Autophagy

The consensus is that autophagy exerts a protective effect on chondrocytes in OA. In mice, as cartilage damage increases, and resulting cell death ensues, the expression levels of autophagy-related genes decrease (Caramés et al., 2015). In cell lines and primary chondrocytes, decreased autophagy leads to cartilage degradation (Ribeiro et al., 2016a). Rapamycin (an autophagy inducer) promotes the degradation and clearance of damaged

mitochondria, reduces IL-1β-induced ROS generation, and reduces the OA-like phenotype of chondrocytes (Sasaki et al., 2012). Decreased levels of autophagy are often accompanied by increased levels of apoptosis [e.g., presentation of activated PARP (the caspase-3 substrate)], further exacerbating OA characteristics (Caramés et al., 2015). Moreover, Beclin-1 silencing which reduces autophagy exacerbates cell death (Bohensky et al., 2007). mTOR overexpression also inhibits chondrocyte autophagy and promotes apoptosis, leading to increased cartilage degeneration (Zhang Y. et al., 2015). Autophagy promoted through oligomycin stimulation can effectively eliminate dysfunctional mitochondria, thereby protecting cells from apoptosis (Lopez de Figueroa et al., 2015).

Exercise promotes autophagy which relieves inflammation (Deretic et al., 2013). During exercise, the innate immune molecule TLR-9 interacts with Beclin-1 to strengthen and regulate AMPK activation in muscles (Liu Y. et al., 2020). AMPK interacts with sestrins to participate in exercise-induced autophagy to maintain skeletal muscle glucose metabolism (Liu et al., 2015), and relieve aging-related muscle atrophy (Fan et al., 2017). Exercise-induced AMPK activation can also inhibit mTOR, thereby alleviating other diseases as well by promoting autophagy, reducing the transformation of fatty liver to hepatitis and tumors (Guarino et al., 2020), and alleviating heart damage caused by exhaustive exercise (Liu and Pan, 2019).

The Negative Side of Autophagy

Excessive autophagy can be a double-edged sword (Carames et al., 2010; Lopez de Figueroa et al., 2015; Ribeiro et al., 2016a,b), with no protective effect on cells (Chang et al., 2013), resulting in cell death (Shapiro et al., 2014) through synergistic participation in the process of cell apoptosis (e.g., ATP-dependent apoptosis). Related genes, such as *Ulk1*, *Beclin-1*, and *LC3*, are highly expressed in the early stage of OA, reflecting the protective effect of autophagy on chondrocytes; while in the late stage of OA, they are weakly expressed, as a consequence of autophagy-induced apoptotic cell death (Almonte-Becerril et al., 2010; Carames et al., 2010; Sasaki et al., 2012; Caramés et al., 2015). The opening of membrane pores induced by the ATP-P2X7R axis in muscle injury mediates autophagic cell death (Young et al., 2015). P2X7R receives ATP signals induced by ivermectin to promote autophagy, leading to tumor cell death. Although the role of P2X7R in infection and inflammation has been confirmed (Di Virgilio et al., 2017), studies have shown that inflammation leads to the downregulation of P2X7R expression, which in turn inhibits the PI3K-AKT-mTOR pathway, and promotes the osteogenesis of periodontal ligament stem cells (Xu et al., 2019).

The Consensual Role of Autophagy in Pyroptosis

Contrary to the uncertain relationship between autophagy and apoptosis, autophagy usually alleviates pyroptosis (Gudipaty et al., 2018). This can be verified through various mechanisms in many studies. First, miR-103 targets BNIP3 (Bcl2/Adenovirus EIB 19 kDa Interacting Protein 3) to mediate late autophagy and relieve H_2O_2-induced oxidative stress and pyroptosis (Wang et al., 2020). Second, electrical stimulation affects THP-1 macrophages, activates Sirt3, promotes autophagy, and relieves ROS-induced pyroptosis (Cong et al., 2020). Third, adrenomedullin promotes autophagy and inhibits pyroptosis in testicular stromal cells through the ROS-AMPK-mTOR pathway (Li et al., 2019). Fourth, resveratrol reduces mitochondrial damage and increases autophagy, thereby inhibiting NLRP3 activation and reducing inflammation (Chang et al., 2015). Fifth, baicalein, a Chinese herbal ingredient, promotes autophagy degradation, and reduces unfolded protein accumulation and mitochondrial dysfunction caused by spinal cord ischemia-reperfusion injury, thereby alleviating pyroptosis (Wu et al., 2020). Sixth, metformin activates AMPK, inhibits mTOR, relieves pyroptosis, and treats diabetic heart disease in obese mice (Yang et al., 2019). And seventh, SP1 transcription increases the expression of lnc ZFS1, which downregulates miR-590-3p, inhibits AMPK, activates mTOR, inhibits autophagy, increases pyroptosis, and aggravates sepsis-induced cardiac dysfunction (Liu Y. et al., 2020).

In addition to removing harmful components in the cell, autophagy can also prevent pyroptosis by degrading inflammasome components. The NLRP3 inhibitor CP-456773 and the NF-κB inhibitor celastrol work together to induce autophagy through the AMPK-mTOR pathway and inhibit HSP-90, thereby increasing the autophagic degradation of NLRP3 to inhibit pyroptosis (Saber et al., 2020). Furthermore, bone marrow-derived mesenchymal stem cell (BMSC)-derived exosomes activate AMPK in hypoglycemic/reoxygenation-induced pheochromocytoma cells, inhibiting mTOR, promoting autophagic flux, while LC3 results in NLRP3 degradation to inhibit pyroptosis (Zeng et al., 2020). Also, immunity-related GTPase M (IRGM) interacts with NLRP3 and ASC to inhibit inflammasome oligomerization, thereby inhibiting its assembly and activation, and selectively degrades NLRP3 and ASC by autophagy, alleviating inflammatory cell death (Mehto et al., 2019).

Sometimes, autophagy is also the trigger point of pyroptosis. Autophagy mediates the release of IL-1β (Claude-Taupin et al., 2018). In macrophages, IL-1β is released outside the cell through a hole in the plasma membrane of N-GSDMD, while in neutrophils, N-GSDMD is not localized on the plasma membrane. IL-1β is released through the $LC3^+$ autophagosome pathway (Karmakar et al., 2020). Arsenic can also promote autophagy, with lysosome degradation releasing cathepsin, resulting in NLRP3 activation (Qiu et al., 2018). Autophagy is often inhibited when pyroptosis occurs. During the resting state of macrophages, NLRC4 and Beclin-1/Atg6 form a complex to inhibit autophagy. Under a low degree of infection, NAIP5 recruits NLRC4 and pro-caspase-1 to form a complex to relieve autophagy inhibition, and induce cell protection. When autophagy cannot eliminate an intracellular infection, caspase-1 is activated to initiate pyroptosis (Byrne et al., 2013). NLRP3 inflammasomes in hepatocellular carcinoma cells inhibit autophagy through the 17β-estradiol (E2)/ ERβ/AMPK/mTOR pathway (Wei et al., 2019).

Autophagy Discordance With Pyroptosis

When the two are activated together, autophagy negatively regulates pyroptosis. Inflammasome activation can induce autophagy, but the recruitment of LC3 and p62 induces the co-localization of inflammasomes with autophagosomes, thereby degrading them (Shi et al., 2012). Furthermore, when acrolein induces NLRP3 activation and autophagy through ROS, autophagy inhibits pyrolysis and mitochondrial damage (Jiang et al., 2018). Moreover, H_2O_2 induces nucleus pulposus cells to produce ROS, inducing autophagy, pyroptosis, and the upregulation of nuclear factor erythroid 2 like 2 (NFE2L2, Nrf2). Both Nrf2 and autophagy can alleviate pyroptosis and intervertebral disc degeneration (Bai et al., 2020). Tumor necrosis factor receptor-associated factor 3 (TRAF3) mediates the ubiquitination and degradation of Ulk1 and induces ROS and pyroptosis, while Ulk1 inhibits ROS and apoptosis inducing factor (AIF) translocation into the nucleus (Shen et al., 2020). In another mechanism, zearalenone inhibits the Akt/mTOR pathway to promote autophagy, while also promoting pyroptosis through NF-κB, but the upregulation of autophagy inhibits pyroptosis (Wang et al., 2019). In macrophages, NF-κB mediates the delayed accumulation of p62, forming the NF-κB-p62-mitophagy regulatory loop eliminating damaged mitochondria caused by pyroptosis, and limiting the intracellular pro-inflammatory activity (Zhong et al., 2016).

Alternative Autophagy Mechanisms in Pyroptosis

Autophagolysosomes formed by the fusion of autophagosomes and lysosomes play an important role in pyroptosis. Lysosomes act as AMPK-mTOR signaling hubs and an instability may lead to apoptosis and pyroptosis (Zhu et al., 2020). An impaired autophagy-lysosomal pathway in macular corneal dystrophic cornea can also lead to pyroptosis (Zheng et al., 2020). Moreover, BpV(phen) increases the ubiquitination of p62, affects the binding of p62 and HDAC6, activates the deacetylation of α-tubulin, and affects the stability of acetylated microtubules, resulting in hindered autophagosome and lysosome fusion, while autophagy inhibition leads to apoptosis and pyroptosis (Chen et al., 2015). Lastly, hypoxia-induced autophagy/lysosomal dysfunction leads to ERS, leading to unfolded protein accumulation and impaired autophagy, which in turn activates NLRP3 inflammasomes and induces pyroptosis (Cheng et al., 2019).

Significance of P2X7R in Cell Death Interplay

The interrelationships among phenotypes, such as autophagy, apoptosis, and pyroptosis, are also reflected in P2X7R-mediated cell metabolism and nutrition (Orioli et al., 2017). P2X4/P2X7/pannexin-1 mediates ROS, Ca^{2+}/CaMK II, mitochondrial membrane potential, and caspase-1 activation caused by NADPH oxidase to promote cell pyroptosis and necrosis (Draganov et al., 2015). In ischemic stroke disease, P2X7R-mediated Ca^{2+} and K^+ flow leads to mitochondrial dysfunction, caspase-8 and MAPK activation, and induces apoptosis. Ca^{2+} influx induces lysosomal dysfunction, which leads to decreased autophagic flow and apoptosis. K^+ efflux leads to the activation of inflammasomes and induces pyroptosis (Zhao et al., 2018). Ca^{2+} overload, caused by P2X7R-mediated Ca^{2+} influx under the stimulation by high ATP concentrations in macrophages, leads to mitochondrial dysfunction, which in turn causes cell pyroptosis. However, when P2X7R is stimulated by low ATP concentrations or is positively allosterically regulated by compound K, the accumulation of mtROS and the activation of caspase-1 and 3 alter cell death mechanism from pyroptosis to apoptosis (Bidula et al., 2019).

In summary, autophagy primarily plays the role of a protector, resisting stimuli that cause damage to cells through key signaling pathways, such as AMPK-mTOR and HIF-1α, and supporting homeostasis. When autophagy decreases, P2X7R-mediated ion flux and damage to organelles, such as mitochondria and lysosomes, prevent autophagy flux, and the balance shifts. At this time, autophagy may induce or convert into apoptosis and pyroptosis. On several occasions, autophagy is the initiator of apoptosis, pyroptosis, and inflammation. Therefore, autophagy is a double-edged sword, and the right balance, together with proper activation of P2X7R, is the key to its power.

THERAPEUTIC SIGNIFICANCE OF P2X7R INHIBITORS

The P2X7 receptor inhibition can occur via synthetic reagents, ions, natural molecular compounds, and Chinese herbal medicines. However, due to P2X7R's central role in inflammation, P2X7R inhibitors are receiving more attention for the development of targeted receptor therapies (Khakh and North, 2006; Arulkumaran et al., 2011; North and Jarvis, 2013; Bartlett et al., 2014; Di Virgilio et al., 2017). Various inhibitors display differences in chemical structure, species selectivity, competitive or non-competitive antagonistic methods, and specificity. The first-generation inhibitors, such as Reactive Blue 2, KN-62, PPADS, brilliant blue G (BBG), and oxidized ATP (oATP), are not highly selective, inhibiting other purinergic receptors as well. Second-generation inhibitors have improved target specificity for P2X7R, such as A438079, A740003, A839977, AZ10606120, AZ11645373, GSK314181, and JNJ-47965567. To date, most *in vivo* experiments have been conducted with first-generation inhibitors, but a select few studies have been carried out with specific inhibitors, like A438079, showing good efficacy *in vitro* and *in vivo*. Pretreatment of a DC/CD4+ T cell co-culture system with A438079, and the ensuing inhibition of P2X7R, can reduce the levels of pro-inflammatory factors IL-1β, IL-6, IL-23p19, and TGF-β1, derived from Th17 cells. In the arthritis mice model, induced by the activation of related collagen, A438079 relieved the swelling of the hind paw and the pathological changes in the ankle joint (Fan et al., 2016).

In view of the positive therapeutic effects of P2X7R inhibitors in rodent studies, drugs targeting human P2X7R are being used in clinical settings for the treatment of several diseases, such as pain, arthritis, and multiple sclerosis (Bartlett et al., 2014).

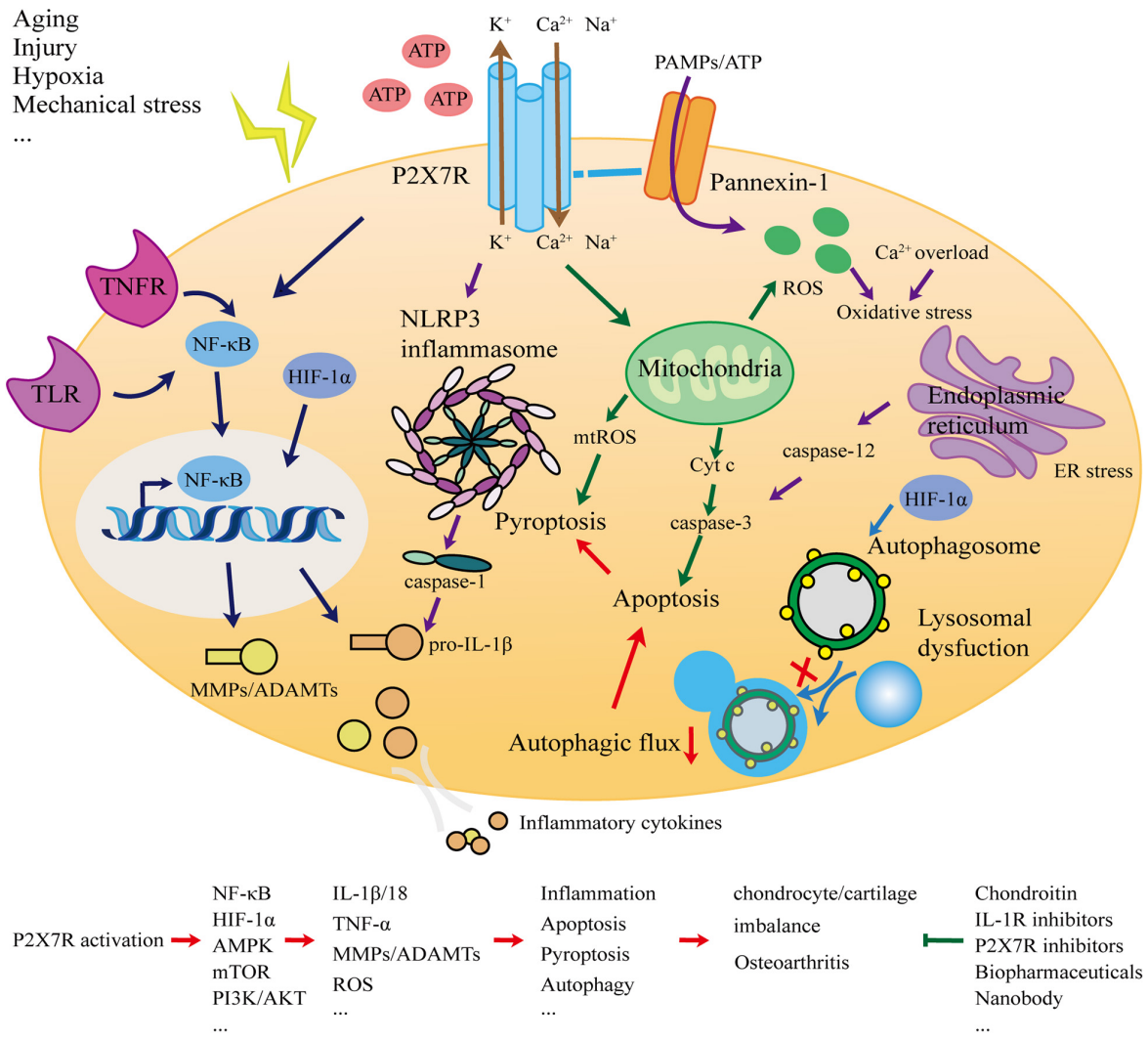

FIGURE 1 | Schematic for the role of the P2X7 receptor in osteoarthritis.

The therapeutic effects of inhibitors, such as oATP, BBG, KN-62, and A438079, have been confirmed in preclinical models of inflammatory diseases, such as contact allergy, inflammatory pain, endotoxin-induced fever, and antibody-induced nephritis (Matute et al., 2007; Taylor et al., 2009; Weber et al., 2010; Barbera-Cremades et al., 2012). Two clinical trials of patients with rheumatoid arthritis receiving P2X7R-specific inhibitors, AZD9056 and CE-224, reported on its safety and clinical efficacy. The dosages were well tolerated, but efficacy was not improved in patients already resistant to methotrexate or sulfasalazine (used in the treatment of joint swelling and pain) (Keystone et al., 2012; Stock et al., 2012). This would point to a need to use P2X7R inhibitors in conjunction with other targeted therapies capable of resensitizing mechanistic pathways involved in drug-resistance.

Although rodent models and receptor inhibitors are regularly encountered in P2X7R research, the selectivity and specificity of inhibitors still require attention. Recent development of therapeutic antibodies, such as nanobodies or single-domain antibodies, can also have the potential to specifically inhibit membrane proteins. Therefore, we expect the development of more effective drugs and treatments targeting P2X7R.

CONCLUSION AND PROSPECTS

This article systematically analyzed and elucidated the association between P2X7R and OA. The most typical manifestation of OA is cartilage degradation. As the only cellular component of cartilage, chondrocytes are in a stable state and balance is crucial. The ECM degradation of chondrocytes and the release of inflammatory factors are important events leading to cartilage degradation. Inflammation is a direct manifestation of OA. To explore whether P2X7, as a key switch of inflammation, is involved in the occurrence and development of OA, we considered the network (**Figure 1**) of interaction from the perspectives of inflammation,

apoptosis, pyroptosis, and autophagy, and presented new OA prevention and treatment strategies.

Currently, there is no treatment method that can completely prevent the occurrence and development of OA. Delaying and reducing the death of chondrocytes to prevent the degradation of the cartilage matrix could be a potential therapeutic focus. As various factors affect chondrocyte cell death progression, including the degree of cartilage degradation, pro-inflammatory cytokines, and ATP availability, we propose the therapeutic focus to begin with the recognition of ATP as the first step in activating inflammation to narrow our approach to anti-inflammatory designs. Caspase-knockout studies have found that cells require both ATP energy and caspases to transform pyroptosis into apoptosis, thereby moving toward programmed death, and away from necrosis (Zeiss, 2003). zVAD-fmk is often used as a caspase inhibitor in OA research (Hwang and Kim, 2015), which can significantly reduce chondrocyte apoptosis and cartilage degradation (D'Lima et al., 2006). Moreover, when these factors are managed, mitochondrial integrity remains intact, reducing oxidative stress levels. Retaining a positive antioxidant balance exerts anti-inflammatory and anti-apoptotic effects. Oxidative stress can further be balanced by promoting autophagy, thus promoting mitochondrial housekeeping. However, autophagy can be a double-edged sword, and needs careful consideration when promoted. Excessive autophagy can trigger cell apoptosis, and the rapid loss of chondrocytes may worsen OA (Shapiro et al., 2014). Nevertheless, the mainstream view remains that autophagy stimulation in the early stages of OA can protect chondrocytes.

Treatment strategies should also focus on the role of P2X7R. Soon after it was cloned, the P2X7R protein received widespread attention as a key switch for inflammation with great therapeutic potential. For some chronic inflammatory diseases, small molecule (drug-like) inhibitors targeting P2X7R have been used in phase I and II clinical studies (Gunosewoyo and Kassiou, 2010; Sluyter and Stokes, 2011; Park and Kim, 2017). To date, more than 30 clinical studies in this regard have been conducted. Although the safety of inhibitors has been satisfactory, the clinical efficacy has been disappointing. In knee OA, rheumatoid arthritis, and chronic obstructive pulmonary disease, the efficacy is poor, while in Crohn's disease fairly positive (Arulkumaran et al., 2011; Keystone et al., 2012; Stock et al., 2012; Eser et al., 2015). Biopharmaceuticals may present a new way to replace small drug-like compounds. Antibodies against non-functional variants of human P2X7R have been used to treat cancer. The highly purified goat IgG can effectively reduce pathological changes in basal cell carcinoma size (Gilbert et al., 2017). In addition, nanobodies (e.g., 13A7 nanobody, single-domain antibody fragments elicited in camelids) that can bind to human or mouse P2X7R with high affinity, after inoculation in mice, effectively relieve the symptoms of experimental allergic contact dermatitis and glomerulonephritis. Dano1 nano antibody is selective for human P2X7R and can effectively reduce the level of IL-1β in the blood after endotoxin treatment (Danquah et al., 2016). Therefore, in the case of poor efficacy of anti-P2X7 receptor active drugs, biologics targeting P2X7R indicate a new direction for future research.

In conclusion, there remains a need for more specific OA therapies to be developed. P2X7R of the purinoceptor family, is closely related to inflammation and a promising drug target for OA. However, research into P2X7R and its role in the pathogenesis of OA requires further investigation. For the benefit of patients and scientific progress, we believe that these expectations will be realized in the near future.

AUTHOR CONTRIBUTIONS

ZL performed the literature review, drafted the manuscript, and prepared the figure. ZH and LB edited and revised the manuscript. All authors contributed to the article and approved the submitted version.

FUNDING

This work was supported by the National Natural Science Foundation of China (Grant Nos. 81772420, 81272050, and 31900847); China Postdoctoral Fund (2019M66169); and Liaoning Provincial Doctor Start-up Fund (2019JH3/10100299).

ACKNOWLEDGMENTS

We thank the lab affiliated to China Medical University for core support.

REFERENCES

Aguirre, A., Shoji, K. F., Saez, J. C., Henriquez, M., and Quest, A. F. (2013). FasL-triggered death of Jurkat cells requires caspase 8-induced, ATP-dependent cross-talk between Fas and the purinergic receptor P2X(7). *J. Cell. Physiol.* 228, 485–493. doi: 10.1002/jcp.24159

Aigner, T., Fundel, K., Saas, J., Gebhard, P. M., Haag, J., Weiss, T., et al. (2006). Large-scale gene expression profiling reveals major pathogenetic pathways of cartilage degeneration in osteoarthritis. *Arthritis Rheum.* 54, 3533–3544. doi: 10.1002/art.22174

Almonte-Becerril, M., Navarro-Garcia, F., Gonzalez-Robles, A., Vega-Lopez, M. A., Lavalle, C., and Kouri, J. B. (2010). Cell death of chondrocytes is a combination between apoptosis and autophagy during the pathogenesis of Osteoarthritis within an experimental model. *Apoptosis* 15, 631–638. doi: 10.1007/s10495-010-0458-z

Amoroso, F., Falzoni, S., Adinolfi, E., Ferrari, D., and Di Virgilio, F. (2012). The P2X7 receptor is a key modulator of aerobic glycolysis. *Cell Death Dis.* 3:e370. doi: 10.1038/cddis.2012.105

Archer, C. W., and Francis-West, P. (2003). The chondrocyte. *Int. J. Biochem. Cell Biol.* 35, 401–404.

Arulkumaran, N., Unwin, R. J., and Tam, F. W. (2011). A potential therapeutic role for P2X7 receptor (P2X7R) antagonists in the treatment of inflammatory diseases. *Expert Opin. Investig. Drugs* 20, 897–915. doi: 10.1517/13543784.2011.578068

Bai, Z., Liu, W., He, D., Wang, Y., Yi, W., Luo, C., et al. (2020). Protective effects of autophagy and NFE2L2 on reactive oxygen species-induced pyroptosis of

human nucleus pulposus cells. *Aging* 12, 7534–7548. doi: 10.18632/aging.103109

Bao, L., Locovei, S., and Dahl, G. (2004). Pannexin membrane channels are mechanosensitive conduits for ATP. *FEBS Lett.* 572, 65–68. doi: 10.1016/j.febslet.2004.07.009

Bao, Q., and Shi, Y. (2007). Apoptosome: a platform for the activation of initiator caspases. *Cell Death Differ.* 14, 56–65. doi: 10.1038/sj.cdd.4402028

Barbera-Cremades, M., Baroja-Mazo, A., Gomez, A. I., Machado, F., Di Virgilio, F., and Pelegrin, P. (2012). P2X7 receptor-stimulation causes fever via PGE2 and IL-1beta release. *FASEB J.* 26, 2951–2962. doi: 10.1096/fj.12-205765

Barbera-Cremades, M., Baroja-Mazo, A., and Pelegrin, P. (2016). Purinergic signaling during macrophage differentiation results in M2 alternative activated macrophages. *J. Leukoc. Biol.* 99, 289–299. doi: 10.1189/jlb.1a0514-267rr

Bartlett, R., Stokes, L., and Sluyter, R. (2014). The P2X7 receptor channel: recent developments and the use of P2X7 antagonists in models of disease. *Pharmacol. Rev.* 66, 638–675. doi: 10.1124/pr.113.008003

Beecher, B. R., Martin, J. A., Pedersen, D. R., Heiner, A. D., and Buckwalter, J. A. (2007). Antioxidants block cyclic loading induced chondrocyte death. *Iowa Orthop. J.* 27, 1–8.

Bian, S., Sun, X., Bai, A., Zhang, C., Li, L., Enjyoji, K., et al. (2013). P2X7 integrates PI3K/AKT and AMPK-PRAS40-mTOR signaling pathways to mediate tumor cell death. *PLoS One* 8:e60184. doi: 10.1371/journal.pone.0060184

Bianco, F., Pravettoni, E., Colombo, A., Schenk, U., Moller, T., Matteoli, M., et al. (2005). Astrocyte-derived ATP induces vesicle shedding and IL-1 beta release from microglia. *J. Immunol.* 174, 7268–7277. doi: 10.4049/jimmunol.174.11.7268

Bidula, S., Dhuna, K., Helliwell, R., and Stokes, L. (2019). Positive allosteric modulation of P2X7 promotes apoptotic cell death over lytic cell death responses in macrophages. *Cell Death Dis.* 10:882.

Bijlsma, J. W. J., Berenbaum, F., and Lafeber, F. P. J. G. (2011). Osteoarthritis: an update with relevance for clinical practice. *Lancet* 377, 2115–2126. doi: 10.1016/s0140-6736(11)60243-2

Blanco, F. J., Guitian, R., Vazquez-Martul, E., de Toro, F. J., and Galdo, F. (1998). Osteoarthritis chondrocytes die by apoptosis. A possible pathway for osteoarthritis pathology. *Arthritis Rheum.* 41, 284–289. doi: 10.1002/1529-0131(199802)41:2<284::aid-art12>3.0.co;2-t

Bobinac, D., Spanjol, J., Zoricic, S., and Maric, I. (2003). Changes in articular cartilage and subchondral bone histomorphometry in osteoarthritic knee joints in humans. *Bone* 32, 284–290. doi: 10.1016/s8756-3282(02)00982-1

Bohensky, J., Leshinsky, S., Srinivas, V., and Shapiro, I. M. (2010). Chondrocyte autophagy is stimulated by HIF-1 dependent AMPK activation and mTOR suppression. *Pediatr. Nephrol.* 25, 633–642. doi: 10.1007/s00467-009-1310-y

Bohensky, J., Shapiro, I. M., Leshinsky, S., Terkhorn, S. P., Adams, C. S., and Srinivas, V. (2007). HIF-1 regulation of chondrocyte apoptosis: induction of the autophagic pathway. *Autophagy* 3, 207–214. doi: 10.4161/auto.3708

Borges da Silva, H., Beura, L. K., Wang, H., Hanse, E. A., Gore, R., Scott, M. C., et al. (2018). The purinergic receptor P2RX7 directs metabolic fitness of long-lived memory CD8(+) T cells. *Nature* 559, 264–268. doi: 10.1038/s41586-018-0282-0

Bortner, C. D., Hughes, F. M. Jr., and Cidlowski, J. A. (1997). A primary role for K+ and Na+ efflux in the activation of apoptosis. *J. Biol. Chem.* 272, 32436–32442. doi: 10.1074/jbc.272.51.32436

Bougault, C., Gosset, M., Houard, X., Salvat, C., Godmann, L., Pap, T., et al. (2012). Stress-induced cartilage degradation does not depend on the NLRP3 inflammasome in human osteoarthritis and mouse models. *Arthritis Rheum.* 64, 3972–3981. doi: 10.1002/art.34678

Burnstock, G. (2006). Purinergic signalling. *Br. J. Pharmacol.* 147(Suppl. 1), S172–S181.

Byrne, B. G., Dubuisson, J. F., Joshi, A. D., Persson, J. J., and Swanson, M. S. (2013). Inflammasome components coordinate autophagy and pyroptosis as macrophage responses to infection. *mBio* 4:e00620-12.

Caramés, B., Olmer, M., Kiosses, W. B., and Lotz, M. K. (2015). The relationship of autophagy defects to cartilage damage during joint aging in a mouse model. *Arthritis Rheum.* 67, 1568–1576. doi: 10.1002/art.39073

Carames, B., Taniguchi, N., Otsuki, S., Blanco, F. J., and Lotz, M. (2010). Autophagy is a protective mechanism in normal cartilage, and its aging-related loss is linked with cell death and osteoarthritis. *Arthritis Rheum.* 62, 791–801. doi: 10.1002/art.27305

Carr, A. J., Robertsson, O., Graves, S., Price, A. J., Arden, N. K., Judge, A., et al. (2012). Knee replacement. *Lancet* 379, 1331–1340.

Chang, J., Wang, W., Zhang, H., Hu, Y., Wang, M., and Yin, Z. (2013). The dual role of autophagy in chondrocyte responses in the pathogenesis of articular cartilage degeneration in osteoarthritis. *Int. J. Mol. Med.* 32, 1311–1318. doi: 10.3892/ijmm.2013.1520

Chang, Y. P., Ka, S. M., Hsu, W. H., Chen, A., Chao, L. K., Lin, C. C., et al. (2015). Resveratrol inhibits NLRP3 inflammasome activation by preserving mitochondrial integrity and augmenting autophagy. *J. Cell. Physiol.* 230, 1567–1579. doi: 10.1002/jcp.24903

Chen, C. T., Burton-Wurster, N., Borden, C., Hueffer, K., Bloom, S. E., and Lust, G. (2001). Chondrocyte necrosis and apoptosis in impact damaged articular cartilage. *J. Orthop. Res.* 19, 703–711. doi: 10.1016/s0736-0266(00)00066-8

Chen, Q., Yue, F., Li, W., Zou, J., Xu, T., Huang, C., et al. (2015). Potassium bisperoxo(1,10-phenanthroline)oxovanadate (bpV(phen)) induces apoptosis and pyroptosis and disrupts the P62-HDAC6 protein interaction to suppress the acetylated microtubule-dependent degradation of autophagosomes. *J. Biol. Chem.* 290, 26051–26058. doi: 10.1074/jbc.m115.653568

Chen, X., Li, H., Wang, K., Liang, X., Wang, W., Hu, X., et al. (2019). Aerobic exercise ameliorates myocardial inflammation, fibrosis and apoptosis in high-fat-diet rats by inhibiting P2X7 purinergic receptors. *Front. Physiol.* 10:1286. doi: 10.3389/fphys.2019.01286

Cheng, S.-B., Nakashima, A., Huber, W. J., Davis, S., Banerjee, S., Huang, Z., et al. (2019). Pyroptosis is a critical inflammatory pathway in the placenta from early onset preeclampsia and in human trophoblasts exposed to hypoxia and endoplasmic reticulum stressors. *Cell Death Dis.* 10:927.

Chevalier, X., Goupille, P., Beaulieu, A. D., Burch, F. X., Bensen, W. G., Conrozier, T., et al. (2009). Intraarticular injection of anakinra in osteoarthritis of the knee: a multicenter, randomized, double-blind, placebo-controlled study. *Arthritis Rheum.* 61, 344–352. doi: 10.1002/art.24096

Claude-Taupin, A., Bissa, B., Jia, J., Gu, Y., and Deretic, V. (2018). Role of autophagy in IL-1beta export and release from cells. *Semin. Cell Dev. Biol.* 83, 36–41. doi: 10.1016/j.semcdb.2018.03.012

Clavijo-Cornejo, D., Martinez-Flores, K., Silva-Luna, K., Martinez-Nava, G. A., Fernandez-Torres, J., Zamudio-Cuevas, Y., et al. (2016). The overexpression of NALP3 inflammasome in knee osteoarthritis is associated with synovial membrane prolidase and NADPH oxidase 2. *Oxid. Med. Cell. Longev.* 2016:1472567.

Cohen, S. B., Proudman, S., Kivitz, A. J., Burch, F. X., Donohue, J. P., Burstein, D., et al. (2011). A randomized, double-blind study of AMG 108 (a fully human monoclonal antibody to IL-1R1) in patients with osteoarthritis of the knee. *Arthritis Res. Ther.* 13:R125.

Coimbra, I. B., Jimenez, S. A., Hawkins, D. F., Piera-Velazquez, S., and Stokes, D. G. (2004). Hypoxia inducible factor-1 alpha expression in human normal and osteoarthritic chondrocytes. *Osteoarthritis Cartilage* 12, 336–345.

Colegio, O. R., Chu, N. Q., Szabo, A. L., Chu, T., Rhebergen, A. M., Jairam, V., et al. (2014). Functional polarization of tumour-associated macrophages by tumour-derived lactic acid. *Nature* 513, 559–563. doi: 10.1038/nature13490

Coll, R. C., Robertson, A. A., Chae, J. J., Higgins, S. C., Munoz-Planillo, R., Inserra, M. C., et al. (2015). A small-molecule inhibitor of the NLRP3 inflammasome for the treatment of inflammatory diseases. *Nat. Med.* 21, 248–255.

Comassi, M., Santini, E., Rossi, C., Vitolo, E., Seghieri, M., Tocchini, L., et al. (2017). The level of physical training modulates cytokine levels through P2X7 receptor in healthy subjects. *Eur. J. Clin. Invest.* 48:e12880. doi: 10.1111/eci.12880

Cong, L., Gao, Z., Zheng, Y., Ye, T., Wang, Z., Wang, P., et al. (2020). Electrical stimulation inhibits Val-boroPro-induced pyroptosis in THP-1 macrophages via sirtuin3 activation to promote autophagy and inhibit ROS generation. *Aging* 12, 6415–6435. doi: 10.18632/aging.103038

Coppe, J. P., Desprez, P. Y., Krtolica, A., and Campisi, J. (2010). The senescence-associated secretory phenotype: the dark side of tumor suppression. *Annu. Rev. Pathol.* 5, 99–118. doi: 10.1146/annurev-pathol-121808-102144

Cui, J., Zhang, M., Zhang, Y. Q., and Xu, Z. H. (2007). JNK pathway: diseases and therapeutic potential. *Acta Pharmacol. Sin.* 28, 601–608. doi: 10.1111/j.1745-7254.2007.00579.x

da Costa, B. R., Nuesch, E., Reichenbach, S., Juni, P., and Rutjes, A. W. (2012). Doxycycline for osteoarthritis of the knee or hip. *Cochrane Database Syst. Rev.* 11:CD007323.

Danquah, W., Meyer-Schwesinger, C., Rissiek, B., Pinto, C., Serracant-Prat, A., Amadi, M., et al. (2016). Nanobodies that block gating of the P2X7 ion channel ameliorate inflammation. *Sci. Transl. Med.* 8:366ra162. doi: 10.1126/scitranslmed.aaf8463

de Gassart, A., and Martinon, F. (2015). Pyroptosis: caspase-11 unlocks the gates of death. *Immunity* 43, 835–837. doi: 10.1016/j.immuni.2015.10.024

Delarasse, C., Gonnord, P., Galante, M., Auger, R., Daniel, H., Motta, I., et al. (2009). Neural progenitor cell death is induced by extracellular ATP via ligation of P2X7 receptor. *J. Neurochem.* 109, 846–857. doi: 10.1111/j.1471-4159.2009.06008.x

Denecker, G., Vercammen, D., Declercq, W., and Vandenabeele, P. (2001). Apoptotic and necrotic cell death induced by death domain receptors. *Cell. Mol. Life Sci.* 58, 356–370. doi: 10.1007/pl00000863

Deretic, V., Saitoh, T., and Akira, S. (2013). Autophagy in infection, inflammation and immunity. *Nat. Rev. Immunol.* 13, 722–737.

Di Virgilio, F. (2013). The therapeutic potential of modifying inflammasomes and NOD-like receptors. *Pharmacol. Rev.* 65, 872–905. doi: 10.1124/pr.112.006171

Di Virgilio, F., Dal Ben, D., Sarti, A. C., Giuliani, A. L., and Falzoni, S. (2017). The P2X7 receptor in infection and inflammation. *Immunity* 47, 15–31. doi: 10.1016/j.immuni.2017.06.020

Dinarello, C. A. (2002). The IL-1 family and inflammatory diseases. *Clin. Exp. Rheumatol.* 20(5 Suppl. 27), S1–S13.

Dinarello, C. A., Simon, A., and van der Meer, J. W. M. (2012). Treating inflammation by blocking interleukin-1 in a broad spectrum of diseases. *Nat. Rev. Drug Discov.* 11, 633–652. doi: 10.1038/nrd3800

Distel, E., Cadoudal, T., Durant, S., Poignard, A., Chevalier, X., and Benelli, C. (2009). The infrapatellar fat pad in knee osteoarthritis: an important source of interleukin-6 and its soluble receptor. *Arthritis Rheum.* 60, 3374–3377. doi: 10.1002/art.24881

D'Lima, D., Hermida, J., Hashimoto, S., Colwell, C., and Lotz, M. (2006). Caspase inhibitors reduce severity of cartilage lesions in experimental osteoarthritis. *Arthritis Rheum.* 54, 1814–1821. doi: 10.1002/art.21874

D'Lima, D. D., Hashimoto, S., Chen, P. C., Colwell, C. W., and Lotz, M. K. (2001). Human chondrocyte apoptosis in response to mechanical injury. *Osteoarthritis Cartilage* 9, 712–719. doi: 10.1053/joca.2001.0468

Donnelly-Roberts, D. L., Namovic, M. T., Faltynek, C. R., and Jarvis, M. F. (2004). Mitogen-activated protein kinase and caspase signaling pathways are required for P2X7 receptor (P2X7R)-induced pore formation in human THP-1 cells. *J. Pharmacol. Exp. Ther.* 308, 1053–1061. doi: 10.1124/jpet.103.059600

Draganov, D., Gopalakrishna-Pillai, S., Chen, Y. R., Zuckerman, N., Moeller, S., Wang, C., et al. (2015). Modulation of P2X4/P2X7/Pannexin-1 sensitivity to extracellular ATP via Ivermectin induces a non-apoptotic and inflammatory form of cancer cell death. *Sci. Rep.* 5:16222.

Dubyak, G. R. (2012). P2X7 receptor regulation of non-classical secretion from immune effector cells. *Cell. Microbiol.* 14, 1697–1706. doi: 10.1111/cmi.12001

Działo, J., Tokarz-Deptuła, B., and Deptuła, W. (2013). Excitotoxicity and Wallerian degeneration as a processes related to cell death in nervous system. *Arch. Ital. Biol.* 151, 67–75.

Elmore, S. (2007). Apoptosis: a review of programmed cell death. *Toxicol. Pathol.* 35, 495–516.

Eser, A., Colombel, J. F., Rutgeerts, P., Vermeire, S., Vogelsang, H., Braddock, M., et al. (2015). Safety and efficacy of an oral inhibitor of the purinergic receptor P2X7 in adult patients with moderately to severely active crohn's disease: a randomized placebo-controlled, double-blind, phase IIa study. *Inflamm. Bowel Dis.* 21, 2247–2253.

Fan, J., Yang, X., Li, J., Shu, Z., Dai, J., Liu, X., et al. (2017). Spermidine coupled with exercise rescues skeletal muscle atrophy from D-gal-induced aging rats through enhanced autophagy and reduced apoptosis via AMPK-FOXO3a signal pathway. *Oncotarget* 8, 17475–17490. doi: 10.18632/oncotarget.15728

Fan, Z. D., Zhang, Y. Y., Guo, Y. H., Huang, N., Ma, H. H., Huang, H., et al. (2016). Involvement of P2X7 receptor signaling on regulating the differentiation of Th17 cells and type II collagen-induced arthritis in mice. *Sci. Rep.* 6:35804.

Felson, D. T., Zhang, Y., Anthony, J. M., Naimark, A., and Anderson, J. J. (1992). Weight loss reduces the risk for symptomatic knee osteoarthritis in women. The Framingham Study. *Ann. Intern. Med.* 116, 535–539. doi: 10.7326/0003-4819-116-7-535

Ferrari, D., Pizzirani, C., Adinolfi, E., Lemoli, R. M., Curti, A., Idzko, M., et al. (2006). The P2X7 receptor: a key player in IL-1 processing and release. *J. Immunol.* 176, 3877–3883.

Festjens, N., Vanden Berghe, T., and Vandenabeele, P. (2006). Necrosis, a well-orchestrated form of cell demise: signalling cascades, important mediators and concomitant immune response. *Biochim. Biophys. Acta* 1757, 1371–1387. doi: 10.1016/j.bbabio.2006.06.014

Forsyth, C. B., Cole, A., Murphy, G., Bienias, J. L., Im, H.-J., and Loeser, R. F. Jr. (2005). Increased matrix metalloproteinase-13 production with aging by human articular chondrocytes in response to catabolic stimuli. *J. Gerontol. A Biol. Sci. Med. Sci.* 60, 1118–1124. doi: 10.1093/gerona/60.9.1118

Fradejas, N., Pastor, M. D., Burgos, M., Beyaert, R., Tranque, P., and Calvo, S. (2010). Caspase-11 mediates ischemia-induced astrocyte death: involvement of endoplasmic reticulum stress and C/EBP homologous protein. *J. Neurosci. Res.* 88, 1094–1105.

Franceschini, A., Capece, M., Chiozzi, P., Falzoni, S., Sanz, J. M., Sarti, A. C., et al. (2015). The P2X7 receptor directly interacts with the NLRP3 inflammasome scaffold protein. *FASEB J.* 29, 2450–2461. doi: 10.1096/fj.14-268714

Fuentes-Prior, P., and Salvesen, G. (2004). The protein structures that shape caspase activity, specificity, activation and inhibition. *Biochem. J.* 384(Pt 2), 201–232. doi: 10.1042/bj20041142

Ganley, I. G., Lam du, H., Wang, J., Ding, X., Chen, S., and Jiang, X. (2009). ULK1.ATG13.FIP200 complex mediates mTOR signaling and is essential for autophagy. *J. Biol. Chem.* 284, 12297–12305. doi: 10.1074/jbc.m900573200

Garber, K. (2012). Autophagy. Explaining exercise. *Science* 335:281. doi: 10.1126/science.335.6066.281

Garcia, D., and Shaw, R. J. (2017). AMPK: mechanisms of cellular energy sensing and restoration of metabolic balance. *Mol. Cell* 66, 789–800. doi: 10.1016/j.molcel.2017.05.032

García-Arnandis, I., Guillén, M. I., Gomar, F., Pelletier, J.-P., Martel Pelletier, J., and Alcaraz, M. J. (2010). High mobility group box 1 potentiates the pro-inflammatory effects of interleukin-1 b in osteoarthritic synoviocytes. *Arthritis Res. Ther.* 12:R165.

Gilbert, S. M., Gidley Baird, A., Glazer, S., Barden, J. A., Glazer, A., Teh, L. C., et al. (2017). A phase I clinical trial demonstrates that nfP2X7 -targeted antibodies provide a novel, safe and tolerable topical therapy for basal cell carcinoma. *Br. J. Dermatol.* 177, 117–124. doi: 10.1111/bjd.15364

Gomez, R., Conde, J., Scotece, M., Gomez-Reino, J. J., Lago, F., and Gualillo, O. (2011). What's new in our understanding of the role of adipokines in rheumatic diseases? *Nat. Rev. Rheumatol.* 7, 528–536. doi: 10.1038/nrrheum.2011.107

Green, D. R. (2003). Overview: apoptotic signaling pathways in the immune system. *Immunol. Rev.* 193, 5–9. doi: 10.1034/j.1600-065x.2003.00045.x

Grishko, V. I., Ho, R., Wilson, G. L., and Pearsall, A. W. (2009). Diminished mitochondrial DNA integrity and repair capacity in OA chondrocytes. *Osteoarthritis Cartilage* 17, 107–113. doi: 10.1016/j.joca.2008.05.009

Guarino, M., Kumar, P., Felser, A., Terracciano, L. M., Guixe-Muntet, S., Humar, B., et al. (2020). Exercise attenuates the transition from fatty liver to steatohepatitis and reduces tumor formation in mice. *Cancers (Basel)* 12:1407. doi: 10.3390/cancers12061407

Gudbergsen, H., Boesen, M., Lohmander, L. S., Christensen, R., Henriksen, M., Bartels, E. M., et al. (2012). Weight loss is effective for symptomatic relief in obese subjects with knee osteoarthritis independently of joint damage severity assessed by high-field MRI and radiography. *Osteoarthritis Cartilage* 20, 495–502. doi: 10.1016/j.joca.2012.02.639

Gudipaty, S. A., Conner, C. M., Rosenblatt, J., and Montell, D. J. (2018). Unconventional ways to live and die: cell death and survival in development, homeostasis, and disease. *Annu. Rev. Cell Dev. Biol.* 34, 311–332. doi: 10.1146/annurev-cellbio-100616-060748

Guha, S., Baltazar, G. C., Coffey, E. E., Tu, L. A., Lim, J. C., Beckel, J. M., et al. (2013). Lysosomal alkalinization, lipid oxidation, and reduced phagosome clearance triggered by activation of the P2X7 receptor. *FASEB J.* 27, 4500–4509. doi: 10.1096/fj.13-236166

Guilak, F. (2011). Biomechanical factors in osteoarthritis. *Best Pract. Res. Clin. Rheumatol.* 25, 815–823. doi: 10.1016/j.berh.2011.11.013

Gunosewoyo, H., and Kassiou, M. (2010). P2X purinergic receptor ligands: recently patented compounds. *Expert Opin. Ther. Pat.* 20, 625–646. doi: 10.1517/13543771003702424

Guo, H., Callaway, J. B., and Ting, J. P. (2015). Inflammasomes: mechanism of action, role in disease, and therapeutics. *Nat. Med.* 21, 677–687. doi: 10.1038/nm.3893

Haseeb, A., and Haqqi, T. M. (2013). Immunopathogenesis of osteoarthritis. *Clin. Immunol.* 146, 185–196. doi: 10.1016/j.clim.2012.12.011

Hashimoto, S., Ochs, R. L., Komiya, S., and Lotz, M. (1998). Linkage of chondrocyte apoptosis and cartilage degradation in human osteoarthritis. *Arthritis Rheum.* 41, 1632–1638. doi: 10.1002/1529-0131(199809)41:9<1632::aid-art14>3.0.co;2-a

He, Y., Hara, H., and Nunez, G. (2016). Mechanism and regulation of NLRP3 inflammasome activation. *Trends Biochem. Sci.* 41, 1012–1021. doi: 10.1016/j.tibs.2016.09.002

Henrotin, Y., Deby-Dupont, G., Deby, C., De Bruyn, M., Lamy, M., and Franchimont, P. (1993). Production of active oxygen species by isolated human chondrocytes. *Br. J. Rheumatol.* 32, 562–567. doi: 10.1093/rheumatology/32.7.562

Henrotin, Y., Labasse, A., Zheng, S. X., Galais, P., Tsouderos, Y., Crielaard, J. M., et al. (2001). Strontium ranelate increases cartilage matrix formation. *J. Bone Min. Res.* 16, 299–308. doi: 10.1359/jbmr.2001.16.2.299

Henrotin, Y., and Lambert, C. (2013). Chondroitin and glucosamine in the management of osteoarthritis: an update. *Curr. Rheumatol. Rep.* 15:361.

Henrotin, Y. E., Bruckner, P., and Pujol, J. P. L. (2003). The role of reactive oxygen species in homeostasis and degradation of cartilage. *Osteoarthritis Cartilage* 11, 747–755. doi: 10.1016/s1063-4584(03)00150-x

Heraud, F., Héraud, A., and Harmand, M. F. (2000). Apoptosis in normal and osteoarthritic human articular cartilage. *Ann. Rheum. Dis.* 59, 959–965. doi: 10.1136/ard.59.12.959

Hwang, H. S., and Kim, H. A. (2015). Chondrocyte apoptosis in the pathogenesis of osteoarthritis. *Int. J. Mol. Sci.* 16, 26035–26054. doi: 10.3390/ijms161125943

Jeon, S. M. (2016). Regulation and function of AMPK in physiology and diseases. *Exp. Mol. Med.* 48:e245. doi: 10.1038/emm.2016.81

Jiang, C., Jiang, L., Li, Q., Liu, X., Zhang, T., Dong, L., et al. (2018). Acrolein induces NLRP3 inflammasome-mediated pyroptosis and suppresses migration via ROS-dependent autophagy in vascular endothelial cells. *Toxicology* 410, 26–40. doi: 10.1016/j.tox.2018.09.002

Jiang, L. H., Baldwin, J. M., Roger, S., and Baldwin, S. A. (2013). Insights into the molecular mechanisms underlying mammalian P2X7 receptor functions and contributions in diseases, revealed by structural modeling and single nucleotide polymorphisms. *Front. Pharmacol.* 4:55. doi: 10.3389/fphar.2013.00055

Jin, C., Frayssinet, P., Pelker, R., Cwirka, D., Hu, B., Vignery, A., et al. (2011). NLRP3 inflammasome plays a critical role in the pathogenesis of hydroxyapatite-associated arthropathy. *Proc. Natl. Acad. Sci. U.S.A.* 108, 14867–14872. doi: 10.1073/pnas.1111101108

Johnson, K., Zhu, S., Tremblay, M. S., Payette, J. N., Wang, J., Bouchez, L. C., et al. (2012). A stem cell-based approach to cartilage repair. *Science* 336, 717–721.

Kaczmarek, A., Vandenabeele, P., and Krysko, D. V. (2013). Necroptosis: the release of damage-associated molecular patterns and its physiological relevance. *Immunity* 38, 209–223. doi: 10.1016/j.immuni.2013.02.003

Kahlenberg, J. M., and Dubyak, G. R. (2004). Mechanisms of caspase-1 activation by P2X 7 receptor-mediated K + release. *Am. J. Physiol. Cell Physiol.* 286, C1100–C1108.

Karasawa, A., and Kawate, T. (2016). Structural basis for subtype-specific inhibition of the P2X7 receptor. *elife* 5:e22153.

Karki, P., Seong, C., Kim, J. E., Hur, K., Shin, S. Y., Lee, J. S., et al. (2007). Intracellular K(+) inhibits apoptosis by suppressing the Apaf-1 apoptosome formation and subsequent downstream pathways but not cytochrome c release. *Cell Death Differ.* 14, 2068–2075. doi: 10.1038/sj.cdd.4402221

Karmakar, M., Minns, M., Greenberg, E. N., Diaz-Aponte, J., Pestonjamasp, K., Johnson, J. L., et al. (2020). N-GSDMD trafficking to neutrophil organelles facilitates IL-1beta release independently of plasma membrane pores and pyroptosis. *Nat. Commun.* 11:2212.

Kerr, J. F., Wyllie, A. H., and Currie, A. R. (1972). Apoptosis: a basic biological phenomenon with wide-ranging implications in tissue kinetics. *Br. J. Cancer* 26, 239–257. doi: 10.1038/bjc.1972.33

Keystone, E. C., Wang, M. M., Layton, M., Hollis, S., McInnes, I. B., and Team, D. C. S. (2012). Clinical evaluation of the efficacy of the P2X7 purinergic receptor antagonist AZD9056 on the signs and symptoms of rheumatoid arthritis in patients with active disease despite treatment with methotrexate or sulphasalazine. *Ann. Rheum. Dis.* 71, 1630–1635.

Khakh, B. S., and North, R. A. (2006). P2X receptors as cell-surface ATP sensors in health and disease. *Nature* 442, 527–532. doi: 10.1038/nature04886

Kim, H. A., Cho, M. L., Choi, H. Y., Yoon, C. S., Jhun, J. Y., Oh, H. J., et al. (2006). The catabolic pathway mediated by Toll-like receptors in human osteoarthritic chondrocytes. *Arthritis Rheum.* 54, 2152–2163. doi: 10.1002/art.21951

Kim, N.-G., Lee, H., Son, E., Kwon, O.-Y., Park, J.-Y., Park, J.-H., et al. (2003). Hypoxic induction of caspase-11/caspase-1/interleukin-1β in brain microglia. *Mol. Brain Res.* 114, 107–114. doi: 10.1016/s0169-328x(03)00135-9

Kong, D., Zheng, T., Zhang, M., Wang, D., Du, S., Li, X., et al. (2013). Static mechanical stress induces apoptosis in rat endplate chondrocytes through MAPK and mitochondria-dependent caspase activation signaling pathways. *PLoS One* 8:e69403. doi: 10.1371/journal.pone.0069403

Kroemer, G., and Reed, J. C. (2000). Mitochondrial control of cell death. *Nat. Med.* 6, 513–519.

Kulbe, J. R., Mulcahy Levy, J. M., Coultrap, S. J., Thorburn, A., and Bayer, K. U. (2014). Excitotoxic glutamate insults block autophagic flux in hippocampal neurons. *Brain Res.* 1542, 12–19. doi: 10.1016/j.brainres.2013.10.032

Kurosaka, K., Takahashi, M., Watanabe, N., and Kobayashi, Y. (2003). Silent cleanup of very early apoptotic cells by macrophages. *J. Immunol.* 171, 4672–4679. doi: 10.4049/jimmunol.171.9.4672

Kyrkanides, S., Tallents, R. H., Miller, J. N., Olschowka, M. E., Johnson, R., Yang, M., et al. (2011). Osteoarthritis accelerates and exacerbates Alzheimer's disease pathology in mice. *J. Neuroinflammation* 8:112. doi: 10.1186/1742-2094-8-112

Laker, R. C., Drake, J. C., Wilson, R. J., Lira, V. A., Lewellen, B. M., Ryall, K. A., et al. (2017). Ampk phosphorylation of Ulk1 is required for targeting of mitochondria to lysosomes in exercise-induced mitophagy. *Nat. Commun.* 8:548.

Latz, E., Xiao, T. S., and Stutz, A. (2013). Activation and regulation of the inflammasomes. *Nat. Rev. Immunol.* 13, 397–411. doi: 10.1038/nri3452

Lee, M. S., Kwon, H., Lee, E. Y., Kim, D. J., Park, J. H., Tesh, V. L., et al. (2016). Shiga toxins activate the NLRP3 inflammasome pathway to promote both production of the proinflammatory cytokine interleukin-1beta and apoptotic cell death. *Infect. Immun.* 84, 172–186. doi: 10.1128/iai.01095-15

Leist, M., Single, B., Castoldi, A. F., Kuhnle, S., and Nicotera, P. (1997). Intracellular adenosine triphosphate (ATP) concentration: a switch in the decision between apoptosis and necrosis. *J. Exp. Med.* 185, 1481–1486. doi: 10.1084/jem.185.8.1481

Li, J., and Dong, S. (2016). The signaling pathways involved in chondrocyte differentiation and hypertrophic differentiation. *Stem Cells Int.* 2016:2470351.

Li, M. Y., Zhu, X. L., Zhao, B. X., Shi, L., Wang, W., Hu, W., et al. (2019). Adrenomedullin alleviates the pyroptosis of Leydig cells by promoting autophagy via the ROS-AMPK-mTOR axis. *Cell Death Dis.* 10:489.

Licastro, F., Candore, G., Lio, D., Porcellini, E., Colonna-Romano, G., Franceschi, C., et al. (2005). Innate immunity and inflammation in ageing: a key for understanding age-related diseases. *Immun. Ageing.* 2:8.

Liu, H. T., and Pan, S. S. (2019). Late exercise preconditioning promotes autophagy against exhaustive exercise-induced myocardial injury through the activation of the AMPK-mTOR-ULK1 pathway. *Biomed. Res. Int.* 2019:5697380.

Liu, J. J., Li, Y., Yang, M. S., Chen, R., and Cen, C. Q. (2020). SP1-induced ZFAS1 aggravates sepsis-induced cardiac dysfunction via miR-590-3p/NLRP3-mediated autophagy and pyroptosis. *Arch. Biochem. Biophys.* 695:108611. doi: 10.1016/j.abb.2020.108611

Liu, X., Niu, Y., Yuan, H., Huang, J., and Fu, L. (2015). AMPK binds to Sestrins and mediates the effect of exercise to increase insulin-sensitivity through autophagy. *Metabolism* 64, 658–665. doi: 10.1016/j.metabol.2015.01.015

Liu, Y., Nguyen, P. T., Wang, X., Zhao, Y., Meacham, C. E., Zou, Z., et al. (2020). TLR9 and beclin 1 crosstalk regulates muscle AMPK activation in exercise. *Nature* 578, 605–609. doi: 10.1038/s41586-020-1992-7

Lo, Y. Y., Wong, J. M., and Cruz, T. F. (1996). Reactive oxygen species mediate cytokine activation of c-Jun NH2-terminal kinases. *J. Biol. Chem.* 271, 15703–15707. doi: 10.1074/jbc.271.26.15703

Lo Verso, F., Carnio, S., Vainshtein, A., and Sandri, M. (2014). Autophagy is not required to sustain exercise and PRKAA1/AMPK activity but is important to prevent mitochondrial damage during physical activity. *Autophagy* 10, 1883–1894. doi: 10.4161/auto.32154

Locovei, S., Scemes, E., Qiu, F., Spray, D. C., and Dahl, G. (2007). Pannexin1 is part of the pore forming unit of the P2X(7) receptor death complex. *FEBS Lett.* 581, 483–488. doi: 10.1016/j.febslet.2006.12.056

Loening, A. M., James, I. E., Levenston, M. E., Badger, A. M., Frank, E. H., Kurz, B., et al. (2000). Injurious mechanical compression of bovine articular cartilage induces chondrocyte apoptosis. *Arch. Biochem. Biophys.* 381, 205–212. doi: 10.1006/abbi.2000.1988

Loeser, R. F. (2011). Aging and osteoarthritis. *Curr. Opin. Rheumatol.* 23, 492–496.

Lopez de Figueroa, P., Lotz, M. K., Blanco, F. J., and Carames, B. (2015). Autophagy activation and protection from mitochondrial dysfunction in human chondrocytes. *Arthritis Rheumatol.* 67, 966–976. doi: 10.1002/art.39025

Lopez-Castejon, G., and Brough, D. (2011). Understanding the mechanism of IL-1beta secretion. *Cytokine Growth Factor Rev.* 22, 189–195. doi: 10.1016/j.cytogfr.2011.10.001

MacKenzie, A., Wilson, H. L., Kiss-Toth, E., Dower, S. K., North, R. A., and Surprenant, A. (2001). Rapid secretion of interleukin-1β by microvesicle shedding. *Immunity* 15, 825–835. doi: 10.1016/s1074-7613(01)00229-1

Man, G., and Mologhianu, G. (2014). Osteoarthritis pathogenesis: a complex process that involves the entire joint. *J. Med. Life* 7, 37–41.

Man, S., and Kanneganti, T. D. (2015). Regulation of inflammasome activation. *Immunol. Rev.* 265, 6–21.

Martin, J. A., and Buckwalter, J. A. (2006). Post-traumatic osteoarthritis: the role of stress induced chondrocyte damage. *Biorheology* 43, 517–521.

Martin-Rincon, M., Perez-Lopez, A., Morales-Alamo, D., Perez-Suarez, I., de Pablos-Velasco, P., Perez-Valera, M., et al. (2019). Exercise mitigates the loss of muscle mass by attenuating the activation of autophagy during severe energy deficit. *Nutrients* 11:2824. doi: 10.3390/nu11112824

Mascanfroni, I. D., Takenaka, M. C., Yeste, A., Patel, B., Wu, Y., Kenison, J. E., et al. (2015). Metabolic control of type 1 regulatory T cell differentiation by AHR and HIF1-alpha. *Nat. Med.* 21, 638–646. doi: 10.1038/nm.3868

Matute, C., Torre, I., Perez-Cerda, F., Perez-Samartin, A., Alberdi, E., Etxebarria, E., et al. (2007). P2X(7) receptor blockade prevents ATP excitotoxicity in oligodendrocytes and ameliorates experimental autoimmune encephalomyelitis. *J. Neurosci.* 27, 9525–9533. doi: 10.1523/jneurosci.0579-07.2007

McGilligan, V. E., Gregory-Ksander, M. S., Li, D., Moore, J. E., Hodges, R. R., Gilmore, M. S., et al. (2013). *Staphylococcus aureus* activates the NLRP3 inflammasome in human and rat conjunctival goblet cells. *PLoS One* 8:e74010. doi: 10.1371/journal.pone.0074010

Mehto, S., Jena, K. K., Nath, P., Chauhan, S., Kolapalli, S. P., Das, S. K., et al. (2019). The Crohn's disease risk factor irgm limits nlrp3 inflammasome activation by impeding its assembly and by mediating its selective autophagy. *Mol. Cell* 73, 429–445.e7.

Mizushima, N., and Komatsu, M. (2011). Autophagy: renovation of cells and tissues. *Cell* 147, 728–741. doi: 10.1016/j.cell.2011.10.026

Mueller, M. B., and Tuan, R. S. (2011). Anabolic/Catabolic balance in pathogenesis of osteoarthritis: identifying molecular targets. *PM R* 3(6 Suppl. 1), S3–S11.

Nicke, A. (2008). Homotrimeric complexes are the dominant assembly state of native P2X7 subunits. *Biochem. Biophys. Res. Commun.* 377, 803–808. doi: 10.1016/j.bbrc.2008.10.042

Nishida, K., Nakatani, T., Ohishi, A., Okuda, H., Higashi, Y., Matsuo, T., et al. (2012). Mitochondrial dysfunction is involved in P2X7 receptor-mediated neuronal cell death. *J. Neurochem.* 122, 1118–1128. doi: 10.1111/j.1471-4159.2012.07868.x

Nishida, Y., Knudson, C. B., and Knudson, W. (2004). Osteogenic Protein-1 inhibits matrix depletion in a hyaluronan hexasaccharide-induced model of osteoarthritis. *Osteoarthritis Cartilage* 12, 374–382. doi: 10.1016/j.joca.2004.01.008

North, R. A. (2002). Molecular physiology of P2X receptors. *Physiol. Rev.* 82, 1013–1067. doi: 10.1152/physrev.00015.2002

North, R. A., and Jarvis, M. F. (2013). P2X receptors as drug targets. *Mol. Pharmacol.* 83, 759–769. doi: 10.1124/mol.112.083758

Olee, T., Hashimoto, S., Quach, J., and Lotz, M. (1999). IL-18 is produced by articular chondrocytes and induces proinflammatory and catabolic responses. *J. Immunol.* 162, 1096–1100.

Orioli, E., Marchi, E. D., Giuliani, A. L., and Adinolfi, E. (2017). P2X7 receptor orchestrates multiple signalling pathways triggering inflammation, autophagy and metabolic/trophic responses. *Curr. Med. Chem.* 24, 2261–2275.

Palmer, A. J., Thomas, G. E., Pollard, T. C., Rombach, I., Taylor, A., Arden, N., et al. (2013). The feasibility of performing a randomised controlled trial for femoroacetabular impingement surgery. *Bone Joint Res.* 2, 33–40. doi: 10.1302/2046-3758.22.2000137

Pan, T., Shi, X., Chen, H., Chen, R., Wu, D., Lin, Z., et al. (2018). Geniposide suppresses interleukin-1beta-induced inflammation and apoptosis in rat chondrocytes via the PI3K/Akt/NF-kappaB signaling pathway. *Inflammation* 41, 390–399. doi: 10.1007/s10753-017-0694-2

Panenka, W., Jijon, H., Herx, L. M., Armstrong, J. N., Feighan, D., Wei, T., et al. (2001). P2X7-like receptor activation in astrocytes increases chemokine monocyte chemoattractant protein-1 expression via mitogen-activated protein kinase. *J. Neurosci.* 21, 7135–7142. doi: 10.1523/jneurosci.21-18-07135.2001

Papp, L., Vizi, E. S., and Sperlagh, B. (2007). P2X7 receptor mediated phosphorylation of p38MAP kinase in the hippocampus. *Biochem. Biophys. Res. Commun.* 355, 568–574. doi: 10.1016/j.bbrc.2007.02.014

Park, J. H., and Kim, Y. C. (2017). P2X7 receptor antagonists: a patent review (2010-2015). *Expert Opin. Ther. Pat.* 27, 257–267. doi: 10.1080/13543776.2017.1246538

Parzych, K. R., and Klionsky, D. J. (2014). An overview of autophagy: morphology, mechanism, and regulation. *Antioxid. Redox Signal.* 20, 460–473. doi: 10.1089/ars.2013.5371

Pelegrin, P., Barroso-Gutierrez, C., and Surprenant, A. (2008). P2X7 receptor differentially couples to distinct release pathways for IL-1β in mouse macrophage. *J. Immunol.* 180, 7147–7157. doi: 10.4049/jimmunol.180.11.7147

Pelegrin, P., and Surprenant, A. (2006). Pannexin-1 mediates large pore formation and interleukin-1beta release by the ATP-gated P2X7 receptor. *EMBO J.* 25, 5071–5082. doi: 10.1038/sj.emboj.7601378

Pellegatti, P., Raffaghello, L., Bianchi, G., Piccardi, F., Pistoia, V., and Di Virgilio, F. (2008). Increased level of extracellular ATP at tumor sites: in vivo imaging with plasma membrane luciferase. *PLoS One* 3:e2599. doi: 10.1371/journal.pone.0002599

Perregaux, D. G., McNiff, P., Laliberte, R., Conklyn, M., and Gabel, C. A. (2000). ATP acts as an agonist to promote stimulus-induced secretion of IL-1 beta and IL-18 in human blood. *J. Immunol.* 165, 4615–4623. doi: 10.4049/jimmunol.165.8.4615

Piccioli, P., and Rubartelli, A. (2013). The secretion of IL-1beta and options for release. *Semin. Immunol.* 25, 425–429. doi: 10.1016/j.smim.2013.10.007

Pivec, R., Johnson, A. J., Mears, S. C., and Mont, M. A. (2012). Hip arthroplasty. *Lancet* 380, 1768–1777.

Pizzirani, C., Ferrari, D., Chiozzi, P., Adinolfi, E., Sandona, D., Savaglio, E., et al. (2007). Stimulation of P2 receptors causes release of IL-1beta-loaded microvesicles from human dendritic cells. *Blood* 109, 3856–3864. doi: 10.1182/blood-2005-06-031377

Plesner, L. (1995). Ecto-ATPases: identities and functions. *Int. Rev. Cytol.* 158, 141–214. doi: 10.1016/s0074-7696(08)62487-0

Qiu, J. H., Asai, A., Chi, S., Saito, N., Hamada, H., and Kirino, T. (2000). Proteasome inhibitors induce cytochrome c-caspase-3-like protease-mediated apoptosis in cultured cortical neurons. *J. Neurosci.* 20, 259–265. doi: 10.1523/jneurosci.20-01-00259.2000

Qiu, T., Pei, P., Yao, X., Jiang, L., Wei, S., Wang, Z., et al. (2018). Taurine attenuates arsenic-induced pyroptosis and nonalcoholic steatohepatitis by inhibiting the autophagic-inflammasomal pathway. *Cell Death Dis.* 9:946.

Qu, Y., Franchi, L., Nunez, G., and Dubyak, G. R. (2007). Nonclassical IL-1 beta secretion stimulated by P2X7 receptors is dependent on inflammasome activation and correlated with exosome release in murine macrophages. *J. Immunol.* 179, 1913–1925. doi: 10.4049/jimmunol.179.3.1913

Rao, Z., Wang, S., and Wang, J. (2017). Peroxiredoxin 4 inhibits IL-1beta-induced chondrocyte apoptosis via PI3K/AKT signaling. *Biomed. Pharmacother.* 90, 414–420. doi: 10.1016/j.biopha.2017.03.075

Rathakrishnan, C., Tiku, K., Raghavan, A., and Tiku, M. L. (1992). Release of oxygen radicals by articular chondrocytes: a study of luminol- dependent chemiluminescence and hydrogen peroxide secretion. *J. Bone Min. Res.* 7, 1139–1148. doi: 10.1002/jbmr.5650071005

Rekha, R. S., Rao Muvva, S. S., Wan, M., Raqib, R., Bergman, P., Brighenti, S., et al. (2015). Phenylbutyrate induces LL-37-dependent autophagy and intracellular killing of *Mycobacterium tuberculosis* in human macrophages. *Autophagy* 11, 1688–1699. doi: 10.1080/15548627.2015.1075110

Ribeiro, M., López de Figueroa, P., Blanco, F. J., Mendes, A. F., and Carames, B. (2016a). Insulin decreases autophagy and leads to cartilage degradation. *Osteoarthritis Cartilage* 24, 731–739. doi: 10.1016/j.joca.2015.10.017

Ribeiro, M., Lopez de Figueroa, P., Nogueira-Recalde, U., Centeno, A., Mendes, A. F., Blanco, F. J., et al. (2016b). Diabetes-accelerated experimental osteoarthritis is prevented by autophagy activation. *Osteoarthritis Cartilage* 24, 2116–2125. doi: 10.1016/j.joca.2016.06.019

Roach, H. I., Aigner, T., and Kouri, J. B. (2004). Chondroptosis: a variant of apoptotic cell death in chondrocytes? *Apoptosis* 9, 265–277. doi: 10.1023/b:appt.0000025803.17498.26

Rutjes, A. W., Jüni, P., da Costa, B. R., Trelle, S., Nüesch, E., and Reichenbach, S. (2012). Viscosupplementation for osteoarthritis of the knee: a systematic review and meta-analysis. *Ann. Intern. Med.* 157, 180–191.

Saber, S., Abd El-Kader, E. M., Sharaf, H., El-Shamy, R., El-Saeed, B., Mostafa, A., et al. (2020). Celastrol augments sensitivity of NLRP3 to CP-456773 by modulating HSP-90 and inducing autophagy in dextran sodium sulphate-induced colitis in rats. *Toxicol. Appl. Pharmacol.* 400:115075. doi: 10.1016/j.taap.2020.115075

Sandell, L. J., and Aigner, T. (2001). Articular cartilage and changes in arthritis. An introduction: cell biology of osteoarthritis. *Arthritis Res.* 3, 107–113.

Sasaki, H., Takayama, K., Matsushita, T., Ishida, K., Kubo, S., Matsumoto, T., et al. (2012). Autophagy modulates osteoarthritis-related gene expression in human chondrocytes. *Arthritis Rheum.* 64, 1920–1928. doi: 10.1002/art.34323

Scanzello, C. R., Plaas, A., and Crow, M. K. (2008). Innate immune system activation in osteoarthritis: is osteoarthritis a chronic wound? *Curr. Opin. Rheumatol.* 20, 565–572. doi: 10.1097/bor.0b013e32830aba34

Schipani, E., Ryan, H. E., Didrickson, S., Kobayashi, T., Knight, M., and Johnson, R. S. (2001). Hypoxia in cartilage: HIF-1alpha is essential for chondrocyte growth arrest and survival. *Genes Dev.* 15, 2865–2876.

Schmidt, T. A., Gastelum, N. S., Nguyen, Q. T., Schumacher, B. L., and Sah, R. L. (2007). Boundary lubrication of articular cartilage: role of synovial fluid constituents. *Arthritis Rheum.* 56, 882–891. doi: 10.1002/art.22446

Schwalm, C., Jamart, C., Benoit, N., Naslain, D., Premont, C., Prevet, J., et al. (2015). Activation of autophagy in human skeletal muscle is dependent on exercise intensity and AMPK activation. *FASEB J.* 29, 3515–3526. doi: 10.1096/fj.14-267187

Sekar, P., Huang, D. Y., Hsieh, S. L., Chang, S. F., and Lin, W. W. (2018). AMPK-dependent and independent actions of P2X7 in regulation of mitochondrial and lysosomal functions in microglia. *Cell Commun. Signal.* 16:83.

Shao, B. Z., Xu, Z. Q., Han, B. Z., Su, D. F., and Liu, C. (2015). NLRP3 inflammasome and its inhibitors: a review. *Front. Pharmacol.* 6:262. doi: 10.3389/fphar.2015.00262

Shapiro, I. M., Layfield, R., Lotz, M., Settembre, C., and Whitehouse, C. (2014). Boning up on autophagy: the role of autophagy in skeletal biology. *Autophagy* 10, 7–19. doi: 10.4161/auto.26679

Sharma, D., and Kanneganti, T. D. (2016). The cell biology of inflammasomes: mechanisms of inflammasome activation and regulation. *J. Cell Biol.* 213, 617–629.

Shen, Y., Liu, W. W., Zhang, X., Shi, J. G., Jiang, S., Zheng, L., et al. (2020). TRAF3 promotes ROS production and pyroptosis by targeting ULK1 ubiquitination in macrophages. *FASEB J.* 34, 7144–7159. doi: 10.1096/fj.201903073r

Shi, C. S., Shenderov, K., Huang, N. N., Kabat, J., Abu-Asab, M., Fitzgerald, K. A., et al. (2012). Activation of autophagy by inflammatory signals limits IL-1beta production by targeting ubiquitinated inflammasomes for destruction. *Nat. Immunol.* 13, 255–263. doi: 10.1038/ni.2215

Signaling, F. B. (2004). Transduction: target in osteoarthritis. *Curr. Opin. Rheumatol.* 16, 616–622. doi: 10.1097/01.bor.0000133663.37352.4a

Sitia, R., and Rubartelli, A. (2020). Evolution, role in inflammation, and redox control of leaderless secretory proteins. *J. Biol. Chem.* 295, 7799–7811. doi: 10.1074/jbc.rev119.008907

Sluyter, R. (2017). P2X7 receptor. *Adv. Exp. Med. Biol.* 1051, 17–53.

Sluyter, R., and Stokes, L. (2011). Significance ofP2X7receptor variants to human health and disease. *Recent Pat. DNA Gene Seq.* 5, 41–54. doi: 10.2174/187221511794839219

Speziali, A., Delcogliano, M., Tei, M., Placella, G., Chillemi, M., Tiribuzi, R., et al. (2015). Chondropenia: current concept review. *Musculoskelet. Surg.* 99, 189–200. doi: 10.1007/s12306-015-0377-9

Stock, T. C., Bloom, B., Wei, N., Ishaq, S., Park, W., Wang, X., et al. (2012). Efficacy and safety of CE-224,535, an antagonist of P2X7 receptor, in treatment of patients with rheumatoid arthritis inadequately controlled by methotrexate. *J. Rheumatol.* 39, 720–727. doi: 10.3899/jrheum.110874

Stolberg-Stolberg, J. A., Furman, B. D., Garrigues, N. W., Lee, J., Pisetsky, D. S., Stearns, N. A., et al. (2013). Effects of cartilage impact with and without fracture on chondrocyte viability and the release of inflammatory markers. *J. Orthop. Res.* 31, 1283–1292. doi: 10.1002/jor.22348

Strowig, T., Henao-Mejia, J., Elinav, E., and Flavell, R. (2012). Inflammasomes in health and disease. *Nature* 481, 278–286. doi: 10.1038/nature10759

Sun, K., Liu, F., Wang, J., Guo, Z., Ji, Z., and Yao, M. (2017). The effect of mechanical stretch stress on the differentiation and apoptosis of human growth plate chondrocytes. *In Vitro Cell. Dev. Biol. Anim.* 53, 141–148. doi: 10.1007/s11626-016-0090-5

Sun, L., Gao, J., Zhao, M., Cui, J., Li, Y., Yang, X., et al. (2015). A novel cognitive impairment mechanism that astrocytic p-connexin 43 promotes neuronic autophagy via activation of P2X7R and down-regulation of GLT-1 expression in the hippocampus following traumatic brain injury in rats. *Behav. Brain Res.* 291, 315–324. doi: 10.1016/j.bbr.2015.05.049

Surprenant, A., Rassendren, F., Kawashima, E., North, R. A., and Buell, G. (1996). The cytolytic P2Z receptor for extracellular ATP identified as a P2X receptor (P2X7). *Science* 272, 735–738. doi: 10.1126/science.272.5262.735

Takenouchi, T., Fujita, M., Sugama, S., Kitani, H., and Hashimoto, M. (2009a). The role of the P2X7 receptor signaling pathway for the release of autolysosomes in microglial cells. *Autophagy* 5, 723–724. doi: 10.4161/auto.5.5.8478

Takenouchi, T., Nakai, M., Iwamaru, Y., Sugama, S., Tsukimoto, M., Fujita, M., et al. (2009b). The activation of P2X7 receptor impairs lysosomal functions and stimulates the release of autophagolysosomes in microglial cells. *J. Immunol.* 182, 2051–2062. doi: 10.4049/jimmunol.0802577

Taylor, S. R., Turner, C. M., Elliott, J. I., McDaid, J., Hewitt, R., Smith, J., et al. (2009). P2X7 deficiency attenuates renal injury in experimental glomerulonephritis. *J. Am. Soc. Nephrol.* 20, 1275–1281. doi: 10.1681/asn.2008060559

Thomas, C. M., Fuller, C. J., Whittles, C. E., and Sharif, M. (2007). Chondrocyte death by apoptosis is associated with cartilage matrix degradation. *Osteoarthritis Cartilage* 15, 27–34. doi: 10.1016/j.joca.2006.06.012

Turrens, J. F. (2003). Mitochondrial formation of reactive oxygen species. *J. Physiol.* 552(Pt 2), 335–344. doi: 10.1113/jphysiol.2003.049478

Uthman, O. A., van der Windt, D. A., Jordan, J. L., Dziedzic, K. S., Healey, E. L., Peat, G. M., et al. (2013). Exercise for lower limb osteoarthritis: systematic review incorporating trial sequential analysis and network meta-analysis. *BMJ* 347:f5555. doi: 10.1136/bmj.f5555

van Lent, P. L., Blom, A. B., Schelbergen, R. F., Sloetjes, A., Lafeber, F. P., Lems, W. F., et al. (2012). Active involvement of alarmins S100A8 and S100A9 in the regulation of synovial activation and joint destruction during mouse and human osteoarthritis. *Arthritis Rheum.* 64, 1466–1476. doi: 10.1002/art.34315

van Lent, P. L., Blom, A. B., van der Kraan, P., Holthuysen, A. E., Vitters, E., van Rooijen, N., et al. (2004). Crucial role of synovial lining macrophages in the promotion of transforming growth factor beta-mediated osteophyte formation. *Arthritis Rheum.* 50, 103–111. doi: 10.1002/art.11422

Vanden Berghe, T., Kaiser, W. J., Bertrand, M. J., and Vandenabeele, P. (2015). Molecular crosstalk between apoptosis, necroptosis, and survival signaling. *Mol. Cell. Oncol.* 2:e975093. doi: 10.4161/23723556.2014.975093

Verbruggen, G., Wittoek, R., Vander Cruyssen, B., and Elewaut, D. (2012). Tumour necrosis factor blockade for the treatment of erosive osteoarthritis of the interphalangeal finger joints: a double blind, randomised trial on structure modification. *Ann. Rheum. Dis.* 71, 891–898. doi: 10.1136/ard.2011.149849

Vigano, E., and Mortellaro, A. (2013). Caspase-11: the driving factor for noncanonical inflammasomes. *Eur. J. Immunol.* 43, 2240–2245. doi: 10.1002/eji.201343800

Wada, T., and Penninger, J. M. (2004). Mitogen-activated protein kinases in apoptosis regulation. *Oncogene* 23, 2838–2849. doi: 10.1038/sj.onc.1207556

Wang, J., and Dahl, G. (2018). Pannexin1: a multifunction and multiconductance and/or permeability membrane channel. *Am. J. Physiol. Cell Physiol.* 315, C290–C299.

Wang, Q., Rozelle, A. L., Lepus, C. M., Scanzello, C. R., Song, J. J., Larsen, D. M., et al. (2011). Identification of a central role for complement in osteoarthritis. *Nat. Med.* 17, 1674–1679.

Wang, X., Jiang, L., Shi, L., Yao, K., Sun, X., Yang, G., et al. (2019). Zearalenone induces NLRP3-dependent pyroptosis via activation of NF-kappaB modulated by autophagy in INS-1 cells. *Toxicology* 428:152304. doi: 10.1016/j.tox.2019.152304

Wang, Y., Song, X., Li, Z., Liu, N., Yan, Y., Li, T., et al. (2020). MicroRNA-103 protects coronary artery endothelial cells against H2O2-induced oxidative stress via BNIP3-mediated end-stage autophagy and antipyroptosis pathways. *Oxid. Med. Cell Longev.* 2020:8351342.

Weber, F. C., Esser, P. R., Muller, T., Ganesan, J., Pellegatti, P., Simon, M. M., et al. (2010). Lack of the purinergic receptor P2X(7) results in resistance to contact hypersensitivity. *J. Exp. Med.* 207, 2609–2619. doi: 10.1084/jem.20092489

Wei, Q., Zhu, R., Zhu, J., Zhao, R., and Li, M. (2019). E2-induced activation of the NLRP3 inflammasome triggers pyroptosis and inhibits autophagy in HCC cells. *Oncol. Res.* 27, 827–834. doi: 10.3727/096504018x15462920753012

Wilhelm, K., Ganesan, J., Muller, T., Durr, C., Grimm, M., Beilhack, A., et al. (2010). Graft-versus-host disease is enhanced by extracellular ATP activating P2X7R. *Nat. Med.* 16, 1434–1438. doi: 10.1038/nm.2242

Wu, C., Xu, H., Li, J., Hu, X., Wang, X., Huang, Y., et al. (2020). Baicalein attenuates pyroptosis and endoplasmic reticulum stress following spinal cord ischemia-reperfusion injury via autophagy enhancement. *Front. Pharmacol.* 11:1076. doi: 10.3389/fphar.2020.01076

Xu, X. Y., He, X. T., Wang, J., Li, X., Xia, Y., Tan, Y. Z., et al. (2019). Role of the P2X7 receptor in inflammation-mediated changes in the osteogenesis of periodontal ligament stem cells. *Cell Death Dis.* 10:20.

Yang, D., He, Y., Munoz-Planillo, R., Liu, Q., and Nunez, G. (2015). Caspase-11 requires the Pannexin-1 channel and the Purinergic P2X7 pore to mediate pyroptosis and endotoxic shock. *Immunity* 43, 923–932. doi: 10.1016/j.immuni.2015.10.009

Yang, F., Qin, Y., Wang, Y., Meng, S., Xian, H., Che, H., et al. (2019). Metformin inhibits the NLRP3 inflammasome via AMPK/mTOR-dependent effects in diabetic cardiomyopathy. *Int. J. Biol. Sci.* 15, 1010–1019. doi: 10.7150/ijbs.29680

Yang, J., Liu, Z., and Xiao, T. S. (2017). Post-translational regulation of inflammasomes. *Cell. Mol. Immunol.* 14, 65–79. doi: 10.1038/cmi.2016.29

Yang, X., Zhou, G., Ren, T., Li, H., Zhang, Y., Yin, D., et al. (2012). Beta-Arrestin prevents cell apoptosis through pro-apoptotic ERK1/2 and p38 MAPKs and anti-apoptotic Akt pathways. *Apoptosis* 17, 1019–1026. doi: 10.1007/s10495-012-0741-2

Yin, W., Park, J. I., and Loeser, R. F. (2009). Oxidative stress inhibits insulin-like growth factor-I induction of chondrocyte proteoglycan synthesis through differential regulation of phosphatidylinositol 3-Kinase-Akt and MEK-ERK MAPK signaling pathways. *J. Biol. Chem.* 284, 31972–31981. doi: 10.1074/jbc.m109.056838

Young, C. N., Sinadinos, A., Lefebvre, A., Chan, P., Arkle, S., Vaudry, D., et al. (2015). A novel mechanism of autophagic cell death in dystrophic muscle regulated by P2RX7 receptor large-pore formation and HSP90. *Autophagy* 11, 113–130. doi: 10.4161/15548627.2014.994402

Yu, S. M., and Kim, S. J. (2014). Withaferin A-caused production of intracellular reactive oxygen species modulates apoptosis via PI3K/Akt and JNKinase in rabbit articular chondrocytes. *J. Korean Med. Sci.* 29, 1042–1053. doi: 10.3346/jkms.2014.29.8.1042

Yu, S. M., and Kim, S. J. (2015). The thymoquinone-induced production of reactive oxygen species promotes dedifferentiation through the ERK pathway and inflammation through the p38 and PI3K pathways in rabbit articular chondrocytes. *Int. J. Mol. Med.* 35, 325–332. doi: 10.3892/ijmm.2014.2014

Zamli, Z., Adams, M. A., Tarlton, J. F., and Sharif, M. (2013). Increased chondrocyte apoptosis is associated with progression of osteoarthritis in spontaneous Guinea pig models of the disease. *Int. J. Mol. Sci.* 14, 17729–17743. doi: 10.3390/ijms140917729

Zamli, Z., and Sharif, M. (2011). Chondrocyte apoptosis: a cause or consequence of osteoarthritis? *Int. J. Rheum. Dis.* 14, 159–166. doi: 10.1111/j.1756-185x.2011.01618.x

Zeiss, C. J. (2003). The apoptosis-necrosis continuum: insights from genetically altered mice. *Vet. Pathol.* 40, 481–495. doi: 10.1354/vp.40-5-481

Zemmyo, M., Meharra, E. J., Kuhn, K., Creighton-Achermann, L., and Lotz, M. (2003). Accelerated, aging-dependent development of osteoarthritis in alpha1 integrin-deficient mice. *Arthritis Rheum.* 48, 2873–2880.

Zeng, Q., Zhou, Y., Liang, D., He, H., Liu, X., Zhu, R., et al. (2020). Exosomes secreted from bone marrow mesenchymal stem cells attenuate oxygen-glucose deprivation/reoxygenation-induced pyroptosis in PC12 cells by promoting AMPK-dependent autophagic flux. *Front. Cell. Neurosci.* 14:182. doi: 10.3389/fncel.2020.00182

Zhang, F., Wang, J., Chu, J., Yang, C., Xiao, H., Zhao, C., et al. (2015). MicroRNA-146a induced by hypoxia promotes chondrocyte autophagy through Bcl-2. *Cell. Physiol. Biochem.* 37, 1442–1453.

Zhang, W., Zhong, B., Zhang, C., Luo, C., and Zhan, Y. (2018). miR-373 regulates inflammatory cytokine-mediated chondrocyte proliferation in osteoarthritis by targeting the P2X7 receptor. *FEBS Open Bio.* 8, 325–331.

Zhang, Y., Cheng, H., Li, W., Wu, H., and Yang, Y. (2019). Highly-expressed P2X7 receptor promotes growth and metastasis of human HOS/MNNG osteosarcoma cells via PI3K/Akt/GSK3beta/beta-catenin and mTOR/HIF1alpha/VEGF signaling. *Int. J. Cancer* 145, 1068–1082.

Zhang, Y., Vasheghani, F., Li, Y. H., Blati, M., Simeone, K., Fahmi, H., et al. (2015). Cartilage-specific deletion of mTOR upregulates autophagy and protects mice from osteoarthritis. *Ann. Rheum. Dis.* 74, 1432–1440.

Zhang, Y. B., Li, S. X., Chen, X. P., Yang, L., Zhang, Y. G., Liu, R., et al. (2008). Autophagy is activated and might protect neurons from degeneration after traumatic brain injury. *Neurosci. Bull.* 24, 143–149.

Zhao, H., Chen, Y., and Feng, H. (2018). P2X7 receptor-associated programmed cell death in the pathophysiology of hemorrhagic stroke. *Curr. Neuropharmacol.* 16, 1282–1295.

Zheng, T., Zhao, C., Zhao, B., Liu, H., Wang, S., Wang, L., et al. (2020). Impairment of the autophagy-lysosomal pathway and activation of pyroptosis in macular corneal dystrophy. *Cell Death Discov.* 6:85.

Zhong, Z., Umemura, A., Sanchez-Lopez, E., Liang, S., Shalapour, S., Wong, J., et al. (2016). NF-kappaB restricts inflammasome activation via elimination of damaged mitochondria. *Cell* 164, 896–910.

Zhou, R., Yazdi, A. S., Menu, P., and Tschopp, J. (2011). A role for mitochondria in NLRP3 inflammasome activation. *Nature* 469, 221–225.

Zhu, S. Y., Yao, R. Q., Li, Y. X., Zhao, P. Y., Ren, C., Du, X. H., et al. (2020). Lysosomal quality control of cell fate: a novel therapeutic target for human diseases. *Cell Death Dis.* 11:817.

Conflict of Interest: The authors declare that the research was conducted in the absence of any commercial or financial relationships that could be construed as a potential conflict of interest.

frontiers in Cell and Developmental Biology

ORIGINAL RESEARCH
published: 18 February 2021
doi: 10.3389/fcell.2021.639851

SLC7A11 Reduces Laser-Induced Choroidal Neovascularization by Inhibiting RPE Ferroptosis and VEGF Production

Xiaohuan Zhao[1,2,3,4†], Min Gao[1,2,3,4†], Jian Liang[1,2,3,4†], Yuhong Chen[1,2,3,4], Yimin Wang[1,2,3,4], Yuwei Wang[1,2,3,4], Yushu Xiao[1,2,3,4], Zhenzhen Zhao[1,2,3,4], Xiaoling Wan[1,2,3,4], Mei Jiang[1,2,3,4], Xueting Luo[1,2,3,4], Feng Wang[5] and Xiaodong Sun[1,2,3,4*]*

[1] Department of Ophthalmology, Shanghai General Hospital, Shanghai Jiao Tong University School of Medicine, Shanghai, China, [2] National Clinical Research Center for Eye Diseases, Shanghai, China, [3] Shanghai Key Laboratory of Fundus Diseases, Shanghai, China, [4] Shanghai Engineering Center for Visual Science and Photomedicine, Shanghai, China, [5] The Center for Microbiota and Immunological Diseases, Shanghai General Hospital, Shanghai Institute of Immunology, Department of Immunology and Microbiology, Shanghai Jiao Tong University School of Medicine, Shanghai, China

In age-related macular degeneration (AMD), one of the principal sources of vascular endothelial growth factor (VEGF) is retinal pigment epithelium (RPE) cells under hypoxia or oxidative stress. Solute carrier family 7 member 11 (SLC7A11), a key component of cystine/glutamate transporter, regulates the level of cellular lipid peroxidation, and restrains ferroptosis. In our study, we assessed the role of SLC7A11 in laser-induced choroidal neovascularization (CNV) and explored the underlying mechanism. We established a mouse model of CNV to detect the expression level of SLC7A11 and VEGF during disease progression. We found the expression of the SLC7A11 protein in RPE cells peaked at 3 days after laser treatment, which was correlated with the expression of VEGF. Intraperitoneal injection of SLC7A11 inhibitor expanded the area of CNV. We examined functional proteins related to oxidative stress and Fe^{2+} and found laser-induced ferroptosis accompanied by increased Fe^{2+} content and GPX4 expression in the RPE-choroidal complex after laser treatment. We verified the expression of SLC7A11 in the ARPE19 cell line and the effects of its inhibitors on cell viability and lipid peroxidation *in vitro*. Application of SLC7A11 inhibitor and SLC7A11 knockdown increased the level of lipid peroxidation and reduced the cell viability of ARPE19 which can be rescued by ferroptosis inhibitors ferrostatin-1 (Fer-1) and liproxstatin-1 (Lip-1). Conversely, SLC7A11 overexpression induced resistance to erastin or RSL3-induced ferroptosis. Moreover, we tested the possible regulatory transcription factor NF-E2-related factor 2 (NRF2) of SLC7A11 by Western blot. Knock-down of NRF2 decreased the expression of SLC7A11. Our study suggests that SLC7A11 plays a key role in the laser-induced CNV model by protecting RPE cells from ferroptosis. SLC7A11 provides a new therapeutic target for neovascular AMD patients.

Keywords: SLC7A11, RPE, ferroptosis, VEGF, CNV

OPEN ACCESS

Edited by:
Yinan Gong,
University of Pittsburgh, United States

Reviewed by:
Xizhi Guo,
Harvard Medical School,
United States
Minghui Gao,
Harbin Institute of Technology, China

***Correspondence:**
Feng Wang
wangfeng16@sjtu.edu.cn;
w.feng2002@163.com
Xiaodong Sun
xdsun@sjtu.edu.cn

† These authors have contributed equally to this work and share first authorship

Specialty section:
This article was submitted to Cell Death and Survival, a section of the journal Frontiers in Cell and Developmental Biology

Received: *10 December 2020*
Accepted: *27 January 2021*
Published: *18 February 2021*

Citation:
Zhao X, Gao M, Liang J, Chen Y, Wang Y, Wang Y, Xiao Y, Zhao Z, Wan X, Jiang M, Luo X, Wang F and Sun X (2021) SLC7A11 Reduces Laser-Induced Choroidal Neovascularization by Inhibiting RPE Ferroptosis and VEGF Production. Front. Cell Dev. Biol. 9:639851. doi: 10.3389/fcell.2021.639851

BACKGROUND

Age-related macular degeneration (AMD) is the leading cause of irreversible vision loss among the elderly in developed countries. It is estimated that there will be 288 million AMD patients by 2040 around the world (Wong et al., 2014). AMD has two clinical subtypes: geographic atrophy (dry) types and neovascular (wet) types. Neovascular AMD (nAMD) causes severe and rapid vision loss in 80% of patients who have it. This loss is characterized by abnormal choroidal neovascularization (CNV) (Ishikawa et al., 2016). CNV is the growth of new blood vessels that originate from the choroid through a break in Bruch's membrane. The blood vessels invade the subretinal pigment epithelial and subretinal space, which causes exudation, hemorrhage, and secondary fibrovascular scarring (Al Gwairi et al., 2016; Al-Zamil and Yassin, 2017).

Multiple regulatory factors mediate the formation and development of CNV, especially the development of new blood vessels (angiogenesis) induced by vascular endothelial growth factor (VEGF) (Nowak et al., 2003). It is believed that VEGF and its receptor are the most important regulators of CNV (Shibuya, 2011). So, targeted VEGF therapy is a primary treatment for nAMD. However, some patients with AMD do not respond to targeted therapy. Because of the short half-life of anti-VEGF drugs, many AMD patients need long-term or even life-long treatment. This has adverse effects such as retinal atrophy (Xiao et al., 2019), and the patients' safety and the economic burden on them must be considered. Besides directly blocking VEGF or inhibiting VEGF signals, it is also worth determining if regulating upstream signals indirectly inhibits the production of VEGF (Al-Latayfeh et al., 2012).

A principal source of VEGF is retinal pigment epithelium (RPE) cells under hypoxia and oxidative stress (Kannan et al., 2006; Paeng et al., 2015; Arjamaa et al., 2017). RPE cells play an important role in phagocytizing the outer segment of the photoreceptor, which is highly enriched with polyunsaturated fatty acids and leaves RPE particularly susceptible to lipid peroxidation (Yang et al., 2006). Moreover, some studies have shown that the development of AMD involves lipid peroxidation and iron metabolism (Yang and Stockwell, 2016; Sun et al., 2018). It is unclear how lipid reactive oxygen species (ROS) and iron dysregulation contribute to CNV.

Ferroptosis is a non-apoptotic, iron-dependent regulated cell death, driven by lipid peroxide accumulation (Yang and Stockwell, 2016). Ferroptosis results in morphological changes, including mitochondrial shrinkage and increased mitochondrial membrane density. Ferroptosis can be induced by glutathione peroxidase 4 (GPX4) inhibitors (Yu et al., 2017). SLC7A11, a key component of cystine/glutamate transporter on the membrane, promotes cystine uptake, and glutathione synthesis (Koppula et al., 2018). Pharmacological inhibition SLC7A11 causes cystine depletion and the accumulation of lipid peroxide.

In this study, we focused on ferroptosis and the regulation of iron metabolism in CNV. We designed experiments to study whether oxidative stress, regulated by SLC7A11, played a role in the progression of CNV. The results showed that oxidative-stress-related protein and SLC7A11 increased in a mouse model of laser-induced CNV. Next, we inhibited SLC7A11 in both CNV mouse and ARPE19 cell to further clarify its protective role and explore its related molecular mechanism. We found that SLC7A11 could serve as a new therapeutic target to AMD.

MATERIALS AND METHODS

Cell Culture

The ARPE19 cell line were cultured in DMEM/F-12 medium added to 10% fetal bovine serum (Sigma-Aldrich, St. Louis, MO, United States) and 1% penicillin/streptomycin (GIBCO). They were cultured at 37°C with 5% CO_2 and treated with different reagents according to experimental design: H_2O_2 (Sigma) and SAS (sulfasalazine, Sigma).

Animals

Female C57BL/6 mice, aged 6–8 weeks (Shanghai, China) were used. The water and food consumed by all mice was sterilized. Each experimental group had five or six mice for laser-induced CNV. All animal experiments were approved by the Ethics Committee of Shanghai Jiao Tong University, Shanghai, China, and they were conducted in compliance with the Association for Research in Vision and Ophthalmology Statement for the Use of Animals in Ophthalmic and Vision Research.

GSH Determination

ARPE19 intracellular GSH was detected using a GSH and GSSG Assay Kit (Beyotime, S0053) according to the manufacturer's instructions. The absorbance was measured at 405 nm with a microplate reader (Infinite F50 microplate reader, Swiss). The glutathione and GSSG content of the sample were calculated according to the standard curve, and the GSH content was obtained by the formula: GSH = total glutathione-GSSG × 2 (μM). Experiments were done in three parallel wells and repeated at least twice.

Lipid Peroxidation Detection

BODIPY^{TM} 581/591 C11 (Thermo Fisher, D3861) was used to measure ARPE19 cell lipid peroxidation as reported (Sun et al., 2018). BODIPY was incorporated into cells seeded in a six-well plate for 30 min at a final concentration of 2 μM. The cells were washed three times with PBS. Then flow cytometry (Beckman Coulter, United States) and fluorescence microscopy were used to detect the changes of the probe emission. When lipid peroxidation occurs, the emission of BODIPY changes from red to green (Christova et al., 2004). Experiments were done in three parallel wells and repeated at least twice.

Measurement of Cell Viability

A CCK-8 kit (Beyotime) was used to detect cell viability. ARPE19 was seeded in a 96-well plate and incubated at 37°C. When the cell density was 80–90% of the well, the cells were washed with PBS and treated with CCK-8 reagent for 1 h at 37°C. Absorbance was measured at 450 nm using a microplate reader (Infinite F50 microplate reader, Swiss). Experiments were done in six parallel wells and repeated at least twice.

Western Blot

Retinal pigment epithelium-choroidal complex or RPE cells were collected and measured with the Pierce bicinchoninic acid (BCA) assay. Approximately 10 μg protein were added to SDS-PAGE gels ranging from 8 to 15% and transferred onto a PVDF membrane (Merck Millipore, Billerica, MA, United States). The membranes were blocked with Tris-buffered saline Tween-20 (TBST) containing 5% skim milk for 1 h. Then they were incubated overnight at 4°C in primary antibody: xCT (Novus Biologicals, NB 300-318, 1:1000), NRF2 (Proteintech, 1:1000), HO-1 (Proteintech, 1:1000), GCLC (Proteintech, 1:1000), NQO1 (Proteintech, 1:1000), GPX4 (Abcam, 1:1000), GAPDH (Proteintech, 1:1000). The membranes were washed with TBST and incubated with secondary antibodies conjugated with horseradish peroxidase (HRP) (Proteintech, 1:5000) for 1 h. Then the plots were exposed to a molecular imaging system (Amersham Imager 600, GE Healthcare, Buckinghamshire, United Kingdom).

Real-Time PCR Analysis

Total RNA was isolated according to the RNAsimple Total Kit protocol (Tiangen Biotech, Beijing, China) and quantified by NanoDrop 2000c spectrophotometer (Thermo Fisher Scientific, Wilmington, DE, United States). cDNA was synthesized according to the RT Master Mix protocol (Takara Bio Inc., Dalian, China). The primers were: mouse *Slc7a11*, 5′- TGGGTGGAACTGCTCGTAAT -3′ (forward) and 5′- AGGATGTAGCGTCCAAATGC -3′ (reverse); mouse *Nrf2*, 5′- CTTTAGTCAGCGACAGAAGGAC-3′ (forward) and 5′-AGGCATCTTGTTTGGGAATGTG-3′ (reverse); mouse *GAPDH*, 5′- TGACCTCAACTACATGGTCTACA -3′ (forward) and 5′- CTTCCCATTCTCGGCCTTG -3′ (reverse); human *SLC7A11*, 5′- GCGTGGGCATGTCTCTGAC -3′ (forward) and 5′-GCTGGTAATGGACCAAAGACTTC-3′ (reverse); human *NRF2*, 5′- TCTGACTCCGGCATTTCACT-3′ (forward) and 5′- GGCACTGTCTAGCTCTTCCA -3′ (reverse); human *VEGFA*, 5′-AGGGCAGAATCATCACGAAGT-3′ (forward) and 5′-AGGGTCTCGATTGGATGGCA-3′ (reverse); human *GAPDH*, 5′-TGTGGGCATCAATGGATTTGG-3′ (forward) and 5′-ACACCATGTATTCCGGGTCAAT-3′ (reverse).

NRF2 RNA Interference

ARPE19 was transfected with double-stranded siRNA to knock down *NRF2* by Lipofectamine 3000 (Thermo Fisher Scientific). The sequences were: si-*NRF2*-1 5′-UAAAGUGGCUGCUCAGAAUUU-3′, si-*NRF2*-2 5′-GACAGAAGUUGACAAUUAUTT-3′, si-*NRF2*-3 5′-CCAGAACACUCAGUGGAAUTT-3′. Double-stranded siRNAs were synthesized by Shanghai GenePharma (Shanghai, China).

Laser-Induced CNV in Mice

C57BL/6J (6–8 weeks old) mice were anesthetized by intraperitoneally injecting 1.5% sodium pentobarbital (100 μl/20g). 0.5% tropicamide and 0.5% noradrenaline hydrochloride eye drops were dripped into the eyes of the mice to dilate the pupils. Laser photocoagulation (350 Mw, 50 ms) was performed in the 2, 5, 8, and 11 o'clock position around the optic disk and kept away from blood vessels. It was focused on RPE, and it disturbed Bruch's membrane when bubbles were observed.

Fundus Fluorescent Angiography (FFA)

0, 1, 3, 7, and 10 days after laser injury, FFA was performed before sacrifice. After being anesthetized, the pupils of mice were dilated and 2% fluorescein sodium (Fluorescite; Alcon, Tokyo, Japan) was injected intraperitoneally. FFA images were made at intervals of 2 min. The FFA images were analyzed using ImageJ software (NIH, United States).

Immunofluorescence Staining

Immunofluorescence stain assay was performed on sections of the eyes (10 μm in thickness), made with a microtome. After fixation, the samples were blocked with PBS containing 0.3% Triton X-100 and 5% goat serum albumin (Beyotime) for 1 h. Then the sections were incubated overnight at 4°C with primary antibodies against SLC7A11 (CST, 1:1000), isolectin (Santa Cruz Biotechnology, 1:1000), RPE65 (Abcam, 1:1000). The sections were stained for 1 h with Alexa Fluor 594 or 488-conjugated secondary antibodies (Proteintech, 1:1000). This step was not required for the immunofluorescence of isolectin. The retinal sections were visualized using a confocal microscope (Leica, United States).

SLC7A11 shRNA Plasmids Construction

The pLKO.1-*SLC7A11* shRNA oligos were: shRNA-1 CCTGTCACTATTTGGAGCTTT, shRNA-2 CCTGCGTATTATCTCTTTATT, and shRNA-3 CCCTGGAGTTATGCAGCTAAT. The pLKO.1-*SLC7A11* and scrambled shRNA with packing plasmids pSPA and pMD2G (Addgene) were transfected into HEK293 packing cells using Lipofectamine 3000 (Thermo Fisher Scientific). *SLC7A11*, shRNA, or scrambled shRNA were introduced into ARPE19 cells by transfection with lentiviral supernatants. RT-PCR and Western blot were used to select stable transfected sequences with a certain knockdown efficiency for subsequent experiments.

Cloning and Transfection

SLC7A11 plasmid was constructed by using the methods described (Nazari et al., 2014; Nasca et al., 2017). Briefly, the SLC7A11 cDNA was subcloned into pAAV-CMS vector. New recombinant plasmids were termed as AAV-SLC7A11. Then the AAV- SLC7A11 was transfected into ARPE19 cells with the Lipofectamine 3000 (Thermo Fisher Scientific). 6 h after transfection, the cells were cultured in fresh medium containing erastin (Sigma-Aldrich) or RSL3 (CAYMAN) for 24 h, then the culture medium was replaced by the fresh medium. The cell viability was measured by the CCK8 48 h after transfection.

PI Staining

Staining with PI (81845, Sigma) was carried out according to the manufacturer's instructions. Briefly, cells were suspended and stained with PI at a final concentration of 30 μM for 30 min (Rosenberg et al., 2019). The samples were counterstained with DAPI for fluorescence observation.

Iron Assay

Fe^{2+} was found in the RPE-choroidal complex by using an iron assay kit (Sigma-Aldrich, MAK025) according to the manufacturer's instructions. Absorbance was measured at 595 nm using a microplate reader (Infinite F50 microplate reader, Swiss).

Statistical Analysis

Statistical analysis was performed using SPSS 21.0 software (GraphPad Prism, San Diego, CA, United States). Data were expressed as the mean ± SD from at least three biological replicates. The differences between the two groups were analyzed by a Student's *t*-test. One-way ANOVA analysis was used to identify differences when there were three or more groups. A value of $p < 0.05$ was considered statistically significant.

RESULTS

Laser-Induced CNV Vascular Leakage and Dynamic Changes of VEGFA

To understand the natural process of CNV, we measured the leakage area and volume of CNV fluorescence at various points in time after laser treatment. Compared with 3 days after laser treatment, there was no significant difference in the fluorescence area at 7 days, but the fluorescence intensity increased (**Figures 1A–C**, $p < 0.05$). In addition, by immunofluorescence, we found that the volume of neovascularization at 7 days post injury (dpi) was larger than that at 3 dpi (**Figures 1D,E**, $p < 0.05$). So, we measured the size of the CNV at 7 dpi. We then detected the level of VEGFA at the corresponding point in time by Western blot. After laser treatment, VEGFA expression was upregulated; it peaked at 3 dpi, then decreased to normal at 7 dpi (**Figures 1F,G**, $p < 0.05$).

The Expression of SLC7A11 in the Natural Course of Laser-Induced CNV in Mice

Next, we evaluated the level of SLC7A11 after laser treatment. Both SLC7A11 protein (**Figures 2A,B**, $p < 0.05$) and mRNA (**Figure 2C**, $p < 0.05$) rose after laser treatment. The mRNA level reached a peak at 3 dpi and fell back at 7 dpi. This showed that SLC7A11 can respond to laser-induced damage in the early stage. The SLC7A11 protein level gradually increased with time, and it peaked at 7 dpi. We used immunofluorescence to identify cells

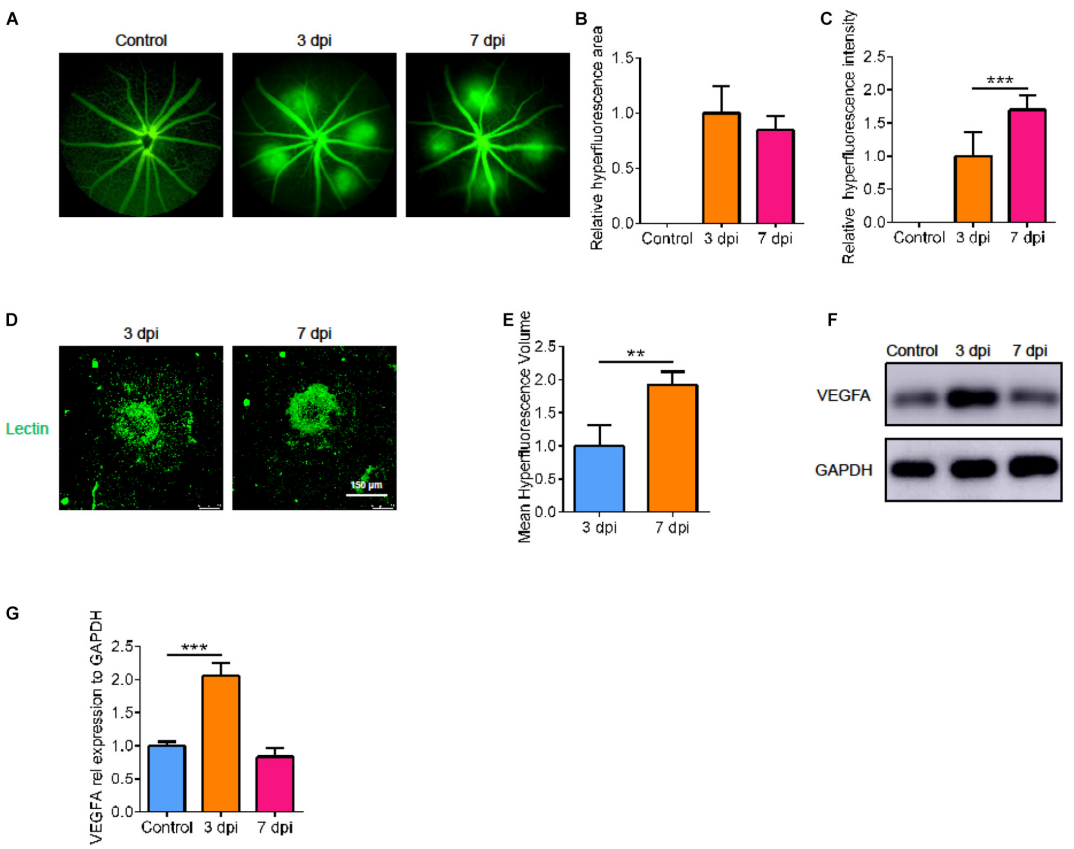

FIGURE 1 | Laser-induced CNV vascular leakage and dynamic changes of VEGFA. **(A)** Fluorescence imaging of mice at various points in time after laser treatment. **(B,C)** The average area and intensity of fluorescence imaging after laser treatment by Image-J ($n = 6$). **(D,E)** Laser spot size at 3 dpi and 7 dpi by immunofluorescence and Image-J ($n = 6$). **(F,G)** The VEGFA protein changes dynamically at the corresponding point in time by Western blot ($n = 3$). Bar graphs show mean ± SD. *P*-values: T-test and One-way ANOVA analysis. (***$p < 0.001$, **$p < 0.01$). Scale bar = 150 μm.

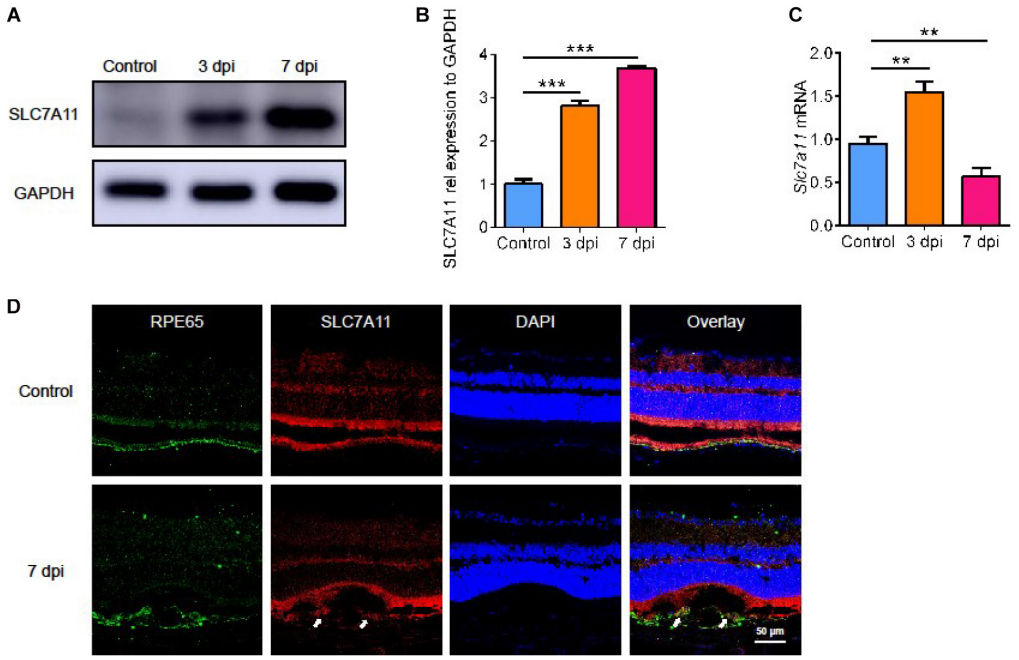

FIGURE 2 | The expression of SLC7A11 in the natural course of laser-induced CNV in mice. **(A,B)** The level of SLC7A11 protein at various points in time after laser by Western blot ($n = 3$). **(C)** The level of *Slc7a11* mRNA after laser by RT-PCR ($n = 6$). **(D)** The location of SLC7A11 (white arrow) by immunofluorescence. Bar graphs show mean ± SD. *P*-values: one-way ANOVA analysis (***$p < 0.001$, **$p < 0.01$). Scale bar = 50 μm.

with high SLC7A11 expression. SLC7A11 was highly expressed and co-stained with RPE cells after 7 days of CNV; while at 0 dpi, almost no SLC7A11 signal was detected (**Figure 2D**). This is consistent with the protein level. In addition, we found that RPE cells became larger and more irregular after laser treatment. This suggests that with the progress of CNV, the RPE layer was destroyed, and the morphology and size changed. In response to injury, RPE cells produced SLC7A11 which increases with time.

The Level of Oxidative Stress in Laser-Induced CNV

SLC7A11 is a key component of glutamate/cystine transporter on the cell membrane. It promotes cystine uptake and glutathione biosynthesis, protecting cells from oxidative stress and ferroptotic death (Koppula et al., 2018). To verify the level of oxidative stress after laser treatment, we detected the expression of three proteins involved in antioxidant effects: heme oxygenase-1 (HO-1), glutamate-cysteine ligase catalytic subunit (GCLC), and NAD(P)H quinone dehydrogenase 1 (NQO1). All of them increased and reached a peak at 3 dpi and decreased slightly by 7 dpi (**Figures 3A–D**, $p < 0.05$). This suggests that there is oxidative stress in the process of laser-induced neovascularization.

Ferroptosis Was Induced in RPE Cells of CNV *in vivo*

Because of the high level of oxidative stress, we looked for signs of damage related to oxidative stress. We found that glutathione peroxidase 4 (GPX4), an antioxidant enzyme, increased significantly by 3 days after CNV, and it decreased after 7 days, the same as HO-1 and NQO1 (**Figures 3A,B,D,E**, $p < 0.05$). GPX4 senses oxidative stress and converts lipid hydroperoxides into non-toxic lipid alcohols (Bersuker et al., 2019) to prevent ferroptosis (Seiler et al., 2008). To determine if ferroptosis occurred after CNV, we measured the iron content in the choroid. We found that the content of Fe^{2+} in the RPE-choroidal complex after CNV was higher in CNV group than in the control group (**Figure 3G**, $p < 0.05$). We used PI staining to measure cell death and BODIPY^{TM} 581/591 C11 to test lipid peroxidation. After CNV treatment, RPE cells death occurred with high level of lipid peroxidation (**Figures 3H,I**). Therefore, we speculated that choroidal ferroptosis occurs after CNV, and the compensatory increase of SLC7A11 and GPX4 in RPE is to reduce the ferroptosis of cells. In addition, a possible regulatory gene upstream of SLC7A11, *Nrf2*, was also upregulated at both protein and mRNA levels after laser treatment, and this lasted at least to 7 dpi (**Figures 3A,F,J**, $p < 0.05$).

The Cell Viability and Lipid Peroxidation Level of RPE Cells After SLC7A11 Inhibition

To further clarify the role of SLC7A11 in RPE, we used ARPE19 cells treated with H_2O_2 for 24 h. We found that the expression of VEGFA and SLC7A11 increased as the concentration of H_2O_2 increased (**Figures 4A–E**, $p < 0.05$). To investigate the critical effect of SLC7A11, we used short hairpin RNA (shRNA) to knock down the expression of *SLC7A11* in ARPE19. The *SLC7A11*^{KD} ARPE19 showed a low

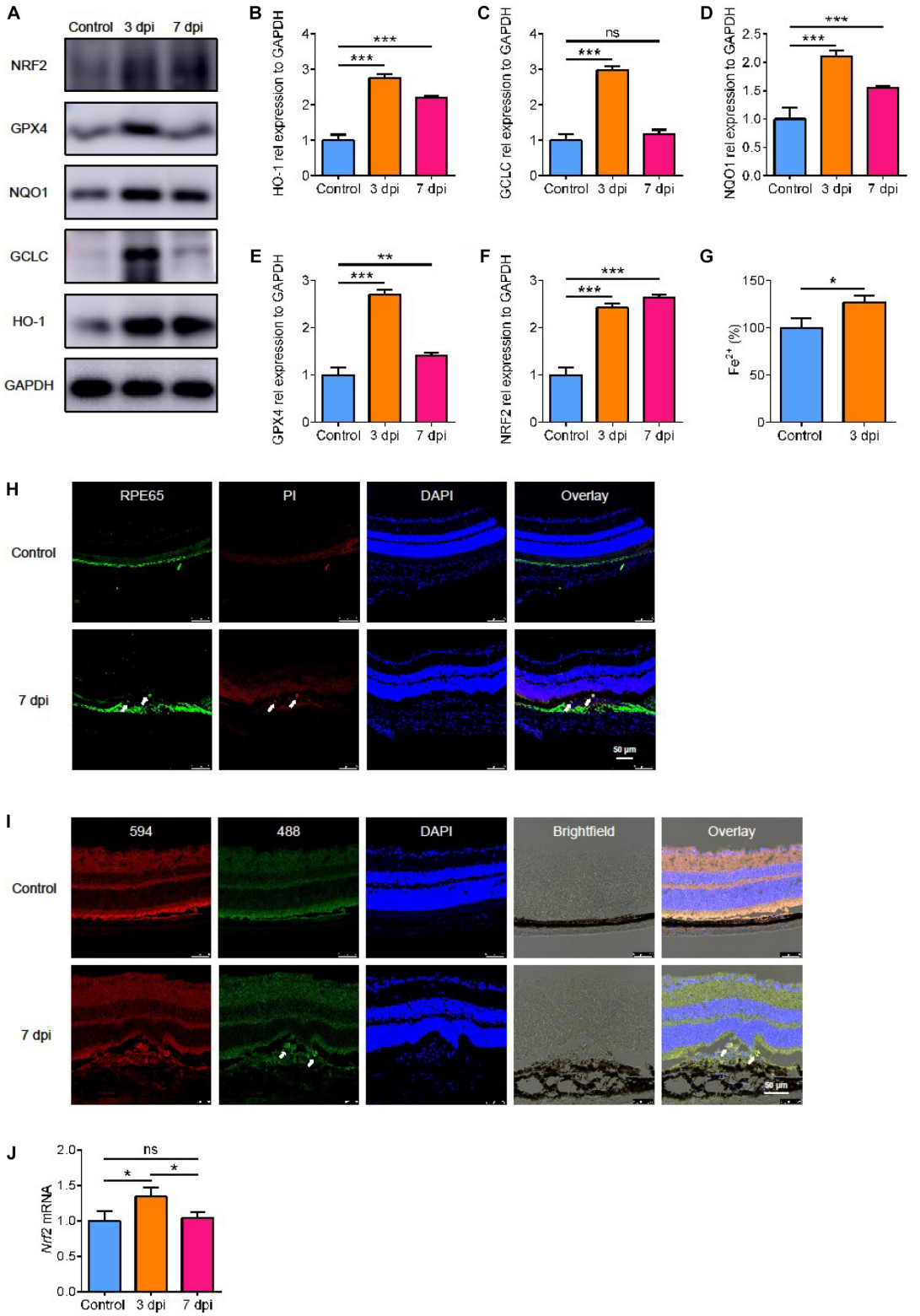

FIGURE 3 | The expression of proteins involved in oxidative stress. **(A–F)** The expression of proteins involved in oxidative stress detected by Western blot ($n = 3$). **(G)** The content of Fe^{2+} in the RPE-choroidal complex after CNV ($n = 6$). **(H)** Cell death (white arrow) after laser by PI staining. **(I)** The level of lipid peroxidation (white arrow) after laser with C11 BODIPY 581/591. **(J)** The expression of *Nrf2* mRNA after laser by RT-PCR ($n = 6$). Bar graphs show mean ± SD. *P*-values: *t*-test and one-way ANOVA analysis (***$p < 0.001$, **$p < 0.01$, *$p < 0.05$). Scale bar = 50 μm.

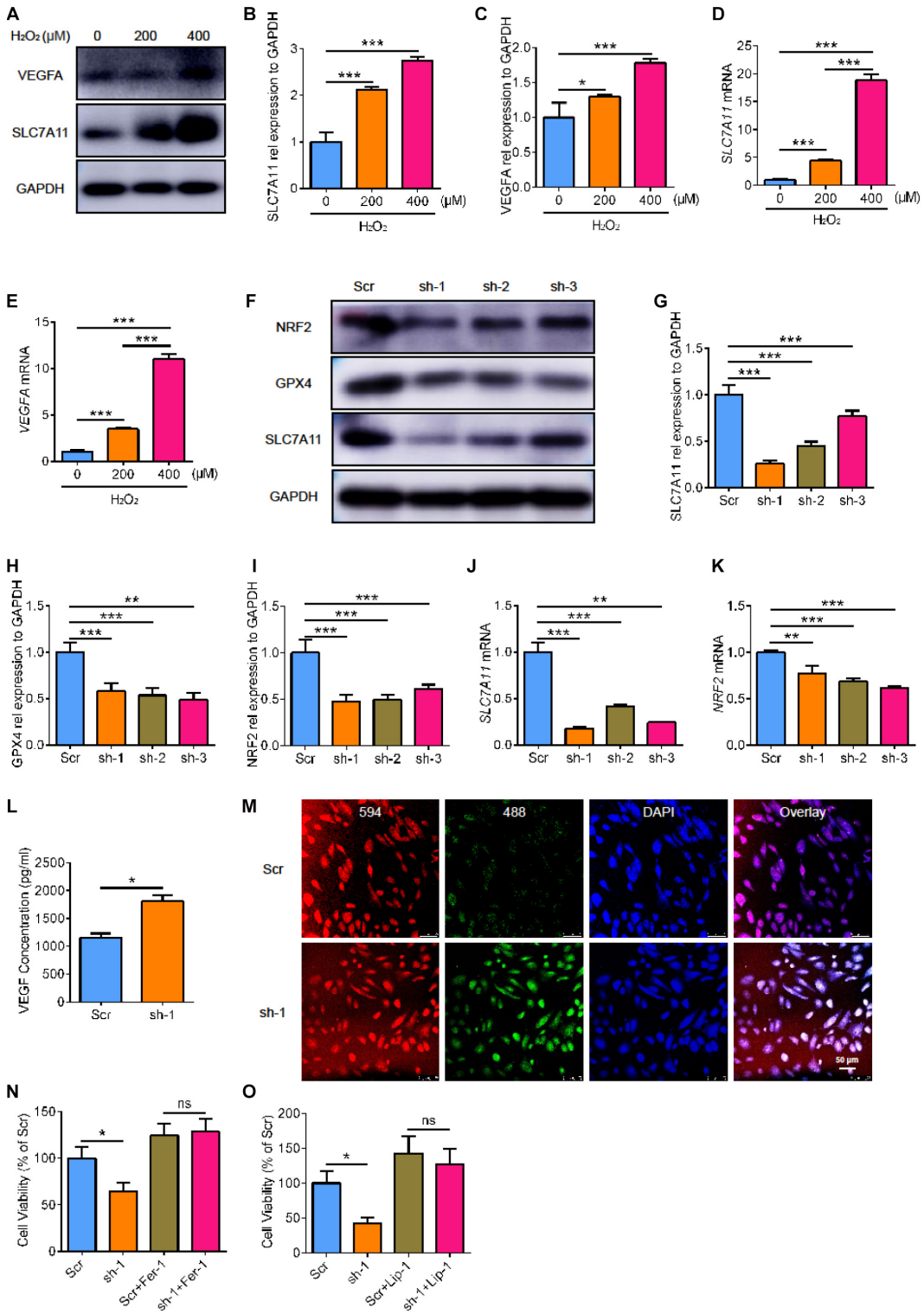

FIGURE 4 | The cell viability and lipid peroxidation level of *SLC7A11*^{KD} ARPE19. **(A–C)** The protein expression of SLC7A11 and VEGFA in ARPE19 with different concentration of H_2O_2, including 0, 200, 400 μM (n = 3). **(D,E)** The mRNA level of *SLC7A11* and *VEGFA* in ARPE19 with different concentration of H_2O_2 (n = 6). **(F–I)** The expression of SLC7A11, GPX4, and NRF2 protein using shRNA to knock down *SLC7A11* (n = 3). **(J,K)** The mRNA of *SLC7A11* and *NRF2* using shRNA to knock down *SLC7A11* (n = 6). **(L)** The concentration of VEGF of *SLC7A11*^{KD} ARPE19 by ELISA (n = 5). **(M)** The level of lipid peroxidation of *SLC7A11*^{KD} ARPE19 by BODIPY^{TM} 581/591 (n = 5). **(N,O)** The cell viability of *SLC7A11*^{KD} ARPE19 with the treatment of Fer-1 (1000 nM) and Lip-1 (20 μM) (n = 6). Bar graphs show mean ± SD. *P*-values: T-test and one-way ANOVA analysis. (***$p < 0.001$, **$p < 0.01$, *$p < 0.05$). Scale bar = 50 μm.

protein and mRNA expression of SLC7A11 (**Figures 4F,G,J**, $p < 0.05$). Interestingly, we found that knocking down *SLC7A11* led to lower expression of NRF2 at both protein and mRNA levels compared to control group (**Figures 4F,I,K**, $p < 0.05$). This suggests that SLC7A11 regulates NRF2 expression at the transcription and translation levels. After exposure to H_2O_2, $SLC7A11^{KD}$ ARPE19 expressed less GPX4 (**Figures 4F,H**, $p < 0.05$). This indicated that SLC7A11 regulated the expression of GPX4. In $SLC7A11^{KD}$ ARPE19 supernatant, we observed upregulation of VEGF which indicated *SLC7A11* loss has an effect on ARPE19 expression of VEGF (**Figure 4L**, $p < 0.05$). We next detected oxidation by the ratiometric fluorescent lipid peroxidation sensor BODIPY^{TM} 581/591. $SLC7A11^{KD}$ ARPE19 exhibited higher levels of lipid peroxidation compared to normal cells, which suggests that SLC7A11 inhibited lipid peroxidation (**Figure 4M** and **Supplementary Figure 1A**). We observed lower cell viability in $SLC7A11^{KD}$ ARPE19 cells rather than control cells (**Figure 4N,O**, $p < 0.05$). To test whether ARPE19 cells undergo ferroptotic death upon *SLC7A11* inhibition, we treated ARPE19 with the potent ferroptosis inhibitors ferrostatin-1 (Fer-1) and liproxstatin-1 (Lip-1) (Zilka et al., 2017). We found that ferroptosis-rescuing antioxidant Fer-1 and Lip-1 rescued the decreased cell viability caused by *SLC7A11* deletion using CCK-8 and PI staining (**Figures 4N,O** and **Supplementary Figure 1B**, $p < 0.05$). This shows that $SLC7A11^{KD}$ ARPE19 undergo ferroptotic death.

Next, we used the SLC7A11 inhibitor, sulfasalazine (SAS), to stimulate the ARPE19 cell line. We examined the level of glutathione (GSH) and found that as the concentration of SAS increased, the level of GSH decreased. This indicated that SAS inhibited the function of SLC7A11 (**Figure 5A**, $p < 0.05$). We detected VEGF in cell supernatant by enzyme linked immunosorbent assay (ELISA) and found that the treatment of SAS increased the concentration of VEGF (**Figure 5B**, $p < 0.05$). This suggests that inhibition of SLC7A11 promoted the expression of VEGF. As the concentration of SAS increased, the expression of GPX4 in ARPE decreased, indicating a decrease in antioxidant capacity (**Figures 5C,D**, $p < 0.05$). We noticed that cell viability decreased as SAS concentration increased, which could be rescued by Fer-1 (**Figures 5E,F** and **Supplementary Figure 2A**, $p < 0.05$). However, Lip-1 only partially alleviates the decline in cell viability caused by SAS, because of the possible toxic effect of SAS itself, which has been reported in previous studies (**Figure 5G** and **Supplementary Figure 2A**, $p < 0.05$) (Linares et al., 2011; Li et al., 2020; Zheng et al., 2020). Similarly, SAS increased the ARPE19 lipid peroxidation level, detected by flow and immunofluorescence (**Figures 5H–J** and **Supplementary Figure 2B**, $p < 0.05$). This shows that inhibition of SLC7A11 enhanced lipid peroxidation and promoted ARPE19 to undergo ferroptosis.

SLC7A11 Overexpression Induces Ferroptosis Resistance

To further investigate the functional relevance of SLC7A11 in RPE biology, SLC7A11 plasmid was transfected into ARPE19 cells ($SLC7A11^{OE}$). SLC7A11 protein and mRNA levels were confirmed by Western blot and quantitative RT-PCR (**Figures 6A,B,D**, $p < 0.05$). We found that fostered *SLC7A11* expression upregulated significantly *NRF2* mRNA (**Figure 6E**, $p < 0.05$). Furthermore, increased NRF2 protein levels were accompanied by enhanced levels of SLC7A11 (**Figures 6A,C**, $p < 0.05$). We then analyzed the *VEGFA* mRNA levels of $SLC7A11^{OE}$ cells. Noteworthy, $SLC7A11^{OE}$ cells expressed lower amounts of *VEGFA* compared to control cells (**Figure 6F**, $p < 0.05$). To test the sensitivity to ferroptosis of $SLC7A11^{OE}$ cells, we treated ARPE19 cells with ferroptosis inducer erastin and GPX4 inhibitors 1S, 3R-RSL3 (RSL3). $SLC7A11^{OE}$ cells were resistant to erastin and RSL3 compared to control cells (**Figures 6G,H** and **Supplementary Figure 3**, $p < 0.05$). To compare the cell viability between $SLC7A11^{OE}$ and anti-VEGF treatment, ARPE19 treated with anti-VEGF or $SLC7A11^{OE}$ were perform*ed sim*ultaneously. As shown below, there is no significant difference between anti-VEGF treatment and NC group, which means anti-VEGF treatment has no effects on the ferroptosis (**Figure 6I**, $p < 0.05$). Altogether, these results demonstrate that SLC7A11 confers a ferroptosis-resistance phenotype in RPE cells and targeting SLC7A11 provides a method for increasing ferroptotic susceptibility in RPE cells.

SLC7A11 Inhibition Promotes the Development of CNV

To further verify the role of SLC7A11 in the process of neovascularization, we intraperitoneally injected SAS or PBS once a day, from 7 days before laser treatment to 7 days after laser treatment. At 7 dpi, we performed fluorescence angiography and isolated choroid for immunofluorescence (**Figure 7A**). After SAS-treatment, the CNV area was larger than PBS group in both fluorescence angiography and immunofluorescence (**Figures 7B–F**, $p < 0.05$). This implies that SLC7A11 plays a protective role in CNV progress.

Regulatory Relationship Between NRF2 and SLC7A11

We found a complex regulatory relationship between SLC7A11 and NRF2, the major antioxidant transcription factor. Considering that after SLC7A11 knocked down or overexpressed, the expression level of NRF2 also changed, so we speculated that the expression of SLC7A11 could regulate the expression of NRF2.

On the other hand, some studies supported NRF2 as one of the upstream regulators of SLC7A11. Therefore, we used small interfering RNA to knock down the expression of *NRF2* in ARPE19 (**Figures 8A,B,E**, $p < 0.05$). After knocking down *NRF2*, we found that the expression of SLC7A11 decreased, which comported with previous studies (**Figures 8A,C,F**, $p < 0.05$) (Liu et al., 2017; Shin et al., 2017). Moreover, the lower level of NRF2 was accompanied by a decrease of GPX4 (**Figures 8A,D**, $p < 0.05$). This suggests that NRF2 and SLC7A11 form a positive feedback loop; they strengthen each other, regulating the downstream GPX4 and ferroptosis.

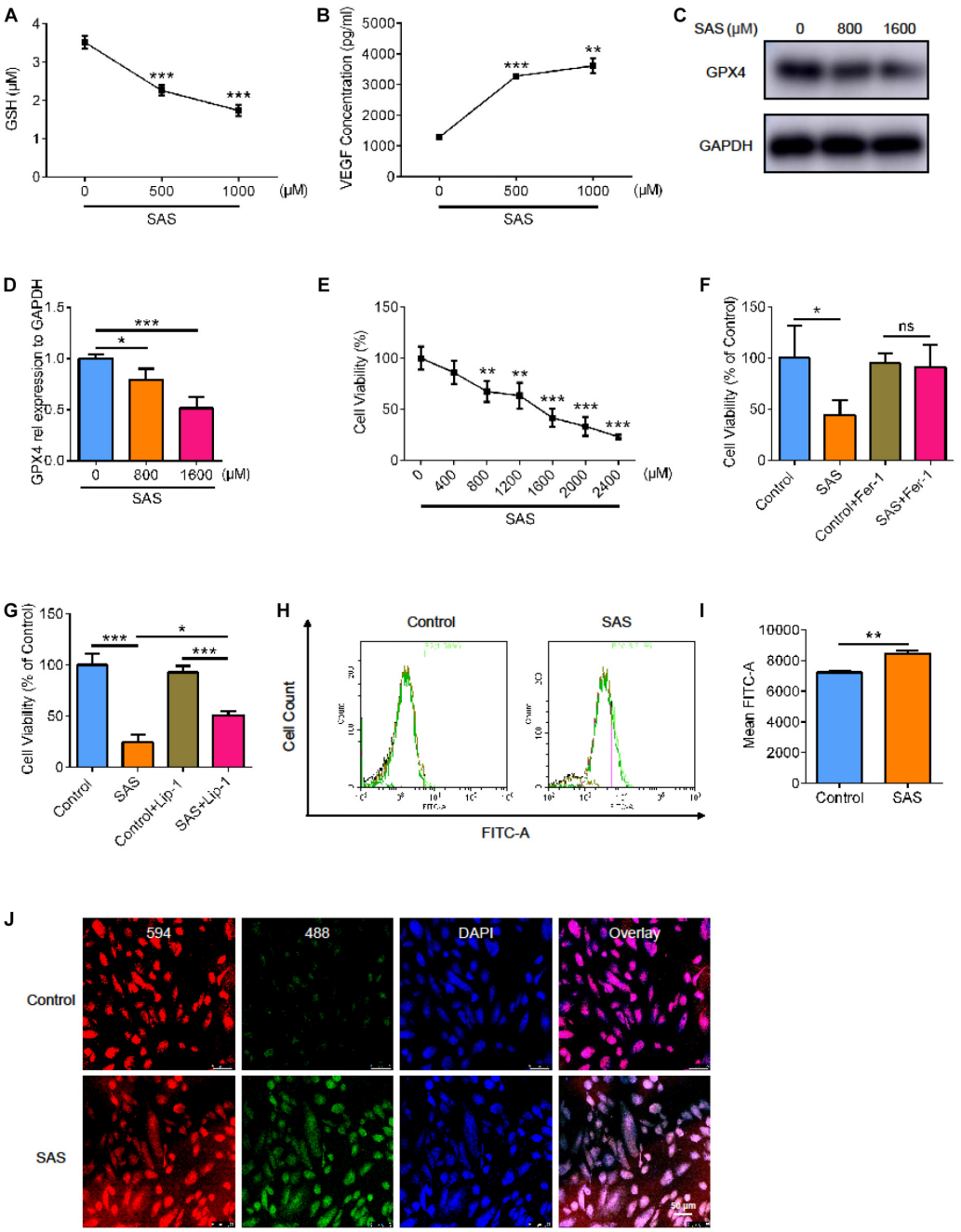

FIGURE 5 | The effect of SLC7A11 inhibitor on ARPE cell line. **(A)** The GSH of ARPE19 with different concentration of SAS ($n = 5$). **(B)** The concentration of VEGF of ARPE19 with SAS stimulation by ELISA ($n = 5$). **(C,D)** The protein expression of GPX4 with different concentration of SAS ($n = 3$). **(E)** The cell viability of ARPE19 with different concentration of SAS ($n = 5$). **(F,G)** The cell viability of ARPE19 with treatment of Fer-1 (1000 nM) or Lip-1 (20 μM) after stimulation of 1600 μM SAS ($n = 6$). **(H–J)** The level of lipid peroxidation under SAS stimulation by BODIPY^{TM} 581/591 ($n = 5$). Bar graphs show mean ± SD. *P*-values: one-way ANOVA analysis and *t*-test (***$p < 0.001$, **$p < 0.01$, *$p < 0.05$). Scale bar = 50 μm.

DISCUSSION

In clinical practice, AMD imposes a huge economic burden on society because of its damage to eyesight. Treatment with anti-vascular endothelial growth factor (anti-VEGF) has greatly improved the vision of AMD patients and their quality of life. However, there are individual differences in the treatment of anti-VEGF (Amoaku et al., 2015; Yang et al., 2016). Despite the more active targeted therapy, some AMD patients still show an unremitting decline in visual acuity accompanied by the aggravation of macular morphology. In addition, many AMD patients require long-term anti-VEGF treatment, and repeated

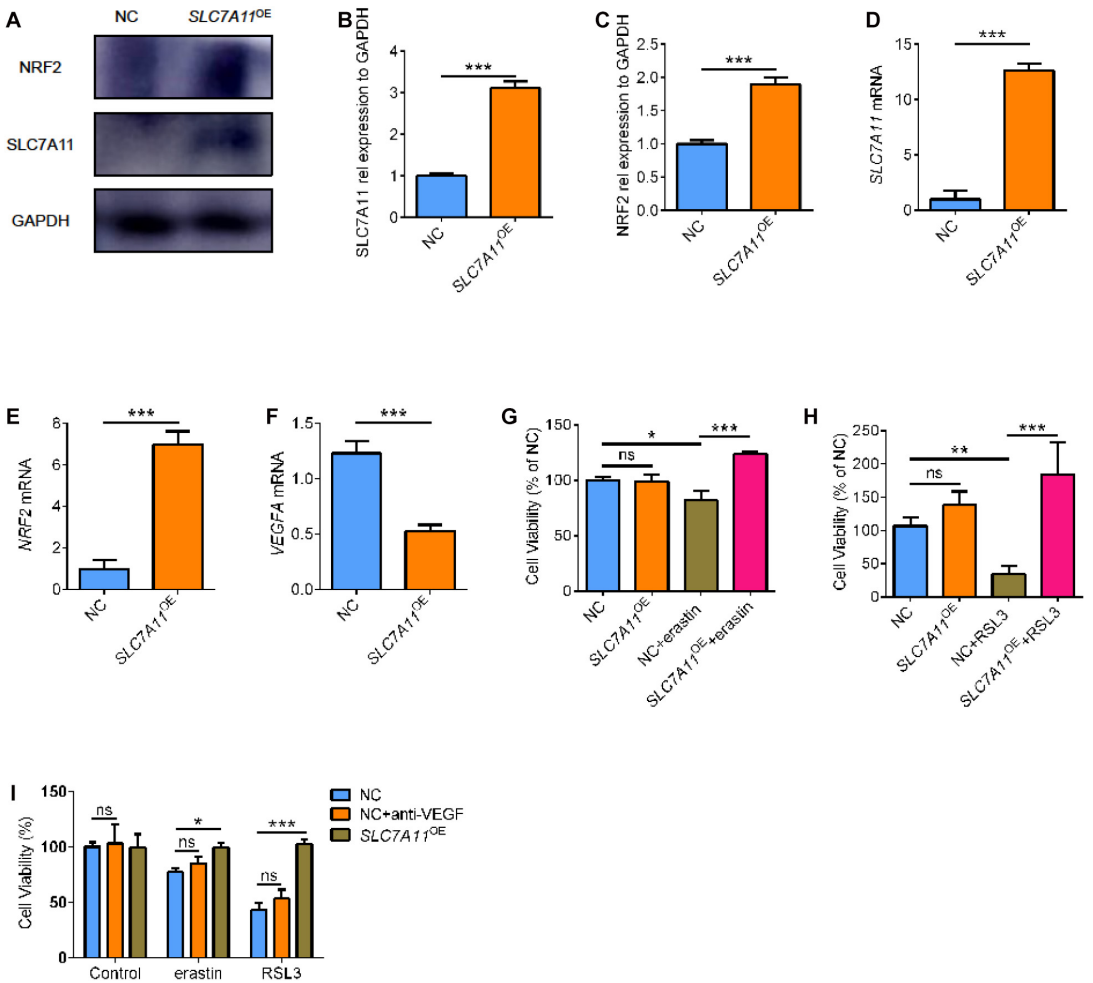

FIGURE 6 | The cell viability of *SLC7A11*^{OE} ARPE19. **(A–C)** SLC7A11 and NRF2 protein in *SLC7A11*^{OE} ARPE19 were evaluated by Western blot (n = 3). **(D–F)** *SLC7A11*, *NRF2*, and *VEGFA* mRNA in *SLC7A11*^{OE} ARPE19 were evaluated by RT-PCR (n = 6). **(G,H)** The cell viability of *SLC7A11*^{OE} ARPE19 with the stimulation of erastin (200 μM) or RSL3 (20 μM) (n = 5). **(I)** The cell viability of anti-VEGF treatment and *SLC7A11*^{OE} ARPE19 with the stimulation of erastin (200 μM) or RSL3 (20 μM) (n = 5). Bar graphs show mean ± SD. P-values: one-way ANOVA analysis and t-test (***$p < 0.001$, **$p < 0.01$, *$p < 0.05$).

intraocular injections may cause atrophy of the retina and choroid, which also causes vision loss (Gemenetzi et al., 2017). We hoped to find a general cellular mechanism to explain neovascularization in the course of AMD to find a solution for non-responding patients and patients who need repeated injections to address the deficiencies of anti-VEGF.

Previous studies have shown that in neovascular AMD, RPE and other cells produce VEGF in a hypoxic environment, which promotes the formation and expansion of neovascularization (Bhutto and Lutty, 2012). RPE absorbs excess light and devours the outer section of the photoreceptor filled with unsaturated fatty acids. Thus, RPE consumes a large amount of oxygen and it requires RPE to reserve sufficient capacity to resist oxidative stress. With the increase of age, RPE accumulates too much active oxygen, and its ability to resist oxidative damage decreases. Previous studies have shown that RPE undergoes necrosis and apoptosis under oxidative stress (Hanus et al., 2015). Recent research has shown that RPE cells induced ferroptosis because of the effects of glutamic acid (Sun et al., 2018) and oxidative stress (Totsuka et al., 2019; Lee et al., 2020). However, the ferroptosis of RPE cells *in vivo* is still poorly understood. Our results suggest that SLC7A11 and its-related ferroptosis are involved in the progress of laser-induced CNV. SLC7A11 protects RPE and reduces the CNV area by preventing ferroptosis in RPE.

First, in the laser-induced CNV model, the expression of SLC7A11 in CNV increased, reaching a peak at 7 days. Besides SLC7A11, many molecules related to oxidative stress, including HO-1, GCLC, and NQO1, also peaked at 3 days after the laser treatment. This indicates that the oxidative damage of CNV also peaked at that time. Moreover, VEGFA, closely related to the occurrence and development of CNV, also peaked. It is no doubt that oxidative stress is involved in the formation and expansion of CNV, and our study once again provides conclusive evidence for this. In our *in vitro* experiments, we found that RPE cells expressed more VEGF with increasing H_2O_2 concentration. To

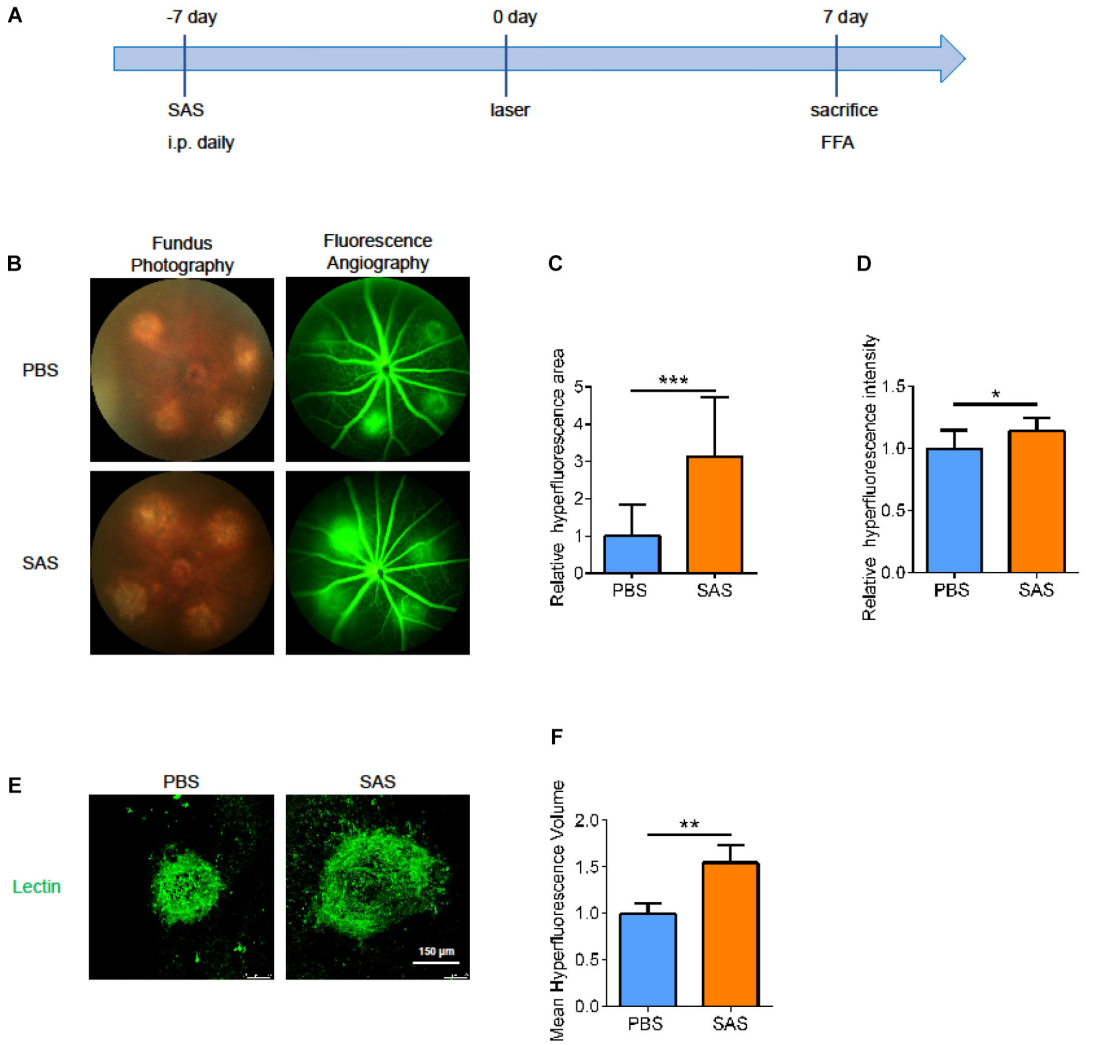

FIGURE 7 | The effect of SLC7A11 inhibitors on CNV areas. **(A)** Schematic diagram of mice administrated SAS. **(B)** Fluorescence imaging of mice after SAS treatment. **(C,D)** The average fluorescence intensity and leakage volume of fluorescence imaging after SAS treatment by Image-J ($n = 6$). **(E,F)** Laser spot size after SAS treatment by immunofluorescence and Image-J ($n = 6$). Bar graphs show mean ± SD. *P*-values: *t*-test (***$p < 0.001$, **$p < 0.01$, *$p < 0.05$). Scale bar = 150 μm.

resist oxidative damage, RPE highly expressed some protective molecules, such as SLC7A11 for compensation.

Second, we also clarified the important regulatory role of SLC7A11 in this process. SLC7A11, as a key component of cystine/glutamate transporter on cell membranes, is an important molecule to buffer oxidative stress injury by regulating the quantity and proportion of intracellular and extracellular GSH (Koppula et al., 2018). In our study, the expression of SLC7A11 increased after laser treatment, and the laser area expanded after using the inhibitor SAS. This illustrates the protective role of SLC7A11 in the progress of CNV. Similarly, ARPE19 expressed more SLC7A11 after being stimulated with H_2O_2. As SAS concentration increased, ARPE19 induced ferroptosis by reducing intracellular GSH levels. It also exhibited lower cell viability and higher lipid peroxidation levels.

Third, we explored the mechanism of SLC7A11 protection on RPE. On the 3rd day after laser irradiation, the expression of SLC7A11 increased and there was an increase of GPX4. The high expression of SLC7A11 shows that, after laser treatment, the tissue needs more cystine to enter the cell and synthesize more GSH. GPX4, as an indispensable regulator of ferroptosis, catalyzes the conversion of GSH to GSSG to exert its antioxidant effect (Yang et al., 2014). Therefore, the simultaneous increase of SLC7A11 and GPX4 suggests that the cells were suffering from powerful oxidative stress and required a strong antioxidant capacity. At 7 dpi, the levels of SLC7A11 increased and GPX4 decreased to some extent, and the expression of oxidative stress-related protein also decreased. Therefore, SLC7A11 and GPX4 were consistent with the level of oxidative stress in the environment, indicating that SLC7A11 is sensitive and timely. In ARPE19, we used SAS to suppress SLC7A11 or shRNA to knock

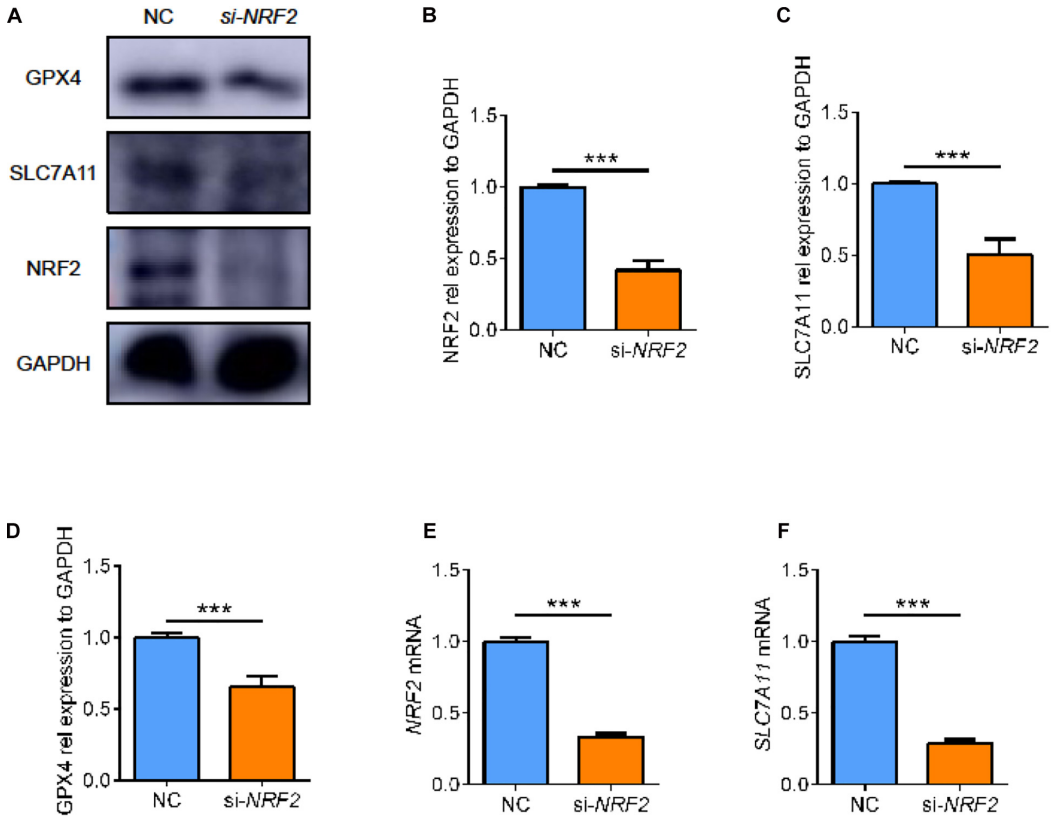

FIGURE 8 | The effect of *NRF2* knockdown on ARPE cell line. **(A–D)** The protein expression level of NRF2, SLC7A11, and GPX4 using siRNA ($n = 3$). **(E,F)** The mRNA expression level of *NRF2* and *SLC7A11* using siRNA ($n = 6$). Bar graphs show mean ± SD. *P*-values: *t*-test (***$p < 0.001$).

it down, and GPX4 showed a consistent downward trend. At the same time, ARPE19 also showed higher lipid peroxidation levels and lower cell viability, implying RPE was undergoing ferroptosis. These results show that SLC7A11 balances the production of effector molecules, and it protects cells from ferroptosis by regulating the expression of GPX4. In oncology, many studies have shown that the inhibition of SLC7A11 is directly related to ferroptosis (Jiang et al., 2015; Lang et al., 2019). But in the eyes, especially neovascular AMD, little is known about the ferroptosis of RPE. Our research fills the gap in the study of ferroptosis in this field, and it proposes some possible mechanisms.

In addition, we found complex interactions between NRF2 and SLC7A11, such that they form a positive feedback loop and strengthen each other to regulate downstream GPX4 and ferroptosis. We used small interfering RNA to knock down NRF2 and found that SLC7A11 fell with it. Interestingly, when we used short-hairpin RNA to knock down SLC7A11, we noticed that NRF2 showed a corresponding decline. Conversely, SLC7A11 overexpression induced higher expression of NRF2 compared to control cells. Previous studies have noted that NRF2 regulates the expression of SLC7A11, but we found a change that SLC7A11 can also affect the expression of NRF2. This has been confirmed by our study. We speculated that the positive feedback regulation between NRF2 and SLC7A11 may function as protection against oxidative stress. More specific regulatory mechanisms for NRF2 and SLC7A11 require more attention.

However, there were some aspects of the experiment worth improving. We lacked more detailed verification and explanation to further prove the complex relationship between NRF2 and SLC7A11.

In conclusion, our study proposed a possible new mechanism in RPE in the laser-induced CNV model, namely SLC7A11 and its suppressed ferroptosis. SLC7A11 could play an antioxidant role, protect cells from ferroptosis, and reduce CNV areas by activating or increasing GPX4. It provides a new therapeutic idea for neovascular AMD patients who are clinically insensitive to anti-VEGF treatment or who require repeated injections that cause side effects. Delivery of target gene DNA to specific tissue by AAV is powerful technology in the field of gene therapy. And in the future, delivery of SLC7A11 to RPE by AAV would become a possible clinical method to protect the cell from ferroptosis in the neovascular AMD patients.

DATA AVAILABILITY STATEMENT

The original contributions presented in the study are included in the article/**Supplementary Material**, further inquiries can be directed to the corresponding authors.

ETHICS STATEMENT

The animal study was reviewed and approved by the Association for Research in Vision and Ophthalmology Statement for the Use of Animals in Ophthalmic and Vision Research. Written informed consent was obtained from the owners for the participation of their animals in this study.

AUTHOR CONTRIBUTIONS

XZ, MG, and JL conceived the study, designed the experiments, and performed the experiments with the help of YC, YiW, YuW, YX, and ZZ. XZ wrote the manuscript. XW, MJ, XL, FW, and XS interpreted the data and contributed to discussion. XS and FW were the guarantor of this work and as such, had full access to all the data in the study and took responsibility for the integrity of the data and the accuracy of the data analysis. All authors reviewed and concurred with the final manuscript.

FUNDING

This study was supported by grants from the National Natural Science Foundation of China (81730026), the National Key R&D Program (2017YFA0105301), the National Major Scientific and Technological Special Project for "Significant New Drugs Development" during the Thirtieth Five-year Plan Period (2019ZX09301113), the Science and Technology Commission of Shanghai Municipality (17411953000 and 19495800700), Shanghai Collaborative Innovation Center for Translational Medicine (TM201917) to XS, the Program for Professor of Special Appointments (Eastern Scholar) at Shanghai Institutions of Higher Learning, and the Top Young Talent Program of Shanghai to FW.

SUPPLEMENTARY MATERIAL

The Supplementary Material for this article can be found online at: https://www.frontiersin.org/articles/10.3389/fcell.2021.639851/full#supplementary-material

Supplementary Figure 1 | The level of lipid peroxidation and cell death of *SLC7A11^{KD}* ARPE19. **(A)** The level of lipid peroxidation of *SLC7A11^{KD}* ARPE19 by BODIPY^{TM} 581/591. **(B)** Immunofluorescence for PI staining of *SLC7A11^{KD}* ARPE19 with the treatment of Fer-1 (1000 nM) and Lip-1 (20 μM). Scale bar = 50 μm.

Supplementary Figure 2 | The level of lipid peroxidation and cell death of ARPE19 after SAS treatment. **(A)** Immunofluorescence for PI staining of ARPE19 with the treatment of Fer-1 (1000 nM) and Lip-1 (20 μM) after SAS treatment. **(B)** The level of lipid peroxidation under SAS stimulation by BODIPY^{TM} 581/591. Scale bar = 50 μm.

Supplementary Figure 3 | The cell death of *SLC7A11^{OE}* ARPE19 with PI staining. Immunofluorescence for PI staining of *SLC7A11^{OE}* ARPE19 with the treatment of erastin (200 μM) or RSL3 (20 μM). Scale bar = 50 μm.

REFERENCES

Al Gwairi, O., Thach, L., Zheng, W. H., Osman, N., and Little, P. J. (2016). Cellular and molecular pathology of age-related macular degeneration: potential role for proteoglycans. *J. Ophthalmol.* 2016:2913612.

Al-Latayfeh, M., Silva, P. S., Sun, J. K., and Aiello, L. P. (2012). Antiangiogenic therapy for ischemic retinopathies. *Cold Spring Harb. Perspec. Med.* 2:a006411. doi: 10.1101/cshperspect.a006411

Al-Zamil, W. M., and Yassin, S. A. (2017). Recent developments in age-related macular degeneration: a review. *Clinical Interv. Aging* 12, 1313–1330. doi: 10.2147/cia.s143508

Amoaku, W. M., Chakravarthy, U., Gale, R., Gavin, M., Ghanchi, F., Gibson, J., et al. (2015). Defining response to anti-VEGF therapies in neovascular AMD. *Eye* 29, 721–731. doi: 10.1038/eye.2015.48

Arjamaa, O., Aaltonen, V., Piippo, N., Csont, T., Petrovski, G., Kaarniranta, K., et al. (2017). Hypoxia and inflammation in the release of VEGF and interleukins from human retinal pigment epithelial cells. *Graefes Arch. Clin. Exp. Ophthalmol.* 255, 1757–1762. doi: 10.1007/s00417-017-3711-0

Bersuker, K., Hendricks, J. M., Li, Z., Magtanong, L., Ford, B., Tang, P. H., et al. (2019). The CoQ oxidoreductase FSP1 acts parallel to GPX4 to inhibit ferroptosis. *Nature* 575, 688–692. doi: 10.1038/s41586-019-1705-2

Bhutto, I., and Lutty, G. (2012). Understanding age-related macular degeneration (AMD): relationships between the photoreceptor/retinal pigment epithelium/Bruch's membrane/choriocapillaris complex. *Mol. Aspects Med.* 33, 295–317. doi: 10.1016/j.mam.2012.04.005

Christova, Y., James, P. S., and Jones, R. (2004). Lipid diffusion in sperm plasma membranes exposed to peroxidative injury from oxygen free radicals. *Mol. Reproduc.Dev.* 68, 365–372. doi: 10.1002/mrd.20084

Gemenetzi, M., Lotery, A. J., and Patel, P. J. (2017). Risk of geographic atrophy in age-related macular degeneration patients treated with intravitreal anti-VEGF agents. *Eye* 31, 1–9. doi: 10.1038/eye.2016.208

Hanus, J., Anderson, C., and Wang, S. (2015). RPE necroptosis in response to oxidative stress and in AMD. *Ageing Res. Rev.* 24, 286–298. doi: 10.1016/j.arr.2015.09.002

Ishikawa, K., Kannan, R., and Hinton, D. R. (2016). Molecular mechanisms of subretinal fibrosis in age-related macular degeneration. *Exp. Eye Res.* 142, 19–25. doi: 10.1016/j.exer.2015.03.009

Jiang, L., Kon, N., Li, T., Wang, S. J., Su, T., Hibshoosh, H., et al. (2015). Ferroptosis as a p53-mediated activity during tumour suppression. *Nature* 520, 57–62. doi: 10.1038/nature14344

Kannan, R., Zhang, N., Sreekumar, P. G., Spee, C. K., Rodriguez, A., Barron, E., et al. (2006). Stimulation of apical and basolateral VEGF-A and VEGF-C secretion by oxidative stress in polarized retinal pigment epithelial cells. *Mol. Vis.* 12, 1649–1659.

Koppula, P., Zhang, Y., Zhuang, L., and Gan, B. (2018). Amino acid transporter SLC7A11/xCT at the crossroads of regulating redox homeostasis and nutrient dependency of cancer. *Cancer Commun.* 38:12. doi: 10.1186/s40880-018-0288-x

Lang, X., Green, M. D., Wang, W., Yu, J., Choi, J. E., Jiang, L., et al. (2019). Radiotherapy and immunotherapy promote tumoral lipid oxidation and ferroptosis via synergistic repression of SLC7A11. *Cancer Discov.* 9, 1673–1685. doi: 10.1158/2159-8290.cd-19-0338

Lee, J. J., Ishihara, K., Notomi, S., Efstathiou, N. E., Ueta, T., Maidana, D., et al. (2020). Lysosome-associated membrane protein-2 deficiency increases the risk of reactive oxygen species-induced ferroptosis in retinal pigment epithelial cells. *Biochem. Biophy. Res. Commun.* 521, 414–419. doi: 10.1016/j.bbrc.2019.10.138

Li, Y. C., Shen, J. D., Lu, S. F., Zhu, L. L., Wang, B. Y., Bai, M., et al. (2020). Transcriptomic analysis reveals the mechanism of sulfasalazine-induced liver injury in mice. *Toxicol. Lett.* 321, 12–20. doi: 10.1016/j.toxlet.2019.12.011

Linares, V., Alonso, V., and Domingo, J. L. (2011). Oxidative stress as a mechanism underlying sulfasalazine-induced toxicity. *Exp. Opin. Drug Safety* 10, 253–263. doi: 10.1517/14740338.2011.529898

Liu, D. S., Duong, C. P., Haupt, S., Montgomery, K. G., House, C. M., Azar, W. J., et al. (2017). Inhibiting the system x/glutathione axis selectively targets cancers with mutant-p53 accumulation. *Nat. Commun.* 8:14844.

Nasca, C., Bigio, B., Zelli, D., de Angelis, P., Lau, T., Okamoto, M., et al. (2017). Role of the astroglial glutamate exchanger xCT in ventral hippocampus in resilience to stress. *Neuron* 96, 402–413. doi: 10.1016/j.neuron.2017.09.020

Nazari, M., Salabi, F., Zhang, L., Zhao, F., Wei, C., Du, L., et al. (2014). AAV2-mediated follistatin overexpression induces ovine primary myoblasts proliferation. *BMC Biotechnol.* 14:87. doi: 10.1186/s12896-014-0087-7

Nowak, M., Swietochowska, E., Wielkoszyński, T., Marek, B., Karpe, J., Górski, J., et al. (2003). Changes in blood antioxidants and several lipid peroxidation products in women with age-related macular degeneration. *Eur. J. Ophthalmol.* 13, 281–286. doi: 10.1177/112067210301300307

Paeng, S. H., Jung, W. K., Park, W. S., Lee, D. S., Kim, G. Y., Choi, Y. H., et al. (2015). Caffeic acid phenethyl ester reduces the secretion of vascular endothelial growth factor through the inhibition of the ROS, PI3K and HIF-1α signaling pathways in human retinal pigment epithelial cells under hypoxic conditions. *Int. J. Mol. Med.* 35, 1419–1426. doi: 10.3892/ijmm.2015.2116

Rosenberg, M., Azevedo, N. F., and Ivask, A. (2019). Propidium iodide staining underestimates viability of adherent bacterial cells. *Sci. Rep.* 9:6483.

Seiler, A., Schneider, M., Förster, H., Roth, S., Wirth, E. K., Culmsee, C., et al. (2008). Glutathione peroxidase 4 senses and translates oxidative stress into 12/15-lipoxygenase dependent- and AIF-mediated cell death. *Cell Metab.* 8, 237–248. doi: 10.1016/j.cmet.2008.07.005

Shibuya, M. (2011). Vascular endothelial growth factor (VEGF) and its receptor (VEGFR) signaling in angiogenesis: a crucial target for anti- and Pro-angiogenic therapies. *Genes Cancer* 2, 1097–1105. doi: 10.1177/1947601911423031

Shin, C. S., Mishra, P., Watrous, J. D., Carelli, V., D'Aurelio, M., Jain, M., et al. (2017). The glutamate/cystine xCT antiporter antagonizes glutamine metabolism and reduces nutrient flexibility. *Nat. Commun.* 8:15074.

Sun, Y., Zheng, Y., Wang, C., and Liu, Y. (2018). Glutathione depletion induces ferroptosis, autophagy, and premature cell senescence in retinal pigment epithelial cells. *Cell. Death Dis.* 9:753.

Totsuka, K., Ueta, T., Uchida, T., Roggia, M. F., Nakagawa, S., Vavvas, D. G., et al. (2019). Oxidative stress induces ferroptotic cell death in retinal pigment epithelial cells. *Exp. Eye Res.* 181, 316–324. doi: 10.1016/j.exer.2018.08.019

Wong, W. L., Su, X., Li, X., Cheung, C. M., Klein, R., Cheng, C. Y., et al. (2014). Global prevalence of age-related macular degeneration and disease burden projection for 2020 and 2040: a systematic review and meta-analysis. *Lancet. Glob. Health* 2, e106–e116.

Xiao, M., Liu, Y., Wang, L., Liang, J., Wang, T., Zhai, Y., et al. (2019). Intraocular VEGF deprivation induces degeneration and fibrogenic response in retina. *FASEB J.* 33, 13920–13934. doi: 10.1096/fj.201901283rr

Yang, P., Peairs, J. J., Tano, R., and Jaffe, G. J. (2006). Oxidant-mediated Akt activation in human RPE cells. *Invest. Ophthalmol. Vis. Sci.* 47, 4598–4606. doi: 10.1167/iovs.06-0140

Yang, S., Zhao, J., and Sun, X. (2016). Resistance to anti-VEGF therapy in neovascular age-related macular degeneration: a comprehensive review. *Drug Design Dev. Ther.* 10, 1857–1867. doi: 10.2147/dddt.s97653

Yang, W. S., SriRamaratnam, R., Welsch, M. E., Shimada, K., Skouta, R., Viswanathan, V. S., et al. (2014). Regulation of ferroptotic cancer cell death by GPX4. *Cell* 156, 317–331. doi: 10.1016/j.cell.2013.12.010

Yang, W. S., and Stockwell, B. R. (2016). Ferroptosis: death by lipid peroxidation. *Trends Cell Biol.* 26, 165–176. doi: 10.1016/j.tcb.2015.10.014

Yu, H., Guo, P., Xie, X., Wang, Y., and Chen, G. (2017). Ferroptosis, a new form of cell death, and its relationships with tumourous diseases. *J. Cell. Mol. Med.* 21, 648–657. doi: 10.1111/jcmm.13008

Zheng, Z., Luo, G., Shi, X., Long, Y., Shen, W., Li, Z., et al. (2020). The X inhibitor sulfasalazine improves the anti-cancer effect of pharmacological vitamin C in prostate cancer cells via a glutathione-dependent mechanism. *Cell. Oncol.* 43, 95–106. doi: 10.1007/s13402-019-00474-8

Zilka, O., Shah, R., Li, B., Friedmann Angeli, J. P., Griesser, M., Conrad, M., et al. (2017). On the mechanism of cytoprotection by ferrostatin-1 and liproxstatin-1 and the role of lipid peroxidation in ferroptotic cell death. *ACS Central Sci.* 3, 232–243. doi: 10.1021/acscentsci.7b00028

Conflict of Interest: The authors declare that the research was conducted in the absence of any commercial or financial relationships that could be construed as a potential conflict of interest.

frontiers in Cell and Developmental Biology

REVIEW
published: 04 March 2021
doi: 10.3389/fcell.2021.634690

Guidelines for Regulated Cell Death Assays: A Systematic Summary, A Categorical Comparison, A Prospective

Xi-min Hu[1], Zhi-xin Li[1], Rui-han Lin[1], Jia-qi Shan[1], Qing-wei Yu[1], Rui-xuan Wang[1], Lv-shuang Liao[1], Wei-tao Yan[1], Zhen Wang[2], Lei Shang[3], Yanxia Huang[1], Qi Zhang[1] and Kun Xiong[1,4]**

[1] Department of Anatomy and Neurobiology, School of Basic Medical Sciences, Central South University, Changsha, China, [2] Wuxi School of Medicine, Jiangnan University, Wuxi, China, [3] Jiangxi Research Institute of Ophthalmology and Visual Sciences, Affiliated Eye Hospital of Nanchang University, Nanchang, China, [4] Hunan Key Laboratory of Ophthalmology, Changsha, China

Over the past few years, the field of regulated cell death continues to expand and novel mechanisms that orchestrate multiple regulated cell death pathways are being unveiled. Meanwhile, researchers are focused on targeting these regulated pathways which are closely associated with various diseases for diagnosis, treatment, and prognosis. However, the complexity of the mechanisms and the difficulties of distinguishing among various regulated types of cell death make it harder to carry out the work and delay its progression. Here, we provide a systematic guideline for the fundamental detection and distinction of the major regulated cell death pathways following morphological, biochemical, and functional perspectives. Moreover, a comprehensive evaluation of different assay methods is critically reviewed, helping researchers to make a reliable selection from among the cell death assays. Also, we highlight the recent events that have demonstrated some novel regulated cell death processes, including newly reported biomarkers (e.g., non-coding RNA, exosomes, and proteins) and detection techniques.

Keywords: regulated cell death, detecting methods, guidelines, biomarkers, clinical application

OPEN ACCESS

Edited by:
Yinan Gong,
University of Pittsburgh, United States

Reviewed by:
Bradlee Heckmann,
University of South Florida Health, United States
Shuting Zhang,
Broad Institute, United States

***Correspondence:**
Qi Zhang
214056@csu.edu.cn
orcid.org/0000-0001-6300-6491
Kun Xiong
xiongkun2001@163.com
orcid.org/0000-0002-3103-6028

Specialty section:
This article was submitted to Cell Death and Survival, a section of the journal Frontiers in Cell and Developmental Biology

Received: *28 November 2020*
Accepted: *08 February 2021*
Published: *04 March 2021*

Citation:
Hu X-m, Li Z-x, Lin R-h, Shan J-q, Yu Q-w, Wang R-x, Liao L-s, Yan W-t, Wang Z, Shang L, Huang Y, Zhang Q and Xiong K (2021) Guidelines for Regulated Cell Death Assays: A Systematic Summary, A Categorical Comparison, A Prospective. Front. Cell Dev. Biol. 9:634690. doi: 10.3389/fcell.2021.634690

INTRODUCTION

Cell death is generally classified into two types: accidental cell death (ACD) and regulated cell death (RCD). RCD is regarded as reversible and can be blocked by small inhibitors (Wang S. et al., 2017; Cheng et al., 2018; Kumar and Sandhir, 2018; Wang et al., 2019c,d). Various programs of RCD have been described and their research continues to progress, including apoptosis (extrinsic and intrinsic), regulated necrosis (namely necroptosis), autophagy-dependent cell death (e.g., autosis), pyroptosis, ferroptosis, NETosis, parthanatos, entotic cell death, anoikis, lysosome-dependent cell death, and mitotic death (Kroemer et al., 2005; Galluzzi et al., 2018). Both in technical research and mechanism mining, the research into these types of RCDs has made great progress, and we have selected in-depth research and rapid recent development of the knowledge of RCDs as an illustration, including apoptosis, necroptosis, autophagy, pyroptosis, ferroptosis, and NETosis.

With the development of RCD studies, the detection methods have been improved simultaneously and diversified for accurate identification and systematic analysis. The history of RCDs began in 1842 when dying cells were noticed by Karl Vogt in toads (Tang et al., 2019). In Lockshin and Williams (1964) reported an orderly and predictable pattern of birth and death at the cellular level, called metamorphosis, a phenomenon with pycnotic nuclei, shrunken and degenerated mitochondria, and conspicuous lysosome-like bodies observed *via* light and electron microscopy (EM) (Lockshin and Williams, 1964, 1965). Apoptosis was termed "shrinkage necrosis" in Kerr (1971); Kerr et al. (1972) distinguished two types of cell death (apoptosis and necrosis) in human pathology samples, focusing on cell morphology, and described necrotic cells as swollen cells with swollen organelles.

The first description of pyroptosis was reported in Zychlinsky et al. (1992), but the term "pyroptosis" was first coined in Cookson and Brennan (2001) after an observation of bacteria-infected macrophages going through a rapidly caspase 1-dependent lytic cell death pathway.

In the early 21st century, necrosis was previously considered to be uncontrollable, but it was recently revised as a partly regulated mechanism, namely necroptosis, involving mitochondrial permeability transition through morphological and biochemical detection (Vercammen et al., 1998; Holler et al., 2000; Baines et al., 2005). The discovery of ferroptosis has come a long way since the 1950s, although it was only named in Dixon et al. (2012). In the following year, the term "autosis" was described by Beth Levine following the observation of a subtype of cell death associated with autophagy induced by nutrient deprivation or Tat-Beclin 1 [one of the peptides inducing autophagy by BECN1 and human immunodeficiency virus (HIV) Tat protein] (Liu et al., 2013). Novel observations regarding neuronal cell death continue to be reported frequently, both refining and redefining known paradigms of cell death, such as apoptosis, necroptosis (Arrazola and Court, 2019), autophagic cell death (Liu and Levine, 2015), ferroptosis (Dixon et al., 2012), and pyroptosis (Fink and Cookson, 2006) (the timeline of the RCDs research is depicted in **Figure 1**).

All of the discovery in RCDs requires accurate identification techniques, including superficial morphological detection, but the changes in detail are indistinguishable at the morphological level. Biochemical detection, which refers to multiple biomarkers, and functional perspectives based on functional changes, such as assays related to the molecular mechanism of the RCD-related genes (Hengartner and Horvitz, 1994), have widely used flow cytometry in RCDs detection, cytosolic DNA assays, and nucleic acid kits (Boldin et al., 1996; Li et al., 1997, 1998; Luo et al., 1998; Paludan et al., 2019). Various signature proteins involved in cell death have been reported and researchers make use of these proteins in cell death assays. The discovery of the main proteins is shown in the timeline in **Figure 1**.

Regulated cell death is closely related to physiological and pathological processes, including inflammation, neurodegenerative diseases, immunological diseases, and cancer (Anderton et al., 2020). Therefore, targeting the regulatory mechanisms of RCD is becoming a great opportunity to discover new therapies to target regulated pathways and identify potential drug targets. They can also act as potential targets in diagnosis and prognostic evaluation. Each of the RCDs has a unique molecular mechanism, with special morphological characteristics, and they have established complex connections with each other. Fully understanding their various detection methods, as well as their advantages, is necessary for the efficiency and accuracy of their detection. We have summarized and compared the signaling pathways regulating cell death, mainly including apoptosis, necrosis, autophagy, ferroptosis, pyroptosis, and NETosis, in these aspects: morphology, biochemistry, and function (a brief summary is available in **Table 1**).

CELL VIABILITY ASSAYS

Once cell death is induced, the plasma membrane integrity would be destroyed, or before losing its integrity, the corpse or fragments of the cell would be engulfed by neighboring cells *in vivo*. The cells' contents can also be exposed or even lost (e.g., the spillage of cytosolic lactate dehydrogenase (LDH), the exposure of DNA), the activity of intracellular enzymes could decline (e.g., succinate dehydrogenase), and a reduction in intracellular adenosine triphosphate (ATP) is observed, which reflects the cellular energy capacity and viability. In view of these phenomena, spectrophotometry, fluorometry, flow cytometry, and microscopy are utilized for cell viability assays.

Spectrophotometry

Spectrophotometry is a qualitative or quantitative analysis of signal material through the absorption of a certain range of wavelengths. Using spectrophotometry to monitor the metabolic activity of cells is regarded as an indicator of cell viability, such as succinate dehydrogenase (SDH) activity analysis, the cytosolic LDH release analysis, certain proteins, and DNA binding by crystal violet staining. The principle of these technologies, in summary, is that the light absorption value of certain markers can be measured by a microplate enzyme for a qualitative or quantitative analysis of cell viability.

Some limitations of SDH activity analysis are as follows: (1) In dead cells, SDH is often still partially active, resulting in being erroneously scored as living cells when it comes to the early stages of apoptosis. (2) Not only cell death, but also other physical and chemical factors can lead to a decrease of enzyme activity, which leads to a false-positive or false-negative result. (3) The activity of an enzyme is variant in different tissue or cells, such as a lesser degree of SDH activity being present in neural and hepatic tissues, which easily leads to errors (Bernocchi and Barni, 1983). (4) The process of MTT conversion is also affected by various conditions, such as the cellular confluency and the culture medium exhaustion, which could lead to under-estimating the cell viability. (5) Some other solutes might elevate background signals by absorbing the same range of wavelengths, such as media containing phenol red, which leads to an increased cell viability range in the assay. All in all, SDH activity analyses of cell viability are usually used in conjunction with other techniques to improve their accuracy.

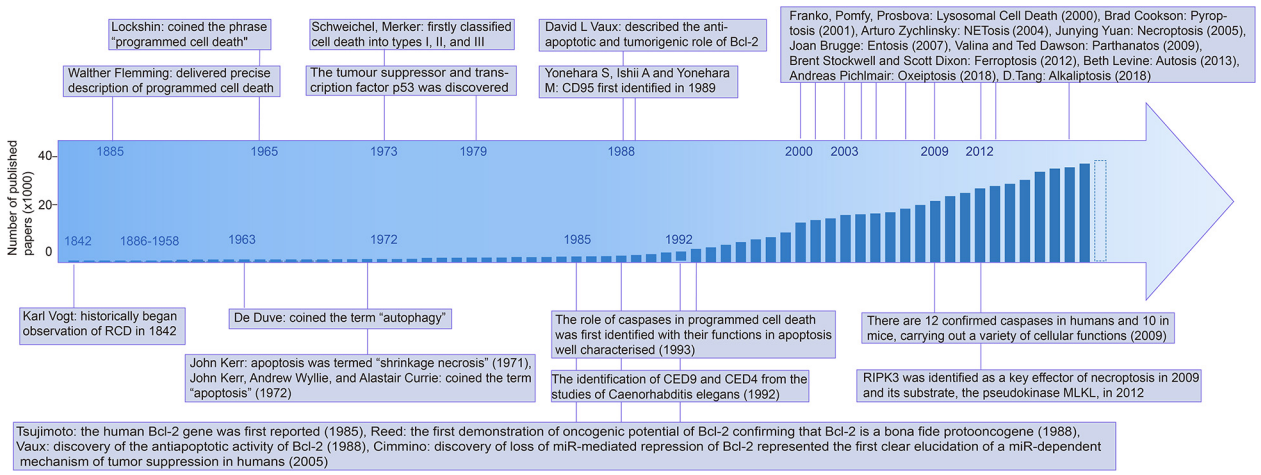

FIGURE 1 | Timeline of the mile stone of cell death research. Abbreviations: Bcl-2: B-cell leukemia/lymphoma-2, CED-9: Cell death abnormality gene 9, RIPK3: Receptor-interacting serine/threonine-protein kinase 3, MLKL: Mixed lineage kinase domain like pseudokinase, PCD: Programmed cell death, CD95: cluster of differentiation 95.

Crystal violet staining binding by certain proteins and DNA is suitable for monitoring the effect of various compounds (e.g., chemotherapeutics) on cell growth or survival as a reliable and quick screening measure (Geserick et al., 2009). However, some of the special cases would be potentially compromised due to the changed adherent properties of cells, such as the proliferative responses that occur in conjunction with cell death responses or the steps of repeated washing, which might sometimes lead to detached living cells, causing artifacts, especially when there is a higher cell density (Feoktistova et al., 2016).

As for the cytosolic LDH release analysis, some caution should be exercised regarding the instability and proteolytic degradation of LDH activity, since some of the factors may interfere with the results, such as the time spent, the pH, and the specific components present in the culture medium (e.g., pyruvate) (Kendig and Tarloff, 2007).

Fluorometry, Flow Cytometry, and Microscopy Assay

The plasma membrane integrity is followed by the exposure of intracellular contents, and the dye could enter and bind to these contents in the dead cell. For identifying leaking cell contents and lost membrane integrity, researchers often use a targeted approach for detection, such as light microscopy to detect trypan blue positive cells, and fluorometry and flow cytometry are used for identifying leaking cell contents. The detailed descriptions of each of these technologies is shown below.

Using technologies such as flow cytometry and light microscopy, the dead cells are indicated indirectly. For example, in DNA-binding, impermeant fluorescent dyes are used for detection, such as propidium iodide (PI), 7-amino actinomycin D (7-AAD) or the Sytox probes (Life Technologies) (Riccardi and Nicoletti, 2006; Zembruski et al., 2012, Thakur et al., 2015). For instance, during apoptosis, PI is able to bind and label DNA fragments and makes it possible to provide a rapid (in about 2 h) and precise method for evaluating intracellular DNA fragments through flow cytometry, and subsequently identifying the hypodiploid cells (Riccardi and Nicoletti, 2006). Compared with crystal violet staining analysis by spectrophotometry as mentioned above, this reduces the steps used to wash cells.

Notably, trypan blue staining could detect all forms of cell death, but differentiating among the specific types of cell death needs further testing (Crowley et al., 2016a). Moreover, other assays for detecting the loss of plasma membrane integrity have been adapted, such as immunocytochemistry to assay protein translocation, and 4′,6′-diamidino-2-phenylindole (DAPI) staining to assay nuclear fragmentation (Crowley et al., 2016b). For example, immunocytochemistry, such as for cytochrome c, is regarded as an essential tool for understanding and characterizing the mitochondrial apoptosis pathway (Crowley et al., 2016c).

DETERMINING CELL MORPHOLOGY OF RCDS

Incipiently, differentiating RCDs usually relied on morphological changes limited by techniques while the three major types of cell death are identified (type I cell death refers to apoptosis, type II cell death corresponds to autophagy-dependent cell death, type III cell death is related to necrosis) (Kerr, 1971; Lin et al., 1973). In Lockshin and Williams (1964) the American biologist Richard A Lockshin thoroughly described PCD (Lockshin and Williams, 1965), and in Kerr et al. (1972), the Australian pathologist John F Kerr and his colleagues coined the term "apoptosis." They analyzed RCDs based on morphological changes. Later, the Nomenclature Committee on Cell Death (NCCD) updated the classification system of cell death through more comprehensive aspects, including classification (Kroemer et al., 2005, 2009), molecular definitions (Galluzzi et al., 2012), essential vs. accessory terms (Galluzzi et al., 2015), and molecular

TABLE 1 | Comparison of five types of RCDs.

Items	Definition	Morphological features	Detecting methods	References
Apoptosis	A vital component of various processes including normal cell turnover, proper development and functioning of the immune system, hormone-dependent atrophy, embryonic development and chemical-induced cell death	Cell shrinkage (pyknosis); DNA fragmentation (karyorrhexis); nuclear condensation; membrane blebbing; apoptotic body formation	DNA fragmentation (DNA ladder assay, TUNEL assay, and comet assay); phosphatidylserine (Annexin V, flow cytometric analysis); bid, p53 (RT-PCR, western blot, immunohistochemistry); caspase activation (western blot, ELISA, flow cytometric analysis); Fas, TNF, TRAIL (RT-PCR, western blot, immunohistochemistry); Cytochrome C release (ELISA)	Saraste and Pulkki, 2000; Hunter et al., 2005; Elmore, 2007; Huerta et al., 2007; Krysko et al., 2008; Majtnerová and Roušar, 2018
Necroptosis	A type of cell death that is caused by the loss of plasma membrane integrity following receptor interacting kinase 3 (RIPK3)-mediated phosphorylation of the pseudokinase mixed lineage kinase domain like (MLKL/pMLKL)	Cell swelling; membrane rupture; retain integral nucleus; translucent cytoplasm	RIPK1, RIPK3, MLKL (immunofluorescent staining); MLKL (quantitative RT-PCR); RIPK1/3, RIP3, MLKL (western blotting); MLKL, RIPK3, RIP1 (ELISA); annexin V–/propidium iodide+ or annexin V+/propidium iodide+ (flow cytometry); RIP1/RIP3 complex (immunoprecipitation and electron microscopy); RIP1 (immunoblotting); membrane translocation (immunofluorescence microscopy and TIRF microscopy);	Aachoui et al., 2013; Chen et al., 2014; He et al., 2016; Gong et al., 2019; Tonnus et al., 2019; Wimmer et al., 2020; Wu Y. et al., 2020
Autophagy	An evolutionarily ancient and highly conserved catabolic process involving the formation of double membraned vesicles called autophagosomes that engulf cellular proteins and organelles for delivery to the lysosome	Lack of chromatin condensation; massive vacuolization of the cytoplasm; accumulation of (double-membraned) autophagic vacuoles; little or no uptake by phagocytic cells	Immune colloidal gold technique; GFP-LC3 or mRFP-GFP-LC3 (immunofluorescence); LC3-II / LC3-I, beclin, ATG5, ATG7, p62 and phosphorylation status of ULK (western blot); LDH sequestration; MDC staining Hsc70 with lysosomal markers (immunofluorescence); LAMP2A (western blot)	Bernocchi and Barni, 1983; Boldin et al., 1996; Broaddus et al., 1996; Boschker and Middelburg, 2002; Brauer, 2003; Brinkmann et al., 2004; Bergsbaken et al., 2009; Burattini and Falcieri, 2013; Braga et al., 2016; Buschhaus et al., 2017, 2018; Bhutia et al., 2019; Yang J. W. et al., 2018
Ferroptosis	An iron-dependent form of regulated cell death caused by unrestricted lipid peroxidation and subsequent membrane damage	The loss of plasma membrane integrity; the leakage of intracellular contents	ATP5G3, PTGS2, IREB2, CS, RPL8 (quantitative real−time PCR); JNK, Erk1/2, p38, LC3I/II, Nrf2, p62, Slc7a11 (western blot); Fe^{2+} release assay; flow cytometry; GPX4 (ELISA); NADP/NADPH, LC3 (fluorescence); immunofluorescence;	Wang H. et al., 2017; Kong et al., 2019; Tang and Kroemer, 2020
Pyroptosis	A form of lytic cell death that is triggered by proinflammatory signals and associated with inflammation	Membranous pore formation; cytoplasmic swelling; rupture of the cell membrane and release of its intra-cellular contents into the immediate cellular milieu	BCA, casp1 (western blot); real-time PCR; caspase-1, CD31 (TUNEL staining and immunostaining); IL-1β, IL-18, pro-IL-1β, IL-1α (ELISA); FAM-FLICA-caspase-1 and PI (flow cytometry); NLRP3, caspase-1, IL-1β, IL-18 (immunofluorescence); Ca^{2+} (fluorescence); IL-1β, casp1, casp8 (immunoblotting); determination of LDH; PLFA (isotope labeling); spectral analysis; DAB, AEC (chromogenic staining)	Boschker and Middelburg, 2002; Schneider et al., 2017; Lei et al., 2018; Wang et al., 2018a; Wu et al., 2018; Yang F. et al., 2018

ATG5/7: Autophagy-Related protein 5/7, ATP5G3: isoform 3 of subunit c of mitochondrial ATP synthase, CD31: platelet/endothelial cell adhesion molecule-1, ELISA: enzyme linked immunosorbent assay, Erk1/2: extracellular signal-regulated kinase 1, FLICA: fluorochrome-labeled inhibitors of caspases, GFP: green fluorescent protein, GPX4: glutathione peroxidase 4, IREB2: iron-responsive element-binding protein 2, LAMP2A: lysosome-associated membrane protein 2A, LC3: light chain 3, LDH: lactate dehydrogenase, MLKL: mixed lineage kinase domain-like pseudokinase, NLRP3: nod-like receptor protein-3, Nrf2: nuclear factor erythroid 2 p45-related factor 2, PLFA: phospholipid fatty acid, PTGS2: prostaglandin endoperoxide synthase 2, RFP: red fluorescent protein, RIPK1/3: Receptor-interacting serine/threonine-protein kinase 1/3, Slc7a11: solute carrier family 7 member 11, TIRF: total internal reflection fluorescent, TNF: tumor necrosis factor, TRAIL: tumor necrosis factor-related apoptosis-inducing ligand, TUNEL: terminal deoxynucleotidyl transferase (TdT) dUTP Nick-End labeling, ULK: Unc-51-like kinas.

mechanisms (Paredes-Gamero et al., 2012). Meanwhile, the technology of RCDs detection is developing rapidly. To date, these detection techniques have been developed for monitoring the morphology of RCDs, such as light microscopy (Paredes-Gamero et al., 2012), EM, transmission electron microscopy (TEM) (ultrastructural changes and chromatin condensation in the cells) (Dong et al., 2015), scanning electron microscopy (surface changes of cells or tissues) (Burattini and Falcieri, 2013), atomic force microscopy (whole-process changes in RCDs) (Kuznetsov et al., 1997; Hessler et al., 2005; Sborgi et al., 2016), fluorescence microscopy (FM) (specific fluorescence labeling such as NAD(P)H-labeled in apoptosis) (Alturkistany et al., 2019), and practical flow cytometry (number and rate of dead cells) (Yasuhara et al., 2003; Paredes-Gamero et al., 2012; Liao S. et al., 2019).

As the most intuitive means, morphologic detection also refers to many different aspects: the alterations of the membrane (e.g., the loss of membrane integrity), the changes in cytoplasmic contents (e.g., mitochondrial damage), and the alterations of the nucleus and DNA. Each of the

RCDs has their own iconic characteristic presented through immunohistochemistry (IHC) or various fluorescent dyes and high-resolution microscopy (**Figure 2**).

Time-Lapse Microscopic Analysis

Time-lapse microscopic analysis, involving a temperature and CO_2-controlled incubator, has benefits for monitoring a biological process over a time period, which may last from a few hours to several days (Wallberg et al., 2016b). It can be suitable for a comparative and dynamic study of single cells *in vivo* or in culture shown as automated imaging of visible cell surface changes. This technique could be recorded *via* using differential interference contrast (DIC) optics either alone or in combination with epifluorescence microscopy specifying a predefined delay between the acquisition of images. The related parts of this technology may be changed slightly, generally including a Leica ASMDW live cell imaging system (Leica Microsystems, Mannheim, Germany), which includes a DM IRE2 microscope equipped with an HCX PL APO 63/1.3 glycerin corrected 37℃ objective and a 12 bit Coolsnap HQ Camera (Cappellini et al., 2005; Krysko et al., 2008; Chan et al., 2011).

After staining with combinations of dyes, cell death can be visualized. These dyes include Alexa Fluor 647-conjugated Annexin V and Sytox Green (SG), or Annexin VFITC and PI. Recently, fluorescent probes have been developed to improve the accuracy during detection, such as two-related fluorescent probes, namely molecular conjugates of one or two zinc dipicolylamine (ZnDPA) coordination complexes with an appended solvatochromic benzothiazolium squaraine dye targeting the anionic phospholipids and phosphatidylserine (PS) exposed on the surface of dead or dying cells (Jarvis et al., 2018). This method is considered the best choice to distinguish between necrosis and apoptosis morphologically (Wallberg et al., 2016b). Annexin V staining using fluorescein isothiocyanate (FITC) could be used to detect apoptosis through binding to PS in the presence of Ca^{2+} (Vermes et al., 1995; Baskic et al., 2006). In necrosis, Annexin V staining can present a positive, so researchers always use double staining of Annexin V and PI to confirm necrosis (Vermes et al., 1995), and it has been proven that ^{99m}Tc-radiolabeled Annexin V is the most successful marker (Brauer, 2003).

Obtaining the data of cell morphology in apoptosis is described as: roundness, blebbing, the breaking up of cell fragments into apoptotic bodies (a process called "budding"), which are eventually degraded within phagolysosomes, and nuclear condensation (karyopyknosis) and fragmentation (karyorrhexis), and it always happens in small clusters of cells or individual cells without inflammation. After that, apoptotic

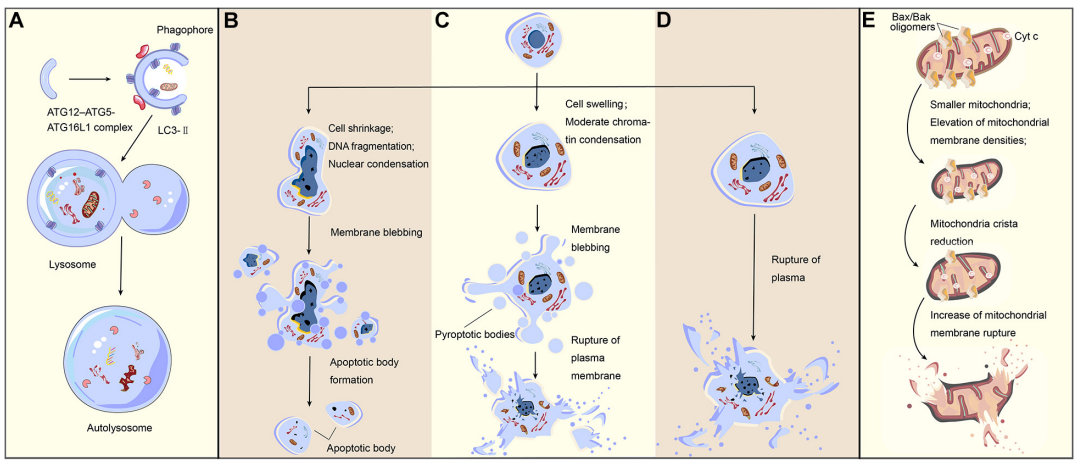

FIGURE 2 | Morphological changes of regulated cell death. Different types of cell death inducing with various pathways present diverse morphological changes. **(A)** The formation of autophagosomes is the typical characteristic of autophagy. ATG12-ATG5-ATG16L1 complex and LC3-II contribute to the extension of the phagophore. When the autophagosome is completely formed, LC3-II will separate from the outer membrane, and the autophagosome fuses with the lysosome so that an autolysosome finally emerged. **(B)** As for apoptosis, in the early stage, the nuclear condensation starts with cell shrinkage. During later stages, nucleus breaks up and the plasma membrane bubbles with no rupture, naturally associating with no inflammation. Finally, it forms apoptotic bodies. **(C)** Being different from apoptosis, after cell swelling and large bubbling, pyroptosis has plasma membrane rupture in the final stage. **(D)** When it comes to necroptosis, the appearance of cell swelling often followed by organelles dilation, and the nucleus disintegrates late. In some cases, chromatin condensation also occurs. Finally, with the rupture of plasma, a massive inflammation in the tissue is triggered. **(E)** The morphological characteristics of ferroptosis, however, mainly reflects on the changes of mitochondria. Compared with organelles swelling in necroptosis, here in the first stage, the mitochondria become smaller and membrane densities are elevated, followed by mitochondria crista reduction and plasma membrane rupture.

cells are consumed via phagocytic systems *in vivo*, or eventually lose the integrity of their plasma membrane and undergo secondary necrosis, which is characterized by plasma membrane permeabilization and osmotic swelling without phagocytosis. As for necroptosis, cellular swelling and a balloon-like-structure formation ("oncosis") are regarded as the major characteristic changes with inflammation.

However, it can also be challenging to distinguish apoptosis from necroptosis because undergoing secondary necrosis might occur in apoptotic cells where Annexin V-binding can enter cells through a broken membrane. To avoid this case, the combination of Annexin V and noncell permeable DNA stains (e.g., PI or SG) is adopted (Wallberg et al., 2016b; Jarvis et al., 2018).

Time-lapse microscopic assays can also be used to show some of the specific molecular markers, such as DNA, RNA or proteins involved in their molecular pathways and functions through using fluorescent molecular probes, such as monitoring autophagy *via* time-lapse microscopy to track Parkin (a protein implicated in mitophagy) fused with fluorescent enhanced yellow fluorescent protein (EYFP) (Di Sante et al., 2016). This method has advantages for collecting information at the single-cell level. However, assays based on time-lapse microscopy are susceptible to some factors (e.g., vibrations, the fluctuations of temperature and humidity, pH and cell motility, etc.) that may interfere with the acquisition of high-quality images (Di Sante et al., 2016).

EM Analysis

Electron microscopy analysis has always supplied us with a great deal of data in cell death research, in which TEM benefits from its much higher resolving power (0.1-0.4 nm) and scanning electron microscope (SEM) also offers high resolving power (about 1 nm). TEM makes it possible to better understand the relationships between a biological structure and its function at the cellular, subcellular, and even molecular levels through two- and three-dimensional images of the cells to distinguish different forms of RCDs, which is considered as a "golden standard" (Ericsson, 1969; Krysko et al., 2008). SEM, a kind of observation at the level between TEM and the light microscope, could emerge as a good method to provide a delicate imaging stereo effect of the surface of the cells with a magnification of 300,000 times or more. SEM is utilized for topographic imaging of bulk samples suited for low energy EM, whose maximum electron energies are at 30 keV (Sun et al., 2018). In addition, SEM combined with other analytical instruments can be used to observe the microscopic morphology and to carry out a composition analysis of the material microregion. However, many researchers consider EM analysis to be time-consuming and expensive.

Meanwhile, the preliminary substrate preparation of dying cells for EM could be difficult during the intermediate process because it may cause damage to the original morphology of the RCDs, especially when they detach the dying cells from their substrate, typically resulting in spinning down these floating cells. Recently, EM has been optimized continuously; for example, using macrophages or cytospinning to capture the cells prevents interference with their cell morphology (Vanden Berghe et al., 2013; Crowley et al., 2016d).

SEM/STEM/TED imaging can capture a wealth of information and focused ion beam scanning electron microscopy (FIB/SEM) (Knott et al., 2011), one of the three-dimensional EMs, is being increasingly adopted in life sciences. It is worth noting that the discovery of cryo-electron microscopy (cryo-EM), leading to a detailed or realistic display of ultrastructure in cells, may provide more convincing evidence in RCDs (Li et al., 2018; Fitzpatrick and Saibil, 2019).

Determining Cell Morphology in Apoptosis

As for apoptosis, people have marked it by the typical morphological changes: cell shrinkage, DNA fragmentation (karyorrhexis), chromatin changes during condensation and margination, a ruffling plasma membrane, and breaking up of cell fragments into apoptotic bodies (a process called "budding"), which are eventually degraded within phagolysosomes. Previously, light microscopy has identified the morphological changes occurring during apoptosis with cellular shrinking and pyknosis (Kerr et al., 1972). After hematoxylin and eosin stain (HE staining), the histologic characteristics of apoptosis are defined as confirming a round or oval mass, a red-stained eosinophilic cytoplasm, and purple-dense nuclear chromatin fragments, usually occurring in small clusters of cells or individual cells without inflammation. Besides, the more detailed morphological changes have been confirmed by EM, which could better present the subcellular changes, such as the most characteristic feature of apoptosis, pyknosis in which uniformly dense masses of chromatin are formed and distributed against the nuclear envelope after chromatin condensation (Hacker, 2000; Zucker et al., 2000). Additionally, the loss of cell-to-cell contacts and microvilli are visible in the images (Kerr et al., 1994; Cummings et al., 1997).

Determining Cell Morphology in Necroptosis

Compared to apoptosis, necrosis emerges as a general swollen cell (oncosis) and the swelling of the cytoplasmic organelles (e.g., swollen mitochondria), poorly demarcated clumps of chromatin, a rapid loss of plasma membrane integrity, and the release of cytoplasmic contents, which is uncontrolled and passive, and eventually, the changes of nuclear morphology are described as pyknosis, karyorhexis, and karyolysis. In detail, the major morphological changes during necrosis could be summarized as: (1) nucleus: pyknosis for the nuclear dehydration, karyorhexis (nuclear fragmentation), karyolysis (without the visible outlines of the nuclei); (2) cytoplasm: cytoplasmic vacuoles forming; endoplasmic reticulum swelling; cytoplasmic blebs forming; mitochondria condensing, swelling or breaking up; ribosomes disaggregating and rupturing; (3) others: cellular swelling; membranes disrupting; eventually; an inflammatory response occurring (Trump et al., 1997). Necrosis is another form of cell death that has some similar aspects to apoptosis, due to several processes like the morphologies and mechanisms shared between them (Kerr et al., 1972; Zeiss, 2003). The characteristic morphology in necrotic cells, such as cytoplasmic swelling, is due to the membrane permeabilization being an early event. Losing membrane permeability in apoptotic cells occurs relatively late.

Determining Cell Morphology in Autophagy

Acting as a non-invasive response to cell death with the formation of large-scale autophagic cavitation, autophagy contributes to maintaining the balance of the cellular structure, metabolism, and biological function for homeostasis (Deter and De Duve, 1967; Mizushima and Komatsu, 2011). There are three types of autophagy according to the pathways in which cargoes or phagocytes are transported into lysosomes: microautophagy, macroautophagy, and chaperone-mediated autophagy (CMA) (Rogoza et al., 2004). A comparison of these three forms of autophagy is shown in **Table 2**. Remarkably, the application of TEM has promoted the progression of autophagy from the phagolysosome to related protein imaging using the cryo-EM structure (Ohsumi, 2014; Hurley and Nogales, 2016).

Macroautophagy

Among the three types of autophagy, macroautophagy has been studied extensively and clearly. It is induced under stress stimulus, resulting in maintaining cell growth through specifically degrading damaged or superfluous organelles or leading to various human pathologies, including lung, heart, neuron, and liver disease, cancer, myopathies, aging and so on, after excessive self-degradation (Yorimitsu and Klionsky, 2005; Parzych and Klionsky, 2014; Pastuhov et al., 2016). Morphologically, the autophagosome is one of the distinct features forming by expansion as well as *de novo* rather than membrane budding from an already contained cargo (du Toit et al., 2018). The membrane expands and bends, and then a spherical autophagosome is generated. Using electron microscopic examination of the obverse, it has been found that the diameter of autophagosomes ranges from 0.5 to 1.5 μm in mammals and ∼0.4 to 0.9 μm in yeast (Takeshige et al., 1992; Gu et al., 2020). Besides autophagosomes, autophagy precursors (which include the cytoplasm, organelles, or bacteria) and autophagolysosomes (autophagosomes that bind to the lysosome) are also vital subcellular structures.

Microautophagy

For microautophagy, most of the research has focused on yeast and describes its transport pathway as cytoplasmic contents are transported into the lysosome within the lysosomal membrane invagination (Marzella et al., 1981). De Duve *et al.* first observed microbodies in autophagy using EM (Baudhuin, 1966). Also, Sakai et al. observed the process of microautophagy using vacuoles and microbodies of yeast with fluorescent double-labeling (Itoh et al., 1998). Then, nucleus microautophagy in yeast was reported by Roberts *et al.* (Fernandez et al., 2003). Early on, using EM, people noticed the free-floating vesicles within the lysosome through englobing Percoll particles by way of cup-like invaginations of the lysosomal membrane (Marzella et al., 1980). Recently, nucleophagy, which targets autophagic degradation as nuclear material, has helped in elucidating the endosomal microautophagy transports detected by indirect immunofluorescence techniques (Otto and Thumm, 2020). Microautophagy is so small that TEM is needed to see it clearly. Due to the limitations of technology, we know little about microautophagy, including the inducing factors, the mechanism, and its role in the disease processes (Mijaljica et al., 2011; Sato et al., 2019; De Falco et al., 2020).

Chaperone-mediated autophagy

Compared with microautophagy and macroautophagy, one of the nonspecific pathways to engulf the cytoplasm, CMA, is highly specific and refers to a specific substrate (a compound formed by a pentapeptide sequence that is biochemically related to KFERQ, namely Lys-Phe-Glu-Arg-Gln and HSPA8/HSC7, the heat shock 70 kDa protein 8) and specific receptor LAMP2A, the lysosomal-associated membrane protein 2A (Chiang et al., 1989; Dice, 1990). The morphological changes of CMA are not obvious, so immunofluorescence analyses, western blots, and other biochemical methods play crucial roles in CMA assays (Wu et al., 2019).

TABLE 2 | Comparison of distinguishing criteria, morphological features and monitoring methods of three kinds of autophagy.

Items	Definition	Morphological features	Detecting methods	References
Microautophagy	Cytoplasmic contents are transported to the lysosome within lysosomal membrane invagination or deformation.	Lysosomal membrane invagination or deformation	Transmission electron microscopy	Mijaljica et al., 2011; Parzych and Klionsky, 2014
Macroautophagy	Cargo is transported to the lysosome by de novo formation of autophagosomes.	Membrane expansion and bend; phagophore nucleation and elongation; autophagosome formation	Electron microscopy; immune colloidal gold technique; GFP-LC3 or mRFP-GFP-LC3 (Immunofluorescence); LC3-II / LC3-I, Beclin, ATG5, ATG7, p62 and phosphorylation status of ULK (western blot); radiolabeling; LDH sequestration; MDC staining	Parzych and Klionsky, 2014; Seglen et al., 2015; Murugan and Amaravadi, 2016; Orhon and Reggiori, 2017; du Toit et al., 2018; Yang F. et al., 2018
CMA	Unfolded proteins containing the KFERQ motif are transported directly across the lysosomal membrane through the action of cytosolic chaperones.	Multimerization of LAMP2A binding to the lumenal side of the lysosomal membrane by HSP90	Hsc70 with lysosomal markers (Immunofluorescence); LAMP2A (western blot); radiolabeling	Cuervo, 2010; Parzych and Klionsky, 2014; Patel and Cuervo, 2015; Arias, 2017; Wu et al., 2019

Abbreviations: LAMP2A: lysosome-associated membrane protein 2A, HSP90: Heat Shock Protein 90, ATG5: Autophagy-Related Gene 5, ATG7: Autophagy-Related Gene 7, Hsc70: heatshockprotein.

Non-canonical autophagy

Besides these classical autophagy pathways, the recent identification of non-canonical autophagy pathways, such as LC3-associated phagocytosis (LAP) and LC3-associated endocytosis are showing impact on cell viability (Martinez et al., 2016). This non-canonical autophagic process relies on Rubicon (rubicon autophagy regulator [RUBCN]), contributes to immunosuppression (Sil et al., 2020). And these specific pathways have been reported to underly the pathogenesis of various diseases. For example, LAP is closely related to systemic lupus erythematosus (SLE) (Bandyopadhyay and Overholtzer, 2016; Martinez et al., 2016), tumor (Cunha et al., 2018). And LC3-associated endocytosis has been shown to be protective against neuronal cell death in Alzheimer's Disease (Heckmann et al., 2020a,b). Similar to canonical autophagy, LAP require ATG-7/-3/-5/-12/-16L for LC3 lipidation (Martinez et al., 2011, 2015). But unlike autophagy, LAP is a process requiring NADPH oxidase-2 (NOX2)5, and Rubicon5 (Martinez et al., 2015), and LAP is independent of the pre-initiation complex containing ULK1 and FIP200 and proceeds with a distinct Beclin 1-VPS34 complex lacking ATG14 (Florey et al., 2011; Martinez et al., 2011; Kim et al., 2013).

All in all, these three canonical autophagy pathways could deliver the cargo to the lysosome to degrade and recycle while each of them features with different morphology. The formation of autophagosome is regarded as characteristic changes during macroautophagy, which is formed by portions of the cytosol and intact organelles (e.g., mitochondria) sequestered into a double-membrane vesicle (Mijaljica et al., 2011). By contrast, microautophagy involves the direct engulfment of cytoplasm at the lysosome surface requiring the EM for detecting, whereas CMA refers to a process delivering soluble and unfolded proteins directly across the limiting membrane of the lysosome (Massey et al., 2004).

Determining Cell Morphology in Ferroptosis

As an oxidative, iron-dependent form of RCD, ferroptosis is induced through an excess accumulation of reactive oxygen species (ROS) and lipid peroxidation products (Dixon et al., 2012; Chen et al., 2020). When undergoing ferroptosis, dysmorphic small mitochondria or mitochondria shrinkage with enlarged and reduced crista, and a condensed and ruptured membrane can be detected morphologically using an electron microscope (Dixon et al., 2012; Friedmann Angeli et al., 2014; Doll et al., 2017). Although relevant research in ferroptosis has made rapid progress, using mitochondrial morphology to distinguish ferroptosis is still highly debatable since there is a lack of studies on the correlation between mitochondria and ferroptosis (Dixon et al., 2012; Gaschler et al., 2018).

Determining Cell Morphology in Pyroptosis

Pyroptosis refers to a process in which the pores on plasma membranes are gradually formed, inflammatory cytokines are released, and the lysed cells are induced through the canonical caspase-1-mediated monocyte death or the non-canonical caspase-4/5/11 inflammasome pathways (He et al., 2019; Wang et al., 2019e). The morphological changes during pyroptosis include cell swelling, which is induced through entering water molecules, the formation of 10-15 nm pores in the plasma membrane, and the eventual release of pro-inflammatory cytokines (interleukin-1β (IL-1β) and interleukin-18 (IL-18)), distinct from apoptosis without inflammatory release (Lu et al., 2020). Activating caspases, an N-terminal cleavage product (GSDMD-NT) would be generated, which triggers inflammatory death (pyroptosis) and the release of inflammatory cytokines such as IL-1β 1,2 (Shi et al., 2015). Notably, it is visible by EM since GSDMD-NT oligomerizes in membranes to form pores to trigger pyroptosis (Liu et al., 2016). These morphological changes have been observed in smooth muscle cells (SMC), endothelial cells (EC), macrophages, phagocytes, astrocytes and neurons, and additional research on its mechanism and technical studies are needed in the future (Liu et al., 2018, 2020).

Determining Cell Morphology in NETosis

NETosis, one of the RCD types which was first described in 2004, is regarded as a program for formation of neutrophil extracellular traps (NETs) initiating a fight against pathogens and linking to various diseases (Brinkmann et al., 2004). According to the viability of cells, NETosis could be divided into two different forms, namely classical or suicidal NETosis resulting in the cell death, and vital NETosis retaining viability. The typical morphological changes of classical NETosis are described as chromatin decondensation associated with histone modification, and the release of granule components into the cytosol, as well as many characteristic features which are the same as other forms of RCDs (such as the changes in the nucleus and in the cytoplasm during apoptosis, necroptosis, pyroptosis, and autophagy (Vorobjeva and Chernyak, 2020). As for vital NETosis, it refers to a massive and very fast release of mitochondrial DNA (mtDNA) without loss of viability, when neutrophils retain their viability and natural effector functions (Yousefi et al., 2008, 2009).

Flow Cytometry Assay

Flow cytometry is used as a general measure for rapid analysis of a large number of cells individually, which detects up to 10,000 cells per second. Based on the cellular characteristics, including the size, granularity and morphology of the cells, the integrity or potential of the cell membrane, the intracellular pH, and the levels of cellular contents such as surface receptors, proteins, the ions (e.g., calcium), DNA, and RNA, flow cytometry could provide data to distinguish RCDs through the use of fluorescence, absorbance measurements, and light-scattering.

Currently, flow cytometry is used not only in cell counting but also in image analysis, namely multispectral imaging cytometry for multiparameter studies on cell demise (Lelliott et al., 2019; Cerrato et al., 2020). Morphology-based flow cytometry assays are used to identify RCDs, such as the percentage of apoptotic cells that are indicated based on the cells exhibiting nuclear fragmentation as well as a low nuclear area and a bright detail intensity. Various staining approaches such as 1 μM camptothecin (CPT; Sigma, a DNA topoisomerase I inhibitor) for 6 hours, fixed and stained with PI, and collected on the ImageStream (George et al., 2004), can be applied. Moreover, cells undergoing autophagy can be identified through visualizing

fluorescently labeled lysosomal markers, and LC3 puncta labeled and/or the co-localization of fluorescently labeled LC3 using flow cytometry provide benefit in an objective, quantitative, and statistically robust manner (Pugsley, 2017). Also, the loss of plasma membrane integrity using cell-impermeant dyes could be assessed through a morphology-based flow cytometry assay to detect cell viability (Vanden Berghe et al., 2013). Furthermore, flow cytometry is often used to monitor RCDs with biomarkers and we will discuss this below.

Confocal Laser Scanning Microscopy

Detection work needs a point scanning confocal microscope with good optical efficiency. Importantly, a good lens with a long working distance and high NA determines the rendering effect. The Leica TCS4D or SP1 with a Leica inverted IRMB microscope and an Argon-Krypton laser (Omnichrome, Chino, CA, United States) emitting 3 wavelengths (488, 568, and 647 nm) have been used in confocal microscopy (Zucker and Rogers, 2019). A 5 × or 10 × objective with a high numerical aperture (NA) and the lenses including Zeiss 5 × fluor (NA 0.25), Zeiss 10 × fluor (NA 0.5), Leica 10 × Plan APO (NA 0.5), and Leica multi-immersion 10 × (NA 0.4), also a Zeiss lens fitting on a Leica microscope whose magnification could be increased by 20%, are available (Zubairova et al., 2019; Zucker and Rogers, 2019). Confocal microscopy could provide a visible three-dimensional structure as a good indicator for RCDs visualization, and it is also flexible and fast except for some cumbersome processes, namely staining, fixation, dehydration, and clearing (Zucker and Rogers, 2019). For example, confocal microscopy is used to provide insights into the dynamics of cell death with the fluorescent dyes fluorescein diacetate (FDA) and PI (Jones et al., 2016). Also, the research into mitophagy using confocal microscopy and the subcellular localization of ceramide in mitochondria were visualized by colocalization of ceramides and mitochondria (Sentelle et al., 2012).

FM

Fluorescence microscopy is often utilized to monitor RCDs *via* not only detecting specific markers, but also for evaluating cell nucleus damage and DNA, leading to direct visualization of pathophysiological processes with sub-cellular resolution. On this basis, FM is constantly being improved for various requirements in detection, such as fluorescence lifetime imaging microscopy (FLIM) being used to monitor caspase-3 activity during apoptosis (Buschhaus et al., 2017, 2018). Moreover, autolysosomes for autophagy detection can be visible via the colocalization of LC3 and lysosomal markers by FM (Yoshii and Mizushima, 2017; Bhutia et al., 2019). Caspase-1 activity assays for pyroptosis detection could also be adapted to FM, such as with a Nikon ECLIPSE TE2000-U FM in Tokyo, Japan (Liao Y. et al., 2019). The changes of the nuclei could therefore be identified through FM to distinguish apoptotic cells from healthy cells or necrotic cells for staining with DAPI or other dyes (Crowley et al., 2016). DAPI or Hoechst 33258, 33342, and 34580 are often used to monitor DNA fragmentation or damaged cell nuclei through binding to A-T base pairs lining the minor groove of double-stranded DNA (Eriksson et al., 1993; Martin et al., 2005). FM has tended to be artificially intelligent, and its probes have become smaller and more prominent with more precise targeting options.

Intravital Multiphoton Microscopy

People also pay more attention to RCDs monitoring *in vivo*. Intravital multiphoton microscopy has been developed in the cell death process for monitoring at the cell level in tissues *in vivo* (Mesa et al., 2015). It is an objective and real-time technique for capturing morphological changes during RCDs (e.g., apoptosis characteristics with membrane blebbing and ApoBD formation) *in vivo* with a fluorescence resonance energy transfer (FRET)-based caspase 3 activation reporter (Garrod et al., 2012; Mayer et al., 2017). For staining, poly ((3-((4-methylthiophen-3-yl)oxy)propyl) triphenylphosphonium chloride) (PMTPP), one of the fluorescent sensors or stains used for monitoring ATP levels in cell membranes to monitor cell death processed *in vivo* through FM, is available (Huang et al., 2017). To make the detection in RCDs more realistic, standard, noninvasive, clinical, magnetic resonance imaging and spectroscopy (MRI/MRS), computed tomography (CT), positron emission tomography (PET), and radionuclide imaging methods are also used for monitoring the biochemical and physiological processes in apoptosis, necrosis, autophagy, and ferroptosis (Brauer, 2003; Lee et al., 2019).

MONITORING AND MEASURING RCDs BY BIOMARKERS

To make the identification of RCDs more objective and quantitative, researchers always combine morphological changes and biomarkers of RCDs. RCDs have different pathways involved with specific proteins; for example, caspase-3 is an important effector of apoptosis, and once activated, it leads to apoptosis (Li X. et al., 2019). Although detection of biomarkers makes RCDs identification more accurate, it can be challenging to distinguish different forms of RCDs clearly for the discovery of new RCDs mechanisms and interlaced protein pathways.

Depending on where the content exists and how the content is extracted, the molecular biomarkers used in RCDs detection are divided into three types: cell surface markers acting at the plasma membrane (e.g., PS (PtdSer), pannexin 1 (PANX1)), intracellular markers working inside the cells (e.g., caspase activity, mitochondrial potential), and soluble extracellular markers as well as released molecules with a potential role as circulating biomarkers of cell death (e.g., caspase-3, cytokeratin 18 (CK18), HMGB1 and the enzyme LDH) (Krysko et al., 2008; Hashimoto et al., 2016; Shukuya et al., 2020; Wimmer et al., 2020). The conventional biomarkers of RCDs are shown in **Table 3**. These vital biomarkers are shown in a schematic diagram (**Figure 3**), which depicts the cross-regulation among different types of cell death.

Biomarker Detection Technology

Western Blot

The main measures for biomarker detection can be considered at three levels, namely DNA, RNA, and proteins. As for

TABLE 3 | Conventional biomarkers for RCDs.

Species of RCDs	Biomarker	Research Model	Death induction	Detecting methods	Expected results	Advantages	Disadvantages	References
Necrosis	Phosphorylation Status of RIPK3, RIPK1 and MLKL	Mice of oligodendrocyte degeneration	N/A	Immunohistochemistry	Upregulated	It is ideal for detecting necrosis in vivo	Most of the antibodies are only suitable for immunoblotting	He et al., 2016
	LDH	Cortical neurons	0.25, 0.5, 1, 2, 3 mM METH and 39°C	Cytotoxicity assay	Upregulated	N/A	It might be influenced by the effect of other species of RCDs	Guo et al., 2020
	Annexin V (FITC)	HT1080^{indRIPK3} cells and L929 cells	10 ng/mL TNF, 500 nM SM	Fluorescence-activated cell sorting	Annexin V^{FITC}, DAPI Upregulated and TMRM Downregulated	It is a fast and quantitative method to record the number of dying cells	It should be combined with a time-course study, and/or the use of specific inhibitors	Wallberg et al., 2016a
Apoptosis	Annexin V (FITC)	HT1080^{indRIPK3} cells and L929 cells	10 ng/mL TNF, 500 nM SM	Fluorescence-activated cell sorting	Annexin V^{FITC} Upregulated and TMRM, DAPI Downregulated	It is a fast and quantitative method to record the number of dying cells	It should be combined with a time-course study, and/or the use of specific inhibitors	Wallberg et al., 2016a
	Caspase3	Platelet	N/A	Flow cytometric analysis and immunofluorescence	Upregulated	It is a specific method for the active form of caspase-3	N/A	Gyulkhandanyan et al., 2012
	PDK1, P-AKT1, BAD, Bcl-2, Bax	C2C12 cells	0.05, 0.5, 1, 2.5, 5- and 10- mM Fluoride	Real-time PCR and western blot	PDK1, P-AKT1 Downregulated and BAD, Bcl-2, Bax Upregulated	N/A	N/A	Zhou et al., 2018
	DNA fragmentation	NIH-3T3 cell line	500 μM Hydrogen peroxide	DNA ladder assay	DNA ladder formed	It is an easily available method and not limited to cells that breed *in vitro*	It is a time-consuming procedure	Rahbar Saadat et al., 2015
Autophagy	GFP-LC3 or mRFP-GFP-LC3 Probe	Zebrafish	Rapamycin or Calpain Inhibitors	Immunofluorescence	Being yellow under neutral pH conditions, and being red under acidic pH conditions	It allows to examining autophagy *in vivo* in vertebrates	It might be influenced by the impairment of autolysosome formation.	Lopez et al., 2018
	GFP-LC3-RFP-LC3ΔG probe	GFP-LC3-RFP-LC3ΔG mice	Starvation	Immunofluorescence	GFP/RFP ratio Downregulated	It can monitor both basal and induced autophagy accurately	It is limited by the level of GFP-LC3-RFP-LC3ΔG currently.	Yoshii and Mizushima, 2017
	LC3-II/p62	Exosome in advanced soild tumor patients'plasma	CQ or HCQ	Western blot	LC3-II/ p62 ratio Upregulated	It can monitor the dynamic changes on autophagic activity	It might be influenced by the effect of apoptosis and necrocytosis	Abdel Karim et al., 2019
	Autophagosome	HCT-116 colon cells	100 nM Rapamycin or overexpression of Beclin1	Immunofluorescence (MDC Staining)	Fluorescence emitted	MDC staining is readily to operate and directly visualize autophagosome formation	MDC staining is non-specific	Yang F. et al., 2018
Pyroptosis	IL-1β, IL-18	Wistar rats and rat chondrocytes	40 mg/mL MIA in 0.9% NaCl solution, 50 μL	Real-time PCR, western blot and enzyme-linked immunosorbent assay	Upregulated	This assay is highly sensitive	Enzyme activity is easily affected and this assay takes many complex measurements	Zu et al., 2019
	NLRP3, caspase-1	Wistar rats and rat chondrocytes	40 mg/mL MIA in 0.9% NaCl solution, 50 μL	Real-time PCR, western blot, flow cytometry, immunofluorescence and immunohistochemistry	Upregulated	This assay is highly sensitive	These multiple steps are time-consuming	Zu et al., 2019
Ferroptosis	ACSL4	HepG2, HL60, LNCaP, and K562 cells	2.5, 5, 10,20 μM Erastin	Western blot	Upregulated	N/A	N/A	Yuan et al., 2016

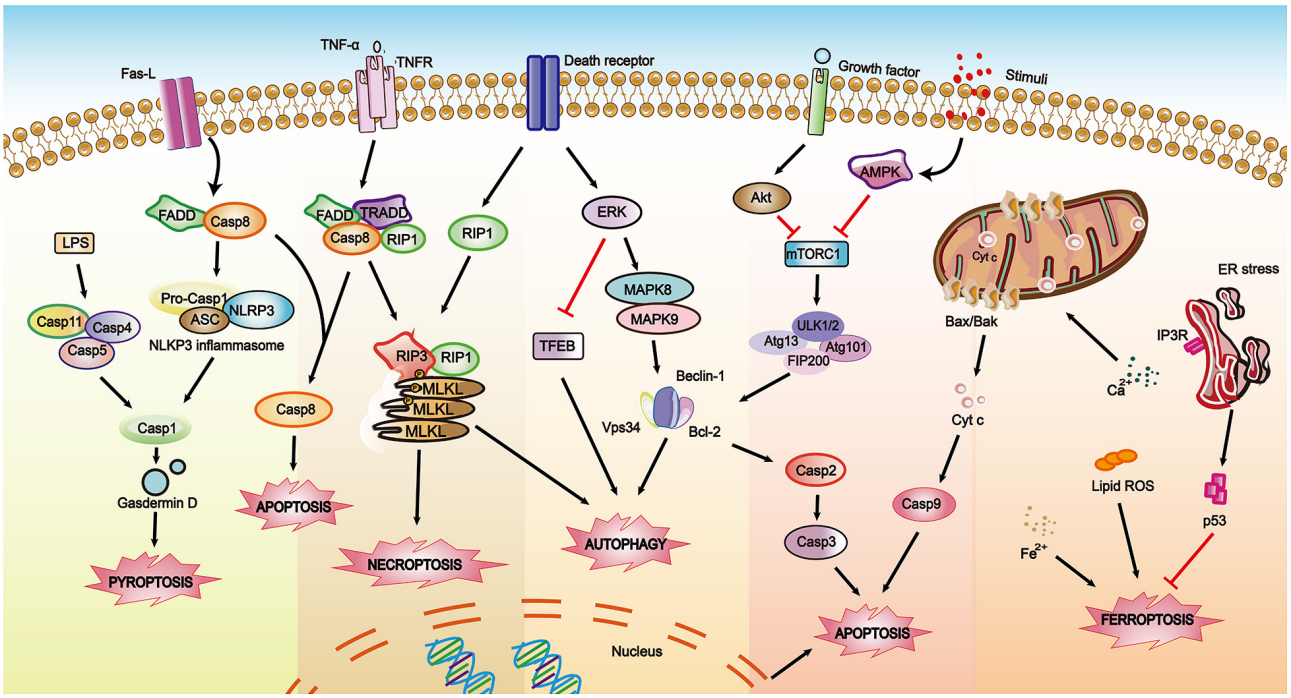

FIGURE 3 | A schematic diagram showing biomarkers involved in RCDs within depicting the cross-regulations among different pathways. The solid arrows indicate activating interactions while the T-shaped lines indicate inhibitory interactions.

gene/mRNA/cfDNA assays, quantitative PCR (qPCR) is a useful and convenient technique. For protein detection, western blots are regarded as a classic technique. The western blot allows for specific identification and characterization of proteins, able to detect specific proteins involved in RCDs to distinguish RCDs. The process is as follows: the proteins are separated through sodium dodecyl sulfate-polyacrylamide gel electrophoresis (SDS-PAGE), then the polyvinylidene fluoride (PVDF) membrane-transferred proteins are incubated with specific antibodies, and the protein of interest is detected by using a fluorescent agent. Remarkably, some of the modifications of proteins related to RCDs could also be detected through western blots, such as phosphorylation, acetylation, ubiquitin, etc. For example, the phosphorylation of RIPK1 could be analyzed via western blotting with special antibodies for research into the regulation of RIPK1 activation by TAK1-mediated phosphorylation, which modulates apoptosis and necroptosis (Geng et al., 2017).

Flow Cytometry

Requiring a high specificity, flow cytometry analysis is utilized to detect the specified cells through an assay of specific markers, volume, form, or any other signal characteristics (Bandura et al., 2009). For detection of apoptosis, PI is excited with a xenon or mercury arc lamp or with the 488 lines of an argon-ion laser and can be detected in the particular fluorescence channel (FL2 or FL3) of a flow fluorocytometer (FACSCalibur flow fluorocytometer, Becton Dickinson) (Bergamaschi et al., 2019). Traditionally, Annexin A5 (A5, PtdSer binding protein) combined with either PI or 7-aminoactinomycin D (7-AAD, membrane impermeable DNA binding dyes) stains are used in flow cytometry to distinguish apoptosis from necrosis (Koopman et al., 1994; Vermes et al., 1995; Broaddus et al., 1996). For the detection of ferroptosis, flow cytometry-based analysis is easy to carry out and is highly sensitive to measure lipid peroxide levels in live cells with the BODIPY^{TM} 581/591 C11 dye (Martinez et al., 2020). This technique is not only used for the separation of positive cells and the capture of special free contents such as vesicles, but also for identifying molecular biomarkers. Recently, flow cytometry assays have been improved to detect and quantify the various forms of RCDs, such as a three-color flow cytometry analysis that has been reported to detect necroptosis and apoptosis in the early and late-stage, and receptor interaction protein 1 (RIP1)-dependent apoptosis simultaneously in a single cell through targeting proteins like caspase-3 and receptor interaction protein 3 (RIP3), and detecting cell viability (Bergamaschi et al., 2019).

Enzyme-Linked Immunosorbent Assay (ELISA)

In the case of biomarkers for RCDs, ELISA is a sensitive, cost-effective and practical option for detection and quantitative or qualitative analysis based on the production of monoclonal or polyclonal antigen-specific antibodies and radioimmunoassay techniques. The ELISA technique is often used to detect RCD-related proteins such as caspase-3/7 up-regulation during apoptosis or cell-free DNA and nucleosomes (Roth et al., 2011), but there are still some constraints that should be of concern, such as the effect of temperature and time on sample storage

since samples stored at −70°C lead to an annual loss of 7% (Holdenrieder et al., 2010).

Cryo-EM

Recently, to present the microenvironment of a protein as much as possible, cryo-EM has been found to be a powerful tool and has been recently used in the research into structural molecular and cellular biology in three-dimensional structures, which was selected by Nature Methods as the Method of the Year 2015, and the Nobel Prize in Chemistry 2017 (Bendory et al., 2020; Garcia-Nafria and Tate, 2020; Guerrero-Ferreira et al., 2020). It provides benefits for a better understanding of how proteins and/or other biological macromolecules are involved in their complex network (Bendory et al., 2020). Cryo-EM is regarded as a suitable method for identifying the structure of isolated biomolecular complexes ranging from a protein sized several tens kilo-Daltons to a virus particle-sized many mega-Daltons and to a whole cell with sub-nanometer resolution (Murata and Wolf, 2018). As for the sample preparations, cryo-EM requires a much smaller amount of sample with tomographic slices of 10-nm thickness; it accepts large image datasets (such as single protein molecules, large protein complexes, thin-protein crystals, virus particles, helical fiber complexes, bacteria, cells, and even entire tissue sections); and near-atomic 3D maps of isolated proteins could be provided (Danev et al., 2019). Kate et al. have shown the reconstructed cryo-tomogram of apoptotic herniating mitochondria to research the classical intrinsic apoptosis pathway by using cryo-EM (McArthur et al., 2018). Meanwhile, cryo-EM has also been used to reveal the morphology of the pores and determine the localization of Bax labeled with nanogold, which allows for understanding the mechanisms of pore formation induced by Bax in apoptosis, necroptosis or ferroptosis (Kuwana, 2019). The proteins of RCD, including their connected macromolecules, microenvironment and even the related signal pathways, can be visualized by using cryo-EM. For example, the filament structure of caspase-8 tandem death effector domain was determined through cryo-EM to achieve a presentation of extensive assembly interfaces and to further confirm with structure-based mutagenesis its filament formation *in vitro*, as well as Fas-induced apoptosis and ASC-mediated caspase-8 recruitment in cells (Fu et al., 2016).

Also, researchers adapted some targeted approaches for the special marker assays, such as the terminal -deoxynucleotidyl transferase mediated nick end labeling (TUNEL) assay that is designed to detect DNA degradation in the late stages of apoptosis. Recently, circulating molecules (e.g., non-coding RNAs, released proteins, heteromeric complexes, enzymatic activity, subcellular vesicles, *etc.*) released from special tissues were found to be detectable in the cerebrospinal fluid, plasma, serum, and any other body fluids, which suggests noninvasive clinical applications.

Biomarkers for Detecting RCDs

Cell Surface Markers

PS (PtdSer) exposure vs. membrane permeability

PS (PtdSer), as a vital content in eukaryotic membranes, is the major anionic phospholipid accounting for 2–10%. PtdSer is generally not externally exposed in normal cells and the exposure of PtdSer could be a hallmark for stressed and dying cells, and a key signal for the removal of apoptotic cells through neighboring phagocytic cells (e.g., macrophages or neutrophils). That is, PtdSer exposure not only occurs in apoptosis but also in other types of cell death, such as necroptosis and autophagy (Galluzzi et al., 2012). It is an interconnected process between the exposing PtdSer and the loss of plasma membrane integrity, whose detections are discussed above. As for PtdSer, Annexin V, one of the imaging probes targeting DNA, is widely used to detect apoptosis when it comes to radionuclide imaging. It is worth mentioning that Annexin V, a nonglycosylated membrane protein probe, has been used as one of the few cell death imaging agents reaching phase II/III clinical trials (Nguyen et al., 2012). Synaptotagmin-I (SynI), synaptic vesicle-related protein, provides another point for probe design by binding to the negatively charged phospholipids PS and phosphatidylinositol in the presence of Ca^{2+} ions (Alam et al., 2010).

Pannexin 1 (PANX1)

The pannexin (Panx) family, consisting of 3 members (Panx1 as the most extensively studied one, Panx2 and Panx3), has been reported as playing a vital role in extracellular ATP release (Baranova et al., 2004). In apoptosis, Panx1 being activated through cleavage mediated by caspase at the C terminus releases ATP as a "find me" signal, which is necessary for macrophage recruitment (Chekeni et al., 2010). Meanwhile, the activation of Panx1 channels contributes to the increase in plasma membrane permeability and the formation of Ca^{2+}-permeable pores at the endoplasmic reticulum, leading to Ca^{2+} leakage and favoring mitochondrial Ca^{2+} uptake, which conveys cytochrome c to the cytosol to induce apoptosis (Chekeni et al., 2010). During research, Panx1 inhibitor carbenoxolone (CBX), pharmacological inhibition or small interfering RNA are used for indirectly inspecting the results *in vivo* and in *vitro*, suggesting PANX1 as a plasma membrane channel that could mediate the regulated release of find-me signals and selective plasma membrane permeability during apoptosis (Chekeni et al., 2010). The quantitative analysis of Panx1 could be detected through qPCR as mRNA levels for *PANX1*, and IHC or western blot for protein expression, whose function is analyzed using patch-clamp methods (Huang et al., 2020). In pyroptosis, caspases-3 and-7 and caspase-11 could not only contribute to cleaving the CT moiety of Panx1, resulting in channel opening and extracellular ATP release, but also induce K+ efflux and the activation of NLRP3 inflammasomes to process and subsequently release IL1β (Yang D. et al., 2015). Dahai et al. identified that Pannexin-1 worked critically for ATP-induced pyroptosis and was induced *via* cytosolic LPS using immunoblotting analysis with or without CBX, probenecid and trovafloxacin (one of the inhibitors of pannexin-1) (Yang D. et al., 2015). As for autophagy, extracellular ATP and engulfing dying cells in the Panx1-dependent pathway could not only recruit immune cells, but was also involved in the pathway of the inflammasome activation in macrophages in which a short hairpin (sh)RNA method for silencing pannexin-1 channels during co-incubation of macrophages with dying autophagic

cells leads to the inhibition of ATP release and inflammasome activation (Ayna et al., 2012). By means of inhibitor targeting the key molecule involved in the pathway of RCDs, this reverse validation is also widely accepted, such as CBX or small interfering RNA being used to inhibit Panx1 for apoptosis detection through qPCR and ELISA.

Intracellular Markers

Oligonucleosomal DNA fragmentation

DNA fragmentation to 180-200 bp and a weight more than 50 kbp is considered as a feature that clearly distinguishes apoptosis (Walker et al., 1999). There are various biochemical techniques to detect DNA ladders, including general-use agarose gel electrophoresis or flow fluorocytometric, which benefits from not being time-consuming and allowing for individual cell analysis. According to different technical principles, there are three main routine assays that were developed to detect DNA fragmentation: DNA ladder assay, TUNEL assay, and comet assay. Firstly, the DNA ladder assay: the DNA fragments (180–200 bp) could be separated into the "DNA ladder" pattern on agarose gel electrophoresis. The DNA ladder assay is used in conjunction with commercial kits that lead to a faster, more accurate, and sensitive assay, but at a greater cost (Micoud et al., 2001). Another approach is the TUNEL assay, which is utilized as a standard histochemical method for tissues, adherent cell lines, and suspension cell lines (Cuello-Carrion and Ciocca, 1999). Different from the DNA ladder assay, the TUNEL assay is more sensitive for the use of specific markers [e.g., bromodeoxyuridine labeling (BrdU), fluorescein labeling, thymidine analogs, 5′-ethynyl2-deoxyuridine labeling (EdU) (Wu et al., 2012), *etc.*] combined with other techniques, such as FM, flow cytometry, or laser scanning cytometry (Darzynkiewicz et al., 2008). As for the comet assay, also named 'single cell gel electrophoresis assay' (SCGE), it has been developed in genotoxicity testing with rapid detection of DNA repair or damage in a single cell (Collins, 2004). According to the quantification of the fluorescent signal in the core (formed of macromolecules and unfragmented DNA) and the tail (formed of predominantly single-stranded DNA) as well as the DNA damage, comets are divided into five groups: none or very low damage, low damage, medium damage, long DNA migration, apoptotic or necrotic DNA migration (Konca et al., 2003).

Although optimized approaches have been developed, various limitations are still a challenge. For instance, DNA damage not only appears in the apoptotic process but also exists in necroptosis, leading to false-positive assay results. And if there is no DNA ladder pattern, it cannot be proven that there is no apoptosis occurring in the sample since it can result from an event of the internucleosomal cleavage of DNA occurring in late apoptosis (Cohen et al., 1992; Collins et al., 1995). There are sometimes mushrooming cases where it is absent with internucleosomal DNA degradation during apoptotic or apoptotic-like cell death so that the intensity of DNA fragment labeling in these assays will be inadequate to distinguish apoptosis (Cohen et al., 1992; Catchpoole and Stewart, 1993; Knapp et al., 1999).

Caspase activation

Caspases, as one of the cysteine aspartate-specific proteases, play a vital role in the early stages of apoptosis, and are regarded as general biomarkers to identify apoptosis. They are synthesized as zymogen precursors that consist of an amino-terminal domain of variable length followed by a p20 and a p10 unit containing the residues. These amino-terminal regions in initiator caspases obtain a caspase recruitment domain (including CARD; caspases 1, 2, 4, 5, 9, 11) or death effector domains (including DED; caspases 8, 10), which are essential for substrate recognition and catalytic activity. After being activated by proximity-induced auto-proteolysis or cleavage via upstream proteases in an intracellular cascade, an active heterotetramer is formed and induces the following pathway (Lamkanfi et al., 2002; Ramirez and Salvesen, 2018). According to the functions and domain architecture, the caspase-family members are classified into two parts: inflammatory (including caspases-1, -4, -5, and -11) or apoptotic (caspases-3, -6, -7, and caspases-8, -9, -10) (Van Opdenbosch and Lamkanfi, 2019). The detection of caspase activation has been used to identify the mitochondrial death pathway of apoptosis in cell-free systems (Chandra and Tang, 2009). Besides caspases, other proteins in response to apoptotic stimuli are also targeted as an indicator, such as Bid, Fas-associated protein with death domain (FADD), Bcl-2 and Bax, cytochrome c, high-mobility group box 1 (HMGβ1), nuclear factor kappa B (NFκB), poly [ADP-Ribose] polymerase 1 (PARP) and other apoptosis-related proteins (Nicholson et al., 1995; Gyulkhandanyan et al., 2012; Del Re et al., 2019; Yang L.L. et al., 2019; Zahran et al., 2020). In pyroptosis, it has been reported that caspase-1 could mediate the cleavage of the cytosolic protein gasdermin D (GSDMD), resulting in promotion of the formation of GSDMD membrane pores and cell lysis, which sheds much-needed light on the necrotic execution mechanism of pyroptosis (de Vasconcelos et al., 2019). As a caspase-independent pathway, necroptosis is also regulated through the caspase regulators in which caspase 8 could work as a potent inhibitor of necroptosis mediated through a heterotrimeric complex involving caspase 8, Fadd, and the long isoform of caspase 8- and FADD-like apoptosis regulator (Dillon et al., 2012). Caspase activity and these related proteins can be detected through flow fluorocytometry, the cleavage of an *in vivo* caspase substrate, FLIM and light microscopy, the Promega Caspase-Glo 3/7 assay, and ELISA, and meanwhile q-PCR is used at the level of the RNAs of the related proteins during cell death. An example of caspase detection, the Promega Caspase-Glo 3/7 assay (Promega Corp., Madison, WI, United States), is utilized for detection, adopting a proluminescent caspase substrate for caspase detection (Mfotie Njoya et al., 2018).

Bid cleavage and the expression of the Bcl-2 protein family

The integrity of the major outer-membrane protein (MOMP) is closely regulated by a group of proteins belonging to the Bcl-2 family and encoded by the *BCL2* genes, which consists of pro-apoptotic and anti-apoptotic members (e.g., Bcl-2 and Bcl-xL) or other classes (e.g., BH3-only proteins with Bcl-2 homology (BH) domains only) (Cheng et al., 2001; Wei et al., 2001; Chipuk et al., 2010). Generally, it is believed that Bcl-2, Bax and Bak are of great

importance in the intrinsic pathway of apoptosis and the Bcl-2/Bax ratio or the level of Bcl-2 is considered as a hall marker for apoptotic detection (Musumeci et al., 2015; Saraste and Pulkki, 2000). The extrinsic pathway of apoptosis, also known as the death receptor pathway, is closely related to the intrinsic pathway (mitochondrial pathway), since the truncated Bid (tBid) protein translocates to the outer mitochondrial membrane (OMM) to promote RCD by engaging Bax/Bak, resulting in MOMP and subsequent caspase-9 activation (Wu X. et al., 2020). Similar to second mitochondria-derived activator of caspases (SMAC) mimetics, MOMP could trigger tumor necrosis factor (NF-κB-dependent production) and coincidentally induce an alternative form of cell death, namely necroptosis (Giampazolias et al., 2017). Remarkably, the Bid is from both the cytosol and the organelle fraction. Because the form of Bid induced by anti-Fas antibodies stays in the cytosolic fraction briefly and only in small amounts, most of the Bid has been associated with the organelle fraction (Krysko et al., 2008). Both the Bid cleavage and the expression of the Bcl-2 protein family are able to be detected through western blot, ELISA, and flow cytometry.

Cytochrome c release

The release of cytochrome c from the mitochondria is a central signal in the intrinsic pathway of apoptosis mediated through OMM permeabilization. The release of cytochrome c activates caspase-3 or -7 *via* the apoptosome, leading to the formation of cyt-c, caspase-9 and Apaf-1, after which apoptosis is induced (Green and Kroemer, 2005; Kroemer et al., 2007). The detection of cytochrome c serves as a biomarker of apoptosis and is also important to understand certain diseases at the cellular level. To detect the level of cytochrome c, multiple existing techniques are adopted, including western blot, ELISA, high-performance liquid chromatography (HPLC), spectrophotometry and flow cytometry. As a special detection method for cytochrome c, fluorescent aptamer/carbon dot-based assays are regarded as a simple, sensitive, rapid and selective label-free assay for apoptosis detection employing the principle of a connection between the surfaces of Carbon Dots (CDs) and nucleic acid aptamer biomolecules. It is very sensitive and selective for apoptotic detection with a 25.90 nM limit in detection and a linear range of 40-240 nM (Ghayyem and Faridbod, 2018). Notably, cytosolic fractions and the organelles should be separated using a mild detergent, digitonin (concentration of 0.02%), in order to leave the mitochondria and lysosomes intact to prevent cytochrome c release from the mitochondria, resulting in artifacts of organelle preparation (Krysko et al., 2008). Moreover, cyt c could accumulate in the culture supernatant during secondary necrosis of anti-Fas-stimulated cells, and cyt c could also accumulate in the culture supernatant from the moment that the plasma membrane loses its integrity in the late necrotic phase of TNF-stimulated cells (Denecker et al., 2001).

The expression and phosphorylation status of RIPK1, RIPK3, and MLKL

Various factors work as key participants in necroptosis, namely in a caspase-independent pathway, such as RIP1, RIP3, and MLKL (Galluzzi et al., 2014; Ding et al., 2015; Wu X. et al., 2020). Combined with traditional methods of detection of necrosis (morphological features, the intracellular-component release, and biochemical features involved in necrosis), specific biomarkers in necrosis allow for more accurate detection of necrosis or even a measure with greater potential for clinical implications (Vanden Berghe et al., 2013; Lu et al., 2017). It has been reported that necrosis is sometimes related to upregulated RIPK1, RIPK3, or MLKL mRNA or protein expression levels *in vivo* in various diseases or physiological conditions (Guo et al., 2020). Activated forms of RIP1, RIP3, and MLKL have emerged as optimal biomarkers for both distinguishing necrosis and the diagnosis or prognostic assessment of diseases related to necrotic injury (He et al., 2016). Some of the specific kinase inhibitors and inducers have been widely used for research into necroptotic signals, such as drug-induced forced dimerization of RIPK1/RIPK3, a means to directly activate RIPK1 or RIPK3 (Rodriguez and Green, 2018). Tissues or cells with increased expression levels of RIPK1, RIPK3, and MLKL may indicate a predisposition to necrosis. However, there are some exceptions to challenge these biomarker indicators while non-necroptotic functions of increased RIPK1 and RIPK3 or necrosis induced without RIPK1 and RIPK3. In detail, the increased expression of RIPK1 and/or RIPK3 could contribute to inflammatory processes as an independent necrotic pathway by regulating pro-inflammatory cytokines (e.g., TNF, IL-1β, and IL-18) (Christofferson et al., 2012; Moriwaki and Chan, 2014; Wong et al., 2014). The phosphorylation status of RIPK3 on S227, and MLKL on Ser358 and Thr357, is considered to reflect activation toward necroptosis (Degterev et al., 2008; McQuade et al., 2013; Wang et al., 2020b). For this biomarker, kinase-dead RIPK3 could function as an anti-necroptotic factor, and similarly, the negative regulation also includes caspase 8, cellular FLICE-inhibitory protein (c-FLIP), chromatin immunoprecipitation (CHIP), MAPK (mitogen-activated protein kinase)-activated protein kinase 2 (MK2), pellino E3 ubiquitin protein ligase 1 (PELI1), and ABIN-1 (A20 binding and inhibitor of NF-κB) (Wang et al., 2018c).

The levels of Atg and LC3

For monitoring autophagy *in vivo*, the 'core' *Atg* genes knockout mouse, GFP-LC3 transgenic mouse, TfLC3 transgenic mouse, and GFP-LC3-RFP-LC3ΔG transgenic mouse are often used as animal models to detect specific protein markers (Kuma et al., 2017). These markers are experimentally adapted as follows: (1) identification of autophagy-related (ATG) genes and proteins related to the initiation of autophagy could be used to assess the activity of autophagy and to study the role of autophagy in the pathophysiological process; (2) for the LC3 (LC3B) and GABARAP family, the ratio of lipidated LC3 (LC3-II) to free LC3 is usually utilized to reflect the number of autophagosomes forming at any given time; 3) tandem fluorescent-tagged LC3 (tfLC3) reporters are used as single-molecule probes to detect autophagosomes labeled with yellow (mRFP and GFP) and autolysosomes labeled with red (mRFP only). Other detections include the GFP-LC3-RFP-LC3ΔG probe, etc. However, some of the Atg proteins may have autophagy-independent functions and the underlying mechanisms are not elucidated so far, such that

the detection of autophagy is still facing challenges (Paunovic et al., 2018; Tan et al., 2019). As for specified autophagy, such as mitophagy, it is related to signaling proteins, such as TOMM20, TIMM23, LC3, and p62 (Wang et al., 2020c).

Meanwhile, the levels of beclin have been used as a marker of autophagy, but there should be more prudent use of it, since in some cases, beclin levels can be transcriptionally upregulated to wild-type levels even in beclin heterozygous or beclin allelic loss cells (Murugan and Amaravadi, 2016). The Atg family are also key proteins, but they are not a reliable reflection of autophagic flux unless combined with LC3 (Murugan and Amaravadi, 2016). According to the functions of LC3 processing for autophagosomes, both its formation and features, western blotting is widely used in autophagy monitoring with antibodies against LC3-I and LC3-II. qPCR-based approaches have also been used for detecting the mRNA levels of autophagy regulators, such as beclin-1, ATG1, DRAM, and LC3 (Kuma et al., 2017).

A brief introduction of biomarkers in pyroptosis

Regarding pyroptosis, there are some proteins used as experimental markers, including caspase-1, propidium, IL-1β, GFP, tdRFP, and LDH. Among these, PI staining is always regarded as a proxy for membrane rupture as it is often found simultaneously for these two things, namely the membrane rupture and the activation of the gasdermin pore (Jorgensen et al., 2016). Recently, researchers have evaluated the reliability of the detection as the molecules and proteins that we detected may pass through the membrane rupture, or through the gasdermin pore, or both (Kovacs and Miao, 2017). For instance, PI and IL-1β (4.5 nm; 5 nm) are small enough to pass through the gasdermin pore (10-15 nm), resulting in a situation that detected significant amounts of PI before the membrane rupture happened (Ding et al., 2016; Liu et al., 2016). On the contrary, tdRFP and LDH are larger, so they seem to be released by the membrane rupture event (Shaner et al., 2004; Russo et al., 2016).

A brief introduction of biomarkers in ferroptosis

As a non-apoptotic form of RCDs, ferroptosis is characterized by iron-dependent accumulation of toxic lipid peroxides in plasma membranes. The cystathionine-β-synthase (CBS) is a marker of transsulfuration pathway activity involved in ferroptosis (Wang et al., 2019b). The lipid peroxide level is closely related to ferroptosis, so it provides a useful means to detect ferroptosis in biological samples, such as measuring the level of cellular lipid peroxide via flow cytometry assays, immunostaining, or colorimetric assays (Uchida et al., 1993: Yagi, 1998; Drummen et al., 2002). Meanwhile, intracellular concentrations of iron and Fe^{2+} and the mitochondrial membrane potential are also used as indicators to distinguish the induction of ferroptosis (Wang et al., 2019b, 2020a). Furthermore, increased ACSL4 is required for lipotoxicity in ferroptosis, and unlike the other ACSL members, it seems to be a marker of ferroptosis since ACSL4 is remarkably downregulated in ferroptosis-resistant cells (e.g., LNCaP and K562) (Yuan et al., 2016; Wenzel et al., 2017). As for the specific detection of ferroptosis, the changes of the mitochondria are regarded as one of the most important indicators, including the morphological and biochemical changes. Increased intracellular concentrations of iron and Fe^{2+} can be monitored by kits, such as an Iron Assay Kit (Sigma Aldrich). Increased mitochondrial superoxide can be detected using a specific fluorescent probe, such as MitoSOX^{TM} Red Mitochondrial Superoxide Indicator for live-cell imaging (Invitrogen). Decreased mitochondrial membrane potential is measured by some kits, such as the Mitochondrial Membrane Potential Kit MAK-159 (Sigma Aldrich) for monitoring fluorescence intensity levels ($\lambda_{ex} = 490/\lambda_{em} = 525$ nm) and ($\lambda_{ex} = 540/\lambda_{em} = 590$ nm) for the ratio analysis (Wang et al., 2019b).

A brief introduction of biomarkers in NETosis

Based on the specific molecules involved in the pathway during NETosis, co-localization of neutrophil-derived proteins (such as myeloperoxidase (MPO) and proteinase 3 (PR3)), and extracellular DNA would suggest the presence of NETosis (Kessenbrock et al., 2009; Nakazawa et al., 2012). Additionally, citrullinated histones could be regarded as a marker for indicating NETs formation. Histones are citrullinated by PAD4 which transport from the cytoplasm to the nucleus activated *via* ROS generation and calcium influx (Remijsen et al., 2011; Wang and Wang, 2013). And cfDNA could also function as one form of NETs remnants which could be detected using PicoGreen® (Zhang et al., 2014).

Release of Extracellular Markers Into the Supernatant or Circulating Biomarkers

The biomarkers released from the cells could remain in the tissue fluid or enter bodily fluids as circulating markers. Some of them could be detected *in vitro* from the supernatant of the samples such as from primary or secondary necrotic cells. Similarly, the monitoring of biomarkers *in vivo* in a liquid biopsy (e.g., plasma samples) also provides another method for detection. These kinds of biomarkers include caspases-3 and -7, high mobility group box 1 protein (HMGB-1), and CK18. Identifying the RCDs *via* the circulating biomarkers is a valid noninvasive alternative in clinical applications.

Caspase-3

Caspase-3, a cysteine protease, could retain its tetrapeptide sequence DEVD (a distinct amino acid sequence of Asp-Glu-Val-Asp), which provides cleaving activity for a long time in various extracellular fluids (Hentze et al., 2001). The p20 subunits of caspase-3 and -7 have been detected in the culture medium following secondary necrosis, whereas there are no such markers but only procaspase-3 and -7 in necrosis (Denecker et al., 2001). Thus, it has been proposed as a specific releasing and circulating biomarker to indicate apoptosis in the tissues (Denecker et al., 2001). Apoptotic cells in the tissue could be measured through various technologies, such as the TdT-mediated X-dUTP nick end labeling method and IHC using antibodies against active caspase 3 or caspase-cleaved proteins to identify the degree of apoptosis (Deng et al., 2019; Kunac et al., 2019).

Cytokeratin 18

CK18 releases a protein cleaved via the effector caspases at two distinct sites (Asp238 and Asp396) during cell death (Ku et al., 2016). The method named the M30-Apoptosense assay

(Peviva AB, Bromma, Sweden) is used to measure the caspase-cleavage CK18 at Asp396 (CK18Asp396-NE M30 neo-epitope) and to specifically discriminate between apoptotic and necrotic cell death (Cummings et al., 2008). The circulating ccCK18 was quantitated through a specific ELISA combined with the antibody, which showed a positive signal in M30 and M65 to indicate apoptosis, whereas an exclusive positive signal in M65 was used to indicate necrosis (Kramer et al., 2004). The time and temperature requirements of this test may bias the results since it requires the samples be placed immediately on ice in order to avoid artificial cell death between acquisition and processing (Greystoke et al., 2008).

HMGB-1

High-mobility group box 1, an architectural chromatin-binding factor, could bind to DNA for increasing protein assembly targeted to specific DNA. It is a protein secreted through activated monocytes or macrophages and is passively released *via* necrotic or damaged cells, but it should be mentioned that HMGB-1 cannot be found in apoptotic cells even after undergoing secondary necrosis and partial autolysis, resulting in a failure to promote inflammation even if not cleared promptly by phagocytic cells (Scaffidi et al., 2002). HMGB-1 released from necrotic cells could activate the macrophages *via* the toll-like receptor 2 (TLR2) and toll-like receptor 4 (TLR4) pathway (Park et al., 2004). HMGB-1 can also chemoattract and activate dendritic cells (DCs) with processing and presentation of tumor antigens (Apetoh et al., 2007; Yang et al., 2007).

Other markers released from cells may also provide indicators for RCD detection, such as DNA laddering signals. The "DNA laddering" resulting from fragmented DNA is cleaved through DNase activated *via* the inhibitor of caspase-activated DNase (iCAT) (Krysko et al., 2008). The 166 base pairs (bp)-length cell-free DNA (cfDNA) consists mainly of nucleosome-protected DNA being released from apoptotic tumor cells into the bloodstream, which might be used in the detection of RCD, providing a target for clinical applications (Krysko et al., 2008; Ulz et al., 2016).

Potential Markers

Recently, non-coding RNA (ncRNA) has been confirmed to have a strong correlation with RCDs, and a positive correlation or a negative correlation might be developed as a useful detection method for monitoring RCDs. For instance, miRNAs (microRNA, one of the non-coding RNAs, 21-23 nucleotides long) is closely related to RCDs, like miR-21 is related to necrosis, miR-137 is related to ferroptosis (Park et al., 2004), miR-184 is related to apoptosis, miRNA-335-5p is related to autophagy, and miR-223 is related to pyroptosis (Wang et al., 2015; Afonso et al., 2018; Luo et al., 2018; Zhang Y. et al., 2018; Zhong et al., 2019). Other ncRNAs like long-coding RNA (lincRNA) and circulating RND (circRNA) may also present the same effect (Zhou et al., 2019; Tao et al., 2020). However, some ncRNAs in RCDs of different healthy or pathological cells or tissues emerge with different expression patterns, so there is still controversy about these biomarkers functioning as indicators to detect RCDs. It is also worth noting that RCDs such as apoptotic cells could release vesicles as apoptotic microvesicles and exosomes-like vesicles that are smaller than ApoBDs (apoptotic bodies). Extracellular vesicles (EVs) like exosomes, microvesicles (MV), ApoBDs (1–5 μm in diameter) and ApoMVs (<1 μm in diameter) released from special cells or tissues may have a close connection with RCDs, which suggests an occurrence of RCDs in pathophysiological processes (Caruso and Poon, 2018; Pavlyukov et al., 2018; Grant et al., 2019; Nooshabadi et al., 2020; Qin et al., 2020). Marat S. et al. investigated the extracellular vesicles secreted by apoptotic glioblastoma cells (apoEVs) for apoptotic research associated with a phenotypic shift of the recipient surviving tumor cells (Pavlyukov et al., 2018).

Notably, cell death has been closely linked to inflammation through various signals such as RIPK1, RIPK3, FADD, FLIP and caspase 8. These molecules are incorporated into compatible and exceedingly dynamic Toll-like receptor, retinoic acid-inducible gene I (RIG-I)-like receptors, and NOD-like receptor which have roles in switching from inflammation to cell death, or perform a programmed execution of both. For example, the overexpression of caspase 11 could induce apoptosis (Wang et al., 1996), and it is also linked to inflammation as an upstream regulator of caspase 1 to promote both pyroptosis and pro-IL-1β processing, or as a molecule releasing after lipopolysaccharide (LPS) or tissue injury (Kang et al., 2000). Caspase 8, involved in the extrinsic pathway of apoptosis, could lead to the development of systemic inflammation (Wallach et al., 2014). Pyroptosis is initiated in response to inflammasome activation in the mobilization of the canonical and/or non-canonical pathways (Bergsbaken et al., 2009). The activation of RIPK3 is crucial for necroptosis induced by TNF. The role for RIPK1 is closely related to other molecules as TNFR1, FADD and caspase 8, and TRIF, IFN and RIPK3 related necroptosis to inflammation, or other types of cell death (Dillon et al., 2014; Kaiser et al., 2014; Rickard et al., 2014). As for autophagy, its proteins play a vital role in inflammation, in which the LC3 conjugation system (vital molecules involved in autophagy, i.e., ATG3, ATG5, ATG7, and ATG16L1) is related to the activation of cells with IFN-γ during inflammation (Zhao et al., 2008; Li et al., 2021). LAP could induce pro-inflammatory gene expression and trigger STING-mediated type I interferon responses in tumor-associated macrophages (Cunha et al., 2018). Compelling evidence showed that ferroptosis have an effect on inflammation where ferroptosis inhibitors exerted anti-inflammatory effects in certain diseases (Sun et al., 2020). Besides the events discussed above, there is still a lot of evidence showing a close connection between cell death and inflammation which suggest these specific inflammation-related factors could function as indicators for adjunctive detection of cell death.

All in all, biomarkers provide pathway-specific measures to distinguish different types of RCDs, but there are still some issues: (1) Protein specificity: the overlap or connected markers involved in different types of RCDs; (2) Misleading results: the specific biomarkers are related to other responses not involving the expected cell death, and the occurrence of cell death is not connected with the targeted proteins; (3) Simultaneous events, such as the induction of cell death may result in another cell death or simultaneous events of two or more types of cell death;

(4) Limited detection technology: some of the subtle changes require more sensitive and comprehensive detection techniques or combined manipulations of pathway-specific markers in cell death pathways.

MONITORING AND MEASURING RCDs FROM *in vivo* TO CLINICAL APPLICATIONS

Monitoring and Measuring RCDs *in vivo*

It is hard to mimic the real microenvironment of cells *in vitro* entirely, and the detection of RCDs *in vivo* is vital for research. The gamma camera imaging, CT, MRI/MRS, PET, and radionuclide imaging methods are usually used to monitor the biochemical and physiological processes of RCDs *in vivo* (Brauer, 2003; Huang et al., 2017). As a common example, MRI is used to monitor the volume reduction of a tumor induced by RCDs. For example, ^{23}Na MRI might be a sufficiently useful and practical method in clinical or laboratory detection of apoptosis. ^{23}Na MRI may be sensitive to high concentrations of Na^+ in tissues and have a close connection to electrolyte-macromolecular interactions during RCDs (Brauer, 2003). The monitoring of cell death *in vivo* provides evidence as to whether or not and how much damage occurs and then guide the clinical assessment and treatment based on the severity of the diseases and the drug choice of anti-bacterial or anti-viral agents.

According to various structural and functional perspectives involved in different types of RCD both *in vivo* and *in vitro*, multiple techniques are required for detection with high repeatability, specificity, and precision. The assays related to morphological, biochemical, and functional changes are presented in **Supplementary Table 1**.

RCDs Detection in Clinic Usage

Regulated cell deaths are closely related to a variety of diseases, and mostly detection of RCDs has been used for early diagnosis and prognosis assessment through monitoring the quality and quantity of the biomarkers involved in RCDs and the various molecular players also used as drug targets for treatment (Thygesen et al., 2007). During development, both the nervous system and the immunogenic cells of the hematopoietic system particularly rely on the overproduction of the cells; in other words, RCDs play a vital role in the nervous and the hematopoietic system. A harmonious process that integrates proliferation, differentiation, and RCDs maintains normal development and the generation of functional circuitry within the nervous system, with elimination of neurons migrating and innervating improper targets or ectopic areas, and the limiting amounts of pro-survival factors produced by targets (including glia) resulting in optimal target innervation through competition with neurons (Fricker et al., 2018). Once the balance breaks, it may lead to various neurodegenerative diseases with a fundamental pathological feature of cell death, such as strokes with a high number of neurons dying by necrosis (Tian et al., 2019; Zhou et al., 2020). Some researchers have

TABLE 4 | Biomarkers of RCDs used in diagnostic, prognostic and research histopathology.

Items	Type	Markers	References
Apoptosis	Diagnostic	Bcl-2, p53, FasL, TNF-α, DNA fragmentation, BBC3, PMAIP1, M30, XIAP, Survivin	Karamitopoulou et al., 2007; Farnebo et al., 2011; Omori et al., 2011; Sen et al., 2015; Heng et al., 2016; Bani-Ahmad et al., 2018; Chen et al., 2019; Henrich et al., 2019; Moledina et al., 2019; Schiffmann et al., 2019
	Prognostic	Bcl-2, Bax, p53, Fas, FasL, caspase-2, caspase-3, caspase-7, caspase-8, caspase-9, TNF-α, DNA fragmentation, Bak, Bok, Bim, PUMA, PMAIP1, MCL1, BCL2L10, TRAIL, TRAIL-R1/2/3, c-FLIP, IAPs	Wang P. et al., 2017; Feng et al., 2018; Huang K.H. et al., 2018
Necroptosis	Diagnostic	NLRP3, AUNIP, RIPK1/3	He et al., 2016; Lee et al., 2016; Yang Z. et al., 2019
	Prognostic	NLRP3, MLKL, RIPK1/3, TLR3/TICAM1, AURKA	Yuan et al., 2015; Yao et al., 2017; Conev et al., 2019; Soleymani Fard et al., 2019; Sun et al., 2019; Malhotra et al., 2020
Autophagy	Diagnostic	LC3, Na+/K+-ATPase, mTOR	Mijatovic et al., 2012; Mete et al., 2018; Sui et al., 2018
	Prognostic	LC3, ATG, BECN1, Na^+/K^+-ATPase, AMPK, mTOR	Cao et al., 2016; Cheng et al., 2016; Schläfli et al., 2016; Li et al., 2017; Gajate et al., 2018; Guo et al., 2019
Ferroptosis	Diagnostic	GPX4, ALOX15, SLC7A11, BAP1, HSP90, HSPB1, FANCD2, TP53	Kamal et al., 2004; Guerriero et al., 2015; Saif et al., 2016; Hui et al., 2017; Davidson et al., 2018; Xu et al., 2019
	Prognostic	GPX4, ACSL4, SLC7A11, TFRC, GLS2, DPP4, NCOA4, BAP1, PEBP1, CARS, VDAC2, HSP90, HSPB1, ITGA6, ITGB4, OTUB1, TP53, HSPA5, FANCD2	Wada et al., 2006; Xu et al., 2010; Zhou et al., 2014; Yang Z. et al., 2015; Chen et al., 2016; Luchini et al., 2016; Lu et al., 2017; Sotgia et al., 2017; Sun and Xu, 2017; Zhao et al., 2017; Dimas et al., 2018; Huang Z.C. et al., 2018; Jiao et al., 2018; Kinowaki et al., 2018; Zhang L. et al., 2018; Li M. et al., 2019; Saha et al., 2019; Dinarvand et al., 2020; Feng et al., 2020; Wu G. et al., 2020
Pyroptosis	Diagnostic	GSDMD, caspase-4	Terlizzi et al., 2018; Xu et al., 2018
	Prognostic	GSDMD, LPS, caspase-1, caspase-4, PKA, IL-1β, IL-18	Del Gobbo et al., 2016; Wędrychowicz et al., 2018; Gao et al., 2018; Hosonaga et al., 2018; Terlizzi et al., 2018; García de Guadiana-Romualdo et al., 2019; Gil and Kim, 2019

used multiple detection methods to achieve signaling pathway mining and clinical guidelines, such as the detection of RIP3 and phosphorylated RIP3s using western blots, and verifying the necroptosis of retinal ganglion cells using EM in retinal diseases research (Liao et al., 2017).

In the immune system, many potentially dangerous or useless immune cells could be eliminated through RCD pathways such as the positive selection and negative selection of T cells (Opferman, 2008; Anuradha et al., 2013). The functions of the immune system are also connected to RCDs, such as apoptotic cells being efficiently cleared in a quiescent manner through the immune system (Kolb et al., 2017). Similarly, the breakage of the steady state is closely related to various immune diseases, such as apoptosis-related autoimmune disease and autophagy-related immune renal disease (Mihaljevic et al., 2018; Ye et al., 2019). Elsewhere, in the circulatory system, platelet apoptosis is characterized by platelet-derived microparticle (MP) formation and cell shrinkage in different cellular compartments (mitochondria, cytosol, and plasma membrane) or at the whole-cell level, has a strong correlation with platelet-related diseases such as vascular restenosis, atherosclerosis, wound healing, angiogenesis, inflammation and immune responses (Smyth et al., 2009; Semple et al., 2011; Gyulkhandanyan et al., 2012). In many cancer types, the value of the apoptotic index (AI) in diagnosis or prognosis has been developed but the results of its accurate evaluation and/or standard settings are controversial (Becker et al., 2014; Fu et al., 2014). It has been reported that the subsequent development of diseases is tied closely to AI, which may be a useful biomarker for prospective studies (Braga et al., 2016), but the results still remain controversial.

Furthermore, we have summarized the biomarkers of RCDs used in diagnostic and prognostic assessment in **Table 4** as well as some related clinical applications in **Supplementary Table 2**. The detection of biomarkers in RCDs are widely used in these assessments, but there are still challenges for their accuracy and effectiveness of detection, tissue and species specificity, etc. Furthermore, targeting RCDs is beneficial for not only diagnosis and prognostication, but also treatment through using drugs to regulate the proteins or genes involved in the RCD pathway.

CONCLUSION AND PERSPECTIVE

Regulated cell deaths, a controlled cellular process during development, contribute to a balance in physiological conditions for cell clearance, tissue integrity, and homeostasis in multi-cellular organisms, whereas the dysregulation of RCDs results in various pathological conditions, such as neurodegenerative diseases, developmental and immunological disorders, and cancer. RCDs include many types of cell death: apoptosis, necrosis, autophagy, ferroptosis, and pyroptosis, each of which plays an important role in different physiological and pathological conditions *via* various proteins, genes, and cofactors, building a complex cell signaling network. In the last few years, tremendous progress has been made in digging out the secrets of RCD and striving toward translational medicine and precision medicine. Our team has been engaged in this field of RCD for many years (Huang et al., 2013; Shang et al., 2014, 2017; Ding et al., 2015; Adams et al., 2016; Xiong et al., 2016; Li et al., 2016; Liao et al., 2017; Wang et al., 2018b,c, 2020b; Guo et al., 2020; Wu X. et al., 2020). Remarkably, cryo-EM, emerging as a powerful technique, has been used in a growing number of structural determinations for the assays of high-resolution protein structures besides the proteins involved in RCDs (Cheng et al., 2015). Even realistic presentation of the proteins in their native cellular microenvironment has been achieved through cryo-electron tomography (cryo-ET) (Danev et al., 2019; Kuwana, 2019; Wang et al., 2019a). Also, flow cytometry is regarded as a preferred method since it is sensitive, fast and multifaceted, and this method is constantly improving and being integrated into clinical applications, such as image-based flow cytometry (Kranich et al., 2020). So many methods also show great potential in research and clinical applications, such as real-time fluorometry, or PET and single-photon emission computed tomography (SPECT) with specific tracers, multicolor labeling and sophisticated morphometric analysis, etc. (Grootjans et al., 2016; Wimmer et al., 2020). Remarkably, combining the special markers as indicators for RCDs monitoring would lead to more accurate ways to identify various types of RCDs. All in all, these powerful and specific methods will provide us with stronger evidence to describe the pattern of cell death by identifying molecular players and unraveling the biochemical pathways of death.

AUTHOR CONTRIBUTIONS

X-MH was the major contributor in reviewing the literature, writing the manuscript, and creating descriptive figures. Z-XL was a major contributor to editing the tables and figures. R-HL and J-QS assisted in literature reviews. KX and QZ was a major contributor in editing the manuscript. All authors read and approved the final manuscript.

FUNDING

This research was supported by the National Natural Science Foundation of China (81772134, 81971891, and 81571939), the Key Research and Development Program of Hunan Province (No. 2018SK2091), and the Wu Jie-Ping Medical Foundation of the Minister of Health of China (No. 320.6750.14118).

ACKNOWLEDGMENTS

We would like to thank Editorial certificate Wordviceat (edit@wordvice.com) for English language editing.

SUPPLEMENTARY MATERIAL

The Supplementary Material for this article can be found online at: https://www.frontiersin.org/articles/10.3389/fcell.2021.634690/full#supplementary-material

REFERENCES

Aachoui, Y., Leaf, I. A., Hagar, J. A., Fontana, M. F., Campos, C. G., Zak, D. E., et al. (2013). Caspase-11 protects against bacteria that escape the vacuole. *Science* 339, 975–978. doi: 10.1126/science.1230751

Abdel Karim, N., Gaber, O., Eldessouki, I., Bahassi, E. M., and Morris, J. (2019). Exosomes as a surrogate marker for autophagy in peripheral blood, correlative data from Phase I study of chloroquine in combination with carboplatin/gemcitabine in advanced solid tumors. *Asian Pac. J. Cancer Prev.* 20, 3789–3796. doi: 10.31557/apjcp.2019.20.12.3789

Adams, C. M., Hiebert, S. W., and Eischen, C. M. (2016). Myc induces miRNA-mediated apoptosis in response to HDAC inhibition in hematologic malignancies. *Cancer Res.* 76, 736–748. doi: 10.1158/0008-5472.can-15-1751

Afonso, M. B., Rodrigues, P. M., Simao, A. L., Gaspar, M. M., Carvalho, T., Borralho, P., et al. (2018). miRNA-21 ablation protects against liver injury and necroptosis in cholestasis. *Cell Death Differ.* 25, 857–872. doi: 10.1038/s41418-017-0019-x

Alam, I. S., Neves, A. A., Witney, T. H., Boren, J., and Brindle, K. M. (2010). Comparison of the C2A domain of synaptotagmin-I and annexin-V as probes for detecting cell death. *Bioconjug. Chem.* 21, 884–891. doi: 10.1021/bc9004415

Alturkistany, F., Nichani, K., Houston, K. D., and Houston, J. P. (2019). Fluorescence lifetime shifts of NAD(P)H during apoptosis measured by time-resolved flow cytometry. *Cytomet. A* 95, 70–79. doi: 10.1002/cyto.a.23606

Anderton, H. I, Wicks, P., and Silke, J. (2020). Cell death in chronic inflammation: breaking the cycle to treat rheumatic disease. *Nat. Rev. Rheumatol.* 16, 496–513. doi: 10.1038/s41584-020-0455-8

Anuradha, R., George, P. J., Hanna, L. E., Chandrasekaran, V., Kumaran, P., Nutman, T. B., et al. (2013). IL- 4-, TGF- beta-, and IL-1-dependent expansion of parasite antigen-specific Th9 cells is associated with clinical pathology in human lymphatic filariasis. *J. Immunol.* 191, 2466–2473. doi: 10.4049/jimmunol.1300911

Apetoh, L., Ghiringhelli, F., Tesniere, A., Criollo, A., Ortiz, C., Lidereau, R., et al. (2007). The interaction between HMGB1 and TLR4 dictates the outcome of anticancer chemotherapy and radiotherapy. *Immunol. Rev.* 220, 47–59. doi: 10.1111/j.1600-065x.2007.00573.x

Arias, E. (2017). Methods to study chaperone-mediated autophagy. *Methods Enzymol.* 588, 283–305. doi: 10.1016/bs.mie.2016.10.009

Arrazola, M. S., and Court, F. A. (2019). Compartmentalized necroptosis activation in excitotoxicity-induced axonal degeneration: a novel mechanism implicated in neurodegenerative disease pathology. *Neural Regen. Res.* 14, 1385–1386. doi: 10.4103/1673-5374.253520

Ayna, G., Krysko, D. V., Kaczmarek, A., Petrovski, G., Vandenabeele, P., and Fesus, L. (2012). ATP release from dying autophagic cells and their phagocytosis are crucial for inflammasome activation in macrophages. *PLoS One* 7:e40069. doi: 10.1371/journal.pone.0040069

Baines, C. P., Kaiser, R. A., Purcell, N. H., Blair, N. S., Osinska, H., Hambleton, M. A., et al. (2005). Loss of cyclophilin D reveals a critical role for mitochondrial permeability transition in cell death. *Nature* 434, 658–662. doi: 10.1038/nature03434

Bandura, D. R., Baranov, V. I., Ornatsky, O. I., Antonov, A., Kinach, R., Lou, X., et al. (2009). Mass cytometry: technique for real time single cell multitarget immunoassay based on inductively coupled plasma time-of-flight mass spectrometry. *Anal. Chem.* 81, 6813–6822. doi: 10.1021/ac901049w

Bandyopadhyay, U., and Overholtzer, M. (2016). LAP: the protector against autoimmunity. *Cell Res.* 26, 865–866. doi: 10.1038/cr.2016.70

Bani-Ahmad, M. A., Al-Sweedan, S. A., Al-Asseiri, M. A., and Alkhatib, A. J. (2018). A proposed kinetic model for the diagnostic and prognostic value of WT1 and p53 in acute myeloid leukemia. *Clin. Lab.* 64, 357–363.

Baranova, A., Ivanov, D., Petrash, N., Pestova, A., Skoblov, M., Kelmanson, I., et al. (2004). The mammalian pannexin family is homologous to the invertebrate innexin gap junction proteins. *Genomics* 83, 706–716. doi: 10.1016/j.ygeno.2003.09.025

Baskic, D., Popovic, S., Ristic, P., and Arsenijevic, N. N. (2006). Analysis of cycloheximide-induced apoptosis in human leukocytes: fluorescence microscopy using annexin V/propidium iodide versus acridin orange/ethidium bromide. *Cell Biol. Int.* 30, 924–932. doi: 10.1016/j.cellbi.2006.06.016

Baudhuin, P. (1966). Lysosomes and cellular autophagy. *Brux Med.* 46, 1059–1070.

Becker, M., Muller, C. B., De Bastiani, M. A., and Klamt, F. (2014). The prognostic impact of tumor-associated macrophages and intra-tumoral apoptosis in non-small cell lung cancer. *Histol. Histopathol.* 29, 21–31.

Bendory, T., Bartesaghi, A., and Singer, A. (2020). Single-particle cryo-electron microscopy: mathematical theory, computational challenges, and opportunities. *IEEE Signal. Process. Mag.* 37, 58–76. doi: 10.1109/msp.2019.2957822

Bergamaschi, D., Vossenkamper, A., Lee, W. Y. J., Wang, P., Bochukova, E., and Warnes, G. (2019). Simultaneous polychromatic flow cytometric detection of multiple forms of regulated cell death. *Apoptosis* 24, 453–464. doi: 10.1007/s10495-019-01528-w

Bergsbaken, T., Fink, S. L., and Cookson, B. T. (2009). Pyroptosis: host cell death and inflammation. *Nat. Rev. Microbiol.* 7, 99–109. doi: 10.1038/nrmicro2070

Bernocchi, G., and Barni, S. (1983). Methodological problems in the histochemical demonstration of succinate semialdehyde dehydrogenase activity. *Histochem. J.* 15, 1161–1176. doi: 10.1007/bf01002737

Bhutia, S. K., Praharaj, P. P., Bhol, C. S., Panigrahi, D. P., Mahapatra, K. K., Patra, S., et al. (2019). Monitoring and measuring mammalian autophagy. *Methods Mol. Biol.* 1854, 209–222. doi: 10.1007/7651_2018_159

Boldin, M. P., Goncharov, T. M., Goltsev, Y. V., and Wallach, D. (1996). Involvement of MACH, a novel MORT1/FADD-interacting protease, in Fas/APO-1- and TNF receptor-induced cell death. *Cell* 85, 803–815. doi: 10.1016/s0092-8674(00)81265-9

Boschker, H. T., and Middelburg, J. J. (2002). Stable isotopes and biomarkers in microbial ecology. *FEMS Microbiol. Ecol.* 40, 85–95. doi: 10.1111/j.1574-6941.2002.tb00940.x

Braga, A., Maesta, I., Rocha Soares, R., Elias, K. M., Custodio Domingues, M. A., Barbisan, L. F., et al. (2016). Apoptotic index for prediction of postmolar gestational trophoblastic neoplasia. *Am. J. Obstet. Gynecol.* 215, 336.e1–336.e12.

Brauer, M. (2003). In vivo monitoring of apoptosis. *Prog. Neuropsychopharmacol. Biol. Psychiatry* 27, 323–331.

Brinkmann, V., Reichard, U., Goosmann, C., Fauler, B., Uhlemann, Y., Weiss, D. S., et al. (2004). Neutrophil extracellular traps kill bacteria. *Science* 303, 1532–1535. doi: 10.1126/science.1092385

Broaddus, V. C., Yang, L., Scavo, L. M., Ernst, J. D., and Boylan, A. M. (1996). Asbestos induces apoptosis of human and rabbit pleural mesothelial cells via reactive oxygen species. *J. Clin. Invest.* 98, 2050–2059. doi: 10.1172/jci119010

Burattini, S., and Falcieri, E. (2013). Analysis of cell death by electron microscopy. *Methods Mol. Biol.* 1004, 77–89.

Buschhaus, J. M., Gibbons, A. E., Luker, K. E., and Luker, G. D. (2017). Fluorescence lifetime imaging of a Caspase-3 apoptosis reporter. *Curr. Protoc. Cell Biol.* 77, 21121–211212.

Buschhaus, J. M., Humphries, B., Luker, K. E., and Luker, G. D. (2018). A Caspase-3 reporter for fluorescence lifetime imaging of single-cell apoptosis. *Cells* 7:57. doi: 10.3390/cells7060057

Cao, Q. H., Liu, F., Yang, Z. L., Fu, X. H., Yang, Z. H., Liu, Q., et al. (2016). Prognostic value of autophagy related proteins ULK1, Beclin 1, ATG3, ATG5, ATG7, ATG9, ATG10, ATG12, LC3B and p62/SQSTM1 in gastric cancer. *Am. J. Transl. Res.* 8, 3831–3847.

Cappellini, A., Mantovani, I., Tazzari, P. L., Grafone, T., Martinelli, G., Cocco, L., et al. (2005). Application of flow cytometry to molecular medicine: detection of tumor necrosis factor-related apoptosis-inducing ligand receptors in acute myeloid leukaemia blasts. *Int. J. Mol. Med.* 16, 1041–1048.

Caruso, S., and Poon, I. K. H. (2018). Apoptotic cell-derived extracellular vesicles: more than just debris. *Front. Immunol.* 9:1486. doi: 10.3389/fimmu.2018.01486

Catchpoole, D. R., and Stewart, B. W. (1993). Etoposide-induced cytotoxicity in two human T-cell leukemic lines: delayed loss of membrane permeability rather than DNA fragmentation as an indicator of programmed cell death. *Cancer Res.* 53, 4287–4296.

Cerrato, G., Liu, P., Martins, I., Kepp, O., and Kroemer, G. (2020). Quantitative determination of phagocytosis by bone marrow-derived dendritic cells via imaging flow cytometry. *Methods Enzymol.* 632, 27–37. doi: 10.1016/bs.mie.2019.07.021

Chan, L. L., Lai, N., Wang, E., Smith, T., Yang, X., and Lin, B. (2011). A rapid detection method for apoptosis and necrosis measurement using the Cellometer imaging cytometry. *Apoptosis* 16, 1295–1303. doi: 10.1007/s10495-011-0651-8

Chandra, D., and Tang, D. G. (2009). Detection of apoptosis in cell-free systems. *Methods Mol. Biol.* 559, 65–75. doi: 10.1007/978-1-60327-017-5_5

Chekeni, F. B., Elliott, M. R., Sandilos, J. K., Walk, S. F., Kinchen, J. M., Lazarowski, E. R., et al. (2010). Pannexin 1 channels mediate 'find-me' signal release and membrane permeability during apoptosis. *Nature* 467, 863–867. doi: 10.1038/nature09413

Chen, J., Wang, Y., Wu, J., Yang, J., Li, M., and Chen, Q. (2020). The potential value of targeting ferroptosis in early Brain injury after acute CNS disease. *Front. Mol. Neurosci.* 13:110. doi: 10.3389/fnmol.2020.00110

Chen, R., Xin, G., and Zhang, X. (2019). Long non-coding RNA HCP5 serves as a ceRNA sponging miR-17-5p and miR-27a/b to regulate the pathogenesis of childhood obesity via the MAPK signaling pathway. *J. Pediatr. Endocrinol. Metab.* 32, 1327–1339. doi: 10.1515/jpem-2018-0432

Chen, W. C., Wang, C. Y., Hung, Y. H., Weng, T. Y., Yen, M. C., and Lai, M. D. (2016). Systematic analysis of gene expression alterations and clinical outcomes for long-chain Acyl-Coenzyme A synthetase family in cancer. *PLoS One* 11:e0155660. doi: 10.1371/journal.pone.0155660

Chen, X., Li, W., Ren, J., Huang, D., He, W. T., Song, Y., et al. (2014). Translocation of mixed lineage kinase domain-like protein to plasma membrane leads to necrotic cell death. *Cell Res.* 24, 105–121. doi: 10.1038/cr.2013.171

Cheng, E. H., Wei, M. C., Weiler, S., Flavell, R. A., Mak, T. W., Lindsten, T., et al. (2001). BCL-2, BCL-X(L) sequester BH3 domain-only molecules preventing BAX- and BAK-mediated mitochondrial apoptosis. *Mol. Cell* 8, 705–711. doi: 10.1016/s1097-2765(01)00320-3

Cheng, J., Shuai, X., Gao, J., Cai, M., Wang, G., and Tao, K. (2016). Prognostic significance of AMPK in human malignancies: a meta-analysis. *Oncotarget* 7, 75739–75748. doi: 10.18632/oncotarget.12405

Cheng, S. Y., Wang, S. C., Lei, M., Wang, Z., and Xiong, K. (2018). Regulatory role of calpain in neuronal death. *Neural Regen. Res.* 13, 556–562. doi: 10.4103/1673-5374.228762

Cheng, Y., Grigorieff, N., Penczek, P. A., and Walz, T. (2015). A primer to single-particle cryo-electron microscopy. *Cell* 161, 438–449. doi: 10.1016/j.cell.2015.03.050

Chiang, H. L., Terlecky, S. R., Plant, C. P., and Dice, J. F. (1989). A role for a 70-kilodalton heat shock protein in lysosomal degradation of intracellular proteins. *Science* 246, 382–385. doi: 10.1126/science.2799391

Chipuk, J. E., Moldoveanu, T., Llambi, F., Parsons, M. J., and Green, D. R. (2010). The BCL-2 family reunion. *Mol. Cell* 37, 299–310. doi: 10.1016/j.molcel.2010.01.025

Christofferson, D. E., Li, Y., Hitomi, J., Zhou, W., Upperman, C., Zhu, H., et al. (2012). A novel role for RIP1 kinase in mediating TNFalpha production. *Cell Death Dis.* 3:e320. doi: 10.1038/cddis.2012.64

Cohen, G. M., Sun, X. M., Snowden, R. T., Dinsdale, D., and Skilleter, D. N. (1992). Key morphological features of apoptosis may occur in the absence of internucleosomal DNA fragmentation. *Biochem. J.* 286(Pt 2), 331–334. doi: 10.1042/bj2860331

Collins, A. R. (2004). The comet assay for DNA damage and repair: principles, applications, and limitations. *Mol. Biotechnol.* 26, 249–261. doi: 10.1385/mb:26:3:249

Collins, A. R., Ma, A. G., and Duthie, S. J. (1995). The kinetics of repair of oxidative DNA damage (strand breaks and oxidised pyrimidines) in human cells. *Mutat. Res.* 336, 69–77. doi: 10.1016/0921-8777(94)00043-6

Conev, N. V., Dimitrova, E. G., Bogdanova, M. K., Kashlov, Y. K., Chaushev, B. G., Radanova, M. A., et al. (2019). RIPK3 expression as a potential predictive and prognostic marker in metastatic colon cancer. *Clin. Invest. Med.* 42, E31–E38.

Cookson, B. T., and Brennan, M. A. (2001). Pro-inflammatory programmed cell death. *Trends Microbiol.* 9, 113–114. doi: 10.1016/s0966-842x(00)01936-3

Crowley, L. C., Marfell, B. J., Christensen, M. E., and Waterhouse, N. J. (2016a). Measuring cell death by trypan blue uptake and light microscopy. *Cold Spring Harb. Protoc.* 7:pdb.prot087155. doi: 10.1101/pdb.prot087155

Crowley, L. C., Marfell, B. J., Scott, A. P., and Waterhouse, N. J. (2016c). Analysis of cytochrome c release by immunocytochemistry. *Cold Spring Harb. Protoc.* 2016:pdb.prot087338. doi: 10.1101/pdb.prot087338

Crowley, L. C., Marfell, B. J., and Waterhouse, N. J. (2016b). Analyzing cell death by nuclear staining with hoechst 33342. *Cold Spring Harb. Protoc.* 2016:pdb.prot087205. doi: 10.1101/pdb.prot087205

Crowley, L. C., Marfell, B. J., and Waterhouse, N. J. (2016d). Morphological analysis of cell death by cytospinning followed by rapid staining. *Cold Spring Harb. Protoc.* 2016:pdb.prot087197. doi: 10.1101/pdb.prot087197

Cuello-Carrion, F. D., and Ciocca, D. R. (1999). Improved detection of apoptotic cells using a modified in situ TUNEL technique. *J. Histochem. Cytochem.* 47, 837–839. doi: 10.1177/002215549904700614

Cuervo, A. M. (2010). Chaperone-mediated autophagy: selectivity pays off. *Trends Endocrinol. Metab.* 21, 142–150. doi: 10.1016/j.tem.2009.10.003

Cummings, J., Ward, T. H., Greystoke, A., Ranson, M., and Dive, C. (2008). Biomarker method validation in anticancer drug development. *Br. J. Pharmacol.* 153, 646–656. doi: 10.1038/sj.bjp.0707441

Cummings, M. C., Winterford, C. M., and Walker, N. I. (1997). Apoptosis. *Am. J. Surg. Pathol.* 21, 88–101.

Cunha, L. D., Yang, M., Carter, R., Guy, C., Harris, L., Crawford, J. C., et al. (2018). LC3-associated phagocytosis in myeloid cells promotes tumor immune Tolerance. *Cell* 175, 429–441. doi: 10.1016/j.cell.2018.08.061

Danev, R., Yanagisawa, H., and Kikkawa, M. (2019). Cryo-electron microscopy methodology: current aspects and future directions. *Trends Biochem. Sci.* 44, 837–848. doi: 10.1016/j.tibs.2019.04.008

Darzynkiewicz, Z., Galkowski, D., and Zhao, H. (2008). Analysis of apoptosis by cytometry using TUNEL assay. *Methods* 44, 250–254. doi: 10.1016/j.ymeth.2007.11.008

Davidson, B., Tötsch, M., Wohlschlaeger, J., Hager, T., and Pinamonti, M. (2018). The diagnostic role of BAP1 in serous effusions. *Hum. Pathol.* 79, 122–126. doi: 10.1016/j.humpath.2018.05.012

De Falco, F., Restucci, B., Urraro, C., and Roperto, S. (2020). Microautophagy upregulation in cutaneous lymph nodes of dogs naturally infected by Leishmania infantum. *Parasitol. Res.* 119, 2245–2255. doi: 10.1007/s00436-020-06718-z

de Vasconcelos, N. M., Van Opdenbosch, N., Van Gorp, H., Parthoens, E., and Lamkanfi, M. (2019). Single-cell analysis of pyroptosis dynamics reveals conserved GSDMD-mediated subcellular events that precede plasma membrane rupture. *Cell Death Differ.* 26, 146–161. doi: 10.1038/s41418-018-0106-7

Degterev, A., Hitomi, J., Germscheid, M. I, Ch'en, L., Korkina, O., Teng, X., et al. (2008). Identification of RIP1 kinase as a specific cellular target of necrostatins. *Nat. Chem. Biol.* 4, 313–321. doi: 10.1038/nchembio.83

Del Gobbo, A., Peverelli, E., Treppiedi, D., Lania, A., Mantovani, G., and Ferrero, S. (2016). Expression of protein kinase A regulatory subunits in benign and malignant human thyroid tissues: a systematic review. *Exp. Cell Res.* 346, 85–90. doi: 10.1016/j.yexcr.2016.06.004

Del Re, D. P., Amgalan, D., Linkermann, A., Liu, Q., and Kitsis, R. N. (2019). Fundamental mechanisms of regulated cell death and implications for heart disease. *Physiol. Rev.* 99, 1765–1817. doi: 10.1152/physrev.00022.2018

Denecker, G., Vercammen, D., Steemans, M., Vanden Berghe, T., Brouckaert, G., Van Loo, G., et al. (2001). Death receptor-induced apoptotic and necrotic cell death: differential role of caspases and mitochondria. *Cell Death Differ.* 8, 829–840. doi: 10.1038/sj.cdd.4400883

Deng, S., Nie, Z. G., Peng, P. J., Liu, Y., Xing, S., Long, L. S., et al. (2019). Decrease of GSK3beta Ser-9 phosphorylation induced osteoblast apoptosis in rat osteoarthritis model. *Curr. Med. Sci.* 39, 75–80. doi: 10.1007/s11596-019-2002-x

Deter, R. L., and De Duve, C. (1967). Influence of glucagon, an inducer of cellular autophagy, on some physical properties of rat liver lysosomes. *J. Cell Biol.* 33, 437–449. doi: 10.1083/jcb.33.2.437

Di Sante, G., Casimiro, M. C., Pestell, T. G., and Pestell, R. G. (2016). Time-Lapse video microscopy for assessment of EYFP-Parkin aggregation as a marker for cellular mitophagy. *J. Vis. Exp.* 111:e53657. doi: 10.3791/53657

Dice, J. F. (1990). Peptide sequences that target cytosolic proteins for lysosomal proteolysis. *Trends Biochem. Sci.* 15, 305–309. doi: 10.1016/0968-0004(90)90019-8

Dillon, C. P., Oberst, A., Weinlich, R., Janke, L. J., Kang, T. B., Ben-Moshe, T., et al. (2012). Survival function of the FADD-CASPASE-8-cFLIP(L) complex. *Cell Rep.* 1, 401–407. doi: 10.1016/j.celrep.2012.03.010

Dillon, C. P., Weinlich, R., Rodriguez, D. A., Cripps, J. G., Quarato, G., Gurung, P., et al. (2014). RIPK1 blocks early postnatal lethality mediated by caspase-8 and RIPK3. *Cell* 157, 1189–1202. doi: 10.1016/j.cell.2014.04.018

Dimas, D. T., Perlepe, C. D., Sergentanis, T. N., Misitzis, I., Kontzoglou, K., Patsouris, E., et al. (2018). The prognostic significance of Hsp70/Hsp90 expression in breast cancer: a systematic review and meta-analysis. *Anticancer Res.* 38, 1551–1562.

Dinarvand, N., Khanahmad, H., Hakimian, S. M., Sheikhi, A., Rashidi, B., and Pourfarzam, M. (2020). Evaluation of long-chain acyl-coenzyme A synthetase 4 (ACSL4) expression in human breast cancer. *Res. Pharm. Sci.* 15, 48–56. doi: 10.4103/1735-5362.278714

Ding, J., Wang, K., Liu, W., She, Y., Sun, Q., Shi, J., et al. (2016). Pore-forming activity and structural autoinhibition of the gasdermin family. *Nature* 535, 111–116. doi: 10.1038/nature18590

Ding, W., Shang, L., Huang, J. F., Li, N., Chen, D., Xue, L. X., et al. (2015). Receptor interacting protein 3-induced RGC-5 cell necroptosis following oxygen glucose deprivation. *BMC Neurosci.* 16:49. doi: 10.1186/s12868-015-0187-x

Dixon, S. J., Lemberg, K. M., Lamprecht, M. R., Skouta, R., Zaitsev, E. M., Gleason, C. E., et al. (2012). Ferroptosis: an iron-dependent form of nonapoptotic cell death. *Cell* 149, 1060–1072. doi: 10.1016/j.cell.2012.03.042

Doll, S., Proneth, B., Tyurina, Y. Y., Panzilius, E., Kobayashi, S., Ingold, I., et al. (2017). ACSL4 dictates ferroptosis sensitivity by shaping cellular lipid composition. *Nat. Chem. Biol.* 13, 91–98. doi: 10.1038/nchembio.2239

Dong, S., Zhao, S., Wang, Y., Pang, T., and Ru, Y. (2015). Analysis of blood cell autophagy distribution in hematologic diseases by transmission electron microscope. *Zhonghua Xue Ye Xue Za Zhi* 36, 144–147.

Drummen, G. P., van Liebergen, L. C., Op den Kamp, J. A., and Post, J. A. (2002). C11-BODIPY(581/591), an oxidation-sensitive fluorescent lipid peroxidation probe: (micro)spectroscopic characterization and validation of methodology. *Free Radic Biol. Med.* 33, 473–490. doi: 10.1016/s0891-5849(02)00848-1

du Toit, A., Hofmeyr, J. S., Gniadek, T. J., and Loos, B. (2018). Measuring autophagosome flux. *Autophagy* 14, 1060–1071.

Elmore, S. (2007). Apoptosis: a review of programmed cell death. *Toxicol. Pathol.* 35, 495–516.

Ericsson, J. L. (1969). Studies on induced cellular autophagy. II. Characterization of the membranes bordering autophagosomes in parenchymal liver cells. *Exp. Cell Res.* 56, 393–405.

Eriksson, S., Kim, S. K., Kubista, M., and Norden, B. (1993). Binding of 4',6-diamidino-2-phenylindole (DAPI) to AT regions of DNA: evidence for an allosteric conformational change. *Biochemistry* 32, 2987–2998. doi: 10.1021/bi00063a009

Farnebo, L., Jerhammar, F., Ceder, R., Grafström, R. C., Vainikka, L., Thunell, L., et al. (2011). Combining factors on protein and gene level to predict radioresponse in head and neck cancer cell lines. *J. Oral Pathol. Med.* 40, 739–746. doi: 10.1111/j.1600-0714.2011.01036.x

Feng, C., Jin, X., Han, Y., Guo, R., Zou, J., Li, Y., et al. (2020). Expression and prognostic analyses of ITGA3, ITGA5, and ITGA6 in head and neck squamous cell carcinoma. *Med. Sci. Monit.* 26:e926800.

Feng, C., Wu, J., Yang, F., Qiu, M., Hu, S., Guo, S., et al. (2018). Expression of Bcl-2 is a favorable prognostic biomarker in lung squamous cell carcinoma. *Oncol. Lett.* 15, 6925–6930.

Feoktistova, M., Geserick, P., and Leverkus, M. (2016). Crystal violet assay for determining viability of cultured cells. *Cold Spring Harb. Protoc.* 2016:pdb.prot087379. doi: 10.1101/pdb.prot087379

Fernandez, S. A., Lobo, A. Z., Oliveira, Z. N., Fukumori, L. M., Robert, A. M. P., and Rivitti, E. A. (2003). Prevalence of antinuclear autoantibodies in the serum of normal blood dornors. *Rev. Hosp. Clin. Fac. Med. Sao Paulo* 58, 315–319. doi: 10.1590/s0041-87812003000600005

Fink, S. L., and Cookson, B. T. (2006). Caspase-1-dependent pore formation during pyroptosis leads to osmotic lysis of infected host macrophages. *Cell Microbiol.* 8, 1812–1825. doi: 10.1111/j.1462-5822.2006.00751.x

Fitzpatrick, A. W., and Saibil, H. R. (2019). Cryo-EM of amyloid fibrils and cellular aggregates. *Curr. Opin. Struct. Biol.* 58, 34–42. doi: 10.1016/j.sbi.2019.05.003

Florey, O., Kim, S. E., Sandoval, C. P., Haynes, C. M., and Overholtzer, M. (2011). Autophagy machinery mediates macroendocytic processing and entotic cell death by targeting single membranes. *Nat. Cell Biol.* 13, 1335–1343. doi: 10.1038/ncb2363

Fricker, M., Tolkovsky, A. M., Borutaite, V., Coleman, M., and Brown, G. C. (2018). Neuronal cell death. *Physiol. Rev.* 98, 813–880.

Friedmann Angeli, J. P., Schneider, M., Proneth, B., Tyurina, Y. Y., Tyurin, V. A., Hammond, V. J., et al. (2014). Inactivation of the ferroptosis regulator Gpx4 triggers acute renal failure in mice. *Nat. Cell Biol.* 16, 1180–1191. doi: 10.1038/ncb3064

Fu, D. R., Kato, D., Watabe, A., Endo, Y., and Kadosawa, T. (2014). Prognostic utility of apoptosis index, Ki-67 and survivin expression in dogs with nasal carcinoma treated with orthovoltage radiation therapy. *J. Vet. Med. Sci.* 76, 1505–1512. doi: 10.1292/jvms.14-0245

Fu, T. M., Li, Y., Lu, A., Li, Z., Vajjhala, P. R., Cruz, A. C., et al. (2016). Cryo-EM structure of caspase-8 Tandem DED filament reveals assembly and regulation mechanisms of the death-inducing signaling complex. *Mol. Cell* 64, 236–250. doi: 10.1016/j.molcel.2016.09.009

Gajate, P., Alonso-Gordoa, T., Martínez-Sáez, O., Molina-Cerrillo, J., and Grande, E. (2018). Prognostic and predictive role of the PI3K-AKT-mTOR pathway in neuroendocrine neoplasms. *Clin. Transl. Oncol.* 20, 561–569. doi: 10.1007/s12094-017-1758-3

Galluzzi, L., Bravo-San Pedro, J. M., Vitale, I., Aaronson, S. A., Abrams, J. M., Adam, D., et al. (2015). Essential versus accessory aspects of cell death: recommendations of the NCCD 2015. *Cell Death Differ.* 22, 58–73.

Galluzzi, L., Kepp, O., Krautwald, S., Kroemer, G., and Linkermann, A. (2014). Molecular mechanisms of regulated necrosis. *Semin. Cell Dev. Biol.* 35, 24–32. doi: 10.1016/j.semcdb.2014.02.006

Galluzzi, L., Vitale, I., Aaronson, S. A., Abrams, J. M., Adam, D., Agostinis, P., et al. (2018). Molecular mechanisms of cell death: recommendations of the nomenclature committee on cell death 2018. *Cell Death Differ.* 25, 486–541.

Galluzzi, L., Vitale, I., Abrams, J. M., Alnemri, E. S., Baehrecke, E. H., Blagosklonny, M. V., et al. (2012). Molecular definitions of cell death subroutines: recommendations of the nomenclature committee on cell death 2012. *Cell Death Differ.* 19, 107–120. doi: 10.1038/cdd.2011.96

Gao, J., Qiu, X., Xi, G., Liu, H., Zhang, F., Lv, T., et al. (2018). Downregulation of GSDMD attenuates tumor proliferation via the intrinsic mitochondrial apoptotic pathway and inhibition of EGFR/Akt signaling and predicts a good prognosis in non-small cell lung cancer. *Oncol. Rep.* 40, 1971–1984.

García de Guadiana-Romualdo, L., Cerezuela-Fuentes, P., Español-Morales, I., Esteban-Torrella, P., Jiménez-Santos, E., Hernando-Holgado, A., et al. (2019). Prognostic value of procalcitonin and lipopolysaccharide binding protein in cancer patients with chemotherapy-associated febrile neutropenia presenting to an emergency department. *Biochem. Med.* 29:010702.

Garcia-Nafria, J., and Tate, C. G. (2020). Cryo-electron microscopy: moving beyond X-Ray crystal structures for drug receptors and drug development. *Annu. Rev. Pharmacol. Toxicol.* 60, 51–71. doi: 10.1146/annurev-pharmtox-010919-023545

Garrod, K. R., Moreau, H. D., Garcia, Z., Lemaitre, F., Bouvier, I., Albert, M. L., et al. (2012). Dissecting T cell contraction in vivo using a genetically encoded reporter of apoptosis. *Cell Rep.* 2, 1438–1447. doi: 10.1016/j.celrep.2012.10.015

Gaschler, M. M., Hu, F., Feng, H., Linkermann, A., Min, W., and Stockwell, B. R. (2018). Determination of the subcellular localization and mechanism of action of ferrostatins in suppressing ferroptosis. *ACS Chem. Biol.* 13, 1013–1020. doi: 10.1021/acschembio.8b00199

Geng, J., Ito, Y., Shi, L., Amin, P., Chu, J., Ouchida, A. T., et al. (2017). Regulation of RIPK1 activation by TAK1-mediated phosphorylation dictates apoptosis and necroptosis. *Nat. Commun.* 8:359.

George, T. C., Basiji, D. A., Hall, B. E., Lynch, D. H., Ortyn, W. E., Perry, D. J., et al. (2004). Distinguishing modes of cell death using the imagestream multispectral imaging flow cytometer. *Cytomet. A* 59, 237–245. doi: 10.1002/cyto.a.20048

Geserick, P., Hupe, M., Moulin, M., Wong, W. W., Feoktistova, M., Kellert, B., et al. (2009). Cellular IAPs inhibit a cryptic CD95-induced cell death by limiting RIP1 kinase recruitment. *J. Cell Biol.* 187, 1037–1054. doi: 10.1083/jcb.200904158

Ghayyem, S., and Faridbod, F. (2018). A fluorescent aptamer/carbon dots based assay for cytochrome c protein detection as a biomarker of cell apoptosis. *Methods Appl. Fluoresc.* 7:015005. doi: 10.1088/2050-6120/aaf0ca

Giampazolias, E., Zunino, B., Dhayade, S., Bock, F., Cloix, C., Cao, K., et al. (2017). Mitochondrial permeabilization engages NF-kappaB-dependent anti-tumour activity under caspase deficiency. *Nat. Cell Biol.* 19, 1116–1129. doi: 10.1038/ncb3596

Gil, M., and Kim, K. E. (2019). Interleukin-18 is a prognostic biomarker correlated with CD8(+) T cell and natural killer cell infiltration in skin cutaneous melanoma. *J. Clin. Med.* 8:1993. doi: 10.3390/jcm8111993

Gong, Y., Fan, Z., Luo, G., Yang, C., Huang, Q., Fan, K., et al. (2019). The role of necroptosis in cancer biology and therapy. *Mol. Cancer* 18:100.

Grant, L. R., Milic, I., and Devitt, A. (2019). Apoptotic cell-derived extracellular vesicles: structure-function relationships. *Biochem. Soc. Trans.* 47, 509–516. doi: 10.1042/bst20180080

Green, D. R., and Kroemer, G. (2005). Pharmacological manipulation of cell death: clinical applications in sight? *J. Clin. Invest.* 115, 2610–2617. doi: 10.1172/jci26321

Greystoke, A., Cummings, J., Ward, T., Simpson, K., Renehan, A., Butt, F., et al. (2008). Optimisation of circulating biomarkers of cell death for routine clinical use. *Ann. Oncol.* 19, 990–995. doi: 10.1093/annonc/mdn014

Grootjans, S., Hassannia, B., Delrue, I., Goossens, V., Wiernicki, B., Dondelinger, Y., et al. (2016). A real-time fluorometric method for the simultaneous detection of cell death type and rate. *Nat. Protoc.* 11, 1444–1454. doi: 10.1038/nprot.2016.085

Gu, S., Tan, J., Li, Q., Liu, S., Ma, J., Zheng, Y., et al. (2020). Downregulation of LAPTM4B contributes to the impairment of the autophagic flux via unopposed activation of mTORC1 signaling during myocardial ischemia/reperfusion injury. *Circ. Res.* 128, e148–e165.

Guerrero-Ferreira, R., Kovacik, L., Ni, D., and Stahlberg, H. (2020). New insights on the structure of alpha-synuclein fibrils using cryo-electron microscopy. *Curr. Opin. Neurobiol.* 61, 89–95. doi: 10.1016/j.conb.2020.01.014

Guerriero, E., Capone, F., Accardo, M., Sorice, A., Costantini, M., Colonna, G., et al. (2015). GPX4 and GPX7 over-expression in human hepatocellular carcinoma tissues. *Eur. J. Histochem.* 59:2540.

Guo, G. F., Wang, Y. X., Zhang, Y. J., Chen, X. X., Lu, J. B., Wang, H. H., et al. (2019). Predictive and prognostic implications of 4E-BP1, Beclin-1, and LC3 for cetuximab treatment combined with chemotherapy in advanced colorectal cancer with wild-type KRAS: analysis from real-world data. *World J. Gastroenterol.* 25, 1840–1853. doi: 10.3748/wjg.v25.i15.1840

Guo, L. M., Wang, Z., Li, S. P., Wang, M., Yan, W. T., Liu, F. X., et al. (2020). RIP3/MLKL-mediated neuronal necroptosis induced by methamphetamine at 39°C. *Neural Regen. Res.* 15, 865–874. doi: 10.4103/1673-5374.268902

Gyulkhandanyan, A. V., Mutlu, A., Freedman, J., and Leytin, V. (2012). Markers of platelet apoptosis: methodology and applications. *J. Thromb. Thrombolys.* 33, 397–411. doi: 10.1007/s11239-012-0688-8

Hacker, G. (2000). The morphology of apoptosis. *Cell Tissue Res.* 301, 5–17.

Hashimoto, K., Besla, R., Zamel, R., Juvet, S., Kim, H., Azad, S., et al. (2016). Circulating cell death biomarkers may predict survival in human lung transplantation. *Am. J. Respir. Crit. Care Med.* 194, 97–105. doi: 10.1164/rccm.201510-2115oc

He, S., Huang, S., and Shen, Z. (2016). Biomarkers for the detection of necroptosis. *Cell Mol. Life Sci.* 73, 2177–2181. doi: 10.1007/s00018-016-2192-3

He, T., Xu, X., Zhang, X. Y., Shen, P., Ling, J. Y., Han, Y. X., et al. (2019). Effectiveness of huai qi huang granules on juvenile collagen-induced arthritis and its influence on pyroptosis pathway in synovial tissue. *Curr. Med. Sci.* 39, 784–793. doi: 10.1007/s11596-019-2106-3

Heckmann, B. L., Teubner, B. J. W., Boada-Romero, E., Tummers, B., Guy, C., Fitzgerald, P., et al. (2020a). Noncanonical function of an autophagy protein prevents spontaneous Alzheimer's disease. *Sci. Adv.* 6:eabb9036. doi: 10.1126/sciadv.abb9036

Heckmann, B. L., Teubner, B. J. W., Tummers, B., Boada-Romero, E., Harris, L., Yang, M., et al. (2020b). LC3-associated endocytosis facilitates beta-amyloid clearance and mitigates neurodegeneration in murine Alzheimer's Disease. *Cell* 183, 1733–1734. doi: 10.1016/j.cell.2020.11.033

Heng, B., Ding, H., Ren, H., Shi, L., Chen, J., Wu, X., et al. (2016). Diagnostic performance of fas ligand mRNA expression for acute rejection after kidney transplantation: a systematic review and meta-analysis. *PLoS One* 11:e0165628. doi: 10.1371/journal.pone.0165628

Hengartner, M. O., and Horvitz, H. R. (1994). The ins and outs of programmed cell death during C. elegans development. *Philos. Trans. R. Soc. Lond. B Biol. Sci.* 345, 243–246. doi: 10.1098/rstb.1994.0100

Henrich, M., Bauknecht, A., Hecht, W., and Reinacher, M. (2019). Lack of Bcl-2 expression in feline follicular lymphomas. *J. Vet. Diagn. Invest.* 31, 809–817. doi: 10.1177/1040638719877916

Hentze, H., Schwoebel, F., Lund, S., Keel, M., Ertel, W., Wendel, A., et al. (2001). In vivo and in vitro evidence for extracellular caspase activity released from apoptotic cells. *Biochem. Biophys. Res. Commun.* 283, 1111–1117. doi: 10.1006/bbrc.2001.4918

Hessler, J. A., Budor, A., Putchakayala, K., Mecke, A., Rieger, D., Banaszak Holl, M. M., et al. (2005). Atomic force microscopy study of early morphological changes during apoptosis. *Langmuir* 21, 9280–9286. doi: 10.1021/la051837g

Holdenrieder, S., Von Pawel, J., Nagel, D., and Stieber, P. (2010). Long-term stability of circulating nucleosomes in serum. *Anticancer Res.* 30, 1613–1615.

Holler, N., Zaru, R., Micheau, O., Thome, M., Attinger, A., Valitutti, S., et al. (2000). Fas triggers an alternative, caspase-8-independent cell death pathway using the kinase RIP as effector molecule. *Nat. Immunol.* 1, 489–495. doi: 10.1038/82732

Hosonaga, M., Arima, Y., Sampetrean, O., Komura, D., Koya, I., Sasaki, T., et al. (2018). HER2 heterogeneity is associated with poor survival in HER2-positive breast cancer. *Int. J. Mol. Sci.* 19:2158. doi: 10.3390/ijms19082158

Huang, B., Geng, Z., Yan, S., Li, Z., Cai, J., and Wang, Z. (2017). Water-soluble conjugated polymer as a fluorescent probe for monitoring adenosine triphosphate level fluctuation in cell membranes during cell apoptosis and in vivo. *Anal. Chem.* 89, 8816–8821. doi: 10.1021/acs.analchem.7b01212

Huang, G., Bao, J., Shao, X., Zhou, W., Wu, B., Ni, Z., et al. (2020). Inhibiting pannexin-1 alleviates sepsis-induced acute kidney injury via decreasing NLRP3 inflammasome activation and cell apoptosis. *Life Sci.* 254:117791. doi: 10.1016/j.lfs.2020.117791

Huang, J. F., Shang, L., Zhang, M. Q., Wang, H., Chen, D., Tong, J. B., et al. (2013). Differential neuronal expression of receptor interacting protein 3 in rat retina: involvement in ischemic stress response. *BMC Neurosci.* 14:16. doi: 10.1186/1471-2202-14-16

Huang, K. H., Fang, W. L., Li, A. F., Liang, P. H., Wu, C. W., Shyr, Y. M., et al. (2018). Caspase-3, a key apoptotic protein, as a prognostic marker in gastric cancer after curative surgery. *Int. J. Surg.* 52, 258–263. doi: 10.1016/j.ijsu.2018.02.055

Huang, Z. C., Li, H., Sun, Z. Q., Zheng, J., Zhao, R. K., Chen, J., et al. (2018). Distinct prognostic roles of HSPB1 expression in non-small cell lung cancer. *Neoplasma* 65, 161–166. doi: 10.4149/neo_2018_102

Huerta, S., Goulet, E. J., Huerta-Yepez, S., and Livingston, E. H. (2007). Screening and detection of apoptosis. *J. Surg. Res.* 139, 143–156. doi: 10.1016/j.jss.2006.07.034

Hui, Y., Chen, S., Lombardo, K. A., Resnick, M. B., Mangray, S., and Matoso, A. (2017). ALOX15 immunohistochemistry aids in the diagnosis of eosinophilic esophagitis on pauci-eosinophilic biopsies in children. *Pediatr. Dev. Pathol.* 20, 375–380. doi: 10.1177/1093526617693106

Hunter, A. L., Choy, J. C., and Granville, D. J. (2005). Detection of apoptosis in cardiovascular diseases. *Methods Mol. Med.* 112, 277–289. doi: 10.1385/1-59259-879-x:277

Hurley, J. H., and Nogales, E. (2016). Next-generation electron microscopy in autophagy research. *Curr. Opin. Struct. Biol.* 41, 211–216. doi: 10.1016/j.sbi.2016.08.006

Itoh, K., Jacob, J., and Sokol, Y. S. (1998). A role for xenopus frizzled 8 in dorsal development. *Mech. Dev.* 74, 145–157. doi: 10.1016/s0925-4773(98)00076-8

Jarvis, T. S., Roland, F. M., Dubiak, K. M., Huber, P. W., and Smith, B. D. (2018). Time-lapse imaging of cell death in cell culture and whole living organisms using turn-on deep-red fluorescent probes. *J. Mater. Chem. B* 6, 4963–4971. doi: 10.1039/c8tb01495g

Jiao, X. D., Qin, B. D., You, P., Cai, J., and Zang, Y. S. (2018). The prognostic value of TP53 and its correlation with EGFR mutation in advanced non-small cell lung cancer, an analysis based on cBioPortal data base. *Lung Cancer* 123, 70–75. doi: 10.1016/j.lungcan.2018.07.003

Jones, K., Kim, D. W., Park, J. S., and Khang, C. H. (2016). Live-cell fluorescence imaging to investigate the dynamics of plant cell death during infection by the rice blast fungus *Magnaporthe oryzae*. *BMC Plant Biol.* 16:69. doi: 10.1186/s12870-016-0756-x

Jorgensen, I., Zhang, Y., Krantz, B. A., and Miao, E. A. (2016). Pyroptosis triggers pore-induced intracellular traps (PITs) that capture bacteria and lead to their clearance by efferocytosis. *J. Exp. Med.* 213, 2113–2128. doi: 10.1084/jem.20151613

Kaiser, W. J., Daley-Bauer, L. P., Thapa, R. J., Mandal, P., Berger, S. B., Huang, C., et al. (2014). RIP1 suppresses innate immune necrotic as well as apoptotic cell death during mammalian parturition. *Proc. Natl. Acad. Sci. U.S.A.* 111, 7753–7758. doi: 10.1073/pnas.1401857111

Kamal, A., Boehm, M. F., and Burrows, F. J. (2004). Therapeutic and diagnostic implications of Hsp90 activation. *Trends Mol. Med.* 10, 283–290. doi: 10.1016/j.molmed.2004.04.006

Kang, S. J., Wang, S., Hara, H., Peterson, E. P., Namura, S., Amin-Hanjani, S., et al. (2000). Dual role of caspase-11 in mediating activation of caspase-1 and caspase-3 under pathological conditions. *J. Cell Biol.* 149, 613–622. doi: 10.1083/jcb.149.3.613

Karamitopoulou, E., Cioccari, L., Jakob, S., Vallan, C., Schaffner, T., Zimmermann, A., et al. (2007). Active caspase 3 and DNA fragmentation as markers for apoptotic cell death in primary and metastatic liver tumours. *Pathology* 39, 558–564. doi: 10.1080/00313020701684375

Kendig, D. M., and Tarloff, J. B. (2007). Inactivation of lactate dehydrogenase by several chemicals: implications for in vitro toxicology studies. *Toxicol. Vitro* 21, 125–132. doi: 10.1016/j.tiv.2006.08.004

Kerr, J. F. (1971). Shrinkage necrosis: a distinct mode of cellular death. *J. Pathol.* 105, 13–20. doi: 10.1002/path.1711050103

Kerr, J. F., Winterford, C. M., and Harmon, B. V. (1994). Apoptosis. Its significance in cancer and cancer therapy. *Cancer* 73, 2013–2026. doi: 10.1002/1097-0142(19940415)73:8<2013::aid-cncr2820730802>3.0.co;2-j

Kerr, J. F., Wyllie, A. H., and Currie, A. R. (1972). Apoptosis: a basic biological phenomenon with wide-ranging implications in tissue kinetics. *Br. J. Cancer* 26, 239–257. doi: 10.1038/bjc.1972.33

Kessenbrock, K., Krumbholz, M., Schonermarck, U., Back, W., Gross, W. L., Werb, Z., et al. (2009). Netting neutrophils in autoimmune small-vessel vasculitis. *Nat. Med.* 15, 623–625. doi: 10.1038/nm.1959

Kim, J. Y., Zhao, H., Martinez, J., Doggett, T. A., Kolesnikov, A. V., Tang, P. H., et al. (2013). Noncanonical autophagy promotes the visual cycle. *Cell* 154, 365–376. doi: 10.1016/j.cell.2013.06.012

Kinowaki, Y., Kurata, M., Ishibashi, S., Ikeda, M., Tatsuzawa, A., Yamamoto, M., et al. (2018). Glutathione peroxidase 4 overexpression inhibits ROS-induced cell death in diffuse large B-cell lymphoma. *Lab. Invest.* 98, 609–619. doi: 10.1038/s41374-017-0008-1

Knapp, P. E., Bartlett, W. P., Williams, L. A., Yamada, M., Ikenaka, K., and Skoff, R. P. (1999). Programmed cell death without DNA fragmentation in the jimpy mouse: secreted factors can enhance survival. *Cell Death Differ.* 6, 136–145. doi: 10.1038/sj.cdd.4400457

Knott, G., Rosset, S., and Cantoni, M. (2011). Focussed ion beam milling and scanning electron microscopy of brain tissue. *J. Vis. Exp.* 2011:e2588.

Kolb, J. P., Oguin, T. H. III, Oberst, A., and Martinez, J. (2017). Programmed cell death and inflammation: winter is coming. *Trends Immunol.* 38, 705–718. doi: 10.1016/j.it.2017.06.009

Konca, K., Lankoff, A., Banasik, A., Lisowska, H., Kuszewski, T., Gozdz, S., et al. (2003). A cross-platform public domain PC image-analysis program for the comet assay. *Mutat. Res.* 534, 15–20. doi: 10.1016/s1383-5718(02)00251-6

Kong, Z., Liu, R., and Cheng, Y. (2019). Artesunate alleviates liver fibrosis by regulating ferroptosis signaling pathway. *Biomed. Pharmacother.* 109, 2043–2053. doi: 10.1016/j.biopha.2018.11.030

Koopman, G., Reutelingsperger, C. P., Kuijten, G. A., Keehnen, R. M., Pals, S. T., and van Oers, M. H. (1994). Annexin V for flow cytometric detection of phosphatidylserine expression on B cells undergoing apoptosis. *Blood* 84, 1415–1420. doi: 10.1182/blood.v84.5.1415.1415

Kovacs, S. B., and Miao, E. A. (2017). Gasdermins: effectors of pyroptosis. *Trends Cell Biol.* 27, 673–684. doi: 10.1016/j.tcb.2017.05.005

Kramer, G., Erdal, H., Mertens, H. J., Nap, M., Mauermann, J., Steiner, G., et al. (2004). Differentiation between cell death modes using measurements of different soluble forms of extracellular cytokeratin 18. *Cancer Res.* 64, 1751–1756. doi: 10.1158/0008-5472.can-03-2455

Kranich, J., Chlis, N. K., Rausch, L., Latha, A., Schifferer, M., Kurz, T., et al. (2020). In vivo identification of apoptotic and extracellular vesicle-bound live cells using image-based deep learning. *J. Extracell Ves.* 9:1792683. doi: 10.1080/20013078.2020.1792683

Kroemer, G., El-Deiry, W. S., Golstein, P., Peter, M. E., Vaux, D., Vandenabeele, P., et al. (2005). Classification of cell death: recommendations of the nomenclature committee on cell death. *Cell Death Differ.* 12(Suppl. 2), 1463–1467. doi: 10.1038/sj.cdd.4401724

Kroemer, G., Galluzzi, L., and Brenner, C. (2007). Mitochondrial membrane permeabilization in cell death. *Physiol. Rev.* 87, 99–163. doi: 10.1152/physrev.00013.2006

Kroemer, G., Galluzzi, L., Vandenabeele, P., Abrams, J., Alnemri, E. S., Baehrecke, E. H., et al. (2009). Classification of cell death: recommendations of the Nomenclature committee on cell death 2009. *Cell Death Differ.* 16, 3–11. doi: 10.1038/cdd.2008.150

Krysko, D. V., Vanden Berghe, T., D'Herde, K., and Vandenabeele, P. (2008). Apoptosis and necrosis: detection, discrimination and phagocytosis. *Methods* 44, 205–221. doi: 10.1016/j.ymeth.2007.12.001

Ku, N. O., Strnad, P., Bantel, H., and Omary, M. B. (2016). Keratins: Biomarkers and modulators of apoptotic and necrotic cell death in the liver. *Hepatology* 64, 966–976. doi: 10.1002/hep.28493

Kuma, A., Komatsu, M., and Mizushima, N. (2017). Autophagy-monitoring and autophagy-deficient mice. *Autophagy* 13, 1619–1628. doi: 10.1080/15548627.2017.1343770

Kumar, M., and Sandhir, R. (2018). Hydrogen sulfide in physiological and pathological mechanisms in brain. *CNS Neurol. Disord. Drug Targets* 17, 654–670. doi: 10.2174/1871527317666180605072018

Kunac, N., Sundov, Z., and Vilovic, K. (2019). Apoptosis as a prognostic factor in colorectal carcinoma: comparison of TUNEL method and immunohistochemical expression of caspase-3. *Appl. Immunohistochem. Mol. Morphol.* 27, e22–e27.

Kuwana, T. (2019). Cryo-electron microscopy to study bax pores and MOMP. *Methods Mol. Biol.* 1877, 247–256. doi: 10.1007/978-1-4939-8861-7_17

Kuznetsov, Y. G., Malkin, A. J., and McPherson, A. (1997). Atomic force microscopy studies of living cells: visualization of motility, division, aggregation, transformation, and apoptosis. *J. Struct. Biol.* 120, 180–191. doi: 10.1006/jsbi.1997.3936

Lamkanfi, M., Declercq, W., Kalai, M., Saelens, X., and Vandenabeele, P. (2002). Alice in caspase land. A phylogenetic analysis of caspases from worm to man. *Cell Death Differ.* 9, 358–361. doi: 10.1038/sj.cdd.4400989

Lee, J. H., Rao, M. V., Yang, D. S., Stavrides, P., Im, E., Pensalfini, A., et al. (2019). Transgenic expression of a ratiometric autophagy probe specifically in neurons enables the interrogation of brain autophagy in vivo. *Autophagy* 15, 543–557. doi: 10.1080/15548627.2018.1528812

Lee, S., Suh, G. Y., Ryter, S. W., and Choi, A. M. (2016). Regulation and function of the nucleotide binding domain leucine-rich repeat-containing receptor, pyrin domain-containing-3 inflammasome in lung disease. *Am. J. Respir. Cell Mol. Biol.* 54, 151–160. doi: 10.1165/rcmb.2015-0231tr

Lei, Q., Yi, T., and Chen, C. (2018). NF-κB-Gasdermin D (GSDMD) Axis Couples oxidative stress and NACHT, LRR and PYD domains-containing protein 3 (NLRP3) inflammasome-mediated cardiomyocyte pyroptosis following myocardial infarction. *Med. Sci. Monit.* 24, 6044–6052. doi: 10.12659/msm.908529

Lelliott, P. M., Momota, M., Lee, M. S. J., Kuroda, E., Iijima, N., Ishii, K. J., et al. (2019). Rapid quantification of NETs in vitro and in whole blood samples by imaging flow cytometry. *Cytomet. A* 95, 565–578. doi: 10.1002/cyto.a.23767

Li, H., Gao, L., Min, J., Yang, Y., and Zhang, R. (2021). Neferine suppresses autophagy-induced inflammation, oxidative stress and adipocyte differentiation in Graves' orbitopathy. *J. Cell Mol. Med.* 25, 1949–1957. doi: 10.1111/jcmm.15931

Li, H., Zhu, H., Xu, C. J., and Yuan, J. (1998). Cleavage of BID by caspase 8 mediates the mitochondrial damage in the Fas pathway of apoptosis. *Cell* 94, 491–501. doi: 10.1016/s0092-8674(00)81590-1

Li, L., Feng, R., Xu, Q., Zhang, F., Liu, T., Cao, J., et al. (2017). Expression of the β3 subunit of Na(+)/K(+)-ATPase is increased in gastric cancer and regulates gastric cancer cell progression and prognosis via the PI3/AKT pathway. *Oncotarget* 8, 84285–84299. doi: 10.18632/oncotarget.20894

Li, M., Jiang, X., Wang, G., Zhai, C., Liu, Y., Li, H., et al. (2019). ITGB4 is a novel prognostic factor in colon cancer. *J. Cancer* 10, 5223–5233. doi: 10.7150/jca.29269

Li, X., Fang, F., Gao, Y., Tang, G., Xu, W., Wang, Y., et al. (2019). ROS Induced by killerred targeting mitochondria (mtKR) enhances apoptosis caused by radiation via Cyt c/Caspase-3 pathway. *Oxid. Med. Cell Longev.* 2019: 4528616.

Li, N., Shang, L., Wang, S. C., Liao, L. S., Chen, D., Huang, J. F., et al. (2016). The toxic effect of ALLN on primary rat retinal neurons. *Neurotox Res.* 30, 392–406. doi: 10.1007/s12640-016-9624-6

Li, P., Nijhawan, D., Budihardjo, I., Srinivasula, S. M., Ahmad, M., Alnemri, E. S., et al. (1997). Cytochrome c and dATP-dependent formation of Apaf-1/caspase-9 complex initiates an apoptotic protease cascade. *Cell* 91, 479–489. doi: 10.1016/s0092-8674(00)80434-1

Li, Y., Fu, T. M., Lu, A., Witt, K., Ruan, J., Shen, C., et al. (2018). Cryo-EM structures of ASC and NLRC4 CARD filaments reveal a unified mechanism of nucleation and activation of caspase-1. *Proc. Natl. Acad. Sci. U.S.A.* 115, 10845–10852. doi: 10.1073/pnas.1810524115

Liao, L., Shang, L., Li, N., Wang, S., Wang, M., Huang, Y., et al. (2017). Mixed lineage kinase domain-like protein induces RGC-5 necroptosis following elevated hydrostatic pressure. *Acta Biochim. Biophys. Sin.* 49, 879–889. doi: 10.1093/abbs/gmx088

Liao, S., Hu, X., Liu, Z., Lin, Y., Liang, R., Zhang, Y., et al. (2019). Synergistic action of microwave-induced mild hyperthermia and paclitaxel in inducing apoptosis in the human breast cancer cell line MCF-7. *Oncol. Lett.* 17, 603–615.

Liao, Y., Zhang, H., He, D., Wang, Y., Cai, B., Chen, J., et al. (2019). Retinal pigment epithelium cell death is associated with NLRP3 inflammasome activation by all-trans retinal. *Invest. Ophthalmol. Vis. Sci.* 60, 3034–3045. doi: 10.1167/iovs.18-26360

Lin, J. Y., Ju, S. T., Wu, H. L., and Tung, T. C. (1973). The binding of abrin and ricin by Ehrlich ascites tumor cells. *Cancer Res.* 33, 2688–2691.

Liu, D., Dong, Z., Xiang, F., Liu, H., Wang, Y., Wang, Q., et al. (2020). Dendrobium alkaloids promote neural function after cerebral ischemia-reperfusion injury through inhibiting pyroptosis induced neuronal death in both in vivo and in vitro models. *Neurochem. Res.* 45, 437–454. doi: 10.1007/s11064-019-02935-w

Liu, W., Chen, Y., Meng, J., Wu, M., Bi, F., Chang, C., et al. (2018). Ablation of caspase-1 protects against TBI-induced pyroptosis in vitro and in vivo. *J. Neuroinflam.* 15:48.

Liu, X., Zhang, Z., Ruan, J., Pan, Y., Magupalli, V. G., Wu, H., et al. (2016). Inflammasome-activated gasdermin D causes pyroptosis by forming membrane pores. *Nature* 535, 153–158. doi: 10.1038/nature18629

Liu, Y., and Levine, B. (2015). Autosis and autophagic cell death: the dark side of autophagy. *Cell Death Differ.* 22, 367–376. doi: 10.1038/cdd.2014.143

Liu, Y., Shoji-Kawata, S., Sumpter, R. M., Wei, Y., Ginet, V., Zhang, L., et al. (2013). Autosis is a Na+,K+-ATPase-regulated form of cell death triggered by autophagy-inducing peptides, starvation, and hypoxia-ischemia. *Proc. Natl. Acad. Sci. U.S.A.* 110, 20364–20371. doi: 10.1073/pnas.1319661110

Lockshin, R. A., and Williams, C. M. (1964). Programmed cell death—II. Endocrine potentiation of the breakdown of the intersegmental muscles of silkmoths. *J. Insect. Physiol.* 10, 643–649. doi: 10.1016/0022-1910(64)90034-4

Lockshin, R. A., and Williams, C. M. (1965). Programmed Cell Death–I. Cytology of degeneration in the intersegmental muscles of the pernyi silkmoth. *J. Insect. Physiol.* 11, 123–133. doi: 10.1016/0022-1910(65)90099-5

Lopez, A., Fleming, A., and Rubinsztein, D. C. (2018). Seeing is believing: methods to monitor vertebrate autophagy in vivo. *Open Biol.* 8:180106. doi: 10.1098/rsob.180106

Lu, A. Y., Turban, J. L., Damisah, E. C., Li, J., Alomari, A. K., Eid, T., et al. (2017). Novel biomarker identification using metabolomic profiling to differentiate radiation necrosis and recurrent tumor following Gamma Knife radiosurgery. *J. Neurosurg.* 127, 388–396. doi: 10.3171/2016.8.jns161395

Lu, F., Lan, Z., Xin, Z., He, C., Guo, Z., Xia, X., et al. (2020). Emerging insights into molecular mechanisms underlying pyroptosis and functions of inflammasomes in diseases. *J. Cell Physiol.* 235, 3207–3221. doi: 10.1002/jcp.29268

Luchini, C., Veronese, N., Yachida, S., Cheng, L., Nottegar, A., Stubbs, B., et al. (2016). Different prognostic roles of tumor suppressor gene BAP1 in cancer: a systematic review with meta-analysis. *Genes Chromosom. Cancer* 55, 741–749. doi: 10.1002/gcc.22381

Luo, M., Wu, L., Zhang, K., Wang, H., Zhang, T., Gutierrez, L., et al. (2018). miR-137 regulates ferroptosis by targeting glutamine transporter SLC1A5 in melanoma. *Cell Death Differ.* 25, 1457–1472. doi: 10.1038/s41418-017-0053-8

Luo, X., Budihardjo, I., Zou, H., Slaughter, C., and Wang, X. (1998). Bid, a Bcl2 interacting protein, mediates cytochrome c release from mitochondria in response to activation of cell surface death receptors. *Cell* 94, 481–490. doi: 10.1016/s0092-8674(00)81589-5

Majtnerová, P., and Roušar, T. (2018). An overview of apoptosis assays detecting DNA fragmentation. *Mol. Biol. Rep.* 45, 1469–1478. doi: 10.1007/s11033-018-4258-9

Malhotra, S., Costa, C., Eixarch, H., Keller, C. W., Amman, L., Martínez-Banaclocha, H., et al. (2020). NLRP3 inflammasome as prognostic factor and therapeutic target in primary progressive multiple sclerosis patients. *Brain* 143, 1414–1430. doi: 10.1093/brain/awaa084

Martin, R. M., Leonhardt, H., and Cardoso, M. C. (2005). DNA labeling in living cells. *Cytom. A* 67, 45–52. doi: 10.1002/cyto.a.20172

Martinez, A. M., Kim, A., and Yang, W. S. (2020). Detection of ferroptosis by BODIPY 581/591 C11. *Methods Mol. Biol.* 2108, 125–130. doi: 10.1007/978-1-0716-0247-8_11

Martinez, J., Almendinger, J., Oberst, A., Ness, R., Dillon, C. P., Fitzgerald, P., et al. (2011). Microtubule-associated protein 1 light chain 3 alpha (LC3)-associated phagocytosis is required for the efficient clearance of dead cells. *Proc. Natl. Acad. Sci. U.S.A.* 108, 17396–17401. doi: 10.1073/pnas.1113421108

Martinez, J., Cunha, L. D., Park, S., Yang, M., Lu, Q., Orchard, R., et al. (2016). Noncanonical autophagy inhibits the autoinflammatory, lupus-like response to dying cells. *Nature* 533, 115–119. doi: 10.1038/nature17950

Martinez, J., Malireddi, R. K., Lu, Q., Cunha, L. D., Pelletier, S., Gingras, S., et al. (2015). Molecular characterization of LC3-associated phagocytosis reveals distinct roles for Rubicon, NOX2 and autophagy proteins. *Nat. Cell Biol.* 17, 893–906. doi: 10.1038/ncb3192

Marzella, L., Ahlberg, J., and Glaumann, H. (1980). In vitro uptake of particles by lysosomes. *Exp. Cell Res.* 129, 460–466. doi: 10.1016/0014-4827(80)90515-7

Marzella, L., Ahlberg, J., and Glaumann, H. (1981). Autophagy, heterophagy, microautophagy and crinophagy as the means for intracellular degradation. *Virchows Arch. B Cell Pathol. Incl. Mol. Pathol.* 36, 219–234. doi: 10.1007/bf02912068

Massey, A., Kiffin, R., and Cuervo, A. M. (2004). Pathophysiology of chaperone-mediated autophagy. *Int. J. Biochem. Cell Biol.* 36, 2420–2434. doi: 10.1016/j.biocel.2004.04.010

Mayer, C. T., Gazumyan, A., Kara, E. E., Gitlin, A. D., Golijanin, J., Viant, C., et al. (2017). The microanatomic segregation of selection by apoptosis in the germinal center. *Science* 358:eaao2602. doi: 10.1126/science.aao2602

McArthur, K., Whitehead, L. W., Heddleston, J. M., Li, L., Padman, B. S., Oorschot, V., et al. (2018). BAK/BAX macropores facilitate mitochondrial herniation and mtDNA efflux during apoptosis. *Science* 359:eaao6047. doi: 10.1126/science.aao6047

McQuade, T., Cho, Y., and Chan, F. K. (2013). Positive and negative phosphorylation regulates RIP1- and RIP3-induced programmed necrosis. *Biochem. J.* 456, 409–415. doi: 10.1042/bj20130860

Mesa, K. R., Rompolas, P., Zito, G., Myung, P., Sun, T. Y., Brown, S., et al. (2015). Niche-induced cell death and epithelial phagocytosis regulate hair follicle stem cell pool. *Nature* 522, 94–97. doi: 10.1038/nature14306

Mete, O., Gucer, H., Kefeli, M., and Asa, S. L. (2018). Diagnostic and prognostic biomarkers of adrenal cortical carcinoma. *Am. J. Surg. Pathol.* 42, 201–213. doi: 10.1097/pas.0000000000000943

Mfotie Njoya, E., Eloff, J. N., and McGaw, L. J. (2018). Croton gratissimus leaf extracts inhibit cancer cell growth by inducing caspase 3/7 activation with additional anti-inflammatory and antioxidant activities. *BMC Complem. Altern. Med.* 18:305. doi: 10.1186/s12906-018-2372-9

Micoud, F., Mandrand, B., and Malcus-Vocanson, C. (2001). Comparison of several techniques for the detection of apoptotic astrocytes in vitro. *Cell Prolif.* 34, 99–113. doi: 10.1046/j.1365-2184.2001.00201.x

Mihaljevic, O., Zivancevic-Simonovic, S., Milosevic-Djordjevic, O., Djurdjevic, P., Jovanovic, D., Todorovic, Z., et al. (2018). Apoptosis and genome instability in children with autoimmune diseases. *Mutagenesis* 33, 351–357. doi: 10.1093/mutage/gey037

Mijaljica, D., Prescott, M., and Devenish, R. J. (2011). Microautophagy in mammalian cells: revisiting a 40-year-old conundrum. *Autophagy* 7, 673–682. doi: 10.4161/auto.7.7.14733

Mijatovic, T., Dufrasne, F., and Kiss, R. (2012). Na+/K+-ATPase and cancer. *Pharm. Pat. Anal.* 1, 91–106.

Mizushima, N., and Komatsu, M. (2011). Autophagy: renovation of cells and tissues. *Cell* 147, 728–741. doi: 10.1016/j.cell.2011.10.026

Moledina, D. G., Wilson, F. P., Pober, J. S., Perazella, M. A., Singh, N., Luciano, R. L., et al. (2019). Urine TNF-α and IL-9 for clinical diagnosis of acute interstitial nephritis. *JCI Insight.* 4:e127456.

Moriwaki, K., and Chan, F. K. (2014). Necrosis-dependent and independent signaling of the RIP kinases in inflammation. *Cytokine Growth Fact. Rev.* 25, 167–174. doi: 10.1016/j.cytogfr.2013.12.013

Murata, K., and Wolf, M. (2018). Cryo-electron microscopy for structural analysis of dynamic biological macromolecules. *Biochim. Biophys. Acta Gen. Subj.* 1862, 324–334. doi: 10.1016/j.bbagen.2017.07.020

Murugan, S., and Amaravadi, R. K. (2016). Methods for studying autophagy within the tumor microenvironment. *Adv. Exp. Med. Biol.* 899, 145–166. doi: 10.1007/978-3-319-26666-4_9

Musumeci, G., Castrogiovanni, P., Trovato, F. M., Weinberg, A. M., Al-Wasiyah, M. K., Alqahtani, M. H., et al. (2015). Biomarkers of chondrocyte apoptosis and autophagy in osteoarthritis. *Int. J. Mol. Sci.* 16, 20560–20575. doi: 10.3390/ijms160920560

Nakazawa, D., Tomaru, U., Suzuki, A., Masuda, S., Hasegawa, R., Kobayashi, T., et al. (2012). Abnormal conformation and impaired degradation of propylthiouracil-induced neutrophil extracellular traps: implications of disordered neutrophil extracellular traps in a rat model of myeloperoxidase antineutrophil cytoplasmic antibody-associated vasculitis. *Arthrit. Rheum.* 64, 3779–3787. doi: 10.1002/art.34619

Nguyen, Q. D., Challapalli, A., Smith, G., Fortt, R., and Aboagye, E. O. (2012). Imaging apoptosis with positron emission tomography: 'bench to bedside' development of the caspase-3/7 specific radiotracer [(18)F]ICMT-11. *Eur. J. Cancer* 48, 432–440. doi: 10.1016/j.ejca.2011.11.033

Nicholson, D. W., Ali, A., Thornberry, N. A., Vaillancourt, J. P., Ding, C. K., Gallant, M., et al. (1995). Identification and inhibition of the ICE/CED-3 protease necessary for mammalian apoptosis. *Nature* 376, 37–43. doi: 10.1038/376037a0

Nooshabadi, V. T., Khanmohammadi, M., Shafei, S., Banafshe, H. R., Malekshahi, Z. V., Ebrahimi-Barough, S., et al. (2020). Impact of atorvastatin loaded exosome as an anti-glioblastoma carrier to induce apoptosis of U87 cancer cells in 3D culture model. *Biochem. Biophys. Rep.* 23:100792. doi: 10.1016/j.bbrep.2020.100792

Ohsumi, Y. (2014). Historical landmarks of autophagy research. *Cell Res.* 24, 9–23. doi: 10.1038/cr.2013.169

Omori, K., Mitsuhashi, M., Ishiyama, K., Nair, I., Rawson, J., Todorov, I., et al. (2011). mRNA of the pro-apoptotic gene BBC3 serves as a molecular marker for TNF-α-induced islet damage in humans. *Diabetologia* 54, 2056–2066. doi: 10.1007/s00125-011-2183-8

Opferman, J. T. (2008). Apoptosis in the development of the immune system. *Cell Death Differ.* 15, 234–242. doi: 10.1038/sj.cdd.4402182

Orhon, I., and Reggiori, F. (2017). Assays to monitor autophagy progression in cell cultures. *Cells* 6:20. doi: 10.3390/cells6030020

Otto, F. B., and Thumm, M. (2020). Mechanistic dissection of macro- and micronucleophagy. *Autophagy* 2020, 1–14. doi: 10.1080/15548627.2020.1725402

Paludan, S. R., Reinert, L. S., and Hornung, V. (2019). DNA-stimulated cell death: implications for host defence, inflammatory diseases and cancer. *Nat. Rev. Immunol.* 19, 141–153. doi: 10.1038/s41577-018-0117-0

Paredes-Gamero, E. J., Martins, M. N., Cappabianco, F. A., Ide, J. S., and Miranda, A. (2012). Characterization of dual effects induced by antimicrobial peptides: regulated cell death or membrane disruption. *Biochim. Biophys. Acta* 1820, 1062–1072. doi: 10.1016/j.bbagen.2012.02.015

Park, J. S., Svetkauskaite, D., He, Q., Kim, J. Y., Strassheim, D., Ishizaka, A., et al. (2004). Involvement of toll-like receptors 2 and 4 in cellular activation by high mobility group box 1 protein. *J. Biol. Chem.* 279, 7370–7377. doi: 10.1074/jbc.m306793200

Parzych, K. R., and Klionsky, D. J. (2014). An overview of autophagy: morphology, mechanism, and regulation. *Antioxid. Redox Signal.* 20, 460–473. doi: 10.1089/ars.2013.5371

Pastuhov, S. I., Fujiki, K., Tsuge, A., Asai, K., Ishikawa, S., Hirose, K., et al. (2016). The core molecular machinery used for engulfment of apoptotic cells regulates the JNK pathway mediating axon regeneration in caenorhabditis elegans. *J. Neurosci.* 36, 9710–9721. doi: 10.1523/jneurosci.0453-16.2016

Patel, B., and Cuervo, A. M. (2015). Methods to study chaperone-mediated autophagy. *Methods* 75, 133–140. doi: 10.1016/j.ymeth.2015.01.003

Paunovic, V. I, Petrovic, V., Milenkovic, M., Janjetovic, K., Pravica, V., Dujmovic, I., et al. (2018). Autophagy-independent increase of ATG5 expression in T cells of multiple sclerosis patients. *J. Neuroimmunol.* 319, 100–105. doi: 10.1016/j.jneuroim.2018.03.001

Pavlyukov, M. S., Yu, H., Bastola, S., Minata, M., Shender, V. O., Lee, Y., et al. (2018). Apoptotic Cell-derived extracellular vesicles promote malignancy of glioblastoma via intercellular transfer of splicing factors. *Cancer Cell* 34, 119–135.e10.

Pugsley, H. R. (2017). Quantifying autophagy: measuring LC3 puncta and autolysosome formation in cells using multispectral imaging flow cytometry. *Methods* 112, 147–156. doi: 10.1016/j.ymeth.2016.05.022

Qin, B., Zhang, Q., Hu, X. M., Mi, T. Y., Yu, H. Y., Liu, S. S., et al. (2020). How does temperature play a role in the storage of extracellular vesicles? *J. Cell Physiol.* 235, 7663–7680. doi: 10.1002/jcp.29700

Rahbar Saadat, Y., Saeidi, N., Vahed, S. Z., Barzegari, A., and Barar, J. (2015). An update to DNA ladder assay for apoptosis detection. *Bioimpacts* 5, 25–28. doi: 10.15171/bi.2015.01

Ramirez, M. L. G., and Salvesen, G. S. (2018). A primer on caspase mechanisms. *Semin. Cell Dev. Biol.* 82, 79–85. doi: 10.1016/j.semcdb.2018.01.002

Remijsen, Q., Kuijpers, T. W., Wirawan, E., Lippens, S., Vandenabeele, P., and Vanden Berghe, T. (2011). Dying for a cause: NETosis, mechanisms behind an antimicrobial cell death modality. *Cell Death Differ.* 18, 581–588. doi: 10.1038/cdd.2011.1

Riccardi, C., and Nicoletti, I. (2006). Analysis of apoptosis by propidium iodide staining and flow cytometry. *Nat. Protoc.* 1, 1458–1461. doi: 10.1038/nprot.2006.238

Rickard, J. A., O'Donnell, J. A., Evans, J. M., Lalaoui, N., Poh, A. R., Rogers, T., et al. (2014). RIPK1 regulates RIPK3-MLKL-driven systemic inflammation and emergency hematopoiesis. *Cell* 157, 1175–1188. doi: 10.1016/j.cell.2014.04.019

Rodriguez, D. A., and Green, D. R. (2018). Generation and use of chimeric RIP kinase molecules to study necroptosis. *Methods Mol. Biol.* 187, 71–83. doi: 10.1007/978-1-4939-8754-2_7

Rogoza, R. M., Fairfax, D. F., Henry, P., Merlin, N., Khan, R. F., Gupta, S. K., et al. (2004). Electron spin resonance spectroscopy reveals alpha-phenyl-N-tert-butylnitrone spin-traps free radicals in rat striatum and prevents haloperidol-induced vacuous chewing movements in the rat model of human tardive dyskinesia. *Synapse* 54, 156–163. doi: 10.1002/syn.20078

Roth, C., Pantel, K., Muller, V., Rack, B., Kasimir-Bauer, S., Janni, W., et al. (2011). Apoptosis-related deregulation of proteolytic activities and high serum levels of circulating nucleosomes and DNA in blood correlate with breast cancer progression. *BMC Cancer* 11:4. doi: : 10.1186/1471-2407-11-4

Russo, H. M., Rathkey, J., Boyd-Tressler, A., Katsnelson, M. A., Abbott, D. W., and Dubyak, G. R. (2016). Active Caspase-1 induces plasma membrane pores that precede pyroptotic lysis and are blocked by lanthanides. *J. Immunol.* 197, 1353–1367. doi: 10.4049/jimmunol.1600699

Saha, S. K., Islam, S. M. R., Abdullah-Al-Wadud, M., Islam, S., Ali, F., and Park, K. S. (2019). Multiomics analysis reveals that GLS and GLS2 differentially modulate the clinical outcomes of cancer. *J. Clin. Med.* 8:355. doi: 10.3390/jcm8030355

Saif, R., Awan, A. R., Lyons, L., Gandolfi, B., Tayyab, M., Ellahi Babar, M., et al. (2016). Hspb1 and Tp53 mutation and expression analysis in cat mammary tumors. *Iran J. Biotechnol.* 14, 202–212. doi: 10.15171/ijb.1480

Saraste, A., and Pulkki, K. (2000). Morphologic and biochemical hallmarks of apoptosis. *Cardiovasc. Res.* 45, 528–537. doi: 10.1016/s0008-6363(99)00384-3

Sato, M., Seki, T., Konno, A., Hirai, H., Kurauchi, Y., Hisatsune, A., et al. (2019). Rapamycin activates mammalian microautophagy. *J. Pharmacol. Sci.* 140, 201–204. doi: 10.1016/j.jphs.2019.05.007

Sborgi, L., Ruhl, S., Mulvihill, E., Pipercevic, J., Heilig, R., Stahlberg, H., et al. (2016). GSDMD membrane pore formation constitutes the mechanism of pyroptotic cell death. *EMBO J.* 35, 1766–1778. doi: 10.15252/embj.201694696

Scaffidi, P., Misteli, T., and Bianchi, M. E. (2002). Release of chromatin protein HMGB1 by necrotic cells triggers inflammation. *Nature* 418, 191–195. doi: 10.1038/nature00858

Schiffmann, L. M., Göbel, H., Löser, H., Schorn, F., Werthenbach, J. P., Fuchs, H. F., et al. (2019). Elevated X-linked inhibitor of apoptosis protein (XIAP) expression uncovers detrimental prognosis in subgroups of neoadjuvant treated and T-cell rich esophageal adenocarcinoma. *BMC Cancer* 19:531. doi: 10.1186/s12885-019-5722-1

Schläfli, A. M., Adams, O., Galván, J. A., Gugger, M., Savic, S., Bubendorf, L., et al. (2016). Prognostic value of the autophagy markers LC3 and p62/SQSTM1 in early-stage non-small cell lung cancer. *Oncotarget* 7, 39544–39555. doi: 10.18632/oncotarget.9647

Schneider, K. S., Groß, C. J., Dreier, R. F., Saller, B. S., Mishra, R., Gorka, O., et al. (2017). The inflammasome drives GSDMD-independent secondary pyroptosis

and il-1 release in the absence of Caspase-1 protease activity. *Cell Rep.* 21, 3846–3859. doi: 10.1016/j.celrep.2017.12.018

Seglen, P. O., Luhr, M. I., Mills, G., Saetre, F., Szalai, P., and Engedal, N. (2015). Macroautophagic cargo sequestration assays. *Methods* 75, 25–36. doi: 10.1016/j.ymeth.2014.12.021

Semple, J. W., Italiano, J. E., and Freedman, J. (2011). Platelets and the immune continuum. *Nat. Rev. Immunol.* 11, 264–274. doi: 10.1038/nri2956

Sen, F., Yildiz, I., Odabas, H., Tambas, M., Kilic, L., Karadeniz, A., et al. (2015). Diagnostic value of serum M30 and M65 in patients with nasopharyngeal carcinoma. *Tumour Biol.* 36, 1039–1044. doi: 10.1007/s13277-014-2708-0

Sentelle, R. D., Senkal, C. E., Jiang, W., Ponnusamy, S., Gencer, S., Selvam, S. P., et al. (2012). Ceramide targets autophagosomes to mitochondria and induces lethal mitophagy. *Nat. Chem. Biol.* 8, 831–838. doi: 10.1038/nchembio.1059

Shaner, N. C., Campbell, R. E., Steinbach, P. A., Giepmans, B. N., Palmer, A. E., and Tsien, R. Y. (2004). Improved monomeric red, orange and yellow fluorescent proteins derived from *Discosoma* sp. red fluorescent protein. *Nat. Biotechnol.* 22, 1567–1572. doi: 10.1038/nbt1037

Shang, L., Ding, W., Li, N., Liao, L., Chen, D., Huang, J., et al. (2017). The effects and regulatory mechanism of RIP3 on RGC-5 necroptosis following elevated hydrostatic pressure. *Acta Biochim. Biophys. Sin.* 49, 128–137.

Shang, L., Huang, J. F., Ding, W., Chen, S., Xue, L. X., Ma, R. F., et al. (2014). Calpain: a molecule to induce AIF-mediated necroptosis in RGC-5 following elevated hydrostatic pressure. *BMC Neurosci.* 15:63. doi: 10.1186/1471-2202-15-63

Shi, J., Zhao, Y., Wang, K., Shi, X., Wang, Y., Huang, H., et al. (2015). Cleavage of GSDMD by inflammatory caspases determines pyroptotic cell death. *Nature* 526, 660–665. doi: 10.1038/nature15514

Shukuya, T., Ghai, V., Amann, J. M., Okimoto, T., Shilo, K., Kim, T. K., et al. (2020). Circulating micrornas and extracellular vesicle-containing MicroRNAs as response biomarkers of anti-programmed cell death protein 1 or programmed death-ligand 1 therapy in NSCLC. *J. Thorac. Oncol.* 15, 1773–1781. doi: 10.1016/j.jtho.2020.05.022

Sil, P., Suwanpradid, J., Muse, G., Gruzdev, A., Liu, L., Corcoran, D. L., et al. (2020). Noncanonical autophagy in dermal dendritic cells mediates immunosuppressive effects of UV exposure. *J. Allergy Clin. Immunol.* 145, 1389–1405. doi: 10.1016/j.jaci.2019.11.041

Smyth, S. S., McEver, R. P., Weyrich, A. S., Morrell, C. N., Hoffman, M. R., Arepally, G. M., et al. (2009). Platelet functions beyond hemostasis. *J. Thromb. Haemost* 7, 1759–1766. doi: 10.1111/j.1538-7836.2009.03586.x

Soleymani Fard, S., Sotoudeh, M., Yazdanbod, M., Ghavamzadeh, A., Malekzadeh, R., Yaghmaie, M., et al. (2019). Evaluation of the association between androgen receptor and AURKA and its prognostic value in gastric cancer. *Int. J. Hematol. Oncol. Stem Cell Res.* 13, 174–182.

Sotgia, F., Fiorillo, M., and Lisanti, M. P. (2017). Mitochondrial markers predict recurrence, metastasis and tamoxifen-resistance in breast cancer patients: early detection of treatment failure with companion diagnostics. *Oncotarget* 8, 68730–68745. doi: 10.18632/oncotarget.19612

Sui, X., Li, Y., Sun, Y., Li, C., Li, X., and Zhang, G. (2018). Expression and significance of autophagy genes LC3, Beclin1 and MMP-2 in endometriosis. *Exp. Ther. Med.* 16, 1958–1962.

Sun, C., Muller, E., Meffert, M., and Gerthsen, D. (2018). On the progress of Scanning Transmission Electron Microscopy (STEM) imaging in a scanning electron microscope. *Microsc. Microanal.* 24, 99–106. doi: 10.1017/s1431927618000181

Sun, W., Yu, W., Shen, L., and Huang, T. (2019). MLKL is a potential prognostic marker in gastric cancer. *Oncol. Lett.* 18, 3830–3836.

Sun, X. J., and Xu, G. L. (2017). Overexpression of Acyl-CoA Ligase 4 (ACSL4) in patients with hepatocellular carcinoma and its prognosis. *Med. Sci. Monit.* 23, 4343–4350. doi: 10.12659/msm.906639

Sun, Y., Chen, P., Zhai, B., Zhang, M., Xiang, Y., Fang, J., et al. (2020). The emerging role of ferroptosis in inflammation. *Biomed. Pharmacother.* 127:110108. doi: 10.1016/j.biopha.2020.110108

Takeshige, K., Baba, M., Tsuboi, S., Noda, T., and Ohsumi, Y. (1992). Autophagy in yeast demonstrated with proteinase-deficient mutants and conditions for its induction. *J. Cell Biol.* 119, 301–311. doi: 10.1083/jcb.119.2.301

Tan, J. M. J., Mellouk, N., and Brumell, J. H. (2019). An autophagy-independent role for ATG16L1: promoting lysosome-mediated plasma membrane repair. *Autophagy* 15, 932–933. doi: 10.1080/15548627.2019.1586261

Tang, D., Kang, R., Berghe, T. V., Vandenabeele, P., and Kroemer, G. (2019). The molecular machinery of regulated cell death. *Cell Res.* 29, 347–364. doi: 10.1038/s41422-019-0164-5

Tang, D., and Kroemer, G. (2020). Ferroptosis. *Curr. Biol.* 30, R1292–R1297.

Tao, P., Yang, B., Zhang, H., Sun, L., Wang, Y., and Zheng, W. (2020). The overexpression of lncRNA MEG3 inhibits cell viability and invasion and promotes apoptosis in ovarian cancer by sponging miR-205-5p. *Int. J. Clin. Exp. Pathol* .13, 869–879.

Terlizzi, M., Colarusso, C., De Rosa, I., De Rosa, N., Somma, P., Curcio, C., et al. (2018). Correction: circulating and tumor-associated caspase-4: a novel diagnostic and prognostic biomarker for non-small cell lung cancer. *Oncotarget* 9:29537. doi: 10.18632/oncotarget.25751

Thakur, S., Cattoni, D. I., and Nollmann, M. (2015). The fluorescence properties and binding mechanism of SYTOX green, a bright, low photo-damage DNA intercalating agent. *Eur. Biophys. J.* 44, 337–348. doi: 10.1007/s00249-015-1027-8

Thygesen, K., Alpert, J. S., White, H. D., and Task Force Members (2007). Universal definition of myocardial infarction. *Eur. Heart J.* 28, 2525–2538.

Tian, J., Shi, R., Xiao, P., Liu, T., She, R., Wu, Q., et al. (2019). Hepatitis E virus induces brain injury probably associated with mitochondrial apoptosis. *Front. Cell Infect. Microbiol.* 9:433. doi: 10.3389/fcimb.2019.00433

Tonnus, W., Meyer, C., Paliege, A., Belavgeni, A., von Mässenhausen, A., Bornstein, S. R., et al. (2019). The pathological features of regulated necrosis. *J. Pathol.* 247, 697–707. doi: 10.1002/path.5248

Trump, B. F. I, Berezesky, K., Chang, S. H., and Phelps, P. C. (1997). The pathways of cell death: oncosis, apoptosis, and necrosis. *Toxicol. Pathol.* 25, 82–88. doi: 10.1177/019262339702500116

Uchida, K., Szweda, L. I., Chae, H. Z., and Stadtman, E. R. (1993). Immunochemical detection of 4-hydroxynonenal protein adducts in oxidized hepatocytes. *Proc. Natl. Acad. Sci. U.S.A.* 90, 8742–8746. doi: 10.1073/pnas.90.18.8742

Ulz, P., Thallinger, G. G., Auer, M., Graf, R., Kashofer, K., Jahn, S. W., et al. (2016). Inferring expressed genes by whole-genome sequencing of plasma DNA. *Nat. Genet.* 48, 1273–1278. doi: 10.1038/ng.3648

Van Opdenbosch, N., and Lamkanfi, M. (2019). Caspases in cell death. *Inflamm. Dis. Immun.* 50, 1352–1364.

Vanden Berghe, T., Grootjans, S., Goossens, V., Dondelinger, Y., Krysko, D. V., Takahashi, N., et al. (2013). Determination of apoptotic and necrotic cell death in vitro and in vivo. *Methods* 61, 117–129. doi: 10.1016/j.ymeth.2013.02.011

Vercammen, D., Brouckaert, G., Denecker, G., Van de Craen, M., Declercq, W., Fiers, W., et al. (1998). Dual signaling of the Fas receptor: initiation of both apoptotic and necrotic cell death pathways. *J. Exp. Med.* 188, 919–930. doi: 10.1084/jem.188.5.919

Vermes, I., Haanen, C., Steffens-Nakken, H., and Reutelingsperger, C. (1995). A novel assay for apoptosis. Flow cytometric detection of phosphatidylserine expression on early apoptotic cells using fluorescein labelled Annexin V. *J. Immunol. Methods* 184, 39–51. doi: 10.1016/0022-1759(95)00072-i

Vorobjeva, N. V., and Chernyak, B. V. (2020). NETosis: molecular mechanisms, role in physiology and pathology. *Biochemistry* 85, 1178–1190. doi: 10.1134/s0006297920100065

Wada, S., Noguchi, T., Takeno, S., and Kawahara, K. (2006). PIK3CA and TFRC located in 3q are new prognostic factors in esophageal squamous cell carcinoma. *Ann. Surg. Oncol.* 13, 961–966. doi: 10.1245/aso.2006.08.006

Walker, P. R., Leblanc, J., Smith, B., Pandey, S., and Sikorska, M. (1999). Detection of DNA fragmentation and endonucleases in apoptosis. *Methods* 17, 329–338. doi: 10.1006/meth.1999.0747

Wallach, D., Kang, T. B., Yang, S. H., and Kovalenko, A. (2014). The in vivo significance of necroptosis: lessons from exploration of caspase-8 function. *Cytokine Growth Fact. Rev.* 25, 157–165. doi: 10.1016/j.cytogfr.2013.12.001

Wallberg, F., Tenev, T., and Meier, P. (2016a). Analysis of apoptosis and necroptosis by fluorescence-activated cell sorting. *Cold Spring Harb. Protoc.* 2016:pdb.prot087387. doi: 10.1101/pdb.prot087387

Wallberg, F., Tenev, T., and Meier, P. (2016b). Time-lapse imaging of cell death. *Cold Spring Harb. Protoc.* 2016:pdb.prot087395.

Wang, H., An, P., Xie, E., Wu, Q., Fang, X., Gao, H., et al. (2017). Characterization of ferroptosis in murine models of hemochromatosis. *Hepatology* 66, 449–465. doi: 10.1002/hep.29117

Wang, P., Liang, J., Wang, Z., Hou, H., Shi, L., and Zhou, Z. (2017). The prognostic value of p53 positive in colorectal cancer: a retrospective cohort study. *Tumour Biol.* 39:1010428317703651.

Wang, S., Liao, L., Wang, M., Zhou, H., Huang, Y., Wang, Z., et al. (2017). Pin1 promotes regulated necrosis induced by glutamate in rat retinal neurons via CAST/Calpain2 pathway. *Front. Cell Neurosci.* 11:425. doi: 10.3389/fncel.2017.00425

Wang, J., Hu, M., Wang, J., Qi, J., Han, Z., Wang, G., et al. (2019a). Reconstitution and structure of a plant NLR resistosome conferring immunity. *Science* 364:eaav5870. doi: 10.1126/science.aav5870

Wang, M., Mao, C., Ouyang, L., Liu, Y., Lai, W., Liu, N., et al. (2019b). Long noncoding RNA LINC00336 inhibits ferroptosis in lung cancer by functioning as a competing endogenous RNA. *Cell Death Differ.* 26, 2329–2343. doi: 10.1038/s41418-019-0304-y

Wang, S., Huang, Y., Yan, Y., Zhou, H., Wang, M., Liao, L., et al. (2019c). Calpain2 but not calpain1 mediated by calpastatin following glutamate-induced regulated necrosis in rat retinal neurons. *Ann. Anat.* 221, 57–67. doi: 10.1016/j.aanat.2018.08.005

Wang, S., Liao, L., Huang, Y., Wang, M., Zhou, H., Chen, D., et al. (2019d). Pin1 is regulated by CaMKII activation in glutamate-induced retinal neuronal regulated necrosis. *Front. Cell Neurosci.* 13:276. doi: 10.3389/fncel.2019.00276

Wang, Y. Y., Liu, X. L., and Zhao, R. (2019e). Induction of pyroptosis and its implications in cancer management. *Front. Oncol.* 9:971. doi: 10.3389/fonc.2019.00971

Wang, J. X., Gao, J., Ding, S. L., Wang, K., Jiao, J. Q., Wang, Y., et al. (2015). Oxidative modification of miR-184 enables it to target Bcl-xL and Bcl-w. *Mol. Cell* 59, 50–61. doi: 10.1016/j.molcel.2015.05.003

Wang, M., Mao, C., Ouyang, L., Liu, Y., Lai, W., Liu, N., et al. (2020a). Correction to: long noncoding RNA LINC00336 inhibits ferroptosis in lung cancer by functioning as a competing endogenous RNA. *Cell Death Differ.* 27:1447. doi: 10.1038/s41418-019-0394-6

Wang, M., Wan, H., Wang, S., Liao, L., Huang, Y., Guo, L., et al. (2020b). RSK3 mediates necroptosis by regulating phosphorylation of RIP3 in rat retinal ganglion cells. *J. Anat.* 237, 29–47. doi: 10.1111/joa.13185

Wang, W., Lu, Y., Wang, Y., Zhang, Y., Xia, B., and Cao, J. (2020c). Siderophores induce mitophagy-dependent apoptosis in platelets. *Ann. Transl. Med.* 8:879. doi: 10.21037/atm-20-4861

Wang, S., Miura, M., Jung, Y., Zhu, H., Gagliardini, V., Shi, L., et al. (1996). Identification and characterization of Ich-3, a member of the interleukin-1beta converting enzyme (ICE)/Ced-3 family and an upstream regulator of ICE. *J. Biol. Chem.* 271, 20580–20587. doi: 10.1074/jbc.271.34.20580

Wang, S., and Wang, Y. (2013). Peptidylarginine deiminases in citrullination, gene regulation, health and pathogenesis. *Biochim. Biophys. Acta* 1829, 1126–1135. doi: 10.1016/j.bbagrm.2013.07.003

Wang, Y. C., Liu, Q. X., Liu, T., Xu, X. E., Gao, W., Bai, X. J., et al. (2018a). Caspase-1-dependent pyroptosis of peripheral blood mononuclear cells predicts the development of sepsis in severe trauma patients: A prospective observational study. *Medicine* 97:e9859. doi: 10.1097/md.0000000000009859

Wang, Z., Guo, L. M., Wang, Y., Zhou, H. K., Wang, S. C., Chen, D., et al. (2018b). Inhibition of HSP90alpha protects cultured neurons from oxygen-glucose deprivation induced necroptosis by decreasing RIP3 expression. *J. Cell Physiol.* 233, 4864–4884. doi: 10.1002/jcp.26294

Wang, Z., Guo, L. M., Zhou, H. K., Qu, H. K., Wang, S. C., Liu, F. X., et al. (2018c). Using drugs to target necroptosis: dual roles in disease therapy. *Histol. Histopathol.* 33, 773–789.

Wędrychowicz, A., Tomasik, P., Zając, A., and Fyderek, K. (2018). Prognostic value of assessment of stool and serum IL-1β, IL-1ra and IL-6 concentrations in children with active and inactive ulcerative colitis. *Arch. Med. Sci.* 14, 107–114. doi: 10.5114/aoms.2017.68696

Wei, M. C., Zong, W. X., Cheng, E. H., Lindsten, T., Panoutsakopoulou, V., Ross, A. J., et al. (2001). Proapoptotic BAX and BAK: a requisite gateway to mitochondrial dysfunction and death. *Science* 292, 727–730. doi: 10.1126/science.1059108

Wenzel, S. E., Tyurina, Y. Y., Zhao, J., St Croix, C. M., Dar, H. H., Mao, G., et al. (2017). PEBP1 wardens ferroptosis by enabling lipoxygenase generation of lipid death signals. *Cell* 171, 628–641.e26.

Wimmer, K., Sachet, M., and Oehler, R. (2020). Circulating biomarkers of cell death. *Clin. Chim. Acta* 500, 87–97. doi: 10.1016/j.cca.2019.10.003

Wong, W. W., Vince, J. E., Lalaoui, N., Lawlor, K. E., Chau, D., Bankovacki, A., et al. (2014). cIAPs and XIAP regulate myelopoiesis through cytokine production in an RIPK1- and RIPK3-dependent manner. *Blood* 123, 2562–2572. doi: 10.1182/blood-2013-06-510743

Wu, G., Wang, Q., Xu, Y., Li, Q., and Cheng, L. (2020). A new survival model based on ferroptosis-related genes for prognostic prediction in clear cell renal cell carcinoma. *Aging* 12, 14933–14948. doi: 10.18632/aging.103553

Wu, X., Hu, X., Zhang, Q., Liu, F., and Xiong, K. (2020). Regulatory role of chinese herbal medicine in regulated neuronal death. *CNS Neurol. Disord. Drug Targets* 19:1. doi: 10.2174/1871527319666200730165011

Wu, Y., Dong, G., and Sheng, C. (2020). Targeting necroptosis in anticancer therapy: mechanisms and modulators. *Acta Pharm. Sin. B* 10, 1601–1618. doi: 10.1016/j.apsb.2020.01.007

Wu, J. Z., Ardah, M., Haikal, C., Svanbergsson, A., Diepenbroek, M., Vaikath, N. N., et al. (2019). Dihydromyricetin and Salvianolic acid B inhibit alpha-synuclein aggregation and enhance chaperone-mediated autophagy. *Transl. Neurodegener.* 8:18.

Wu, L., Prins, H. J., Helder, M. N., van Blitterswijk, C. A., and Karperien, M. (2012). Trophic effects of mesenchymal stem cells in chondrocyte co-cultures are independent of culture conditions and cell sources. *Tissue Eng. Part A* 18, 1542–1551. doi: 10.1089/ten.tea.2011.0715

Wu, X., Zhang, H., Qi, W., Zhang, Y., Li, J., Li, Z., et al. (2018). Nicotine promotes atherosclerosis via ROS-NLRP3-mediated endothelial cell pyroptosis. *Cell Death Dis.* 9:171.

Xiong, K., Liao, H., Long, L., Ding, Y., Huang, J., and Yan, J. (2016). Necroptosis contributes to methamphetamine-induced cytotoxicity in rat cortical neurons. *Toxicol. Vitro* 35, 163–168. doi: 10.1016/j.tiv.2016.06.002

Xu, B., Jiang, M., Chu, Y., Wang, W., Chen, D., Li, X., et al. (2018). Gasdermin D plays a key role as a pyroptosis executor of non-alcoholic steatohepatitis in humans and mice. *J. Hepatol.* 68, 773–782. doi: 10.1016/j.jhep.2017.11.040

Xu, S., Zhao, F., Liang, Z., Feng, H., Bao, Y., Xu, W., et al. (2019). Expression of FANCD2 is associated with prognosis in patients with nasopharyngeal carcinoma. *Int. J. Clin. Exp. Pathol.* 12, 3465–3473.

Xu, Y. F., Yi, Y., Qiu, S. J., Gao, Q., Li, Y. W., Dai, C. X., et al. (2010). PEBP1 downregulation is associated to poor prognosis in HCC related to hepatitis B infection. *J. Hepatol.* 53, 872–879. doi: 10.1016/j.jhep.2010.05.019

Yagi, K. (1998). Simple assay for the level of total lipid peroxides in serum or plasma. *Methods Mol. Biol.* 108, 101–106. doi: 10.1385/0-89603-472-0:101

Yang, D., Chen, Q., Yang, H., Tracey, K. J., Bustin, M., and Oppenheim, J. J. (2007). High mobility group box-1 protein induces the migration and activation of human dendritic cells and acts as an alarmin. *J. Leukoc Biol.* 81, 59–66. doi: 10.1189/jlb.0306180

Yang, D., He, Y., Munoz-Planillo, R., Liu, Q., and Nunez, G. (2015). Caspase-11 requires the Pannexin-1 channel and the purinergic P2X7 pore to mediate pyroptosis and endotoxic shock. *Immunity* 43, 923–932. doi: 10.1016/j.immuni.2015.10.009

Yang, Z., Zhuang, L., Szatmary, P., Wen, L., Sun, H., Lu, Y., et al. (2015). Upregulation of heat shock proteins (HSPA12A, HSP90B1, HSPA4, HSPA5 and HSPA6) in tumour tissues is associated with poor outcomes from HBV-related early-stage hepatocellular carcinoma. *Int. J. Med. Sci.* 12, 256–263. doi: 10.7150/ijms.10735

Yang, F., Qin, Y., Wang, Y., Li, A., Lv, J., Sun, X., et al. (2018). LncRNA KCNQ1OT1 mediates pyroptosis in diabetic cardiomyopathy. *Cell Physiol. Biochem.* 50, 1230–1244. doi: 10.1159/000494576

Yang, J. W., Zhang, Q. H., and Liu, T. (2018). Autophagy facilitates anticancer effect of 5-fluorouracil in HCT-116 cells. *J. Cancer Res. Ther.* 14, S1141–S1147.

Yang, L. L., Chen, H., Wang, J., Xia, T., Sun, H., Yuan, C. H., et al. (2019). 4-HNE induces apoptosis of human retinal pigment epithelial cells by modifying HSP70. *Curr. Med. Sci.* 39, 442–448. doi: 10.1007/s11596-019-2057-8

Yang, Z., Liang, X., Fu, Y., Liu, Y., Zheng, L., Liu, F., et al. (2019). Identification of AUNIP as a candidate diagnostic and prognostic biomarker for oral squamous cell carcinoma. *eBio Med.* 47, 44–57. doi: 10.1016/j.ebiom.2019.08.013

Yao, C., Li, G., Cai, M., Qian, Y., Wang, L., Xiao, L., et al. (2017). Expression and genetic polymorphism of necroptosis related protein RIPK1 is correlated with severe hepatic ischemia-reperfusion injury and prognosis after hepatectomy in hepatocellular carcinoma patients. *Cancer Biomark.* 20, 23–29. doi: 10.3233/cbm-170525

Yasuhara, S., Zhu, Y., Matsui, T., Tipirneni, N., Yasuhara, Y., Kaneki, M., et al. (2003). Comparison of comet assay, electron microscopy, and flow cytometry for detection of apoptosis. *J. Histochem. Cytochem.* 51, 873–885. doi: 10.1177/002215540305100703

Ye, X., Zhou, X. J., and Zhang, H. (2019). Autophagy in immune-related renal disease. *J. Immunol. Res.* 2019:5071687.

Yorimitsu, T., and Klionsky, D. J. (2005). Autophagy: molecular machinery for self-eating. *Cell Death Differ.* 12(Suppl. 2), 1542–1552. doi: 10.1038/sj.cdd.4401765

Yoshii, S. R., and Mizushima, N. (2017). Monitoring and measuring autophagy. *Int. J. Mol. Sci.* 18:1865. doi: 10.3390/ijms18091865

Yousefi, S., Gold, J. A., Andina, N., Lee, J. J., Kelly, A. M., Kozlowski, E., et al. (2008). Catapult-like release of mitochondrial DNA by eosinophils contributes to antibacterial defense. *Nat. Med.* 14, 949–953. doi: 10.1038/nm.1855

Yousefi, S., Mihalache, C., Kozlowski, E., Schmid, I., and Simon, H. U. (2009). Viable neutrophils release mitochondrial DNA to form neutrophil extracellular traps. *Cell Death Differ.* 16, 1438–1444. doi: 10.1038/cdd.2009.96

Yuan, H., Li, X., Zhang, X., Kang, R., and Tang, D. (2016). Identification of ACSL4 as a biomarker and contributor of ferroptosis. *Biochem. Biophys. Res. Commun.* 478, 1338–1343. doi: 10.1016/j.bbrc.2016.08.124

Yuan, M. M., Xu, Y. Y., Chen, L., Li, X. Y., Qin, J., and Shen, Y. (2015). TLR3 expression correlates with apoptosis, proliferation and angiogenesis in hepatocellular carcinoma and predicts prognosis. *BMC Cancer* 15:245. doi: 10.1186/s12885-015-1262-5

Zahran, R., Ghozy, A., Elkholy, S. S., El-Taweel, F., and El-Magd, M. A. (2020). Combination therapy with melatonin, stem cells and extracellular vesicles is effective in limiting renal ischemia-reperfusion injury in a rat model. *Int. J. Urol.* 27, 1039–1049. doi: 10.1111/iju.14345

Zeiss, C. J. (2003). The apoptosis-necrosis continuum: insights from genetically altered mice. *Vet. Pathol.* 40, 481–495. doi: 10.1354/vp.40-5-481

Zembruski, N. C., Stache, V., Haefeli, W. E., and Weiss, J. (2012). 7-Aminoactinomycin D for apoptosis staining in flow cytometry. *Anal. Biochem.* 429, 79–81. doi: 10.1016/j.ab.2012.07.005

Zhang, L., Huang, Y., Ling, J., Zhuo, W., Yu, Z., Luo, Y., et al. (2018). Overexpression of SLC7A11: a novel oncogene and an indicator of unfavorable prognosis for liver carcinoma. *Future Oncol.* 14, 927–936. doi: 10.2217/fon-2017-0540

Zhang, Y., Liu, X., Bai, X., Lin, Y., Li, Z., Fu, J., et al. (2018). Melatonin prevents endothelial cell pyroptosis via regulation of long noncoding RNA MEG3/miR-223/NLRP3 axis. *J. Pineal. Res.* 64:12449.

Zhang, S., Lu, X., Shu, X., Tian, X., Yang, H., Yang, W., et al. (2014). Elevated plasma cfDNA may be associated with active lupus nephritis and partially attributed to abnormal regulation of neutrophil extracellular traps (NETs) in patients with systemic lupus erythematosus. *Intern. Med.* 53, 2763–2771. doi: 10.2169/internalmedicine.53.2570

Zhao, H., Ji, B., Chen, J., Huang, Q., and Lu, X. (2017). Gpx 4 is involved in the proliferation, migration and apoptosis of glioma cells. *Pathol. Res. Pract.* 213, 626–633. doi: 10.1016/j.prp.2017.04.025

Zhao, Z., Fux, B., Goodwin, M., Dunay, I. R., Strong, D., Miller, B. C., et al. (2008). Autophagosome-independent essential function for the autophagy protein Atg5 in cellular immunity to intracellular pathogens. *Cell Host Microb.* 4, 458–469. doi: 10.1016/j.chom.2008.10.003

Zhong, G., Long, H., Ma, S., Shunhan, Y., Li, J., and Yao, J. (2019). miRNA-335-5p relieves chondrocyte inflammation by activating autophagy in osteoarthritis. *Life Sci.* 226, 164–172. doi: 10.1016/j.lfs.2019.03.071

Zhou, B. H., Tan, P. P., Jia, L. S., Zhao, W. P., Wang, J. C., and Wang, H. W. (2018). PI3K/AKT signaling pathway involvement in fluoride-induced apoptosis in C2C12?cells. *Chemosphere* 199, 297–302. doi: 10.1016/j.chemosphere.2018.02.057

Zhou, L., Zhou, M., Tan, H., and Xiao, M. (2020). Cypermethrin-induced cortical neurons apoptosis via the Nrf2/ARE signaling pathway. *Pestic Biochem. Physiol.* 165:104547. doi: 10.1016/j.pestbp.2020.02.013

Zhou, Y., Wu, J., Fu, X., Du, W., Zhou, L., Meng, X., et al. (2014). OTUB1 promotes metastasis and serves as a marker of poor prognosis in colorectal cancer. *Mol. Cancer* 13:258. doi: 10.1186/1476-4598-13-258

Zhou, Z. B., Huang, G. X., Fu, Q., Han, B., Lu, J. J., Chen, A. M., et al. (2019). circRNA.33186 contributes to the pathogenesis of osteoarthritis by sponging miR-127-5p. *Mol. Ther.* 27, 531–541. doi: 10.1016/j.ymthe.2019.01.006

Zu, Y., Mu, Y., Li, Q., Zhang, S. T., and Yan, H. J. (2019). Icariin alleviates osteoarthritis by inhibiting NLRP3-mediated pyroptosis. *J. Orthop. Surg. Res.* 14:307.

Zubairova, U. S., Verman, P. Y., Oshchepkova, P. A., Elsukova, A. S., and Doroshkov, A. V. (2019). LSM-W(2): laser scanning microscopy worker for wheat leaf surface morphology. *BMC Syst. Biol.* 13:22. doi: 10.1186/s12918-019-0689-8

Zucker, R. M., Hunter, E. S. III, and Rogers, J. M. (2000). Confocal laser scanning microscopy of morphology and apoptosis in organogenesis-stage mouse embryos. *Methods Mol. Biol.* 135, 191–202. doi: 10.1385/1-59259-685-1:191

Zucker, R. M., and Rogers, J. M. (2019). Confocal laser scanning microscopy of morphology and apoptosis in organogenesis-stage mouse embryos. *Methods Mol. Biol.* 1965, 297–311. doi: 10.1007/978-1-4939-9182-2_20

Zychlinsky, A., Prevost, M. C., and Sansonetti, P. J. (1992). *Shigella flexneri* induces apoptosis in infected macrophages. *Nature* 358, 167–169. doi: 10.1038/358167a0

Conflict of Interest: The authors declare that the research was conducted in the absence of any commercial or financial relationships that could be construed as a potential conflict of interest.

frontiers in Cell and Developmental Biology

ORIGINAL RESEARCH
published: 08 November 2021
doi: 10.3389/fcell.2021.630166

Granule Leakage Induces Cell-Intrinsic, Granzyme B-Mediated Apoptosis in Mast Cells

Sabrina Sofia Burgener[1,2†], Melanie Brügger[1,2,3], Nathan Georges François Leborgne[1,2], Sophia Sollberger[1,2], Paola Basilico[3,4], Thomas Kaufmann[5], Phillip Ian Bird[6] and Charaf Benarafa[1,2]*

[1] Institute of Virology and Immunology (IVI), Mittelhäusern, Switzerland, [2] Department of Infectious Diseases and Pathobiology, Vetsuisse Faculty, University of Bern, Bern, Switzerland, [3] Graduate School for Cellular and Biomedical Science, University of Bern, Bern, Switzerland, [4] Theodor Kocher Institute, Department of Preclinical Medicine, Faculty of Medicine, University of Bern, Bern, Switzerland, [5] Institute of Pharmacology, Department of Preclinical Medicine, Faculty of Medicine, University of Bern, Bern, Switzerland, [6] Department of Biochemistry and Molecular Biology, Monash Biomedicine Discovery Institute, Monash University, Clayton, VIC, Australia

OPEN ACCESS

Edited by:
Yinan Gong, University of Pittsburgh, United States

Reviewed by:
Julian Pardo, Fundacion Agencia Aragonesa para la Investigacion y el Desarrollo, Spain
Satoshi Tanaka, Kyoto Pharmaceutical University, Japan

***Correspondence:**
Charaf Benarafa
charaf.benarafa@vetsuisse.unibe.ch

†Present address:
Sabrina Sofia Burgener, Institute for Molecular Bioscience and IMB Centre for Inflammation and Disease Research, The University of Queensland, St. Lucia, QLD, Australia

Specialty section:
This article was submitted to Cell Death and Survival, a section of the journal Frontiers in Cell and Developmental Biology

Received: *16 November 2020*
Accepted: *14 October 2021*
Published: *08 November 2021*

Citation:
Burgener SS, Brügger M, Leborgne NGF, Sollberger S, Basilico P, Kaufmann T, Bird PI and Benarafa C (2021) Granule Leakage Induces Cell-Intrinsic, Granzyme B-Mediated Apoptosis in Mast Cells. Front. Cell Dev. Biol. 9:630166. doi: 10.3389/fcell.2021.630166

Mast cells are multifunctional immune cells scattered in tissues near blood vessels and mucosal surfaces where they mediate important reactions against parasites and contribute to the pathogenesis of allergic reactions. Serine proteases released from secretory granules upon mast cell activation contribute to these functions by modulating cytokine activity, platelet activation and proteolytic neutralization of toxins. The forced release of granule proteases into the cytosol of mast cells to induce cell suicide has recently been proposed as a therapeutic approach to reduce mast cell numbers in allergic diseases, but the molecular pathways involved in granule-mediated mast cell suicide are incompletely defined. To identify intrinsic granule proteases that can cause mast cell death, we used mice deficient in cytosolic serine protease inhibitors and their respective target proteases. We found that deficiency in Serpinb1a, Serpinb6a, and Serpinb9a or in their target proteases did not alter the kinetics of apoptosis induced by growth factor deprivation *in vitro* or the number of peritoneal mast cells *in vivo*. The serine protease cathepsin G induced marginal cell death upon mast cell granule permeabilization only when its inhibitors Serpinb1a or Serpinb6a were deleted. In contrast, the serine protease granzyme B was essential for driving apoptosis in mast cells. On granule permeabilization, granzyme B was required for caspase-3 processing and cell death. Moreover, cytosolic granzyme B inhibitor Serpinb9a prevented caspase-3 processing and mast cell death in a granzyme B-dependent manner. Together, our findings demonstrate that cytosolic serpins provide an inhibitory shield preventing granule protease-induced mast cell apoptosis, and that the granzyme B-Serpinb9a-caspase-3 axis is critical in mast cell survival and could be targeted in the context of allergic diseases.

Keywords: serpins, lysosomal peptidases, cell death, granzyme B, lysosomal permeabilization, mast cells, serine protease

INTRODUCTION

Developing from bone marrow precursors, mature mast cells are scattered in tissues and found strategically placed in the proximity of blood vessels, nerves, hair follicles and mucosal surfaces. Since their discovery by Paul Ehrlich 140 years ago, physiological and pathological functions of mast cells have been debated (Maurer et al., 2003; Bradding and Pejler, 2018). The textbook view is that mast cells contribute prominently to IgE-mediated allergic reactions and control parasite infections via the rapid release of mast cell granule contents (Galli et al., 2008). Beyond essential contributions to allergy and the control of helminth infection, novel functions linked to degranulation of mast cells have been demonstrated in innate and adaptive immune responses against various microbes, neoplasia, and chronic non-allergic inflammatory diseases (Galli et al., 2015; Oskeritzian, 2015).

Among the preformed factors released by degranulation of mast cells, specialized proteases act to amplify or dampen inflammation and, importantly, to inactivate endogenous and exogenous toxins (Metz et al., 2006; Piliponsky et al., 2008, 2012; Akahoshi et al., 2011; Galli et al., 2015; Waern et al., 2016). Among these granule proteases are chymases, which are serine proteases that evolved by gene duplication from a common ancestor shared with granzymes, cathepsin G (CatG) and complement factor D. These protease genes are located on three conserved loci in vertebrates (Ahmad et al., 2014). Mast cell granules also store soluble α- and β-tryptases, which are serine proteases that evolved from membrane-bound γ-tryptases independently of chymases (Trivedi et al., 2007). Finally, mast cell granules also contain other serine proteases such as granzyme B (GzmB) and CatG, which are not restricted to mast cells. Thus, mast cells store a range of serine proteases in their granules, and these proteases may also induce proteolysis and cell suicide if released from granules into the cytosol.

Protease inhibitors such as clade B serpins have a nuclear and/or cytoplasmic intracellular localization and promote survival of neutrophils, NK and activated cytotoxic T cells (Kaiserman and Bird, 2010; Benarafa and Simon, 2017). The specific function of intracellular serpins in mast cell homeostasis has not been elucidated but expression analysis from the literature and publicly available resources support the hypothesis that intracellular serpins may provide a survival shield in mast cells against their own granule proteases. Indeed, the cytosolic inhibitor SERPINB6 is expressed in mast cells in the lung, skin and tonsils, as well as in mastocytoma and systemic mastocytosis (Strik et al., 2004). SERPINB6 forms inhibitory complexes with monomeric β-tryptase (Strik et al., 2004) and is one of the best-characterized inhibitors of CatG (Scott et al., 1999). In addition to SERPINB6, mast cells express SERPINB1, a related cytosolic serpin that inhibits CatG and chymase, as well as other leukocyte granule proteases such as neutrophil elastase, proteinase-3, and granzyme H (Cooley et al., 2001; Benarafa et al., 2002; Wang et al., 2013). SERPINB9 inhibits GzmB and is expressed in natural killer cells, cytotoxic T lymphocytes, dendritic cells as well as mast cells (Bird et al., 1998; Hirst et al., 2003; Bladergroen et al., 2005). Here, we used mice deficient in Serpinb1a (*Sb1a*$^{-/-}$), Serpinb6a (*Sb6a*$^{-/-}$), Serpinb9a (*Sb9a*$^{-/-}$), and their target proteases to investigate serpin function in mast cell homeostasis and survival upon granule permeabilization and growth factor deprivation *in vitro*. We identify a cytoprotective function for these serpins and a major function for GzmB in inducing mast cell apoptosis following cell-intrinsic granule leakage.

RESULTS

Serine Proteases and Caspases Induce Cell Death in Mouse and Human Mast Cells

Permeabilization of granules with L-leucyl-L-leucine methyl ester (LLME), a well-characterized lysosomotropic agent, induces cell death in various leukocytes containing granules (Thiele and Lipsky, 1986, 1990a,b). Melo et al. (2011a, 2015) reported that mast cells are sensitive to LLME-induced death, but the precise molecular mechanisms and whether proteases are involved remain unclear. We replicated their findings showing that treatment of mouse bone marrow-derived mast cells (BMDMCs) with LLME rapidly induces cell death (**Figure 1A**). Inhibition of serine proteases with Pefabloc [a.k.a. 4-benzenesulfonyl fluoride hydrochloride (AEBSF)] inhibited cell death in a dose-dependent manner with optimal concentrations between 10 and 40 μM, although it was toxic at higher concentrations (**Figure 1A**). Inhibition of caspases with Q-VD-OPh also reduced death of BMDMCs treated with LLME, with or without Pefabloc, suggesting multiple proteases operate in this cell death pathway (**Figure 1B**). In addition, we observed a synergistic pro-survival effect of the inhibitors of serine proteases and caspases in the human mast cell line HMC-1.2 treated with LLME (**Figure 1C**). Importantly, LLME induced a strong activation of caspase-3, which was inhibited by both Q-VD-OPh and by Pefabloc (**Figures 1D,E**), suggesting that granule serine proteases may contribute to caspase-3 activation leading to apoptosis.

Expression of Proteases and Corresponding Cytosolic Inhibitors in Mouse Bone Marrow-Derived Mast Cells

To start identifying the protease(s) responsible for inducing cell death, we then evaluated the expression of a broad range of serine proteases in WT BMDMCs during *in vitro* differentiation with recombinant mouse IL-3 for 4, 6, and 8 weeks. mRNA expression levels in WT BMDMCs revealed relatively high expression of the mast cell-restricted serine proteases chymases mMCP-2 and mMCP-5, and the tryptase mMCP-6, whereas mMCP-4, -7, -9, and -10 expression was weak or not detected (**Figure 2A**). Furthermore, we found that serine proteases cathepsin G (CatG), granzyme B (GzmB), and granzyme A (GzmA), which are not restricted to mast cells, are expressed at levels similar to MCP-2, independently of the maturation state of the BMDMCs. Perforin expression, in contrast, was not detected. Expression of the metalloprotease carboxypeptidase 3 (MC-CPA3) was also detected (**Figure 2A**).

Since BMDMCs expressed appreciable mRNA levels of CatG, GzmA, and GzmB, we investigated the expression of their

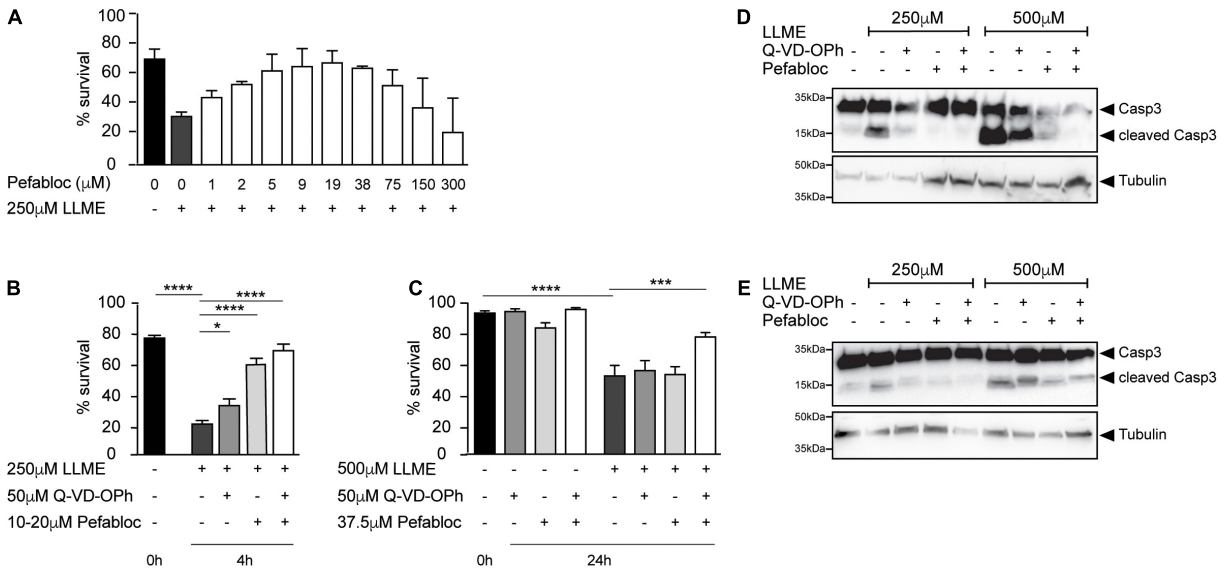

FIGURE 1 | Serine protease- and caspase-dependent cell death in human and mouse mast cells. **(A–C)** Survival of mast cells treated with L-leucyl-L-leucine methyl ester (LLME) in presence of indicated concentrations of serine protease inhibitor (Pefabloc) and pancaspase inhibitor (Q-VD-OPh). Cell viability was determined by flow cytometry as shown in **Supplementary Figure 3**. Data are shown as mean ± SEM. **(A)** WT mouse BMDMCs ($n = 3$). **(B)** BMDMCs of WT mice ($n = 10$). **(C)** Human mast cell line HMC1.2 ($n = 7$–9). **(B,C)** Data are shown as mean ± SEM and were analyzed by one-way ANOVA (****$p < 0.0001$; ***$p < 0.001$; *$p < 0.05$; ns, not significant). **(D,E)** Western blot analysis of caspase-3 cleavage in WT BMDMCs treated with LLME and inhibitors. **(D)** cell lysates and **(E)** cell lysate and supernatant combined are shown. Fifteen μg of protein was loaded in each lane.

respective cytosolic inhibitors in WT BMDMCs during *in vitro* differentiation. We found that two CatG inhibitors *Serpinb1a* (Benarafa et al., 2002) and *Serpinb6a* (Sun et al., 1997) had the highest expression levels. In contrast, transcription of *Serpinb1b*, which also inhibits CatG, was not detectable. Expression of the inhibitors of GzmA and GzmB, *Serpinb6b* (Kaiserman et al., 2014) and *Serpinb9a* (Sun et al., 1997), respectively, were also strongly expressed in all preparations and time points. Expression of *Serpinb6c*, which has no known target protease identified to date, was lower and not consistently detectable (**Figure 2B**). Previous studies reported that GzmA protein is not expressed in mast cells (Pardo et al., 2007; Ronnberg et al., 2014). Using a GzmA-specific antibody and intracellular staining, we found specific staining of GzmA in wild-type NK cells, but not peritoneal mast cells nor BMDMCs, suggesting that GzmA is post-transcriptionally regulated in mast cells (**Supplementary Figures 1A, 2**). Because $Sb6a^{-/-}$ and $Sb9a^{-/-}$ mice express green fluorescent protein (GFP) under the control of the respective endogenous serpin promoter, expression of the GFP reporter was quantified in BMDMCs by flow cytometry. In agreement with the transcription data, higher GFP levels were reported in mast cells when driven by endogenous *Serpinb6a* promoter then when driven by the endogenous *Serpinb9a* promoter. Furthermore, $Sb6a^{-/-}$ and double-deficient $Sb1a.Sb6a^{-/-}$ mast cells had similar levels of GFP expression (**Figure 2C**), indicating that deletion of *Serpinb1a* does not alter basal expression of Serpinb6a in BMDMCs. Co-expression of granule serine proteases and their respective cytosolic inhibitory serpins in BMDMCs suggest cell-intrinsic regulatory mechanisms as shown for other leukocytes (Kaiserman and Bird, 2010; Benarafa and Simon, 2017). We then compared the relative frequency of peritoneal mast cells in mice lacking *Serpinb1a* ($Sb1a^{-/-}$), *Serpinb6a* ($Sb6a^{-/-}$), *Serpinb9a* ($Sb9a^{-/-}$), or both *Serpinb1a* and *Serpinb6a* ($Sb1a.Sb6a^{-/-}$) and found no statistically significant differences compared to WT mice (**Figure 2D** and **Supplementary Figures 1A,B**). Together, these findings show that these cytosolic serpins are not required for development and maturation of mast cells under steady state conditions.

$Sb9a^{-/-}$ Bone Marrow-Derived Mast Cells Are Highly Sensitive to Granule Permeabilization Induced Cell Death

Treatment of WT BMDMCs with LLME rapidly induced cell death (**Figure 3A** and **Supplementary Figure 3**). The effect of LLME on WT BMDMCs was partly reduced by caspase inhibition with Q-VD-OPh (**Figure 3B**). $Sb9a^{-/-}$ BMDMCs treated with LLME for 2 and 4 h showed significantly reduced survival compared to WT BMDMCs with and without Q-VD-OPh (**Figures 3A,B**). In contrast, $Sb1a^{-/-}$, $Sb6a^{-/-}$, and $Sb1a.Sb6a^{-/-}$ BMDMCs treated with LLME showed comparable survival to WT BMDMCs in the absence of Q-VD-OPh. Treatment with Q-VD-OPh was less efficient at improving survival in $Sb1a^{-/-}$, $Sb6a^{-/-}$, and $Sb1a.Sb6a^{-/-}$ BMDMCs treated with LLME compared to WT, suggesting that multiple proteolytic pathways contribute to the fate of mast cells upon granule permeabilization and that cytosolic serpins, particularly Serpinb9a, are important for survival following leakage of granule proteases into the cytosol.

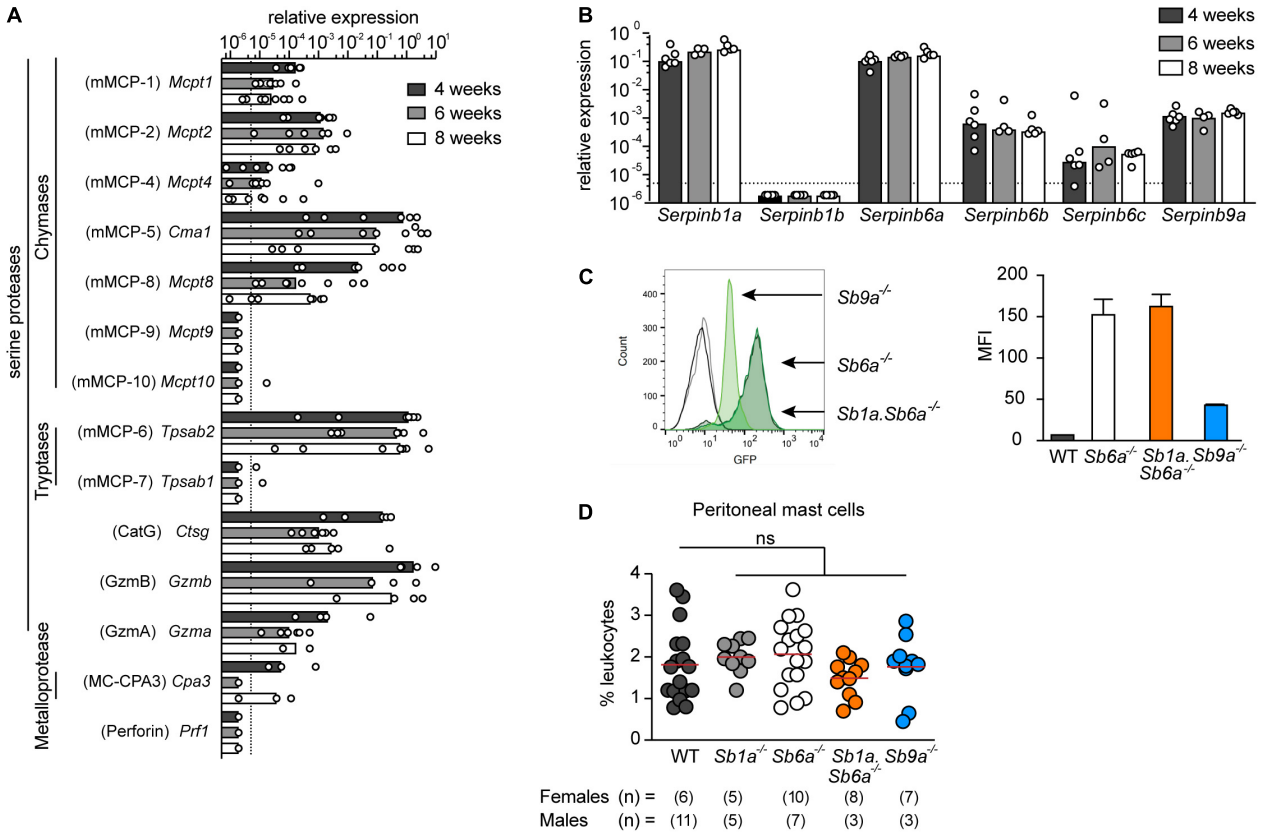

FIGURE 2 | Expression of serine proteases and clade B serpins in BMDMCs. **(A)** Relative mRNA expression of mouse mast cell proteases (mMCP), including chymases (*Mcpt*), tryptases (*Tpsab*), cathepsin G (*Ctsg*), granzymes (*Gzm*), carboxypeptidase 3 (*Cpa3*); and expression of perforin (*Prf1*) in WT mouse BMDMCs at indicated time of *in vitro* differentiation with IL-3. **(B)** Relative mRNA expression of mouse serpin homolog genes in WT mouse BMDMCs at indicated time of *in vitro* differentiation with IL-3. Data are shown as mean relative expression (bars) with individual BMDMC preparation (dots) (n = 4–6). Data are shown as median with range. **(C)** Representative flow cytometry histogram (left) and mean ± SD (right) of mean fluorescence intensity (MFI) of reporter GFP signal in BMDMCs of *Sb6a*$^{-/-}$, *Sb1a.Sb6a*$^{-/-}$, and *Sb9a*$^{-/-}$ mice. **(D)** Percentage of mast cells (IgE^{+}, FcεR1a^{+}, c-Kit^{+}) in peritoneal cavity of WT, *Sb1a*$^{-/-}$, *Sb6a*$^{-/-}$, *Sb1a.Sb6a*$^{-/-}$, and *Sb9a*$^{-/-}$ female and male mice. Data were analyzed by one-way ANOVA and showed no difference relative to WT mice; data are shown as median (red line) and for individual mice (n = 5–11/sex/genotype).

Granzyme B Is the Main Inducer of Apoptosis in Mast Cells Upon Granule Leakage

We then investigated BMDMCs of mice deficient for the target proteases of the three serpins. In particular, *GzmB*$^{-/-}$ BMDMCs were highly resistant to LLME-induced cell death compared to WT BMDMCs (**Figure 3C**). Moreover, *GzmB.Sb9a*$^{-/-}$ BMDMCs had similar resistance to LLME treatment as *GzmB*$^{-/-}$ BMDMCs, and notably demonstrated higher survival than WT BMDMCs. Therefore, the susceptibility of *Sb9a*$^{-/-}$ BMDMCs to granule protease-mediated suicide is principally due to unleashed GzmB activity (**Figure 3B**). In the presence of Q-VD-OPh, survival improved in WT BMDMCs, reaching the levels of *GzmB*$^{-/-}$ and *GzmB.Sb9a*$^{-/-}$ BMDMCs, suggesting activation of caspases downstream of GzmB (**Figure 3C**). In contrast, *CatG*$^{-/-}$ BMDMCs had no survival benefit compared to WT BMDMCs (**Figure 3D**). The survival of *CatG.Sb1a.Sb6a*$^{-/-}$ BMDMCs was also similar to WT BMDMCs. Taken together, we conclude that GzmB is the principal mediator of apoptosis following granule leakage in mast cells, and that CatG detectably contributes to cell death only in the absence of its two inhibitory serpins.

Deletion of Cathepsin G, Granzyme B or Their Inhibitors Does Not Alter Bone Marrow-Derived Mast Cell Differentiation and Apoptosis Induced by Growth Factor Deprivation

Survival and differentiation of BMDMCs *in vitro* is dependent on the supply of growth factors, such as IL-3, which sustain survival in part by inhibiting the intrinsic pathway of apoptosis (Karlberg et al., 2010b; Ottina et al., 2015). To test whether intracellular serpins are also involved in this intrinsic apoptosis pathway, we measured survival of BMDMCs for 96 h after IL-3 withdrawal. Survival of WT BMDMCs was substantially enhanced by the caspase inhibitor Q-VD-OPh (**Figure 4**). In paired experiments, we observed no significant difference in survival of *Sb1a*$^{-/-}$,

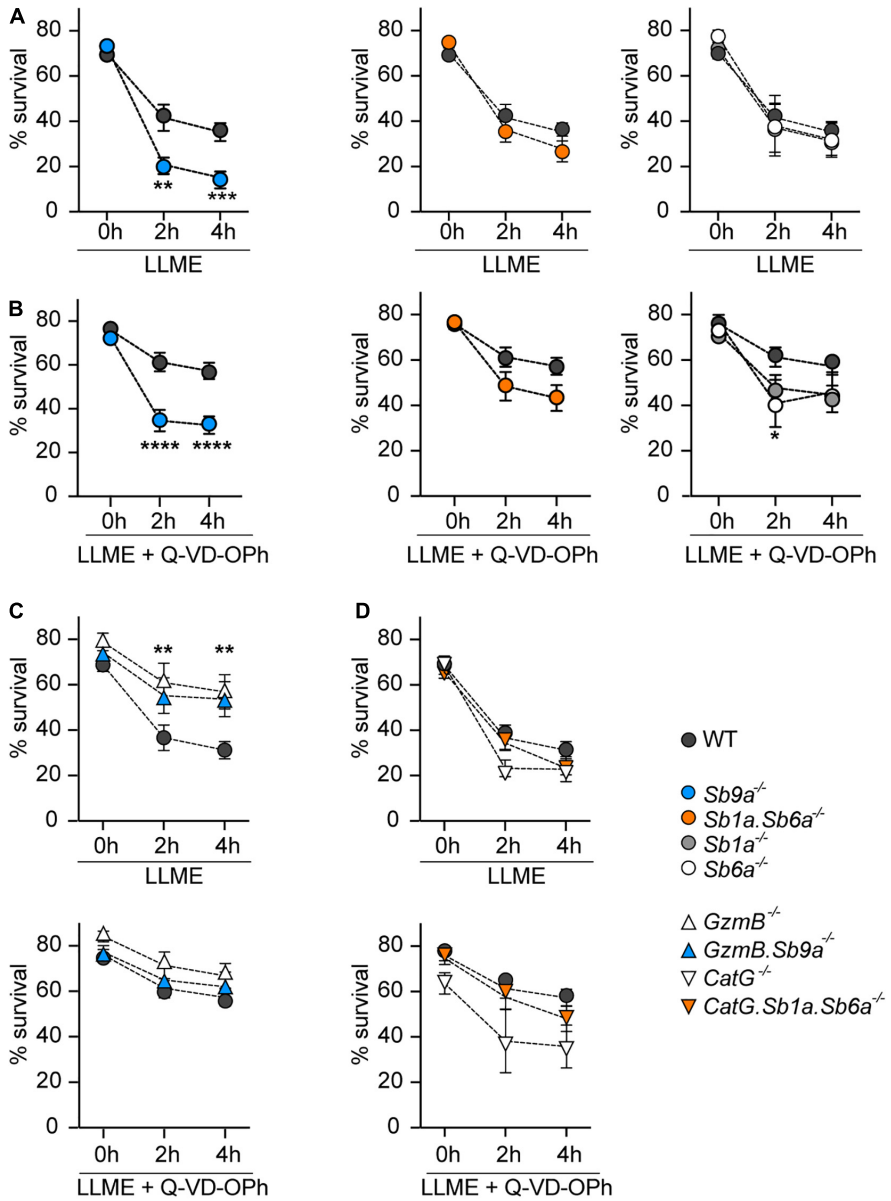

FIGURE 3 | Kinetics of cell death induced by granule permeabilization of BMDMCs. BMDMCs were treated with 250 μM L-leucyl-L-leucine methyl ester (LLME) with or without 50 μM Q-VD-OPh as indicated: **(A)** serpin-deficient BMDMCs, **(B)** serpin-deficient BMDMCs with Q-VD-OPh, **(C)** *GzmB*$^{-/-}$ and *GzmB.Sb9a*$^{-/-}$ BMDMCs with or without Q-VD-OPh, **(D)** *CatG*$^{-/-}$ and *CatG.Sb1a.Sb6a*$^{-/-}$ BMDMCs with or without Q-VD-OPh. **(A–D)** Viability was measured by flow cytometry using annexin V-APC and PI/7-AAD labeling as shown in **Supplementary Figure 3**. WT BMDMCs in each panel are from paired experiments with the corresponding mutant BMDMCs. Data are shown as mean ± SEM and were analyzed by two-way ANOVA (**$p < 0.01$; ***$p < 0.001$; ****$p < 0.0001$) (n = 5–14).

Sb6a$^{-/-}$, *Sb9a*$^{-/-}$, and *Sb1a.Sb6a*$^{-/-}$ BMDMCs compared to WT with or without caspase inhibition (**Figure 4A**). Similarly, BMDMCs derived from mice lacking GzmB and CatG showed no significant protection against cell death induced by IL-3 withdrawal in presence or absence of Q-VD-OPh (**Figure 4B**). Finally, we tested the survival of BMDMCs lacking the serpins as well as their respective target protease. *GzmB.Sb9a*$^{-/-}$ and *CatG.Sb1a.Sb6a*$^{-/-}$ BMDMCs were comparable in their survival as paired cultures of WT BMDMCs (**Figure 4C**). These findings indicate that although IL-3 removal triggers caspase activation and apoptosis, this pathway does not require granule proteases GzmB and CatG, and it is not regulated by cytosolic serpins.

Granzyme B Triggers the Activation of Caspase-3 Following Granule Leakage

GzmB is a known inducer of apoptosis when delivered with perforin to target cells by cytotoxic T lymphocytes and natural killer cells. In the cytosol, GzmB processes multiple targets including direct proteolytic activation of procaspase-3 and

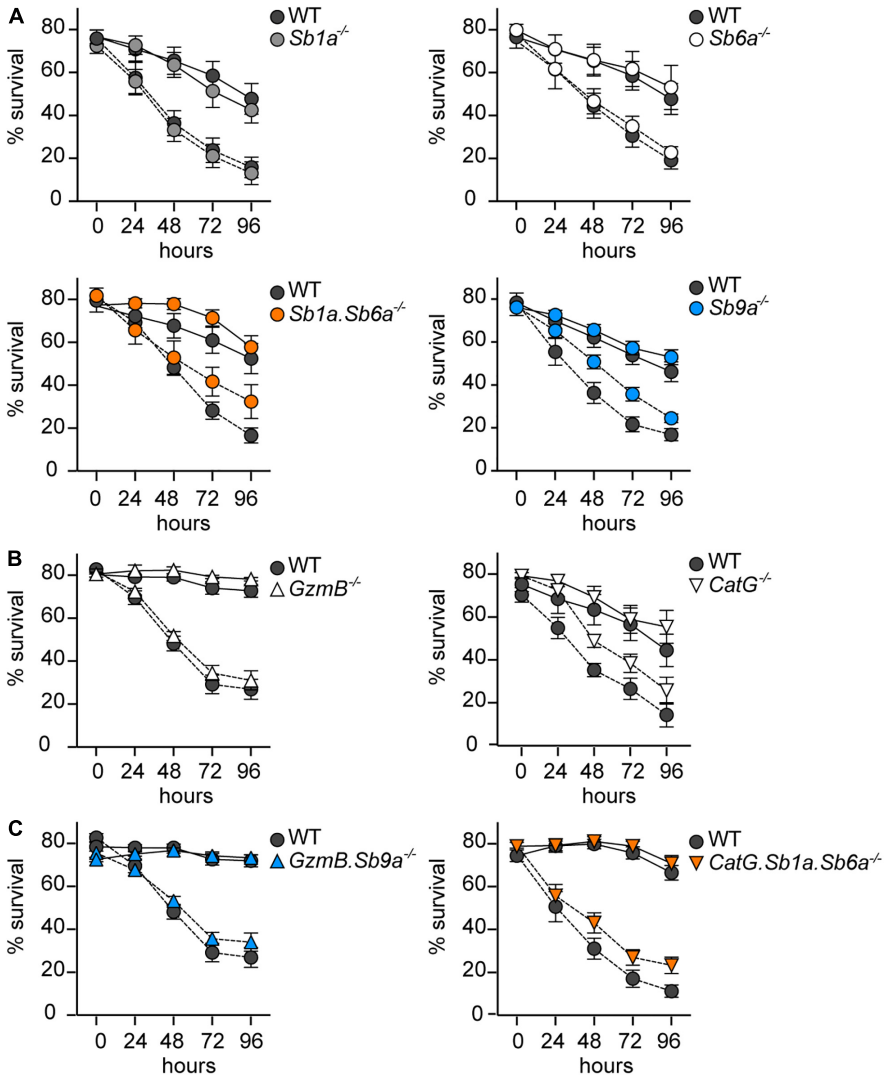

FIGURE 4 | Kinetics of apoptosis of BMDMCs after growth factor deprivation. BMDMCs differentiated *in vitro* for 6–9 weeks were cultured for 96 h in the absence of recombinant IL-3 with (black line) or without (dashed line) of 50 μM Q-VD-OPh. Viability was assessed daily by flow cytometry using annexin V-APC/PI/7-AAD exclusion: **(A)** serpin-deficient BMDMCs, **(B)** *GzmB*$^{-/-}$ and *CatG*$^{-/-}$ BMDMCs, **(C)** *GzmB.Sb9a*$^{-/-}$ and *CatG.Sb1a.Sb6a*$^{-/-}$ BMDMCs. WT BMDMCs in each panel are from paired experiments with the corresponding mutant BMDMCs. Data are shown as mean ± SEM and were analyzed by two-way ANOVA (n = 5–15).

indirect activation via mitochondrial apoptotic events (Lord et al., 2003). As caspase inhibition in *GzmB*$^{-/-}$ BMDMCs treated with LLME only marginally improved survival (**Figure 3B**), we tested whether GzmB is required for caspase activation upon permeabilization of granules. Western blot analysis of LLME-treated BMDMCs revealed that the active caspase-3 p17 fragment is generated in a dose-dependent manner in WT and *Sb9a*$^{-/-}$ BMDMCs. Most importantly, absence of GzmB in *GzmB*$^{-/-}$ and in *GzmB.Sb9a*$^{-/-}$ BMDMCs prevented the cleavage of pro-caspase-3 p35 into p19 and the active p17 fragment. Conversely, caspase-3 processing was accelerated in *Sb9a*$^{-/-}$ BMDMCs showing a complete conversion into the active p17 fragment even treated at a low LLME concentration (**Figures 5A,B**). Overall, our findings indicate that GzmB is the most effective serine protease inducing apoptosis in mast cells after leakage from granules. Sb9a acts as a gatekeeper for caspase-3 activation by inhibiting GzmB. The higher survival of *GzmB*$^{-/-}$ compared to WT BMDMCs (**Figure 3C**) suggest that the protease eventually overwhelms its inhibitor to induce caspase-dependent and caspase-independent cell death.

DISCUSSION

Mast cells contribute to severe symptoms associated with allergic disorders (Galli et al., 2008). Reducing mast cell numbers at disease-specific locations may therefore provide a novel therapeutic axis (Karra et al., 2009; Hagforsen et al., 2015; Cildir et al., 2017). Studies by Melo et al. (2011a,b) and Paivandy et al. (2014) showed that mast cells are sensitive to death in

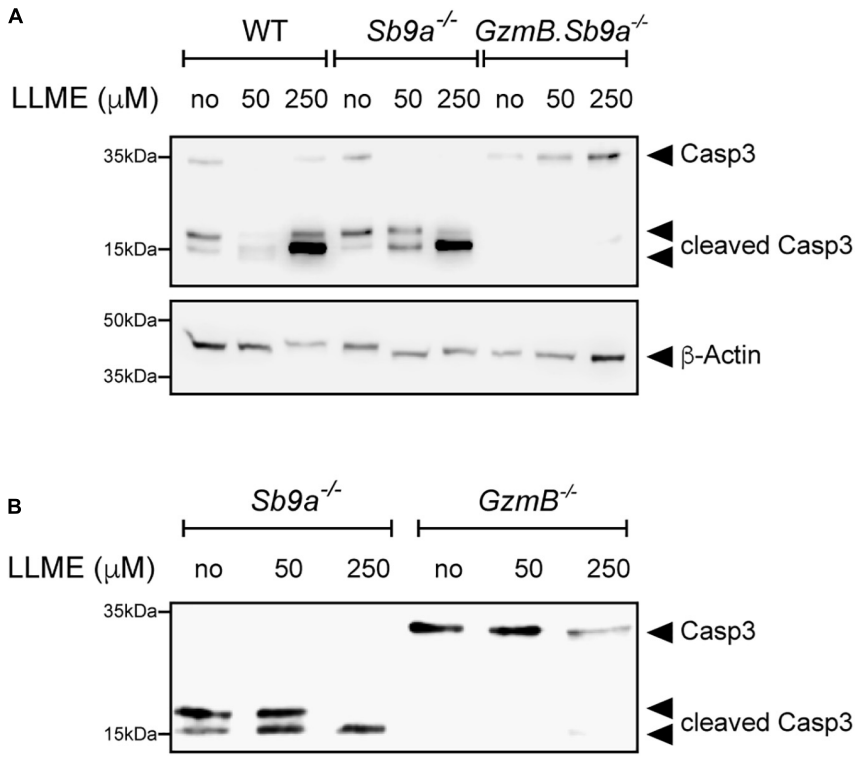

FIGURE 5 | GzmB-dependent cleavage of caspase-3 in LLME-treated BMDMCs. Western Blot analysis of caspase-3 cleavage in BMDMC of **(A)** WT, *Sb9a*$^{-/-}$ and *GzmB.Sb9a*$^{-/-}$ mice **(B)** *Sb9a*$^{-/-}$ and *GzmB*$^{-/-}$ mice stimulated with 50 and 250 μM L-leucyl-L-leucine methyl ester (LLME) for 30 min.

response to lysosomotropic agents such as LLME and mefloquine (an anti-malaria drug) due to cell-intrinsic leakage of their secretory granules and that this form of cell death is mediated by serine proteases and caspases. However, the serine protease(s) involved in this cell death pathway remain incompletely defined: BMDMCs deficient in the tryptase mMCP-6 were only marginally protected against cell death and deletion of the chymase mMCP-4 or the carboxypeptidase A (CPA) had no effect (Melo et al., 2011b). Here we have confirmed that cell death induced by LMME in human HMC-1.2 and mouse BMDMCs is efficiently blocked by the combined use of inhibitors of caspases and serine proteases.

We found that the serine proteases GzmB and CatG, previously associated with granule-mediated suicide in other leukocyte classes (Kaiserman and Bird, 2010; Benarafa and Simon, 2017), are also present at appreciable levels in mast cells, comparable to levels of the signature mast cell protease, chymase. We hypothesized that these proteases may be involved in LLME-mediated mast cell death, and that their cognate cytosolic serpins might act to block this death pathway. Indeed, *Sb1a* $^{-/-}$, *Sb6a*$^{-/-}$ and, most severely, double-deficient *Sb1a.Sb6a*$^{-/-}$ neutrophils have increased susceptibility to this form of cell death as both serpins contribute additively to inhibit CatG (Burgener et al., 2016, 2019). Moreover, granule permeabilization induces cell death in LLME-treated neutrophils in a CatG-dependent manner (Baumann et al., 2013; Burgener et al., 2019). Here, we found that Serpinb1a, Serpinb6a (and their target CatG) are highly expressed in mast cells. Yet, Serpinb1a and Serpinb6a had limited protective effects on mast cells following LLME exposure and this protection was only noticeable when caspases were inhibited. *Sb1a.Sb6a*$^{-/-}$ BMDMCs did not show increased death compared to single knockout *Sb1a*$^{-/-}$ or *Sb6a*$^{-/-}$ BMDMCs. CatG deletion rescued this mild phenotype in *CatG.Sb1a.Sb6*$^{-/-}$ BMDMCs, demonstrating that CatG has a real but minor effect on mast cell suicide.

Similarly, Serpinb9 protects activated cytotoxic T lymphocytes and natural killer cells against cell intrinsic death induced by GzmB stored in their granules (Hirst et al., 2003; Ida et al., 2003; Bird et al., 2014; Mangan et al., 2017). GzmB and its inhibitor Serpinb9a are expressed in BMDMCs as well as in human mast cells and cell lines (Bladergroen et al., 2005; Pardo et al., 2007; Strik et al., 2007). Importantly, we found that *GzmB*$^{-/-}$ BMDMCs are resistant to mast cell death induced by LLME and that their survival was significantly improved compared to WT BMDMCs. Conversely, Serpinb9a deletion increased death of BMDMCs. The cytoprotective function of Serpinb9a is principally through inhibition of GzmB since *GzmB.Sb9a*$^{-/-}$ BMDMCs were as resistant to LLME as *GzmB*$^{-/-}$ BMDMCs. We found that Pefabloc (AEBSF) protects against LLME-induced death in WT BMDMCs, yet Pefabloc inhibits most serine proteases but not GzmB. This suggests that other Pefabloc-sensitive mast cell proteases, such as mMCP-6, may contribute in part in this pathway via inactivation of Serpinb9a; such a hypothesis remains to be explored.

Our findings suggest multiple pathways leading to death in mast cells via the activity of granule serine proteases GzmB and, to a lesser extent, CatG. The GzmB pathway appears to be the most prominent as GzmB induces apoptosis even in the presence of its endogenous inhibitor Serpinb9a, whereas CatG appears to be well under control of the abundant basal levels of Serpinb1a and Serpinb6a. The relative contribution of serine proteases thus depends on their abundance, especially relative to the levels of cytosolic serpins and to the expression of downstream targets that will accelerate cellular demise.

Our data indicates that GzmB contributes to the direct or indirect activation of caspase-3 upon granule permeabilization. Yet, caspase inhibition was not sufficient to block cell death. This may be due in part to the ability of GzmB to induce apoptosis via multiple independent pathways (Chowdhury and Lieberman, 2008; Martinvalet, 2015). It has been proposed that pro-caspase-3 is also stored and activated in a granzyme B-dependent manner in mast cell secretory granules (Garcia-Faroldi et al., 2013; Zorn et al., 2013). While we cannot exclude the possibility that granule caspase-3 contributes to mast cell death, our data support the view that caspase-3 activation classically occurs in the cytosol. Indeed, Serpinb9a has a nucleo-cytosolic localization and is not found in granules (Bird et al., 2001), while *Sb9a*$^{-/-}$ BMDMCs treated with LLME showed increased cleavage of caspase-3 into p17 active fragment. The composition of granule cargo is regulated at several levels: the presence of signal peptide is found at the N-terminus of serine and cysteine proteases but not caspases, which are found in the cytosol. The storage of some serine proteases in different granules is further regulated by serglycin. Serglycin is required for the packaging of most mast cell proteases, including chymases and carboxylpeptidase and to a lesser extent tryptases (Ronnberg et al., 2012). GzmB also requires serglycin for localization in granules (Sutton et al., 2016), while CatG does not (Niemann et al., 2007). Interestingly, mast cells of *Serglycin*$^{-/-}$ mice are protected against LLME-induced apoptotic cell death (Melo et al., 2011b). Our findings on GzmB are thus in agreement with previous work demonstrating that a serglycin-dependent protease is responsible for apoptotic death in mast cells following granule permeabilization (Melo et al., 2012).

Mast cells are long-lived in tissues and their survival depends on pro-survival signals and the regulation of the mitochondrial pathway of apoptosis by B-cell lymphoma-2 (Bcl-2) family proteins (Karlberg et al., 2010b; Garrison et al., 2012). Growth factors such as IL-3 and the c-kit ligand stem cell factor (SCF) sustain the survival of mast cells through increased expression of anti-apoptotic Bcl-2 family proteins such as MCL-1 and A1 (Xiang et al., 2001; Reinhart et al., 2018). Conversely, withdrawal of IL-3 or SCF triggers the mitochondrial pathway of apoptosis by increasing the expression of the BH3 only proteins Puma and Bim, respectively (Moller et al., 2005; Ekoff et al., 2007). In support of this model, we found that deletion of Serpinb1a, Serpinb6a and Serpinb9a or their target proteases CatG and GzmB does not alter the cell death kinetics of apoptosis mediated by IL-3 withdrawal. Similarly, *Serglycin*$^{-/-}$ BMDMCs undergo apoptosis normally upon IL-3 withdrawal (Melo et al., 2011b). Targeting mast cells in allergic disorders or in systemic mastocytosis using BH3 mimetics holds promise (Aichberger et al., 2009; Karlberg et al., 2010a; Reinhart et al., 2018). Our findings suggest that induction of GzmB-mediated death in mast cells would provide an additional independent mechanism to target mast cells that could be used in synergy with BH3 mimetics.

In conclusion, we have shown that cytosolic clade B serpins provide a key protective shield in mast cells and prevent the onset of a very rapid apoptotic-like cell death associated with granule serine protease activity. The balance between GzmB and Serpinb9a is particularly important to maintain mast cell survival and the targeted release of GzmB in mast cells and/or downregulation of Serpinb9 may be an interesting therapeutic avenue to target mast cells.

MATERIALS AND METHODS

Mice

All animal studies were approved by the Cantonal Veterinary Office of Bern and conducted in accordance with the Swiss federal legislation on animal welfare. Mice were kept in SPF facilities, in individually ventilated cages, with 12/12 light/dark cycle, autoclaved acidified water, autoclaved cages including food, bedding and environmental enrichment. Age and gender of mice is indicated for each *in vivo* or *ex vivo* model described below as well as in figure legends. All gene targeted mice were on the C57BL/6J background or had been backcrossed to the C57BL/6J background for at least 10 generations. *Sb1a*$^{-/-}$ (*Serpinb1a*$^{tm1.1Cben}$), *Sb6a*$^{-/-}$ (*Serpinb6a*$^{tm1.1Pib}$), *Sb9a*$^{-/-}$ (*Serpinb9a*$^{tm1.1Pib}$) were described previously (Scarff et al., 2003; Benarafa et al., 2007; Rizzitelli et al., 2012). *CatG*$^{-/-}$ (*Ctsg*^{tm1Ley}) and *GzmB*$^{-/-}$ (*Gzmb*^{tm1Ley}) mice were kindly provided by Christine Pham (Washington University, St. Louis, MO) (MacIvor et al., 1999) and Australian Phenome Facility (Heusel et al., 1994), respectively. *Sb1a.Sb6a*$^{-/-}$ mice were generated by mating compound heterozygous F1 mice as described previously (Burgener et al., 2019). All double and triple knockout mice as *GzmB.Sb9a*$^{-/-}$ and *CatG.Sb1a.Sb6a*$^{-/-}$ mice were generated in our facility by compound heterozygote mating.

Peritoneal Mast Cells and Flow Cytometry

Peritoneal lavage was performed using 5 mL PBS supplemented with 1% heat-inactivated FBS on healthy female and male mice. Total cell numbers were evaluated by counting cells manually in a Neubauer chamber. Relative percentages of live mast cells were determined by flow cytometry; analysis was performed using FlowJo with single cell gating, dead cell exclusion using propidium iodide (PI) and, mast cells identified as FcεRI^{+}, IgE^{+}, and, c-kit^{+}. Single cell suspensions blocked with anti-CD16/CD32 (clone 2.4G2) and stained for 30–40 min on ice with fluorescently labeled antibodies (BioLegend, BD Biosciences) were acquired using a 4-color FACS Calibur (BD Biosciences). Mast cells were permeabilized using the Foxp3 buffer (eBioscience) and stained using an anti-mouse granzyme A antibody (eBioscience, clone 3G8.5).

Cell Culture

The human mast cell leukemia cell line HMC-1.2 was generated as previously described (Dr. J. Butterfield) and kindly provided by Prof. G. Nilsson (Karolinska Institute, Stockholm) (Butterfield et al., 1988; Nilsson et al., 1994). HMC-1.2 cells were cultured as previously described (Sundstrom et al., 2003). Bone marrow derived mast cells (BMDMCs) were obtained by flushing femurs and tibias bone marrow cells of 6–12 week old female and male mice and cultured in DMEM with 2 mM L-glutamine, supplemented with 10% heat-inactivated FBS, 50 μM β-mercaptoethanol, 1% penicillin/streptomycin, and 10 ng/mL recombinant mouse IL-3 (Peprotech). The cells were maintained at a concentration of 2.5×10^5–1×10^6 cells/mL, at 37°C in 5–7% CO_2. Maturity was assessed by analysis of the expression of c-Kit, IgE, and FcεRI by flow cytometry 4–5 weeks after isolation (**Supplementary Figure 4**). In various assays, BMDMCs were seeded at 1×10^6 cells/mL and incubated at indicated concentrations with L-leucyl-L-leucine methyl ester (LLME) (Bachem, # G-2550), Q-VD-OPh (ApexBio, #A1901) or Pefabloc SC (Sigma, #PEFBSC-RO). In some experiments, mature BMDMCs (1.0×10^6/mL) were cultured in absence of rmIL-3 with DMEM, 1% heat-inactivated FBS, 1% penicillin/streptomycin up to 96 h with or without 50 μM Q-VD-OPh (ApexBio, #A1901). Apoptosis and necrosis of mast cells *in vitro* was determined by staining with Annexin V-fluorescein isothiocyanate (FITC) or Annexin V-allophycocyanin (APC) and propidium iodide (PI) or 7-aminoactinomycin D (7-AAD) at RT for 15 min and measured with a 4-color flow cytometer (FACScalibur, BD Biosciences).

Quantitative RT-PCR

RNA-isolation was performed using RNA-Bee (AMS Biotechnology, #CS-501B). In brief, $3–5 \times 10^6$ BMDMCs were resuspended in 1 mL RNA-Bee and total RNA extracted following the manufacturers protocol. After DNAse treatment, 300 ng total RNA was reverse transcribed using ProtoScript III reverse transcriptase and random primer mix (New England Biolabs). Real-time quantitative PCR amplification was carried out in duplicate or triplicate using Mastermix Plus SYBR Assay-Low Rox (Eurogentec, #RT-SY2X-03+WOULRF) in a Vii7 thermocycler (Applied Biosystems). Sequences of the validated specific primers for proteases, serpins and S16 ribosomal protein (RPS16) are shown in **Supplementary Table 1** (Chen et al., 2005; Martin et al., 2005; Ekoff et al., 2007; Malbec et al., 2007; Andrew et al., 2008; Cremona et al., 2013). For each sample, mRNA levels were expressed relative to S16 expression.

Western Blot

BMDMCs were treated for 0.5 h with 50–500 μM L-leucyl-L-leucine methyl ester (LLME) (Bachem, #G-2550) and lysed in 0.1% Triton-X-100 lysis buffer without protease inhibitors followed by 2×30 s sonication (Soniprep 150 plus, MSE). Lysates were centrifuged at 10,000 g for 10 min at 4°C and supernatant was collected. Total protein concentration in lysates were determined by the BCA assay (Thermo Fisher Scientific, #23225). Cell lysates were pooled with methanol/chloroform-precipitated cell-free supernatants or cell lysates alone (30 μg total protein) were resolved in SDS-PAGE under reducing conditions using Tris-Glycine Buffer. After transfer on nitrocellulose, blocking was performed using 5% skimmed milk and blots were probed with rabbit anti-mouse caspase-3 (Cell Signaling, #9662) and then stripped and reprobed with anti-β-Actin antibody (Abcam, #ab8227).

Statistical Analysis

Statistical analysis was performed using Prism 8.0c (GraphPad, San Diego, CA). Non-parametric tests were used to analyze data from *in vivo* and *ex vivo* studies. Independent experiments were performed and pooled, scatter plots represent individual mice and horizontal lines indicate mean ± SEM or median with range. Experiments were analyzed by one-way or two-way ANOVA with Tukey *post-test* and *p*-values of $p < 0.05$ were considered statistically significant ($^{****}P < 0.0001$; $^{***}P < 0.001$; $^{**}P < 0.01$; $^{*}P < 0.05$). Tests used and number of replicates are indicated in figure legends.

DATA AVAILABILITY STATEMENT

The original contributions presented in the study are included in the article/**Supplementary Material**, further inquiries can be directed to the corresponding author.

ETHICS STATEMENT

Animal experimentation was conducted in compliance with the Swiss Animal Welfare legislation and animal studies were reviewed and approved by the commission for animal experiments of the canton of Bern, Switzerland under licenses BE8/16 and BE35/19.

AUTHOR CONTRIBUTIONS

SB designed, performed the experiments, analyzed the data, and wrote the manuscript. MB, NL, SS, and PB performed the experiments and analyzed the data. TK and PIB provided key reagents, scientific advice, and revised the manuscript. CB supervised the project, designed the experiments, analyzed the data, and wrote the manuscript. All authors contributed to the article and approved the submitted version.

FUNDING

This work was supported by the grants from the Swiss National Science Foundation to CB (310030-149790 and 310030-173137).

ACKNOWLEDGMENTS

We thank Joseph Butterfield, Gunnar Nilsson, Christine Pham for cells, mice and reagents. We thank Isabelle Wymann,

Roman Troxler, Jan Salchli, Katarzyna Sliz, Daniel Brechbühl, and Hans-Peter Lüthi for dedicated animal care. We thank Aurélie Godel and Debora Lind for help with mouse colony maintenance and genotyping.

SUPPLEMENTARY MATERIAL

The Supplementary Material for this article can be found online at: https://www.frontiersin.org/articles/10.3389/fcell.2021.630166/full#supplementary-material

Supplementary Figure 1 | Analysis of peritoneal mast cells. **(A)** Flow cytometry gating strategy of steady state peritoneal lavage cells to identify mast cells as IgE$^+$, FcεR1a$^+$, and, c-Kit$^+$. **(B)** Mast cells (IgE$^+$, FcεR1a$^+$, c-Kit$^+$) in peritoneal cavity of WT, serpin-deficient and protease-deficient mice. Data were analyzed by one-way ANOVA and no difference was found for any deficient mouse relative to WT mice; data are shown as median (red line) and for individual mice (n = 3–11/sex/genotype).

Supplementary Figure 2 | BMDMCs and peritoneal mast cells do not express granzyme A protein. **(A)** Representative flow cytometry plots of peritoneal mast cells and identified as IgE$^+$, FcεR1a$^+$, and, c-Kit$^+$. Data are representative of three preparations of C57BL/6 wild-type mice at 6–12 weeks. **(B)** Representative flow cytometry plots of BMDMCs cultured with IL-3 for 5 weeks. **(C)** Representative flow cytometry plots of mouse spleen NK cells and CD8 T cells. Data are representative of four C57BL/6 wild-type (WT) and five *GzmA*$^{-/-}$ mice at 6–12 weeks. **(A–C)** Expression of granzyme A was assessed in fixed and permeabilized cells with a specific antibody.

Supplementary Figure 3 | Flow cytometry analysis of mast cells viability. Representative flow cytometry dot plots and gating strategy for evaluating mast cell survival with annexin V and propidium iodide staining. BMDMCs were treated or not with LLME as indicated.

Supplementary Figure 4 | Maturity of BMDMCs after 4 weeks of *in vitro* differentiation in presence of IL-3. **(A)** Flow cytometry gating strategy. **(B)** Percentage of IgE$^+$FcεR1a$^+$c-Kit$^+$ BMDMCs of each genotype after 4 weeks of maturation *in vitro* with recombinant mouse IL-3.

Supplementary Figure 5 | Uncropped western blot of **Figures 1**, **5**. Representative uncropped western blots.

REFERENCES

Ahmad, J., Bird, P. I., and Kaiserman, D. (2014). Analysis of the evolution of granule associated serine proteases of immune defence (GASPIDs) suggests a revised nomenclature. *Biol. Chem.* 395, 1253–1262. doi: 10.1515/hsz-2014-0174

Aichberger, K. J., Gleixner, K. V., Mirkina, I., Cerny-Reiterer, S., Peter, B., Ferenc, V., et al. (2009). Identification of proapoptotic Bim as a tumor suppressor in neoplastic mast cells: role of KIT D816V and effects of various targeted drugs. *Blood* 114, 5342–5351. doi: 10.1182/blood-2008-08-175190

Akahoshi, M., Song, C. H., Piliponsky, A. M., Metz, M., Guzzetta, A., Abrink, M., et al. (2011). Mast cell chymase reduces the toxicity of Gila monster venom, scorpion venom, and vasoactive intestinal polypeptide in mice. *J. Clin. Invest.* 121, 4180–4191. doi: 10.1172/JCI46139

Andrew, K. A., Simkins, H. M., Witzel, S., Perret, R., Hudson, J., Hermans, I. F., et al. (2008). Dendritic cells treated with lipopolysaccharide up-regulate serine protease inhibitor 6 and remain sensitive to killing by cytotoxic T lymphocytes in vivo. *J. Immunol.* 181, 8356–8362. doi: 10.4049/jimmunol.181.12.8356

Baumann, M., Pham, C. T., and Benarafa, C. (2013). SerpinB1 is critical for neutrophil survival through cell-autonomous inhibition of cathepsin G. *Blood* 121:455022. doi: 10.1182/blood-2012-09-455022

Benarafa, C., and Simon, H. U. (2017). Role of granule proteases in the life and death of neutrophils. *Biochem. Biophys. Res. Commun.* 482, 473–481. doi: 10.1016/j.bbrc.2016.11.086

Benarafa, C., Cooley, J., Zeng, W., Bird, P. I., and Remold-O'Donnell, E. (2002). Characterization of four murine homologs of the human ov-serpin monocyte neutrophil elastase inhibitor MNEI (SERPINB1). *J. Biol. Chem.* 277, 42028–42033. doi: 10.1074/jbc.M207080200

Benarafa, C., Priebe, G. P., and Remold-O'Donnell, E. (2007). The neutrophil serine protease inhibitor serpinb1 preserves lung defense functions in *Pseudomonas aeruginosa* infection. *J. Exp. Med.* 204, 1901–1909. doi: 10.1084/jem.20070494

Bird, C. H., Blink, E. J., Hirst, C. E., Buzza, M. S., Steele, P. M., Sun, J., et al. (2001). Nucleocytoplasmic distribution of the ovalbumin serpin PI-9 requires a nonconventional nuclear import pathway and the export factor Crm1. *Mol. Cell Biol.* 21, 5396–5407. doi: 10.1128/MCB.21.16.5396-5407.2001

Bird, C. H., Christensen, M. E., Mangan, M. S., Prakash, M. D., Sedelies, K. A., Smyth, M. J., et al. (2014). The granzyme B-Serpinb9 axis controls the fate of lymphocytes after lysosomal stress. *Cell Death Differ.* 21, 876–887. doi: 10.1038/cdd.2014.7

Bird, C. H., Sutton, V. R., Sun, J., Hirst, C. E., Novak, A., Kumar, S., et al. (1998). Selective regulation of apoptosis: the cytotoxic lymphocyte serpin proteinase inhibitor 9 protects against granzyme B-mediated apoptosis without perturbing the Fas cell death pathway. *Mol. Cell Biol.* 18, 6387–6398. doi: 10.1128/mcb.18.11.6387

Bladergroen, B. A., Strik, M. C., Wolbink, A. M., Wouters, D., Broekhuizen, R., Kummer, J. A., et al. (2005). The granzyme B inhibitor proteinase inhibitor 9 (PI9) is expressed by human mast cells. *Eur. J. Immunol.* 35, 1175–1183. doi: 10.1002/eji.200425949

Bradding, P., and Pejler, G. (2018). The controversial role of mast cells in fibrosis. *Immunol. Rev.* 282, 198–231. doi: 10.1111/imr.12626

Burgener, S. S., Baumann, M., Basilico, P., Remold-O'Donnell, E. I, Touw, P., and Benarafa, C. (2016). Myeloid conditional deletion and transgenic models reveal a threshold for the neutrophil survival factor Serpinb1. *Biol. Chem.* 397, 897–905. doi: 10.1515/hsz-2016-0132

Burgener, S. S., Leborgne, N. G. F., Snipas, S. J., Salvesen, G. S., Bird, P. I., and Benarafa, C. (2019). Cathepsin G Inhibition by Serpinb1 and Serpinb6 Prevents Programmed Necrosis in Neutrophils and Monocytes and Reduces GSDMD-Driven Inflammation. *Cell Rep.* 27, 3646–3656e5. doi: 10.1016/j.celrep.2019.05.065

Butterfield, J. H., Weiler, D., Dewald, G., and Gleich, G. J. (1988). Establishment of an immature mast cell line from a patient with mast cell leukemia. *Leuk Res.* 12, 345–355. doi: 10.1016/0145-2126(88)90050-1

Chen, C. C., Grimbaldeston, M. A., Tsai, M., Weissman, I. L., and Galli, S. J. (2005). Identification of mast cell progenitors in adult mice. *Proc. Natl. Acad. Sci. U S A.* 102, 11408–11413. doi: 10.1073/pnas.0504197102

Chowdhury, D., and Lieberman, J. (2008). Death by a thousand cuts: granzyme pathways of programmed cell death. *Annu. Rev. Immunol.* 26, 389–420. doi: 10.1146/annurev.immunol.26.021607.090404

Cildir, G., Pant, H., Lopez, A. F., and Tergaonkar, V. (2017). The transcriptional program, functional heterogeneity, and clinical targeting of mast cells. *J. Exp. Med.* 214, 2491–2506. doi: 10.1084/jem.20170910

Cooley, J., Takayama, T. K., Shapiro, S. D., Schechter, N. M., and Remold-O'Donnell, E. (2001). The serpin MNEI inhibits elastase-like and chymotrypsin-like serine proteases through efficient reactions at two active sites. *Biochemistry* 40, 15762–15770.

Cremona, T. P., Tschanz, S. A., von Garnier, C., and Benarafa, C. (2013). SerpinB1 deficiency is not associated with increased susceptibility to pulmonary emphysema in mice. *Am. J. Physiol. Lung Cell Mol. Physiol.* 305, L981–L989. doi: 10.1152/ajplung.00181.2013

Ekoff, M., Kaufmann, T., Engstrom, M., Motoyama, N., Villunger, A., Jonsson, J. I., et al. (2007). The BH3-only protein Puma plays an essential role in cytokine deprivation induced apoptosis of mast cells. *Blood* 110, 3209–3217. doi: 10.1182/blood-2007-02-073957

Galli, S. J., Tsai, M., and Piliponsky, A. M. (2008). The development of allergic inflammation. *Nature* 454, 445–454. doi: 10.1038/nature07204

Galli, S. J., Tsai, M., Marichal, T., Tchougounova, E., Reber, L. L., and Pejler, G. (2015). Approaches for analyzing the roles of mast cells and their proteases in vivo. *Adv. Immunol.* 126, 45–127. doi: 10.1016/bs.ai.2014.11.002

Garcia-Faroldi, G., Melo, F. R., Ronnberg, E., Grujic, M., and Pejler, G. (2013). Active caspase-3 is stored within secretory compartments of viable mast cells. *J. Immunol.* 191, 1445–1452. doi: 10.4049/jimmunol.1300216

Garrison, S. P., Phillips, D. C., Jeffers, J. R., Chipuk, J. E., Parsons, M. J., Rehg, J. E., et al. (2012). Genetically defining the mechanism of Puma- and Bim-induced apoptosis. *Cell Death Differ.* 19, 642–649. doi: 10.1038/cdd.2011.136

Hagforsen, E., Paivandy, A., Lampinen, M., Westrom, S., Calounova, G., Melo, F. R., et al. (2015). Ablation of human skin mast cells in situ by lysosomotropic agents. *Exp. Dermatol.* 24, 516–521. doi: 10.1111/exd.12699

Heusel, J. W., Wesselschmidt, R. L., Shresta, S., Russell, J. H., and Ley, T. J. (1994). Cytotoxic lymphocytes require granzyme B for the rapid induction of DNA fragmentation and apoptosis in allogeneic target cells. *Cell* 76, 977–987. doi: 10.1016/0092-8674(94)90376-x

Hirst, C. E., Buzza, M. S., Bird, C. H., Warren, H. S., Cameron, P. U., Zhang, M., et al. (2003). The intracellular granzyme B inhibitor, proteinase inhibitor 9, is up-regulated during accessory cell maturation and effector cell degranulation, and its overexpression enhances CTL potency. *J. Immunol.* 170, 805–815. doi: 10.4049/jimmunol.170.2.805

Ida, H., Nakashima, T., Kedersha, N. L., Yamasaki, S., Huang, M., Izumi, Y., et al. (2003). Granzyme B leakage-induced cell death: a new type of activation-induced natural killer cell death. *Eur. J. Immunol.* 33, 3284–3292. doi: 10.1002/eji.200324376

Kaiserman, D., and Bird, P. I. (2010). Control of granzymes by serpins. *Cell Death Differ.* 17, 586–595. doi: 10.1038/cdd.2009.169

Kaiserman, D., Stewart, S. E., Plasman, K., Gevaert, K., Van Damme, P., and Bird, P. I. (2014). Identification of Serpinb6b as a species-specific mouse granzyme A inhibitor suggests functional divergence between human and mouse granzyme A. *J. Biol. Chem.* 289, 9408–9417. doi: 10.1074/jbc.M113.525808

Karlberg, M., Ekoff, M., Labi, V., Strasser, A., Huang, D., and Nilsson, G. (2010b). Pro-apoptotic Bax is the major and Bak an auxiliary effector in cytokine deprivation-induced mast cell apoptosis. *Cell Death Dis.* 1:e43. doi: 10.1038/cddis.2010.20

Karlberg, M., Ekoff, M., Huang, D. C., Mustonen, P. I, Harvima, T., and Nilsson, G. (2010a). The BH3-mimetic ABT-737 induces mast cell apoptosis in vitro and in vivo: potential for therapeutics. *J. Immunol.* 185, 2555–2562. doi: 10.4049/jimmunol.0903656

Karra, L., Berent-Maoz, B., Ben-Zimra, M., and Levi-Schaffer, F. (2009). Are we ready to downregulate mast cells? *Curr. Opin. Immunol.* 21, 708–714. doi: 10.1016/j.coi.2009.09.010

Lord, S. J., Rajotte, R. V., Korbutt, G. S., and Bleackley, R. C. (2003). Granzyme B: a natural born killer. *Immunol. Rev.* 193, 31–38. doi: 10.1034/j.1600-065x.2003.00044.x

MacIvor, D. M., Shapiro, S. D., Pham, C. T., Belaaouaj, A., Abraham, S. N., and Ley, T. J. (1999). Normal neutrophil function in cathepsin G-deficient mice. *Blood* 94, 4282–4293.

Malbec, O., Roget, K., Schiffer, C., Iannascoli, B., Dumas, A. R., Arock, M., et al. (2007). Peritoneal cell-derived mast cells: an in vitro model of mature serosal-type mouse mast cells. *J. Immunol.* 178, 6465–6475. doi: 10.4049/jimmunol.178.10.6465

Mangan, M. S., Melo-Silva, C. R., Luu, J., Bird, C. H., Koskinen, A., Rizzitelli, A., et al. (2017). A pro-survival role for the intracellular granzyme B inhibitor Serpinb9 in natural killer cells during poxvirus infection. *Immunol. Cell Biol.* 95, 884–894. doi: 10.1038/icb.2017.59

Martin, P., Wallich, R., Pardo, J., Mullbacher, A., Munder, M., Modolell, M., et al. (2005). Quiescent and activated mouse granulocytes do not express granzyme A and B or perforin: similarities or differences with human polymorphonuclear leukocytes? *Blood* 106, 2871–2878. doi: 10.1182/blood-2005-04-1522

Martinvalet, D. (2015). ROS signaling during granzyme B-mediated apoptosis. *Mol. Cell Oncol.* 2:e992639. doi: 10.4161/23723556.2014.992639

Maurer, M., Theoharides, T., Granstein, R. D., Bischoff, S. C., Bienenstock, J., Henz, B., et al. (2003). What is the physiological function of mast cells? *Exp. Dermatol.* 12, 886–910.

Melo, F. R., Grujic, M., Spirkoski, J., Calounova, G., and Pejler, G. (2012). Serglycin proteoglycan promotes apoptotic versus necrotic cell death in mast cells. *J. Biol. Chem.* 287, 18142–18152. doi: 10.1074/jbc.M112.344796

Melo, F. R., Lundequist, A., Calounova, G., Wernersson, S., and Pejler, G. (2011a). Lysosomal membrane permeabilization induces cell death in human mast cells. *Scand. J. Immunol.* 74, 354–362. doi: 10.1111/j.1365-3083.2011.02589.x

Melo, F. R., Waern, I., Ronnberg, E., Abrink, M., Lee, D. M., Schlenner, S. M., et al. (2011b). A role for serglycin proteoglycan in mast cell apoptosis induced by a secretory granule-mediated pathway. *J. Biol. Chem.* 286, 5423–5433. doi: 10.1074/jbc.M110.176461

Melo, F. R., Wernersson, S., and Pejler, G. (2015). Induction of mast cell apoptosis by a novel secretory granule-mediated pathway. *Methods Mol. Biol.* 1220, 325–337. doi: 10.1007/978-1-4939-1568-2_20

Metz, M., Piliponsky, A. M., Chen, C. C., Lammel, V., Abrink, M., Pejler, G., et al. (2006). Mast cells can enhance resistance to snake and honeybee venoms. *Science* 313, 526–530. doi: 10.1126/science.1128877

Moller, C., Alfredsson, J., Engstrom, M., Wootz, H., Xiang, Z., Lennartsson, J., et al. (2005). Stem cell factor promotes mast cell survival via inactivation of FOXO3a-mediated transcriptional induction and MEK-regulated phosphorylation of the proapoptotic protein Bim. *Blood* 106, 1330–1336. doi: 10.1182/blood-2004-12-4792

Niemann, C. U., Abrink, M., Pejler, G., Fischer, R. L., Christensen, E. I., Knight, S. D., et al. (2007). Neutrophil elastase depends on serglycin proteoglycan for localization in granules. *Blood* 109, 4478–4486. doi: 10.1182/blood-2006-02-001719

Nilsson, G., Blom, T., Kusche-Gullberg, M., Kjellen, L., Butterfield, J. H., Sundstrom, C., et al. (1994). Phenotypic characterization of the human mast-cell line HMC-1. *Scand. J. Immunol.* 39, 489–498. doi: 10.1111/j.1365-3083.1994.tb03404.x

Oskeritzian, C. A. (2015). Mast cell plasticity and sphingosine-1-phosphate in immunity, inflammation and cancer. *Mol. Immunol.* 63, 104–112. doi: 10.1016/j.molimm.2014.03.018

Ottina, E., Lyberg, K., Sochalska, M., Villunger, A., and Nilsson, G. P. (2015). Knockdown of the antiapoptotic Bcl-2 family member A1/Bfl-1 protects mice from anaphylaxis. *J. Immunol.* 194, 1316–1322. doi: 10.4049/jimmunol.1400637

Paivandy, A., Calounova, G., Zarnegar, B., Ohrvik, H., Melo, F. R., and Pejler, G. (2014). Mefloquine, an anti-malaria agent, causes reactive oxygen species-dependent cell death in mast cells via a secretory granule-mediated pathway. *Pharmacol. Res. Perspect.* 2:e00066. doi: 10.1002/prp2.66

Pardo, J., Wallich, R., Ebnet, K., Iden, S., Zentgraf, H., Martin, P., et al. (2007). Granzyme B is expressed in mouse mast cells in vivo and in vitro and causes delayed cell death independent of perforin. *Cell Death Differ.* 14, 1768–1779. doi: 10.1038/sj.cdd.4402183

Piliponsky, A. M., Chen, C. C., Nishimura, T., Metz, M., Rios, E. J., Dobner, P. R., et al. (2008). Neurotensin increases mortality and mast cells reduce neurotensin levels in a mouse model of sepsis. *Nat. Med.* 14, 392–398. doi: 10.1038/nm1738

Piliponsky, A. M., Chen, C. C., Rios, E. J., Treuting, P. M., Lahiri, A., Abrink, M., et al. (2012). The chymase mouse mast cell protease 4 degrades TNF, limits inflammation, and promotes survival in a model of sepsis. *Am. J. Pathol.* 181, 875–886. doi: 10.1016/j.ajpath.2012.05.013

Reinhart, R., Rohner, L., Wicki, S., Fux, M., and Kaufmann, T. (2018). BH3 mimetics efficiently induce apoptosis in mouse basophils and mast cells. *Cell Death Differ.* 25, 204–216. doi: 10.1038/cdd.2017.154

Rizzitelli, A., Meuter, S., Vega Ramos, J., Bird, C. H., Mintern, J. D., Mangan, M. S., et al. (2012). Serpinb9 (Spi6)-deficient mice are impaired in dendritic cell-mediated antigen cross-presentation. *Immunol. Cell Biol.* 90, 841–851. doi: 10.1038/icb.2012.29

Ronnberg, E., Calounova, G., Sutton, V. R., Trapani, J. A., Rollman, O., Hagforsen, E., et al. (2014). Granzyme H is a novel protease expressed by human mast cells. *Int. Arch. Allergy Immunol.* 165, 68–74. doi: 10.1159/000368403

Ronnberg, E., Melo, F. R., and Pejler, G. (2012). Mast cell proteoglycans. *J. Histochem. Cytochem.* 60, 950–962. doi: 10.1369/0022155412458927

Scarff, K. L., Ung, K. S., Sun, J., and Bird, P. I. (2003). A retained selection cassette increases reporter gene expression without affecting tissue distribution in SPI3 knockout/GFP knock-in mice. *Genesis* 36, 149–157. doi: 10.1002/gene.10210

Scott, F. L., Hirst, C. E., Sun, J., Bird, C. H., Bottomley, S. P., and Bird, P. I. (1999). The intracellular serpin proteinase inhibitor 6 is expressed in monocytes and granulocytes and is a potent inhibitor of the azurophilic granule protease, cathepsin G. *Blood* 93, 2089–2097.

Strik, M. C., de Koning, P. J., Kleijmeer, M. J., Bladergroen, B. A., Wolbink, A. M., Griffith, J. M., et al. (2007). Human mast cells produce and release the cytotoxic lymphocyte associated protease granzyme B upon activation. *Mol. Immunol.* 44, 3462–3472. doi: 10.1016/j.molimm.2007.03.024

Strik, M. C., Wolbink, A., Wouters, D., Bladergroen, B. A., Verlaan, A. R., van Houdt, I. S., et al. (2004). Intracellular serpin SERPINB6 (PI6) is abundantly

expressed by human mast cells and forms complexes with beta-tryptase monomers. *Blood* 103, 2710–2717. doi: 10.1182/blood-2003-08-2981

Sun, J., Ooms, L., Bird, C. H., Sutton, V. R., Trapani, J. A., and Bird, P. I. (1997). A new family of 10 murine ovalbumin serpins includes two homologs of proteinase inhibitor 8 and two homologs of the granzyme B inhibitor (proteinase inhibitor 9). *J. Biol. Chem.* 272, 15434–15441. doi: 10.1074/jbc.272.24.15434

Sundstrom, M., Vliagoftis, H., Karlberg, P., Butterfield, J. H., Nilsson, K., Metcalfe, D. D., et al. (2003). Functional and phenotypic studies of two variants of a human mast cell line with a distinct set of mutations in the c-kit proto-oncogene. *Immunology* 108, 89–97. doi: 10.1046/j.1365-2567.2003.01559.x

Sutton, V. R., Brennan, A. J., Ellis, S., Danne, J., Thia, K., Jenkins, M. R., et al. (2016). Serglycin determines secretory granule repertoire and regulates natural killer cell and cytotoxic T lymphocyte cytotoxicity. *FEBS J.* 283, 947–961. doi: 10.1111/febs.13649

Thiele, D. L., and Lipsky, P. E. (1986). The immunosuppressive activity of L-leucyl-L-leucine methyl ester: selective ablation of cytotoxic lymphocytes and monocytes. *J. Immunol.* 136, 1038–1048.

Thiele, D. L., and Lipsky, P. E. (1990a). Mechanism of L-leucyl-L-leucine methyl ester-mediated killing of cytotoxic lymphocytes: dependence on a lysosomal thiol protease, dipeptidyl peptidase I, that is enriched in these cells. *Proc. Natl. Acad. Sci. U S A.* 87, 83–87. doi: 10.1073/pnas.87.1.83

Thiele, D. L., and Lipsky, P. E. (1990b). The action of leucyl-leucine methyl ester on cytotoxic lymphocytes requires uptake by a novel dipeptide-specific facilitated transport system and dipeptidyl peptidase I-mediated conversion to membranolytic products. *J. Exp. Med.* 172, 183–194. doi: 10.1084/jem.172.1.183

Trivedi, N. N., Tong, Q., Raman, K., Bhagwandin, V. J., and Caughey, G. H. (2007). Mast cell alpha and beta tryptases changed rapidly during primate speciation and evolved from gamma-like transmembrane peptidases in ancestral vertebrates. *J. Immunol.* 179, 6072–6079.

Waern, I., Karlsson, I., Pejler, G., and Wernersson, S. (2016). IL-6 and IL-17A degradation by mast cells is mediated by a serglycin:serine protease axis. *Immun. Inflamm. Dis.* 4, 70–79. doi: 10.1002/iid3.95

Wang, L., Li, Q., Wu, L., Liu, S., Zhang, Y., Yang, X., et al. (2013). Identification of SERPINB1 as a physiological inhibitor of human granzyme H. *J. Immunol.* 190, 1319–1330. doi: 10.4049/jimmunol.1202542

Xiang, Z., Ahmed, A. A., Moller, C., Nakayama, K., Hatakeyama, S., and Nilsson, G. (2001). Essential role of the prosurvival bcl-2 homologue A1 in mast cell survival after allergic activation. *J. Exp. Med.* 194, 1561–1569. doi: 10.1084/jem.194.11.1561

Zorn, C. N., Pardo, J., Martin, P., Kuhny, M., Simon, M. M., and Huber, M. (2013). Secretory lysosomes of mouse mast cells store and exocytose active caspase-3 in a strictly granzyme B dependent manner. *Eur. J. Immunol.* 43, 3209–3218. doi: 10.1002/eji.201343941

Conflict of Interest: The authors declare that the research was conducted in the absence of any commercial or financial relationships that could be construed as a potential conflict of interest.

Publisher's Note: All claims expressed in this article are solely those of the authors and do not necessarily represent those of their affiliated organizations, or those of the publisher, the editors and the reviewers. Any product that may be evaluated in this article, or claim that may be made by its manufacturer, is not guaranteed or endorsed by the publisher.

Advantages of publishing in Frontiers

OPEN ACCESS
Articles are free to read for greatest visibility and readership

FAST PUBLICATION
Around 90 days from submission to decision

HIGH QUALITY PEER-REVIEW
Rigorous, collaborative, and constructive peer-review

TRANSPARENT PEER-REVIEW
Editors and reviewers acknowledged by name on published articles

Frontiers
Avenue du Tribunal-Fédéral 34
1005 Lausanne | Switzerland

Visit us: www.frontiersin.org
Contact us: frontiersin.org/about/contact

REPRODUCIBILITY OF RESEARCH
Support open data and methods to enhance research reproducibility

DIGITAL PUBLISHING
Articles designed for optimal readership across devices

FOLLOW US
@frontiersin

IMPACT METRICS
Advanced article metrics track visibility across digital media

EXTENSIVE PROMOTION
Marketing and promotion of impactful research

LOOP RESEARCH NETWORK
Our network increases your article's readership